START

0003824 RHO-ST-14

Copy 201

High-Level Waste Leakage from the 241-T-106 Tank at Hanford

R. C. Routson
W. H. Price
D. J. Brown
K. R. Fecht

Earth Sciences Group
Research Department

February 1979

Prepared for the United States
Department of Energy
Under Contract EY-77-C-06-1030

SEP 1989
RECEIVED
EDMC

Rockwell International

Rockwell Hanford Operations
Energy Systems Group
Richland, WA 99352

Rockwell International
Rockwell Hanford Operations
Energy Systems Group
Richland, WA 99352

9 2 1 2 4 6 6 1 2 3 6

NOTICE

This Report was prepared as an account of work sponsored by the United States Government. Neither the United States nor the United States Department of Energy, nor any of their Employees, nor any of their Contractors, Subcontractors, or their Employees, makes any warranty, express or implied, or assumes any legal liability or responsibility for the accuracy, completeness, or usefulness of any information, apparatus, product or process disclosed, or represents that its use would not infringe privately owned rights.

AVAILABLE FROM THE
NATIONAL TECHNICAL INFORMATION SERVICE
SPRINGFIELD, VA. 22161

PRICE: MICROFICHE: $3.00
PAPER COPY: $9.50

RHO-ST-14
Distribution Category UC-70

HIGH-LEVEL WASTE LEAKAGE FROM THE 241-T-106 TANK AT HANFORD

R. C. Routson
W. H. Price
D. J. Brown
K. R. Fecht

Earth Sciences Group
Research Department

February 1979

Prepared for the United States
Department of Energy
Under Contract EY-77-C-06-1030

Rockwell International
Rockwell Hanford Operations
Energy Systems Group
Richland, Washington 99352

9 2 1 2 4 6 6 1 2 3 7

THIS PAGE INTENTIONALLY
LEFT BLANK

ABSTRACT

The history, status, fate and impact of the 4.34×10^5-liter (115,000-gallon) radioactive waste tank leak from the 241-T-106 tank have been studied since 1973. As of May 1978, the maximum detected depth of the 1-microcurie per liter (μCi/ℓ) concentration of ruthenium-106 (^{106}Ru) penetration was 33 meters (108 feet) below the ground surface or 29 meters (95 feet) above the regional water table. This maximum depth of penetration was detected in two of the dry wells in the 241-T tank farm. In no other well has radioactivity greater than 1.0-μCi/ℓ been found deeper than 29 meters (95 feet). This is approximately 43% of the distance from the bottom of the tank to the water table. The maximum horizontal movement of the 1-μCi/ℓ ^{106}Ru concentration front from the tank was approximately 23 meters (75 feet) at a depth of 25 meters (82 feet). This distance is approximately equal to the diameter of the tank.

The rate of frontal movement of radioactivity was qualitatively estimated. A large portion of the movement occurred in 1973, prior to the publication of an initial tank leak status report. From 1973 to 1974, detectable lateral movement occurred in at least some sediment layers. From 1974 to 1978, movement could not generally be detected. However, migration in wells near the leak perimeter was detected in 1978, and the probable cause defined.

Calculations on vadose zone moisture and wetting frontal movement were found to be essentially in qualitative agreement in their assessed lack of movement of any waste above concentration guidelines to the Hanford ground water. Thus, during the hazardous lifetime of the fission products, there will likely be no amount of radioactivity enter the Hanford ground water. Therefore, there appears to be no impact of the leak on the Columbia River (the nearest point of uncontrolled access).

ACKNOWLEDGEMENTS

Thanks are expressed to the many individuals and companies who made this report possible. These include: (1) Dr. R. L. Brodzinski of Pacific Northwest Laboratory for directing the measurements of in-well GEA; (2) R. E. Isaacson of Rockwell Hanford Operations for directing, overviewing, and reviewing the project; (3) V. W. Hall and L. L. Weaver, Rockwell Hanford Operations, for conducting GEA analysis of sediments; (4) T. J. Wood of Rockwell Hanford Operations for assistance in drilling and sampling; (5) Dr. L. L. Ames of Pacific Northwest Laboratory for determining hydrologic and engineering properties of sediments; (7) F. Stone of Rockwell Hanford Operations for editorial services; (8) Radiation Monitoring Group of Rockwell Hanford Operations for radiation monitoring support; and (9) J. A. Jones Construction Company for providing field support and drilling.

9 2 1 2 4 6 6 1 2 3 9

CONTENTS

Glossary vii

Introduction 1

241-T-106 Tank Environment 3
- Climate 3
- Stratigraphy 3
  - Middle Ringold 3
  - Upper Ringold 3
  - Eolian Silt 5
  - Hanford Formation 5
  - Backfill 5
- Regional Ground-Water Levels and Travel Times 7
- Construction of 241-T-106 Tank 7
- Composition of the 241-T-106 Tank Contents 7

1978 Status of 241-T-106 Leak Boundary 10
- Dry-Well Monitoring Results 10
- In-Well Gamma Analyses Instrumentation Results 10
  - Comparison Views of Sediment Concentrations 19
  - Ground-Water Radionuclide Concentration Near Leak Site . . . 25
  - Foil Activation Assay 25

Fate and Impact of 241-T-106 Tank Leak 27
- Decay Rate of the Gamma Radioactivity 27
- Vadose Zone Moisture Movement 29
- Wetting Frontal Movement Calculations 29
- Sorption Effects 32

Conclusion and Recommendations 35

References 36

Appendices:

A. Chronology of the 241-T-106 Tank Leak A-1
B. Rockwell Hanford Operations High-Level Radioactive Tank Leak Criteria, Monitoring, and Detection Levels B-1
C. Climate C-1
D. Geology of the 241-T Tank Farm D-1
E. Regional Ground-Water Levels and Travel Times to the Columbia River E-1
F. Ground-Water Measurements F-1
G. Composition of 241-T-106 Tank Contents G-1
H. 1973 Gamma-Energy Analysis of Radionuclide Sediment Samples . . . H-1
J. Analysis Methods J-1
K. In-Well Radioactivity Data K-1
L. 1978 Plan and Section Views of the ^{106}Ru, ^{144}Ce and ^{137}Cs Activity Near the 241-T-106 Tank L-1
M. Regression Analysis of the Logarithm of the In-Well Total Gamma Counts with Time M-1

CONTENTS (Contd.)

Figures:

1. Location of 241-T-106 Tank in Relation to the Hanford Site and the State of Washington 1
2. Three-Dimensional Drawing of the Distribution of Sedimentary Lithologies Beneath the 241-T-106 Tank. 4
3. Typical Horizontal and Vertical Movement of Liquids in Hanford Formation Sediments Under Partially Saturated Conditions 6
4. Structural Details of 241-T-106 Tank 8
5. Relationship of the 241-T-106 Tank to Neighboring Tanks in 241-T Tank Farm. 11
6. In-Well Total Gamma Logs for Well 111 13
7. In-Well Total Gamma Logs for Well 106 14
8. In-Well Total Gamma Logs for Well 120 15
9. In-Well ^{106}Ru Concentration as a Function of Depth in Wells 106, 111, and 120 17
10. In-Well ^{137}Cs Concentration as a Function of Depth in Wells 106, 111, and 120 18
11. Composite Drawing of Plan and Section Views of the 1.0-μCi/ℓ Concentrations of ^{144}Ce, ^{137}Cs and ^{106}Ru in 1973 . . . 20
12. Plan View of the 241-T-106 Tank, the Surrounding Tanks, and Dry Wells in the T-Tank Farm in 1978 22
13. Plan and Cross Section View Through a Portion of 241-T Tank Farm with 1-μCi/ℓ Ruthenium-106 Isopleth Distribution Pattern . . 23
14. Plan and Cross Section View Through a Portion of 241-T Tank Farm with 1-μCi/ℓ Cesium-137 Isopleth Distribution Pattern. . . . 24

Tables:

1. Chemical Composition of the 241-T-106 Tank Supernatant Solution 9
2. Radionuclide Composition of the 241-T-106 Tank Supernatant Solution 9
3. Estimated Plutonium Plus Americium Concentrations (ng/cm^3) in Wells Near the 241-T-106 Tank 26
4. Linear Regression Analysis of ln of In-Well Total Gamma Activity as a Function of Time. 28
5. Radionuclide Composition and Properties and Retardation Factors for Hanford Tank Farm Sediments 34

GLOSSARY

Audit - An official AEC examination and verification of contractor operating procedures.

Boiling Waste - Radioactive liquid waste that generates sufficient fission product decay heat to boil the stored solution.

Breakthrough - First detectable concentration of a nuclide in a column effluent.

Carbon Steel - Steel containing carbon up to about 2%.

Cation Exchange Capacity - Concentration of an exchangeable cation adsorbed by a soil at pH 7 determined by a standard method.

Caustic Waste Solutions - Coating waste solutions with a high concentration of sodium hydroxide (caustic) or acid wastes which have been neutralized and made caustic to about pH 10 for storage in underground carbon steel tanks.

C/C_0 - Amount of a nuclide in the effluent of a soil column divided by the amount of that nuclide added in the effluent.

Cesium-137 - A fission product having a half-life of 30.2 years. It is a long-lived heat producer which is removed in 221-B Plant and will be packaged in high integrity containers and stored. (See Fractionization Processing Facility.)

Chemical Processing of Fuels - The separation and recovery of valuable nuclear materials and removal of undesirable wastes by chemical methods. It may involve dissolution and solvent extraction.

Crib - An underground framework or structure into which liquid wastes are discharged, located so that the radioactivity is sorbed on the soil before the liquid reaches groundwater.

Curie (Ci) - A unit of radioactivity; it is the quantity of any radioactive material in which 3.7×10^{10} nuclear disintegrations occur per second.

Denuded Supernate - The solution which remains after ion exchanging tank farm supernates to recover cesium.

Dry Well - A drill hole which does not reach the water table and is used for radiation monitoring measurements.

Dry Well Data - A measurement, group of measurements, or statistics on the radiation readings in a dry well.

Evaporation System (242-T) - One of the Hanford solidification units which concentrates high-level wastes and produces immobile salt cake for storage in underground waste storage tanks.

Fission Product Isotopes - A general term for the complex mixture of substances produced as a result of nuclear fission.

Fractionization Processing Facility (221-B Plant) - A facility which processes current and accumulated waste by ion exchange, solvent extraction, and precipitation to remove cesium and strontium as purified fractions which will be packaged for storage and will thereby permit solidification of the waste which remains.

Ground Water - Water within the earth, below the unsaturated zone of percolation, the upper surface of which is called the water table.

Half-life - Time required for a radioactive substance to lose 50% of its activity by decay.

Heat-Producing Isotopes - Isotopes which generate heat during the decay process. The two long-lived heat-producing isotopes are strontium-90 and cesium-137.

Interstitial Liquors - The liquid that fills in the space between the crystalline salts that have precipitated out in tanks in the Hanford Waste Solidification System. It is equal to approximately 20 to 30% of the salt cake volume.

Ion Exchange - The equivalent replacement of an adsorbed ion on a solid adsorbent by another ion from the solution.

Isopleth (radioactivity) - A line on a geologic cross section drawn through points of equal radioisotopic composition.

Isotopes - Forms of the same element having identical chemical properties but differing in their atomic masses and nuclear properties.

K_d - Term representing the equilibrium distribution coefficient of a nuclide, A, between the solid adsorbent and the solution at equilibrium:

$$K_d = \frac{A_{solid}}{A_{soln}} \times \frac{cc_{soln.}}{g_{solid}}$$

where:

A_{solid} = the amount of A that is associated with the adsorbent.

$A_{soln.}$ = the amount of A that remains in the solution.

$cc_{soln.}$ = the total volume of solution in cc.

g_{solid} = the total weight of adsorbent in g.

Liquid Level Data - A measurement, group of measurements, or statistics on the level of liquid waste in a storage tank.

Mineral Replacement - Substitution of a crystal lattice ion by another ion from the solution governed by the laws of solubility.

Natural Decay - The decrease in activity of any radioactive material with the passage of time.

Plutonium-239 - The desired activation product of the Hanford production reactors having a half-life of 24,390 years. It is separated in 202-A (Purex) as a nitrate solution and reduced to metal or oxide in 234-5Z Plant, for use as an energy source of atomic weapons and as a fuel for nuclear reactors.

Purex - A chemical processing flowsheet for the extraction and recovery of plutonium and uranium from nuclear fuels using solvent extraction equipment and tributyl phosphate as the organic solvent.

Quality Assurance - The planned and systematic actions necessary to provide adequate confidence that a material, component, system or facility will perform satisfactorily in service.

Radiation Sorption Qualities - The ability of soil or sediment particles to hold on to specific radioisotopes by ionic exchange or other chemical reactions.

Radiochemical Analysis - Measurement of radioactive isotopes by a combination of chemical and instrumental methods.

Radionuclides - A general term referring to any radioactive nuclear species.

Redox - A chemical processing flowsheet for the extraction and recovery of plutonium and uranium from nuclear fuels using solvent extraction equipment and hexone as the organic solvent.

Salt Cake - The product of the Hanford In-Tank Solidification Program, the objective of which is to concentrate and solidify high-level solidifiable wastes as immobile salt in underground waste storage tanks.

Sludge - A precipitated alkaline sediment, usually containing ^{90}Sr, that forms on the bottom of waste storage tanks during interim storage while awaiting decay of most of the short-lived radioisotopes.

Sluicing - The removal of sludge from a boiling waste storage tank, after the overlying liquid is removed, by using a high pressure nozzle to produce a slurry. The slurry is then processed to remove the strontium for encapsulation.

Solvent Extraction - A process for separating selected compounds from an aqueous solution by the use of an organic solvent, such as tributyl phosphate, through selective adsorption or reaction by intimately contacting the aqueous and organic liquids.

Standard Operating Procedure (SOP) - The formal procedures for operating facilities which are designed and implemented to provide maximum safety and protection of all employees, the general public, and environment.

Strontium-90 - A fission product having a half-life of 28.9 years. It is a long-lived heat producer which is removed in 221-B Plant and will be packaged in high integrity containers and stored.

Tank Farm - A group of interconnected underground storage tanks originally built to contain radioactive liquid wastes.

Total Gamma Profiles - Total radioactivity detected either by in-well scintillation or Geiger Müller detectors as a function of depth. The detected radioactivity is essentially gamma because alpha and beta are nearly absorbed by the sediments, well casing and detector casing.

Vadose Zone - The unsaturated sediments above the ground-water table.

9 2 1 2 4 6 6 1 2 4 5

INTRODUCTION

On June 8, 1973, a 2.02 x 10^6-liter (533,000-gallon) capacity 241-T-106 high-level radioactive waste storage tank was confirmed as leaking by the Atlantic Richfield Hanford Company* (ARHCO) day-shift supervisor (Reference 1). This tank is located in the 241-T-tank farm, 200 West Area of the Department of Energy's Hanford Site in south-central Washington State (Figure 1).

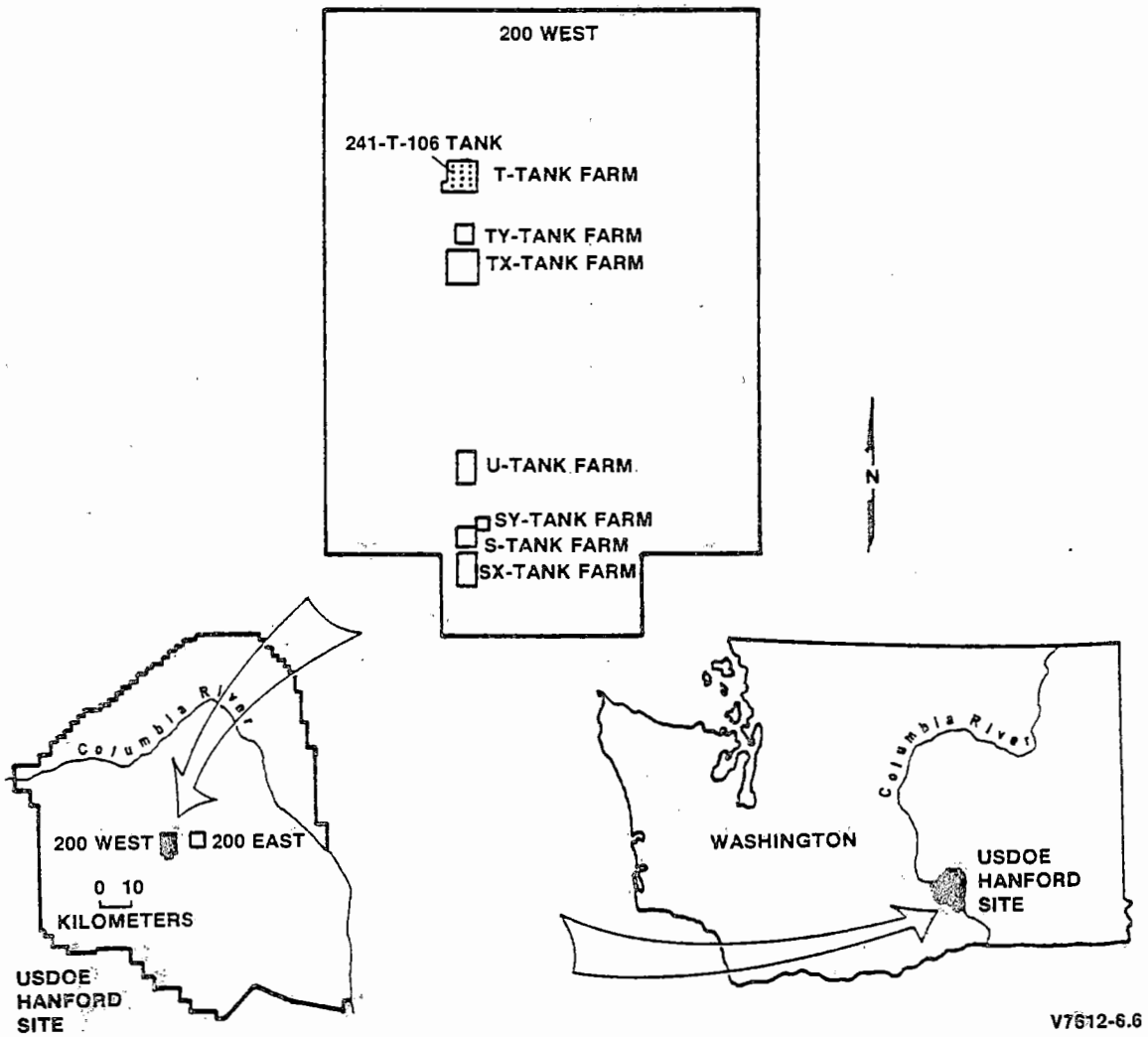

FIGURE 1. Location of 241-T-106 Tank in Relation to the Hanford Site and the State of Washington.

*Atlantic Richfield Hanford Company held the U. S. Department of Energy contract for chemical processing, waste management and site support from January 1, 1966 to June 30, 1977.

It is the purpose of this report to: (1) give the May 1978 241-T-106 tank leak status; (2) make a comprehensive integration of all the 241-T-106 tank leak studies and data; and (3) estimate the future impact of this leak on surrounding uncontrolled areas near the Hanford Site. A summary will be issued in parallel with this technical report.

Two previous reports have been published on the 241-T-106 tank leak. The first was published by the Atomic Energy Commission (AEC). Circumstances surrounding the 241-T-106 tank leak were presented and recommendations were made for improving ARHCO's tank farm monitoring activities and leak detection procedures (Reference 1). Appendix A contains the official chronology of the events leading up to the discovery of the 241-T-106 tank leak. Appendix B contains the present Rockwell Hanford Operations (Rockwell) leak detection criteria, tank farm monitoring activities, and leak evaluation capabilities which evolved in response to the AEC report. The second 241-T-106 tank leak report was published in late 1973 by ARHCO (Reference 2). The extent of the leak and the volume of contaminated sediments, as judged from 1 μCi/ℓ isopleth of ^{106}Ru were determined (Reference 2). The parent-daughter pair, ^{106}Ru-^{106}Rh, (rodium-106) will be given as ^{106}Ru in the balance of this report. Waste penetrated to approximately 27 meters (89 feet) below the ground surface or to about 35 meters (116 feet) above the regional water table. As a result of the ARHCO study, it was estimated that additional waste movement from the 1973 location would be negligible.

On June 9, 1973, the volume of the leak was determined to be approximately 4.35 x 10^5 liters (115,000 gallons) containing approximately 14,000 Ci of strontium-90, 40,000 Ci of ^{137}Cs, and 4 Ci of plutonium (^{239}Pu and ^{240}Pu). In addition, the leak contained approximately 270,000 Ci of radionuclides with half-lives of less than 3 years (99% of which were 1 year half-life ^{106}Ru). Thus, this leak was the largest single accidental release in the AEC's operational history (Reference 3).

To put the volume of this leak into perspective, it can be compared to specific retention disposal at Hanford. Specific retention is defined as the maximum quantity of water (aqueous solution) that a soil or sediment will retain against gravity drainage, and is usually expressed on a volumetric basis (Reference 4). The specific retention capacity of the sediments below a Hanford crib was found to be 10% of a column volume. If a column volume for a tank leak is defined as the area of the bottom of the tank times the depth to ground water (References 5 and 6), the specific retention capacity for the 241-T-106 tank would be 1.8 x 10^6 liters (480,000 gallons). Thus, the 241-T-106 tank leak represents only 24% of the specific retention disposal value. At least 24 monitored specific retention cribs have been used on the Hanford Site for the disposal of unsorbed or poorly sorbed wastes (Reference 7). Of these, none show any radioactivity penetrating to the ground water as judged by scintillation profiles. All these releases were planned, engineered, and proved safe with respect to ground-water management.

241-T-106 TANK ENVIRONMENT

To evaluate the impact of a high-level radioactive waste tank leak, it is essential to consider the position of the tank and its contents in relation to its environment.

CLIMATE

The climate at Hanford can be described as one of low rainfall, 15.9 cm/yr (6.25 in/yr), low relative humidity, dry, hot summers, and frequent periods of dry, moderate-to-high winds. These factors tend to restrict the amount of moisture for percolation and potential leaching of waste released to underground sediments to a low value (see Appendix C).

STRATIGRAPHY

The major sedimentary units in the vadose zone underlying the 241-T tank farm, from the ground water to ground surface, are: (1) middle and upper units of Ringold Formation (the lower Ringold unit is not present in this area); (2) eolian silt; (3) the Hanford Formation; and (4) backfill. The thickness of these unsaturated sediments is approximately 62 meters (203 feet). The major sedimentary lithologies found between the ground surface and water table are depicted in Figure 2.

Middle Ringold

Beneath the 241-T tank farm, the middle Ringold unit predominantly consists of well-rounded cobbles and pebbles with an arkosic sand matrix. The lower portion of the unit is partially cemented with silica and/or calcium carbonate. The predominate conglomerate is massively bedded and poorly sorted. Numerous discontinuous arkosic sand and silt lenses, ranging from 1 centimeter (0.5 inch) to 5 meters (16 feet) in thickness, are interlayered in the conglomerate. The water table, 62 meters (203 feet) below the ground surface, lies within the middle Ringold unit.

Upper Ringold

The upper Ringold unit occurs between elevations 167 to 177 meters (550 to 580 feet) at the site of the 241-T tank farm. The unit consists of well-sorted, fine-grained, arkosic sands and silts. The sediments are crudely-to-well laminated with alternating fine sands and silts about 1.5 centimeters (0.8 inch) in thickness. Two distinct caliche (calcium carbonate) horizons are present near the top of the unit. The lower caliche horizon is very well developed, forming a duricrust with low saturated permeability (0.4 cm/day) values.

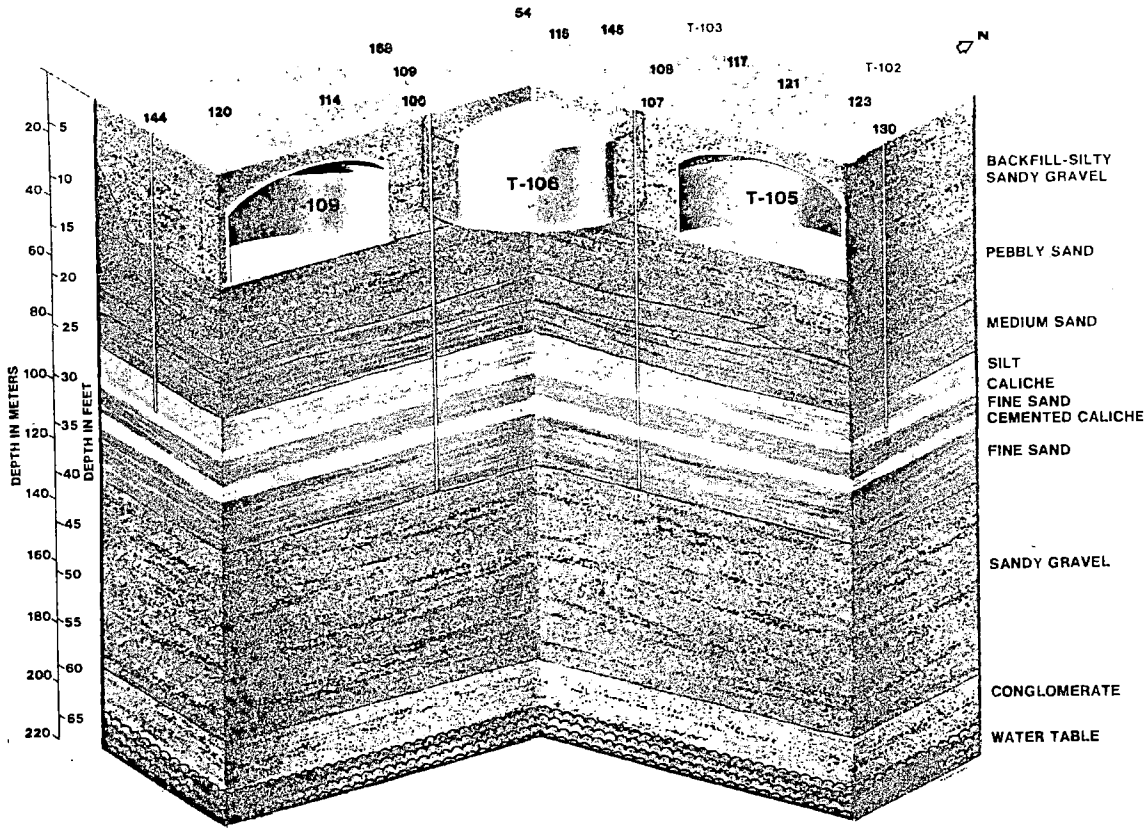

Figure 2. Three-Dimensional Drawing of the Distribution of Sedimentary Lithologies Beneath the 241-T-106 Tank.

Eolian Silt

After deposition of the upper Ringold, the top of the Ringold Formation was subjected to subaerial erosion by winds which reworked and redeposited the fine-grained sands and silts to form the Early Palouse soil or eolian silt (References 8 and 9). Beneath the 241-T tank farm, this unit occurs between 117 to 180 meters (580 to 590 feet) above mean sea level. These sediments are generally compact and massively bedded with no observable internal laminations or cross stratification. Near the base of the eolian silt, a moderately well-developed caliche horizon has developed.

Hanford Formation*

The 241-T tank farm waste storage tanks rest on the Hanford Formation comprised of glaciofluvial deposits. The principal units of the Hanford Formation are pebbly sand and medium sand. These sediments grade downward from poorly sorted, well-rounded cobbles and pebbles with very coarse-to-medium arkosic sand filling the interstitial spaces to well-sorted, subangular-to-subrounded coarse-to-medium arkosic sand.

Each of the principal Hanford Formation units displays complex sedimentary structures which control the unsaturated flow of waste liquids in the vadose zone. Bedding within the structures consists of thin, nearly horizontal, discontinuous laminations and cross-stratified sedimentary beds. These sedimentary structures tend to impede downward migration and enhance lateral spreading of aqueous liquids under partially saturated conditions as shown in Figure 3.

The finer grain sizes (which account for a relatively small weight percent of these sediments) are the important fraction in the sorption of radionuclides. The fractions contain montmorillonite, mica (illite) and chlorite, which have high cation exchange capacities for sorbing radionuclides.

Backfill

In preparation for tank construction, Hanford Formation material was excavated at the 241-T tank farm site. This material, consisting predominantly of cobbles, pebbles, and coarse-to-medium sands to silt, was subsequently used as backfill from the base of the completed tank (193 meters (632 feet) above mean sea level) to the ground surface (205 meters (672 feet) above mean sea level). An inherent characteristic of the backfill is poor sorting from the mixing of numerous stratigraphic layers.

Background information on the regional geologic setting and additional information on stratigraphy, mineralogy, and sedimentary structures are contained in Appendix D.

---

*Informal name.

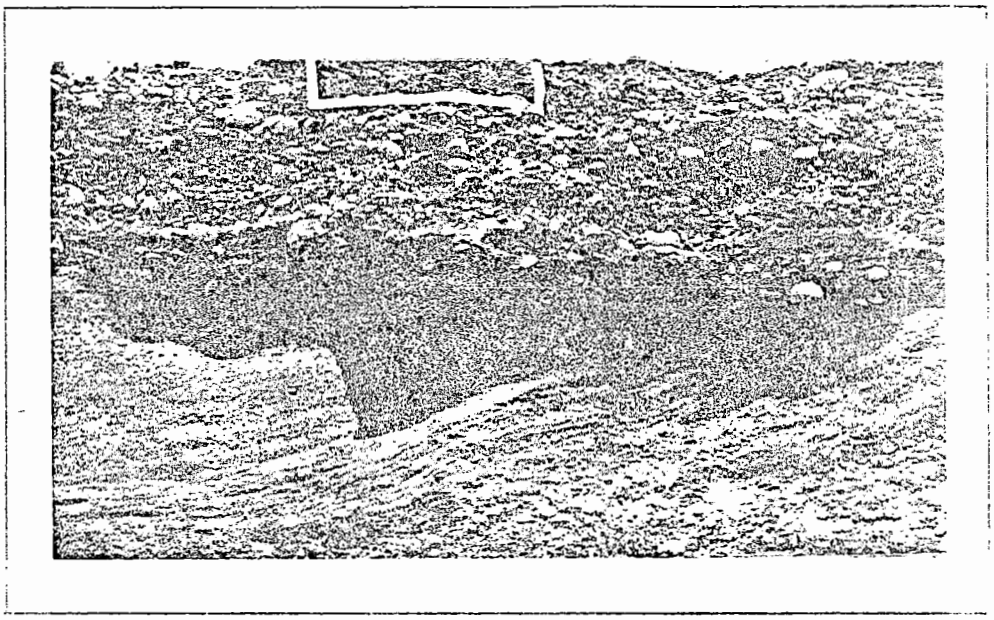

(a) After 6 hours

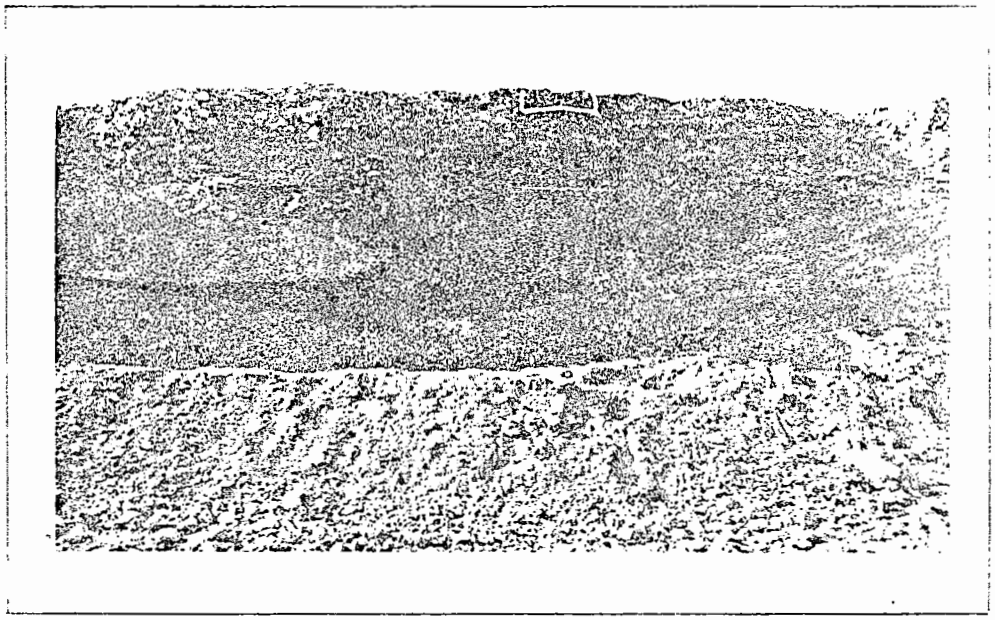

(b) After 24 hours

FIGURE 3. Typical Horizontal and Vertical Movement of Liquids in Hanford Formation Sediments Under Partially Saturated Conditions. Taped area outlines position of water addition.

REGIONAL GROUND-WATER LEVELS AND TRAVEL TIMES

The Columbia River is the nearest area, not controlled by the Department of Energy, accessible to ground water from Hanford. For any waste released to impact the Columbia River, it must be transported through the vadose zone to the water table and by ground water to the Columbia River. Thus, the depth to ground water and the ground-water travel times to the Columbia River are vital environmental parameters to an assessment of impact. Depth to ground water in the vicinity of the 241-T-106 tank is 62 meters (203 feet). A regional ground-water map is provided in Appendix E.

The Hanford Pathline Calculational Procedure (HPCP) computer program was recently developed to determine minimum ground-water travel times from points on the Hanford Site to the Columbia River (Appendix E). Application of the model to seven 200 West Area pathline streams to the Columbia River gave average travel times of 1.2×10^2 years and average water velocities of 61 cm/day (24 in/day).

To further confirm the water travel time in the immediate vicinity of the 241-T tank farm, a four-well tracer test was conducted. The ground-water velocity was found to average 41 cm/day (15 in/day). Since ground-water velocity within the 200 West Area is known to be lower than the average velocity from the 200 West Area to the Columbia River, tracer test result is in agreement with the HPCP value. The physical well configuration and details of the ground-water velocity study are given in Appendix F.

CONSTRUCTION OF 241-T-106 TANK

The 2.02×10^6-liter (533,000-gallon) capacity 241-T-106 tank is one of 12 identical steel-lined tanks constructed in 1943-1944 in the T tank farm. The 241-T-106 tank was the first used for liquid storage in 1944. A drawing of the 241-T-106 tank showing important structural details is presented in Figure 4. The waste storage tanks are constructed of reinforced concrete with a 0.65-centimeter (0.25-inch), PL-type, single-carbon, steel-welded liner on the base and sides of the vessel. They are cylindrical in shape with a domed top and are positioned with at least 1.8 meters (6 feet) of earth cover above the tank dome. The 241-T-106 tank is approximately 23 meters (75 feet) in diameter and 10 meters (33 feet) high. The top of the tank is approximately 2 meters (7 feet) below the surface of the ground, and the bottom of the tank is 49.4 meters (162 feet) above the water table.

COMPOSITION OF THE 241-T-106 TANK CONTENTS

The chemical and radionuclide composition of the 241-T-106 tank supernatant is given in Tables 1 and 2, respectively. In addition, the 241-T-106 tank contained 2.42×10^5 liters (64,000 gallons) of sludge and interstitial liquor (Reference 1). The processes which generate the waste are given in general terms in Appendix G.

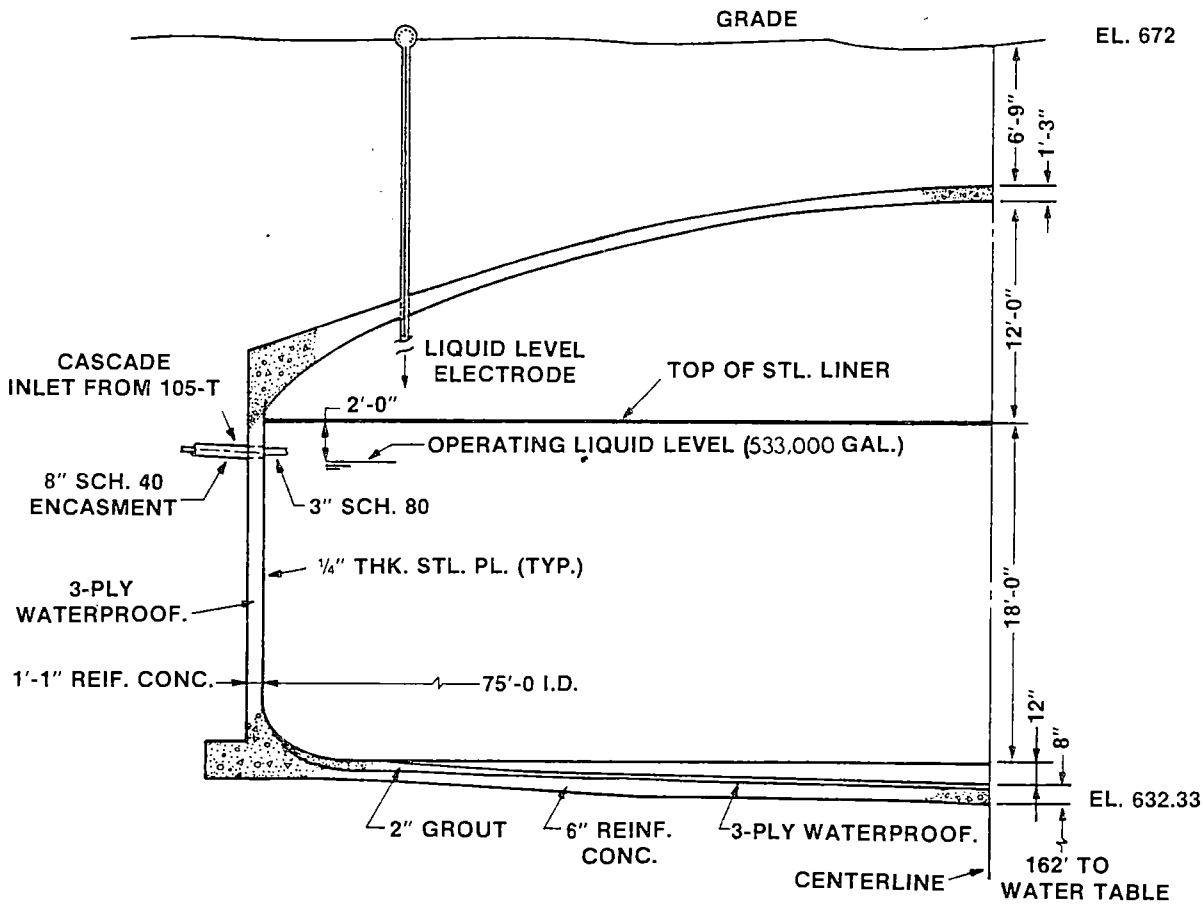

FIGURE 4. Structural Details of 241-T-106 Tank. (Reference 1)

TABLE 1

Chemical Composition of the 241-T-106 Tank Supernatant Solution[a]

Chemical Component	M
Sodium	4.0
Ammonium	0.065
Potassium	0.016
Calcium	0.0022
Nitrite	1.18
Carbonate	0.79
Nitrate	0.77
Sulphate	0.25
Hydroxide	0.24
Aluminum	0.064
pH	11.9

TABLE 2

Radionuclide Composition of the 241-T-106 Tank Supernatant Solution[a]

Radioactive Component	μCi/ℓ	μCi/gal
Cerium-144/Praseodymium-144	1.18×10^4	4.48×10^4
Cesium-137	8.85×10^4	3.35×10^5
Europium-155	1.69×10^3	6.40×10^3
Cesium-134	1.32×10^3	5.00×10^3
Antimony-125	1.12×10^3	4.24×10^3
Strontium-89/Strontium-90	2.98×10^4	1.13×10^5
Ruthenium-106/Rhodium-106	6.12×10^5	2.32×10^6
Plutonium-239	9	34
Plutonium-240[b]	2	8
Americium-241[b]	2	6

[a]Reference 1.

[b]Calculated by ARHCO.

1978 STATUS OF 241-T-106 TANK LEAK BOUNDARY

DRY WELL MONITORING RESULTS

Following confirmation that the 241-T-106 tank was leaking, determining the horizontal and vertical boundaries of the contaminated zone around the tank was an immediate and continuing requirement for making an assessment of the leak.

Only two dry wells (for monitoring purposes) existed in the immediate vicinity of the tank at the time the leak occurred. Several additional dry wells were drilled to obtain adequate delineation of the contaminated zone. The locations of the 241-T-106 tank, five neighboring tanks, and dry wells are shown in Figure 5. Dry well locations are shown as points and are identified by well numbers.

Before the initial leak status report (Reference 2) was released, wells 106 through 121 (16 wells) were drilled. The initial determination/evaluation was based on the in-well total gamma profiles and laboratory gamma energy analysis (GEA) of sediment samples from various depths from these dry wells. In the original 1973 assessment, the limit of maximum horizontal movement of radioactivity at the 1-μCi/ℓ level of ^{106}Ru was delineated by wells 54, 112 through 115, 120, and 121. These dry wells were uncontaminated at the 1-μCi/ℓ ^{106}Ru concentration.

Radioactivity was found at a maximum depth of 27 meters (89 feet), which is 35 meters (116 feet) above the water table (Reference 2). The laboratory GEA of sediment samples from dry wells 106 through 121 and analyses methods on which the original evaluation was made are given in Appendix H and J, respectively.

Since the 1973 evaluation, dry wells 122 through 168 have been drilled. Dry wells 123 through 128, 130, 145, 147, 148, 150, 162, 164, 166 and 167 are particularly useful in the continued monitoring of the maximum extent of the 241-T-106 tank leak (Figure 5). In the 5 years since the initial evaluation, only dry wells 112 and 113 have been reached by the leak plume at $\geq$1 μCi/ℓ of ^{106}Ru value; and dry wells 54, 113, 115, 117, 120, 121, and 145 currently define the maximum extent of horizontal leak migration.

IN-WELL GAMMA ANALYSES INSTRUMENTATION RESULTS

Prior to mid-1974, the most sensitive in-well total gamma radiation measurement capability at Hanford was a thallium-activated sodium iodide scintillation crystal coupled to a photomultiplier tube. Total gamma radiation was measured in counts per minute (cpm). In dry wells where the radioactivity levels were too high to be counted by this scintillation probe, a much less sensitive Geiger-Müller (GM) probe was used. The relative data graphed are designated as in-well total gamma profiles. This method of in-well total gamma detection by the use of an in-well scintillation probe system as a function of depth is continually being improved.

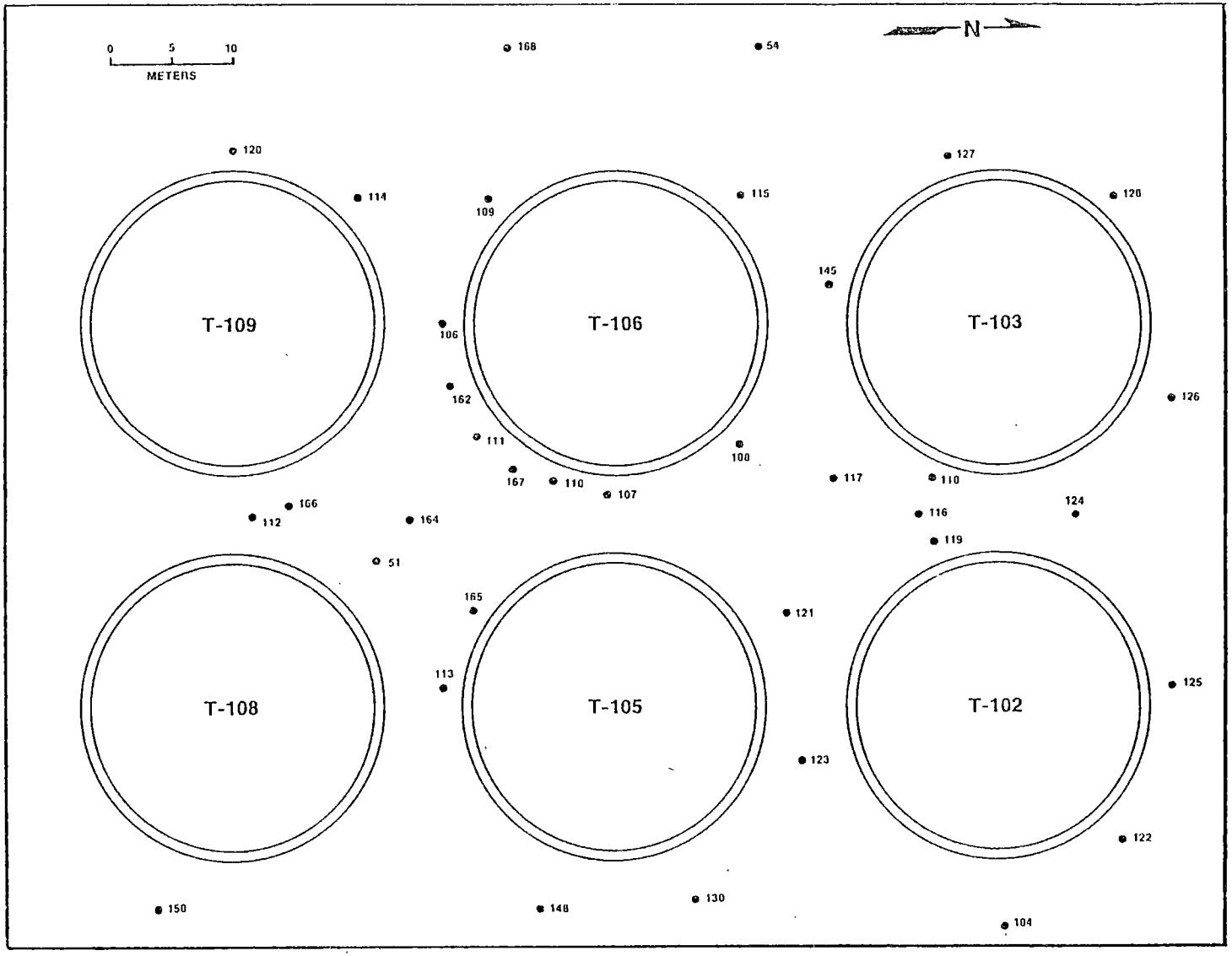

FIGURE 5. Relationship of the 241-T-106 Tank to Neighboring Tanks in the 241-T Tank Farm.

Total gamma measuring systems are maintained at or near the state-of-the-art (Reference 5). Due to these instrument system changes, the total gamma profiles were taken on two slightly different but comparable systems. The total gamma profiles for 1973 and 1974 were taken using one system; in 1975, 1976, 1977 and 1978, an improved system was used. This improved system has a better collimated crystal system, higher fidelity electronics, and a log count rate meter and chart readout. The 1973 and 1974 system, in contrast, had only a linear count rate readout.

Since in-well total gamma profiles are the only continuous 1973 through 1978 radioactivity levels of sediments data, a comparison of profile changes from year to year is the best indication of radionuclide migration.

In-well total gamma profiles from wells 111, 106, and 120 are presented in Figures 6, 7, and 8 respectively. These wells were closest to the leak, near a mid-point of the horizontal distribution of the radioactivity, and near the outer boundary of the leak (Figure 5). Other combinations of wells could have been chosen; however, the same general trends occur. Wells 111 and 106 contained sufficient radioactivity and were monitored with the less sensitive GM probe, while well 120 was monitored with the scintillation probe (1975 through 1978). Additional in-well total gamma profiles for wells 106 through 121 for the years 1973 through 1978 are shown in Appendix K.

From 1973 to 1974, total gamma count levels increased in all wells in at least some sediment layers. The increased activity levels were due to the lateral movement of the waste in the various sediment layers. In contrast to the 1973-1974 period, there is no evidence that the lateral movement of waste has continued at a measurable rate below the backfill since 1974, although limited redistribution may have occurred in the backfill from 1975 to 1976. In fact, the levels have steadily decreased since 1974. This is primarily due to the radioactive decay of ^{106}Ru. Ruthenium-106 was a major gamma activity contribution (>82%) in the 241-T-106 tank supernatant when the leak occurred and has a 1-year half-live. Thus, since 1973, ^{106}Ru has decayed through several half-lives. In addition, ^{106}Ru is the most mobile of the readily detectable radionuclides and is the best waste solution tracer. Since 1974, the waste solution has generally moved so slowly that its movement cannot be detected because the rate of radioactive decay of ^{106}Ru exceeds the rate of further lateral spreading of moisture. This does not indicate, however, that the movement has totally ceased.

The approximately 400-cpm peak at a depth of 31 to 34 meters (100 to 110 feet) of well 111 (Figure 6) and the 20-cpm peak at the 29- to 30-meter (95- to 100-foot) depth of well 106 (Figure 7) may represent lateral movement between 1976 and 1977, but probably do not. In early to mid-1977, several wells were deepened to more clearly define the maximum depth of waste penetration. Prior to then, wells 106 and 111 were only 28 meters (92 feet) deep. Thus, 1977-1978 is the only period of record for the deeper-than-28-meter (92-foot) portion of these gamma curves.

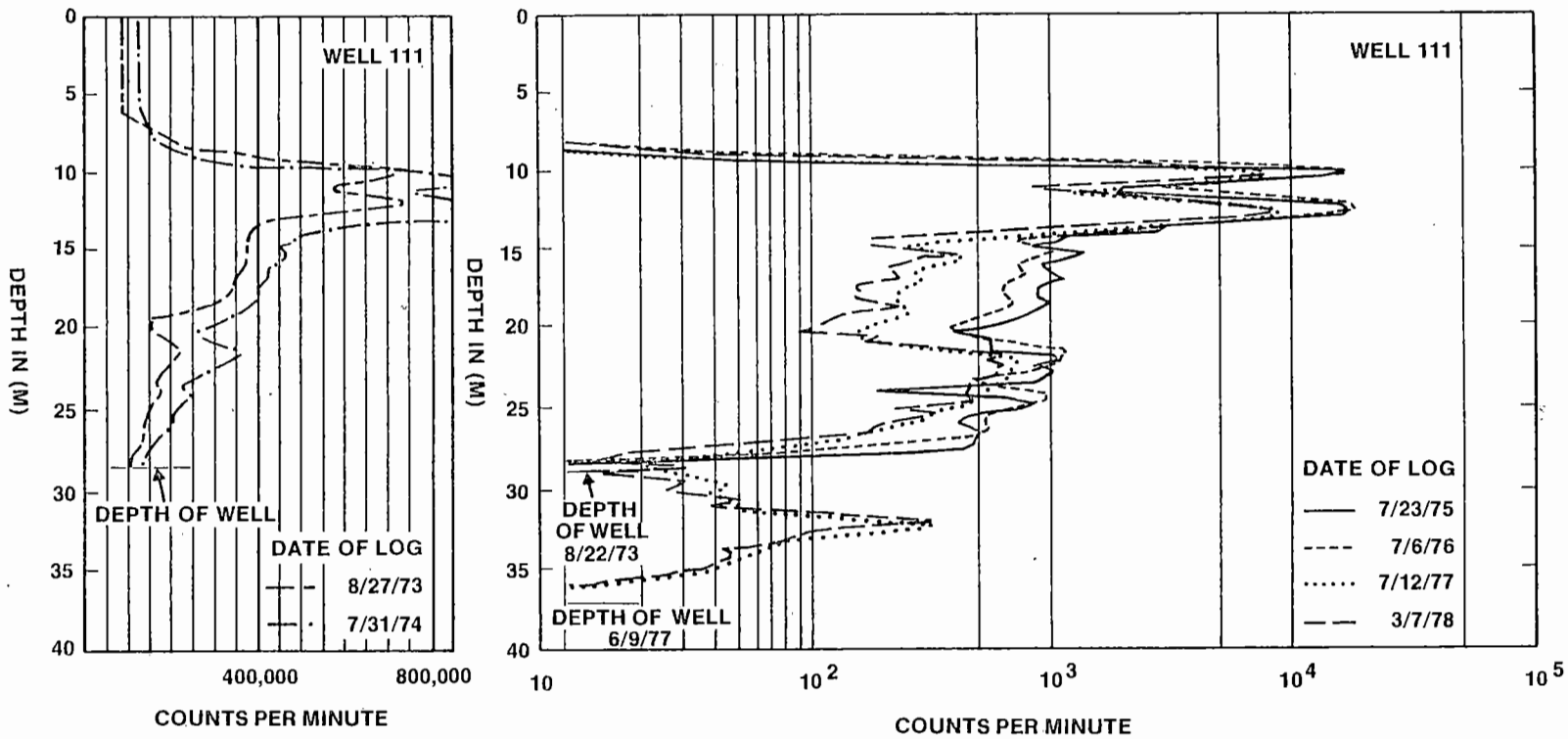

FIGURE 6. In-Well Total Gama Logs for Well 111.

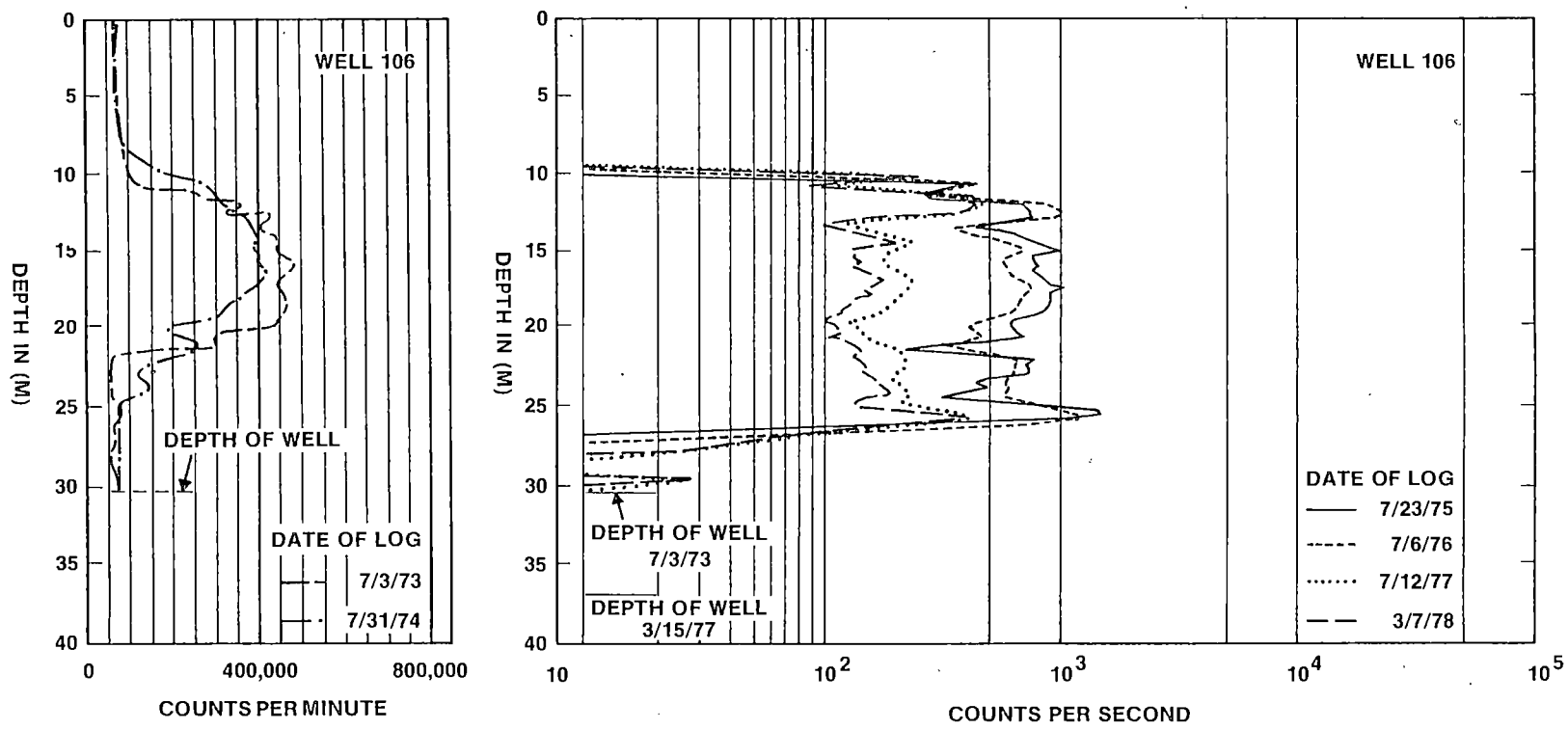

FIGURE 7. In-well Total Gamma Logs for Well 106.

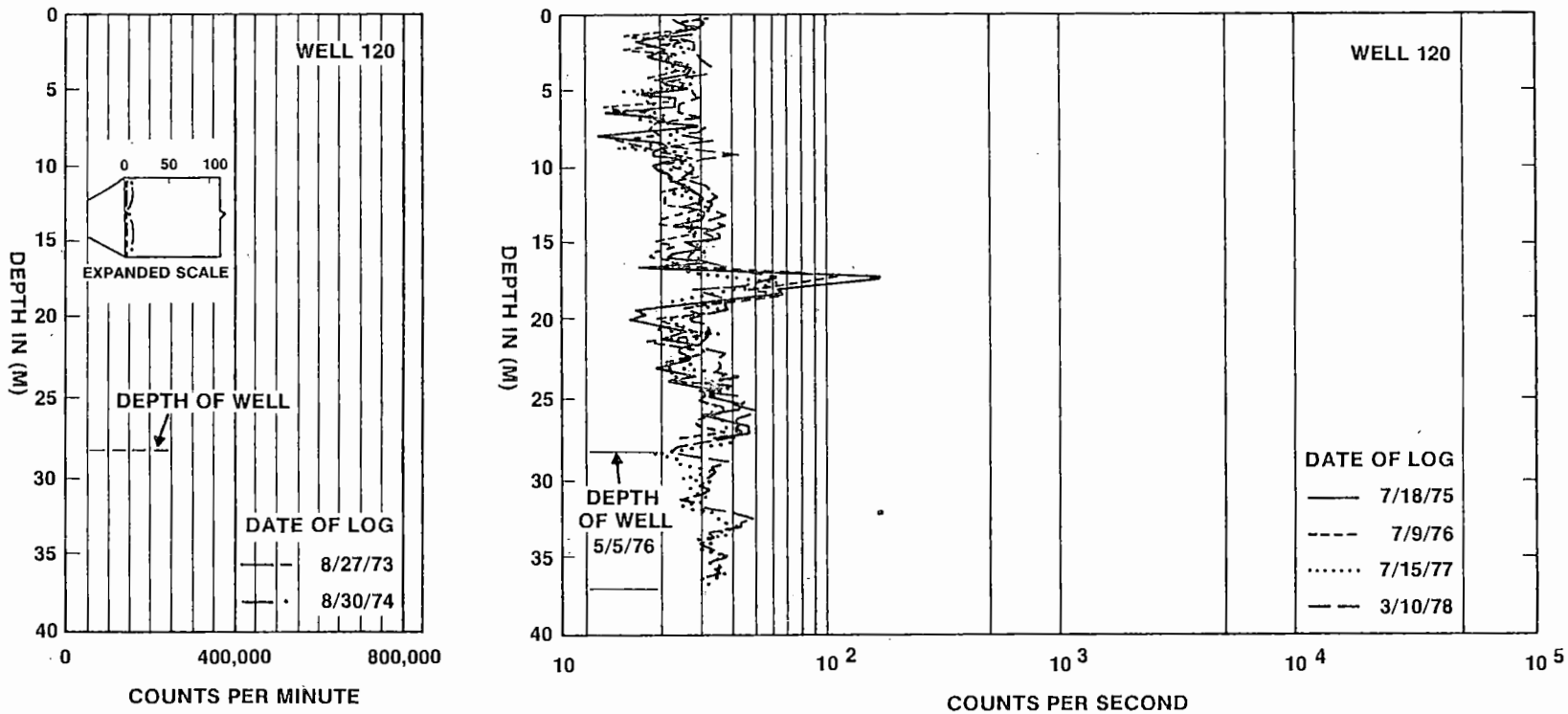

FIGURE 8. In-well Total Gamma Logs for Well 120.

The approximately 200-cpm peak at the 17- to 19-meter (55- to 62-foot) depth in well 120 (Figure 8) indicates how slowly the waste could be moving. In 1975, this sediment depth must have been near the wetting front and near a point of maximum change in radioactivity. This point is where movement could most readily be detected - none is evident.

Although changes in the total gamma profiles generally indicate little or no movement since 1974, at least three examples of measurable lateral movement were detected in 1978. Total gamma scans of wells 112, 113 and 114 (Appendix K) indicate that lateral movement occurred. The level of radioactivity measured by 1978 scintillation gamma scan did not decrease in 1978 relative to 1977 at 20- to 25-meter (69- to 82-foot) depths. These wells are near the perimeter of the leak and ^{106}Ru is detectable above the 1-μCi/ℓ level. This movement could have resulted from the addition of water to the system down a well casing during an unusual climatic event which occurred during the winter of 1977-1978. Snow which had previously accumulated was melted by a sudden warm rainfall. This accumulation of water failed to infiltrate into the soil because the ground was frozen and possibly ran down a well casing. As support for the above suggestion, a grouted well in the T-tank farm is known to have filled with water during the above event. No indication of waste movement has been detected in any well below a depth of approximately 25 meters (82 feet) due to this occurrence.

In mid-1974, a second in-well capability was added on the Hanford Site. In-well high-resolution GEA was developed for making rapid, accurate, and in situ measurements of the concentrations of individual radionuclides in sediments. The detailed method used in these analyses is given in Appendix J.

Radionuclide concentrations of ^{106}Ru and ^{137}Cs in the sediments are represented as a function of depth in Figures 9 and 10, respectively. The comparison of these curves with relative in-well total gamma profiles (Figures 6, 7 and 8) demonstrates the sensitivity of the total gamma scintillation probe. The 1977 and 1978 total gamma curves should be proportional to the summation of the ^{106}Ru and ^{137}Cs concentration curves with appropriate corrections for attenuation through the sediments, solutions, well casing, and air. All other radionuclides were present in the waste at an order of magnitude or lower concentration level than ^{106}Ru plus ^{137}Cs level decayed to 1978 (Table 2). There is general agreement between the total gamma profiles and summation of the ^{106}Ru and ^{137}Cs concentrations. In well 111, a major portion of the total gamma activity in the 10- to 14-meter (32- to 45-foot) and 21- to 23-meter (70- to 75-foot) depths is due to ^{137}Cs activity. These indicate a lesser amount of decay from 1975 to 1978 than the other depth levels of well 111 and depth levels of wells 106 and 120. In contrast, approximately 70% of the gamma activity in well 106 is due to ^{106}Ru, and decay from one year to the next is a higher percentage of the total radioactivity than in well 111. The total measurable gamma radioactivity in well 120 is due to ^{106}Ru at a maximum concentration of <0.1 μCi/ℓ, which is an order of magnitude lower concentration than the lowest graphed in this study.

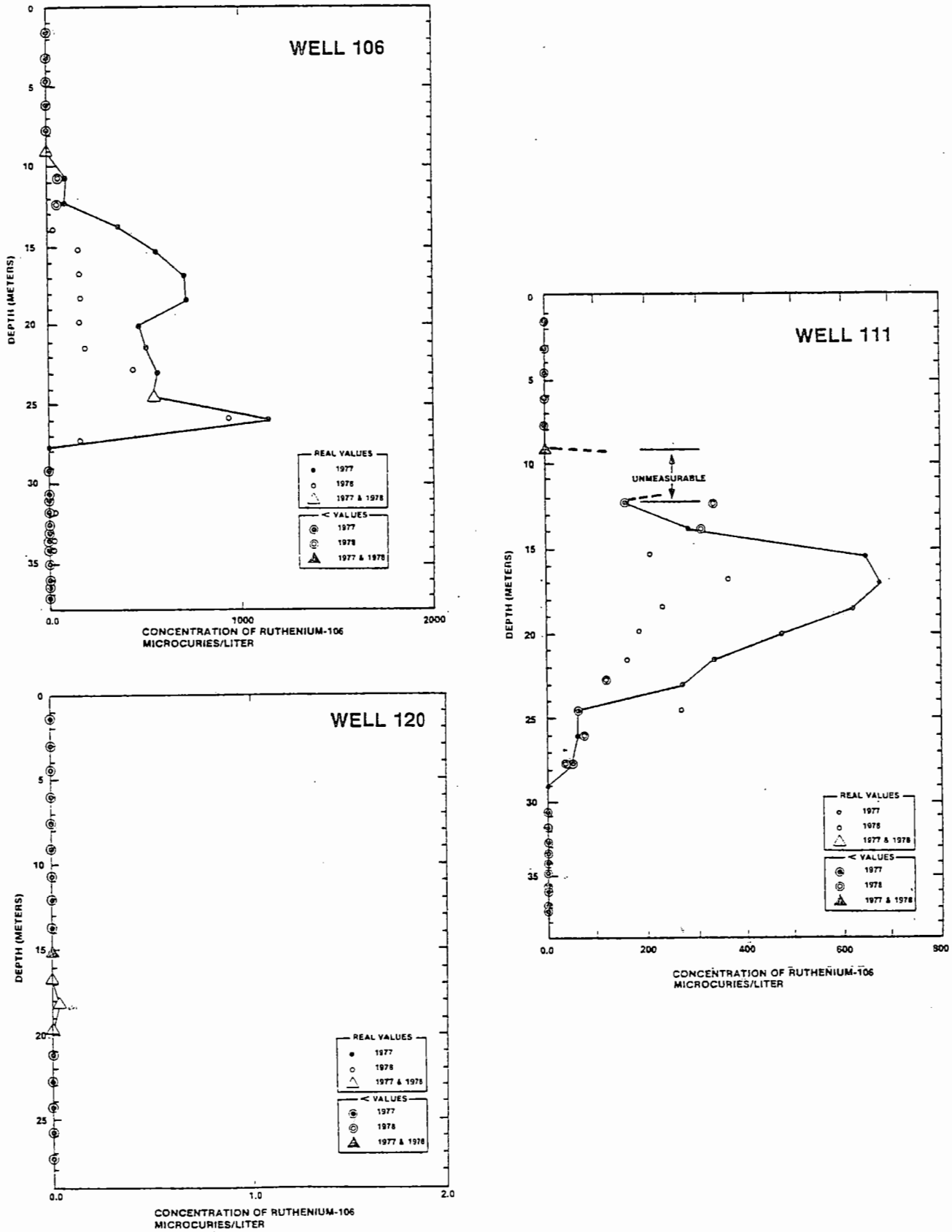

FIGURE 9. In-Well ^{106}Ru Concentration as a Function of Depth in Wells 106, 111, and 120.

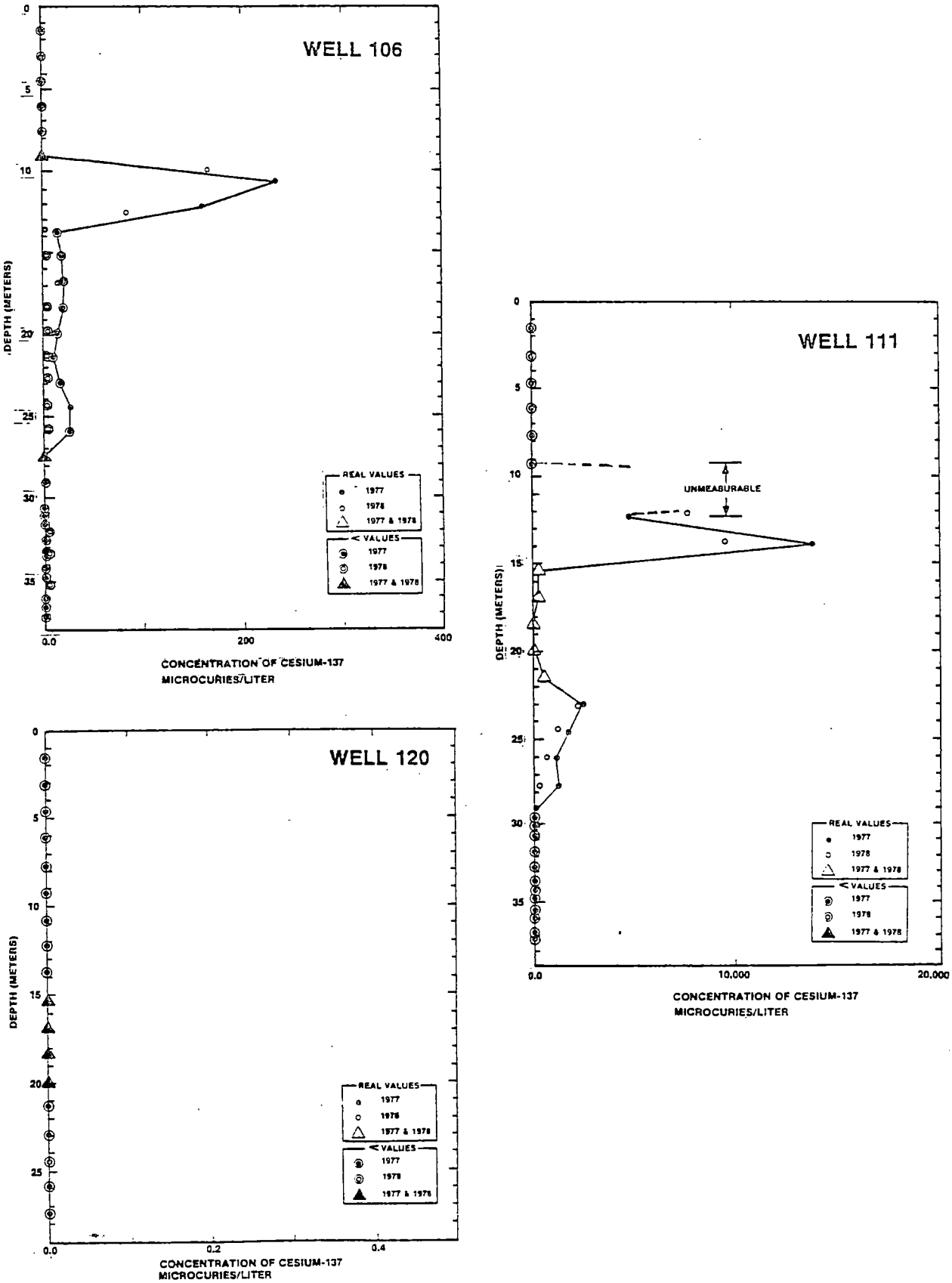

FIGURE 10. In-Well ^{137}Cs Concentration as a Function of Depth in Wells 106, 111, and 120.

The distribution of radionuclides in wells 111, 106 and 120 is controlled to a major extent by sorption and unsaturated flow characteristics of the surrounding sediments. As the edge of the leak plume is approached, the concentration of the lesser sorbed nuclide increases relative to that of a nuclide which is better sorbed. The concentration ratio increases with increasing lateral distance or depth from the leak. Ruthenium-106 is poorly sorbed compared to ^{137}Cs. From well 111 to 106, the $^{106}Ru/^{137}Cs$ concentration ratio increases. In well 120, only ^{106}Ru is measurable. Likewise, from the bottom of the tank to deeper in wells 111 and 106, the $^{106}Ru/^{137}Cs$ concentration ratio increases. Radionuclide concentrations of ^{106}Ru, ^{144}Ce, ^{137}Cs, ^{60}Co and ^{154}Eu for wells 106 through 121, 123, 130, 145, 162, and 164 through 168 of sediments are given in Appendix K.

Comparison Views of Sediment Concentrations

The initial assessment of the movement of radionuclides, made immediately after the leak in 1973, was based on plan and section views of the concentration distributions of ^{106}Ru, ^{144}Ce and ^{137}Cs (Reference 2). These three radionuclides were chosen for evaluation because they span much of the radionuclide mobility range exhibited in the 241-T-106 tank leak system. Cesium-137 is the least mobile and ^{106}Ru is the most mobile. A composite of the plan and section views of the 1-μCi/ℓ concentration isopleths for ^{106}Ru and ^{137}Cs in 1973 (shortly after the leak) is provided in Figure 11. The positions of these isopleths were based on total gamma activity analyses in wells 106 through 121 and on selected sediment samples. Data for the GEA for dry wells 106 through 121 and total gamma profiles are given in Appendices H and K, respectively.

By 1978, the ^{144}Ce ($T_{1/2}$ = 0.8 year) was reduced to such a low level by radioactive decay that the 1-μCi/ℓ concentration could no longer be measured by in-well GEA. With few exceptions, only less-than values are given in Appendix K. Thus, only the 1978 distribution of ^{106}Ru and ^{137}Cs can be compared with the 1973 composite plan and section views. The ^{144}Ce plan and section views given in Appendix L are only approximations based on less-than values.

A plan view of the location of 241-T-106 tank in relationship to immediate neighboring tanks, location of the dry wells around the 241-T-106 tank, and the location of the section views produced for this document is shown in Figure 12. Only section view D-D', showing the ^{106}Ru and ^{137}Cs sediment concentrations for November 1977 and May 1978, are given and described in comparison to the section views of the 1973 evaluation. Section views A-A' contain no radioactivity above the 1-μCi/ℓ level and, therefore, were omitted. Section views B-B' and C-C' are presented in Appendix L to allow a better three-dimensional conceptual view of the leak distributions. Plan views of the 241-T-106 tank and immediate neighboring tanks at the 21- to 23-meter (70- to 75-foot) depth are also given in Appendix L.

PLAN VIEW

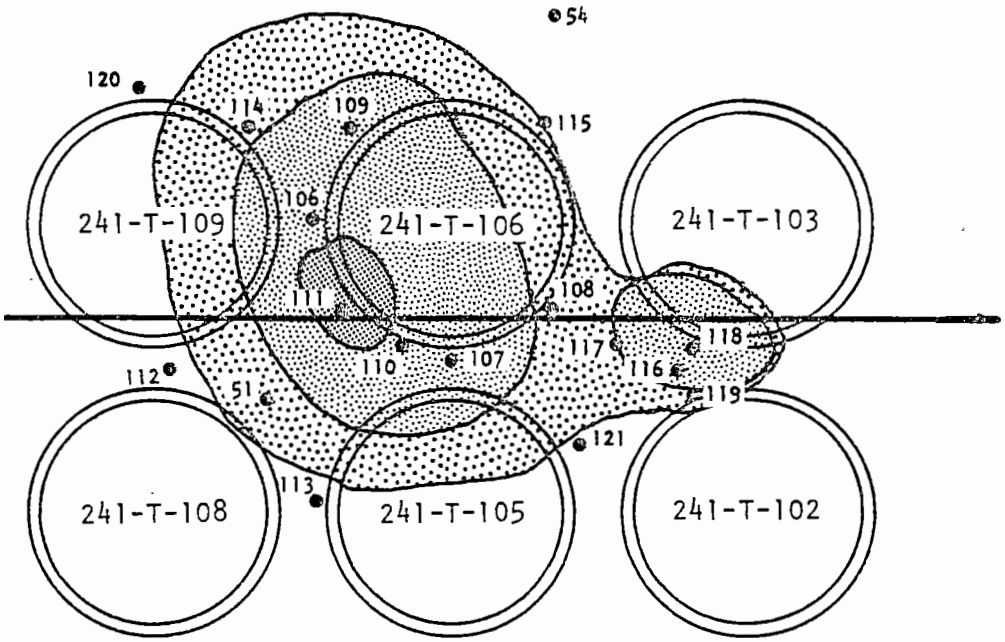

CROSS SECTION VIEW

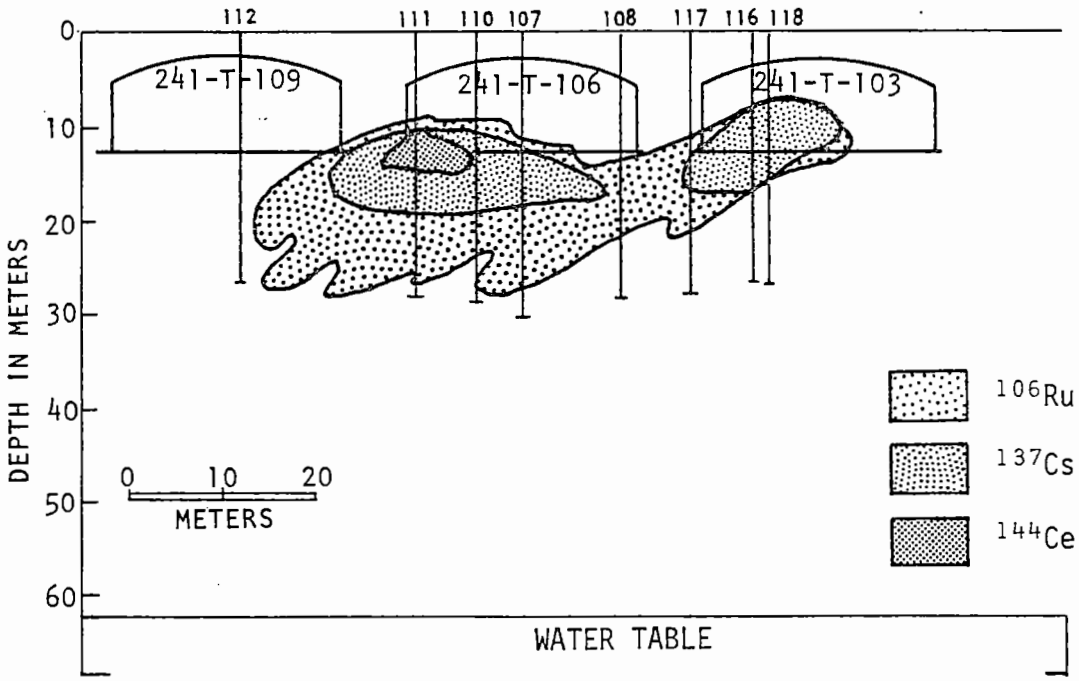

FIGURE 11. Composite Drawing of Plan and Section Views of the 1.0-μCi/ℓ Concentrations of ^{144}Ce, ^{137}Cs and ^{106}Ru in 1973 (Reference 2).

Views of section D-D' for the ^{106}Ru and ^{137}Cs sediment concentrations and plan views of concentrations at the 13.7-meter (45-foot) depth on May 1978 are given in Figures 13 and 14, respectively. The plan and section views are based on the in-well GEA measured by methods discussed in Appendix J and graphed in Appendix K for November 1977 and May 1978. These data are analyses from wells 106 through 121, 123, 130, 146, 162, and 164 through 168.

From comparing 1973 and 1978 isopleths (Figure 13), the volume of soil enclosed by the 1978 ^{106}Ru 1-μCi/ℓ isopleth is only slightly greater than that enclosed by the 1973 isopleth. Only wells 112 and 113 have been intercepted by the 1-μCi/ℓ ^{106}Ru concentration isopleth since 1973. Total gamma profiles for wells near the perimeter of the leak (Appendix K) show that essentially all detectable ^{106}Ru movement occurred between 1973 and 1974. After 5 years, the maximum horizontal distance of the 1-μCi/ℓ ^{106}Ru isopleth from any edge of the 241-T-106 tank is approximately equal to the diameter of the 241-T-106 tank. In 1978, ^{106}Ru concentrations above 1-μCi/ℓ were found at a maximum depth of 33 meters (108 feet) or 29 meters (95 feet) above the water table in well 107 of this cross section and well 168 (not of this cross section). This depth of penetration is only 43% of the distance from the bottom of the tank to ground water. From other wells, the vertical movement does not exceed 29 meters (95 feet).

A second area where the 1973 isopleth shows a change compared to the 1978 isopleth for ^{106}Ru is between wells 117 and 108. In the 1978 case, there is a discontinuity between two segments of the 1-μCi/ℓ isopleths which were joined in 1973. As shown in the 1973 evaluation, the contamination in the well 116 to 118 region was from the 241-T-103 tank.* By 1978, radioactive decay of ^{106}Ru ($T_{1/2}$ = 1 year) primarily had reduced the activity of the second leak to such a low concentration that the two leak plumes no longer merged.

From comparing 1973 and 1978 isopleths (Figure 14), the volume of sediment enclosed by the 1978 ^{137}Cs 1-μCi/ℓ isopleth is greater than that enclosed by the 1973 isopleth. The activity increase in well 111 probably represents the lateral movement of ^{137}Cs from closer to the leak. Well 111 must be near the leak site as judged by the sharpness that the ^{137}Cs front moved. Sediments containing mica characteristically have high sorption selectivities for ^{137}Cs, but relatively low capacities (Reference 10). Thus, essentially all ^{137}Cs is sorbed until the capacity is exceeded and ^{137}Cs moves as a sharp front near a source. As judged from a comparison of 1973 and 1974 in-well total gamma profiles, a large portion of the ^{137}Cs movement occurred during 1973 and between 1973 and 1974.

---

*The 241-T-103 tank leak resulted from a failed grout seal in a spare fill entry line (Reference 2).

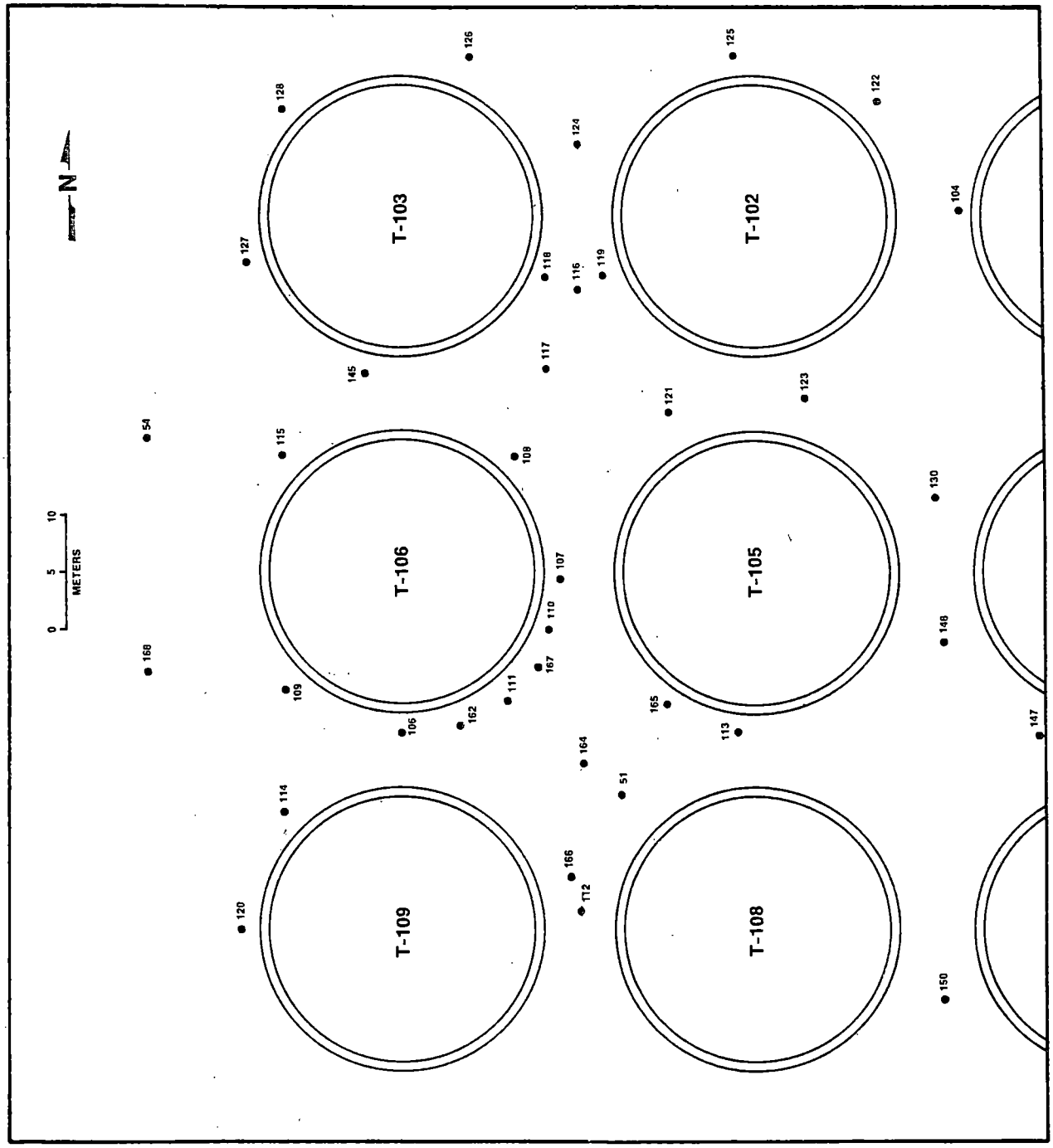

FIGURE 12. Plan View of the 241-T-106 Tank, the Surrounding Tanks, and Dry Wells in the T-Tank Farm in 1978.

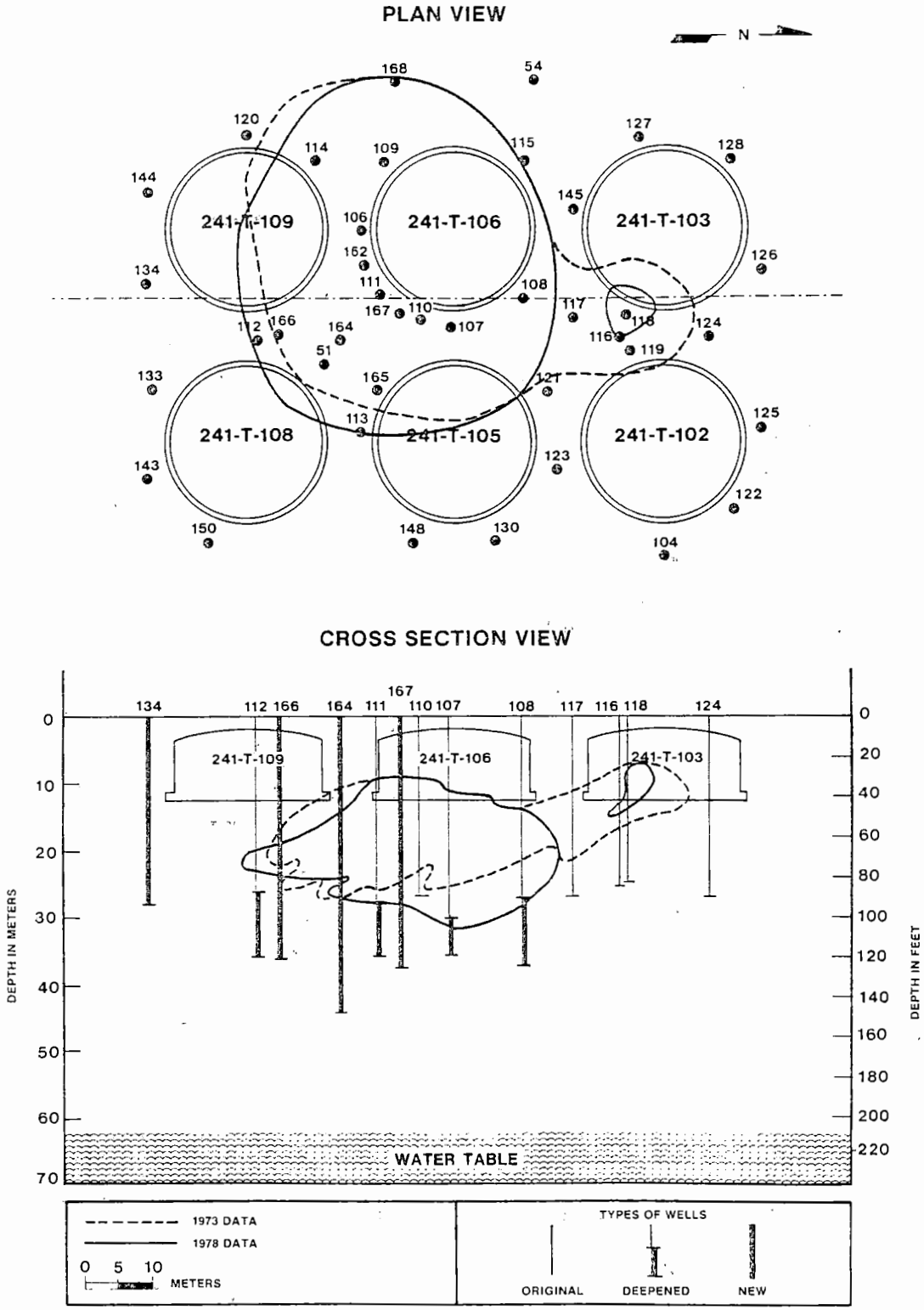

FIGURE 13. Plan and Cross Section View Through a Portion of 241-T Tank Farm with 1-μCi/ℓ Ruthenium-106 Isopleth Distribution Pattern.

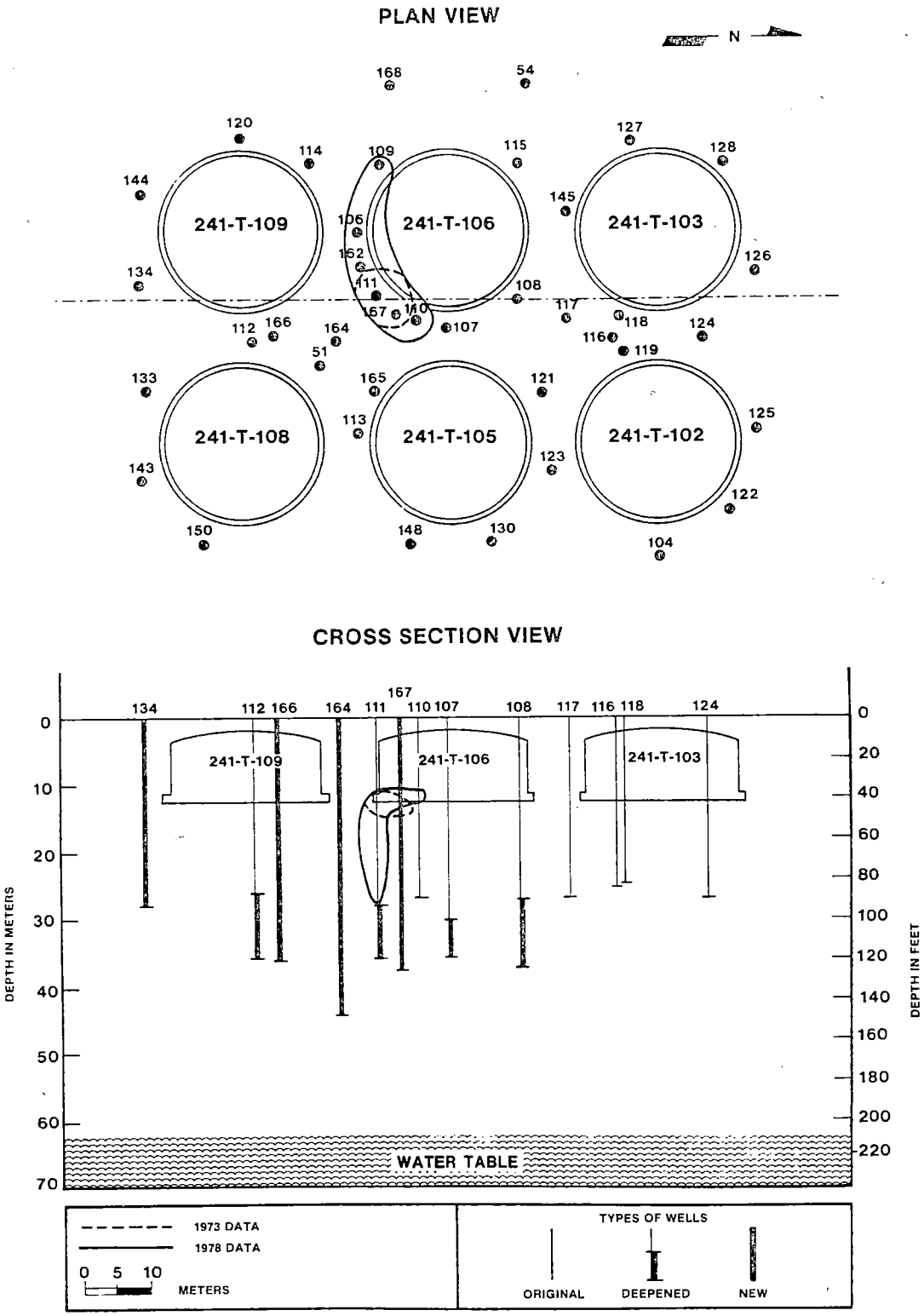

FIGURE 14. Plan and Cross Section View Through a Portion of 241-T Tank Farm with 1-μCi/ℓ Cesium-137 Isopleth Distribution Pattern.

Ground-Water Radionuclide Concentration Near Leak Site

Although there is no evidence that waste from the 241-T-106 tank leak has penetrated to the water table, radionuclide concentrations in ground water are routinely examined as confirmation. Hanford ground-water measurements are taken semiannually as a part of the Hanford on-site environmental monitoring effort. Routine monitoring wells 299-W10-1, 299-W10-4, 299-W11-9, and 299-W11-24 are in the vicinity of the 241-T-106 tank. Data for before and after the 241-T-106 tank leak are given in Appendix F. There is no evidence of ground-water contamination from the 241-T-106 tank leak based on these data.

Foil Activation Assay

The alpha particle emitters, actinides ^{239}Pu and ^{241}Am, are not generally detectable by in-well GEA at the low concentration levels anticipated in the sediments around the 241-T-106 tank. Thus, a more sensitive method is required. Passive foil neutron activation analysis can be used to measure quantities of ^{239}Pu and ^{241}Am at the tens of nanograms per cubic centimeter (ng/cm^3) level in the presence of a high field of gamma radioactivity.

In the foil activation technique, foils of high neutron cross section elements are activated in situ to a radioactive species. The gamma radiation emitted by the activated species is measured and is proportional to the concentration of plutonium and americium. Details of the foil activation method are given in Appendix J. Plutonium-239 plus ^{241}Am concentrations in the 241-T-106 tank are given in Table 3. Low levels of plutonium were detectable at the 99% confidence limit in eight sediment locations of four monitoring wells. In addition, plutonium was detectable at the 95% confidence limit in an additional nine sediment locations of six monitoring wells. All of the sediment locations where plutonium was found were near the bottom of the 241-T-106 tank and in the wells nearest the leak. The maximum plutonium concentration found was 980±200 ng/cm^3 at the 9.2-meter (35-foot) depth of well 111.

TABLE 3

Estimated Plutonium Plus Americium Concentrations (ng/cm^3) in Wells Near the 241-T-106 Tank

Depth, m	Well Number					
	107	110	164	111	166	106
4.2	109±98		<120	<200	<95	340±170
10.8	<96	330±140[a]	330±140[a]	980±200[b]	80±45	125±65
12.0	<85	220±110[a]	900±160[b]	310±180[a]	350±120[b]	330±110[b]
12.6	121±85	180±110	110±76	300±120[a]	430±140[b]	660±190[b]
13.8	85±38[b]	<100	199±78[a]	232±87[b]	290±110[b]	45±20[a]

[a]Significant at the 95% confidence level.

[b]Significant at the 99% confidence level.

9 2 1 2 4 6 6 1 2 7 1

FATE AND IMPACT OF 241-T-106 TANK LEAK

An assessment of the long-term impact of the 241-T-106 tank leak on any uncontrolled area in the environs of the Hanford Site requires an evaluation of liquid transport and sorption of the radionuclides in the vadose zone from the leak to the water table and in the saturated sediments from the water table to the Columbia River, which is the nearest area of uncontrolled access. Since the bottom of the 241-T-106 tank is nearly 50 meters (165 feet) above the regional ground water, the quantity of solution leaked is less than the Hanford specific retention capacity, and no specific retention quantity of liquid is known to have reached the Hanford ground water, it is unlikely that any amount of waste leaked from the 241-T-106 tank will reach the water table, much less be transported to the Columbia River.

DECAY RATE OF THE GAMMA RADIOACTIVITY

Statistical methods were employed to determine if the change (decrease) in the level of in-well total gamma activity as a function of time is relatable to radioactive decay. The decay of all radioactive atoms is a first order kinetic reaction, which is equivalent to stating that the rate of decay is proportional to the number of radioactive atoms. Expressing the above statement mathematically gives:

$$-\frac{dN}{dt} = \frac{0.693}{T_{1/2}} N \qquad (1)$$

where:

$-\frac{dN}{dt}$ = the decay rate in disintegrations per month

N = the number of radioactive atoms

$T_{1/2}$ = the half-life of the radioactive element in months (Reference 11).

Multiplication of equation 1 by dt gives:

$$-\frac{dN}{N} = \frac{0.693}{T_{1/2}} dt \qquad (2)$$

Integrating equation 2 between N_1 and N_2 and times between t_1 and t_2 gives:

$$\ln \frac{N_1}{N_2} = \frac{0.693}{T_{1/2}} (t_2 - t_1) \qquad (3)$$

where:

N_1 = the number of atoms at time t_1

N_2 = the number of atoms at time t_2.

The activity of a radionuclide is proportional to the number of radioactive atoms which gives:

$$A = \frac{0.693}{T_{1/2}} N \tag{4}$$

where:

A = the activity in disintegrations per month.

Substitution of equation 4 into equation 3 gives:

$$\ln \frac{A_1}{A_2} = \frac{-0.693}{T_{1/2}} (t_2 - t_1) \tag{5}$$

If the ln (natural logarithm) of activity is plotted against elapsed time, a straight line of slope $(-0.693/T_{1/2})$ is obtained.

Linear regression analysis was used to determine if the decrease of total gamma activities in wells 51, 106, 107, 108, 109, 110, and 114 as a function of time was due to radioactive decay. The linear regression analyses are summarized in Table 4. The linear regression analysis data are listed in Appendix M. The squared regression coefficients (r^2) vary from 0.826 to 0.999, demonstrating that ln of the in-well total gamma activity is significantly correlated with the elapsed time (decay) at the 95% confidence limit. This strongly suggests 82.6 to 99.9% of the variability in the ln of the in-well total gamma activity is relatable to elapsed time (decay). From the slopes of the lines, the estimation of the half-life of the gamma activity was found to be 13.7 months with a 95% confidence interval of 10.4 to 20.2 months. This range is in fair agreement with the 12-month half-life of ^{106}Ru, which is the primary radionuclide controlling the decay of activity in the selected wells due both to its high relative concentration and short half-life. From this analysis, it can be inferred that the movement of radionuclides in the analyzed wells is so slow relative to the decay of ^{106}Ru that it cannot be generally detected by analyzing the activity change with time.

TABLE 4

Linear Regression Analysis of ln of In-Well Total Gamma Activity as a Function of Time

Well	r^2	Standard Error of Estimate	Slope	Intercept
51	0.896	0.10	-0.060	5.85
106	0.937	0.10	-0.085	6.22
107	0.826	0.10	-0.051	6.13
108	0.934	0.12	-0.089	5.90
109	0.904	0.13	-0.078	5.94
110	0.992	0.14	-0.063	6.25
114	0.999	0.22	-0.079	5.23

VADOSE ZONE MOISTURE MOVEMENT

High-level waste tanks in the tank farms are 43 to 70 meters (141 to 300 feet) above the regional water table. Movement toward the water table will largely be by unsaturated flow.

Although the 241-T-106 tank leak case has not been specifically analyzed, a preliminary analysis was performed which allowed a prediction of the movement of liquids through the Hanford vadose zone sediments toward the water table as a function of sediments-type hydraulic properties, leak-solution properties, and time (Reference 12). The leak size studied was 3×10^6 liters (800,000 gallons) as compared to the 4.35×10^5 liters (115,000 gallons) estimated to have leaked from the 241-T-106 tank. The conclusion of the study was that "it was difficult to imagine that the waste liquid would reach the water table in significant amounts" (Reference 12). Exact models, conditions, and assumptions used in the study are reported in detail elsewhere, but sediments-type hydraulic properties and leak-solution properties were similar (or conservative) to those which could be expected for the 241-T-106 tank leak case. Thus, it seems unlikely that the 241-T-106 tank leak will have a significant effect on any uncontrolled area if little or none of a much larger leak can be expected to reach the water table.

WETTING FRONTAL MOVEMENT CALCULATIONS

Other empirical studies which were conducted on the movement of wetting fronts through Hanford vadose zone sediment columns are in essential agreement with the conclusions of the above leak study (Reference 13). In these column studies of the wetting frontal movement from liquid pulses (10% of the column volume of liquid is added), the distance that the wetting front moved as a function of time was found to be predictable from an empirical equation of the form:

$$S = ET^F \qquad (6)$$

where:

S = the distance of the wetting frontal movement from column surface in centimeters

T = the elapsed time in hours

E and F = empirical parameters which must be evaluated for each sediment.

Parameters E and F were evaluated by converting equation 6 to a linear log - log form, plotting the log S versus the log T, and using linear regression analysis to determine the intercept, slope of the resulting line, and the goodness of fit of the experimental data for predicting intermediate wetting frontal movement values. Parameter E was found from the intercept

of statistical line at T equal at 1 hour and is equal to $10^{\log E}$. Parameter F was equal to the slope of the statistical line. By normalizing the data to the column length, equation 6 takes the form:

$$S' = \frac{S}{L} = \frac{E}{L} T^F = E' T^F \qquad (7)$$

where:

S' = the fractional column distance

E' = the normalized parameter E

L = the column length.

If valid, equation 7 can be used to predict the frontal movement in a column of any length of a 10% liquid pulse. Equation 7 was found to be valid for Hanford sandy sediment columns varying in length by greater than an order of magnitude (Reference 13). Parameters E' and F were found to be constant regardless of column length and to have values of 0.37 and 0.13, respectively, for a typical Hanford sediment (Reference 13). For light sandy sediment columns varying in length by more than order of magnitude, linear regression analysis gave r - values of 0.95 and a standard error of estimate of 0.015 (1.5%). Thus, greater than 90% of the variability in the fractional distance the wetting front moves is attributable to the elapsed time variables for a given sediment; and, the small standard error of the estimate strongly indicates that S can be measured with good accuracy.

Thus, equation 7 can be used to predict the length of time required for solution front to attain any column depth in a homogeneous given sediment column by choosing a column diameter value. This type of analysis is important because no activity will enter the water table until the wetting front intercepts the water table.

For example (using tank and sediment data for the 241-T-106 tank leak case), consider a sediment column 23 meters (75 feet) in diameter and 49 meters (160 feet) long. If 4.35×10^5 liters (115,000 gallons) pulse of solution is added to the above column, the length of time for the wetting front to reach the bottom of the column (distance to ground water) would be calculated as follows.

First the cross-sectional area of the column is calculated from the column diameter which gives 0.14×10^3 m2 (4.4×10^3 ft^2). The 4.4×10^5-liter (1.5×10^4-ft^3) pulse of solution would fill an empty column to the depth of 1.1 meter (3.5 feet). Since this pulse represents 10% of the column volume, the L in equation 7 is 11 meters (36.1 feet) and the values of parameter E' and F determined for a representative Hanford sand give:

$$\frac{49}{11} = 4.4 = 0.37\ T^{0.13} \qquad (8)$$

Solving equation 8 for T gives:

$$T^{0.13} = \frac{4.4}{0.37} = 12 \tag{9}$$

Converting equation 9 to ln form gives:

$$0.13 \ln T = \ln 12 \tag{10}$$

or

$$\ln T = \frac{\ln 12}{.13} = 19 \tag{11}$$

and

$$T = e^{19} = 2.0 \times 10^{8} \text{ hours} = 2.3 \times 10^{4} \text{ years.} \tag{12}$$

In summary, if a 23- x 49-meter (75- x 160-foot) column is filled homogeneously with a representative Hanford sediment and a 4.4 x 10^5-liter (115,000-gallon) pulse of water is added, 2.3 x 10^4 years would elapse before the wetting front reached the bottom of the column.

This calculation for a homogeneous, one-dimensional sediment column is not based on a precise model of the 241-T-106 tank leak. There are several factors which make this a conservative model. First, sediments are not one-dimensional columns; but three-dimensional systems. When a liquid is added slowly as a point source in a leak, to a relatively dry porous media (Hanford sediment), lateral flow (due primarily to capillary, not gravitation forces) at the wetting front assures that essentially all liquid flow in the wetted sediment except near the leak point will be by unsaturated flow. This will be true unless the leak is very large and/or persists for a very long time: neither of which were the case for the 241-T-106 tank leak. Unsaturated flow will have the effect of spreading the leak to a larger volume and decrease the velocity of wetting frontal movement relative to what it would be in a column.

Indeed, in the 241-T-106 tank leak case, the lateral spread was much greater than the 23-meter (75-foot) tank diameter which was used as column diameter as judged from the ^{106}Ru contamination volume (Figure 13). However, this is due not only to unsaturated flow, but also in part, perhaps in large part, to sediment layering.

Layering is the second factor which makes the column model conservative for the 241-T-106 tank leak. The geologic processes which resulted in the glaciofluvial sediments (Hanford Formation) being deposited were of such a nature that sharp boundaries often exist between sediment types based

both on mineralogy and particle size distributions. When a wetting front encounters such a boundary, moisture accumulates and flow is restricted. This is true when the wetting front encounters either coarser or finer sediments. During the time (often a long time relative to the rate of unsaturated flow within the sediment) that the wetting front is stopped at the boundary, the wetting front within the sediment continues to advance. These sharp boundaries tend to be parallel to the surface of the ground, and the spreading tends to be laterally. Figure 3 photographically illustrates the spreading due to unsaturated flow and layering.

A third factor which makes the column model conservative is that the column data used in the above calculation are based on water and the viscosity of water (about 0.01 poise at 20°C for distilled water); the viscosity of the leaked supernatant was approximately 0.15 poise at 20°C. The hydraulic conductivity is proportional to the unsaturated flow rate of water (Reference 14) and inversely proportional to the viscosity. Thus, the wetting frontal movement rate of the 241-T-106 tank leak supernatant would be expected to be ∿10% of the movement rate of distilled water which was used in the column study or nearly an order of magnitude slower.

A final factor which makes the column model a conservative one is that in a soil column bounded by glass, there is an assured conservation of all of the liquid added to the column. This is not true in 241-T-106 tank leak case. Liquid is transported both in the vapor phase and the liquid phase. While the quantitative effect of vapor phase loss to the liquid is unknown, qualitatively vapor phase flow will have the effect of subtracting liquid from the system and thus, will decrease the rate of wetting frontal movement.

Thus, the effects of spreading, layering, viscosity, and vapor phase transport combine to make the wetting frontal movement model conservative for the 241-T-106 tank leak case. All four factors qualitatively indicate that the 241-T-106 tank aqueous solution will move at a slower rate than that of water movement in a column. Thus, the calculation made using the column model can be considered to be a conservative estimate of the time required for the 241-T-106 tank leak aqueous solution to reach ground water, probably by orders of magnitude. Thus, the frontal movement travel time calculated for the hypothetical column of 2.3×10^4 years will be a conservative estimate of the minimal time required for the 241-T-106 tank leak aqueous solution to reach the Hanford ground water.

SORPTION EFFECTS

Radionuclides are transported in solution predominately as solutes. These solutes are capable of undergoing chemical and physical reactions with solid phases (sediments). Sorption is the reaction with, and retention of a solute by a solid phase. Sorption has the effect of retarding the movement of sorbed radionuclides relative to that of transporting liquid. A retardation factor can be calculated from the equation (Reference 15):

$$\frac{Vi}{Vw} = \frac{1}{1 + \frac{Kd\rho}{\Theta}} \qquad (13)$$

9 2 1 2 4 6 6 1 2 7 7

where:

V_i = the velocity of sorbed radionuclides in distance per year

V_w = the velocity of water in distance per year

V_i/V_w = the retardation factor

K_d = the equilibrium distribution coefficient for the sorbed radionuclide in ml/g

ρ = the sediment bulk density in g/cm^3

Θ = the sediment's pore fraction.

Hanford Site sediments have average bulk densities and pore fractions of 1.6 and 0.4, respectively. Thus, equation 13 reduces to:

$$\frac{V_i}{V_w} = \frac{1}{1 + 4K_d} \qquad (14)$$

Kd values measured for Hanford Site and 241-T tank farm sediments are given in Column 5 of Table 5. Retardation factors calculated from equation 14 are given in column 6 of Table 5. The minimum radionuclide travel times can be calculated from the minimum water travel time which was calculated as 2.3×10^4 years by dividing the water travel time by the retardation factor, since the water travel time is inversely proportional to the velocity. These values are given in column 7 of Table 5. Radioactive decay will reduce the activity ratio (C/Co) to 4×10^{-11} in 40 half-lives (Reference 16). By multiplying column 2 of Table 5 by 4×10^{-11}, it can be seen that radioactive decay will reduce activities of all radionuclides in the leak supernatant to values of less than drinking water standards in an uncontrolled area which are given in column 7 of Table 5. Thus, if the minimum radionuclide travel times all exceed 40 half-lives for each radionuclide, no radioactivity will enter the water table at concentrations above drinking water standards. Column 8 of Table 5 indicates that the minimum radionuclide travel times all exceed their 40 half-life values. Furthermore, if some of the activity were to reach the water table, it would require many additional years to move through the saturated zone to the Columbia River, which is the nearest area of uncontrolled access. Moreover, sorption, diffusion, and hydrodynamic dispersion in the saturated groundwater would further reduce the concentration of radionuclides at the Columbia River (Reference 12). Thus, under the environmental conditions of this analysis, it appears there will be no impact of the 241-T-106 tank leak on any uncontrolled area.

TABLE 5

Radionuclide Composition and Properties and Retardation Factors for Hanford Tank Farm Sediments

Radionuclide	Concentration, µCi/gal[1]	Half-Life, ($T_{1/2}$), Yr[2]	40 $T_{1/2}$, Yr	Kd, ml/g	Vi/Vw, unit less	MPC µCi/gal[3]	Minimum Radionuclide Travel Time, Yr
Cerium-144	4.48×10^4	0.78	32	>(0.4 - 1.4)[4]	0.38	4×10^{-2}	1,600
Praseodymium-144		--[5]	--	--	--	--	--
Cesium-137	3.35×10^5	30.00	1,200	7.1 - 12.0	0.034	2×10^{-2}	17,000
Cesium-134	5.00×10^3	2.00	80	7.1 - 12.0	0.034	3×10^{-2}	17,000
Europium-155	6.40×10^3	1.80	72	>(0.4 - 1.4)[4]	0.38	8×10^{-2}	16,000
Antimony-125	4.24×10^3	2.70	110	0.05 - 0.23	0.83	4×10^{-1}	720
Strontium-89	1.13×10^5	--[5]	--	--	--	--	--
Strontium-90		28.00	1,100	170	0.0015	1×10^{-3}	400,000
Ruthenium-106	2.32×10^6	1.0	40	0.41 - 1.4[6]	1.0	1×10^{-2}	600
Rhodium-106		--[5]	--	--	--	--	--
Plutonium-239	34	24,000	1,200,000	>1,500[7]	0.00017	5×10^{-3}	3,600,000
Plutonium-240	8	6,600	260,000	>1,500[7]	0.00017	4×10^{-3}	3,600,000
Americium-241	6	460	18,000	>1,200[8]	0.00021	2×10^{-2}	2,900,000

[1] Reference 1.
[2] Reference 16 (rounded to two places).
[3] Maximum permissible concentrations (Reference 17).
[4] Not actually measured, but known to have a higher Kd than sorbable ruthenium.
[5] Half lives of <0.5 year are not reported.
[6] Hanford studies have shown ~50% of ruthenium is complexed and unsorbable and ~50% sorbable (Reference 18)
[7] Reference 19.
[8] Reference 20.

CONCLUSIONS AND RECOMMENDATIONS

The 1978 status of the 1973 241-T-106 tank leak has been given in this document. Five years after leak occurrence, the maximum depth of the 1-μCi/ℓ ^{106}Ru concentration was found to be 33 meters (108 feet) below the ground surface in two wells; or, approximately 43% of the vertical distance from the bottom of the tank to ground water. In other wells, the vertical movement does not exceed 29 meters (95 feet). The maximum horizontal extent of the 1-μCi/ℓ ^{106}Ru concentration was found to be approximately 23 meters (75 feet) or about equivalent to the diameter of the tank. The rate of frontal movement of the leak was qualitatively estimated. A large portion of the movement occurred in 1973, prior to the publication of the initial status report by ARHCO. From 1973 to 1974, lateral movement occurred in at least some sediment layers (types) in all monitoring wells. From 1974 through 1977, waste movement could not be generally detected due to the radiodecay of mobile ^{106}Ru ($T_{1/2}$ = 1 year), although some movement undoubtedly occurred. However, lateral movement was detected in three wells near the perimeter of the leak from 1977 to 1978. This movement probably resulted from the addition of water to the system down a well casing during an unusual climatic event during the winter of 1977-1978.

The above general pattern of waste movement is about what would be expected by an infiltration of a pulse of water into a soil or sediment system. This generally consists of an initial rapid movement followed by an exponential decrease with time.

Calculations on vadose zone moisture and wetting frontal movements were found to be essentially in qualitative agreement in their assessed lack of movement of any waste above concentration guidelines to the Hanford ground water. Thus, during the hazardous lifetime of the fission products, there will likely be no amount of radioactivity enter the Hanford ground water. Therefore, there appears to be no impact of the leak on the Columbia River (the nearest point of uncontrolled access).

The 241-T-106 tank leak studies conducted up to the present time offer a sufficient basis of understanding of the 1973 leak. Thus, efforts will go from an active study and monitoring mode to a monitoring mode, exclusively. Since ungrouted wells can offer a path to deeper sediments of unexpected sources of water, all ungrouted wells in the T tank farm have been grouted and any new wells drilled in the T tank farm will be grouted as soon as the drilling is completed. In-well scintillation probe total gamma scans were run as soon as these wells were grouted to provide a basis for on-going monitoring. All T tank farm dry wells will continue to be monitored at least quarterly for the foreseeable future.

9212456128 0

REFERENCES

1. AEC-RL Staff, (1973), "Report on the Investigation of the 106-T Tank Leak at the Hanford Reservation, Richland, Washington", TID 26431.

2. ARHCO Research Dept. Staff, (1973), "241-T-106 Tank Leak Investigation", ARH-2874.

3. Gillette, R., (1973), "Radiation Spill at Hanford: The Anatomy of an Accident", Sci. 181:728-730.

4. Routson, R. C., (1969), "Effect of the Prior Disposal of Uncontaminated Solution on the Waste Retention Capacity of a Hanford Crib", BNWL-1163.

5. Haney, W. A., (1958), "A History and Discussion of Specific Retention Disposal of Radioactive Liquid Waste in the 200 Areas", General Electric Company, Richland, WA, HW-61544.

6. Bierschenk, W. H., (1959), "Techniques for Estimating the Specific Retention Properties of Hanford Soils", General Electric Company, Richland, WA, HW-61544.

7. Fecht, K. R., G. V. Last, and K. R. Price, (1977), "Evaluation of Scintillation Probe Profiles From 200 Area Crib Monitoring Wells", ARH-ST-156.

8. Brown, D. J., and R. E. Brown, (1958), "Subsurface Eolian Deposit at the Hanford Project, Washington (Abstract), Geological Society of American Bulletin, 69:1676-1677.

9. Brown, D. J., (1960), "An Eolian Deposit Beneath 200 West Area", General Electric Company, Richland, WA, HW-67549.

10. Bolt, G. H., M. E. Summer, and A. Kamphorst, (1963), "A Study of the Equilibria Between Three Catagories of Potassium in Illitic Soil", Soil Sci. Soc., 27:294-299.

11. Chase, G. D., and J. L. Rabinowitz, (1964), "Principles of Radioisotope Methodology", Burgess Publishing Co., Minneapolis, MN, p. 372.

12. Arnett, R. C., D. J. Brown, and R. G. Baca, (1973), "Hanford Groundwater Transport Estimates for Hypothetical Radioactive Waste Incidents", ARH-LD-162.

13. Routson, R. C., and D. J. Brown, (1978), "Frontal Movements of Aqueous Solutions During Redistribution Through Air-Dry Sand Columns as a Function of Column Length and Time", Soil Sci. 125:320-326.

14. Rose, C. W., (1969), "Agricultural Physics", Pergamon Press, New York, pp. 239.

15. Schroeder, M. C. and A. R. Jenning, (1964), "Laboratory Studies of the Radioactive Contamination of Aquifiers". UCRL-13074.

16. Lederer, C. M., J. M. Hollander, and I. Perlman, (1968), "Table of Isotopes", (6th Ed). John Wiley and Sons, Inc., New York. Pg. 594.

17. Department of Energy, (1978), "Standards for Radiation Protection", Manual Chapter 0524, Annex A. (Formerly Atomic Energy Commission Manual Chapter 0524, 1968). Table II, Column 2.

18. Routson, R. C., (1973), "A Review of Studies on Soil-Waste Relationships on the Hanford Reservation from 1944-1967. BNWL-1464.

19. Rhodes, D. W., (1952), "Preliminary Studies of Plutonium Adsorption in Hanford Soil". HW-24548.

20. Routson, R. C., A. V. Robinson, and G. Jansen, (1977), "^{241}Am, ^{237}Np, and ^{99}Tc Sorption on Two United States Subsoils From Differing Weathering Intensity Areas". Health Physics. 33:311-317.

9 2 1 2 1 5 6 1 2 8 2

THIS PAGE INTENTIONALLY
LEFT BLANK

APPENDIX A

CHRONOLOGY OF THE 241-T-106 TANK LEAK

The following is the official record of the events leading up to the discovery of the 216-T-106 Tank leak (Reference 1).

"1. Between January and April 4, 1973, the liquid level in Tank 241-T-106 was essentially stable at 24 inches. This volume consisted of approximately 35,000 gallons of liquid and 39,000 gallons of sludge.

2. On Wednesday, April 4, the planned filling of 241-T-106 Tank with ion exchange waste (denuded supernate) was started. Tank 241-T-106 was being emptied. Tank 241-T-106 is the last in the cascade series of T-104, T-105, and T-106 (T-104 is filled with solidified waste - salt cake). The waste was pumped to T-105 to fill T-106 via cascade overflow. The transfer was a day-shift operation and liquid level readings in T-107, T-105, and T-106 were taken three to four times a shift during pumping operations.

3. On or about Friday, April 20, leaking began. (The leak beginning could not have been determined from the early liquid level readings taken during pumping operations, but was determined after the fact, based on the material balances obtained for transfers up to this point.)

4. On Monday, April 23, the weekly liquid level reading in Tank T-106 was recorded during pumping operations at 153.3 inches.

5. On Tuesday, April 24, pumpings from Tank T-107 ended. The liquid level for Tank T-106 was recorded at 175.4 inches. Because of the cascading effect from Tank T-105 into T-106, liquid continued to enter Tank T-106 until an estimated level of 183.7 inches was reached on Wednesday, April 24. This constituted the end of the filling operation.

6. On Wednesday, May 2, the first weekly liquid level reading for Tank T-106 after completion of the pumping operation was taken. It was recorded at 178.9 inches on the 200 West Area waste storage tank inventory form. The information was recorded in the static tank farm inventory log and left on the office desk of the 200 West Area day-shift supervisor in Room 224 of U Building. The day-shift supervisor stated that he did not review the information because of the press of other duties. (The process control technician, who records and initially evaluates all waste operations, stated that he never received the 200 West Area waste storage tank inventory form for May 2.) In this, and subsequent cases discussed regarding data never received or belatedly found, the Committee was unable to locate the missing data or determine where the data were placed.

7. On Monday, May 7, the weekly liquid level reading for Tank T-106 was recorded at 174.0 inches. The information was logged in the static tank farm inventory log in the day-shift supervisor's office. He did not review it. (The Process Control Group never received the 200 West Area waste storage tank inventory form for May 7.)

8. On Tuesday, May 8, the monthly dry well readings for T Tank Farm for May were taken and the resultant strip charts were left on the desk of the day-shift supervisor. The reading for Well 299-W10-51, which is 47 feet from the outside edge (in closest proximity to Tank T-106), indicated no abnormalities.

9. On Monday, May 14, the weekly liquid level reading for Tank T-106 was recorded at 167.9 inches. The information was logged in the static tank farm inventory log. It was not reviewed by the day-shift supervisor, but a waste storage tank inventory form was prepared by the operator and transmitted to the Process Control Group. The latter received these data on Tuesday, May 22. However, because the readings for the two previous weeks (178.9 and 174.0 inches, respectively) were not received and since the Process Control Group does not routinely review pumping reports such as that which ended on April 24, the only weekly inventory information with which to compare the 167.9-inch reading was for April 23 (153.5 inches) and was taken during actual pumping operation. Therefore, as of May 14, the process control technician was unable to determine that there had been a decrease in the liquid level of Tank T-106 subsequent to the end of the filling process.

10. On Monday, May 21, the weekly liquid level reading for Tank T-106 was recorded at 160.4 inches. The information was logged in the static tank farm inventory log. The day-shift supervisor did not review it. He stated that he transmitted the data on a waste storage tank inventory form.

11. On Wednesday, May 30, the weekly liquid level reading was recorded at 152.0 inches and logged on the static tank farm inventory log. The day-shift supervisor did not review it. He stated that he transmitted the data to the Process Control Group on a waste storage tank inventory form. This form did not reach Process Control until sometime during the middle of the week of June 4.

12. On May 30, the Process Control Group team leader notified Manufacturing Department personnel in a regularly scheduled meeting that the only liquid level inventory form received since April 23 was the one for May 14 and requested that the missing data be furnished to Process Control.

13. On Thursday, May 31, the monthly dry well readings on T Tank Farm for June were taken. Well 299-W10-51 was checked with a scintillation probe and went off-scale at 10,000 counts per minute (cpm). The dry well monitoring operator left the strip chart with the day-shift supervisor and mentioned the problem on the well to him. The supervisor asked him to take another reading on the following day. The chart for May 31 was not received by the Process Control Group until June 15.

14. On Friday, June 1, the dry well monitoring operator took another reading on Well 299-W10-51 and informed his supervisor of the continued high reading. The reading was off-scale at 1,000,000 cpm. The day-shift supervisor requested that this well be checked on a daily basis, but did nothing further about the data. The dry well chart for June 1 was not received by the Process Control Group until June 15.

15. On Monday, June 4, the dry well reading on Well 299-W10-51 was again taken by the monitoring operator, using a less sensitive probe than the previous week. It registered 300,000 cpm using a Geiger-Müller (GM) probe. The strip chart was placed on the desk of the day-shift supervisor, who did not review it. This chart was received by the Process Control Group on Saturday, June 9. On the same date, the weekly liquid level reading for Tank T-106 was recorded at 149.2 inches on the waste storage tank inventory form and logged in the static tank farm inventory log. The day-shift supervisor did not review it, but he did transmit the data to the Process Control Group. However, by the time the Process Control Group received this information, during the week of June 11, the fact that Tank T-106 was leaking had already been determined.

During the week of June 4, but on separate days, the process control technician received the liquid level data for May 21 and May 30 which reflected decreases from the previous weeks' readings. The technician checked his records on June 7 for possible tank transfers that he might not have been aware of and reviewed other available documents for any information that might provide the reason for the decrease.

16. On Tuesday, June 5, the dry well monitoring operator took another reading on Well 299-W10-51. Using a GM probe, the well was recorded at 290,000 cpm on the same range as used the previous day. He placed the chart on the desk of the day-shift supervisor. The day-shift supervisor did not review it. The chart for June 5 was received by the Process Control Grup, Saturday, June 19.

17. On Wednesday, June 6, the dry well monitoring operator took another reading on Well 299-W10-51. Using the same probe and range as the previous day, the well was recorded at 310,000 cpm. He placed the chart on the desk of the day-shift supervisor. The day-shift supervisor did not review it. The chart for June 6 was received by the Process Control Group on Saturday, June 9.

18. On Thursday, June 7, the dry well monitoring operator took another reading for Well 299-W10-51. Using the same probe and power range as the previous day, the well was recorded at 290,000 cpm. He placed the chart on the desk of the day-shift supervisor. The day-shift supervisor did not review it until sometime during the early evening, when he reviewed all the charts taken during that week for Well 299-W10-51. The day-shift supervisor stated to the Investigation Committee that he had informed the Tank Farm Subsection Manager by telephone at home that evening about the problem while discussing other nonrelated problems.

Also, on June 7, the Process Control Technician, after a check of all the records available regarding an answer to the decrease in the liquid level for Tank T-106, requested the day-shift supervisor to check his records. The day-shift supervisor did not return the call that afternoon. The process control technician, in the absence of a return call, thereupon informed his supervisor that he suspected that Tank T-106 was a "leaker".

19. On Friday, June 8, the day-shift supervisor confirmed that all data indicated a leak in Tank T-106. At 9:00 a.m., during a regularly scheduled meeting held by Manufacturing and Process Control personnel, emergency plans to pump out Tank T-106 were initiated.

Atlantic Richfield Hanford Company (ARHCO) informed AEC-RL Director of Production and Waste Management of the leaking tank at approximately 4:25 p.m. The Manager, AEC-RL, was informed at his home that evening of the leak and that emergency pumping operations were being initiated.

20. On Saturday morning, June 9, a meeting attended by Manufacturing and Process Engineering personnel was held to review the leak data and pumping operations. During that meeting, the leak volume was determined to be approximately 115,000 gallons. Nearby monitoring wells were identified and preliminary plans for the placement of new monitoring dry wells and groundwater wells were discussed.

21. On Sunday, June 10, at approximately noon, all of the liquid waste not retained in sludges had been pumped out of Tank T-106, with a net loss from the leak of approximately 115,000 gallons, amounting to approximately 14,000 Ci of strontium-90, 40,000 Ci of cesium-137, and four Ci of plutonium. The residual amount of waste (sludge, interstitial liquors and supernate) remaining in the tank was approximately 64,000 gallons."

REFERENCE

1. AEC-RL Staff, (1973), "Report on the Investigation of the 106-T Tank Leak at the Hanford Reservation, Richland, Washington," TID 26431.

9 2 1 2 4 6 5 1 2 8 7

APPENDIX B

ROCKWELL HANFORD OPERATIONS HIGH-LEVEL RADIOACTIVE TANK LEAK CRITERIA, MONITORING, AND DETECTION LEVELS

As a response to the 1973 AEC-RL investigation of the 241-T-106 tank leak, certain portions of the Standard Operating Procedure (SOP) for the Tank Farm Operations and Tank Farm Surveillance functions were upgraded. This appendix summarizes the present Rockwell SOP for monitoring, leak detection, and detection criteria and capabilities. The nature, scope, and frequency of the monitoring, as well as the required response to data deviation criteria, are systematically given for each tank farm and tank in a four-volume official Rockwell operation manual. The report on the investigation of the 241-T-106 tank leak (Reference 1) can be consulted for a comparison of the present procedure with the 1973 procedures.

Several types of monitoring activities are routinely conducted on the Hanford Site's 15 tank farms which are A, AX, AY, AZ, B, BX, BY, C, S, SX, T, TX, TY, and U tank farms. Five routine categories of tank leak detection monitoring are employed. The first is the measurement of liquid levels in all tanks by manual methods and/or liquid gauges. A second is the measurement of total gamma levels in dry wells around all tanks by the scintillation methods described in Appendix J. A third monitoring category is the measurement of total gamma by scintillation methods in lateral tubes located approximately 3 meters below the concrete base of A farm tanks and tanks SX-105, SX-107 through SX-112, SX-114, and SX-115 in the SX tank farm. A fourth is the measurement of total gamma, weight, specific gravity, and temperature of any leaked solution in leak detection pits in the AX and AY tank farms by scintillation methods, weighing measurements, and thermocouple readouts, respectively. The final monitoring category is the detection of leakage from the primary means of detection for double-shell tanks in the annulus air sampler, analyzed for the presence of long-lived beta emitters. In addition, conductivity probes at 16 levels monitor the height of any liquid leaked into the annulus space.

Different data collection frequencies are in effect for the five monitoring categories. Liquid level readings are taken in each boiling or nonboiling waste storage tank containing liquid on a minimum frequency of one per shift. During high-level waste transfers, the procurement of liquid level readings is increased to a 2-hour frequency for all involved tanks. For tanks in which automatic liquid gauges are installed, a computer-initiated scan is made hourly. Most dry wells are monitored each Monday, Wednesday, and Friday for a minimum of 3 weeks after the tank has been filled, or until readings stabilize. Laterals with radioactivity levels of less than 330 cpm are monitored three times per week. The AX and AY farm leak detection pits weight factor, specific gravity, and radiation readings are recorded on a once-per-shift frequency. The record of the annulus conductivity probe data is collected once per shift.

All leak-detection monitoring data are evaluated for deviation from specified levels. In the event a limit is exceeded and the potential for a tank leak is indicated, immediate action steps are mandatory. These are the notification of the Manager - Operations, issuance of a Rockwell Hanford Operations Occurrence Report, and development of a plan for corrective action.

ACTION CRITERIA

Liquid level decreases in nonboiling active tanks are limited to 1.27 centimeters for Food Instrument Corporation (FIC) gauges, and 2.54 centimeters for manual liquid level measurements. However, tanks that primarily contain sludge with little associated solution show greater than the above decreases in "liquid level" measurements, particularly if a salt well system is in operation. Such losses are due to sludge slumping, tape flushes, and perforation of the exposed sludge at the point of probe contact. In addition, some of the tanks in which salt well systems are installed have liquid observation wells. These are bottom-screened pipes which extend through the sludge to the tank bottom. Liquid migrating into the well is an approximate indication of interstitial liquid level. Measurements in these wells vary considerably from day to day. Therefore, such tanks require special evaluation prior to any definition of status based on liquid level data. The liquid level action criteria for the individual A, AX, AY, and SX farm tanks are reviewed in relation to these factors monthly. In leak-detection pits of AX and AY farms, any unusual increase in weight factor or radiation level readings are reported immediately. Annulus leak detection in the AY farm is by conductivity probes. If liquid is contacted by any of these probes, it is reported.

In dry well monitoring of waste storage tanks, it is immediately reported and action steps are immediately required when:

1. The scintillation probe (shielded or unshielded) indicates a doubling of the radiation (wells with a background of >500 cps) or a peak exceeds four times the background radiation (wells with a background of from 200 to 500 cps).

2. The GM probe indicates a tripling of the radiation in any area of the well (wells with a background of from 100 to 1,000 cps). (Significant trends can be established before the lower limits, and, in those cases, notification is given earlier.)

3. The radiation increase is within 6.1 meters of the ground surface and cannot be attributed to background from a transfer line or other contained material.

In laterals of A and SX farms, a radiation level increase of >1 cps over background is significant and is reported. For laterals monitoring old contamination >1 cps, there is a large variation in the readings and notification is not given until any part of the baseline profile changes by a factor of 2.

9 2 1 2 4 6 6 1 2 8 9

Actions to be applied in the event of deviate data suggesting a loss of tank integrity vary for specific tanks; however, the general plan for action after issuance of a Rockwell Occurrence Report is: (1) the tank may be placed in a quarantine status pending review of all data pertinent to the occurrence during which time no transfers into the tank are allowed; (2) if the routine data discrepancies cannot be satisfactorily explained, the tank is either removed from service or disposition may await the development of additional information*; and (3) analysis of all new information becomes the basis for a decision to either remove the tank from service or declare it to be sound. Removal from service involves the planned transfer of all liquid, including interstitial liquor, stabilizing the residual material, and ultimately isolating the tank from all liquid sources.

REFERENCE

1. AEC-RL Staff, (1973), "Report on the Investigation of the 106-T Tank Leak at the Hanford Reservation, Richland, Washington," TID 26431.

9212466129 0

*For liquid level losses, special studies are conducted to determine the effect of other mechanisms to explain the decrease, including in-tank photography. Further information relating to dry well and lateral radiation increases may involve the drilling of new wells or augering in the vicinity of a suspect leak to obtain soil samples for analysis of radionuclide content.

THIS PAGE INTENTIONALLY
LEFT BLANK

APPENDIX C

CLIMATE

The area in and around the Hanford Site is characteristic of an arid shrub-steppe region featuring low rainfall, low relative humidity, dry, hot summers, cool-to-moderate winters, and frequent periods of high-to-moderate wind velocity (Reference 1). All of the climatic data reported herein were taken at the Hanford Meteorlogical Station, located approximately 5 kilometers from the 241-T-106 tank leak site, and are based on up to 58 years of record. Due to the nearness of the weather station, these climatic data are particularly applicable to 241-T-106 tank leak situation.

Precipitation is 15.9 centimeters per annum with the months of November to January contributing 42% of the annual total. In contrast, the months of July through September contribute only 10% of the annual total. Mean annual relative humidity at 0600 and 1300 P.S.T. are 74 and 50% respectively. Relative humidity is reported at the hours of 0600 and 1300 as they are at or near the times of diurnal maximum and minimum relative humidity, respectively. November through January mean relative humidity at 0600 and 1300 P.S.T. are 45 and 25% respectively. Mean July relative humidity at 1300 P.S.T. is 22%.

Mean annual temperature at Hanford is 11.5°C. Mean November through January temperature at Hanford is 1.4°C. Mean June through August temperature is 22.8°C. The average number of days with maximum temperatures $\geq$ 32.3°C are 13 and 56, respectively. The average number of days with minimum temperatures below -17.8°C and 0°C are 4 and 115, respectively; however, only half of the years of record have any days below -17.8°C. Table C1 gives the highest average, lowest average, and monthly average wind speed at Hanford. Hanford has an environment of frequent periods of moderate-to-high wind velocities.

In summary, the climatic conditions of low rainfall, low relative humidity, dry, hot summers, and frequent periods of moderate-to-high wind tend to restrict the amount of moisture available for leaching waste released to underground sediment to a low value.

REFERENCE

1. Stone, W. A., D. E. Jenne and J. M. Thorp, (1972), "Climatography of the Hanford Area". BNWL-1605.

TABLE C1

Monthly and Annual Hanford Winds: 1945-1970
(kilometers per hour)

Month	Prev Dir.	Avg Speed	Highest Avg	Year	Lowest Avg	Year	Peak Gust		
							Speed	Dir	Year
Jan	NW	10.3	15.4*	1953	5.0	1955	104.6**	S	1967
Feb	NW	11.3	15.1	1961	7.4	1963	101.4	SW	1965
Mar	WNW	13.5	17.2	1964	9.5	1958	112.7	SW	1956
Apr	WNW	14.5	17.9	1959	11.9	1958	96.6	WSW	1969
May	WNW	14.2	16.9	1965+	9.3	1957	114.3	SSW	1948
Jun	WNW	14.8	17.2	1949	12.4	1950+	115.9	SW	1957
Jul	WNW	13.8	15.4	1963	10.9	1955	88.5	WSW	1968
Aug	WNW	12.8	14.6	1946	9.7	1956	106.2	SW	1961
Sep	WNW	12.1	14.8	1961	8.7	1957	104.6	SSW	1953
Oct	WNW	10.8	14.6	1946	7.1	1952	101.4	SSW	1950
Nov	NW	10.0	12.7	1945	4.7	1956	103.0	SSW	1949
Dec	NW	9.7	13.4	1968	6.3	1963+	114.3	SW	1955
Year	WNW	12.2	13.4	1968+	10.1	1957	115.9**	SW	June 1957

*The average speed for January, 1972, was 15.6 kilometers per hour.

**On January 11, 1972, a new all-time record peak gust of 128.7 kilometers per hour was established.

9 2 1 2 4 6 6 1 2 9 2

APPENDIX D

GEOLOGY OF THE 241-T TANK FARM

REGIONAL GEOLOGIC SETTING

Central Washington lies within the Columbia River Plateau Physiographic Province, formed by a thick accumulation of basaltic lava flows extending laterally from central Washington eastward into Idaho and southward into Oregon (Figure D-1). In south-central Washington State, deformation of the lava flows has formed a broad structural and topographic basin (the Pasco Basin) in which the Hanford Site lies.

The basin is bounded on the north by the Saddle Mountains; on the west by Umtanum Ridge, Yakima Ridge, and the Rattlesnake Hills; on the south by the Rattlesnake Hills and a series of doubly plunging anticlines which merge with the Horse Heaven Hills; and on the east by the Jackass Mountain Monocline (Figure D-2).

Three major stratigraphic units (Figures D-3 and D-4) lie below the Hanford Site: (1) Columbia River Basalt Group which forms the bedrock beneath the Site; (2) semiconsolidated sediments of the Ringold Formation which directly overlie the bedrock; and (3) unconsolidated sand, silts, and gravels of the Hanford Formation, carried into the area by glacial flood waters during the Ice Ages.

Between 20 and 40 million years ago, a series of fissures opened around the periphery of the Pasco Basin and large volumes of basaltic lava were extruded intermittently from these fissures until approximately 8 million years ago (References 1 and 2). The fluidity (viscosity) of the basaltic lava was about the same as water. Under these conditions, the molten rock, insulated by a thin skin of cooled lava, quickly ran downhill filling the lowland areas in the center of the basin. Subsidence; however, kept pace with the inflow of lava accounting for the great thickness now observed in the Pasco Basin. Deep exploratory drilling by the Standard Oil Company of California has shown that the basalt flows in the Pasco Basin have accumulated to a thickness of over 3,200 meters.

Folding of the region started about 12 to 14 million years ago during the extrusion of the middle Yakima Basalts (Reference 3). The Pasco Basin began a slow and prolonged period of subsidence while the margins of the basin began to emerge as anticlinal ridges. During quiescent periods of the Columbia River Basalt volcanism, lakes were formed in the basin when ancestral rivers were impeded by the rising anticlines. Continental, non-marine, clastic, and pyroclastic sedimentary deposits of gravel, sand, silt and clay, and volcanic ash accumulated in the shallow basins. Subsequent basalt flows covered the sediments and the slowly emerging anticlines.

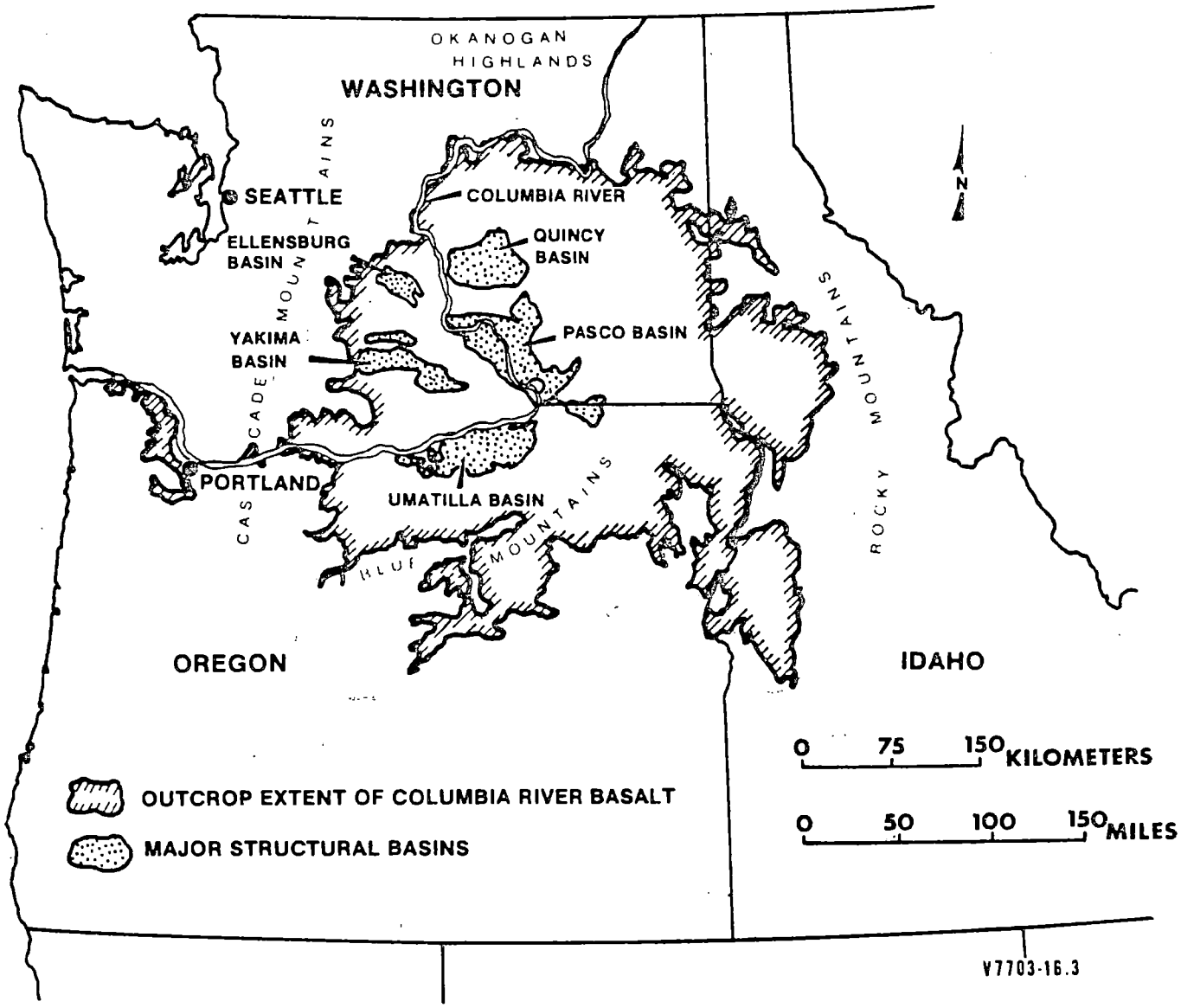

FIGURE D-1. Areal Distribution of Columbia River Plateau Flood Basalts (modified after Wright, et al, 1973, Reference 4).

9 2 1 2 4 6 6 1 2 9 4

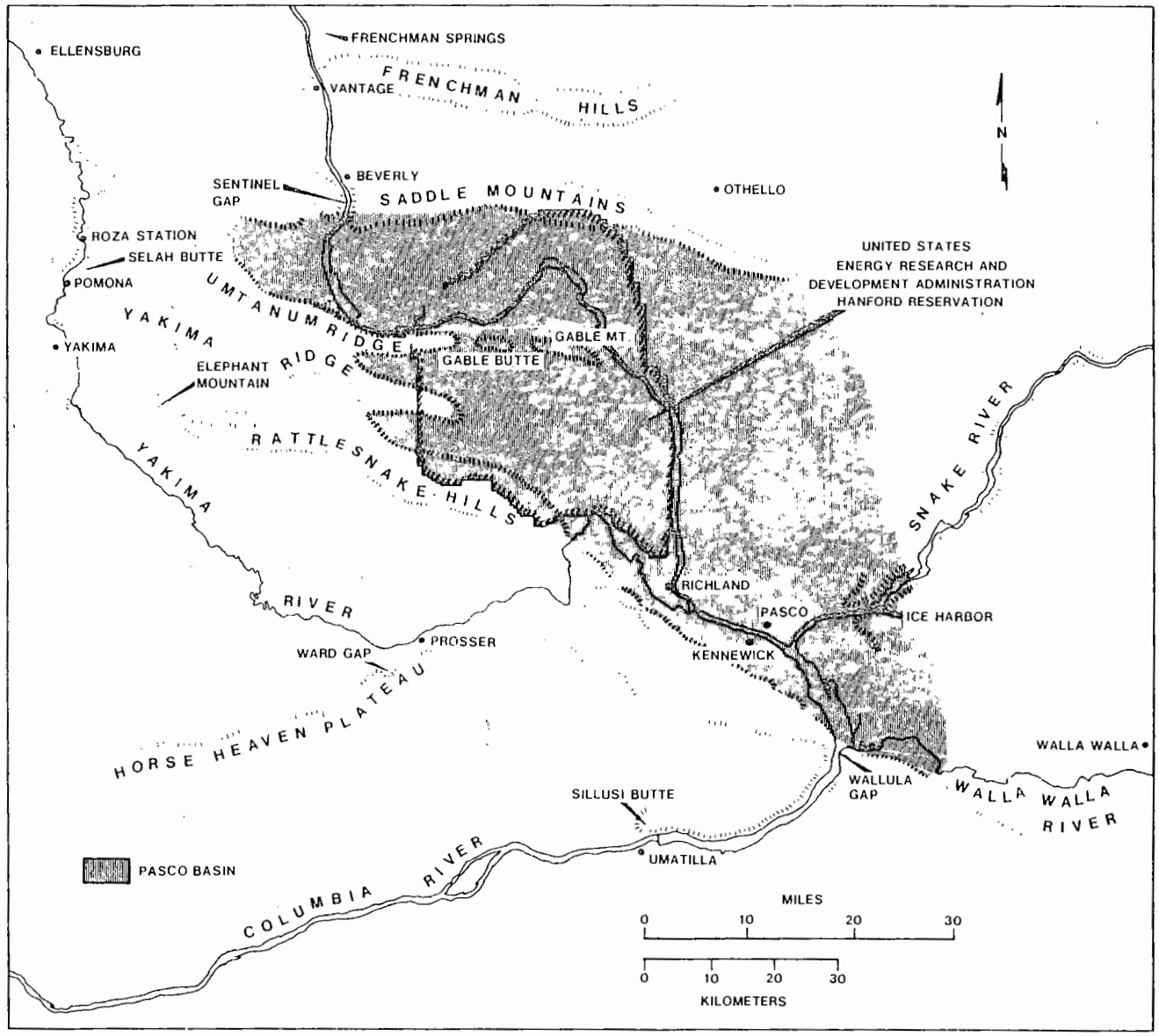

FIGURE D-2. Topography of the Hanford Site and Vicinity (Reference 5).

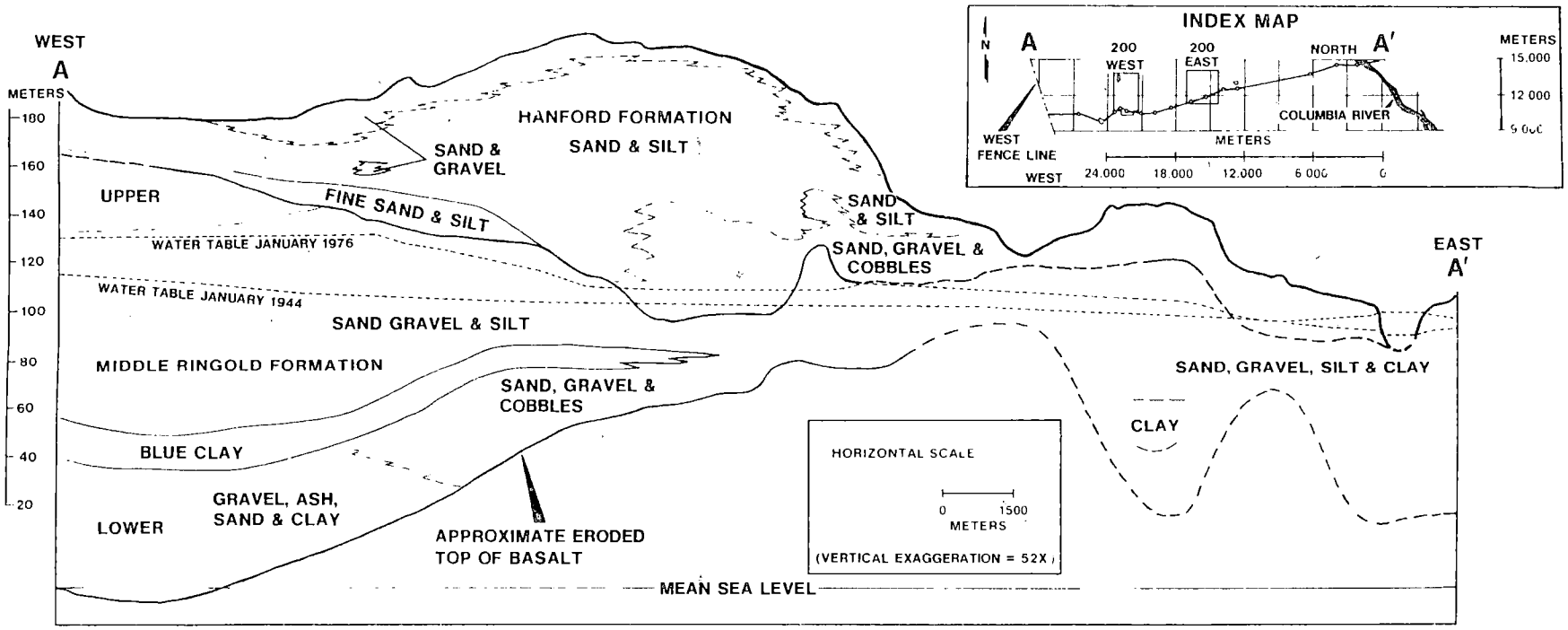

FIGURE D-3. Geologic Cross Section - Hanford Site (modified after Veatch, 1971, Reference 6).

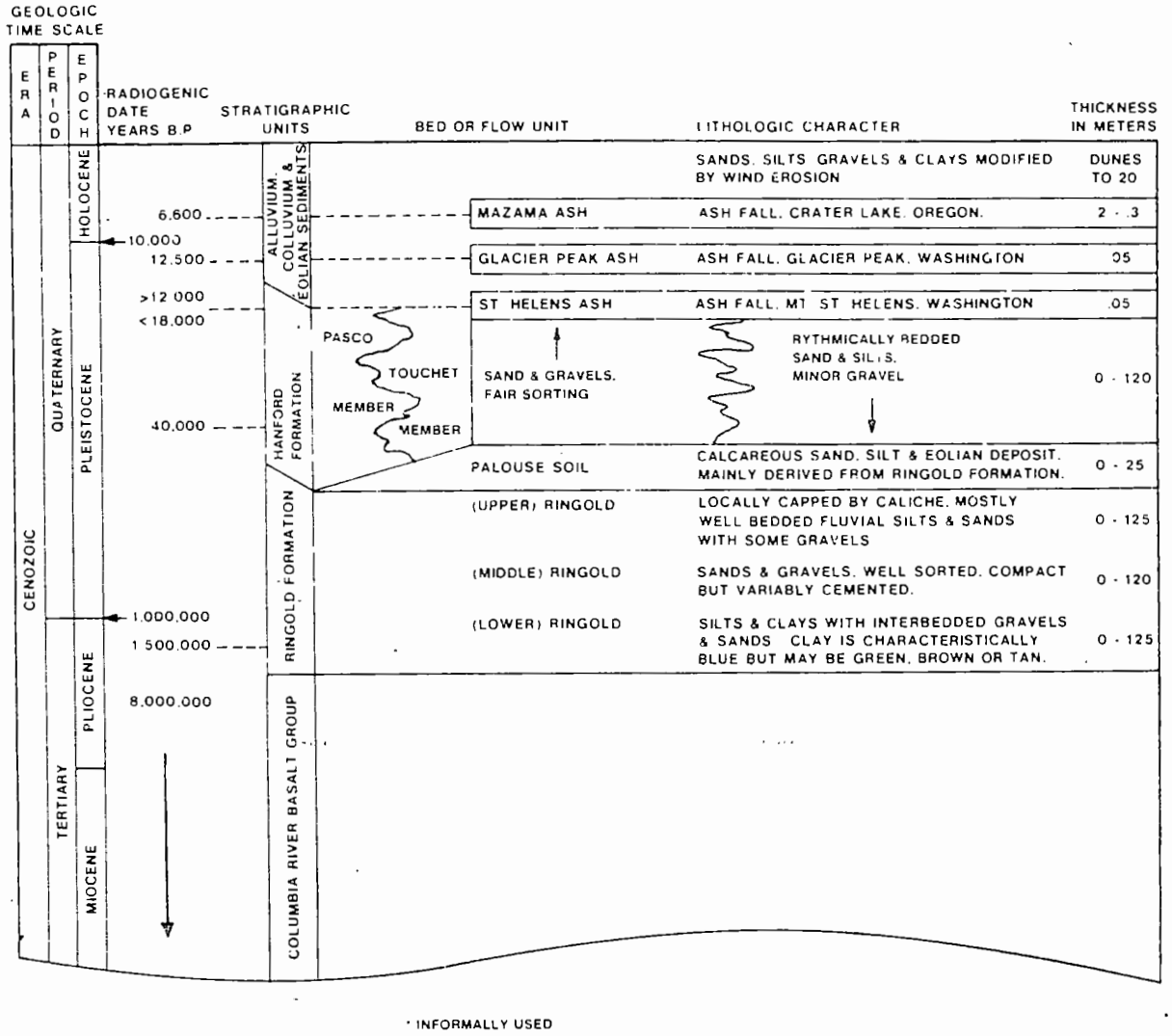

FIGURE D-4. Stratigraphic Chart of the Pasco Basin (References 7, 8 and 9).

The Ringold Formation was formed following the cessation of the Columbia River Basalt volcanism during the Pliocene-Pleistocene epochs. The ancestral Columbia River transported nonmarine, clastic sediments from the surrounding highlands into the subsiding Pasco Basin where they accumulated to a thickness of over 400 meters. The lower portion of the Ringold Formation is, in general, conformable with the surface of the underlying basalt bedrock. Beneath the Hanford Site, this formation is up to 370 meters thick and generally can be divided into three units on the basis of texture: clays and silts of the lower Ringold unit; occasionally cemented sand and gravel of the middle Ringold unit; and silts and fine sands of the upper Ringold unit (Figure D-5, Reference 10).

During the close of the Ice Ages, 10,000 to 20,000 years ago, a continental ice sheet covered much of northern Washington, Idaho, and Montana. As the ice sheet retreated northward, breakup of ice dams resulted in catastrophic floods in which large volumes of glacial meltwaters were released, periodically flooding the Pasco Basin. During one of these floods, over 2×10^{12} cubic meters of water is estimated to have poured into the Pasco Basin at a rate of more than 4×10^{10} cubic meters of water per hour (Reference 11). In places, the floods scoured the then-existing land surfaces, the eolian silt and upper and middle Ringold units, deeply eroding the Ringold Formation. The glacial meltwaters were hydraulically dammed at Wallula Gap, and water was impounded in the Pasco Basin to an elevation of 335 meters above sea level. The velocity of flood waters diminished and unconsolidated sediments up to 122 meters thick were deposited in the Pasco Basin. These sediment deposits became the Hanford Formation (Figure D-4).

The land surface has been only slightly modified since the deposition of the Hanford Formation. Subaerial erosion by wind has aggraded extensive areas in the southwestern portion of the Hanford Site. The silt and sand moved by the wind are redeposited on the ground surface forming dunes. Other Holocene deposits consist of alluvium along the Columbia River, colluvium along the anticlinal ridges, and volcanic ash beds from at least three major eruptions in the Cascade Mountains to the west.

STRATIGRAPHY BENEATH 241-T TANK FARM

The major sedimentary units underlying the 241-T tank farm are: (1) middle and upper units of Ringold Formation; (2) eolian silt; (3) the Hanford Formation; and (4) backfill (Figure D-6). These geologic units are described with emphasis on the sediment types, mineralogy, and structure of sediments in the vadose zone. The thickness of these unsaturated sediments is approximately 62 meters.

SEDIMENT CLASSIFICATION
(modified after R. L. Folk,
1968, Reference 12).

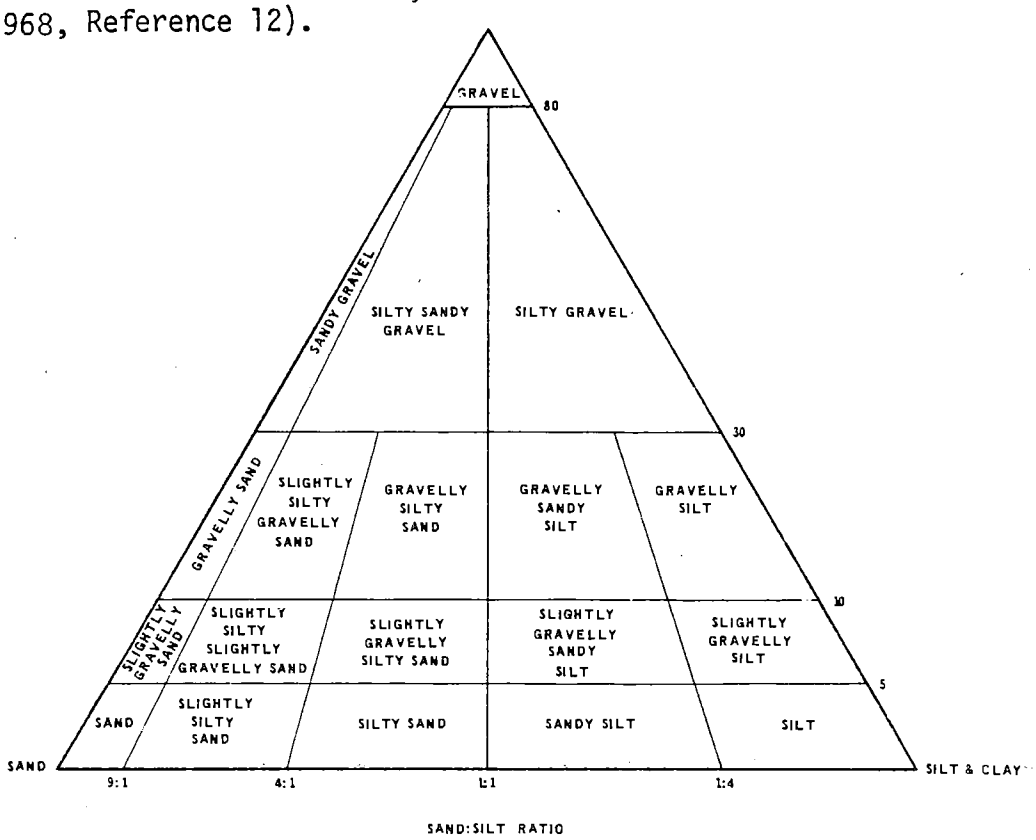

GRAIN SIZE NOMENCLATURE
(modified after C. K. Wentworth, 1922
Reference 13).

PARTICLE DESIGNATION			PARTICLE DIAMETER (MM)
GRAVEL		BOULDER	>256
GRAVEL	COBBLE	LARGE	256-128
GRAVEL	COBBLE	SMALL	128-64
GRAVEL	PEBBLE	VERY COARSE	64-32
GRAVEL	PEBBLE	COARSE	32-16
GRAVEL	PEBBLE	MEDIUM	16-8
GRAVEL	PEBBLE	FINE	8-4
GRAVEL	PEBBLE	VERY FINE	4-2
SAND		VERY COARSE	2-1
SAND		COARSE	1-0.5
SAND		MEDIUM	0.5-0.25
SAND		FINE	0.25-0.125
SAND		VERY FINE	0125-0.0625
SILT & CLAY			<0.0625

FIGURE D-5. Hanford Sediment Classification Index.

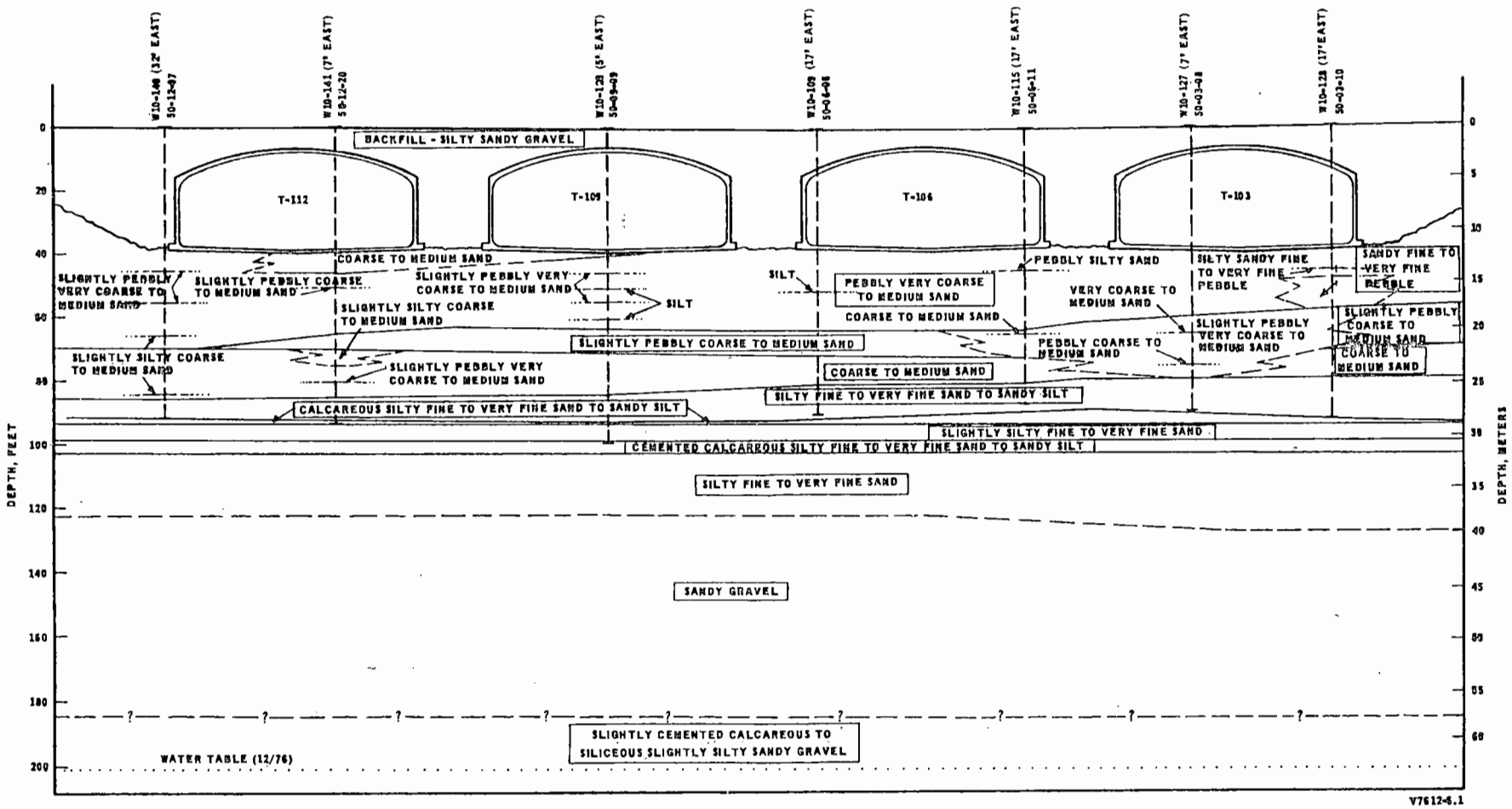

FIGURE D-6. Stratigraphy of the Unsaturated Zone Beneath the 241-T Tank Farm (Reference 8).

9 2 1 2 4 6 6 1 3 0 1

Middle Ringold

Beneath the 241-T tank farm, the 111-meter-thick middle Ringold unit lies unconformably on the Elephant Mountain Member of the Columbia River Basalt Group and dips to the southeast about 9.3 m/km. The unit consists of well-rounded cobbles and pebbles with interstitial spaces filled with coarse-to-fine sands and silt, and partially cemented in the lower portion of the unit (Figure D-7). Inlayed in the conglomerate are numerous thin silt and sand lenses. Measured sediment properties of the conglomerate unit are summarized in Table D1. Grain size and calcium carbonate values for the major middle Ringold unit lithologies are summarized in Table D2.

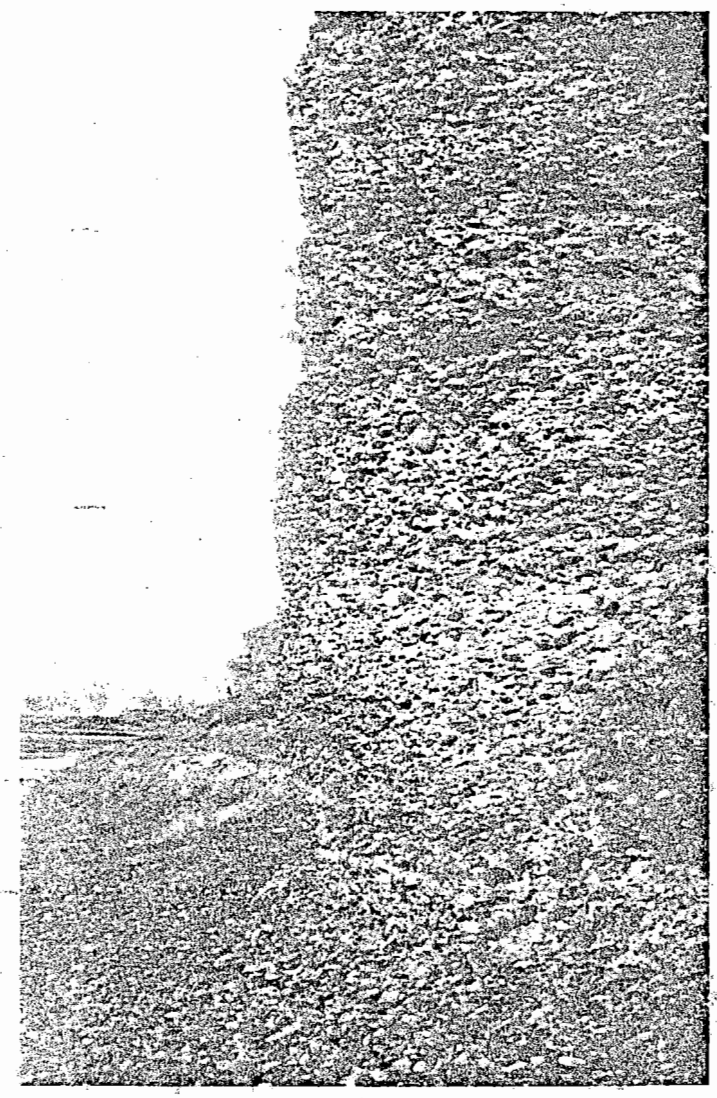

Figure D-7. Middle Ringold Unit at White Bluffs

TABLE D1

Sediment Property Summary

	SEDIMENTARY UNIT	SATURATED PERMEABILITY (cm/day)	POROSITY Percent	BULK DENSITY (g/cm^3)	PARTICLE DENSITY (g/cm^3)	CATION EXCHANGE CAPACITY (meq/g soil)	$CaCO_3$ (meq/g soil)
Backfill	Backfill - Silty Sand Gravel	29.8	34	1.85	2.76	0.0673	10.9
Hanford Formation	Pebbly very coarse to medium Sand	61.0	38	1.81	2.30	.0616	13.0
	Slightly pebbly coarse to medium Sand	290.3	39	1.81	2.92	-	-
	Coarse to medium Sand	187.9	37	1.70	2.64	.0595	26.0
Eolian	Silty fine to very fine Sand to sandy Silt	8.6	43	1.65	2.60	.0696	132.0
Upper Ringold	Slighty silty fine to very fine Sand	49.4	38	1.79	2.84	.0528	76.5
	Cemented silty fine to very fine Sand to sandy Silt	0.4	22	1.65	2.60	.0788	370.0
	Silty fine to very fine Sand	-	36	1.64	2.57	-	-
Middle Ringold	Sandy Gravel	-	-	-	-	-	-
	Sandy gravelly Silt	335.3	-	1.88	2.63	-	-

TABLE D2

Summary of Middle Ringold Typical Grain Size and Calcium Carbonate Content (References 8 and 14)

Lithology	% Pebbles & Cobbles	% Sand					% Silt & Clay	% $CaCO_3$
		Very Coarse	Coarse	Medium	Fine	Very Fine		
Sandy Gravel	77	2	3	4	9	5	1	0.3
Cemented Calcareous to Siliceous Slightly Silty Sandy Gravel	70	4	6	6	8	5	1	0-12.0
Coarse-to-Medium Sand	1	9	26	36	15	10	4	1.0
Cemented Calcareous to Siliceous Slightly Silty Sandy Gravel	67	8	7	6	6	5	2	0-12.0

The predominant conglomerate is an aggregation of massive-bedded, poorly sorted, well-rounded cobbles and pebbles. The color is typically greyish brown to brownish buff, due to the well-developed weathering rinds (up to 1-cm thick) of ferric oxide (hematite) coatings on the gravel fraction. The nonbasaltic gravel fraction lithologies are predominantly quartzites with other clastic, continental metamorphic, granitic and volcanic porphyry rocks derived from the Columbia River drainage basin to the north. The basalt gravel fraction consists of basalt lithologies of the Columbia River type and generally is highly altered due to hydration and physical disintegration.

The conglomerate is divided into two units based on degree of induration. The lower conglomerate is moderately-to-well cemented with silica and/or calcium carbonate. Zones of poorly indurated conglomerate occur within this division. The mineralogical composition of the moderately-to-well indurated conglomerate is predominantly quartzite, basalt, and porphyry pebbles and cobbles with an arkosic sand matrix. The water table is near the top of the indurated conglomerate zone, approximately 143 meters above mean sea level. The upper unit consists of unconsolidated sands and gravels and has similar mineralogical compositions. Beneath the 241-T tank farm, this unit is between the 40- and 50-meter depths.

Sand and silt lenses, ranging from 1 cm to 5 m in thickness, form interlayered discontinuous stringers throughout the conglomerate and gravel. The silt lenses are massive-bedded to horizontally-laminated. The sand lenses are typically coarse-to-medium in grain size, and composed of largely upriver

9212466130 3

arkosic materials (quartz and feldspar) and are commonly cross laminated (Figure D-8). These lenses, up to 5 meters in thickness, represent either lacustrine or fluvial deposits laid down during periods of decreased velocity of the Columbia River.

FIGURE D-8. Sand Lenses of Middle Ringold Unit at White Bluffs.

9212461304

Upper Ringold

The upper Ringold unit, which overlies the middle Ringold unit, occurs between elevations 167 and 177 meters above mean sea level (Figure D-6). The unit consists of predominantly well-sorted, fluvial sands and silts, compact and light brown to light tan in color. These sediments, like the sand units of the middle Ringold unit, represent a period of decreased velocity of the Columbia River or temporary ponding. Bedding is crudely-to-well laminated with alternating fine sands (1.5- to 6-cm thick) and silts (<1-cm thick) similar to the bedding exposed on the White Bluffs in Figure D-9. The boundaries between alternating grain sizes are usually sharp. The sediments are typically fine-grained sands and silts with at least two distinct caliche (calcium carbonate) horizons. Grain size and calcium carbonate values for the upper Ringold unit are summarized in Table D3. The caliche horizons indicate a late upper-Ringold, post-Ringold arid climate similar to the present Hanford climate. The lower caliche horizon is very well developed,

forming a duricrust with low porosity (22%) and low saturated permeability (0.4 cm/day) values (Table D1). The major mineral constituents of the upper Ringold unit are quartz and feldspar (microcline and plagioclase). The calcite present is attributed to the caliche development within this unit.

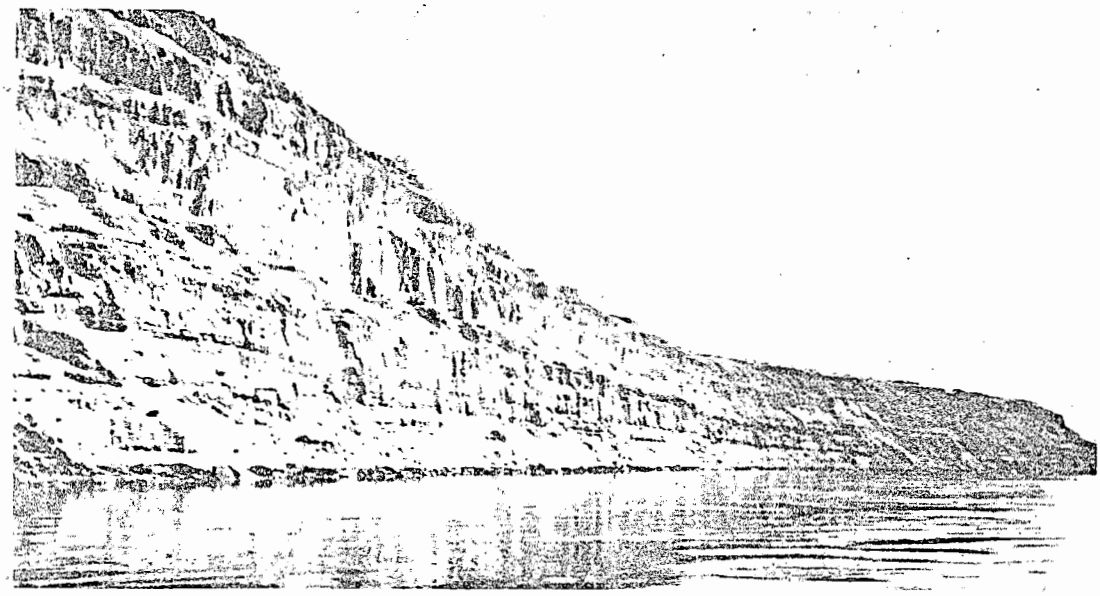

FIGURE D-9. Bedding in Upper Ringold Unit at White Bluffs.

TABLE D3

Upper Ringold Typical Grain Size and Calcium Carbonate Contents (References 8 and 14)

Lithology	% Pebbles & Cobbles	% Sand					% Silt & Clay	% $CaCO_3$
		Very Coarse	Coarse	Medium	Fine	Very Fine		
Calcareous Silty Fine to Very Fine Sand to Sandy Silt	0	0	2	6	8	20	54	12.0
Slightly Silty Fine to Very Fine Sand	0	2	4	15	33	29	16	1.8
Cemented Calcareous Silty Fine to Very Fine Sandy Silt	0	0	3	5	9	19	54	30.0
Silty Fine to Very Fine Sand	0	4	6	13	18	21	38	1.9

9212466130 5

Eolian Silt

After deposition of the upper Ringold, the top of the unit was subjected to subaerial erosion. The surface of the unit was altered by wind which reworked and redeposited the fine grained sands and silts. These wind-deposited sediments, termed Early Palouse soil or eolian silt (References 15 and 16), occur beneath the 241-T tank farm between elevations 177 to 180 meters above mean sea level (Figure D-6).

These sediments are generally compacted, buff colored, and massively bedded with no observable internal laminations or cross stratification. The lack of internal structure suggests the absence of particle traction and migrating dunes. The sediments are typically fine grained, consisting of very fine sands, silts and clays (Table D4). The major mineral constituents are quartz and feldspar (plagioclase and microcline) with approximately 50% of the quartz grains frosted from wind action. The mineral constituents present in corewell DH-6, immediately southeast of the tank farm, and an eolian silt composite sample, collected during drilling tank farm monitoring wells, are described in "Mineralogical Analyses". In addition, mineral constituents for the <50-μm various grain size fractions were determined. The finest fraction (<2 μm), containing montmorillonite, chlorite and mica, have high cation exchange capacities and the ability to sorb radionuclides relative to quartz and feldspar which have low cation exchange capacities (Table D5). Other measured sediment properties of the eolian silt are given in Table D1.

Hanford Formation

The glaciofluvial channel deposits of the Hanford Formation beneath the 241-T tank farm are of the Pasco sands and gravel facies. The three principal units (based on disaggregated grain size morphology) are: (1) pebbly, very coarse-to-medium sand; (2) slightly pebbly, coarse-to-medium sand; and (3) coarse-to-medium sand. These levels represent major surges or meandering of wave current action during one or more of the glaciofluvial floods. The sediments grade downward from poorly sorted, well-rounded cobbles and pebbles with very coarse-to-medium sand filling the interstitial spaces to well-sorted, subangular to subrounded coarse-to-medium sand (Table D6). Sediment color is typically black and tan, "salt-and-pepper".

TABLE D4

Typical Grain Size and Calcium Carbonate Content for 241-T Tank Farm Eolian Silt (References 8 and 14)

Lithology	% Pebbles & Cobbles	% Sand					% Silt & Clay	% $CaCO_3$
		Very Coarse	Coarse	Medium	Fine	Very Fine		
Silty Fine to Very Fine Sand to Sandy Silt	0	0	2	6	8	20	64	3.2

9 2 1 2 4 6 6 1 3 0 6

TABLE D5

Representative Cation-Exchange Capacities (CEC) for Minerals Typical of Hanford Sediments

Mineral	CEC, meq/100 g
Kaolinite	3-10
Mica	20-30
Chlorite	20-30
Montmorillonite	80-150
Feldspars	1-2
Quartz	1-2
Basaltic Fragments	1-3

TABLE D6

Typical Grain Size and Calcium Carbonate Content for Major Hanford Formation Lithologies Beneath 241-T Tank Farm (References 8 and 14)

Lithology	% Pebbles & Cobbles	% Sand					% Silt & Clay	% $CaCO_3$
		Very Coarse	Coarse	Medium	Fine	Very Fine		
Pebbly, Very Coarse-to-Medium Sand	15	28	28	17	6	3	3	1.4
Slightly Pebbly-to-Medium Sand	8	15	25	32	12	5	3	1.5
Coarse-to-Medium Sand	5	10	42	27	8	4	4	2.6

The gravels in the upper and middle units are crudely bedded with thick bedding units and predominantly consist of quartzite, granite and granite porphyry, diorite and diorite porphyry, and basalt with minor constituents of gneiss, schist, and pebble-chert conglomerate. The sands which tend to be well-bedded, are laminated and cross-stratified with thin laminae. These sands, throughout the various Hanford Formation units beneath the tank farm, are predominantly arkosic.

9 2 1 2 4 8 6 1 3 9 7

The finer grain sizes, which account for a relatively small weight percent of the sediments, are the important fraction (as in the eolian silt) in the sorption of radionuclides. These grains contain montimorillonite, mica, and chlorite, which account for the cation exchange capacities of the glaciofluvial sediments given in Table D2. These capacities are relatively low due to the minor amounts of high exchange minerals present in basically all Hanford sediments.

Unsaturated flow of waste liquids and sorption of radionuclides in the vadose zone sediments beneath the 241-T tank farm are partially controlled by the sedimentary structures present. Each of the three principal Hanford Formation units display complex sedimentary structures. Bedding in the Hanford Formation is dominated by thin, nearly horizontal, discontinuous laminations and cross-stratified sedimentary beds. These sedimentary structures impede downward migration and enhance lateral spreading of waste liquids leaked or discharged to the ground under partially saturated conditions as shown in Figure D-10. Additional data on the sedimentary structures typical of the Hanford Formation are presented.

9 2 1 2 4 6 6 1 3 0 8

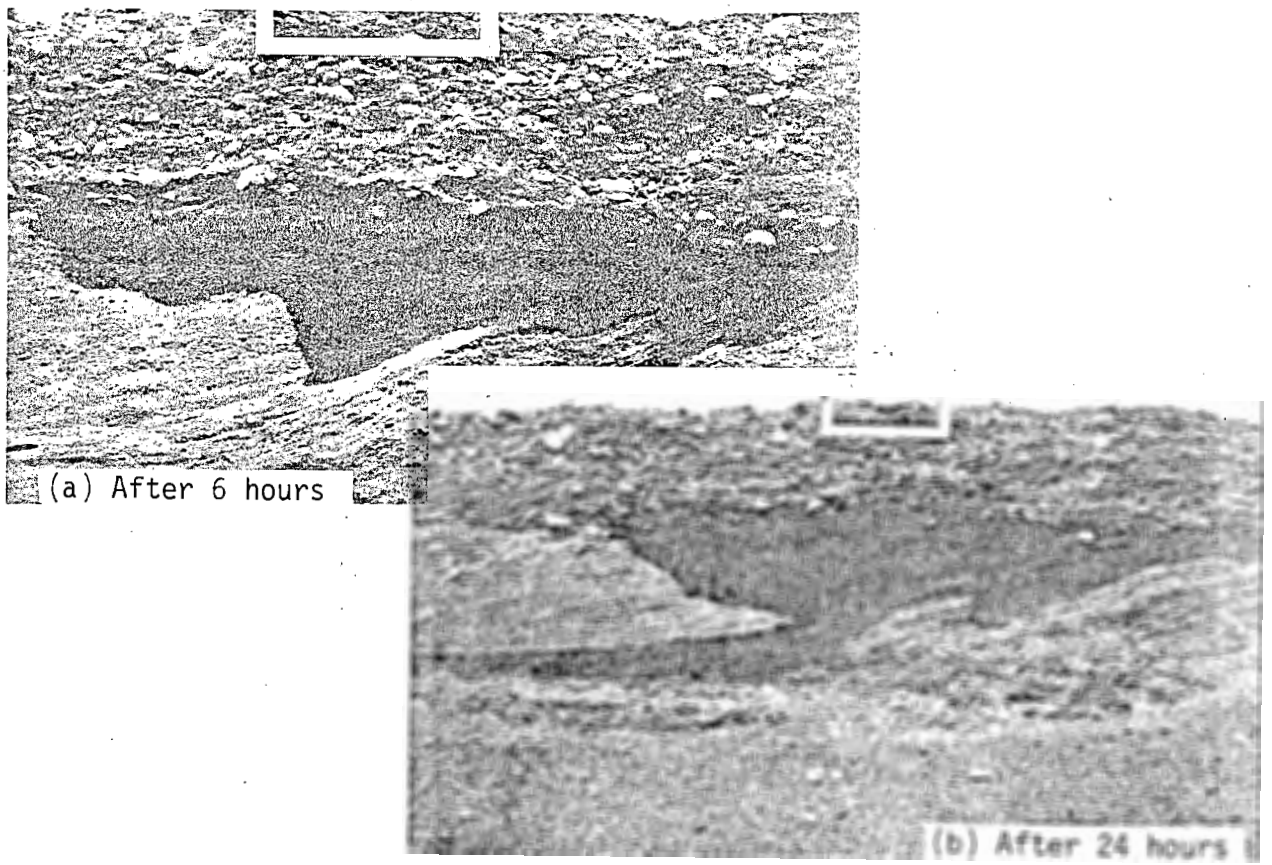

FIGURE D-10. Typical Horizontal and Vertical Movement of Liquids in Hanford Formation Sediments Under Partially Saturated Conditions. Taped area outlines position of water addition.

Backfill

In preparation for tank construction, Hanford Formation material was excavated at 241-T tank farm site (Figure D-11). This material, consisting predominantly of cobbles, pebbles, and coarse-to-medium sands to silt, was subsequently used as backfill from the base of the completed tank (193 meters above mean sea level) to the ground surface (203 meters). An inherent characteristic of the backfill is poor sorting from mixing of numerous stratigraphic layers. Granulometric data and calcium carbonate content for the backfill are given in Table D7. A petrographic examination of the larger-than-medium pebble gravel reveals the backfill is composed of approximately 40% basaltic gravels of the Columbia River Basalt Group types and 60% non-basaltic gravels (Table D8). The sand and silt matrix of the backfill has mineralogy constituents similar to the Hanford Formation sands beneath the backfill. Other measured properties of the backfill sediments are given in Table D2.

9 2 1 2 4 6 6 1 3 0 9

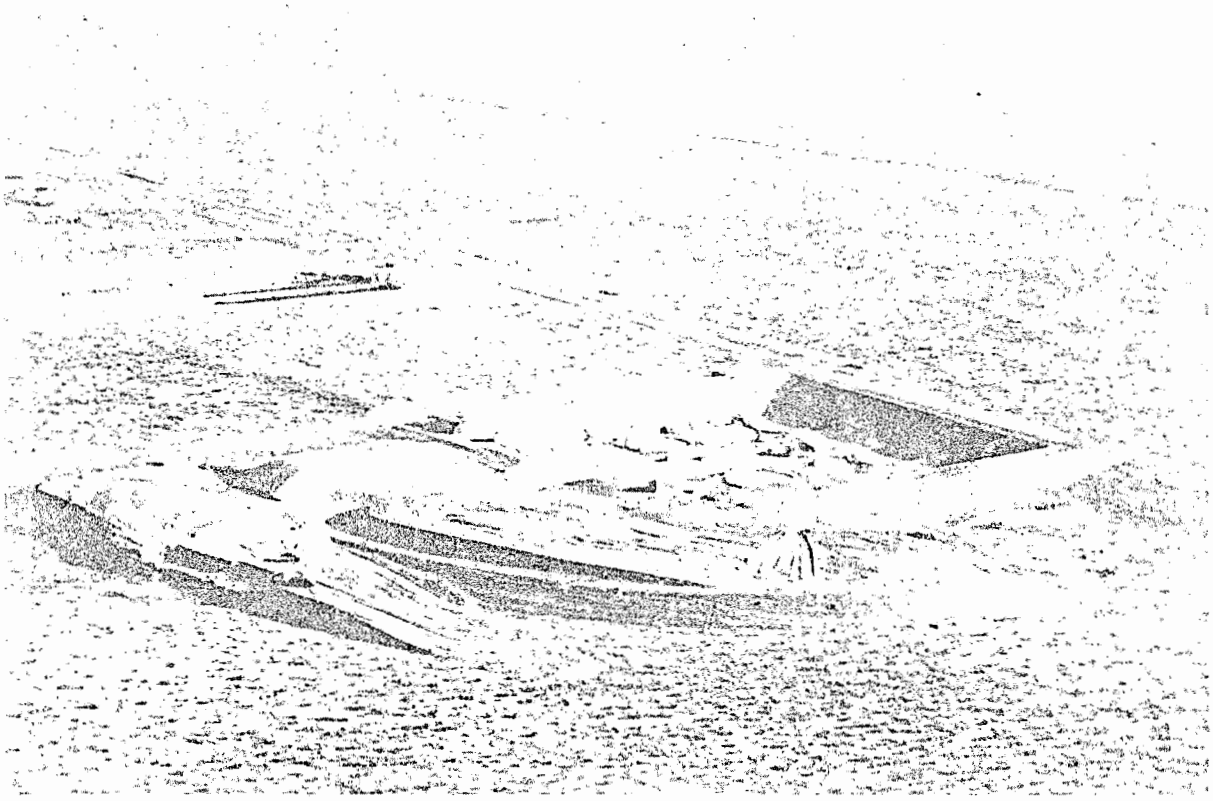

FIGURE D-11. 241-T Tank Farm Excavation.

TABLE D7

Typical Grain Size and Calcium Carbonate Content for the 241-T Tank Farm Backfill (References 8 and 14)

Lithology	% Pebbles & Cobbles	% Sand					& Clay	% $CaCO_3$
		Very Coarse	Coarse	Medium	Fine	Very Fine		
Silty Sandy Gravel	42	7	15	12	8	5	11	1.0

TABLE D8

Hand Specimen Petrography Results for >16-mm Size Fraction from 241-T Tank Farm Backfill

Rock Type	Relative Percentage
Basalt	36
Diorite and Diorite Porphyry	22
Granite and Granite Porphyry	21
Quartzite	14
Gneiss	1
Others	6

9 2 1 2 4 5 6 1 3 1 0

MINERALOGICAL ANALYSIS

Mineralogical analysis of sediments underlying the 241-T tank farm were conducted as part of sediment-tank waste reaction studies to provide more accurate predictive capability than is presently possible on the mobility of radionuclides in the 200 Area sediments and to facilitate the determination of the spacial distribution of the radionuclides beneath waste management facilities. The mineralogical analyses were designed to emphasize study of the finer sediment fractions which contain the higher ion exchange minerals (e.g., smectite, chlorite, and mica). Mineral identification was determined using the X-ray diffractometer and scanning electron microprobe.

X-ray diffraction tracings were used to determine the relative abundance of mineral constituents of the total sample and various size fractions. The x-ray diffraction results of the mineralogy for major sedimentary units found beneath the 241-T tank farm are shown in Tables D9 through D

The mineralogical content of the sand and/or finer sediment fractions also were determined from elemental distributions obtained on the electron microprobe. The electron microprobe results of the mineralogy for major sedimentary units found beneath the 241-T tank farm are shown in Tables D14 and D15. Minerals were identified by referring to their elemental contents as shown in x-ray emission photomicrographs for silicon, aluminum, iron, calcium, magnesium, titanium, potassium, and sodium (Figure D-12).

TABLE D9

Middle Ringold Unit Major Mineral Constituents from Corewell DH-6

Depth, m	Size Fraction	Mineralogy*
89	-200 mesh	Quartz, feldspar, opal, calcite
119	-2 m	Quartz, feldspar, montmorillonite
	2-5 m	Quartz, calcite, feldspar
	5-50 m	Quartz, calcite, feldspar
	As received	Quartz, feldspar
149	-2 m	Montmorillonite
	2-5 m	Montmorillonite, quartz, feldspar, mica
	5-50 m	Montmorillonite, quartz, feldspar, mica
	As received	Quartz, feldspar

*Mineral constituents listed in order of abundance.

TABLE D10

Middle Ringold Unit Major Mineral Constituents from Corewell DH-6 at 130-Meter Depth.

Size Fraction	Mineralogy*
Total sample	Quartz, feldspar
+200 mesh	Quartz, feldspar, mica
2-5 m	Quartz, feldspar, mica
-2 m	Quartz, feldspar, mica, montmorillonite, chlorite

TABLE D11

Upper Ringold Unit Major Mineral Constituents from Corewell DH-6 at 42-Meter Depth.

Size Fraction	Mineralogy*
Total sample	Quartz, feldspar
+200 mesh	Quartz, feldspar
2-5 m	Quartz, feldspar, mica
-2 m	Quartz, mica, montmorillonite

TABLE D12

Mineral Constituents of the 241-T Tank Farm Eolian Silt.

Size Fraction	Mineralogy*
Total sample	Quartz, feldspar, mica
5-50 m	Quartz, feldspar, mica
2-5 m	Quartz, feldspar, mica
-2 m	Quartz, mica, montmorillonite, chlorite

TABLE D13

Hanford Formation Mineral Constituents of Sands from Well 299-W10-148 at 24-Meter Depth.

Size Fraction	Mineralogy*
Total sample	Quartz, feldspar, mica
5-50 m	Quartz, feldspar, mica, chlorite
2-5 m	Quartz, mica, montmorillonite, chlorite, calcite
-2 m	Feldspar, mica, montmorillonite

*Mineral constituents listed in order of abundance.

TABLE D14

Middle Ringold Mineral Composition from Corewell DH-6.

Mineral	Wt %				
	89 m[a]	119 m[a]	149 m[a]	62 m[b]	130 m[c]
Quartz	34.8	47.0	43.5	33.0	51.9
Microcline	26.8	28.8	12.0	23.2	38.0
Plagioclase	19.7	9.2	20.0	20.1	3.0
Amphiboles	4.0	--	10.3	1.8	--
Pyroxenes	--	--	--	--	--
Epidote	--	--	--	7.0	3.3
Sphene	--	--	--	--	--
Apatite	4.4	--	--	--	--
Calcite	--	12.3	3.8	2.2	--
Biotite	--	--	--	--	--
Magnetite	4.9	2.7	7.9	7.8	2.5
Nontronite	--	--	--	--	--
Albite	--	--	--	--	--
Ilmenite	5.5	--	--	1.3	--
Rutile	--	--	2.5	--	1.3
Garnet	--	--	--	3.5	--
Olivine	--	--	--	--	--
Glass	--	--	--	--	--
Zircon	--	--	--	--	--

[a]40- to 200-mesh size fraction is 16.4, 18.3 and 5.4 wt % of the total sample for the 89- , 119- , and 149-meter depths, respectively.

[b]Unconsolidated 40- to 200-mesh size fractions is 9.7 wt % of the total sample.

[c]Sand lense composition.

TABLE D15

Mineral Compositions for Major Sedimentary Units Beneath the 241-T Tank Farm.

Mineral	Wt %			
	42 m[a]	33.5 m[b]	33.5 m[c]	24 m[d]
Quartz	40.5	25.3	27.9	41.0
Microcline	21.8	16.1	17.8	18.3
Plagioclase	10.6	17.8	15.1	18.8
Amphiboles	6.7	10.0	7.9	3.7
Proxenes	--	--	--	5.5
Epidote	3.4	--	--	4.0
Sphene	--	--	0.9	0.4
Apatite	3.4	2.6	0.4	0.3
Calcite	8.0	8.8	8.0	0.7
Biotite	--	1.3	2.9	5.9
Magnetite	4.0	8.2	16.1	1.1
Nontronite	--	--	--	0.4
Albite	--	0	--	--
Ilmenite	1.4	3.5	1.7	--
Rutile	--	3.6	--	--
Garnet	--	1.9	1.3	--
Olivine	--	0	--	--
Glass	--	0	--	--
Zircon	--	1.0	--	--

[a]Upper Ringold 200-mesh particle size fraction from Corewell DH-6.

[b]Composite sample of eolian silt from beneath the 241-T tank farm.

[c]Hanford Formation 10-mesh particle size fraction from Well 299-W10-148.

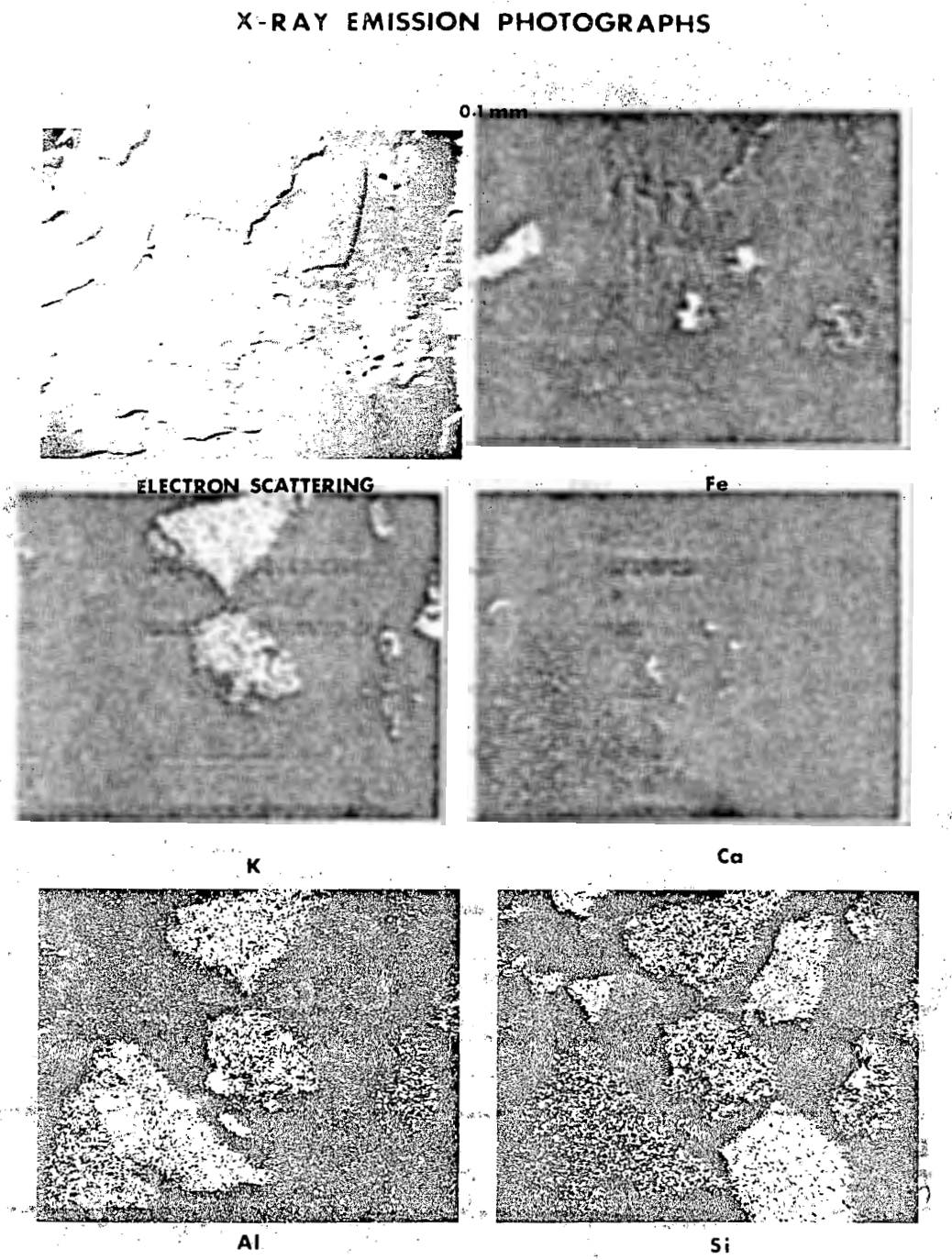

FIGURE D-12. Mineral Assemblages and Hematite Coatings in Middle Ringold Unit at a Depth of 89 to 90 Meter 40-200 Mesh Size Fraction.
(photographs by R. H. Beauchamp, Pacific Northwest Laboratory)

FIGURE D-12. (Continued)

(photographs by R. H. Beauchamp, Pacific Northwest Laboratory)

SEDIMENTARY STRUCTURES OF THE HANFORD FORMATION

Unsaturated flow of waste liquids and filtration of radionuclides in the vadose zone sediments beneath the 241-T tank farm is partially controlled by the sedimentary structures present. Each of the three principal Hanford Formation units displays complex sedimentary structures. Bedding in the Hanford Formation is dominated by thin, nearly horizontal, discontinuous laminations and cross-stratified sedimentary beds. These sedimentary structures impede downward migration and enhance lateral spreading of waste liquids leaked or discharged to the ground under partially saturated conditions.

The glaciofluvial sediments are highly laminated with discontinuous laminae. The laminae generally are composed of nearly horizontal layers parallel to the plane of stratification. There are sharp boundary conditions in the finer grained sediments and gradational boundary conditions in the coarser grained sediments. These boundaries differ in grain size characteristics from the laminae above and below (Figure D-13). Laminations are found throughout the glaciofluvial sediments as they are produced during various wave current action conditions during a glacial floodwater sequence: (1) steady flow conditions and traction on a plane bed; (2) the result of steady decelerating wave current action (Reference 17; (3) periodic stirring of the sediments from meandering of wave current action; and (4) the result of the accumulation of lag deposits from wave current action during the waving stages of the floods.

Another primary sedimentary structure prevalent in the Hanford Formation is cross-stratification in which strata are arranged inclined (up to 34 degrees) to the main planes of stratification. These structures are produced by deposition down the lee slope of ripples, bars, and small deltas. Deposition on the lee slope occurs in response to oversteepening produced by deposition of bed load at the crest of sedimentary structures. Lamination associated with these structures shows a distinct alternation of grain size which occurs from two depositional processes, the avalanching from oversteeping and the deposition of finer grained sediments from suspension between avalanches.

Different types of cross-stratification have been observed in the Hanford Formation; most common are foreset bedding, festoon bedding, and lateral accretion bedding. Foreset bedding generally is a tabular body with inclined cross-stratification along straight lines (Figure D-14). Festoon bedding is marked by inclined cross-stratification curves and concaved downcurrent (Figure D-15). Lateral accretion bedding is low angle, inclined cross-stratification formed on the lee side of meanders during the waning stages of the floods.

Although the Hanford Formation sediments indicate complex internal structures, they also reveal graded bedding and massive bedding (Figures D-16 and D-17). Graded bedding is identified by a gradation in grain size generally normal to the planes of stratification. Bedding of this type is deposited during the waning current action and is a result of terminated deposition of bed load. Massive bedding as observed in the middle Ringold unit displays a lack of internal structure. The lack of traction phases during sedimentary deposition and probable rapid disposition or highly concentrated sediment dispersion is suggested from massive bedding (Reference 9).

Clastic dikes, which are secondary sedimentary structures discordant to the planes of stratification (Figure D-18) have been observed during drilling operations in the 241-T tank farm. Although these structures were not observed during the drilling of leak investigation wells around the 241-T-106 tank, they potentially represent a sedimentary structure which could enhance downward movement of liquid wastes. Clastic dikes vary in width from <1 cm to >1 m. The larger dikes typically are laminated with laminae alternating from very fine sand and silt to a highly variable coarse fraction ranging from fine sand to very fine pebbly sand. Only one indication of downward channeling was evident in the various tank leak investigations. In well 299-W10-111, downward channeling was observed, but is attributed to rapid movement through the Hanford Formation sediments by saturated flow.

Sedimentary structures other than those described above have been observed during the drilling of monitoring wells in the 241-T tank farm, (e.g., cut-and-fill structures), but movement of liquids under unsaturated conditions and sorption of radionuclides would behave similar to the laminated and cross-stratified bedding described herein.

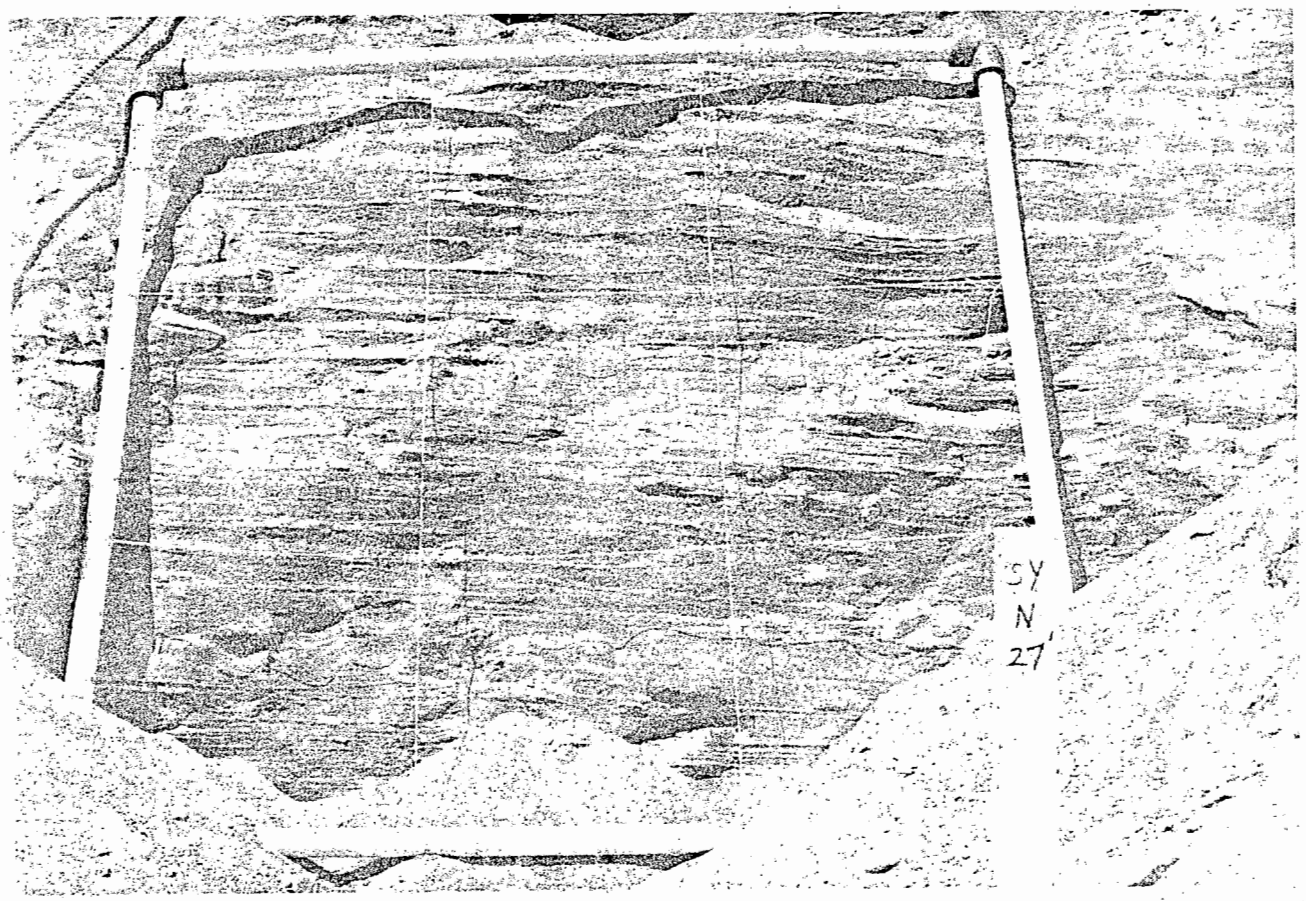

FIGURE D-13. Laminated Bedding in Hanford Formation Sediments.

FIGURE D-14. Foreset Bedding in Hanford Formation Sediments.

FIGURE D-15. Festoon Bedding in Hanford Formation Sediments.

9212461320

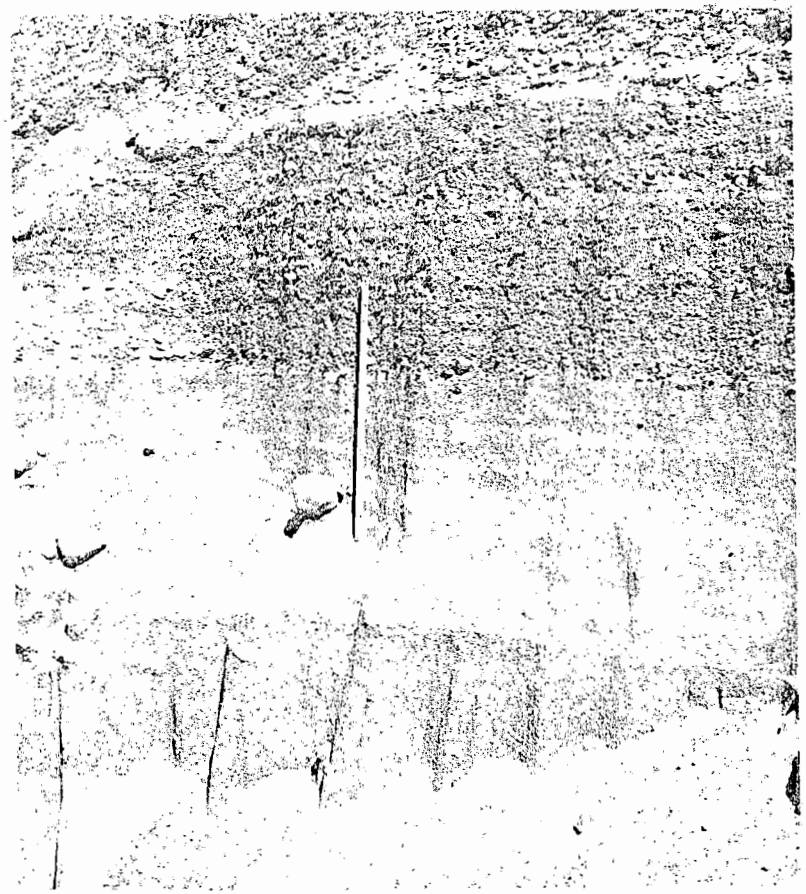

FIGURE D-16. Graded Bedding in Hanford Formation Sediments.

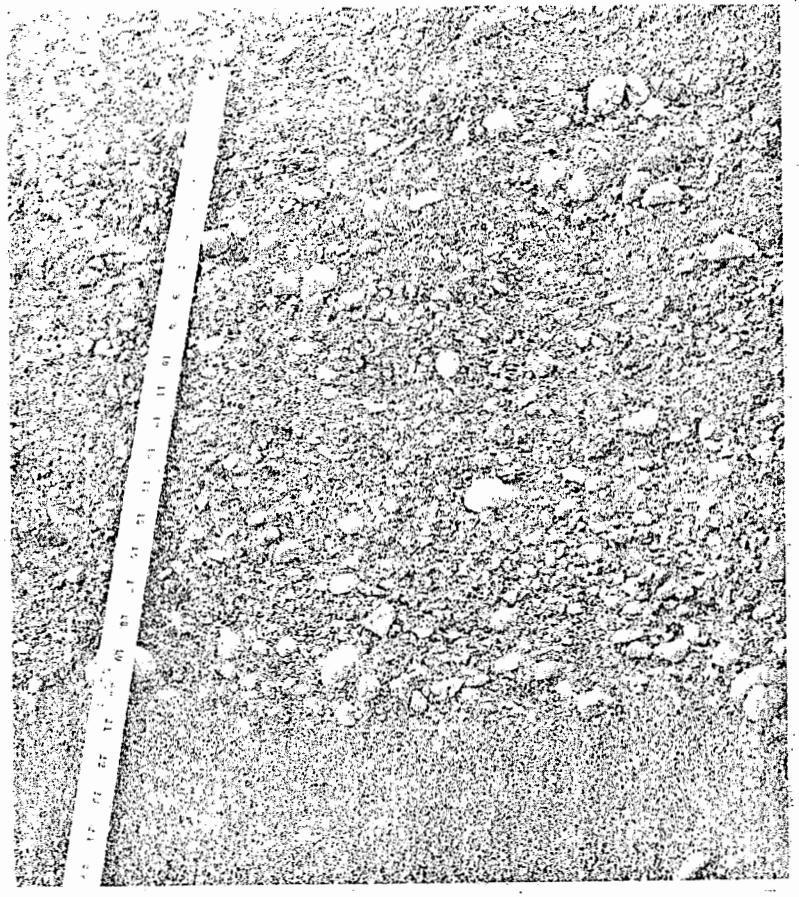

FIGURE D-17. Massive Bedding in Hanford Formation Sediments.

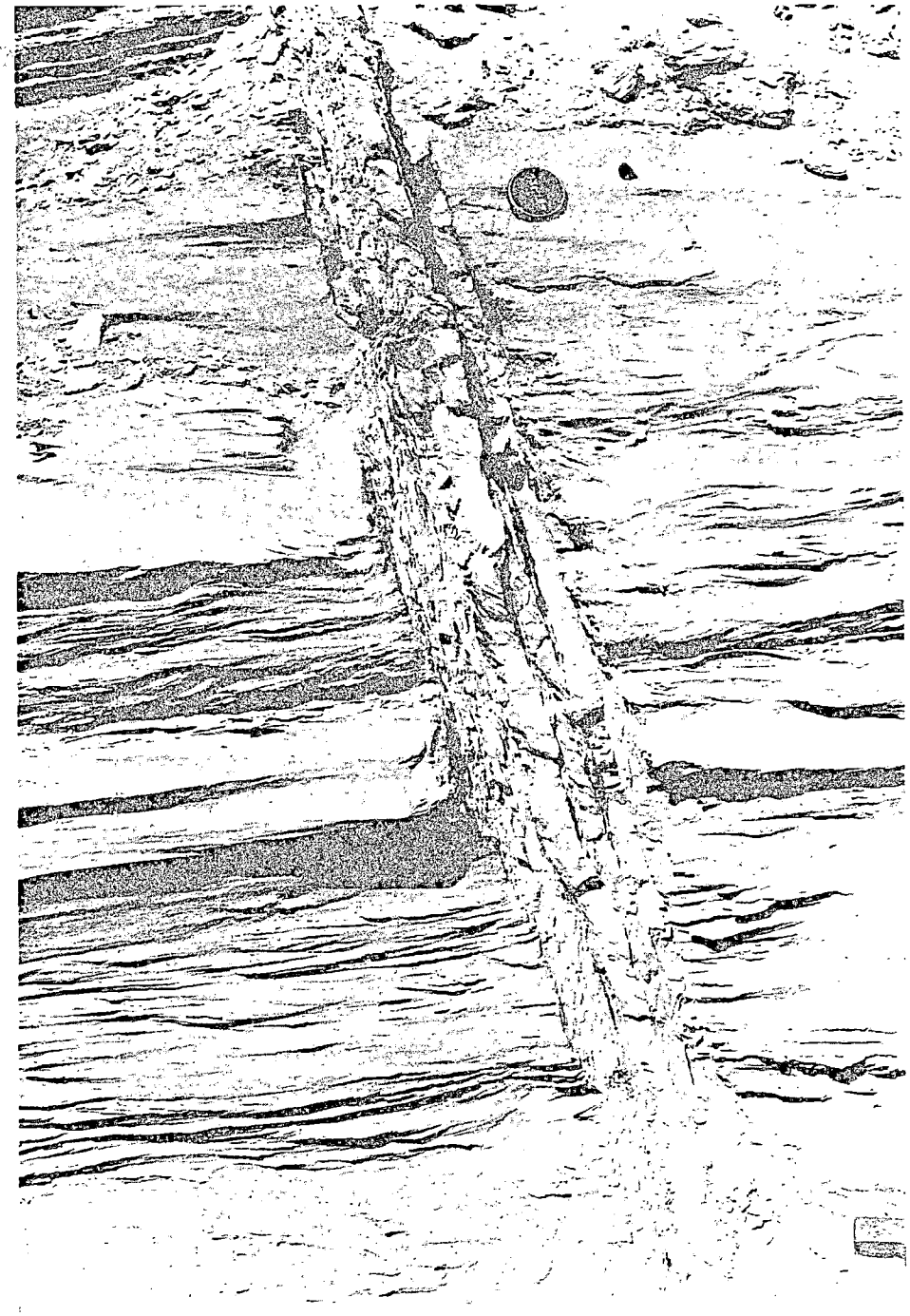

FIGURE D-18. Clastic Dike in Hanford Formation Sediments.

REFERENCES

1. Raymond, J. R., and D. D. Tillson, (1968) "Geophysical Exploration of the Rattlesnake Hills No. 1 Well", BNWL-776, Battelle Northwest, Richland, Washington.

2. Waters, A. C. (1961) "Stratigraphic and Lithologic Variations in the Columbia River Basalt", American Journal of Science 259:583-611.

3. Bentley, R. D. (1977) "Stratigraphy of the Yakima Basalts and Structural Evolution of the Yakima Ridges in the Western Columbia Plateau.

4. Wright, T. L., M. J. Grolier, and D. A. Swanson (1973) "Chemical Variation Related to the Stratigraphy of the Columbia River Basalt", Geological Society of America Bulletin, 84:371-386.

5. ARHCO Research and Engineering Division (1976) "Preliminary Feasibility Study on Storage of Radioactive Wastes in Columbia River Basalts, ARH-ST-137, Atlantic Richfield Hanford Company.

6. Veatch, M. D. (1971) "Anticipated Effect of Discharging 242-S Cooling Water to the Ground", ARH-2214, Atlantic Richfield Hanford Company.

7. Brown, D. J. (1959) "Subsurface Geology of the Hanford Separations Area", HW-61780, General Electric Company.

8. Price, W. H. and K. R. Fecht (1976) "Geology of the 241-T Tank Farm", ARH-LD-135, Atlantic Richfield Hanford Company.

9. Brown, D. J. and R. E. Isaacson (1977) "The Hanford Environment as Related to Radioactive Waste Burial Grounds and Transuranium Waste Storage Facilities", ARH-ST-155, Atlantic Richfield Hanford Company.

10. Newcomb, R. C., J. R. Strand and F. J. Frank (1972) "Geology and Groundwater Characteristics of the Hanford Reservation of the U. S. Atomic Energy Commission, Washington", U. S. Geological Survey Professional Paper 717.

11. Baker, R. V. (1973) "Paleohydrology and Sedimentology of the Lake Missoula Flooding in Eastern Washington", Geological Society of America Special Paper 144.

12. Folk, R. L. (1968) "Petrology of Sedimentary Rocks", University of Texas Press.

13. Wentworth, C. K. (1922) "A Scale of Grade and Class Terms for Clastic Sediments", Journal of Geology, 30:377-392.

14. Fecht, K. R. and W. H. Price (1977) "Granulometric Data 241-T Tank Farm Monitoring Well Sediments", RHO-LD-19, Rockwell Hanford Operations, Richland, Washington.

15. Brown, D. J. and R. E. Brown (1958) "Subsurface Eolian Deposit at the Hanford Projection Washington" Abstract, Geological Society of America Bulletin, 69:1976-1977.

16. Brown, D. J. (1960) "An Eolian Deposit Beneath 200 West Area", HW-67549, General Electric Company.

17. Kuenen, P. H. (1966) "Experimental Turbidite Lamination in a Circular Flume", Journal of Geology, 74:523-545.

9 2 1 2 4 6 6 1 3 2 4

APPENDIX E

REGIONAL GROUND-WATER LEVELS AND TRAVEL TIMES TO THE COLUMBIA RIVER

Regional ground-water contours for the Hanford Site are given in Figure E-1. For the sake of comparison, the elevations of the ground surface above and of the bottom of the 241-T-106 tank are 205 meters and 193 meters, respectively (Reference 1).

A computer program has been developed for predicting the minimum ground-water flow times to the boundary of the Hanford Site. The Hanford Pathline Calculational Procedure (HPCP) is a numerical model developed to predict the movement of fluid "particles" from one location to another within the Hanford ground-water system (Reference 2).

The procedure was designed to calculate pathline starting coordinates in a uniform manner by spacing the coordinates in a flow field so that equal flow exists between any two adjacent pathlines. To accomplish this, it is necessary to: (1) calculate the signed flows in the x and y direction and build a binary data file for each, (2) use these data files to calculate the starting coordinates, and (3) plot the resulting coordinates and the associated circular arc.

This computational routine can be considered a simplified transport model which primarily considers advective changes. The HPCP uses a prediction of the transient ground-water potential field as an input from the variable thickness transient (VTT) flow model (Reference 3). Application of the HPCP model to test cases with semi-analytical results available for comparison have given good results (Reference 2).

Application of the HPCP to predict ground-water travel times from the 200 West Area of the Hanford Site to the Columbia River requires streamlines as well as pathlines be calculated due to long travel times. For a given two-dimensional representation of a ground-water surface, the ground-water velocity vector is perpendicular to the water level contour lines and points in the direction of decreasing water table elevation. Therefore, for any instantaneous ground-water water table elevation distribution, flow directions are drawn in the direction of ground-water movement at a given point in time; a line which is everywhere tangent to velocity vectors in an instantaneous streamline. Such a streamline is only the path of a water particle as long as the water table elevations do not change with time or are at "steady-state".

In the 200 West Area, application pathlines were calculated for the initial 20 years of calculation and streamlines for the remainder of the flow time (Reference 2). The resulting combined units are labeled path-streamlines. Plots of path-streamlines for ground-water travel times from the 200 West Area to the Columbia River are shown in Figure E-2 and travel times are given in Table E1. The average velocity and travel times of the path-streamlines are approximately 61 cm/day and 120 years, respectively.

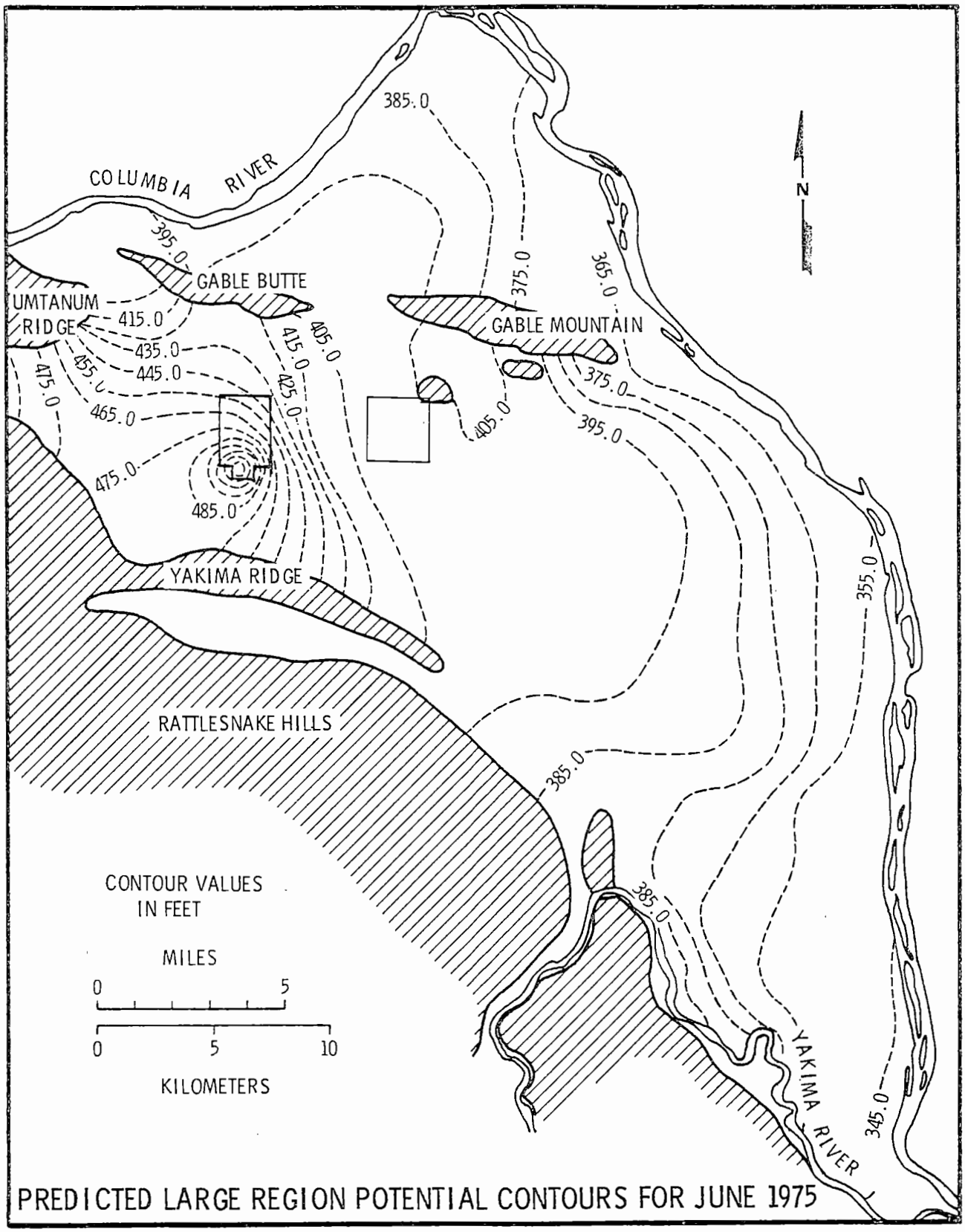

FIGURE E-1. Plot of Potential Contours (Ground Water Surface Contours) for June 1975.

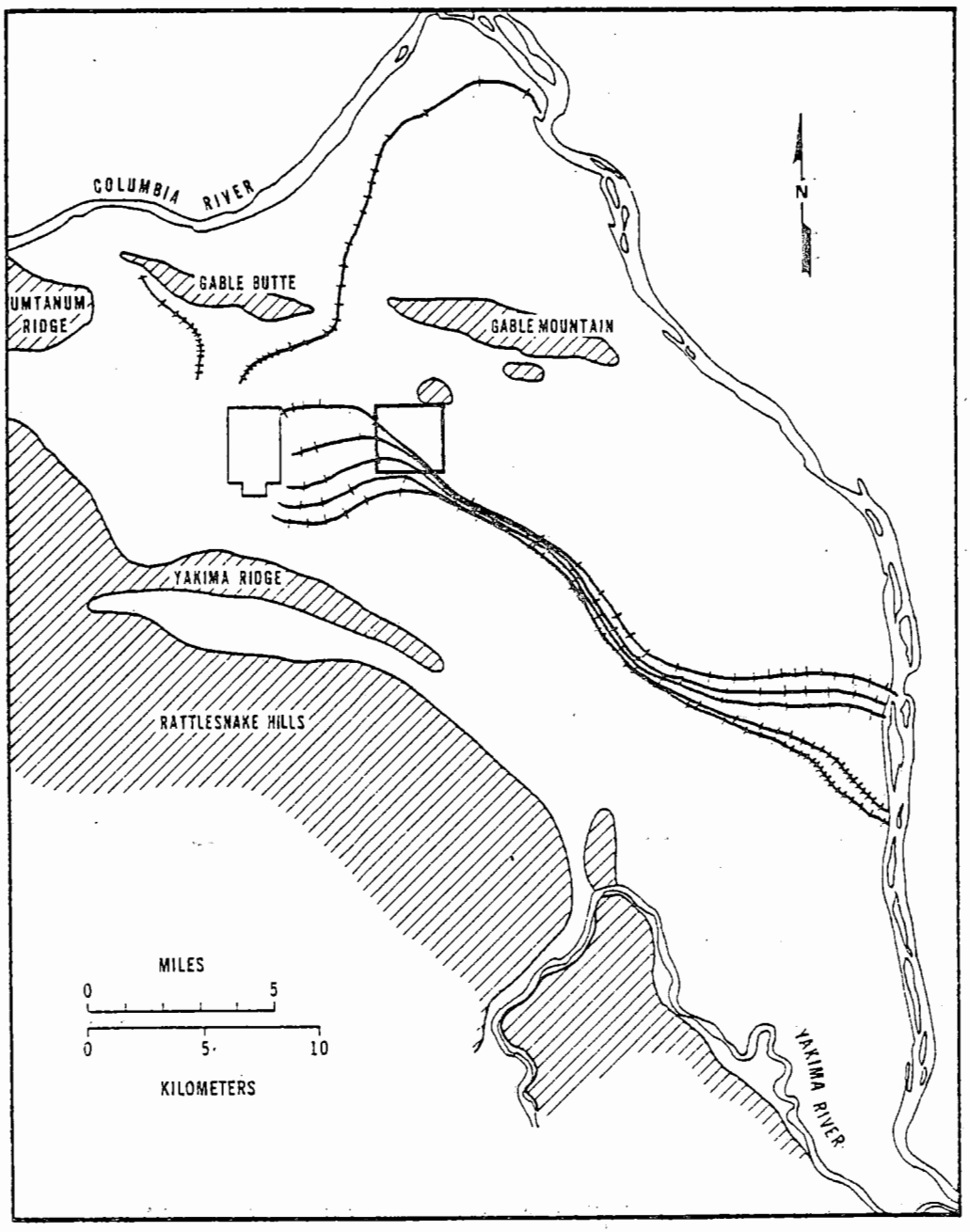

FIGURE E-2. Predicted Path Streamlines for 200 West Area.

TABLE E1

Travel Time-Distance Summary
for Path Streamlines

Path Streamline	Total Distance, m	Total Time, days
1	32,200	58,790
2	31,800	52,400
3	30,000	30,530
4	30,100	31,880
5	31,300	47,090
6	21,400	50,590
7	4,300	27,460

Average Distance = 26,000 m
Average Time = 42,700 days

To produce the binary data files, the desired potential matrix is generated using the source term in the selected region and calculations are performed to produce the signed flows in the x and y direction at each VTT node which does not have an 01 calculational type (Reference 4). A y direction flow from low to high y node numbers has a positive sign as does an x direction flow from low to high x node numbers. The transmissivity, gradients, and flow channel widths are the same as used by the VTT calculational codes. Figure E-3 illustrates the method used to calculate the signed x flow (Fx) and signed y flow (Fy) at a VTT node.

The pathline starting locations are calculated by beginning at the specified location on the circumference of the circle which has its center at (Xc, YX) and a radius, R. The starting location on the circle is specified in the local Cartesian coordinate system with the (0c0) at (Xc, Yc). A delta angle increment is also specified. The initial starting point is taken as the first pathline starting point, a delta angle increment of arc is added, and the flow through that portion of arc is calculated and added to a running sum. Delta arc increments and their flow contributions are added until the running sum has equaled or just surpassed the desired flow spacing between pathlines specified in the input file. The current location on the circumference is then taken as the next starting point; the running sum is set to zero; and the process is repeated until all the desired pathline starting points have been defined.

Figure E-4 shows the mathematics used to calculate the flow through any delta arc segment. Delta arc steps are taken whenever possible unless the delta step crosses the boundary between nodes. The delta step is then cut back so that the entire arc length lines within one set of four nodes as shown in Figure E-4.

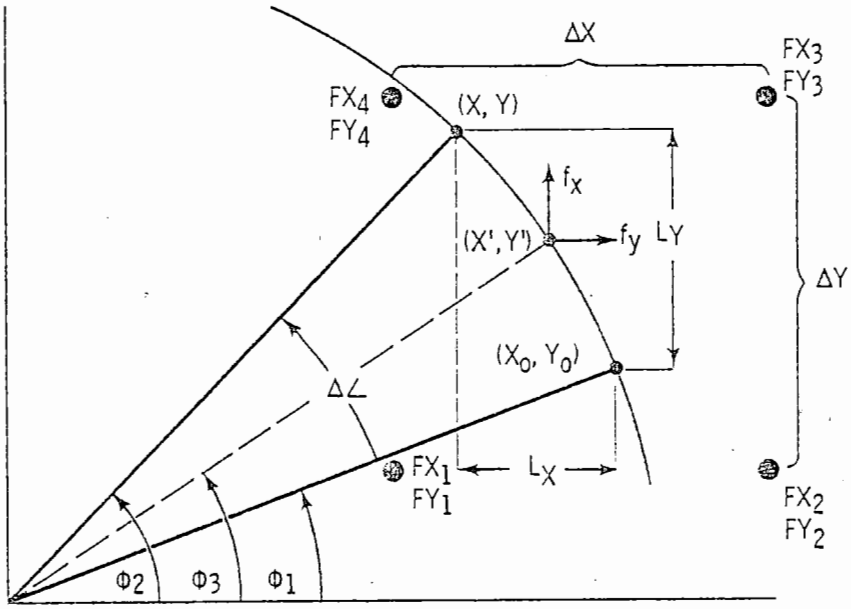

$$T_i = (h_i - h_i^0)\, K_i \quad (i = 1,5)$$

where:

- T = transmissivity
- h = hydraulic potential
- h^0 = aquifer bottom elevation
- K = vertically averaged hydraulic conductivity
- i = node number

$$F_1 = \left[\left(\frac{T_1 + T_2}{2}\right)\left(\frac{h_1 - h_2}{\Delta x}\right)\right] A_1 \Delta_y$$

$$F_2 = \left[\left(\frac{T_1 + T_3}{2}\right)\left(\frac{h_3 - h_1}{\Delta y}\right)\right] A_2 \Delta x$$

$$F_3 = \left[\left(\frac{T_1 + T_4}{2}\right)\left(\frac{h_4 - h_1}{\Delta x}\right)\right] A_3 \Delta y$$

$$F_4 = \left[\left(\frac{T_1 + T_5}{2}\right)\left(\frac{h_1 - h_5}{\Delta y}\right)\right] A_4 \Delta x$$

$$Fx = \frac{F_1 + F_3}{2}, \quad Fy = \frac{F_2 + F_4}{2}$$

where:

- F_i = signed flow
- A_i = function of calculational type of node (= fraction of total width available for flow)
- i = flow channel (1→4)
- Δx = grid spacing in y direction
- Δy = grid spacing in x direction
- Fx = total signed flow in x direction
- Fy = total signed flow in y direction

FIGURE E-3. Method Used to Calculate Signed Flow at a Node.

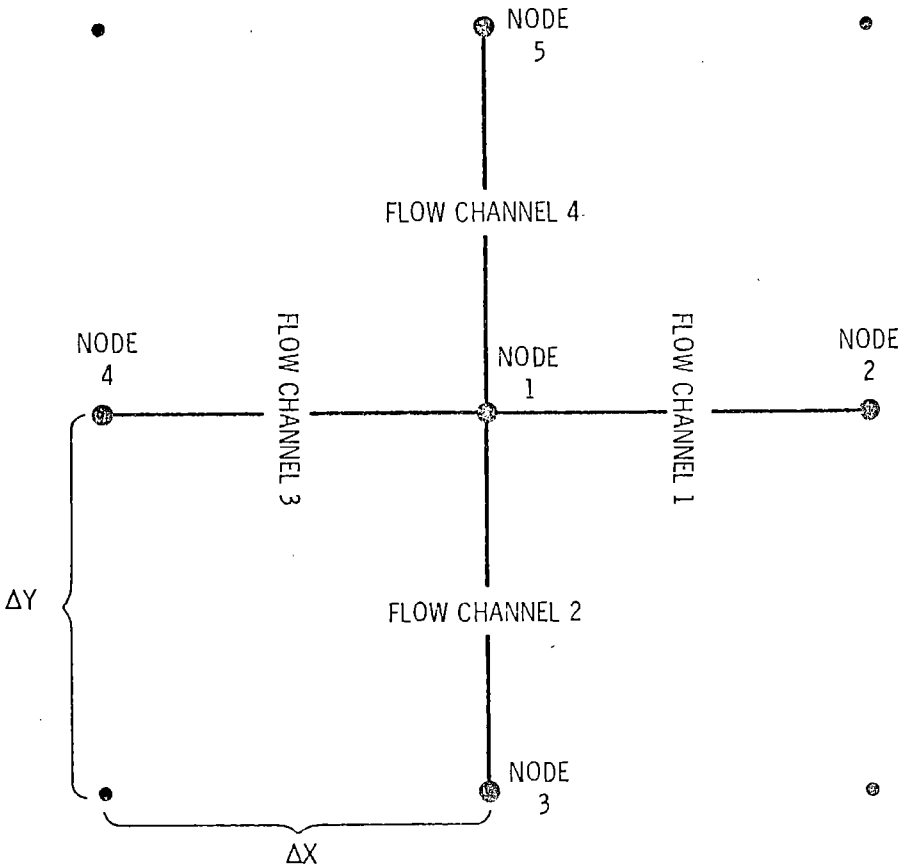

where:

L_x = width of y flow channel = abs(x_p-x_1)

L_y = width of x flow channel = abs(y_p-y_1)

FRC_x = fraction of interpolated x flow for point (x', y') passing through the arc = $\frac{L_x}{\Delta y}$

FRC_y = same as FRC_x but for y flow = $\frac{L_y}{\Delta y}$

FY' = bilinear interpolated Y flow at (x', y') from FY_1→FY_4 values

FX' = bilinear interpolated X flow at (x',y') from FX_1→FX_4 values

then:

fx = FY' * FRC_y * SIGNY (quadrant)

fy = FX' * FRC_x * SIGNX (quadrant)

where:

SIGNX (quadrant) = +1 (quadrant 1 and 4)
-1 (quadrant 2 and 3)

SIGNY (quadrant) = +1 (quadrant 1 and 2)
-1 (quadrant 3 and 4)

TOTAL ARC FLOW = fy + fx

FIGURE E-4. Diagram Illustrating How the Flow from a Δ Arc is Calculated From the Arc Parameters and the X and Y Flow Files.

Once the x and y flow files have been calculated, these data are used to calculate the pathline starting coordinates along the circumference of an arc with specified center and radius and a specified flow increment in cubic meters per day between locations. Three cases were used in this study. The first case used a VTT-generated surface with one source and one sink with three test circles; the second case used a VTT-generated Hanford potential surface to determine if the procedure could reproduce the calculated flow at 200 East and 200 West Areas; and the final case used the same VTT-generated Hanford potential surface to produce the starting locations of the pathlines used in the Hanford Study.

The potential plot in Figure E-5 illustrates the steady-state potential contours and calculational types for the first test problem used to analyze this procedure. This test problem is for a 305-m, 35 x 35 grid system with a uniform K of 1,500 m/day, held node potentials at 30.5 m and bottom elevation at 305 m. There is one source and one sink. The source is at line 17, column 20 at 91,000 m^3/day. This test problem was set up and run to steady-state with the VTT calculational code, and the x and y flow data files were created. Three circles were then used to demonstrate the procedure. The first test circle was centered at the sink location with a radius of 914 m so the source would not be included. The total flow calculated was 91,000 m^3/day (only 0.4% in error). The second test circle was centered at the source location with 915 m radius and the calculated flow was 91,000 m^3/day (only 0.6% in error). The third test circle was centered between the source and the sink with a radius of 1,800 m, so 178 m^3/day (again, less than 1% error when compared to the magnitude of the source and sink values).

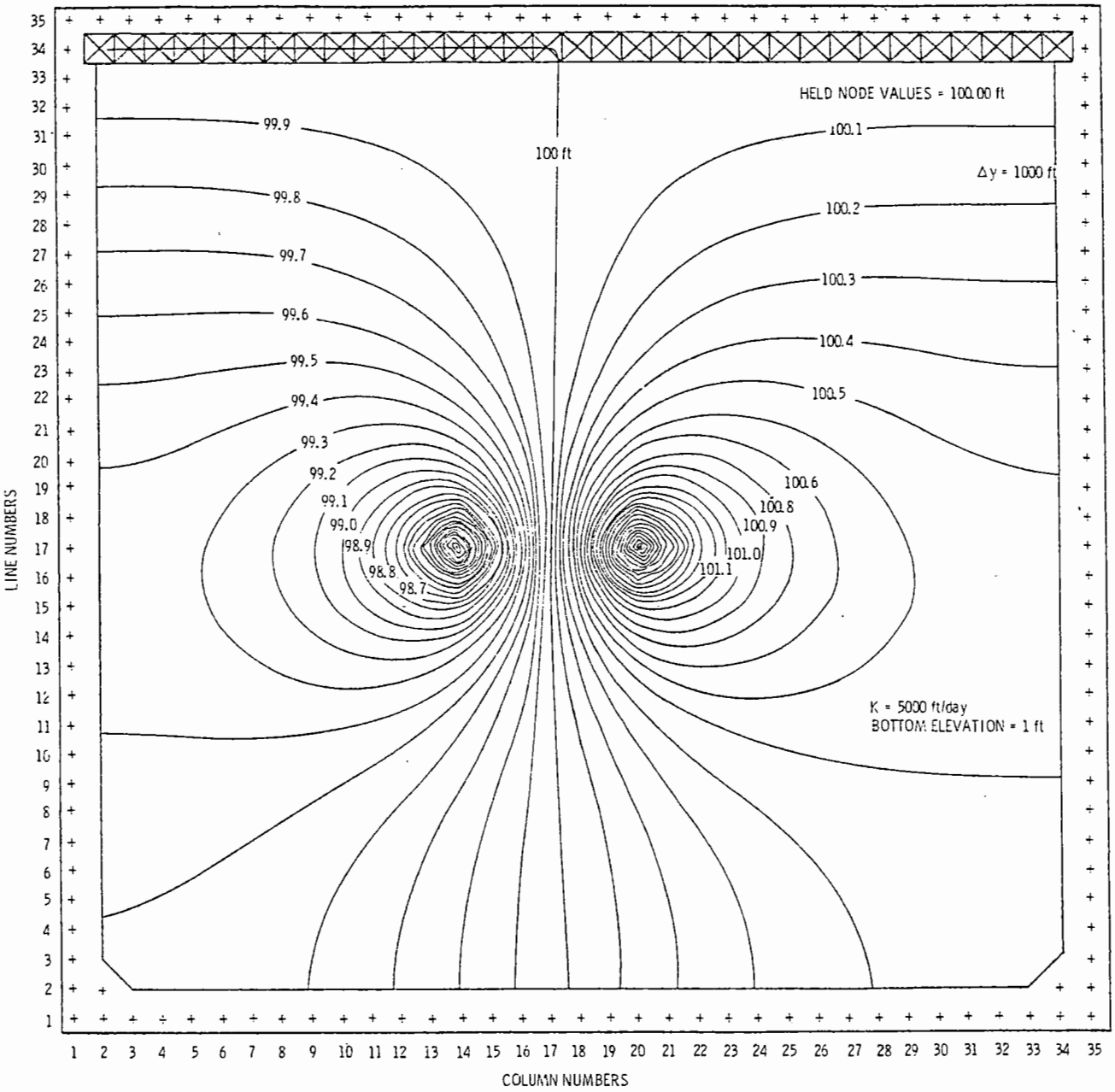

FIGURE E-5. Steady-State Potential Contours and Calculational Types for Test Surface Used to Check Equal Flow Procedure.

REFERENCES

1. AEC-RL Staff, (1973), "Report on the Investigation of the 106-T Tank Leak at the Hanford Reservation, Richland, Washington", TID 26431.

2. Friedricks, D. R., C. R. Cole, R. C. Arnett, R. W. Nelson, (1977), "Hanford Pathline Calculation Program: Theory, Error Analysis and Applications". ARH-ST-149.

3. W. V. DeMier, A. E. Reisenauer, and K. L. Kipp, (1974), "Variable Thickness Transient Groundwater Flow Model User's Manual", BNWL-1704, Battelle, Pacific Northwest Laboratories, Richland, Washington.

9 2 1 2 4 6 6 1 3 3 3

THIS PAGE INTENTIONALLY
LEFT BLANK

0 2 1 2 4 6 6 1 3 3 4

APPENDIX F

GROUND-WATER MEASUREMENTS

GROUND-WATER MONITORING

The ground-water monitoring network in the northern portion of the 200 West Area and immediately surrounding the 241-T tank farm is shown in Figure F-1. As noted, the monitoring wells are used for both water level measurements and ground-water sampling.

Ground-water measurements are taken twice per year as part of the on-site environmental monitoring effort. This information is issued yearly as a set of water table maps and is entered in the Hanford hydrologic data base.* Figure F-2 shows the ground-water level beneath the 241-T tank farm.

Table F1 lists the present ground sampling schedule for the wells shown in Figure F-1. Most monitoring wells are sampled quarterly with the remainder sampled either semi-annually or once every 2 months. Special analyses or sampling schedules are done on request by the Quality Assurance and Safety Division of the Rockwell Hanford Operations. Four monitoring wells immediately surround the 241-T tank farm: 299-W10-1, 299-W10-4, 299-W10-9, and 299-W11-24. Table F2 is a brief of the analytical results dating back to 1970 for the first two wells. Monitoring wells 299-W10-9 and 299-W11-24 were added to the routine monitoring schedule in 1976 and their monthly analytical results are listed in Table F3. The established drinking water standards for each analysis type are listed at the bottom of each table (Reference 1).

GROUND-WATER MIGRATION NEAR THE 241-T TANK FARM

As part of the 241-T-106 tank leak assessment study, knowledge of the unconfined ground-water velocity and direction in the vicinity of the 241-T tank farm is essential to the early detection of potentially released waste entering the ground water. The general ground-water flow pattern within the tank farm area was determined qualitatively through the examination of the Hanford Site water table contour map. The quantitative determination of ground-water velocity and movement; however, requires a tracer study.

Based on the water table contour map, a tracer test site was located immediately north of the 241-T tank farm parallel to the direction of ground-water flow. Four test wells were drilled at locations in Figures F-2 and F-3.

---

*Water Table Measurement Maps, Staff, Research and Engineering Division, "H-2-38396, Rev. 2, H-2-38397, Rev. 2, H-2-38877, Rev. 2, H-2-38398, Rev. 2, and H-2-38399, Rev. 2", Richland, Washington 99352.

On October 5, 1977, one liter of sodium fluorescein dye solution with a concentration of 240 g/ℓ was released into the water table in test well 299-W10-9. Water samples were bailed periodically from the other three test wells, which had been located in the down gradient flow direction. Samples were collected daily for a period of about 5 weeks. Flourescein was first detected in test well 299-W10-10 on 24 October 1977 and the concentration progressively decreased during the remainder of the monitoring period. Test wells 299-W10-11 and 299-W10-12 did not contain detectable concentrations during the entire test. Although the tracer test procedure was simple, it provided valuable information on the general movement of unconfined ground water near the 241-T tank farm. The ground-water velocity as determined from the test was 0.41 m/day. This value is a reasonable estimate of the velocity. However, because of dispersion effects, this velocity determination should not be considered an exact measurement. More importantly, the test results suggest that any contaminants which may enter the ground-water flow system in the 241-T tank farm would be detected in water samples collected from wells in the area.

9212456613336

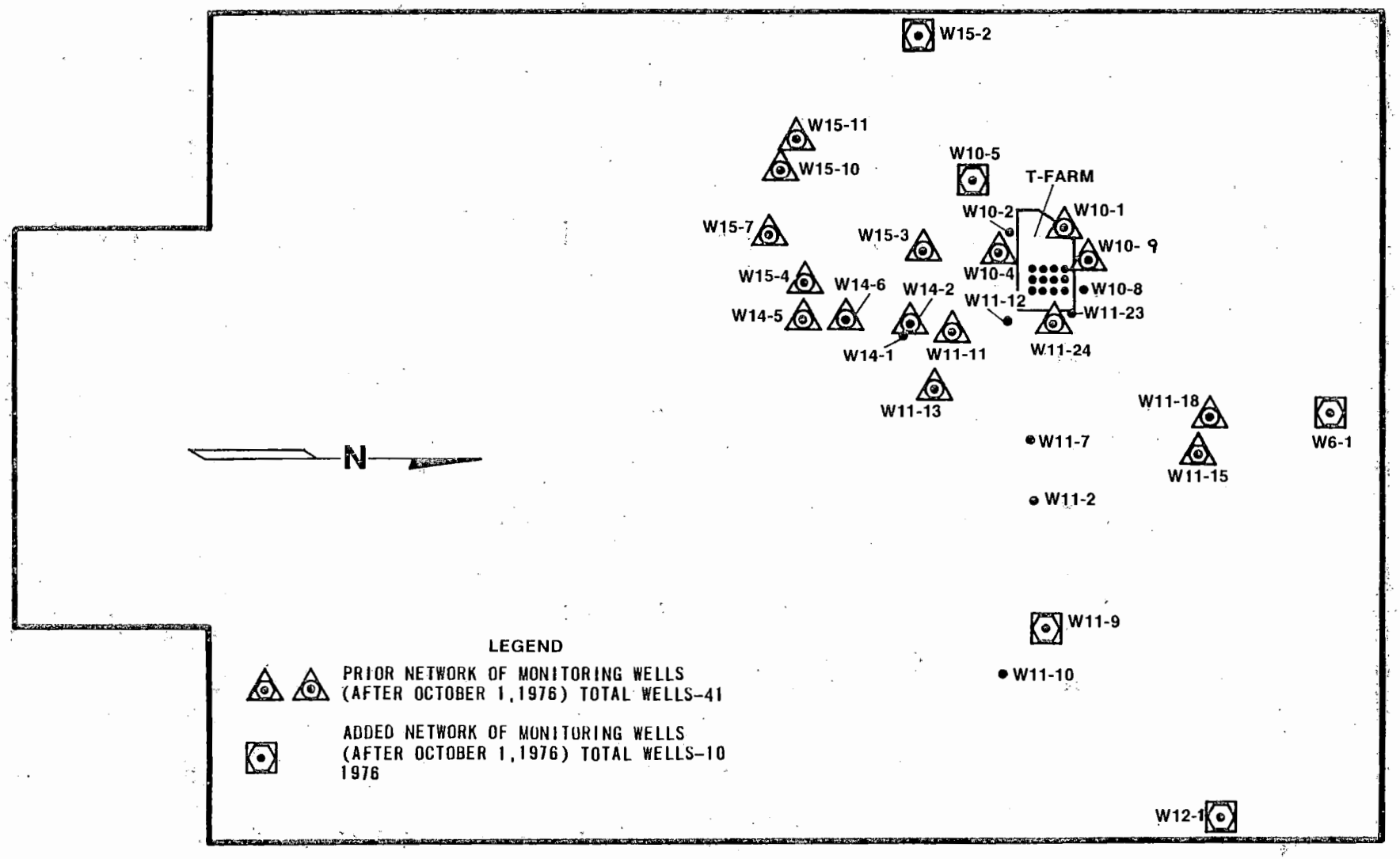

FIGURE F-1. Ground-Water Monitoring Network in 200 West Area of the Hanford Site.

TABLE F1

Ground-Water Monitoring Schedule in the 200 West Area

Well	Site Monitored	Frequency and Analysis					
		Total Alpha	Total Beta	^{60}Co	^{137}Cs	Tritium	Nitrate
299-W6-1	Background data		Q			Q	Q
299-W10-1	216-T-5		Q				
299-W10-4	216-T-36		Q	Q			
299-W10-5	Background data		Q			Q	Q
299-W10-9	241-T tank farm		Q		Q		
299-W11-9	Background data		Q			Q	Q
299-W11-11	216-T-18	Q	Q	Q			
299-W11-13	Background data		S			S	S
299-W11-15	216-T-34		Q				
299-W11-18	216-T-35		Q				
299-W11-24	241-T tank farm		Q				
299-W12-1	Background data		Q			Q	Q
299-W14-2	216-T-26,27,28		Q				Q
299-W14-5	241-TX tank farm		Q			Q	
299-W14-6	241-TX tank farm		Q			Q	
299-W15-2	Background data		Q			Q	Q
299-W15-3	241-TY tank farm		Q	Q	Q		
299-W15-4	216-T-19		Q			Q	Q
299-W15-7	216-Z-7		Q	Q			
299-W15-10		B	B				
299-W15-11	216-Z-16	B	B				

S = Semi-annually Q = Quarterly B = Every 2 months

9 2 1 2 4 6 6 1 3 3 8

TABLE F2

Ground-Water Sampling Results at Wells 299-W10-1 and 299-W10-4

Date	Total Alpha	Total Beta	^{60}Co, pCi/ℓ	$^{89\ 90}Sr$, pCi/ℓ	^{137}Cs, pCi/ℓ	Nitrate, mg/ℓ	^{106}Ru, pCi/ℓ
Well 299-W10-1							
03/11/70		<150					
03/24/71		<160					
03/09/72		<150					
03/19/73		<150					
1/12/73		<75	<21	<28	<30		
03/13/74		<80					
03/10/75		<75					
03/08/76		<80					
1/20/77		<75					
4/12/77		<75					
7/12/77		<75					
10/19/77		<75					
1/25/78		<75					
4/04/78		<75					
6/26/78		<75					
Well 299-W10-4							
3/11/70	<17	160	<18	<27	<300	450	
3/24/71	<17	<160	38±22	<25	<15	470	
3/13/72	-	1000	61±15	<25	120±15		400±72
3/19/73	-	180	80±30	<26	<10		
3/13/74	<85	87±31	<24	<22			
3/10/75	90	120±34	<3	<23			220±150
3/08/76	87	63±22	43±14	<10			
1/20/77		<140	<70±8	<3	<14		
4/12/77		<75	80				
7/12/77		93	52±10		<12		
10/19/77		130	76±8		15±11		
1/25/78		120	69		<15		
4/04/78		95					
6/26/78		110	81				
Drinking Water Standard							
	30	10,000	$3x10^4$	$2x10^4$	45		$1x10^4$

TABLE F3

Ground-Water Sampling Results

Date	Total Beta, pCi/ℓ	Date	Total Beta, pCi/ℓ
Well 299-W10-9		Well 299-W11-24	
1/13/76	<75	1/13/76	95
2/09/76	96	2/09/76	<75
3/08/76	85	3/08/76	-
4/12/76	110	4/12/76	<80
5/11/76	<75	5/11/76	96
6/10/76	110	6/10/76	88
7/15/76	89	7/15/76	120
8/17/76	97	9/13/76	110
9/13/76	130	11/09/76	89
10/11/76	120	12/14/76	<75
11/09/76	130	1/20/77	120
12/14/76	120	2/15/77	110
1/02/77	<75	4/12/77	75
1/20/77	75	7/12/77	75
2/15/77	78	10/19/77	110
4/12/77	75	1/25/78	130
7/12/77	89	4/04/78	75
10/09/77	120	6/26/78	110
1/25/77	130		
4/04/77	75		
6/26/78	75		

9 2 1 2 4 3 6 1 3 4 0

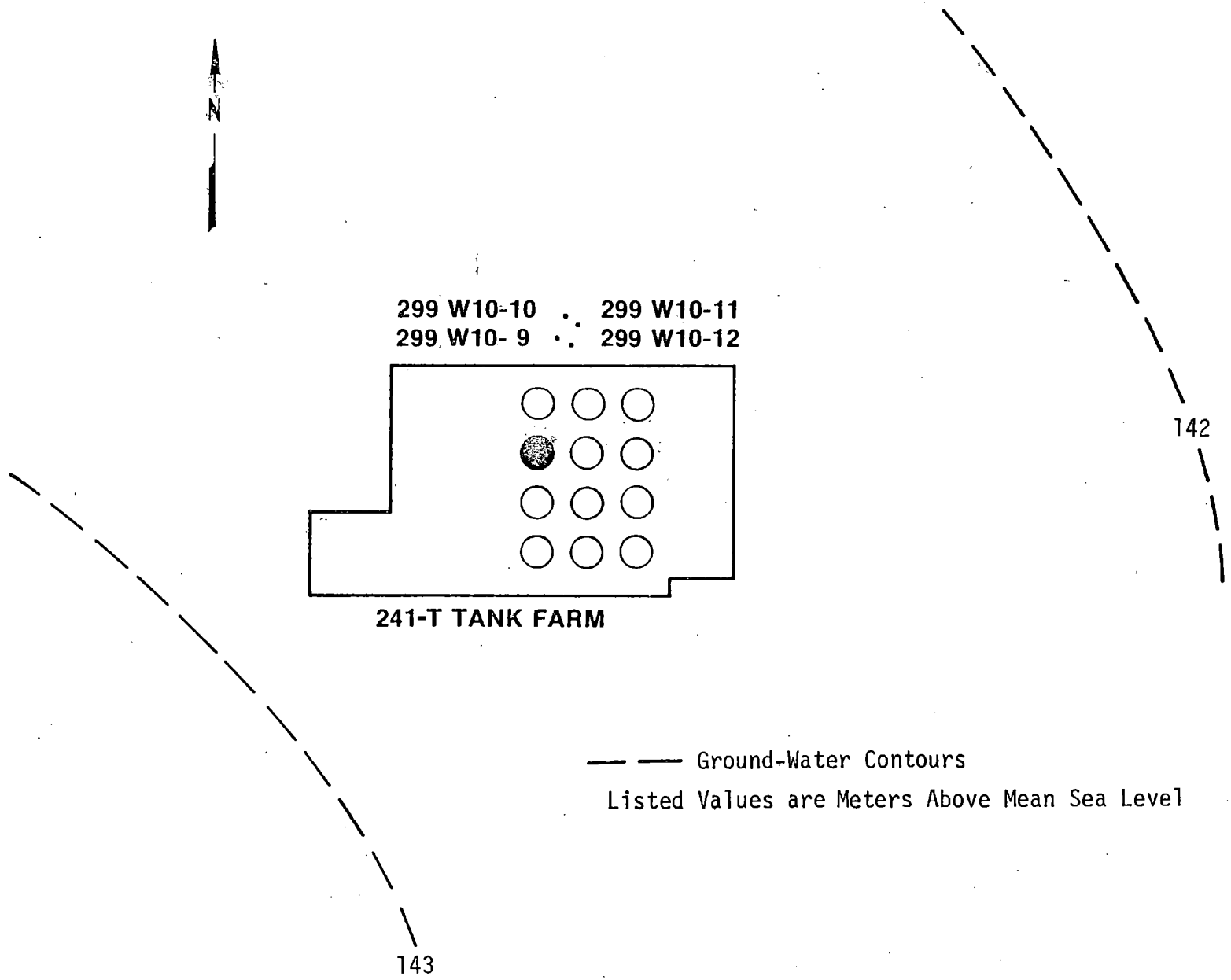

FIGURE F-2. Location of Four Water Wells Near the 241-T Tank Farm.

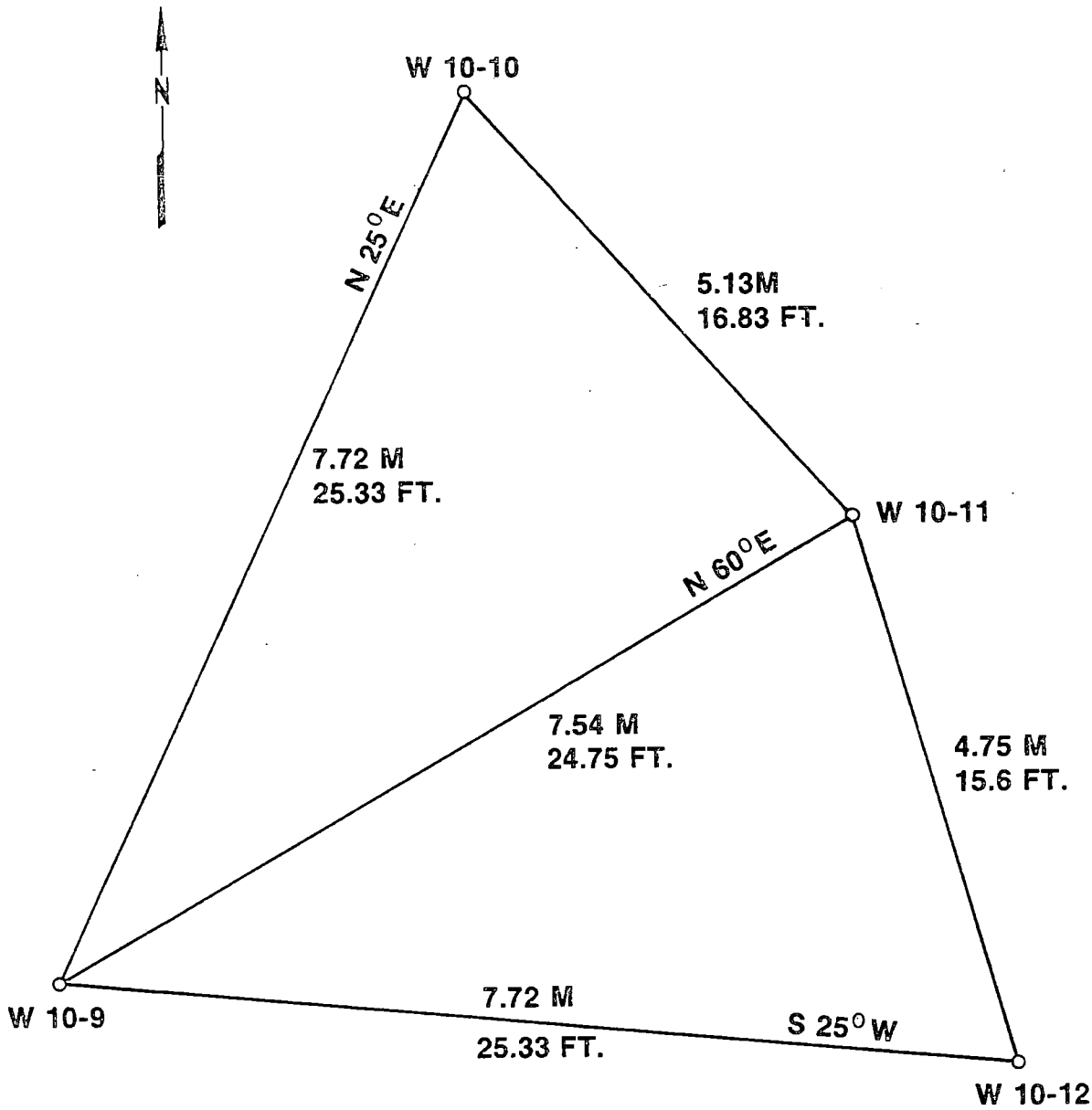

(All Well Numbers
Preceded by 299-)

SCALE
1" = 4'

FIGURE F-3. Relative Location of Four Water Wells North of 241-T Tank Farm.

APPENDIX G

COMPOSITION OF 241-T-106 TANK CONTENTS

For nearly 33 years, radioactive liquid wastes have been generated at Hanford as a result of the chemical processing of fuels from the reactors to separate the plutonium, uranium, and by-product isotopes. In the early Hanford operations, up to 38,000 liters of liquid waste was produced with each ton of uranium processing using a bismuth phosphate precipitation process. These wastes were sufficiently dilute that the fission product generated heat contained in the waste did not present any thermal problems with regard to storage in underground tanks. Such dilute wastes and other wastes that were processed to remove isotopes with long half-lives and subsequently aged (to decay short half-lived isotopes) were designated as "low heat wastes". Heat generated from the low heat wastes in underground tanks constructed during the 1943-1950 period was dissipated without attaining a boiling temperature. (Although the heat output of these wastes is relatively low, they are defined as high level wastes because of the total fission product content in relation to other low level wastes generated during chemical processing.)

With the advent of the second generation (REDOX) and the third generation (PUREX) separations processes, plant technology had improved to the point that a much smaller volume of waste was generated per ton of fuel processed. This, plus longer exposures of fuel, created a potential thermal problem. The radiodecay heat from these plant wastes could not be dissipated in the early "conventional" waste tanks without heat dissipation improvements. This type of waste was designated "high heat waste" and was stored in modified tanks designed to permit boiling under controlled conditions. The steam vapors were condensed and the condensate either discharged to a "crib" or returned to the tank as a cooled liquid, thereby providing a supplementary cooling mechanism. The recycle liquid also was used as make-up water to maintain a stable liquid level in the boiling tank.

In 1965, operations were implemented using evaporative processes to solidify the low heat wastes to a salt cake, which would render the wastes less mobile and less likely to migrate in the event a breach should occur in the containment structure. Earlier, a research and development effort had been initiated to determine methods of removing enough of the long-lived heat-producing isotopes from the high heat wastes so that they, too, could become low heat wastes and be solidified by the same evaporative processes.

In late 1967, a fractionization processing facility (B Plant) was placed in operation to selectively remove cesium and strontium from high heat wastes. In addition, the natural decay mechanism was relied on for removal of a large portion of the heat-generating capacity associated with ^{106}Ru and other fission products having half-lives of less than 1 year.

The resultant composite program for solidification of liquids includes removal of cesium and strontium followed by aging of about 5 years for short-lived fission product decay to convert the high heat wastes to low

heat wastes, and the subsequent evaporation of the low heat waste to produce an immobile salt cake which could be stored more safely than liquids in the existing tanks. The program also includes solidification of the removed cesium and strontium by other processes, and subsequent storage of the cesium and strontium in doubly encapsulated packages in a specially constructed water-cooled basin.

The waste which was stored in the 241-T-106 tank on June 9, 1973, was originally generated at the Purex plant. It had been subjected to an appropriate decay period in boiling waste tanks during which the majority of the strontium precipitated, and the supernate was processed in B Plant by ion exchange for cesium removal. The ion exchange waste was pumped to 241-T-106 tank for storage prior to salt cake solidification in the 242-T evaporator system.

9212456134 4

APPENDIX H

1973 GAMMA-ENERGY ANALYSIS OF RADIONUCLIDE SEDIMENT SAMPLES

A listing of radionuclide concentrations (microcuries per liter) from each well as a function of depth is presented in Table H1.

For comparative purposes, radionuclide values were recalculated (to compensate for radioactive decay) as if all samples were analyzed June 21, 1973 (time zero). Dash indicates radionuclide is absent or below limit of detection. An asterisk indicates that samples were not submitted to laboratory for analysis.

Samples from wells 115, 116, and 121 were not submitted for gamma-energy analyses (GEA) due to the low gamma activity as judged by in-well total gamma profiles. Gamma well logs indicated no radioactivity in Wells 112, 113 and 120; consequently, samples were not submitted for GEA.

1 2 1 2 4 6 6 1 3 4 5

TABLE H1

Gamma-Energy Analyses of Samples

Depth, m	μCi/ℓ						
	^{155}Eu	^{144}Ce	^{125}Sb	^{106}Ru	^{137}Cs	^{154}Eu	^{60}Co
WELL 106							
9.1*							
10.7	127.0	1,070.0	103.0	15,600.0		221.0	68.9
12.2	71.1	612.0	57.1	3,870.0	-	130.0	-
13.7	88.7	886.0	74.0	7,300.0	-	155.0	37.1
15.2	78.1	536.0	57.7	9,160.0	-	131.0	67.8
16.8	98.6	787.0	71.9	9,290.0	-	162.0	50.1
18.3	51.7	346.0	48.5	12,000.0	-	97.0	60.4
19.8	-	-	-	67.5	-	-	-
21.3	-	-	-	2.21	-	-	-
22.9	-	-	-	0.171	0.0075	-	-
24.4	-	-	-	10.2	-	-	-
25.9*							
27.4	-	-	-	0.0394	-	-	-
29.0	-	-	-	0.0533	-	-	-
WELL 107							
9.1*							
10.7*							
12.2*							
13.7	57.6	278.0	49.7	10,700.0	-	16.5	5.92
15.2*							
16.8*							
18.3	-	-	-	3.57	-	-	-
19.8*							
21.3*							
22.9*							
24.4	-	-	2.29	613.0	-	-	-
25.9*							
27.4	-	-	-	1.73	-	-	-
29.0*							

TABLE H1 (Contd)

Depth, m	μCi/ℓ						
	^{155}Eu	^{144}Ce	^{125}Sb	^{106}Ru	^{137}Cs	^{154}Eu	^{60}Ru
WELL 108							
9.1*							
10.7*							
12.2*							
13.7*							
15.2	-	-	-	3,530.0	-	-	-
16.8	-	-	-	36.7	-	-	-
18.3	-	-	-	7.04	-	-	-
19.8	-	-	5.39	1,720.0	0.489	-	-
21.3*							
22.9*							
24.4*							
25.9*							
27.4*							
WELL 109							
9.1*							
10.7	-	-	-	95.1	-	-	-
12.2	26.4	215.0	8.11	1,080.0	-	49.0	10.0
13.7	-	-	-	4,540.0	-	-	-
15.2	-	-	-	4,739.0	-	-	-
16.8	-	-	-	3.20	-	-	-
18.3	-	-	-	0.133	-	-	-
19.8	-	-	-	0.0344	-	-	-
21.3*							
22.9*							
24.4*							
25.9*							
27.4*							

TABLE H1 (Contd)

Depth, m	μCi/ℓ						
	^{155}Eu	^{144}Ce	^{125}Sb	^{106}Ru	^{137}Cs	^{154}Eu	^{60}Co
WELL 110							
9.1*							
10.7	-	155.0	41.5	11,400.0	-	-	9.04
12.2	-	43.4	-	3,880.0	-	-	3.50
13.7	51.0	326.0	48.3	9,130	-	12.7	5.95
15.2	-	122.0	-	10,600.0	-	-	4.94
16.8	-	-	2.67	896.0	-	-	-
18.3	-	-	-	0.095	-	-	-
19.8	-	-	-	18.2	-	-	-
21.3	-	-	1.26	403.0	-	-	-
22.9	-	-	-	0.072	-	-	-
24.4	0.0009	-	-	0.0018	-	-	-
25.9*							
27.4*							
WELL 111							
9.1*							
10.7	15.1	131.0	5.62	324.0	5.08	4.15	0.536
12.2	78.8	764.0	-	5,590.0	207.0	-	-
13.7	145.0	1,500.0	110.0	7,840.0	11.9	36.3	-
15.2	-	-	-	7,270.0	-	-	-
16.8	-	373.0	-	11,500.0	-	-	-
18.3	-	-	-	7,680.0	-	-	-
19.8	-	-	-	3,140.0	-	-	-
21.3	-	-	-	2,540.0	-	-	-
22.9	-	-	-	750.0	-	-	-
24.4*							
25.9*							
27.4*							

TABLE H1 (Contd)

Depth, m	μCi/ℓ						
	^{155}Eu	^{144}Ce	^{125}Sb	^{106}Ru	^{137}Cs	^{154}Eu	^{60}Co
WELL 114							
9.1*							
10.7*	-	-	-		-	-	-
12.2	-	-	-	78.9	-	-	-
13.7	-	0.420	-	1.56	-	-	-
15.2	-	-	-	3,100.0	-	-	-
16.8	-	-	11.0	3,430.0	-	-	-
18.3*							
19.8*							
21.3*							
22.9*							
24.4*							
25.9*							
27.4*							
WELL 117							
9.1*							
10.7*							
12.2*							
13.7	0.957	2.23	-	42.5	-	0.274	0.351
15.2*							
16.8	0.0366	0.0601	-	1.46	-	-	-
18.3*							
19.8	-	-	-	3.71	0.032	-	-
21.3	-	0.0677	-	0.795	-	-	-
22.9*							
24.4*							
25.9*							
27.4*							

TABLE H1 (Contd)

Depth, m	μCi/ℓ						
	^{155}Eu	^{144}Ce	^{125}Sb	^{106}Ru	^{137}Cs	^{154}Eu	^{60}Co
WELL 118							
7.3	4.98	77.2	7.40	34.6	-	-	0.398
7.6	4.15	56.4	1.35	72.7	-	0.943	0.816
7.9	5.91	84.7	0.898	116.0	-	1.33	1.55
8.2	2.29	47.0	0.846	33.2	-	0.534	0.349
8.5	7.34	153.0	0.706	108.0	-	1.70	1.12
8.8*							
9.1	2.92	49.3	0.510	57.4	-	0.680	0.674
10.7	3.03	18.9	-	80.9	-	0.679	0.979
12.2	3.12	22.1	0.443	93.1	-	0.760	0.967
14.0*							
WELL 119							
9.1*							
10.7*							
12.2*							
13.7	0.123	0.217	-	4.97	-	-	0.0408
15.2*							
16.8*							
18.3*							
19.8	-	-	-	0.0358	-	-	-
21.3*							
22.9*							
24.4*							
25.9*							
27.4*							

2124561350

APPENDIX J

ANALYSIS METHODS

IN-WELL TOTAL GAMMA DETECTOR

The van-mounted, gamma-counting system is basically assembled from a Gearhart-Owen Industries, Inc., draw works and main frame, with Harshaw-supplied counting system electronics. Low-level gamma activity is normally monitored with a gross counting scintillation probe which utilizes a 2.5 by 2.5-cm NaI(Tl) scintillation crystal, optically coupled to a photomultiplier tube. The probe assembly also may be used with a lead shield to increase the gamma range capability. Higher level gamma activities are normally monitored with a gross counting GM probe. The probe assemblies are Hanford fabricated. Electrical power is provided by a 115-Vac, 60-Hz, van-mounted auxiliary gasoline engine and driven alternator with over/under voltage protection.

To obtain a well scan, the van is positioned adjacent to a well and the probe rapidly lowered to the bottom by means of the draw works. A turns-counting dial indicates the detector probe depth as it descents. As the probe reaches the bottom, the operator enters the date, well number, probe type, and van number by means of thumbwheel switches. This information is encoded on paper tape by means of a pushbutton. The well data scan is obtained automatically on probe withdrawal. This is done at fixed-reel speed by the draw works speed controller. The count data and time of traverse for each scanned centimeter are output automatically by the counting system electronics for encoding on paper tape. Simultaneously, the output of a count rate meter is graphically recorded on a strip chart recorder for review by the operator.

After field data acquisition is accomplished, the strip charts and paper punched tape are submitted for analysis. The latter is computer processed to yield a graph of the radiation profile of the well and pertinent reports.

GAMMA-ENERGY ANALYSIS OF SEDIMENT SAMPLES

Tank 241-T-106 soil samples were quantitatively analyzed for gamma ray emissions using a three germanium-lithium (Ge(Li)) drifted detector system (References 1 and 2) for radionuclide activity in the nanocurie to microcurie range and a single Ge(Li) detector system (Reference 2) for activity greater than this range. The Gamma X-ray Data Reduction (GXDR) System (Reference 3) was used to calculate the radionuclide activities for each sample gamma-ray spectrum. These systems are routinely used by Rockwell for gamma-ray analysis of 0.5- and 0.025-liter soil samples.

Counting Systems

The three-detector system consists of three Ge(Li) detectors, housed in separate cryostat dewars, which are arranged to form three sides of a square box which presents the maximum detector surface area to the sample. Each of the detectors is in a closed-end coaxial configuration with nominally a 10% relative efficiency, and a full width of half maximum (fwhm) of 2.0 KeV for the 1,332-KeV photopeak from a ^{60}Co source. The shield for the detector system is build with 10-cm-thick lead brick and is graded on the inside with 0.56 mm of cadmium and 0.25 mm of copper to cut down the re-emission of lead K fluorescence X-rays which result from sample-emitted gamma photons absorbed in the shield. The shield for this system stands between the detector and the dewars, thus reducing the level of background radiation from the molecular sieve material in the dewar walls.

The detector signals are preamplified with room temperature Princeton Gamma Tech (PGT) model RG-11 preamplifiers that have been pole-zero matched. This signal is mixed in a PGT Model 308 preamplifier mixer module, then amplified and baseline restored in a Canberra 1413 amplifier using a 4.0-μsec shaping time constant. The signal is routed to a 100-MHz analog-to-digital convertor (ADC) for analysis in a 4,096-channel analyzer. The energy calibration is 500 eV per channel.

The single-detector system consists of a Ge(Li) detector which is a closed-end, coaxially drifted cylinder with its axis parallel to the floor and aligned with the sample positions. The relative efficiency for this detector is 9%. Resolution is 1.885 KeV (fwhm) for the 1,332-KeV photopeak from a ^{60}Co source.

The shield is 10-cm lead, graded with 0.56 mm of cadmium and 0.25 mm of copper to cut down the re-emission of leak K fluorescence X-rays which result from sample-emitted gamma photons absorbed in the shield. The shield cross section is 61 by 61 cm.

The detector signal is preamplified with a room temperature PGT model RG-11 preamplifier and amplified and baseline restored with a 4.0-μsec shaping time constant using a Canberra 1413 amplifier. The signal is routed to a 100-MHz ADC for analysis in a 4,096-channel analyzer. The energy calibration is 500 eV per channel.

System Calibration

All calibration solutions were standardized using the single-detector system. This calibration was made with a National Bureau of Standards Mixed Radionuclide Solution Source. A series of 0.50- and 0.025-liter sea sand matrix radionuclide standards were prepared with known masses of sea sand and with standard solutions of known radionuclide activity. The three-detector system was calibrated with both the 0.50- and 0.025-liter sample geometrics, whereas the single detector was only calibrated with the 0.025-liter sample geometry.

The three-detector system is designed to analyze the low range of gamma activities, nCi/ℓ to μCi/ℓ level, whereas the single-detector system is designed to analyze the middle range of gamma activities, from 0.2 microcurie to 1.0 millicurie.

241-T-106 Samples

The counting geometries used for gamma-ray analyses of the 241-T-106 soil samples were 0.50- and 0.025-liter volumes. Sample activity was administratively limited to 15% dead time (c.a. 10,000 cps) on a pulse height analyzer. If a 0.50-liter sample exceeded this value on the three-detector system, a 0.025-liter sample was prepared. If the sample still exceeded the limit value, it was analyzed on the single-detector system where the sample could be positioned far enough away from the detector.

Sample Spectra Acquisition and Reduction

A Tracor Northern NS-720 pulse height analyzer interfaced to a Tracor Northern NS-111 magnetic tape cassette deck was used for acquisition and storage of the spectra. The data reduction was performed on the GXDR system. The gamma data reduction hardware portion of this system consisted of a Tracor Northern NS-111A magnetic tape cassette deck to receive the spectra data, a NS-636 multichannel analyzer with 8K hard-wired memory for spectral data storage, and an 8K Nova 1200 computer for data reduction. The software program used in data reduction was NS660/Nova ARIS II, version G.

Only the data reduction calculation as it relates to the 241-T-106 spectra is discussed here.

Calculations

A background spectrum was time-normalized and stripped from the sample spectrum. Discrete areas of the spectrum, established by a table of radionuclides suspected of being present in the sample, were searched for the presence of gamma-ray peaks. Gamma-ray peaks with a precision <30% at the 95% confidence level (CL) were used to calculate radionuclides activity. Gamma-ray peaks which had a precision $\leq$ 30% at the 95% CL were used to calculate the "detection level" for the radionuclide.

The following was used to calculate radionuclide activity:

$$\text{Activity, } \mu\text{Ci}/\ell = \frac{[(GP - (NC)]\ (BN)(IS)}{(BD)(T)(UF)}$$

where:

GP = gross count peak area

NC = peak noise continuum

BD = (detector recovery factor) (random summing corrections)

T = acquisition time, sec

$$BN = \frac{1}{(\text{detector efficiency})\ (\text{gamma/decay})}$$

IS = internal sorber corrections

UF = conversion factor for units of μCi/ℓ.

The GP is the sum of 11 pulse height analyzer channels centered at peak center.

The NC is determined by searching for the lowest value of the average of the counts in three consecutive channels on each side of the peak within 20 channels of peak center and is equal to 11 times the average of the lowest values.

The BD is a division which includes a random summing correction and a detector recovery factor. Random summing, which occurs during spectrum acquisition, results in loss in peak area due to random addition of energies from two or more photons, resulting in the recording of an event at the combined energies and not in the full energy peak(s) of the emitter. For 241-T-106 Tank sample analyses, an electronic pulser of 9 cps was used to determine the amount of random summing occurring:

$$\text{Random summing correction} = \frac{\text{pulser peak area, counts}}{9T}$$

In applying this correction, it was assumed that anything that happened to a pulse from the detector also happened to the pulser, pulse introduced at the input to the ADC. The three-detector system was monitored daily for recovery on a 0.50- and 0.025-liter ^{137}Cs standard. The single-detector system was monitored for recovery on the 0.025-liter ^{137}Cs standard.

$$\text{Detector recovery factor} = \frac{\text{measured activity}}{\text{known activity}}$$

Variations >0.5% from day to day were verified by re-analysis of the standard. Variations greater than this normally indicated that one of the detectors had been moved out of alignment.

The BN is defined as being equal to the reciprocal efficiency, measured for a radionuclide, divided by the gamma/decay/sec for the radionuclide gamma-ray.

The IS is a correction for attenuation of a gamma-ray in the sample matrix. An aluminum matrix model was assumed to represent the elemental composition of the 241-T-106 samples. Photon cross-sections were assigned based on this matrix model.

$$IS = \frac{ux}{(1-e^{-ux})}$$

where:

u = photon cross-section, cm^2/g

x = density, g/cm^3

The density of the sample was estimated to be equal to net weight divided by volume of sample.

Precision

The precision value for each spectra peak was calculated as a percentage of the activity at the 95% CL (2T).

$$\% \text{ @ } 95\% \text{ CL} = \frac{196\ [(NP)(T)(BD) + (2)(NC)]^{1/2}}{(NP)(T)(BD)}$$

Detection Limit

When the spectra peak precision value at the 95% CL exceeded 30%, the limit of detection (Reference 4) for the radionuclide was calculated.

$$\text{detection limit} = \frac{(SD)(BN)(IS)\ [(NS + SD^2) + SD]}{T\ 4\ 2}$$

where:

SD = standard deviation = 196/30.

IN-WELL GAMMA-ENERGY ANALYSIS INDIVIDUAL RADIONUCLIDES

The ability to make in situ determinations of the identity and concentration of each radionuclide released to the sediments was necessary to establish their location and sediment retention characteristics as well as to predict future movement and possible consequences. Another desired objective was to determine the location of a leak to facilitate tank repair or permanent in situ waste fixation with, for example, asphaltic emulsions.

Extensive field and laboratory studies using high resolution gamma-ray spectrometry techniques have demonstrated the feasibility of making such in situ measurements. This appendix describes the special instrumentation and techniques developed for making rapid and accurate in situ concentration measurements of in-well gamma-emitting radionuclides.

The developed technology utilizes several types of detectors, including a 20-cm^3 Ge(Li), a 0.5-cm^3 intrinsic germanium, NaI(Tl) crystals, and plastic phosphor scintillation detectors. Both germanium diodes were modified to fit inside a cylindrical housing, capable of passing through a 15-cm well casing. Since germanium diodes are operated at liquid nitrogen temperatures, provisions were made for immersing their copper cold finger heat transfer rods in a 2 1/4-liter stainless steel dewar filled with liquid nitrogen (Figure J-1). This is sufficient to allow either probe to be operated continuously for up to 8 hours without replenishment of the cryogen.

The choice of detector is governed by the amount, type, and location of radioactivity to be measured. In regions of sufficiently high intensity radiation, where operation of the 20-cm^3 Ge(Li) diode is unsuitable due to excessive pulse pileup, the lower efficiency 0.5-cm^3 intrinsic germanium diode is used. NaI(Tl) detectors and plastic phosphors are used for measurements in locations inaccessible with the diode devices, such as lateral pipes which would cause the liquid nitrogen to spill or in wells less than 15 cm in diameter. In general, however, the inferior resolution of the photomultiplier operated crystals renders the germanium detectors preferable choices when possible.

Provisions are made to cover each detector with a lead cap for added shielding where necessary, i.e., high radiation areas. By removing a 5.1-cm diameter side plug from the lead caps, a radial directional capability is provided. In vertical wells, the window direction is indicated by various colored light beams radiating from the top of the detector housing which can be directly observed from the grade level. In horizontal operation, an electronic device contained in the detector housing indicates the window position by means of photocells and a gravity action pendulum.

For vertical wells, the probe assembly is attached to a 305-meter power and signal cable which is lowered mechanically to measured depths by means of a drum and winch. Signals are fed through slip-ring contacts attached to the drum, and pulses are stored in a 2098 channel NS-715 pulse height analyzer calibrated at 1 KeV per channel. A Franklin parallel line printer is used for hard copy printout of the gamma-ray spectrum after each count.

The analyzer, printer, and ancillary electronic equipment are conveniently transported in a light vehicle, and the cable is readily mounted in a pickup truck. In remote areas, power is supplied by a portable 1500-W alternator through a voltage stabilizer.

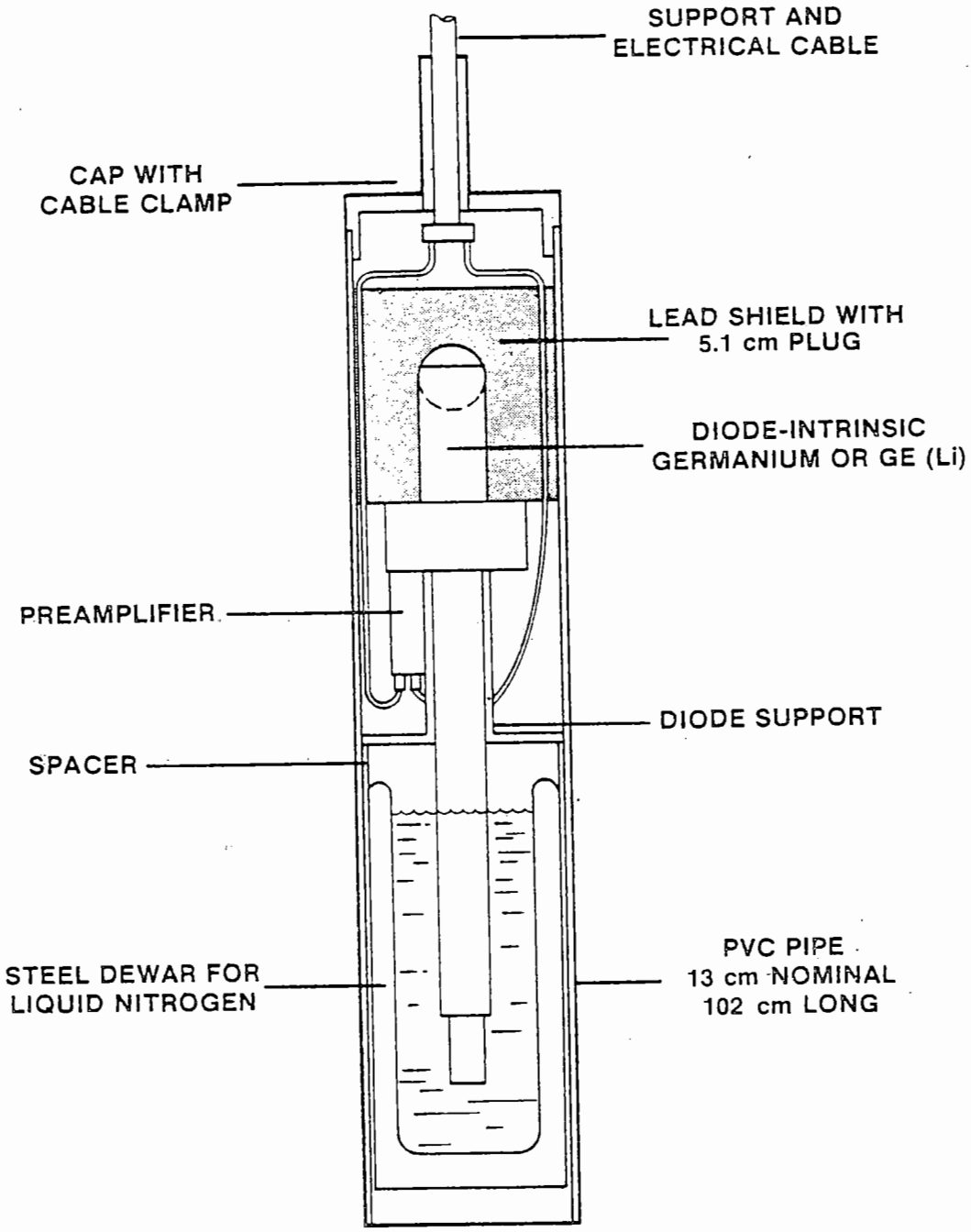

FIGURE J-1. Ge(Li) Well Logging Diode Assembly.

In lateral wells, the probes are pushed to the desired locations with "screw-together sections" of stainless steel rods. NaI(Tl) crystals with 2.5-, 5.1-, or 7.6-cm diameters or a 2.5-cm-diameter by 0.16-cm-thick plastic phospor are used depending on the level of activity and size of the casing.

Calibration of all detectors was done in test well mockups. These consisted of vertically mounted well casings placed in soil with six parallel source tubes located at distances of 2.5, 7.6, 15, 30, 46, and 61 cm from the main casing. The various probe assemblies were placed in the calibration well, and known quantities of ^{60}Co, ^{90}Sr, ^{106}Ru, ^{137}Cs and ^{144}Ce, mounted in sealed capsules, were measured at various locations in tubes. Gamma-ray spectra were obtained for each isotope as a function of vertical and horizontal distance from the detector.

Figure J-2 illustrates the spectra obtained in 10-minute counting periods with the 20-cm^3 Ge(Li) diode using a 1-millicurie source of ^{137}Cs at various horizontal distances from the well casing. By normalizing each spectrum to the same concentration of radioisotope in concentric spherical shells and summing all significant shells, efficiency curves, such as shown in Figures J-3, J-4, and J-5 are generated. The curves, both with and without lead shielding around the diodes, give the number of counts per minute in the photopeak per microcurie of activity per liter of soil (assuming 100% branching fraction). An infinite source constant concentration is assumed; however, soil attenuation renders a maximum effective sphere radius of approximately 0.6 meter for cobalt and less for lower energy photon-emitters for the unshielded diodes. Although a complete efficiency curve for the 0.5-cm^3 diode with lead shielding is not shown, the measured efficiency value for 662 KeV gamma-rays is 0.462 cpm/μCi/ℓ. The final calibration was made in a 6.5 m^3 stainless steel tank with appropriate well casings passing through it which gave a more precise calibration of the spectrometers for radionuclides uniformly distributed in soil. The tank was filled with soil uniformly spiked with known concentrations of ^{106}Ru, ^{137}Cs, ^{125}Sb, ^{154}Eu, and ^{144}Ce and is shown in Figure J-6.

Due to the inherently poor resolution of NaI(Tl) crystals and plastic phosphors relative to germanium diodes and to Compton scattering in soil, it is not possible to adequately resolve radionuclide mixtures with these detector systems to determine concentrations. However, where only a single radioisotope is present or is, by far, the major component, NaI(Tl) crystals or plastic phosphors can be used for concentration measurements in the same manner as described for the diodes.

Figures J-7 through J-9 illustrate the type of data obtainable from different detectors when operated as directional probes. The various curves indicate the relative sensitivity of the detectors for measurements as a function of angle, distance, and gamma energy. The germanium diodes have a much smaller angular resolution than the NaI(Tl) crystal, primarily due to a thicker lead shield in nonwindow directions. However, all the systems are shown to be adequate for determining the directions of high or low concentrations of radionuclides, regardless of relative distance or gamma-ray energy.

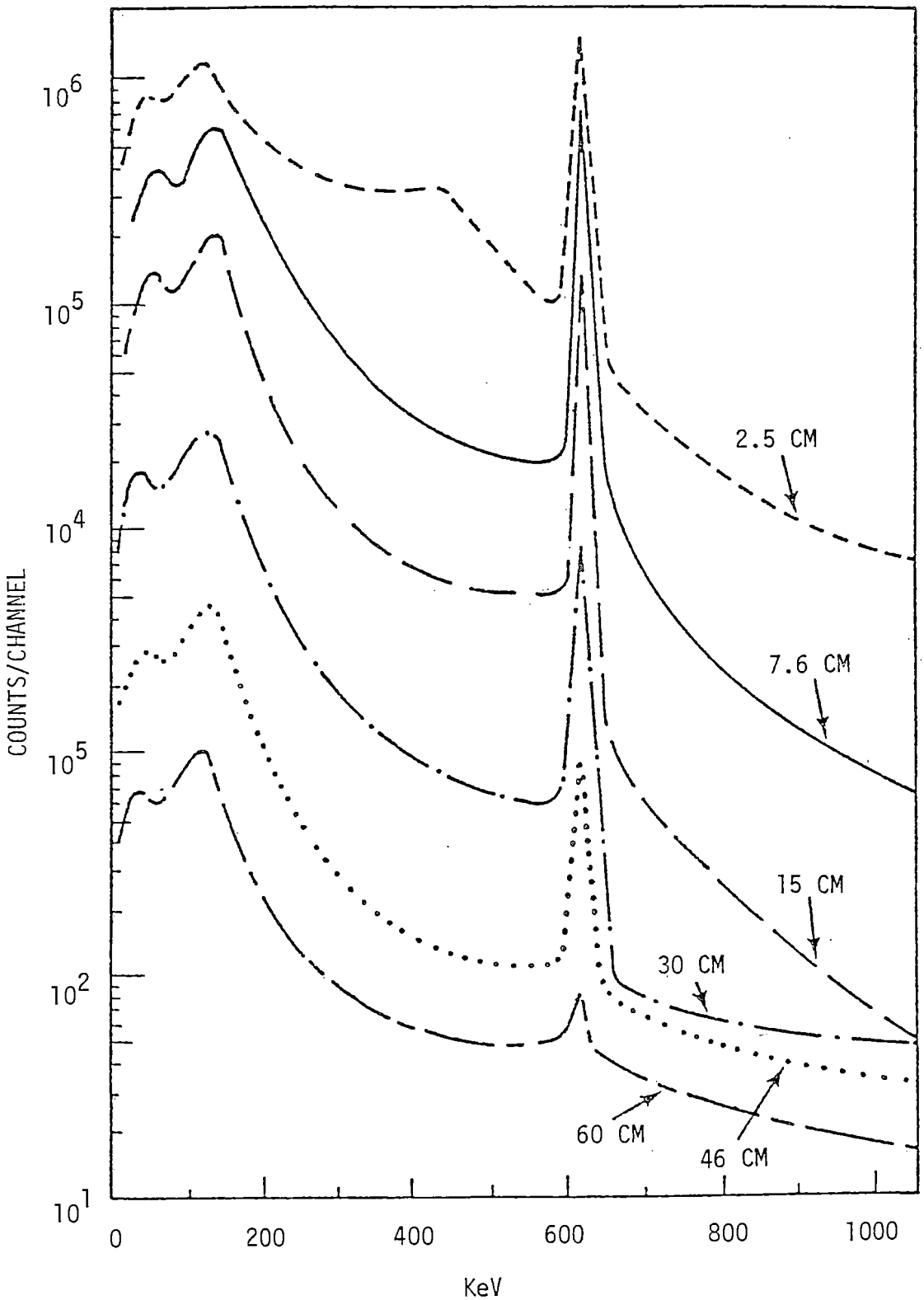

FIGURE J-2. Counts Accumulated by a Ge(Li) Diode as a Function of Distance From a 15-Centimeter Well Casing.

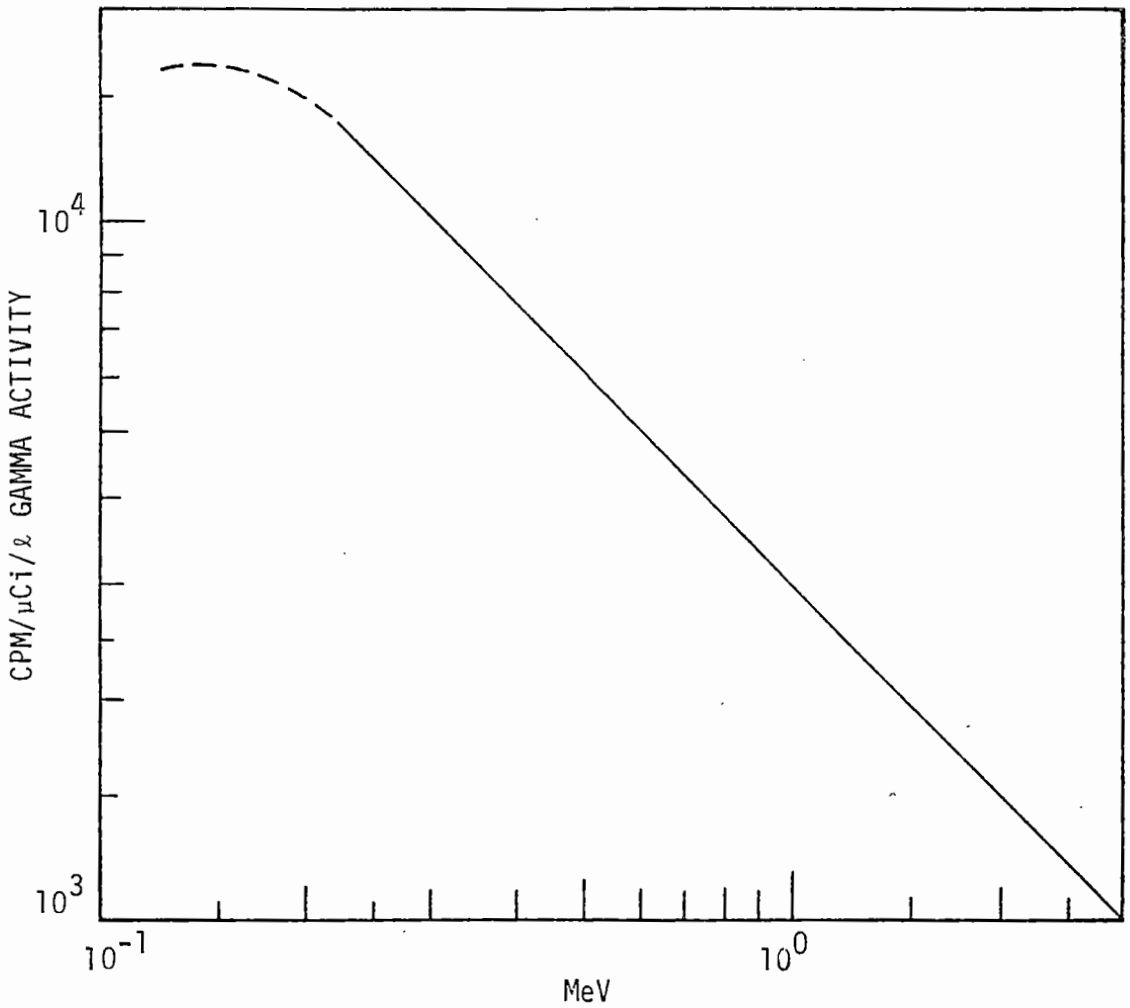

FIGURE J-3. Efficiency of a 20-cc Ge(Li) Diode in Soil, Based on a Relatively Uniform Concentration for a Radius of ∿0.6 Meter.

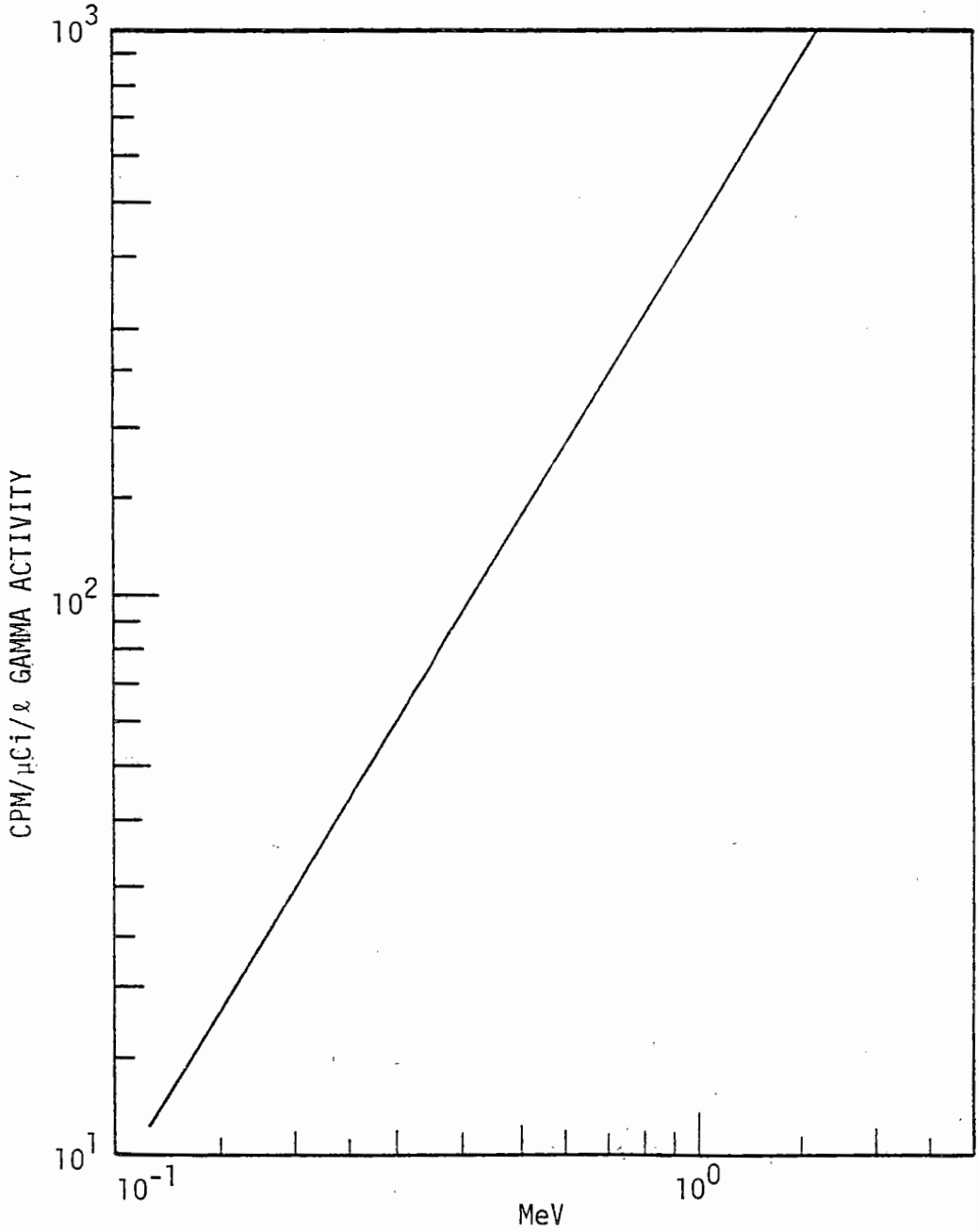

FIGURE J-4. Efficiency of a 20-cc Ge(Li) Diode with Lead Cap for Radionuclides in Soil, Based on a Relatively Uniform Concentration for a Radius of ∿0.6 Meter.

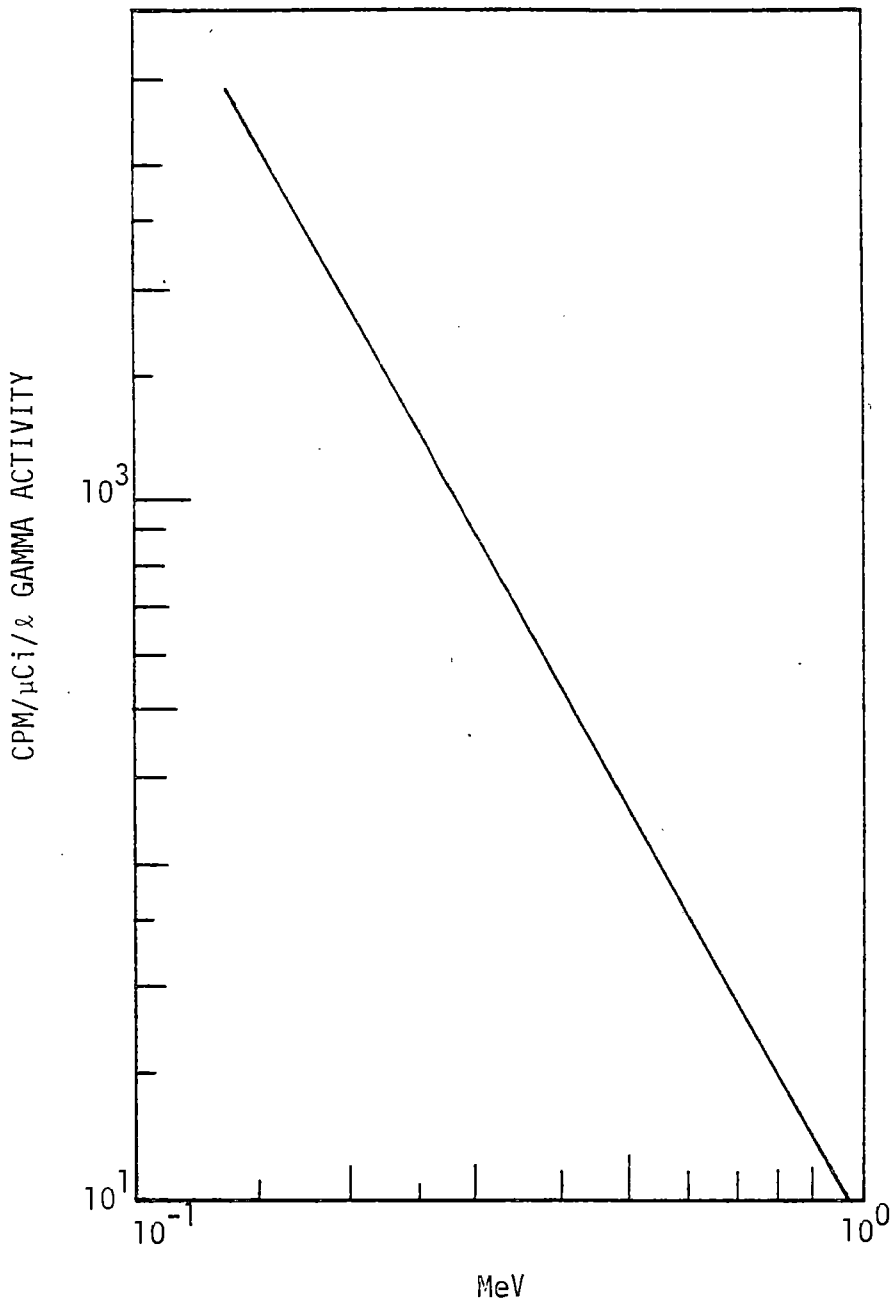

FIGURE J-5. Efficiency of a 0.5-cc Ge(Li) Diode for Radionuclides in Soil, Based on a Relatively Uniform Concentration for a Radius of ∿0.6 Meter.

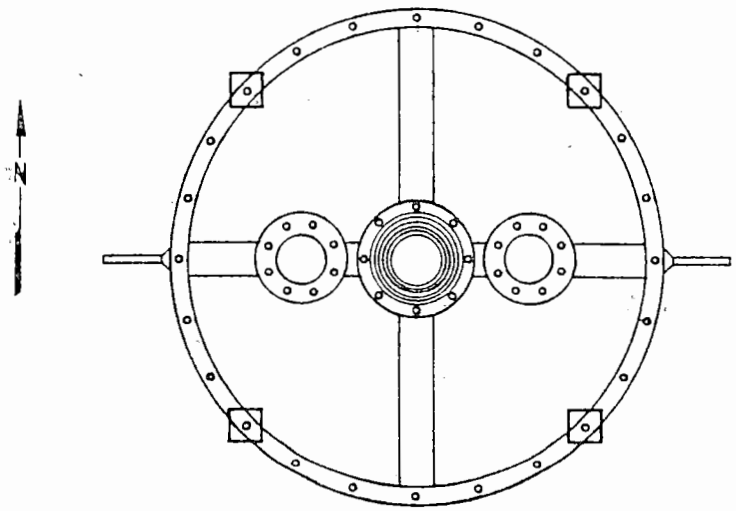

PLAN

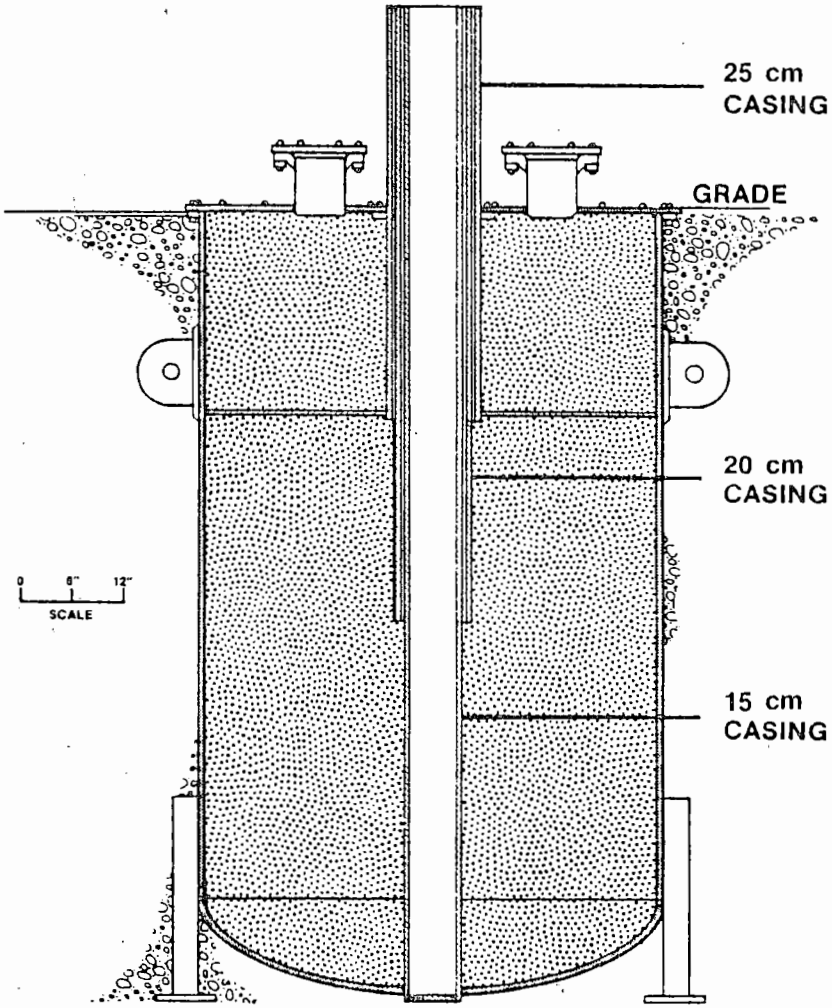

ELEVATION

TANK FILLED WITH HOMOGENEOUSLY SPIKED COARSE TO MEDIUM SAND.
SPIKE CONSISTS OF THE FOLLOWING:

ISOTOPE	μCi/L SOIL*		
137 Cs	10.402	±	0.038
106 Ru	4.570	±	0.023
144 Ce	1.941	±	0.018
134 Cs	0.2125	±	0.0030
125 Sb	0.1158	±	0.0016
154 Eu	-0.02152		0.00052

*CONCENTRATION AS OF JANUARY 1, 1977

FIGURE J-6. In-Well Calibration Facility.

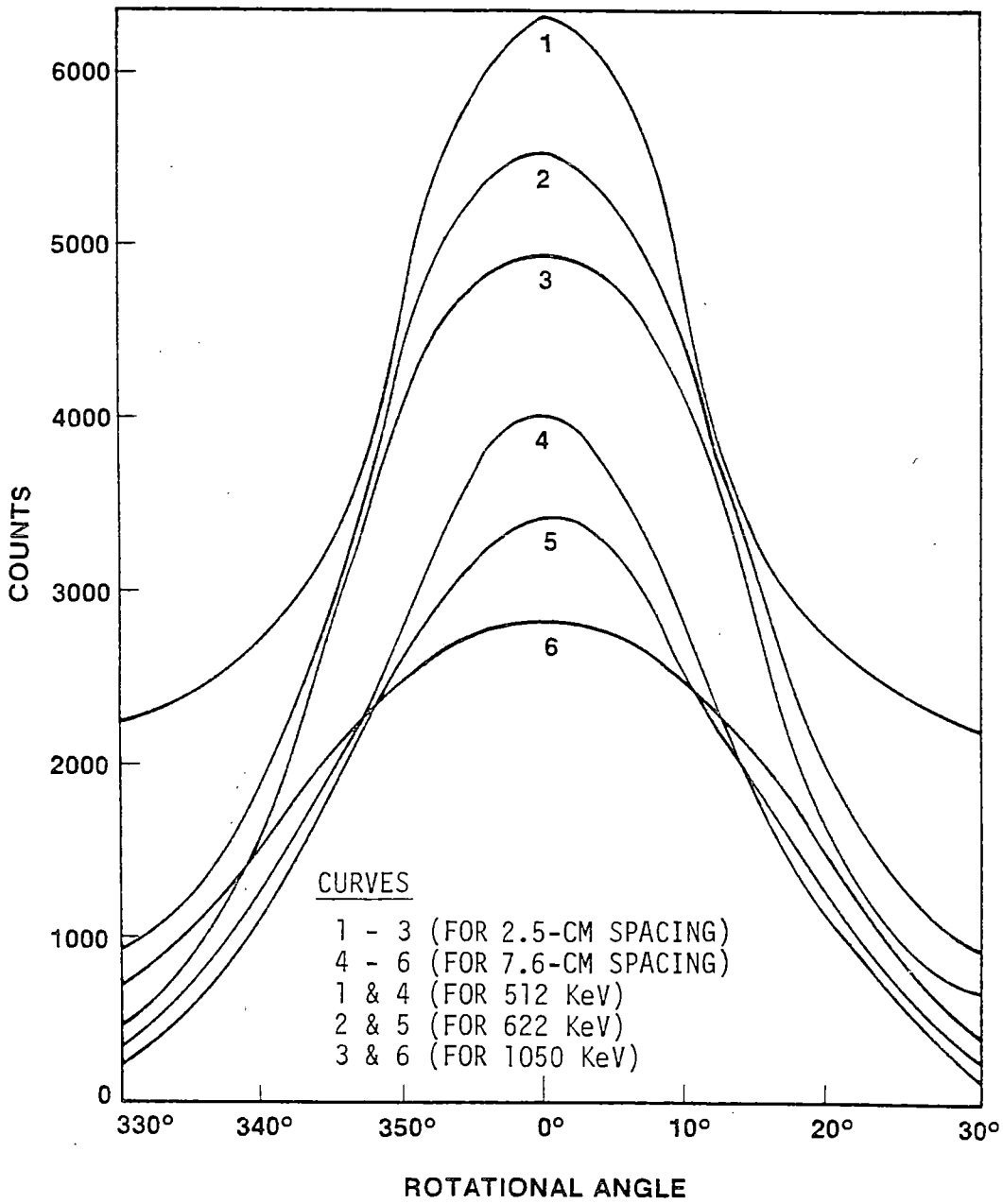

FIGURE J-7. Relative Directional Sensitivity of a 20-cc Ge(Li) Diode for Point Sources of Different Energies and at Different Distances.

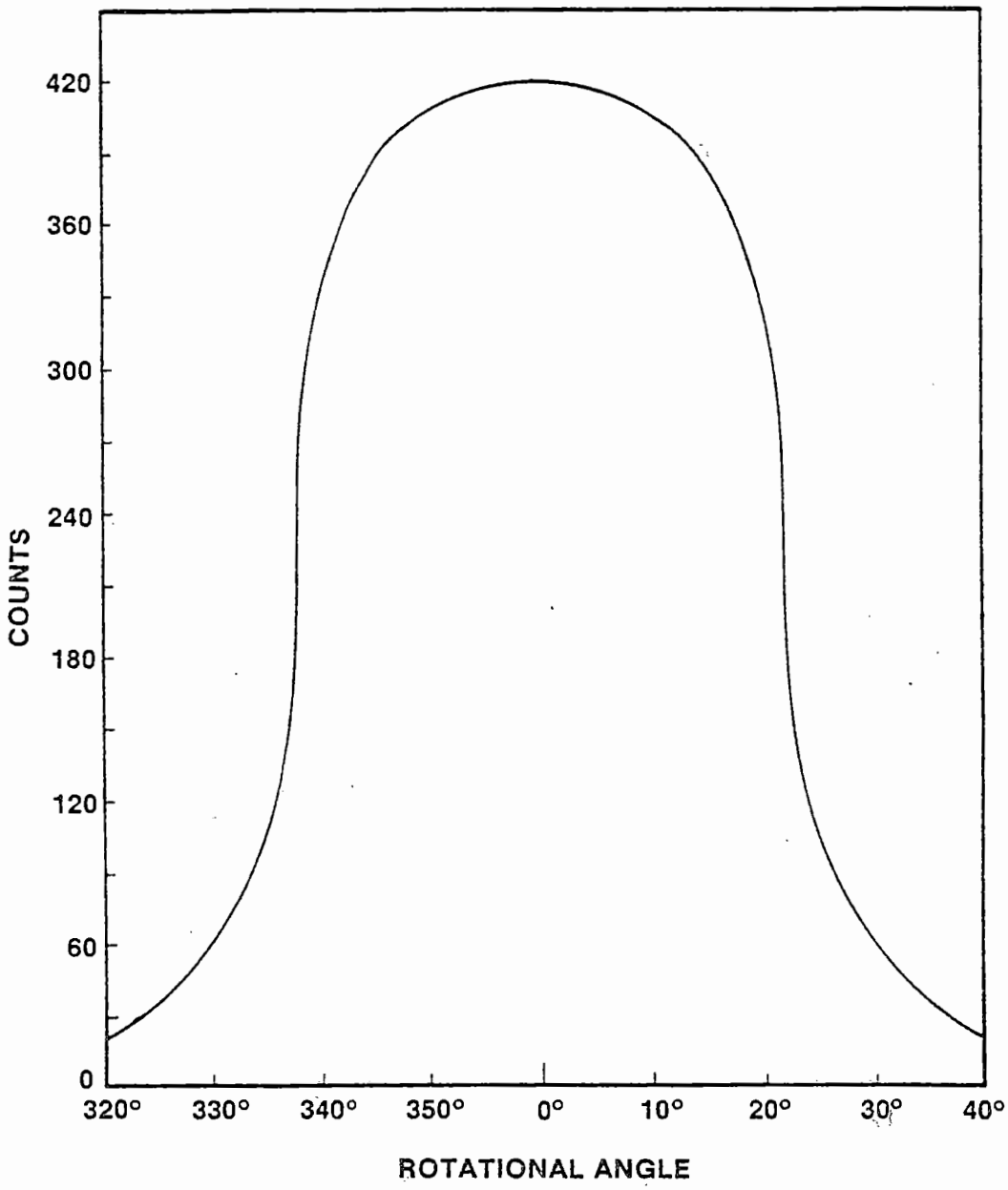

FIGURE J-8. Relative Directional Sensitivity of 0.5-cc Ge(Li) Diode for Point Source of ^{137}Cs at 2.5-Centimeter Spacing.

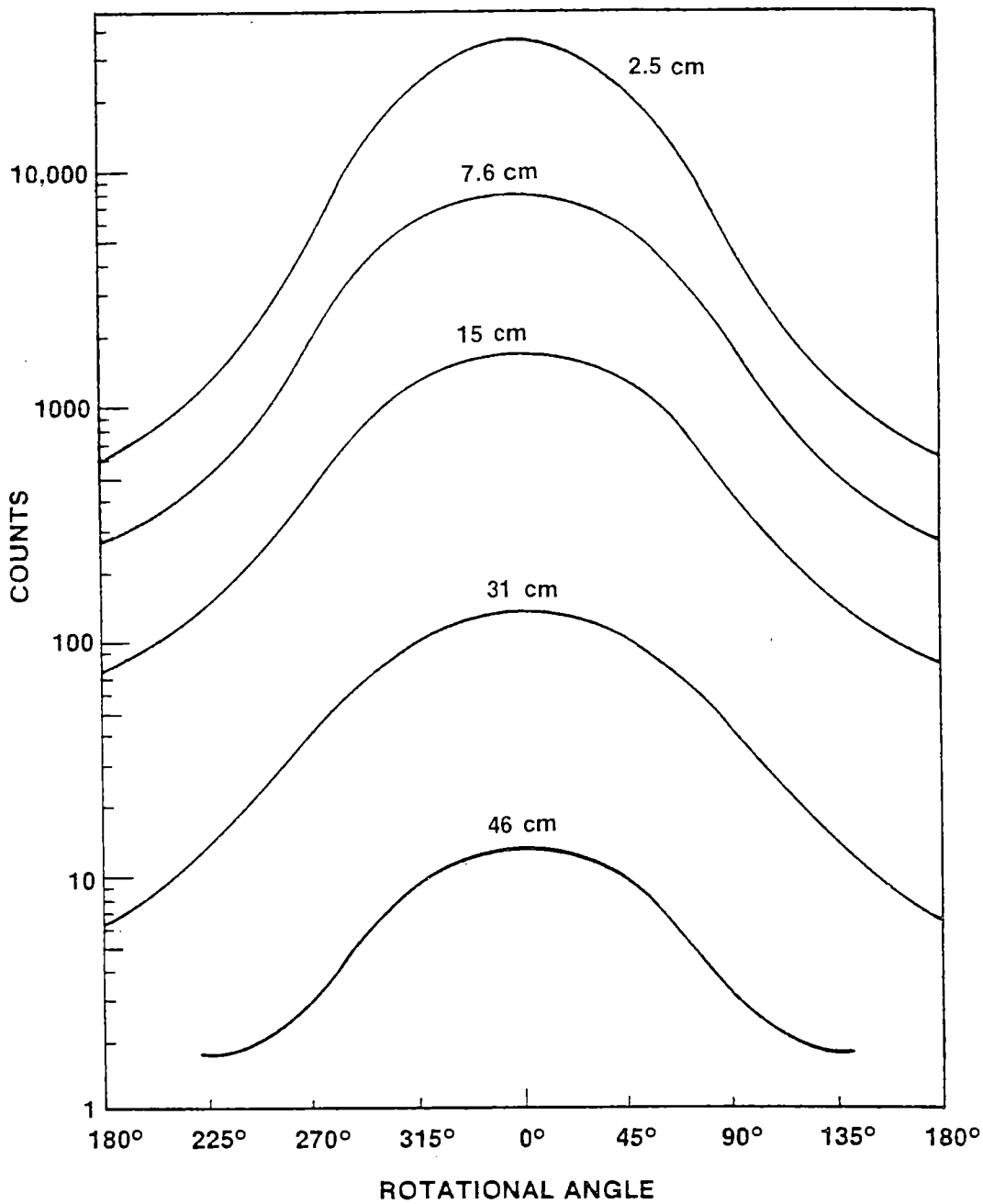

FIGURE J-9. Relative Directional Sensitivity of 1-Inch Diameter by 1-Inch-Thick NaI(Tl) Detector for Point Source of ^{106}Ru at Various Spacings.

FOIL ACTIVATION FOR ALPHA (Pu and Am) ANALYSIS

Plutonium can be assayed at the 10 nCi/g of Pu level in the presence of high gamma fields. This is accomplished by activating metal foils with the neutrons from the contaminated zone. The neutron bombardment of the foils activates atoms of the metal radioactive species. The foil is then removed from the contaminated zone to a low background high efficiency counting laboratory. The gamma emission from the activated atoms is measured and calculations are made to determine the plutonium present.

Problems associated with this approach: (1) varying plutonium, americium and other neutron-emitting species; (2) different isotopic levels of plutonium; and (3) ability to distinguish between plutonium, americium, cerium and other neutron-emitting elements.

The history of the solutions going to the 241-T-106 tank shows that the Pu-O bond should prevail as the only species to consider. Hence, γ,n reactions (like PuF_4) should not be a problem. Also, the isotopic level of plutonium was all weapon grade. Hence, this problem is essentially eliminated. Based on the age of the 241-T-106 tank waste, about 5 to 10% of the total neutron activity comes from the ^{241}Am, the daughter of ^{241}Pu. The variation of 5 to 10% is due to the greater mobility of americium. Americium can be obtained by gamma-energy analysis and from this, the plutonium can be estimated.

Copper was used as the neutron-sensitive foil. It has the following reaction:

$$^{63}_{29}Cu + ^{1}_{0}n \longrightarrow ^{64}_{29}Cu + \beta^-, \gamma(0.51\ MeV) \longrightarrow ^{64}_{30}Zn$$

The excited ^{64}Cu beta decays to ^{64}Zn with a 12.9-hour half-life and emits a gamma with energy of 0.51 MeV. The amount of gamma counts is proportional to the neutron flux corrected back to the time zero (time removed from contaminated source); the neutron flux is proportional to the plutonium plus americium.

REFERENCES

1. W. H. Zimmer, "Automatic Radioactive Inventory System". ARH-SA-134, Atlantic Richfield Hanford Company, Richland, Washington. November 1972; and (IEEE Transactions on Nuclear Science, 19th Nuclear Science Symposium, February 1973), Vol. NS20, No. 1, P. 352.

2. W. H. Zimmer, "Names and Descriptions of Chemical Technology Laboratory Detector Systems". ARH-CD-276, Atlantic Richfield Hanford Company, Richland, Washington, March 1975.

3. W. H. Zimmer, "Gamma X-ray Data Reduction System, Volume 1 - Gamma". ARH-ST-114-1, Atlantic Richfield Hanford Company, Richland, Washington, December 1974.

4. E. Storm and H. I. Israel, "Photon Cross-Sections from 1 KeV to 100 MeV for Elements Z=1 to Z=100". Nuclear Data Tables, Vol. 7, No. 6, Academic Press, New York, 1970.

9212466136 8

APPENDIX K

IN-WELL RADIOACTIVITY DATA

Pages K-2 through K-9 illustrate the in-well total gamma profiles for Wells 106 through 121 for 1973, 1974, 1975, 1976, 1977 and 1978. All well numbers are preceded by the prefix 299-W10-. All 1973 and 1974 measurements were made with a GM probe. Measurements for 1975 through 1978 for Wells 106 through 111 and 114 were made with a GM probe. Measurements for 1975 through 1978 for Wells 112, 113, and 115 through 121 were made with a scintillation probe.

Pages K-11 through K-131 illustrate the ^{106}Ru, ^{144}Ce, ^{137}Cs, ^{60}Co and ^{154}Eu concentrations ($\mu Ci/\ell$) for Wells 106 through 121, 123, 145, 162 and 164-168 for 1977 and 1978. 1977 data points are connected by straight lines (1 Nov 1977). 1978 data points are not connected (1 May 1978). 1977 ^{106}Ru data points must be multiplied by a factor of 0.707 to correct for radioactive decay for direct comparison with 1978 data points. 1977 ^{144}Ce data points must be multiplied by 0.638 to correct for radioactive decay for direct comparison with 1978 data points. Radionuclide concentrations in Wells 162 and 164 through 167 could not be measured in 1978 because these wells were grouted in 1977. All well numbers are prefixed by 299-W10-. Less than values are below the minimum detectable activity for a radionuclide in the gamma radiation field of the measurement.

9212456136 9

TOTAL GAMMA PROFILES FOR WELLS 106 THROUGH 121
1973, 1974, 1975, 1976, 1977 AND 1978

1. All well numbers are preceded by 299-W10-.
2. All 1973 and 1974 measurements were made with a GM probe.
3. Measurements for 1975 through 1978 for Wells 106 through 111 and 114 were made with a GM probe.
4. Measurements through 1978 for Wells 112, 113, and 115 through 121 were made with a scintillation probe.

3 2 1 2 4 6 6 4 3 7 0

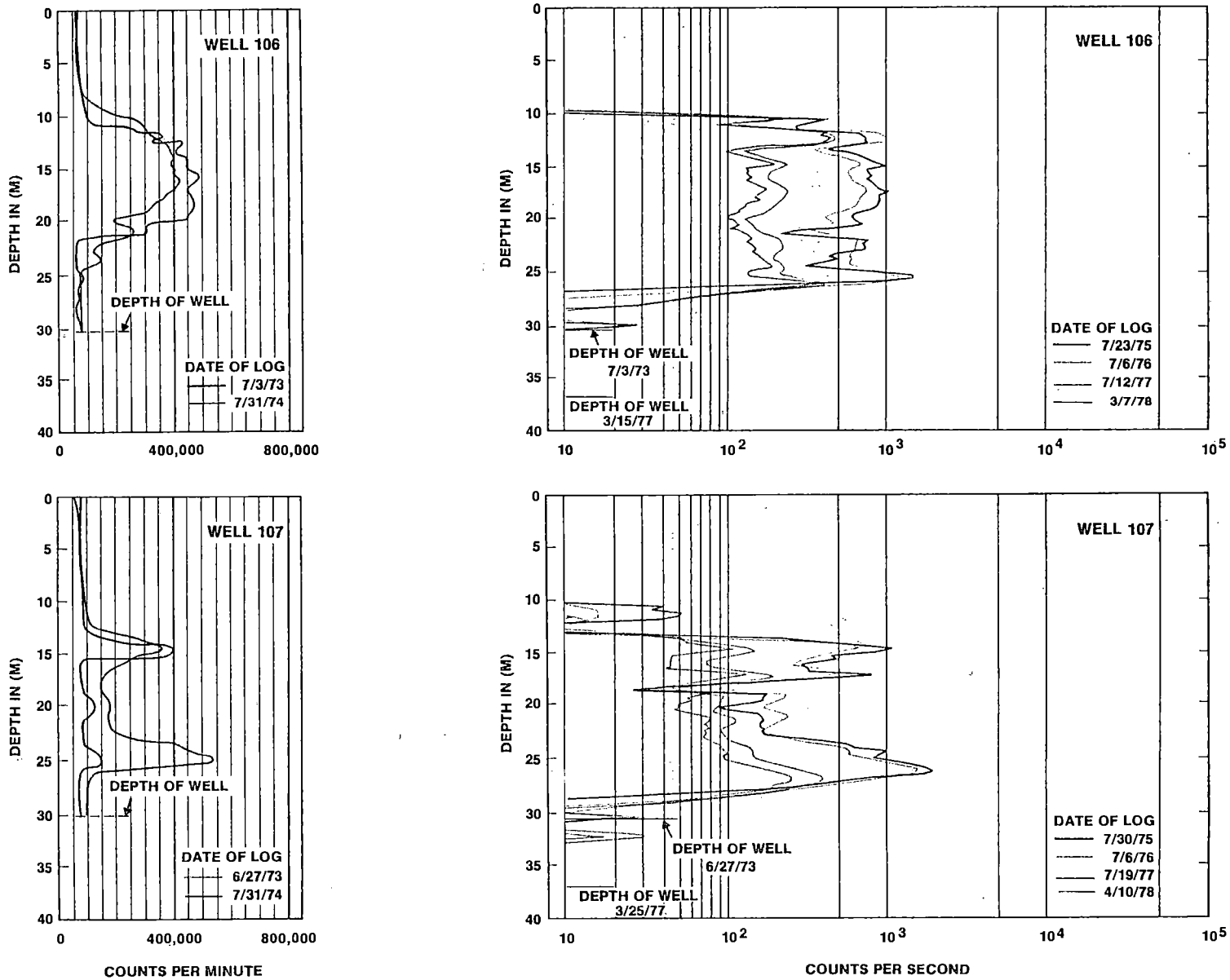
WELL 106
DEPTH IN (M)
DEPTH OF WELL
DATE OF LOG
7/3/73
7/31/74
0
400,000
800,000
WELL 106
DEPTH OF WELL
7/3/73
DEPTH OF WELL
3/15/77
DATE OF LOG
7/23/75
7/6/76
7/12/77
3/7/78
10
10^2
10^3
10^4
10^5
WELL 107
DEPTH OF WELL
DATE OF LOG
6/27/73
7/31/74
COUNTS PER MINUTE
WELL 107
DEPTH OF WELL
6/27/73
DEPTH OF WELL
3/25/77
DATE OF LOG
7/30/75
7/6/76
7/19/77
4/10/78
COUNTS PER SECOND

THIS PAGE INTENTIONALLY
LEFT BLANK

2 2 1 2 4 6 6 1 3 7 2

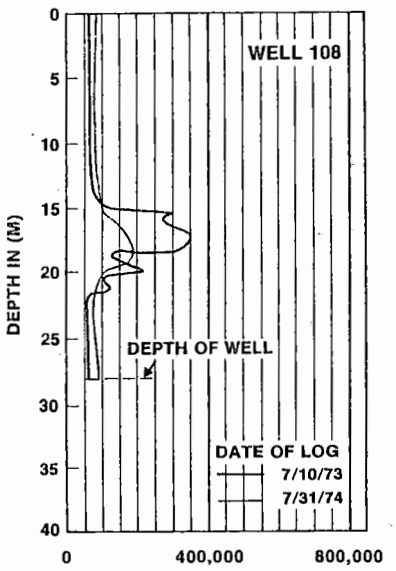
WELL 108
DEPTH IN (M)
DEPTH OF WELL
DATE OF LOG
7/10/73
7/31/74
0
400,000
800,000

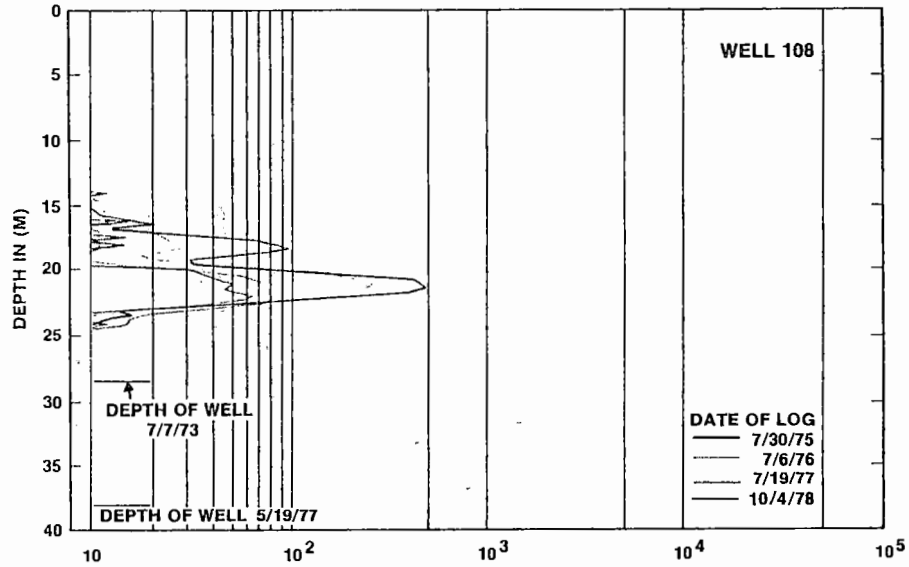
WELL 108
DEPTH IN (M)
DEPTH OF WELL
7/7/73
DEPTH OF WELL 5/19/77
DATE OF LOG
7/30/75
7/6/76
7/19/77
10/4/78
10
10^2
10^3
10^4
10^5

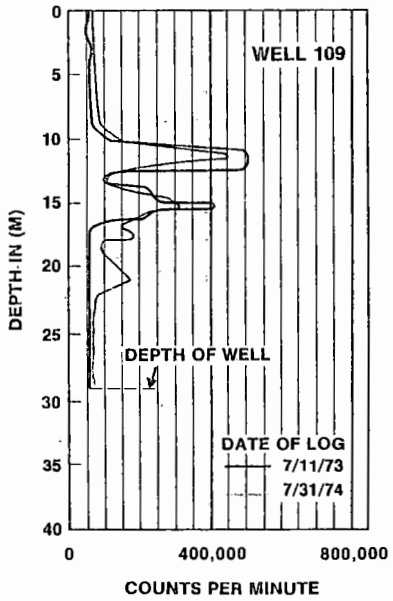
WELL 109
DEPTH IN (M)
DEPTH OF WELL
DATE OF LOG
7/11/73
7/31/74
0
400,000
800,000
COUNTS PER MINUTE

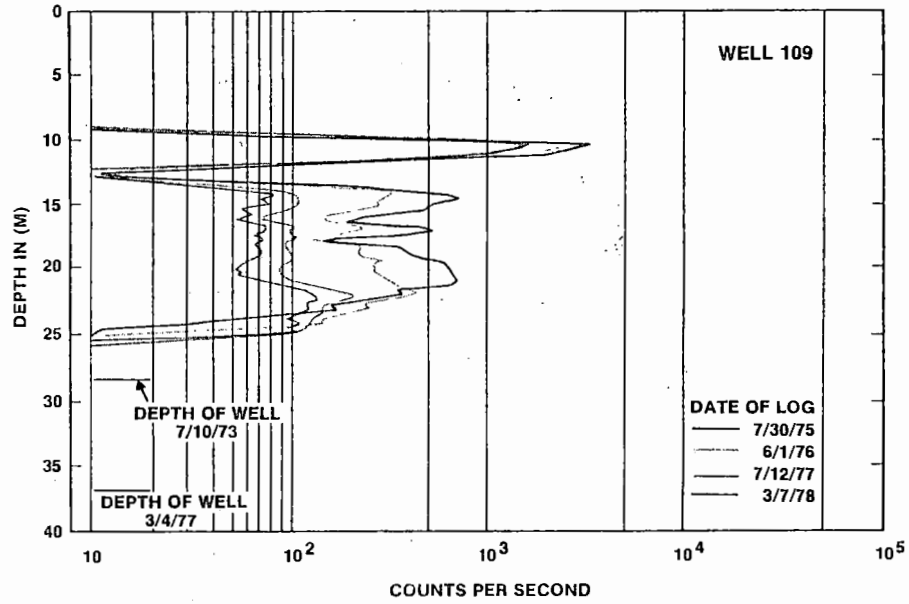
WELL 109
DEPTH IN (M)
DEPTH OF WELL
7/10/73
DEPTH OF WELL
3/4/77
DATE OF LOG
7/30/75
6/1/76
7/12/77
3/7/78
10
10^2
10^3
10^4
10^5
COUNTS PER SECOND

THIS PAGE INTENTIONALLY
LEFT BLANK

4 7 3 1 9 6 4 2 1 2

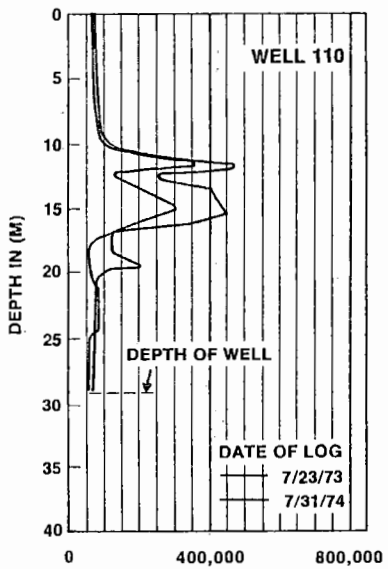
WELL 110
DEPTH IN (M)
DEPTH OF WELL
DATE OF LOG
7/23/73
7/31/74
0
400,000
800,000

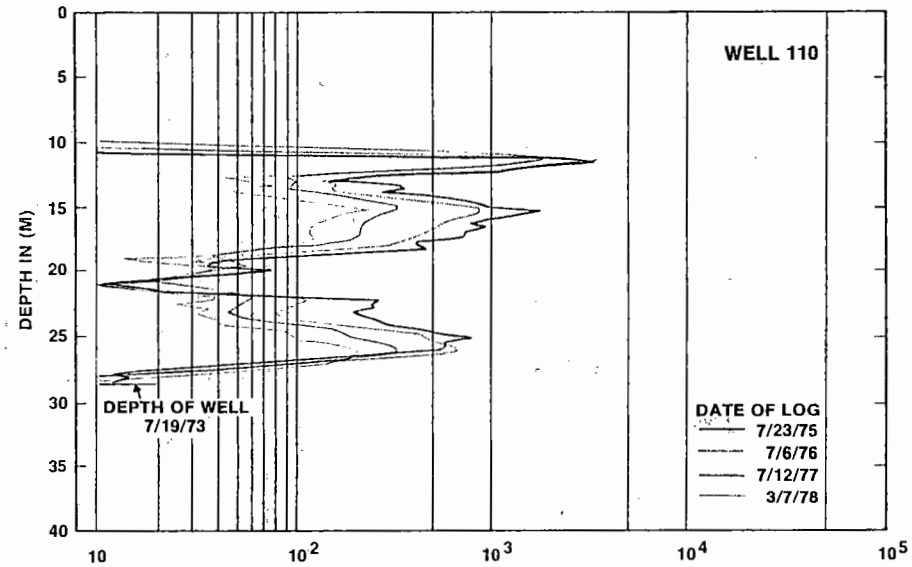
WELL 110
DEPTH IN (M)
DEPTH OF WELL
7/19/73
DATE OF LOG
7/23/75
7/6/76
7/12/77
3/7/78
10
10^2
10^3
10^4
10^5

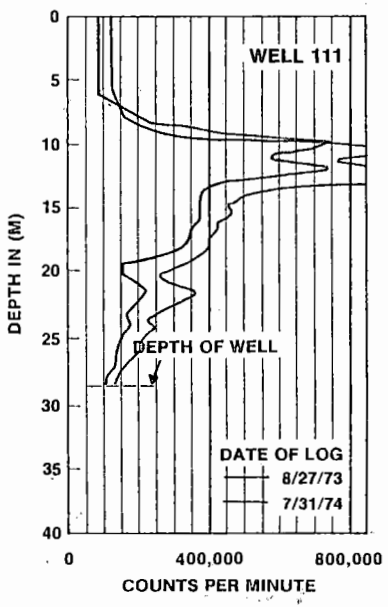
WELL 111
DEPTH IN (M)
DEPTH OF WELL
DATE OF LOG
8/27/73
7/31/74
0
400,000
800,000
COUNTS PER MINUTE

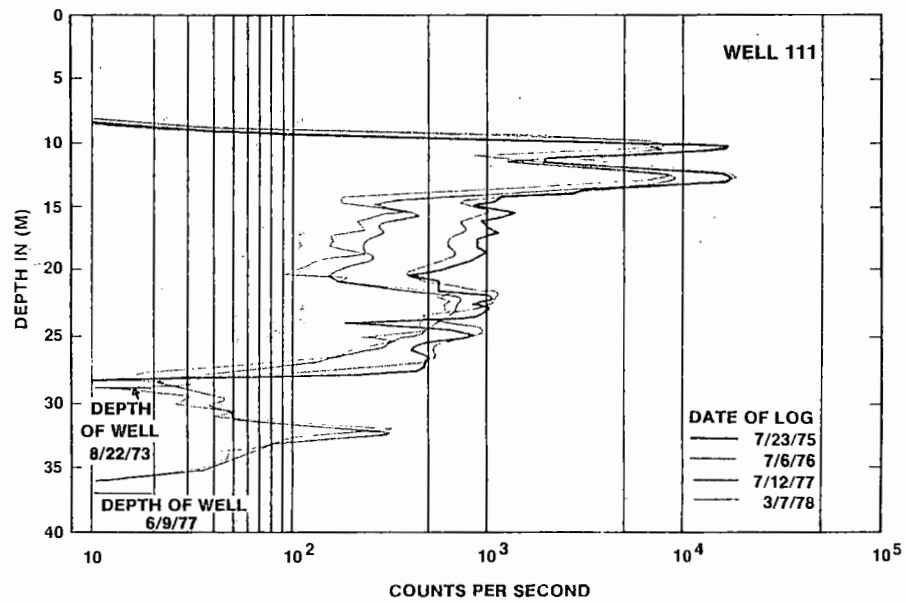
WELL 111
DEPTH IN (M)
DEPTH
OF WELL
8/22/73
DEPTH OF WELL
6/9/77
DATE OF LOG
7/23/75
7/6/76
7/12/77
3/7/78
10
10^2
10^3
10^4
10^5
COUNTS PER SECOND

THIS PAGE INTENTIONALLY
LEFT BLANK

2 2 1 2 4 5 6 1 3 7 5

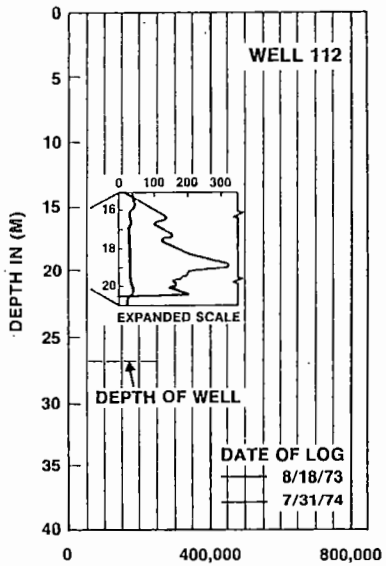
WELL 112
DEPTH IN (M)
0
5
10
15
20
25
30
35
40
0
400,000
800,000
0 100 200 300
16
18
20
EXPANDED SCALE
DEPTH OF WELL
DATE OF LOG
8/18/73
7/31/74

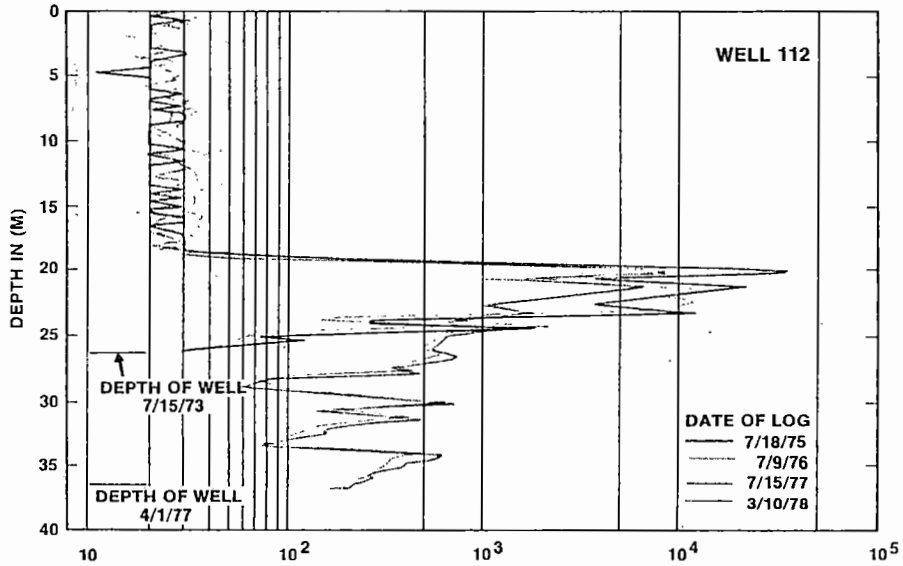
WELL 112
DEPTH IN (M)
0
5
10
15
20
25
30
35
40
10
10^2
10^3
10^4
10^5
DEPTH OF WELL
7/15/73
DEPTH OF WELL
4/1/77
DATE OF LOG
7/18/75
7/9/76
7/15/77
3/10/78

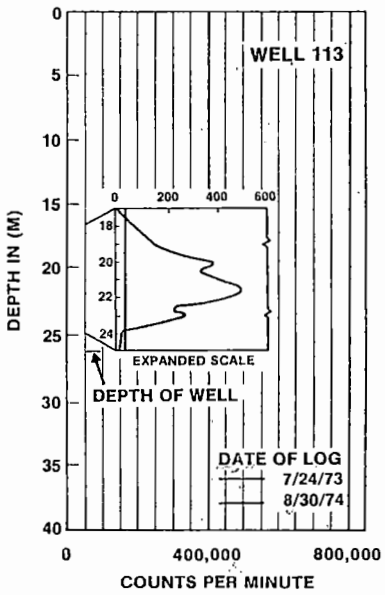
WELL 113
DEPTH IN (M)
0
5
10
15
20
25
30
35
40
0
400,000
800,000
COUNTS PER MINUTE
0 200 400 600
18
20
22
24
EXPANDED SCALE
DEPTH OF WELL
DATE OF LOG
7/24/73
8/30/74

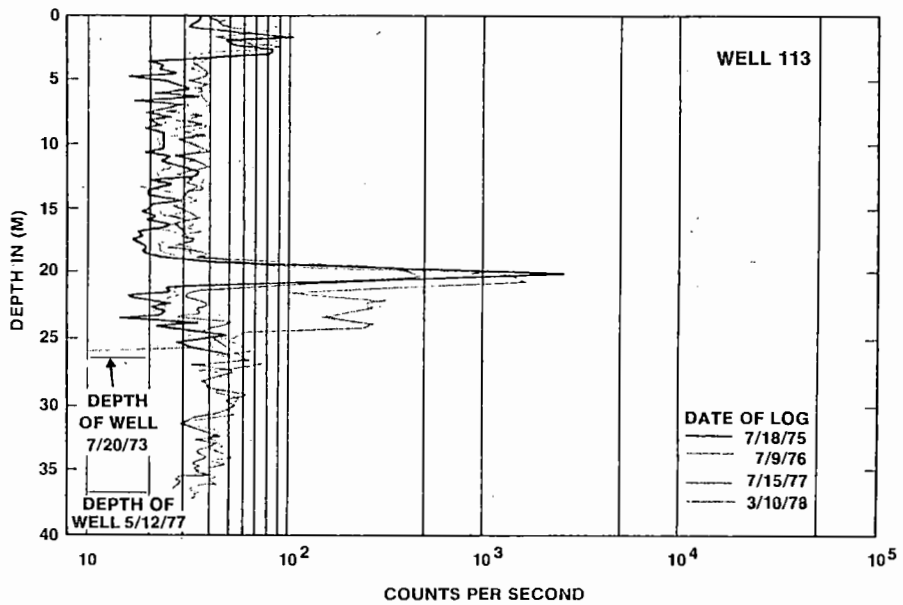
WELL 113
DEPTH IN (M)
0
5
10
15
20
25
30
35
40
10
10^2
10^3
10^4
10^5
COUNTS PER SECOND
DEPTH
OF WELL
7/20/73
DEPTH OF
WELL 5/12/77
DATE OF LOG
7/18/75
7/9/76
7/15/77
3/10/78

THIS PAGE INTENTIONALLY
LEFT BLANK

0 2 1 2 4 6 6 1 3 7 8

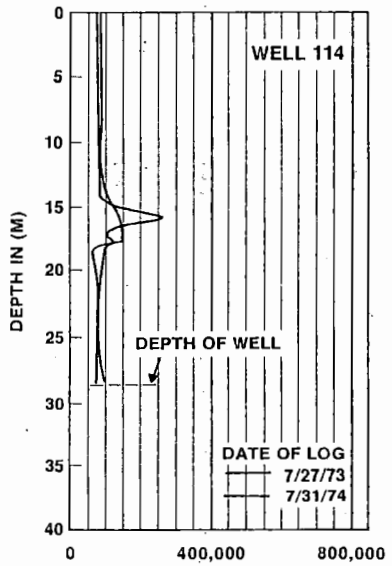
WELL 114
DEPTH IN (M)
DEPTH OF WELL
DATE OF LOG
7/27/73
7/31/74
0
400,000
800,000

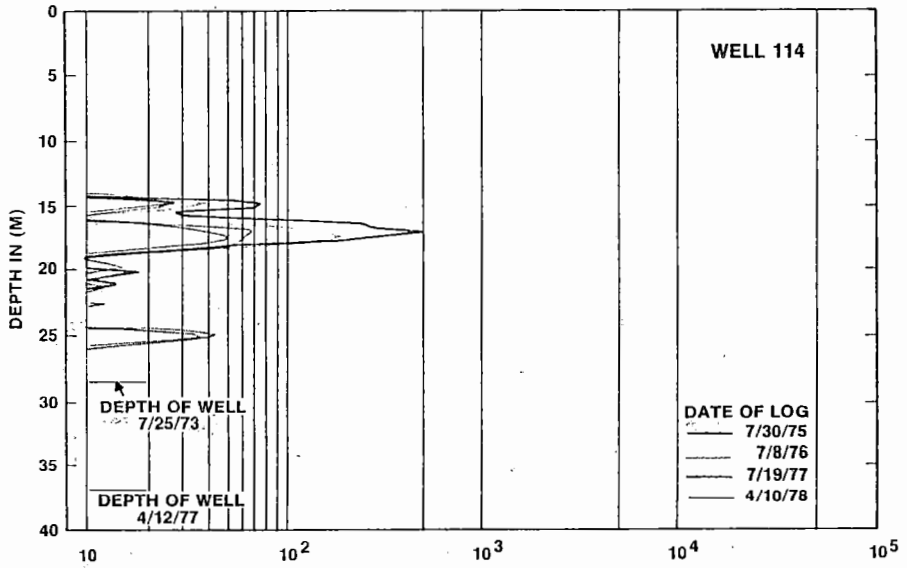
WELL 114
DEPTH IN (M)
DEPTH OF WELL
7/25/73
DEPTH OF WELL
4/12/77
DATE OF LOG
7/30/75
7/8/76
7/19/77
4/10/78
10
10^2
10^3
10^4
10^5

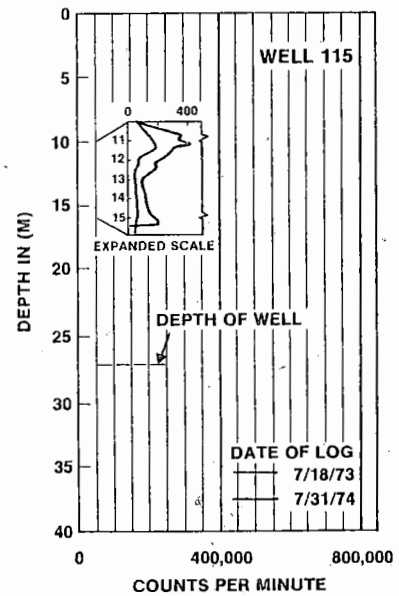
WELL 115
EXPANDED SCALE
DEPTH IN (M)
DEPTH OF WELL
DATE OF LOG
7/18/73
7/31/74
0
400,000
800,000
COUNTS PER MINUTE

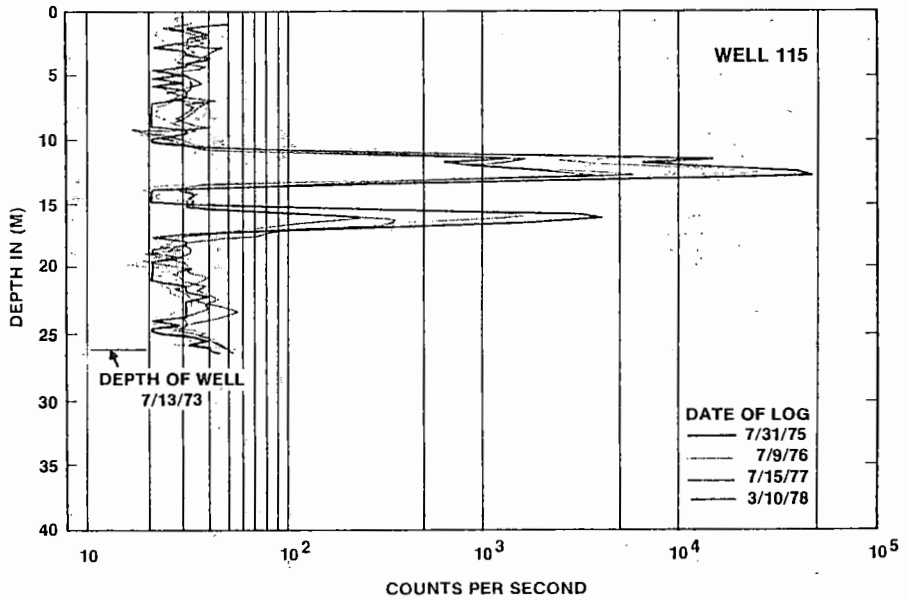
WELL 115
DEPTH IN (M)
DEPTH OF WELL
7/13/73
DATE OF LOG
7/31/75
7/9/76
7/15/77
3/10/78
10
10^2
10^3
10^4
10^5
COUNTS PER SECOND

THIS PAGE INTENTIONALLY
LEFT BLANK

0 8 3 1 9 6 4 2 1 2

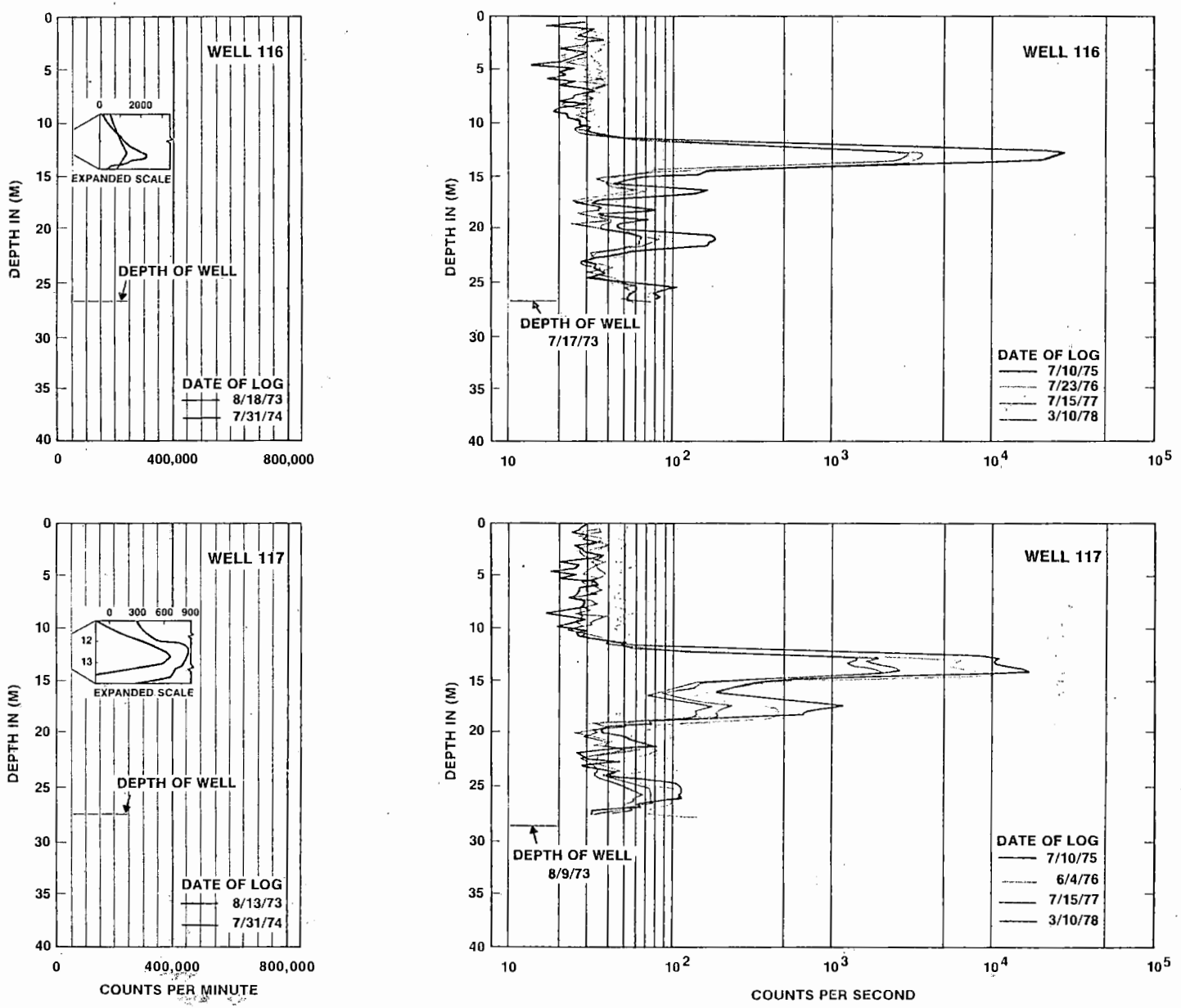
WELL 116
0 2000
EXPANDED SCALE
DEPTH OF WELL
DATE OF LOG
8/18/73
7/31/74
DEPTH IN (M)
0 400,000 800,000
WELL 116
DEPTH OF WELL
7/17/73
DATE OF LOG
7/10/75
7/23/76
7/15/77
3/10/78
10 10^2 10^3 10^4 10^5
WELL 117
0 300 600 900
12
13
EXPANDED SCALE
DEPTH OF WELL
DATE OF LOG
8/13/73
7/31/74
COUNTS PER MINUTE
WELL 117
DEPTH OF WELL
8/9/73
DATE OF LOG
7/10/75
6/4/76
7/15/77
3/10/78
COUNTS PER SECOND

THIS PAGE INTENTIONALLY
LEFT BLANK

0 2 1 2 4 6 6 1 3 8 2

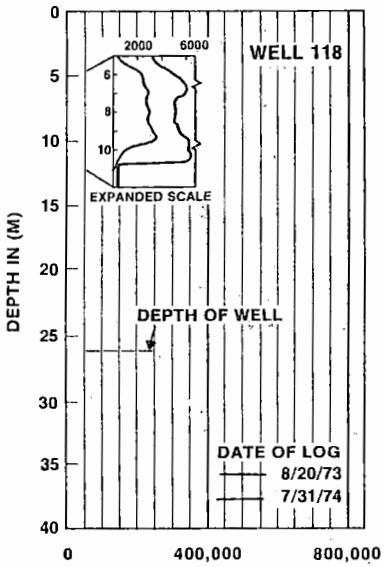
WELL 118
2000
6000
6
8
10
EXPANDED SCALE
DEPTH OF WELL
DATE OF LOG
8/20/73
7/31/74
DEPTH IN (M)
0
400,000
800,000

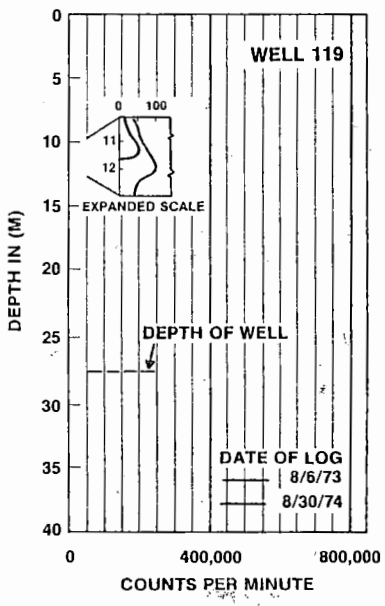
WELL 119
0
100
11
12
EXPANDED SCALE
DEPTH OF WELL
DATE OF LOG
8/6/73
8/30/74
DEPTH IN (M)
0
400,000
800,000
COUNTS PER MINUTE

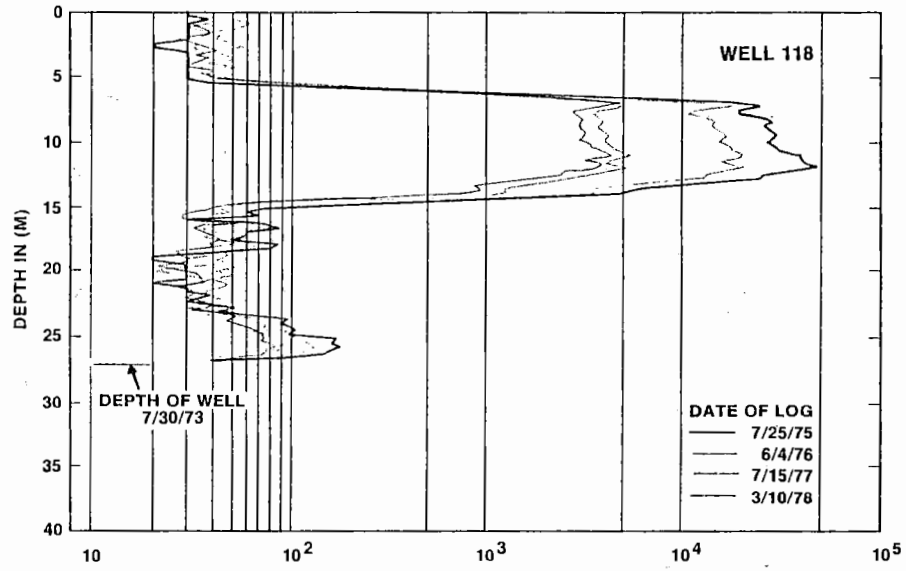
WELL 118
DEPTH OF WELL
7/30/73
DATE OF LOG
7/25/75
6/4/76
7/15/77
3/10/78
DEPTH IN (M)
10
10^2
10^3
10^4
10^5

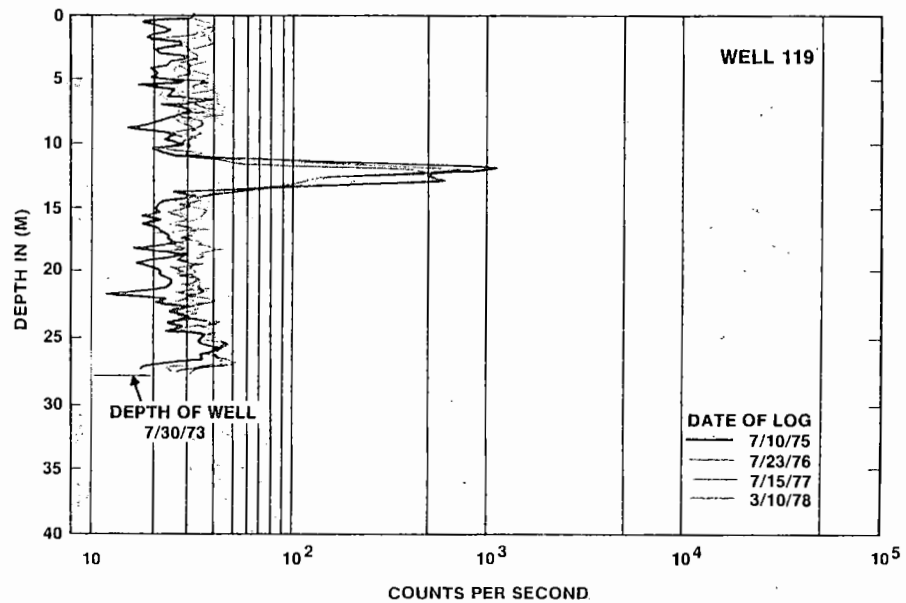
WELL 119
DEPTH OF WELL
7/30/73
DATE OF LOG
7/10/75
7/23/76
7/15/77
3/10/78
DEPTH IN (M)
10
10^2
10^3
10^4
10^5
COUNTS PER SECOND

THIS PAGE INTENTIONALLY
LEFT BLANK

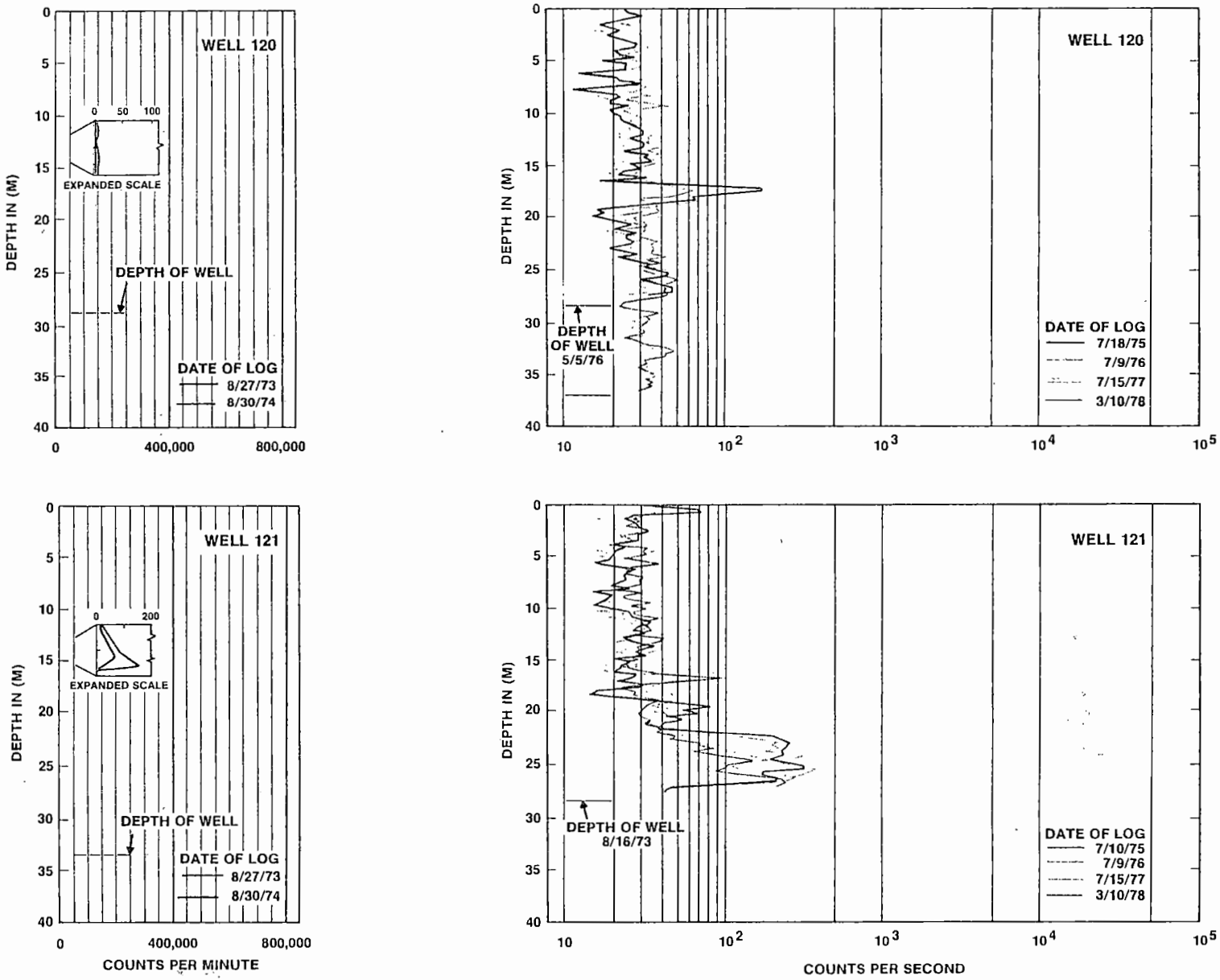
WELL 120
EXPANDED SCALE
0 50 100
DEPTH OF WELL
DATE OF LOG
8/27/73
8/30/74
DEPTH IN (M)
0 400,000 800,000
WELL 120
DEPTH OF WELL 5/5/76
DATE OF LOG
7/18/75
7/9/76
7/15/77
3/10/78
10 10^2 10^3 10^4 10^5
WELL 121
EXPANDED SCALE
0 200
DEPTH OF WELL
DATE OF LOG
8/27/73
8/30/74
COUNTS PER MINUTE
WELL 121
DEPTH OF WELL 8/16/73
DATE OF LOG
7/10/75
7/9/76
7/15/77
3/10/78
COUNTS PER SECOND

THIS PAGE INTENTIONALLY
LEFT BLANK

9 2 1 2 4 5 5 1 3 8 6

^{106}Ru, ^{144}Ce, ^{137}Cs, ^{60}Co and ^{154}Eu
FOR SEDIMENT CONCENTRATIONS FOR 1977 AND 1978

1. 1977 data points are connected by straight lines (1 Nov 77).
2. 1978 data points are not connected (1 May 78).
3. 1977 ^{106}Ru data points must be multiplied by a factor of 0.707 to correct for radioactive decay for direct comparison with the 1978 data points.
4. 1977 ^{144}Ce data points must be multiplied by a factor of 0.638 to correct for radioactive decay for direct comparison with the 1978 data points.
5. Radionuclide concentrations in Wells 162 and 164 through 167 could not be measured in 1978 because these wells were grouted in 1977.
6. All well numbers are preceded by 299-W10-.
7. Less than values are below the minimum detectable activity for a radionuclide in the gamma radiation field of the measurement.

9 2 1 2 4 6 6 1 3 9 7

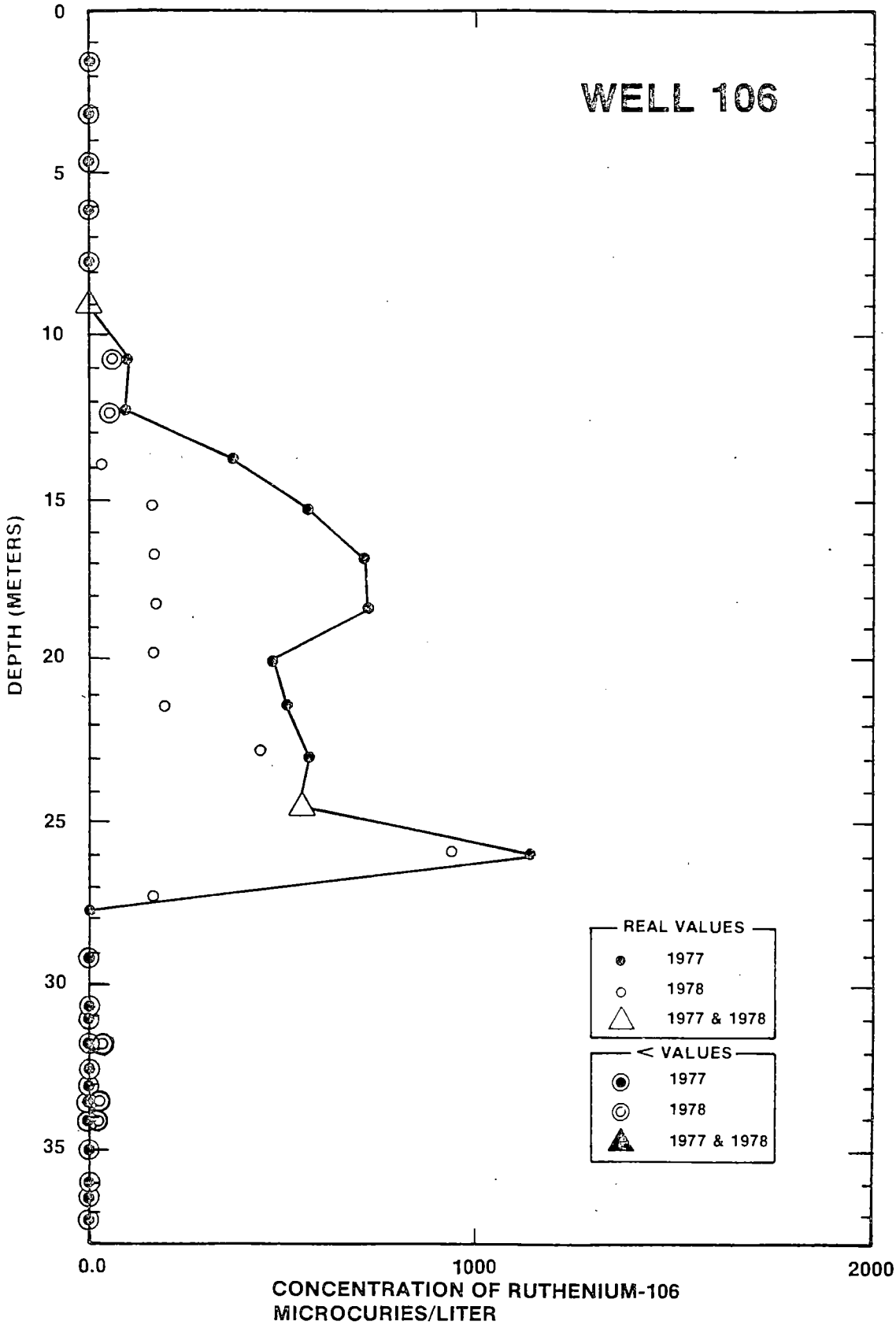
WELL 106
DEPTH (METERS)
0
5
10
15
20
25
30
35
0.0
1000
2000
CONCENTRATION OF RUTHENIUM-106
MICROCURIES/LITER
REAL VALUES
1977
1978
1977 & 1978
< VALUES
1977
1978
1977 & 1978

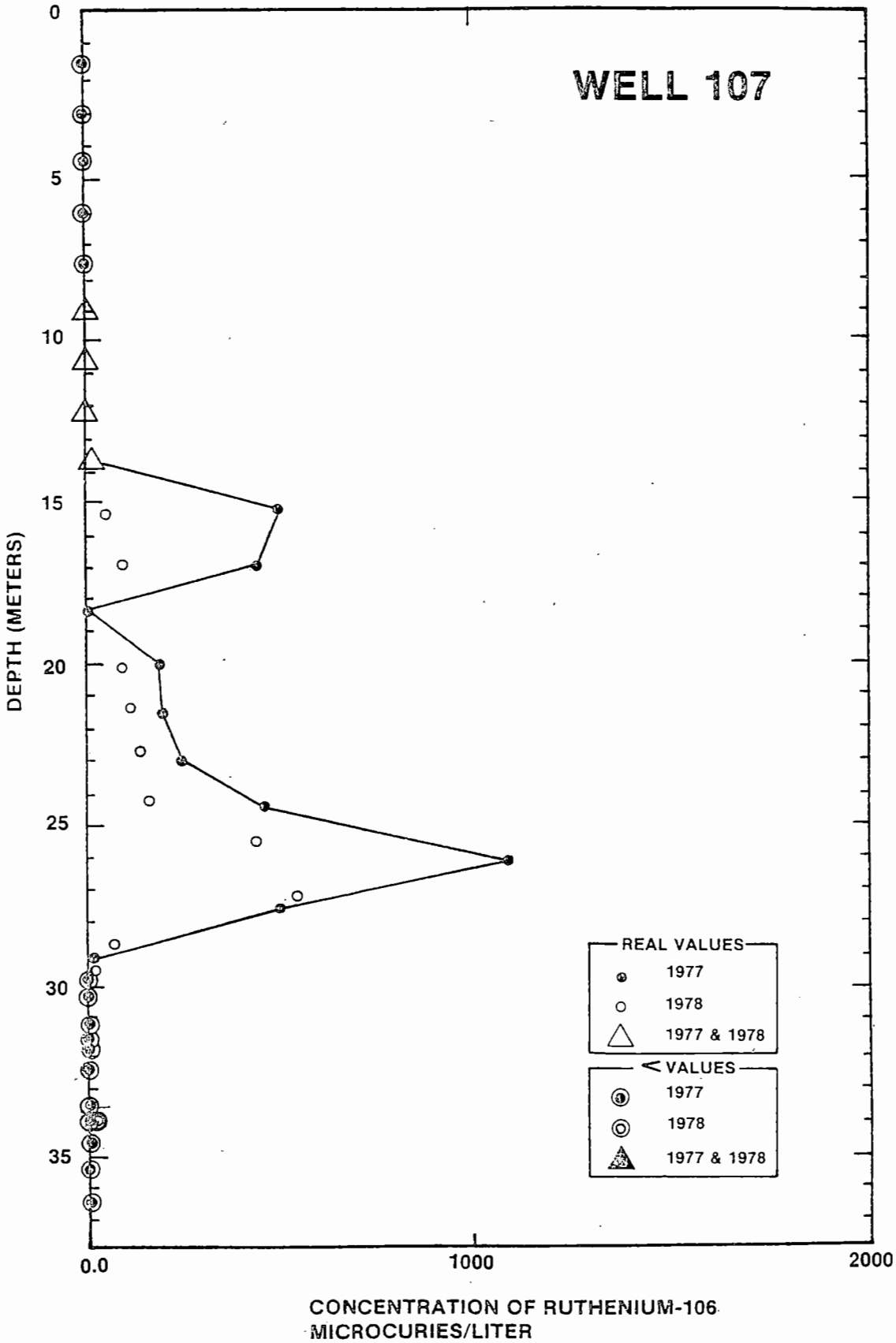
WELL 107
DEPTH (METERS)
0
5
10
15
20
25
30
35
0.0
1000
2000
CONCENTRATION OF RUTHENIUM-106
MICROCURIES/LITER
REAL VALUES
1977
1978
1977 & 1978
< VALUES
1977
1978
1977 & 1978

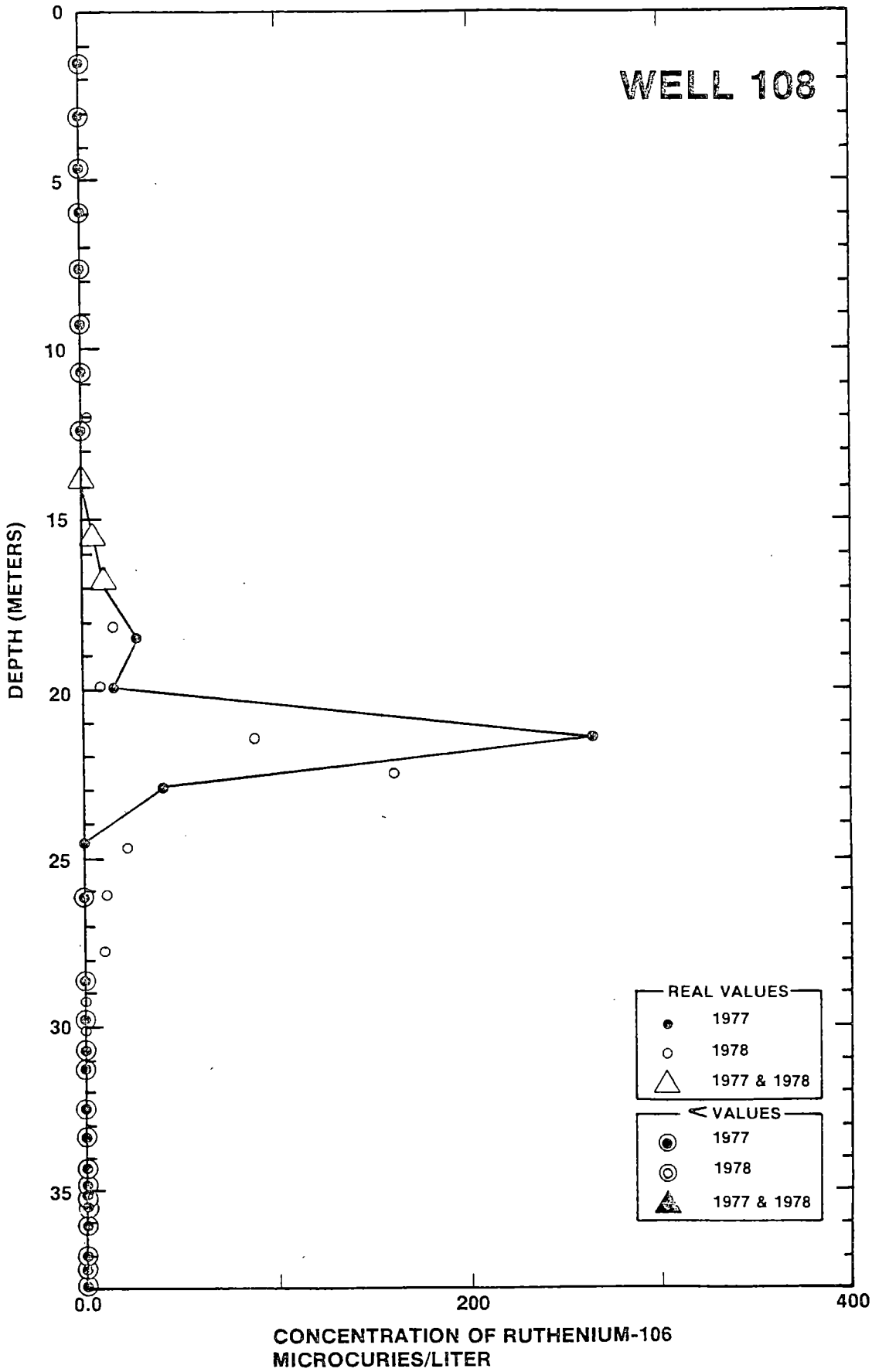
WELL 108
DEPTH (METERS)
0
5
10
15
20
25
30
35
0.0
200
400
CONCENTRATION OF RUTHENIUM-106
MICROCURIES/LITER
REAL VALUES
1977
1978
1977 & 1978
< VALUES
1977
1978
1977 & 1978

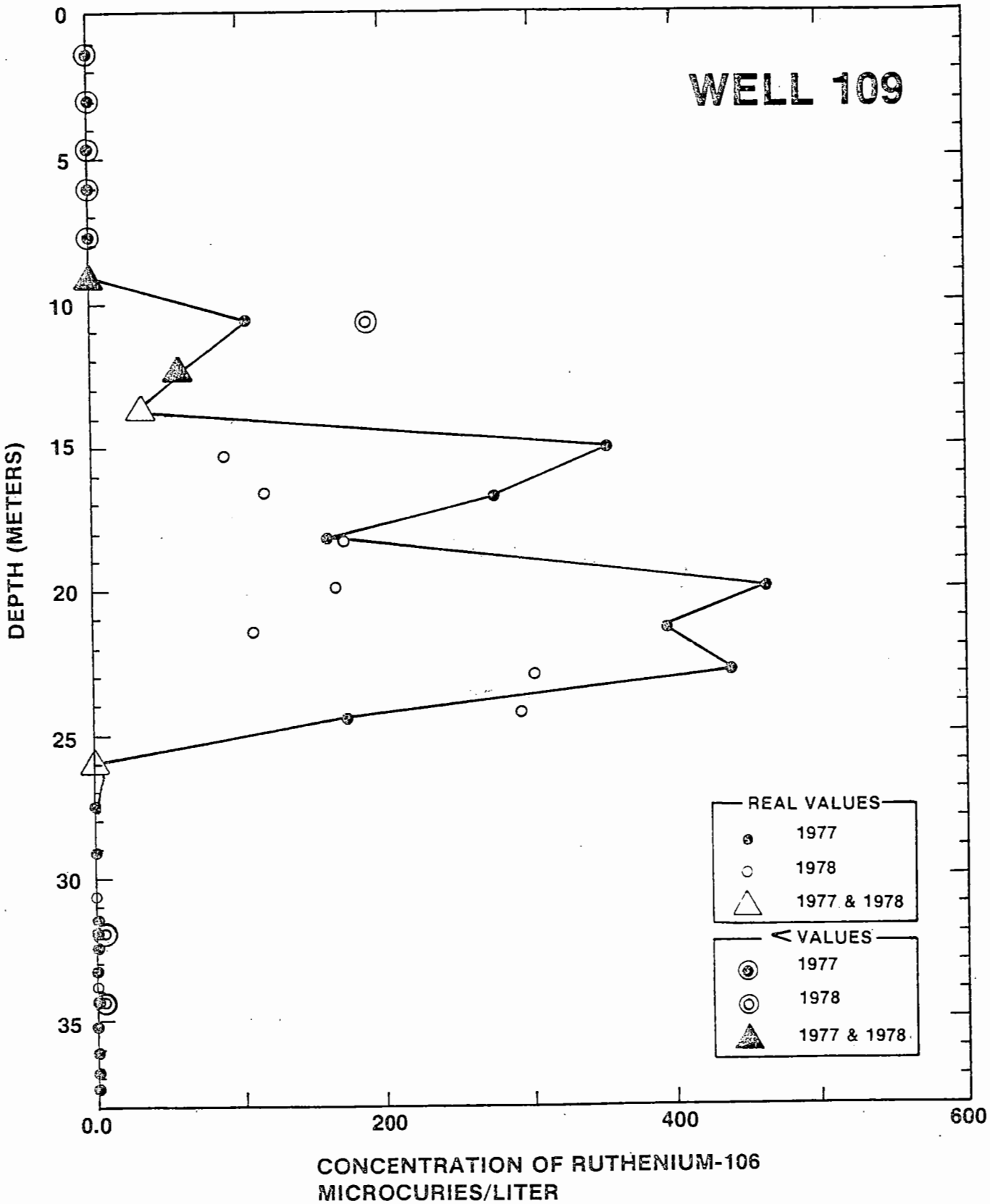
WELL 109
DEPTH (METERS)
0
5
10
15
20
25
30
35
0.0
200
400
600
CONCENTRATION OF RUTHENIUM-106
MICROCURIES/LITER
REAL VALUES
1977
1978
1977 & 1978
< VALUES
1977
1978
1977 & 1978

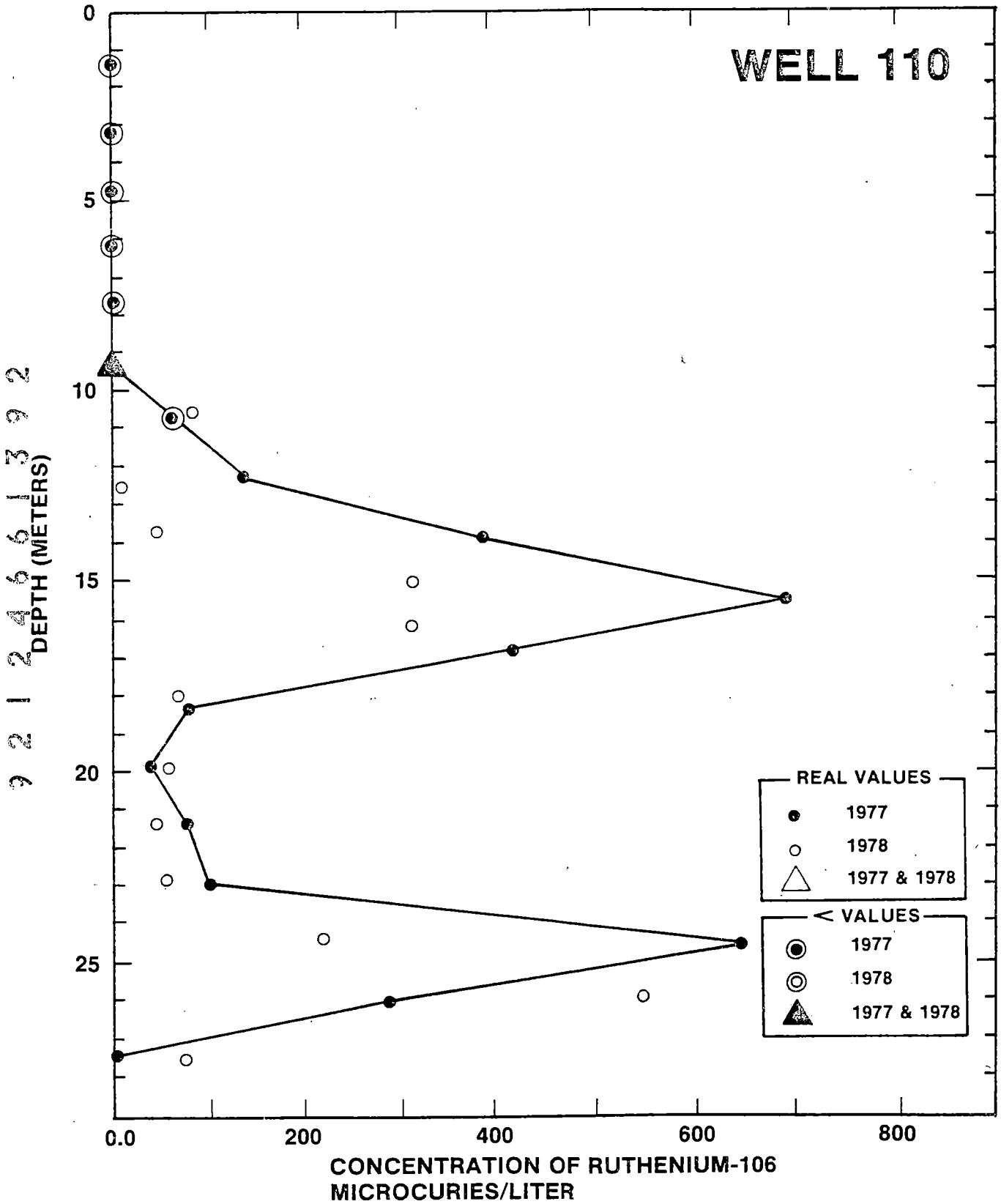
WELL 110
DEPTH (METERS)
0
5
10
15
20
25
0.0
200
400
600
800
CONCENTRATION OF RUTHENIUM-106
MICROCURIES/LITER
REAL VALUES
1977
1978
1977 & 1978
< VALUES
1977
1978
1977 & 1978

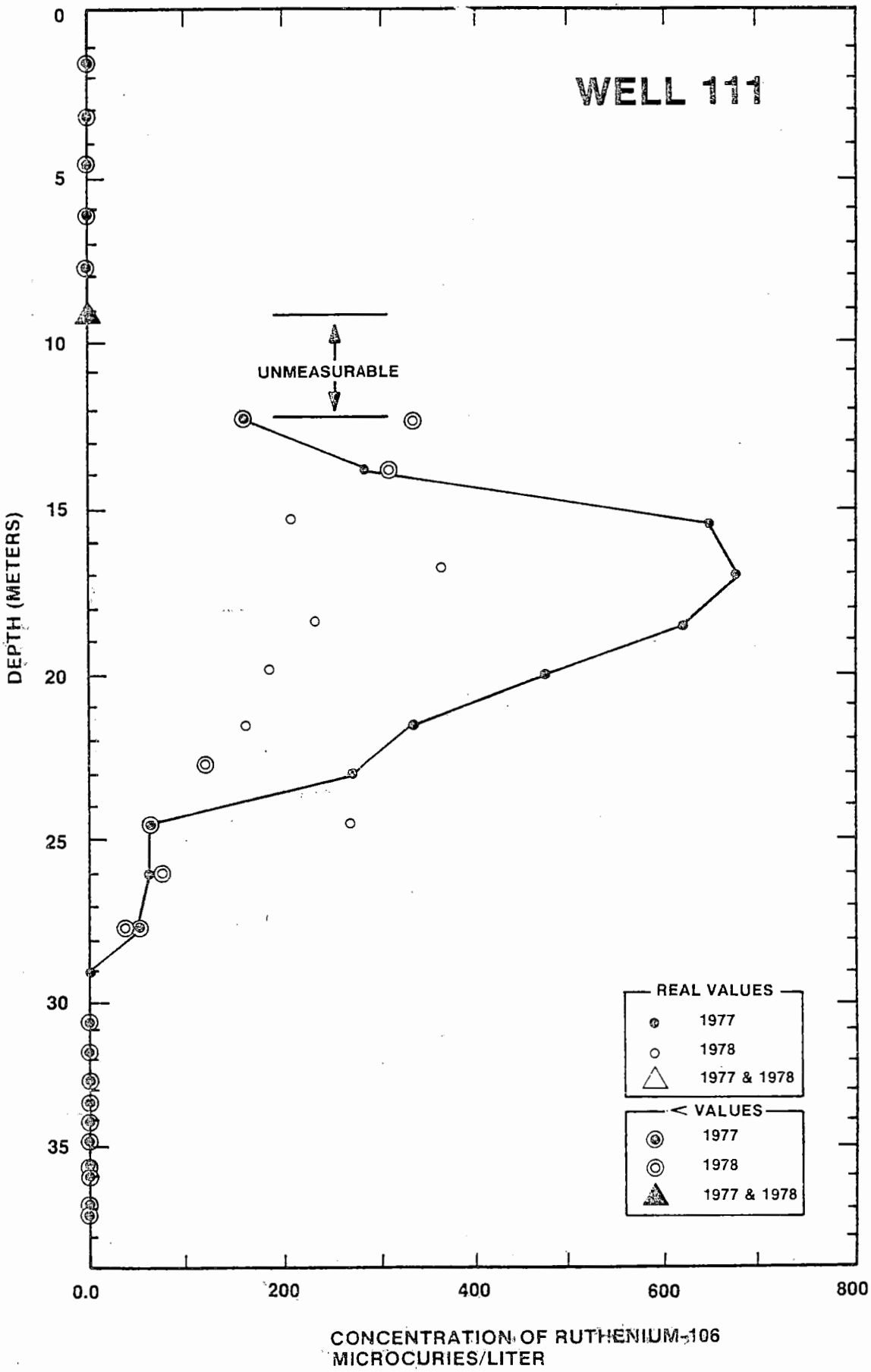
WELL 111
UNMEASURABLE
DEPTH (METERS)
0
5
10
15
20
25
30
35
0.0
200
400
600
800
CONCENTRATION OF RUTHENIUM-106
MICROCURIES/LITER
REAL VALUES
1977
1978
1977 & 1978
< VALUES
1977
1978
1977 & 1978

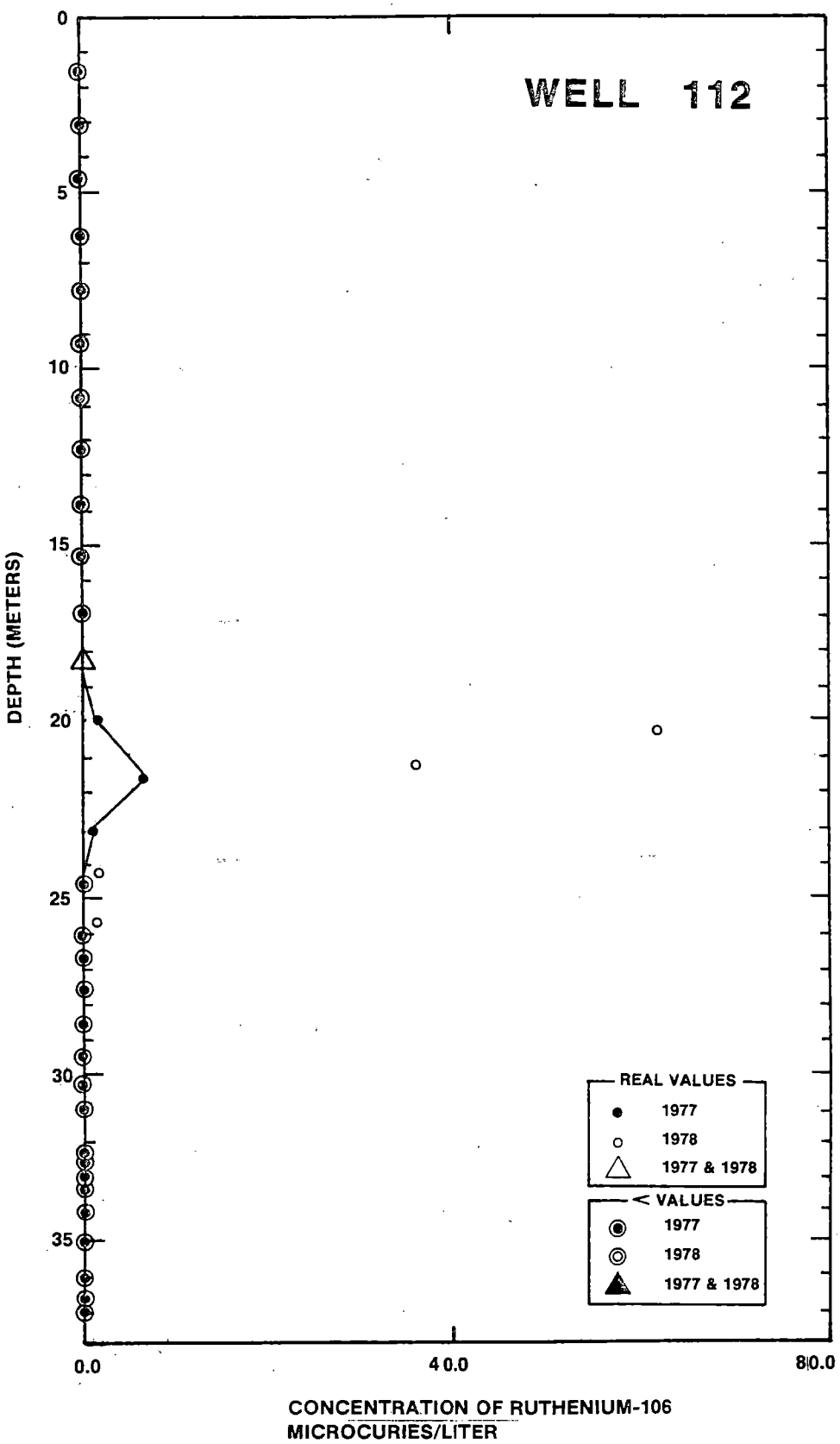

9 2 1 2 4 6 6 1 3 9 4

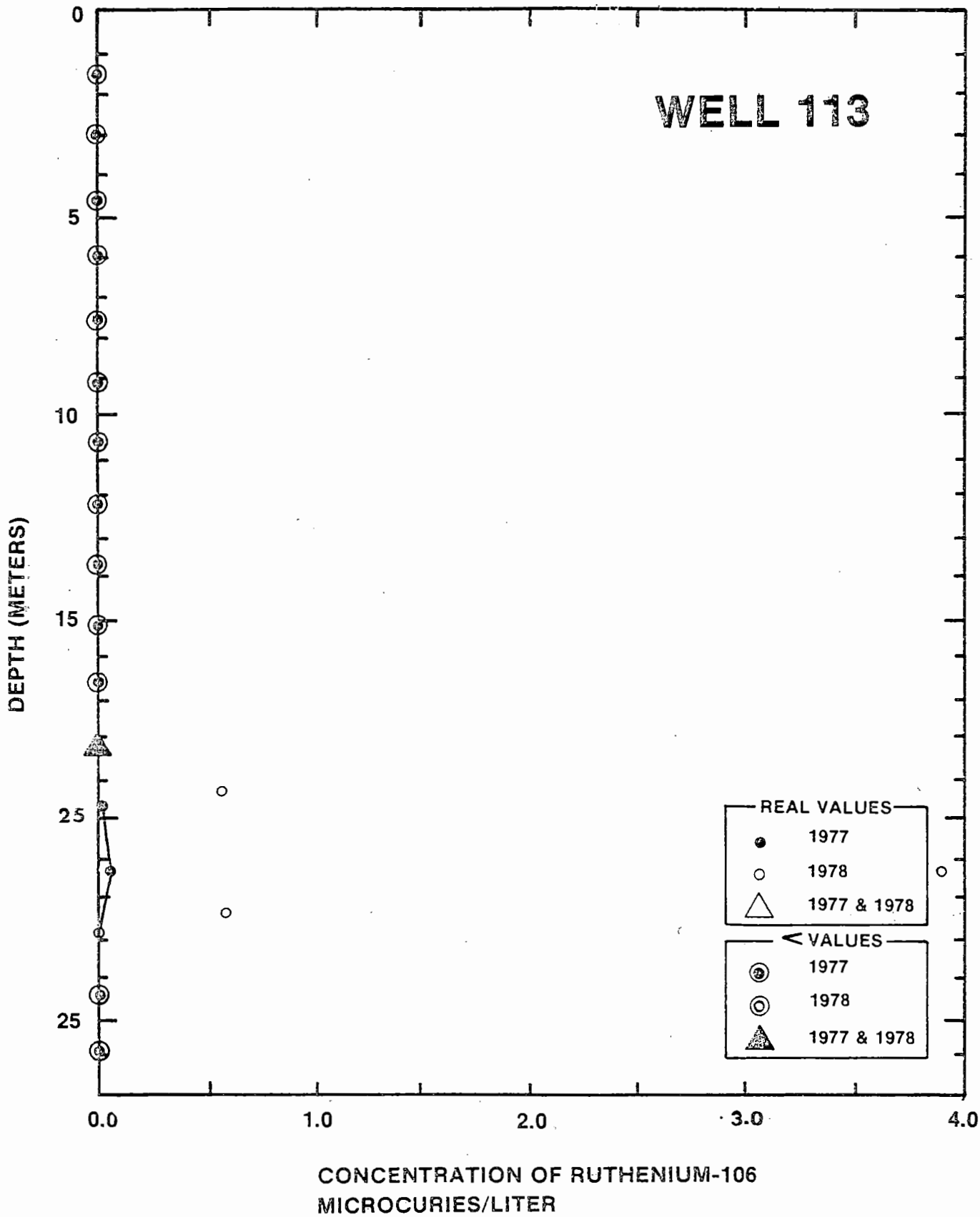

9 2 1 2 4 6 6 1 3 9 5

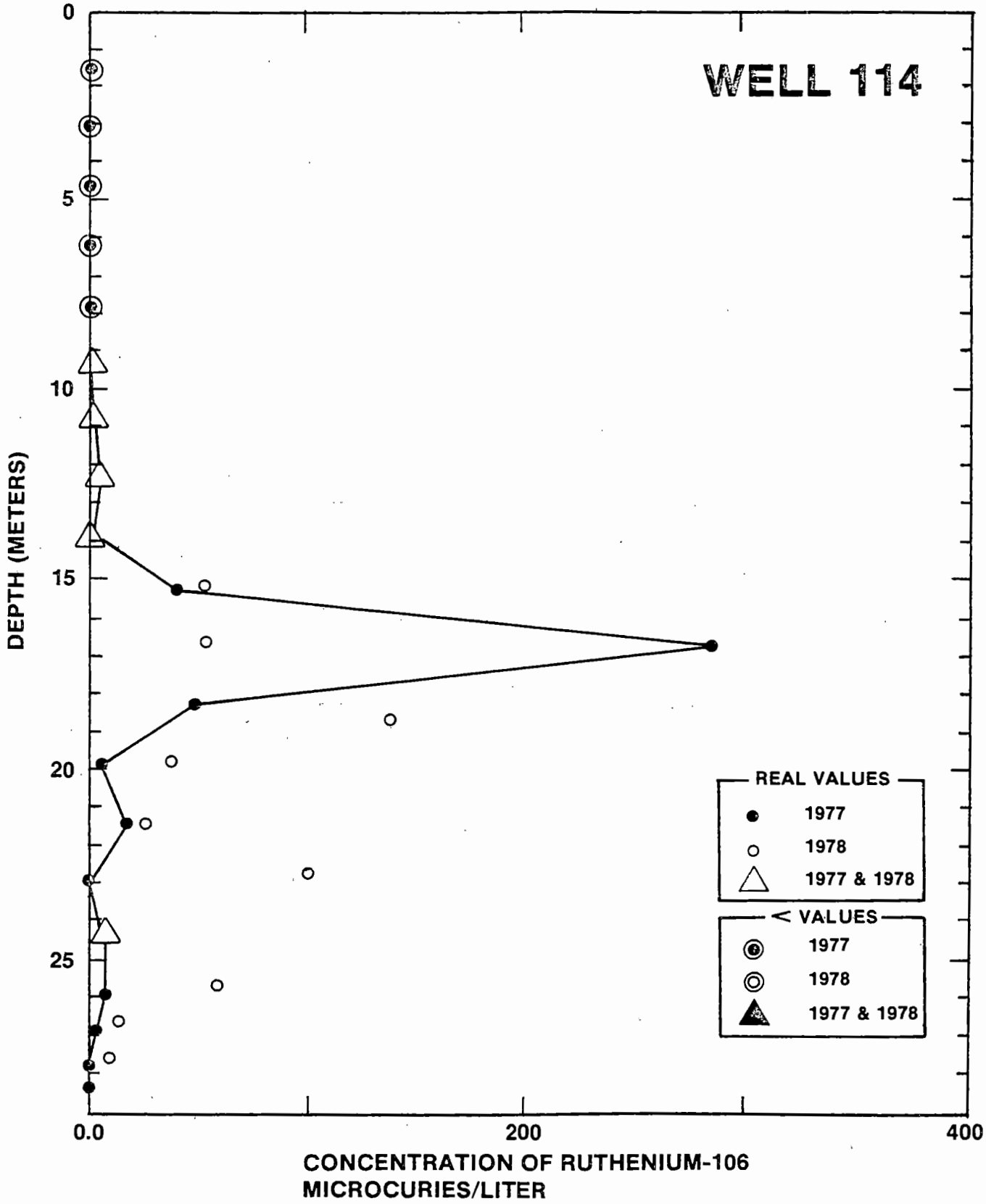

9 2 1 2 4 6 6 1 3 9 6

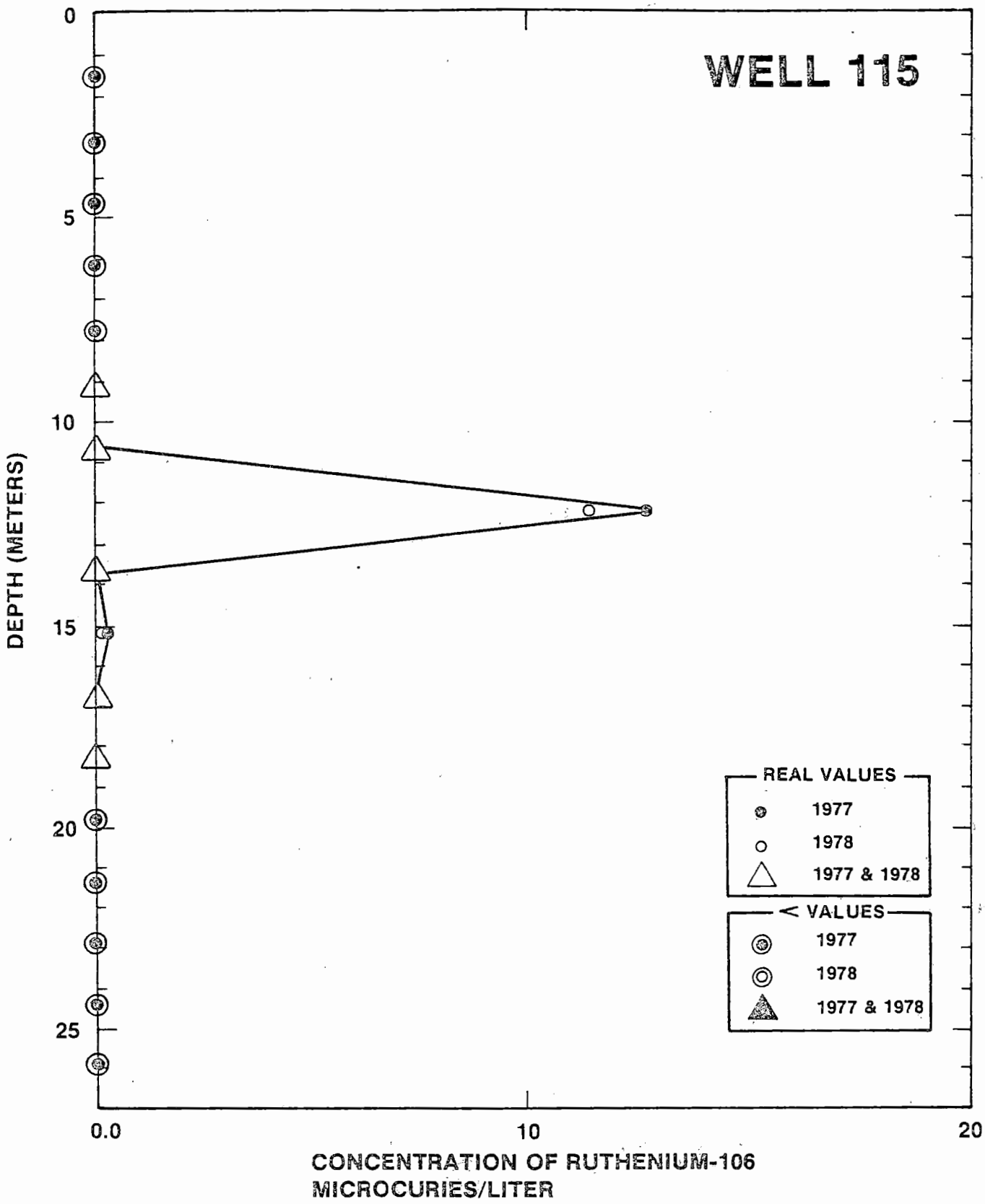

9 2 1 2 4 5 6 1 3 9 7

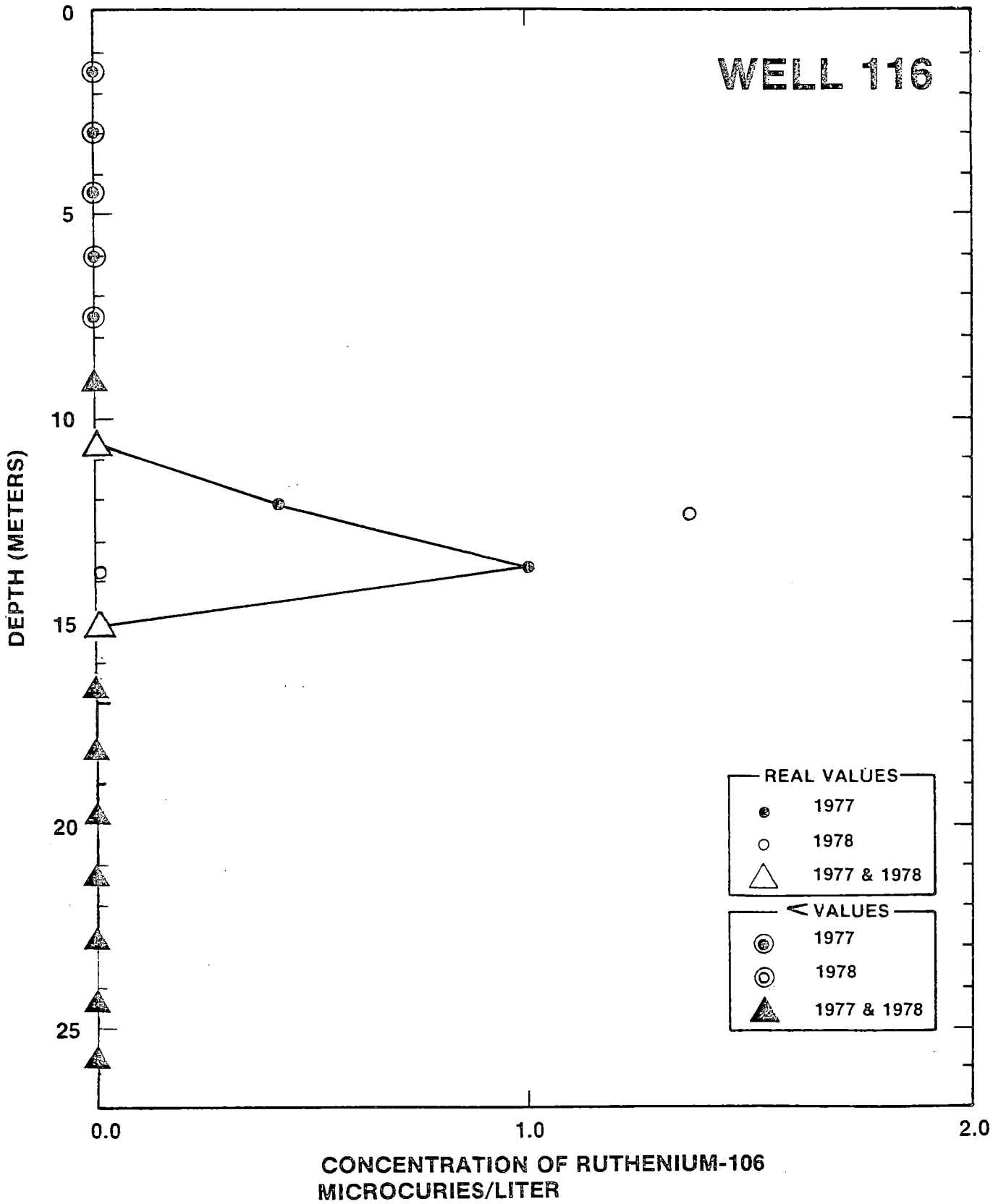

9 2 1 2 4 5 6 1 3 9 8

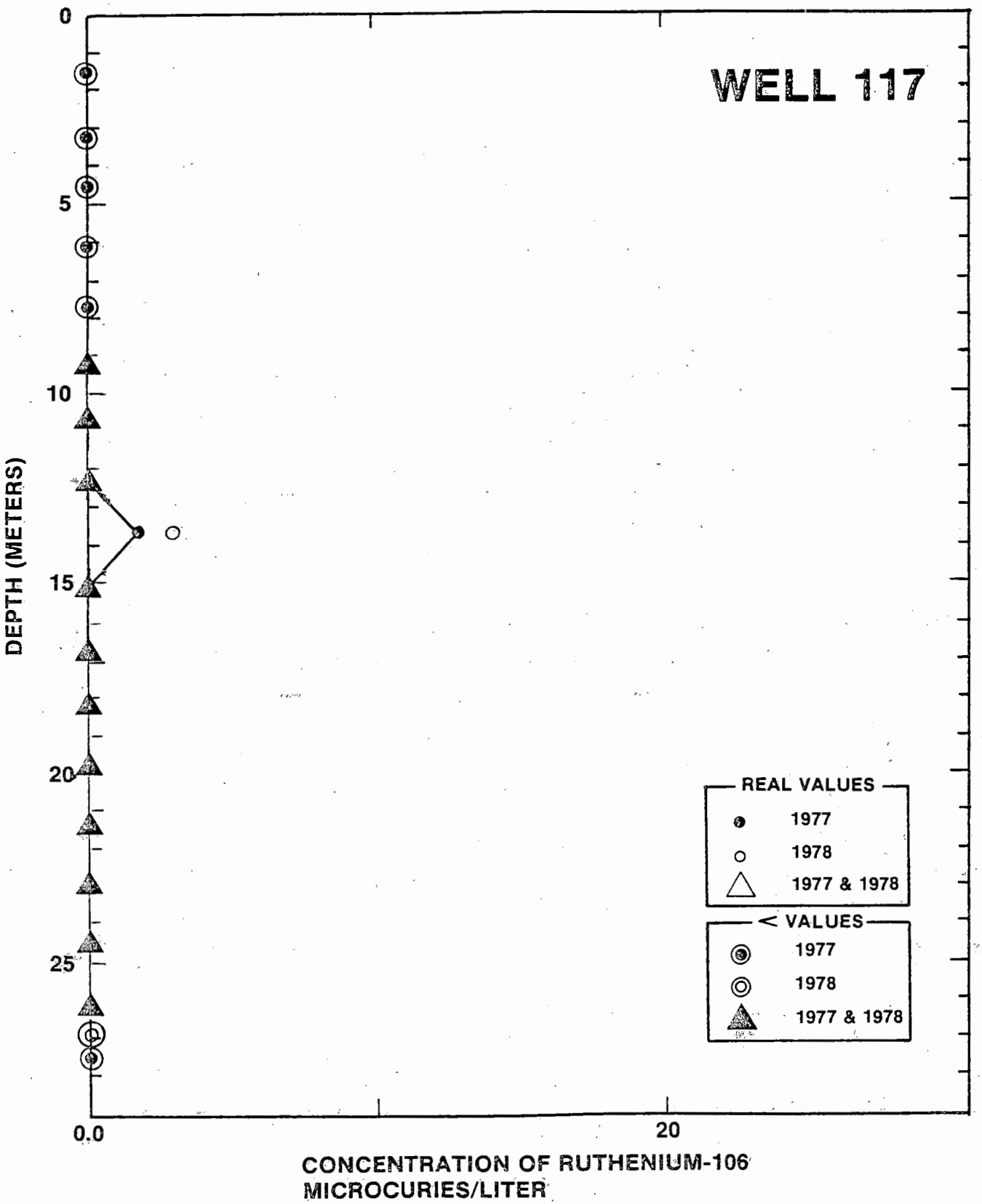

9 2 1 2 4 6 6 1 3 9 9

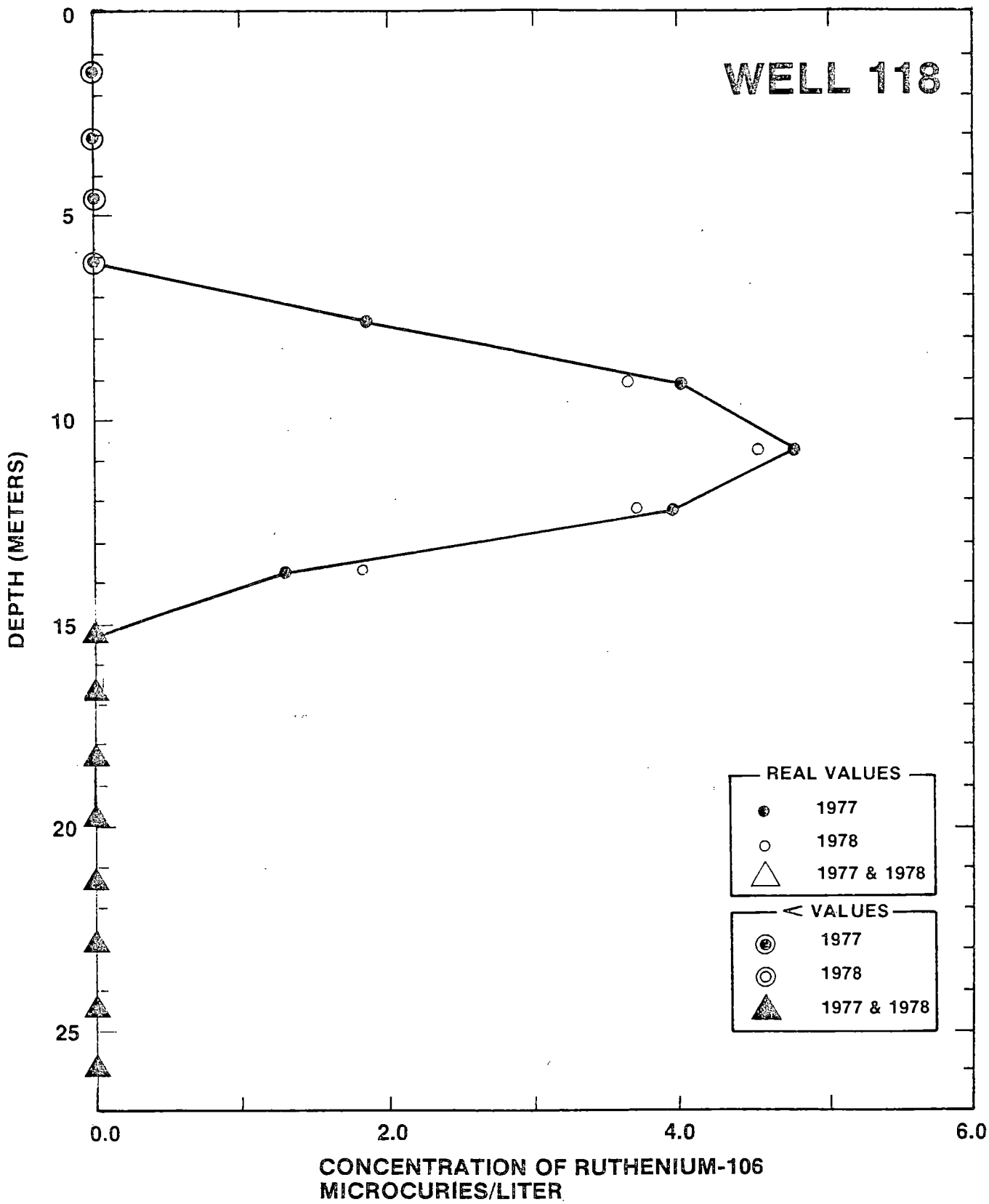

9 2 1 2 4 5 6 1 4 0 0

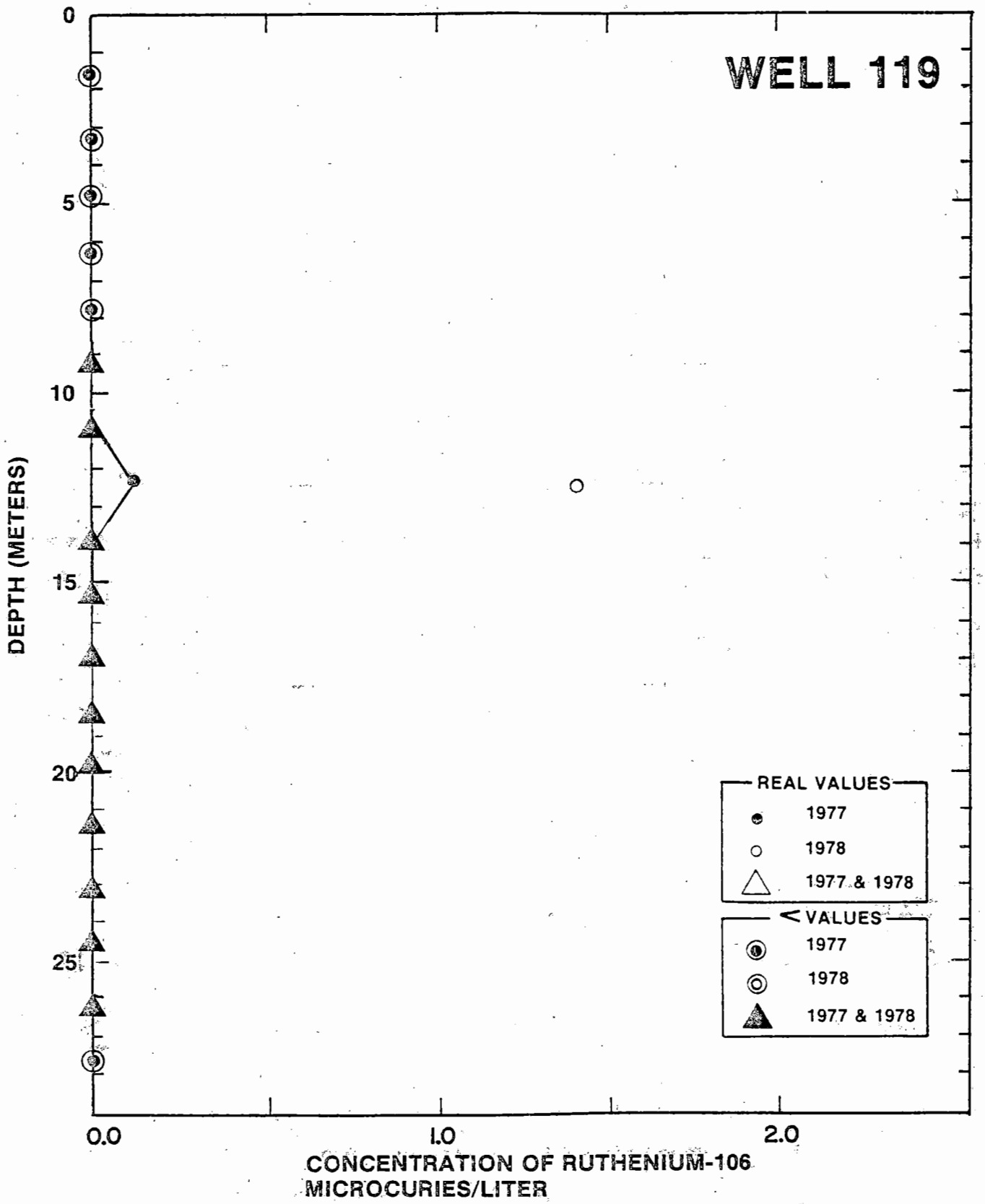

9 2 1 2 4 6 6 1 4 0 1

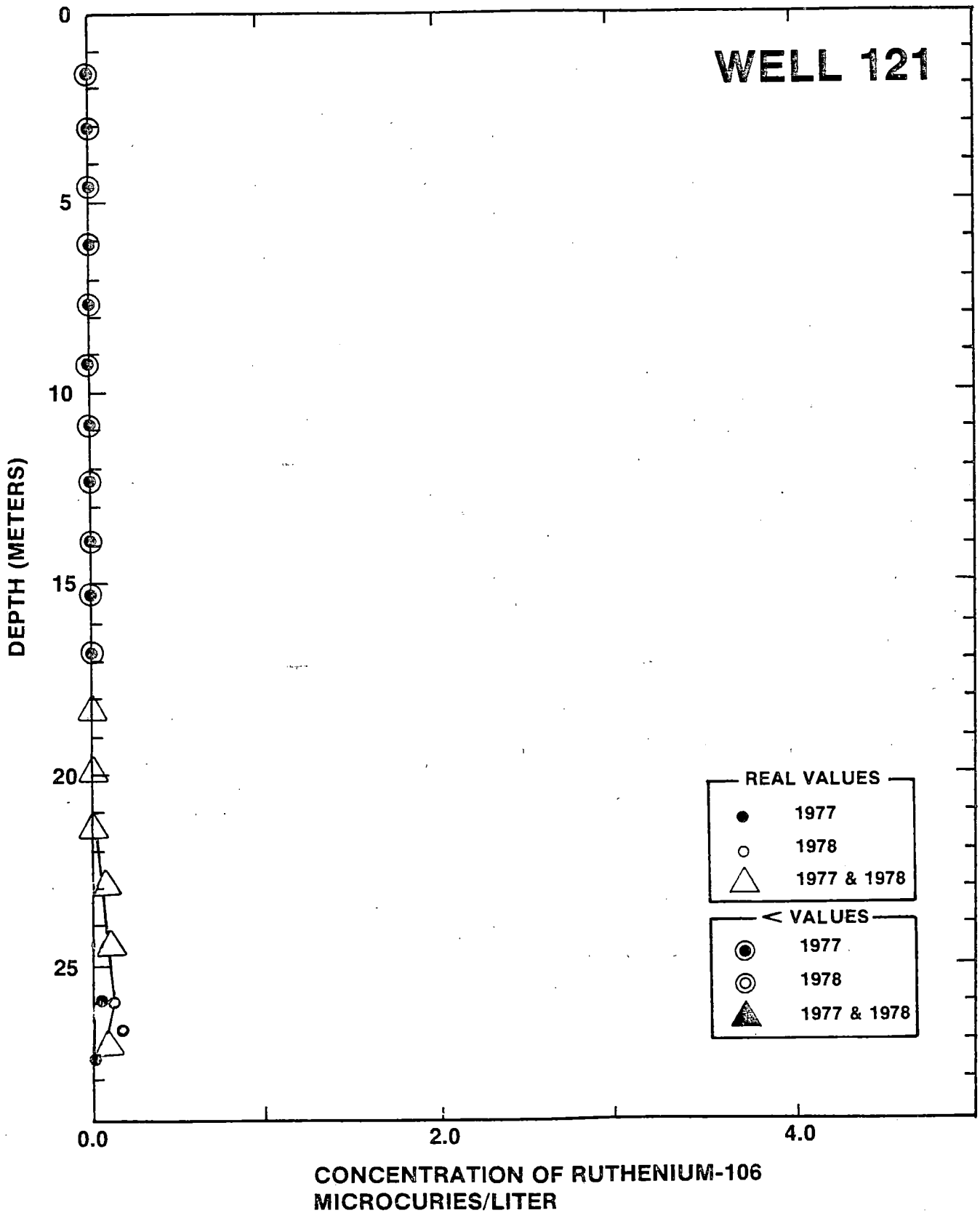

9 2 1 2 4 6 6 1 4 0 2

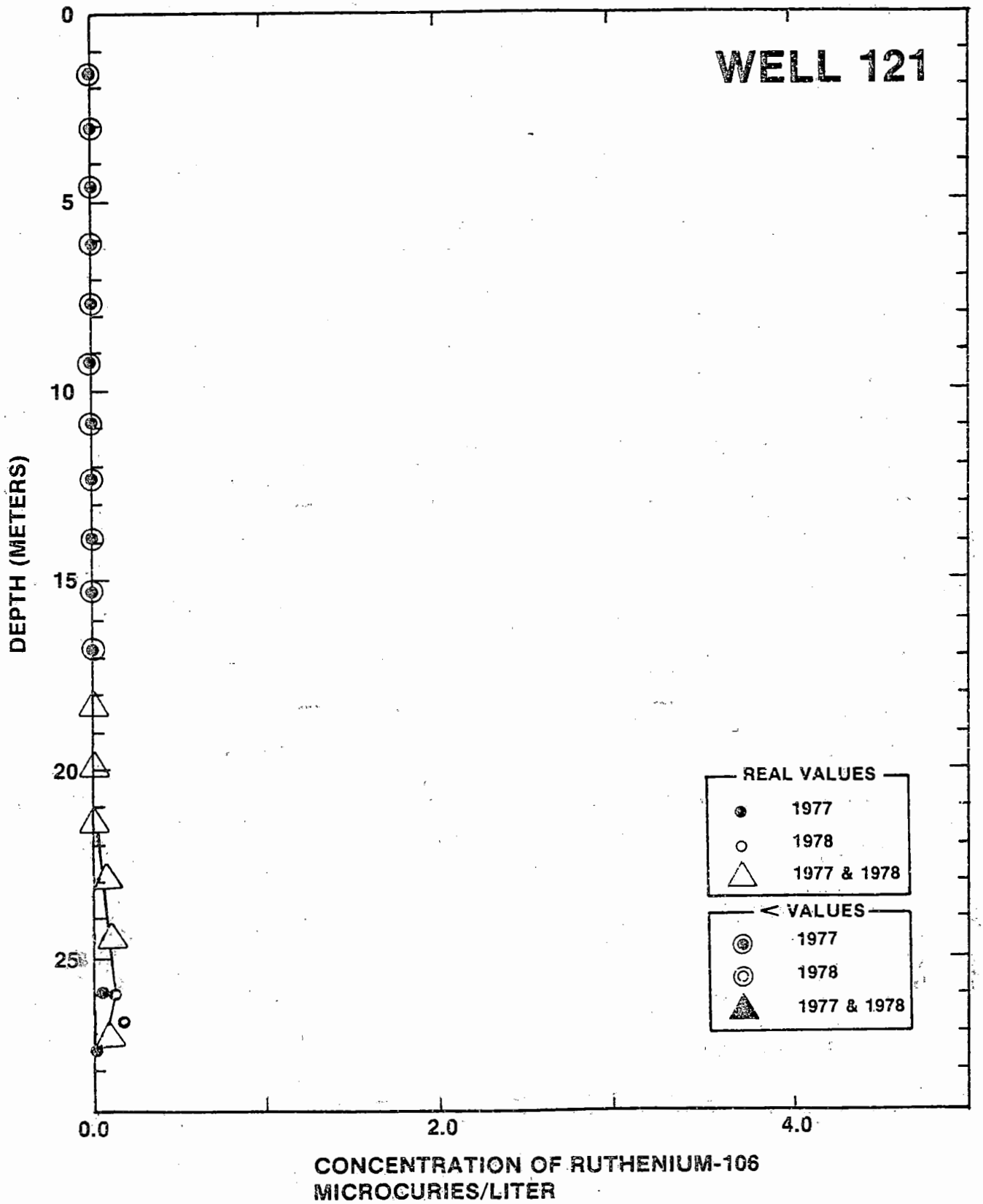

9 2 1 2 4 6 6 1 4 0 3

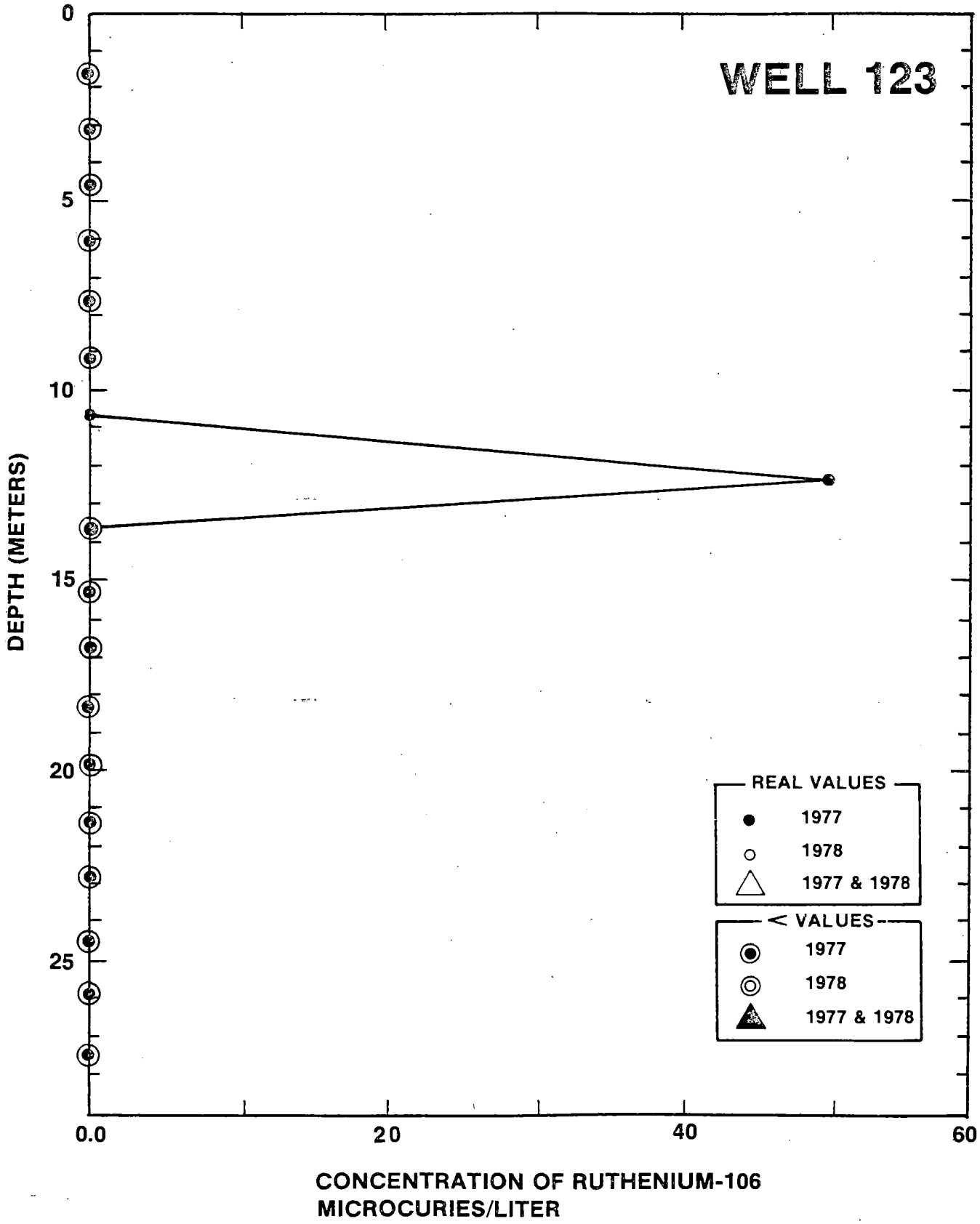

9 2 1 2 4 6 6 1 4 0 4

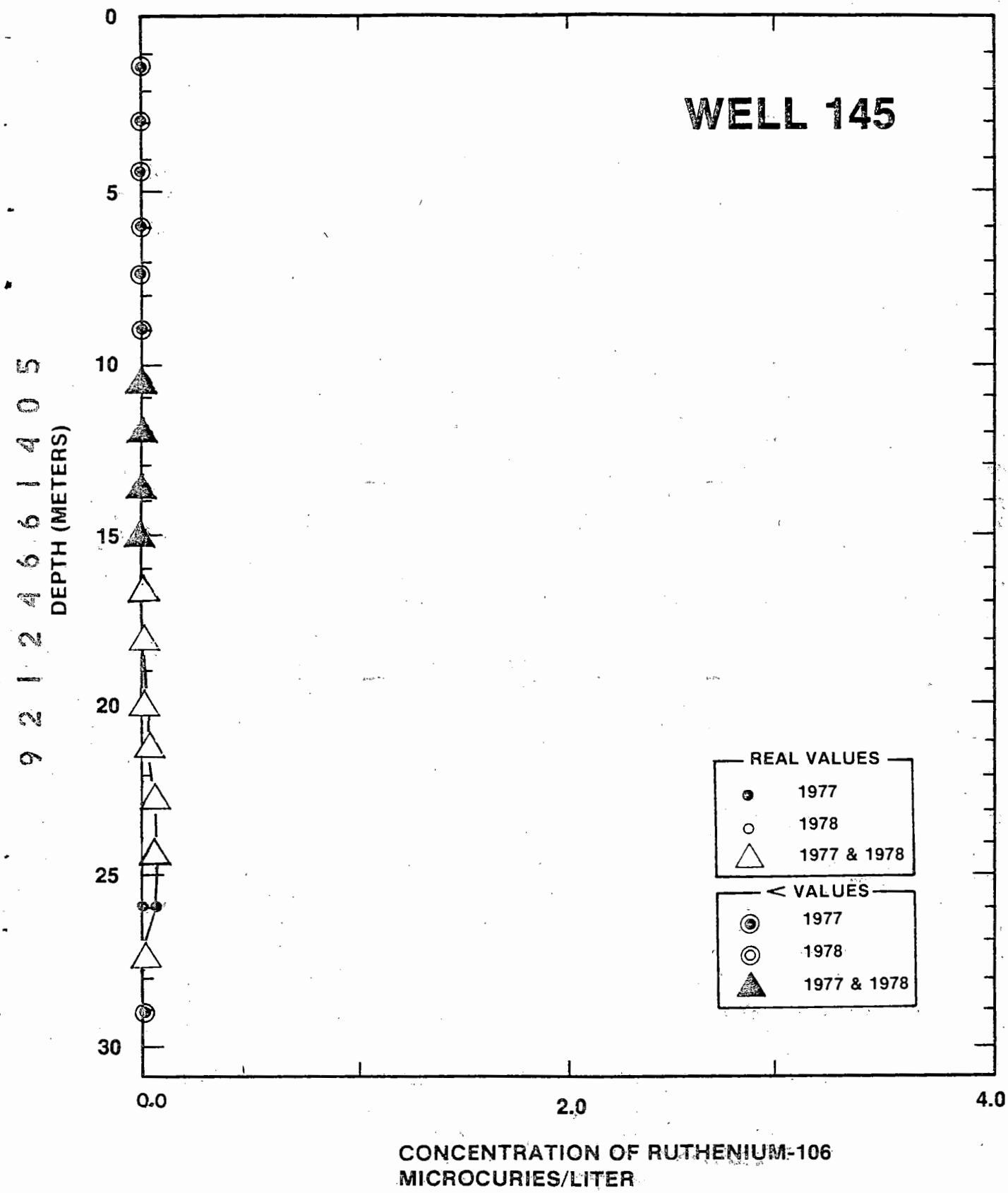
WELL 145
0
5
10
15
20
25
30
DEPTH (METERS)
0.0
2.0
4.0
CONCENTRATION OF RUTHENIUM-106
MICROCURIES/LITER
REAL VALUES
1977
1978
1977 & 1978
< VALUES
1977
1978
1977 & 1978

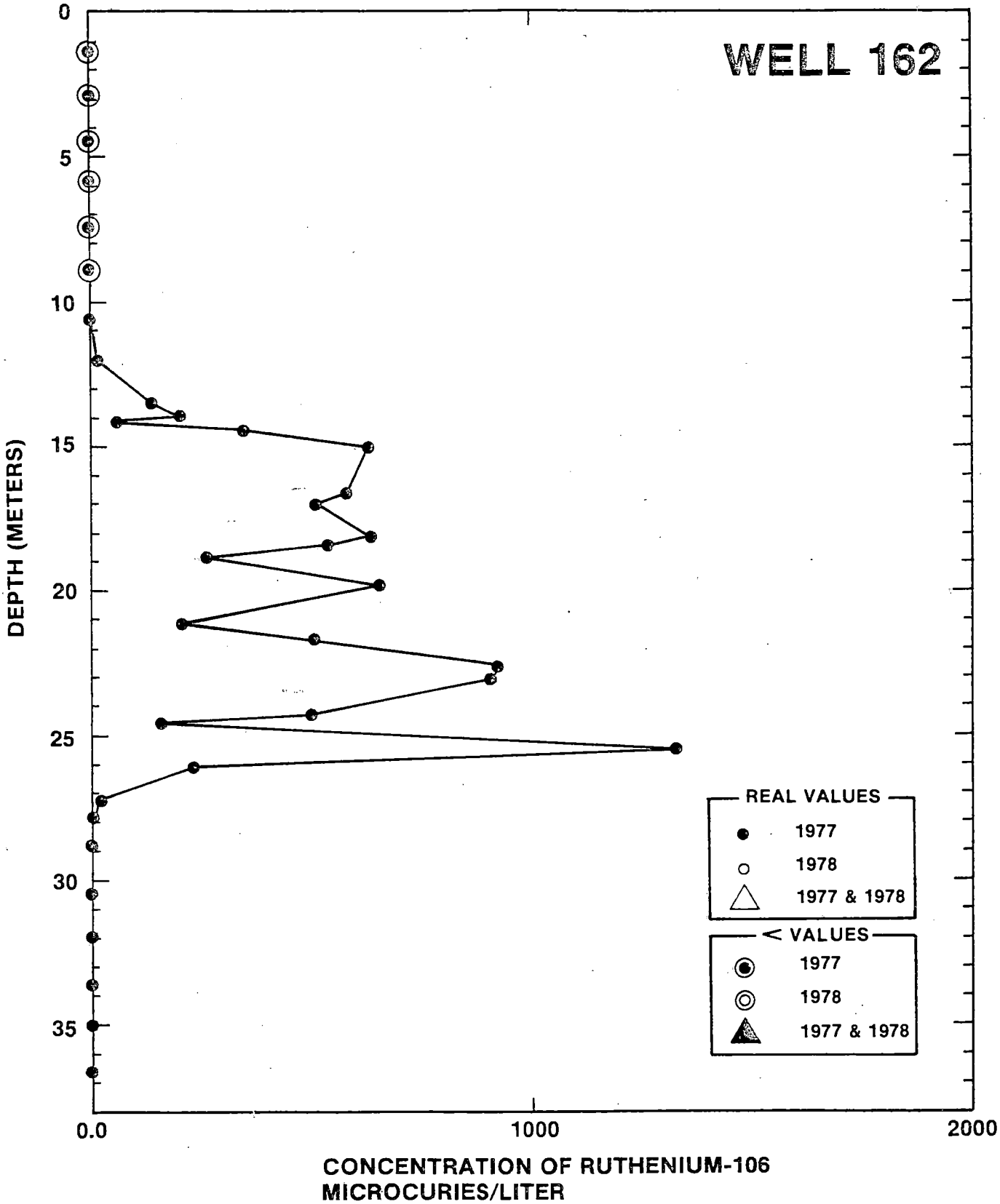

9 2 1 2 4 6 6 1 4 0 6

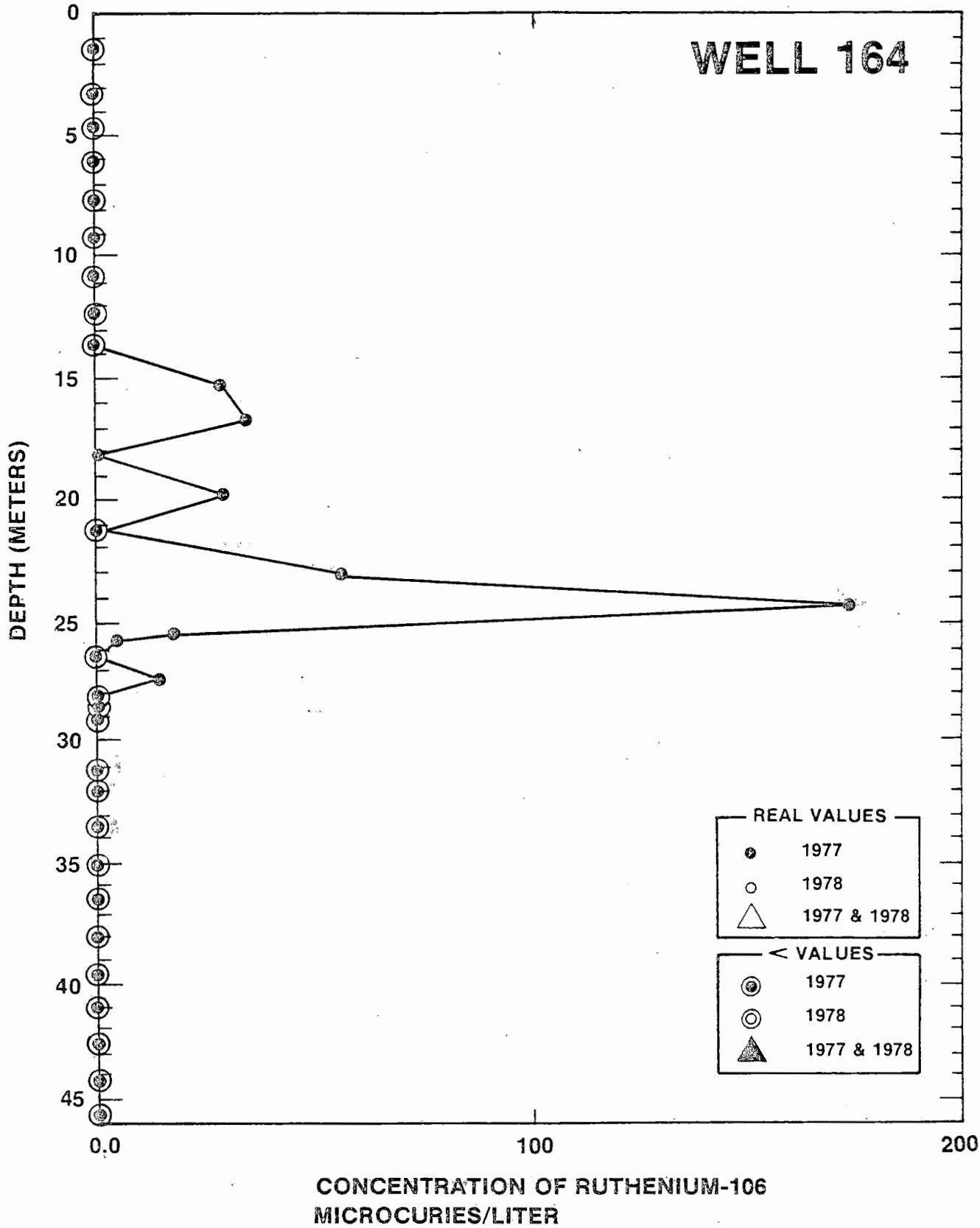

9 2 1 2 4 6 6 1 4 0 7

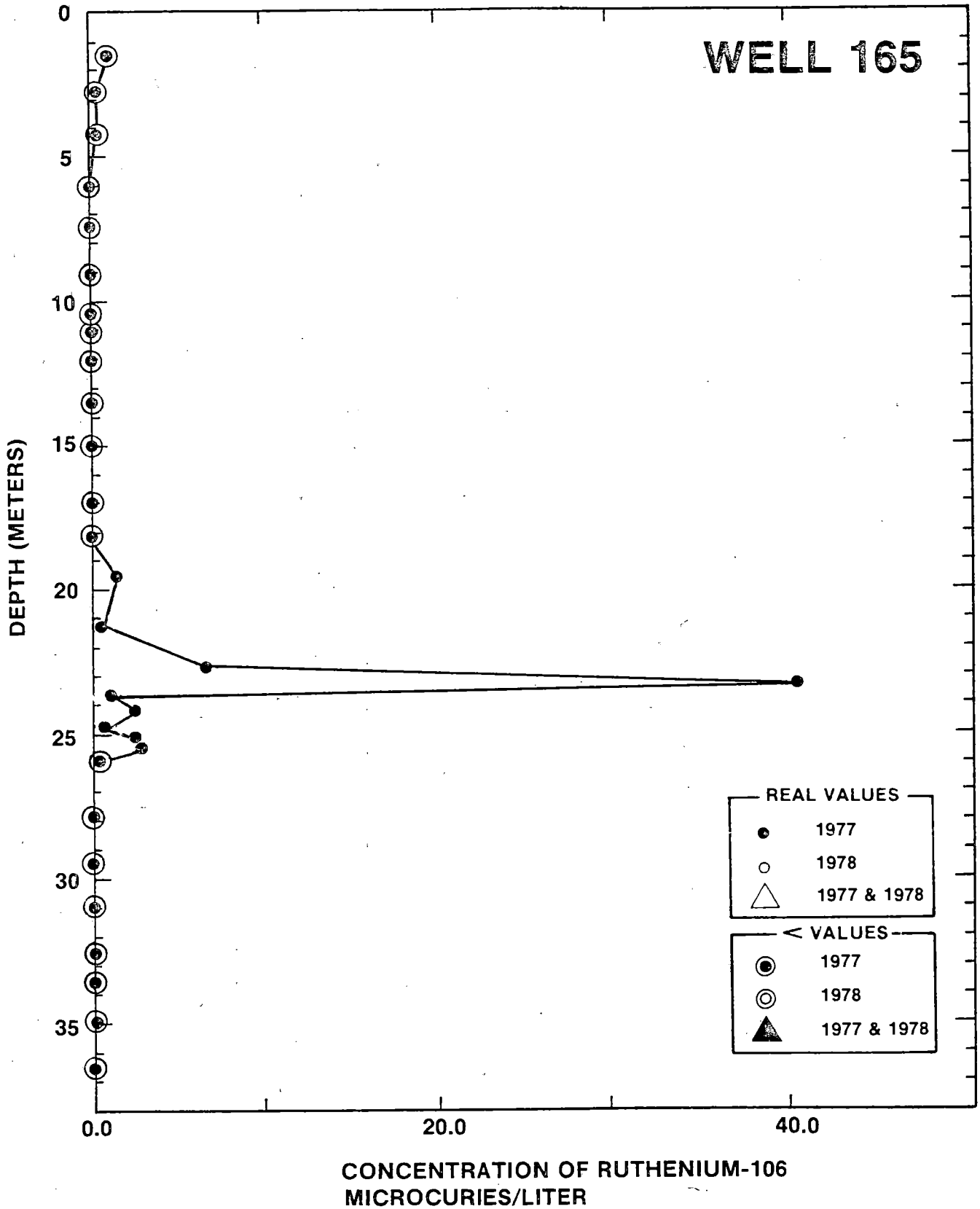

9 2 1 2 4 5 6 1 4 0 8

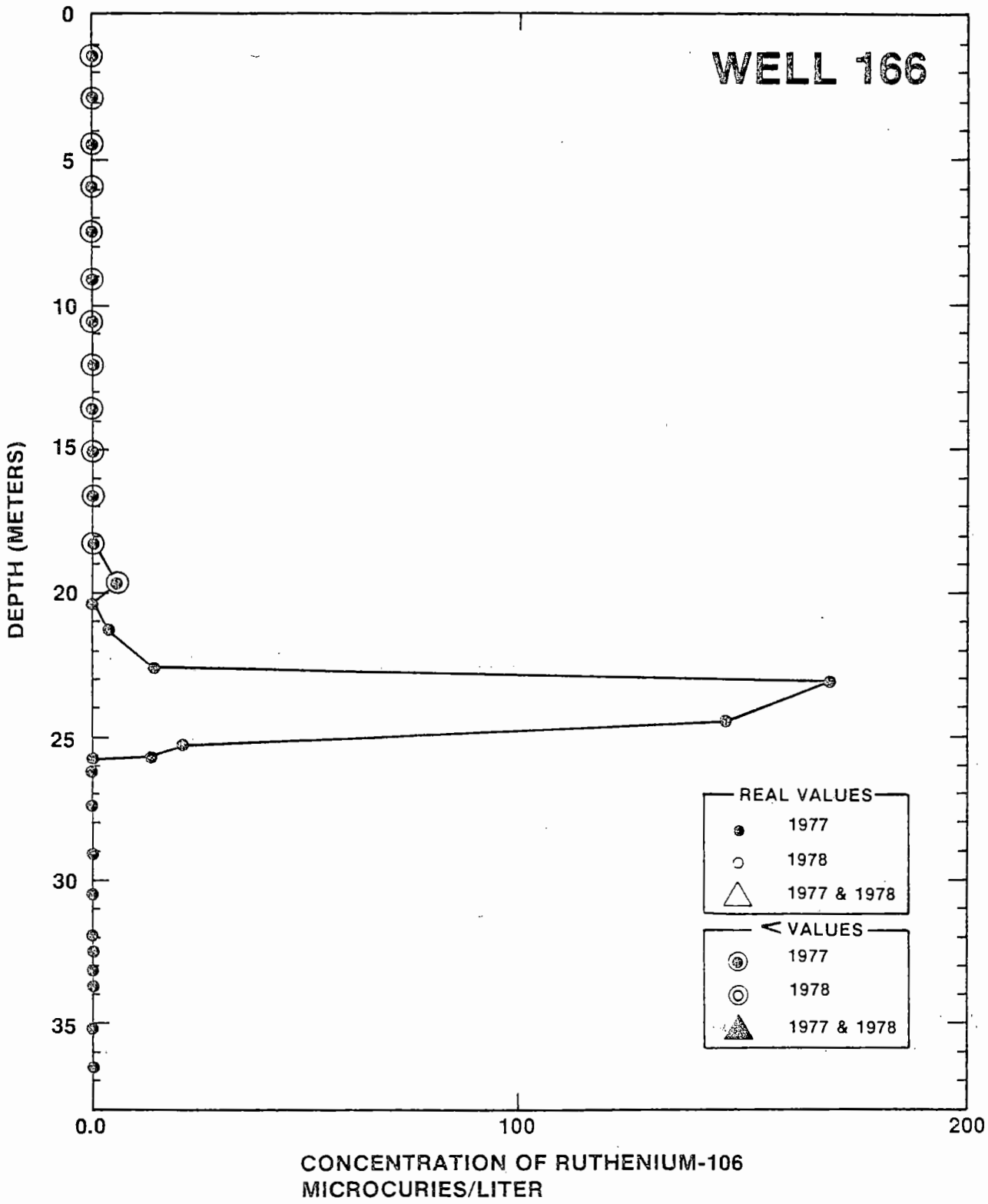

9212246614 09

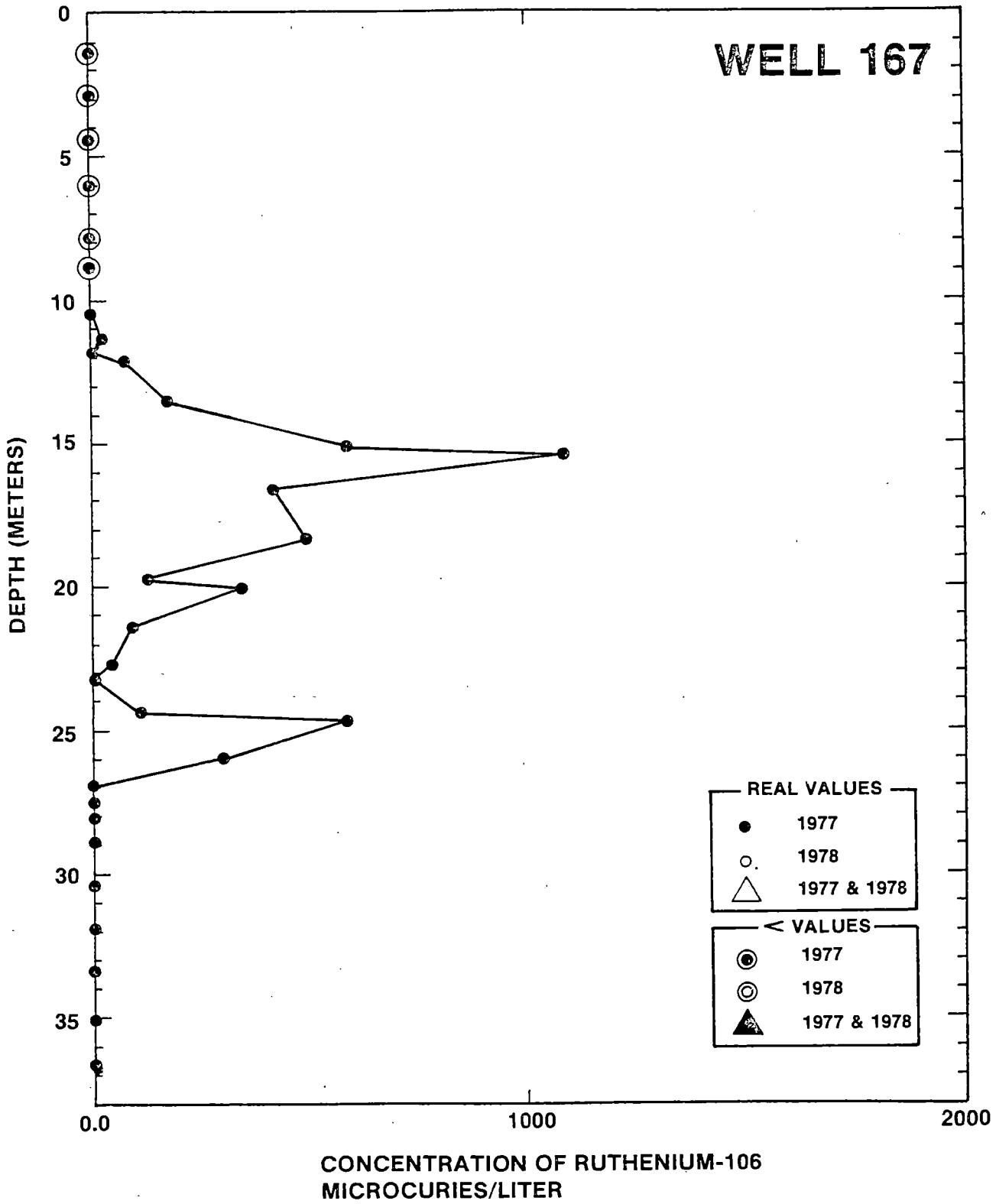

9 2 1 2 4 6 6 1 4 1 0

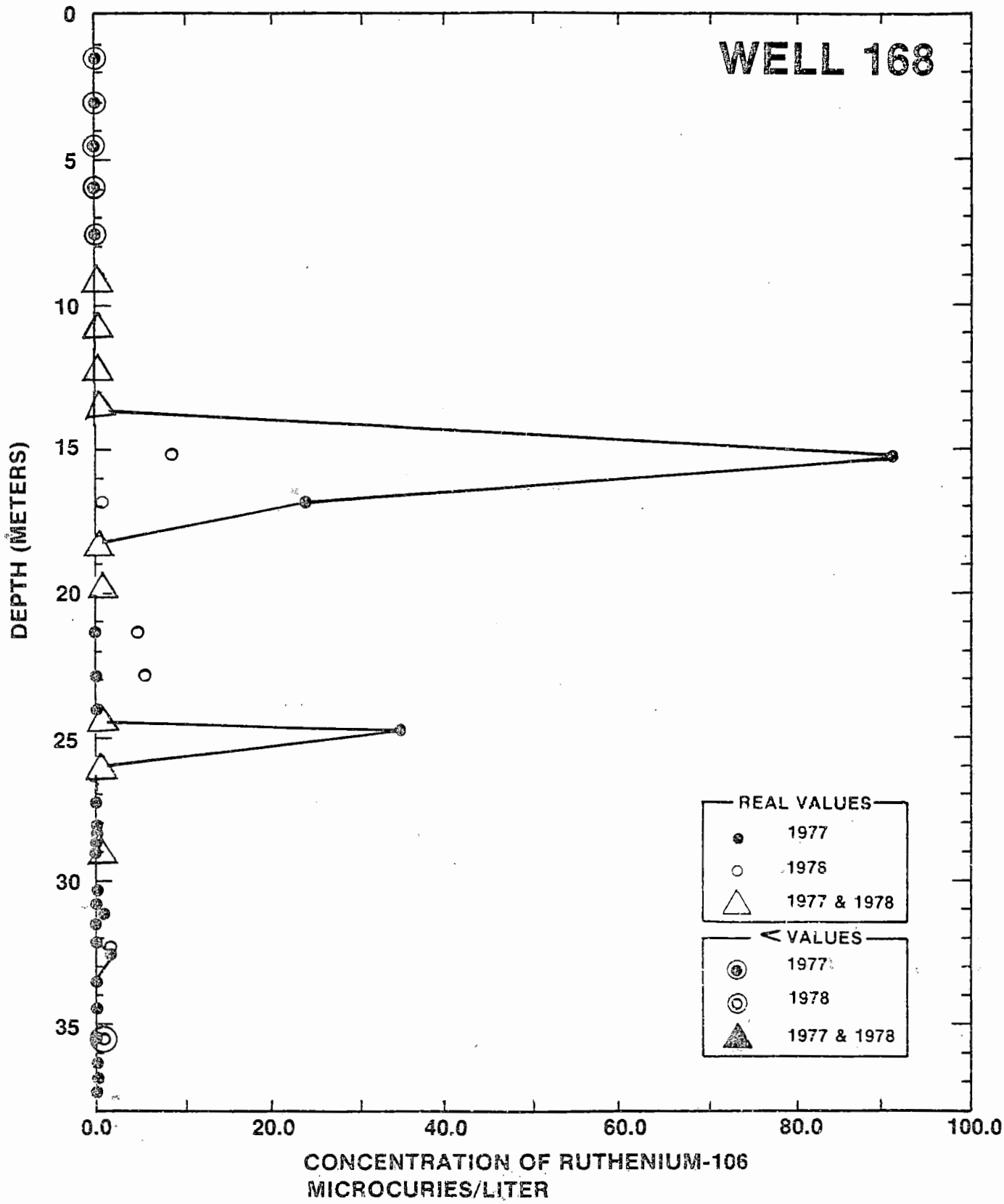
WELL 168
DEPTH (METERS)
0
5
10
15
20
25
30
35
0.0
20.0
40.0
60.0
80.0
100.0
CONCENTRATION OF RUTHENIUM-106
MICROCURIES/LITER
REAL VALUES
1977
1978
1977 & 1978
< VALUES
1977
1978
1977 & 1978

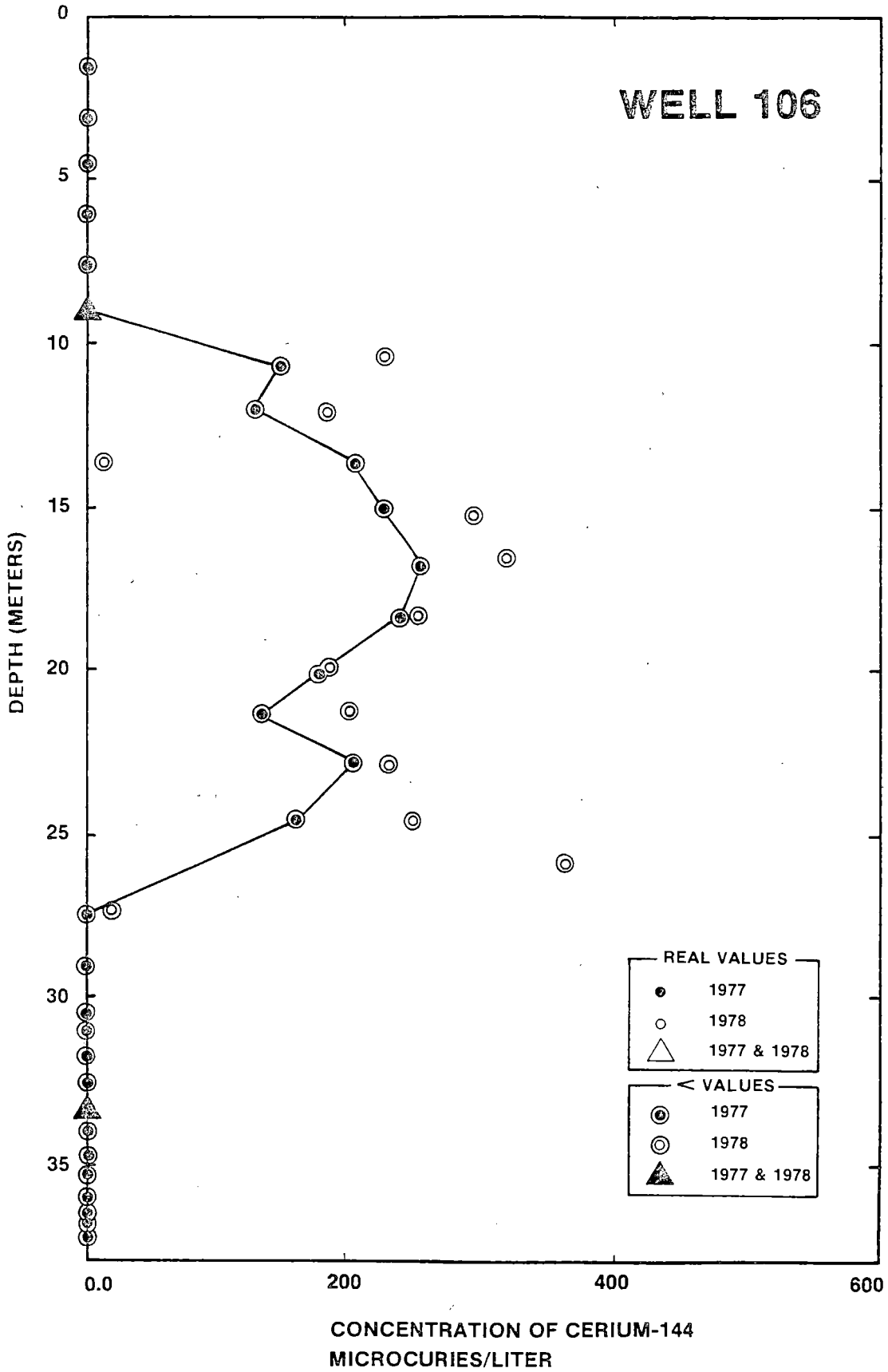
WELL 106
DEPTH (METERS)
0
5
10
15
20
25
30
35
0.0
200
400
600
CONCENTRATION OF CERIUM-144
MICROCURIES/LITER
REAL VALUES
1977
1978
1977 & 1978
< VALUES
1977
1978
1977 & 1978

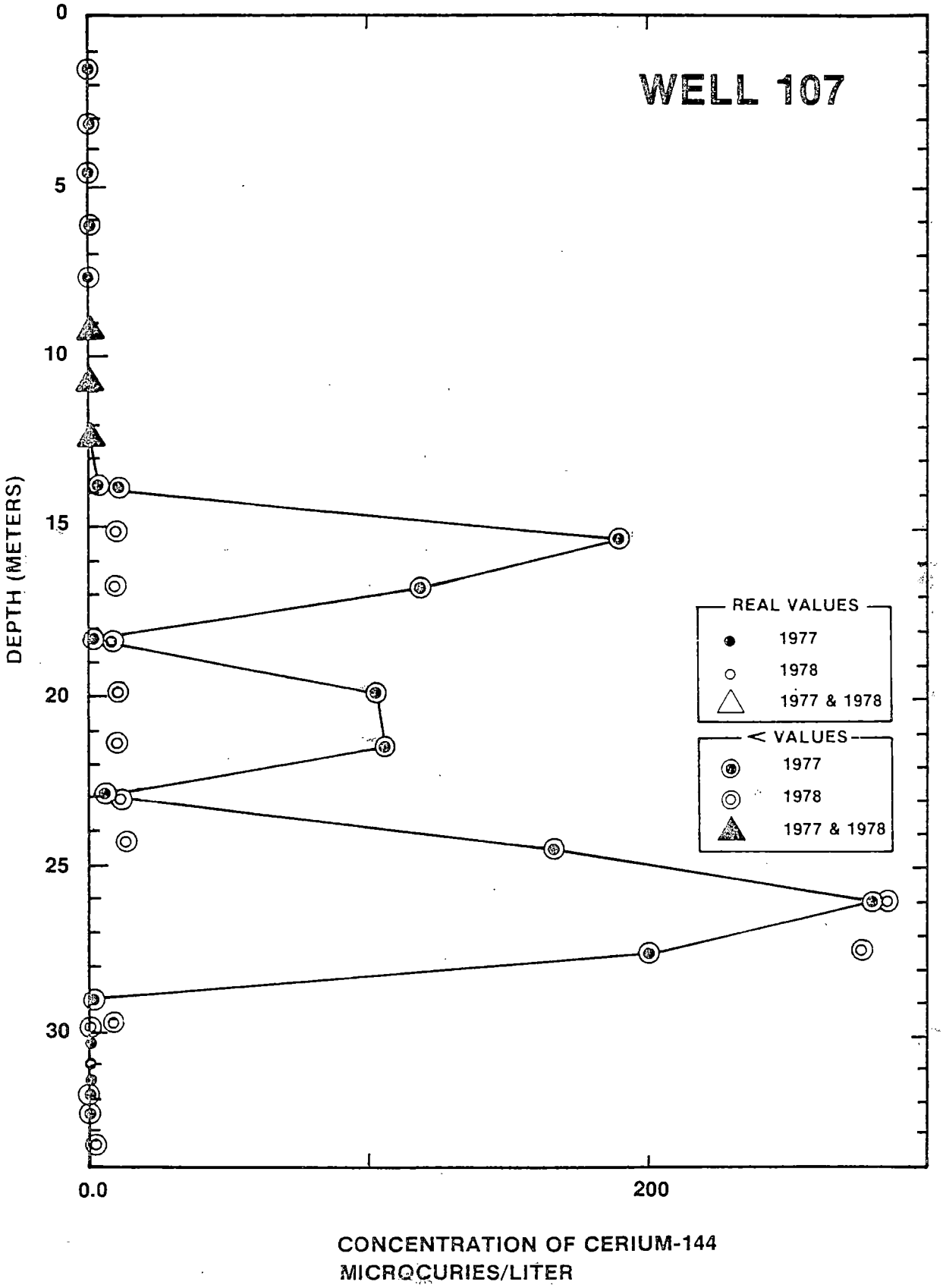

9 2 1 2 4 6 6 1 4 1 3

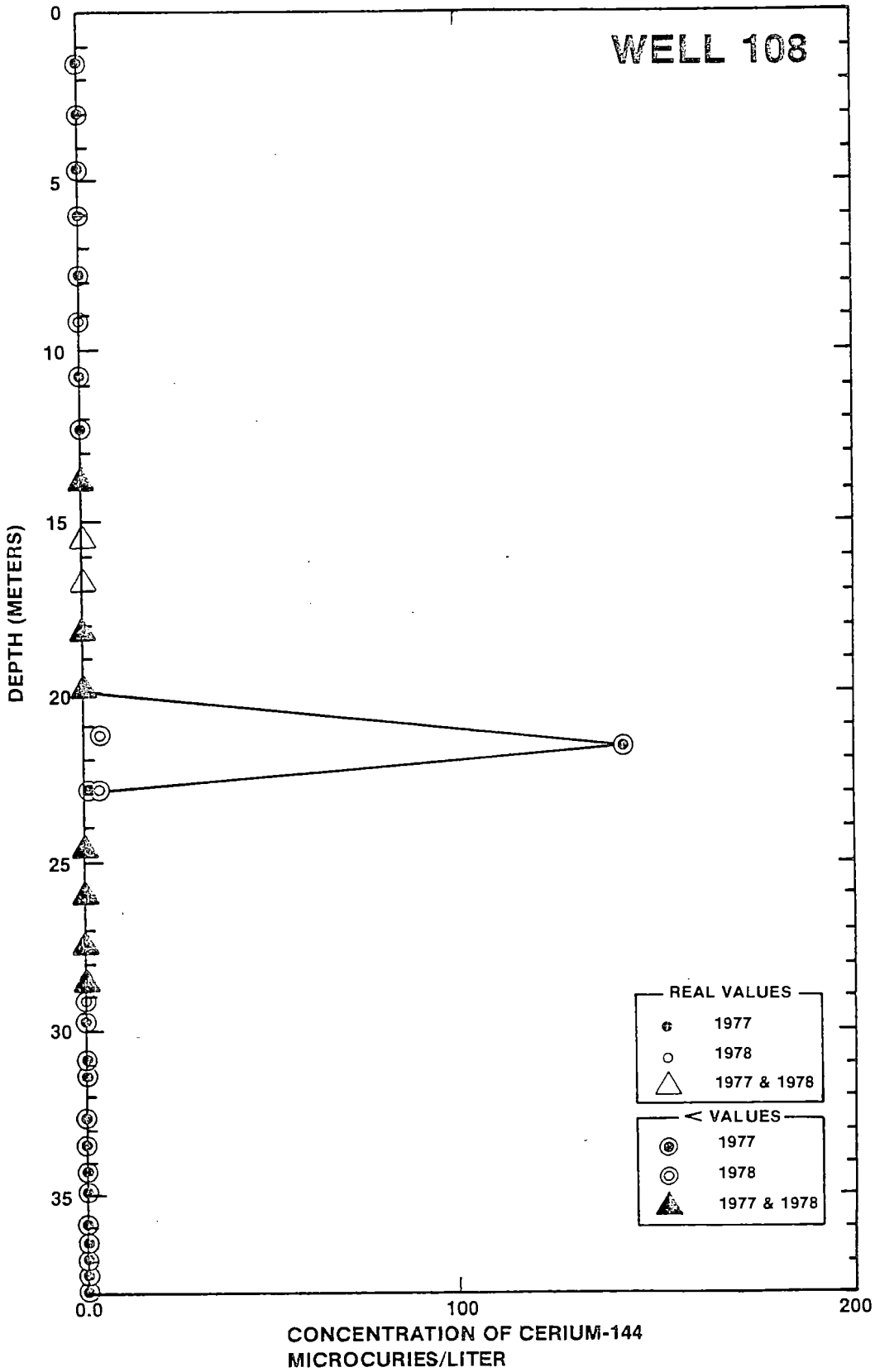
WELL 108
DEPTH (METERS)
0
5
10
15
20
25
30
35
0.0
100
200
CONCENTRATION OF CERIUM-144
MICROCURIES/LITER
REAL VALUES
1977
1978
1977 & 1978
< VALUES
1977
1978
1977 & 1978

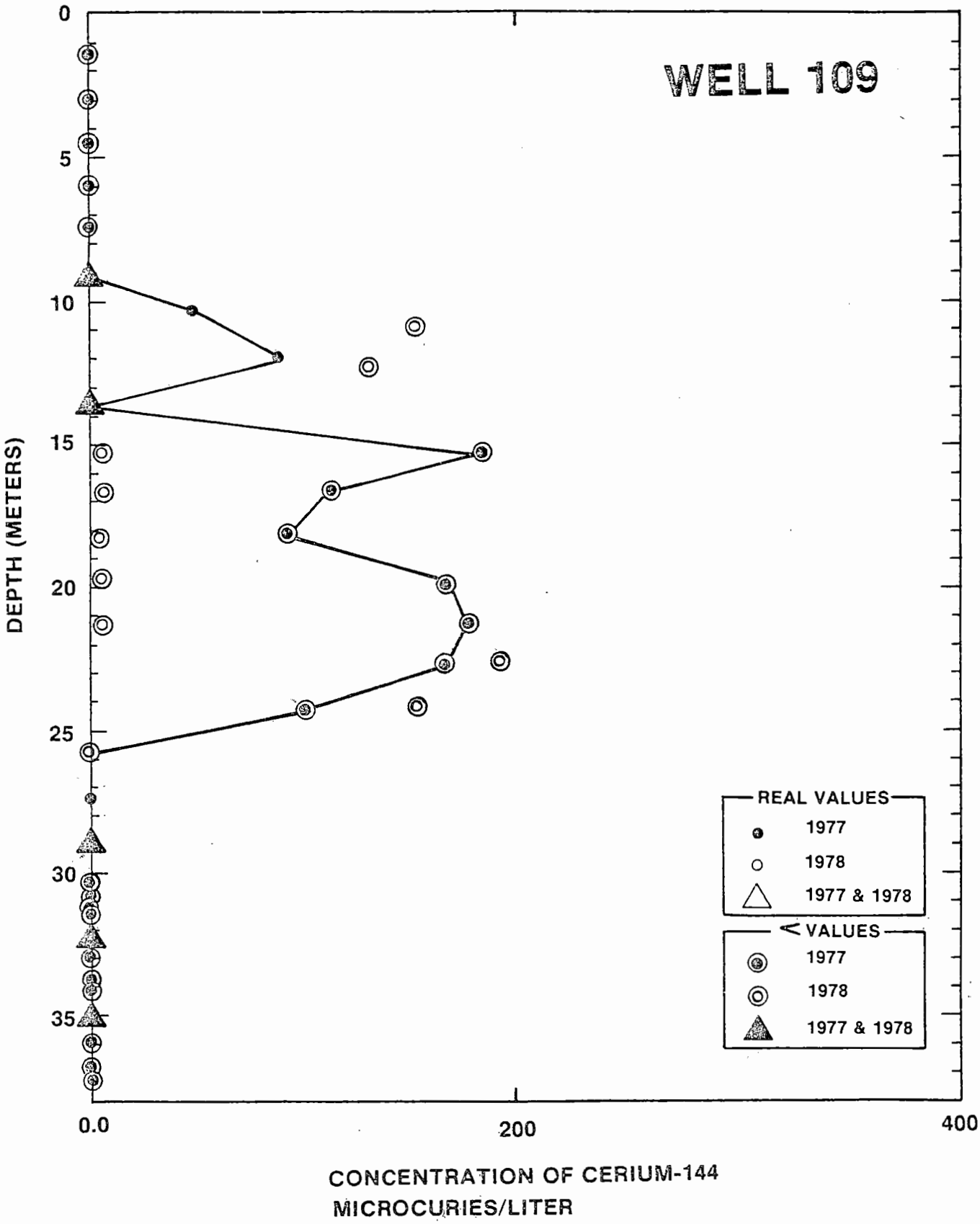
WELL 109
DEPTH (METERS)
0
5
10
15
20
25
30
35
0.0
200
400
CONCENTRATION OF CERIUM-144
MICROCURIES/LITER
REAL VALUES
1977
1978
1977 & 1978
< VALUES
1977
1978
1977 & 1978

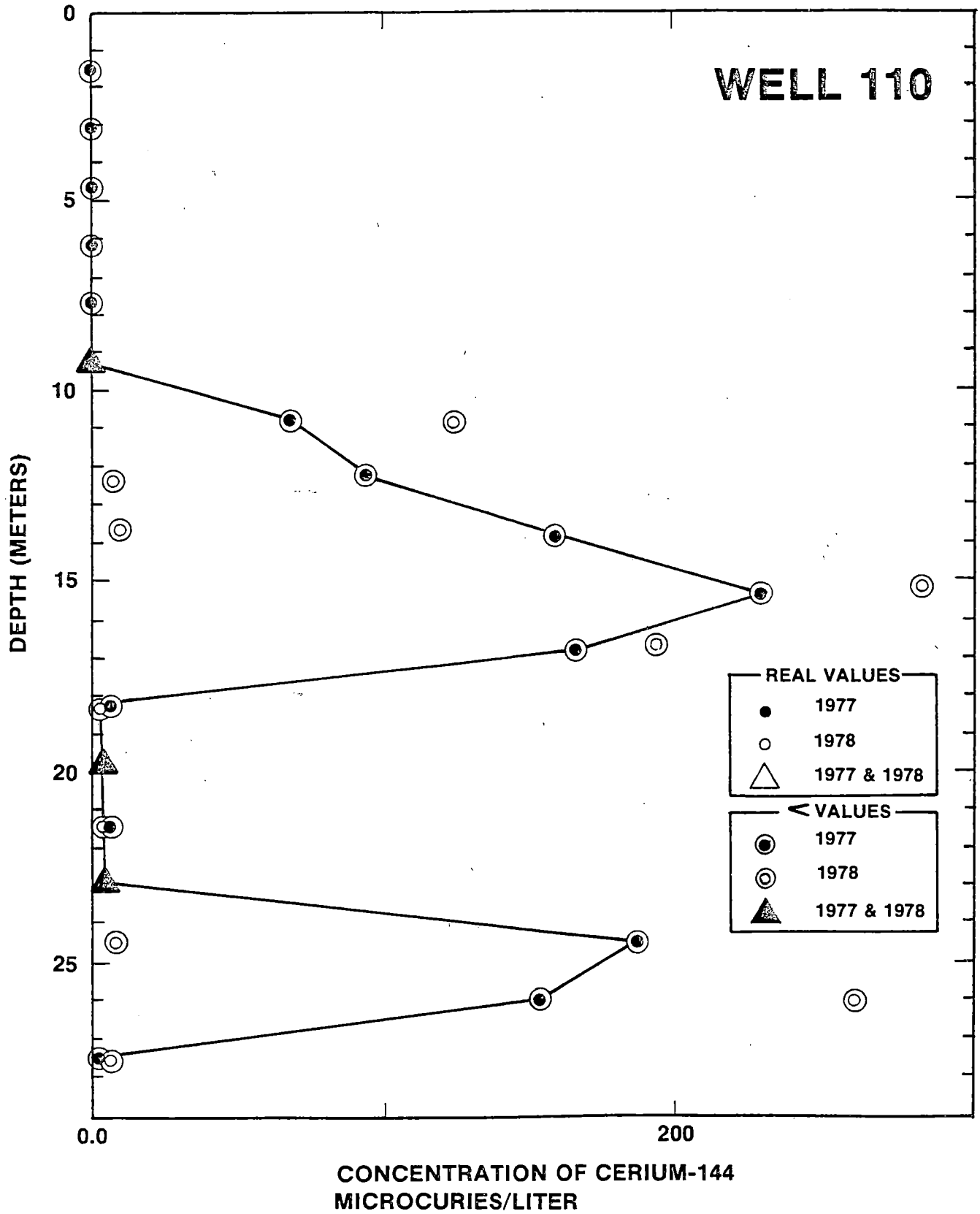
WELL 110
DEPTH (METERS)
0
5
10
15
20
25
0.0
200
CONCENTRATION OF CERIUM-144
MICROCURIES/LITER
REAL VALUES
1977
1978
1977 & 1978
< VALUES
1977
1978
1977 & 1978

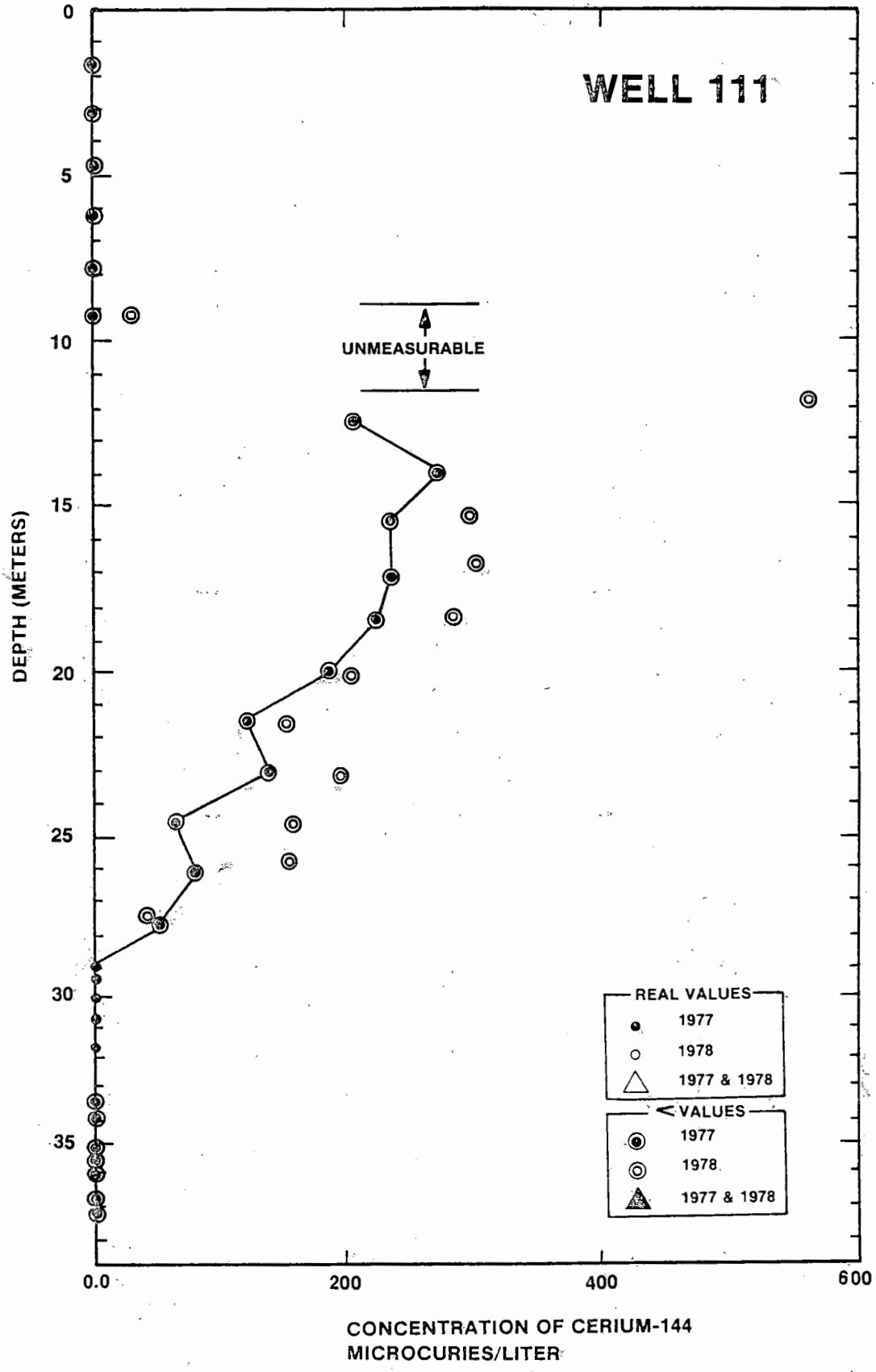
WELL 111
UNMEASURABLE
DEPTH (METERS)
0
5
10
15
20
25
30
35
0.0
200
400
600
CONCENTRATION OF CERIUM-144
MICROCURIES/LITER
REAL VALUES
1977
1978
1977 & 1978
< VALUES
1977
1978
1977 & 1978

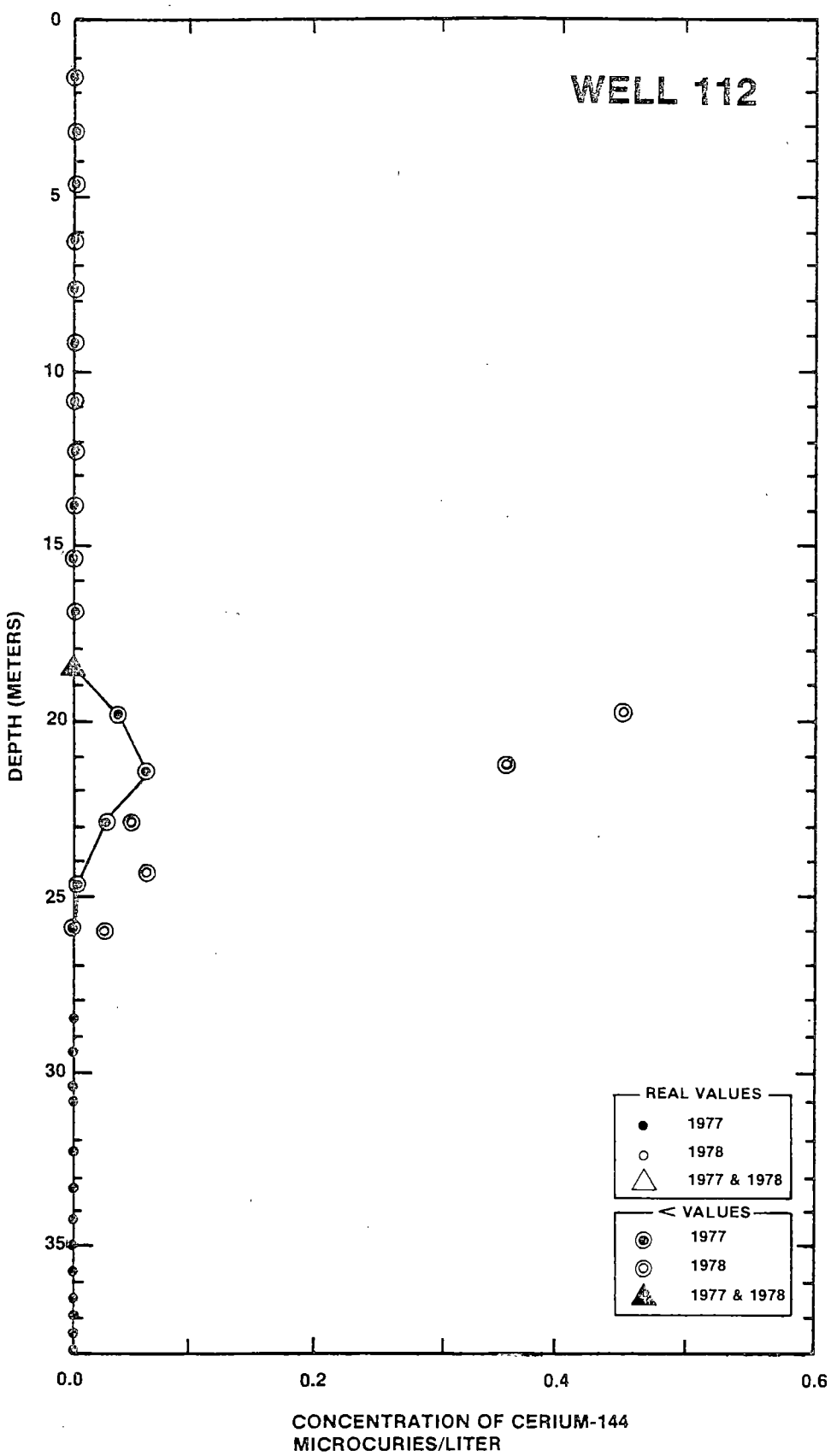
WELL 112
DEPTH (METERS)
0
5
10
15
20
25
30
35
0.0
0.2
0.4
0.6
CONCENTRATION OF CERIUM-144
MICROCURIES/LITER
REAL VALUES
1977
1978
1977 & 1978
< VALUES
1977
1978
1977 & 1978

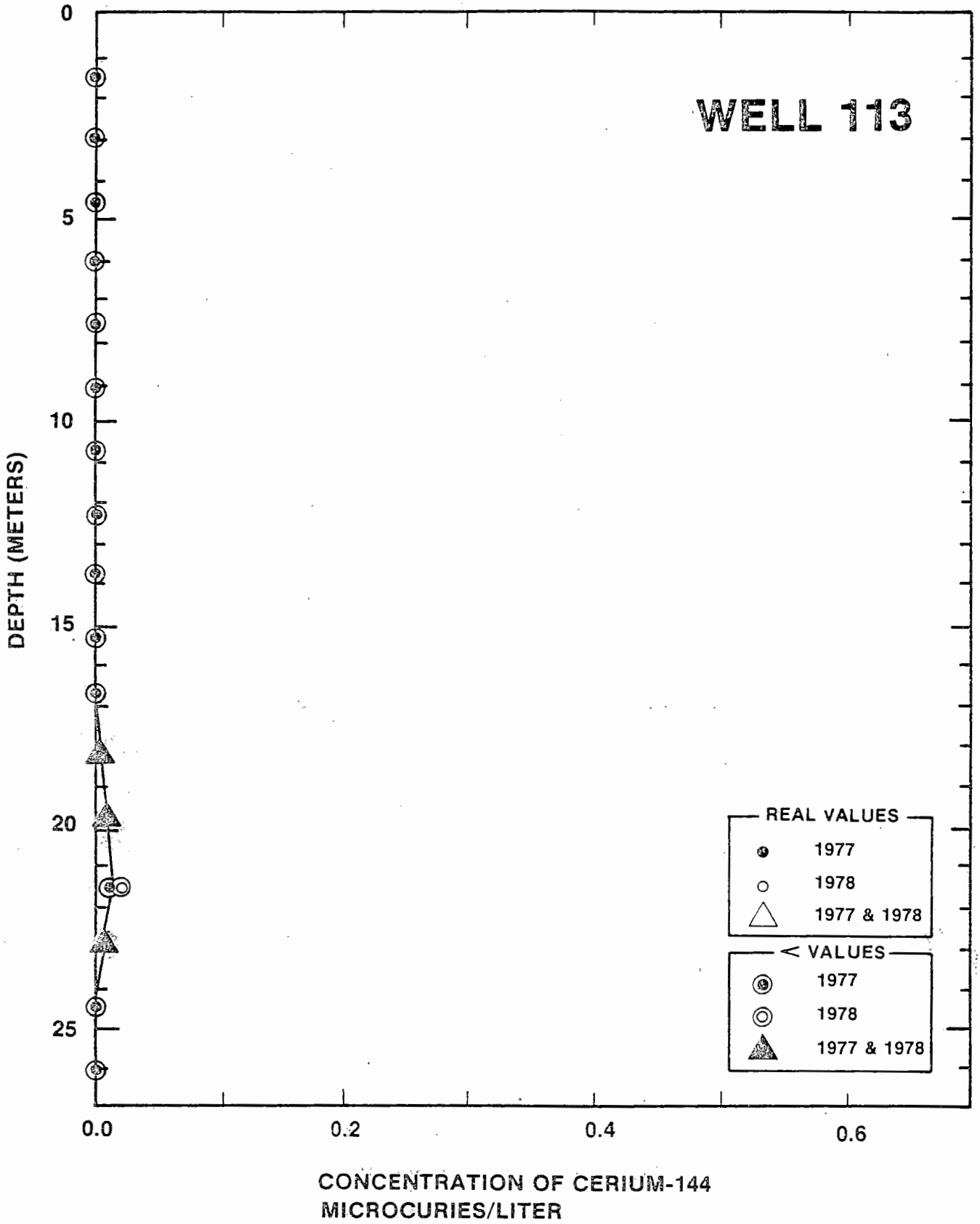
WELL 113
DEPTH (METERS)
0
5
10
15
20
25
0.0
0.2
0.4
0.6
CONCENTRATION OF CERIUM-144
MICROCURIES/LITER
REAL VALUES
1977
1978
1977 & 1978
< VALUES
1977
1978
1977 & 1978

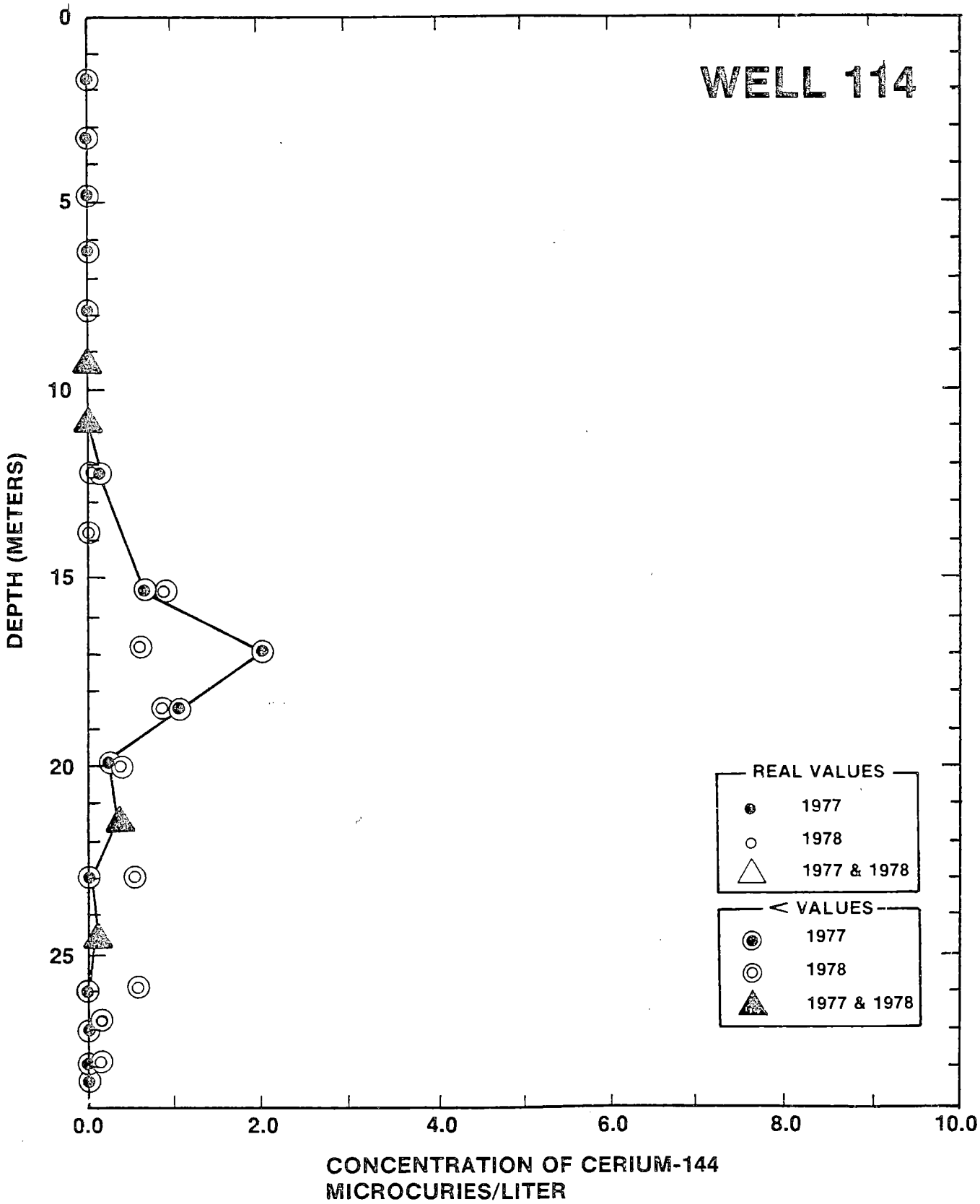
WELL 114
DEPTH (METERS)
0
5
10
15
20
25
0.0
2.0
4.0
6.0
8.0
10.0
CONCENTRATION OF CERIUM-144
MICROCURIES/LITER
REAL VALUES
1977
1978
1977 & 1978
< VALUES
1977
1978
1977 & 1978

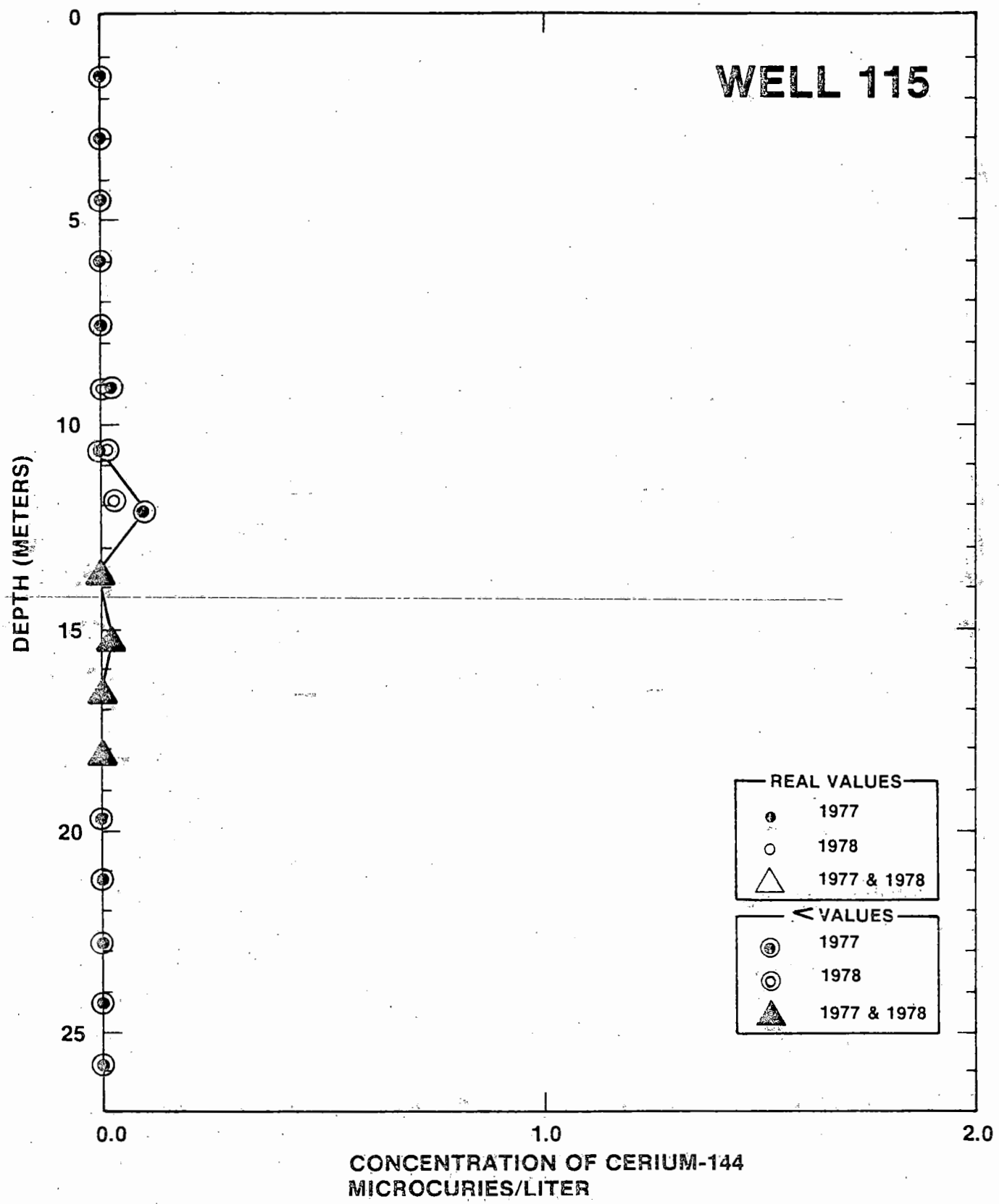
WELL 115
DEPTH (METERS)
0
5
10
15
20
25
0.0
1.0
2.0
CONCENTRATION OF CERIUM-144
MICROCURIES/LITER
REAL VALUES
1977
1978
1977 & 1978
< VALUES
1977
1978
1977 & 1978

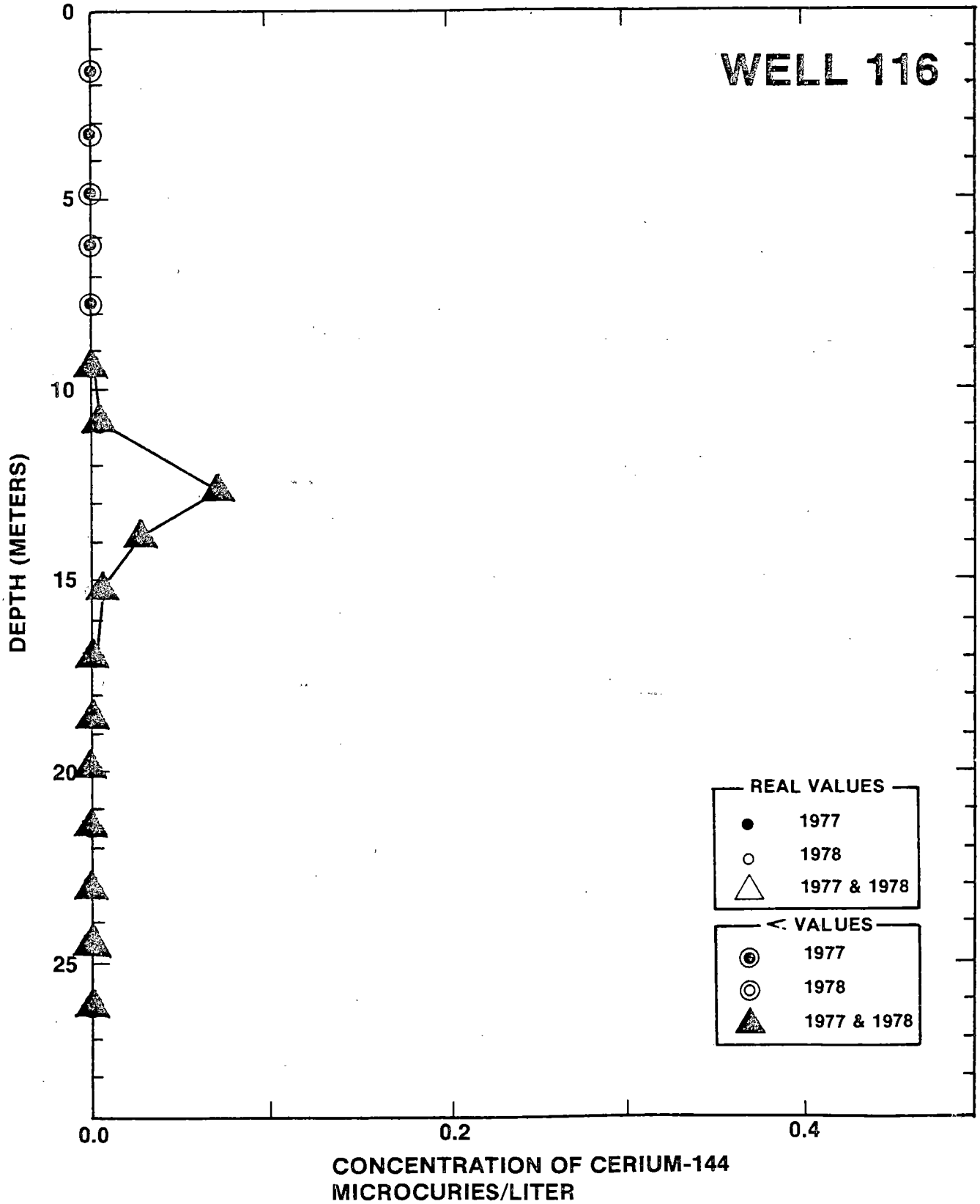

9 2 1 2 4 5 6 1 4 2 2

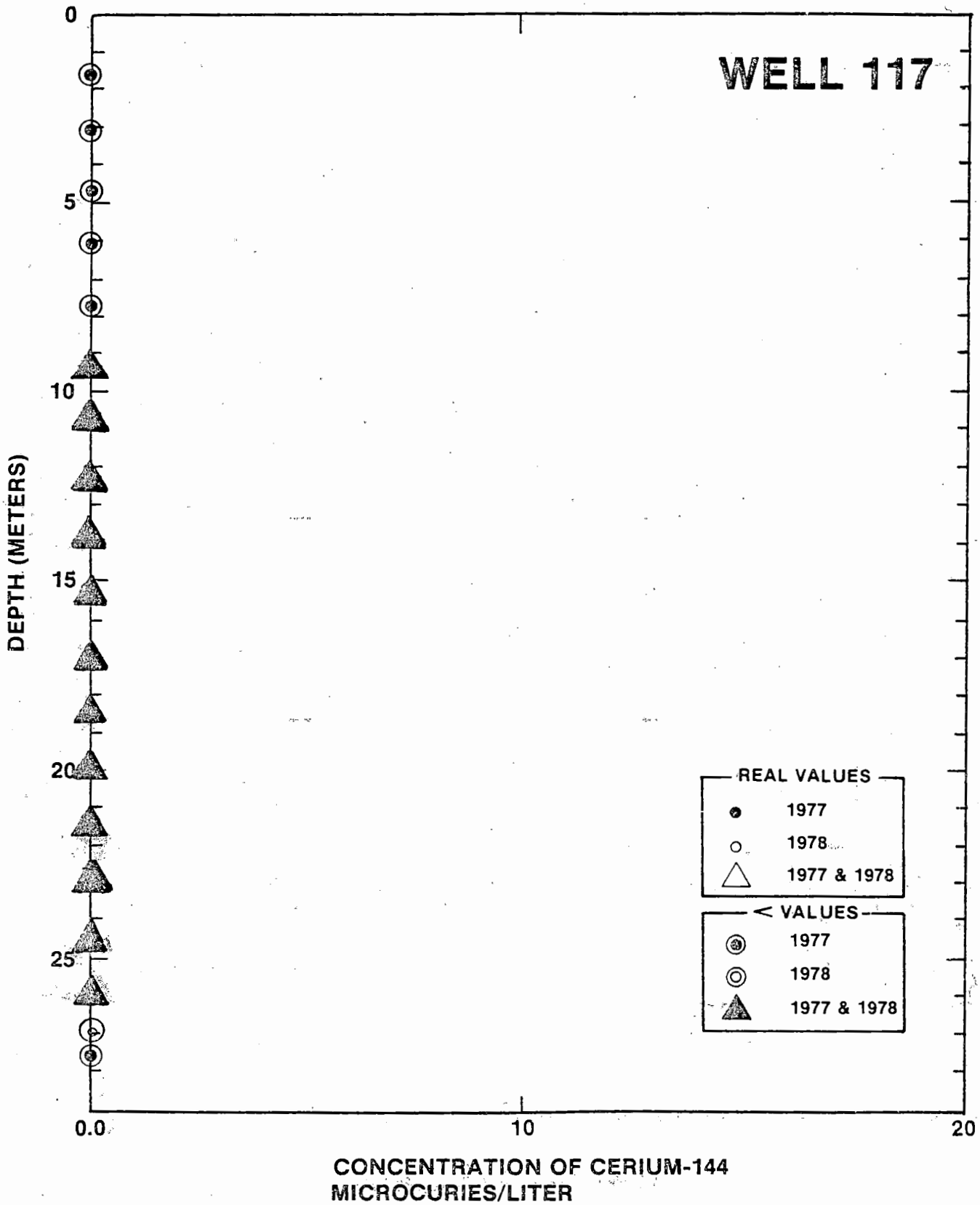
WELL 117
DEPTH (METERS)
0
5
10
15
20
25
0.0
10
20
CONCENTRATION OF CERIUM-144
MICROCURIES/LITER
REAL VALUES
1977
1978
1977 & 1978
< VALUES
1977
1978
1977 & 1978

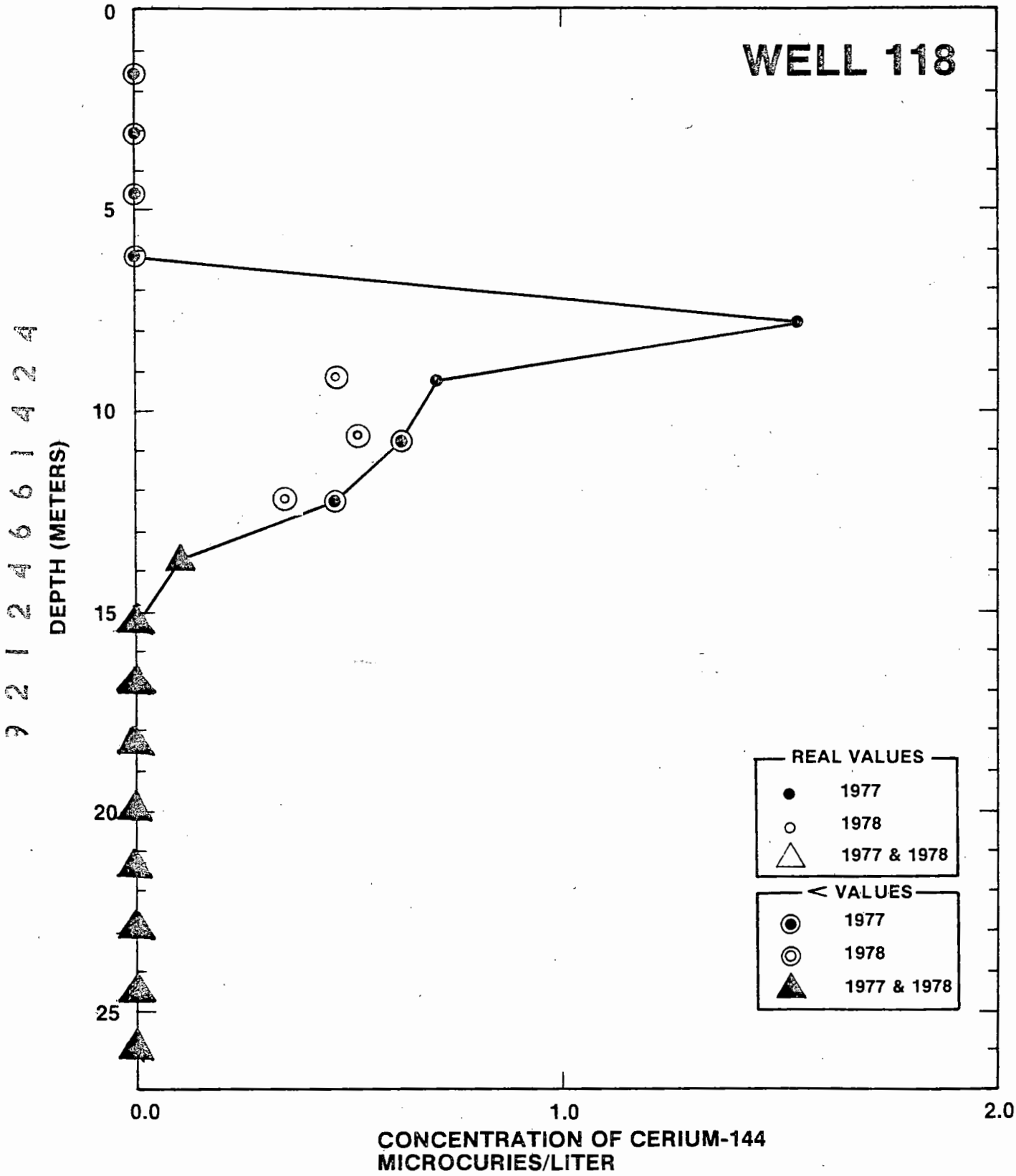
WELL 118
DEPTH (METERS)
0
5
10
15
20
25
0.0
1.0
2.0
CONCENTRATION OF CERIUM-144
MICROCURIES/LITER
REAL VALUES
1977
1978
1977 & 1978
< VALUES
1977
1978
1977 & 1978

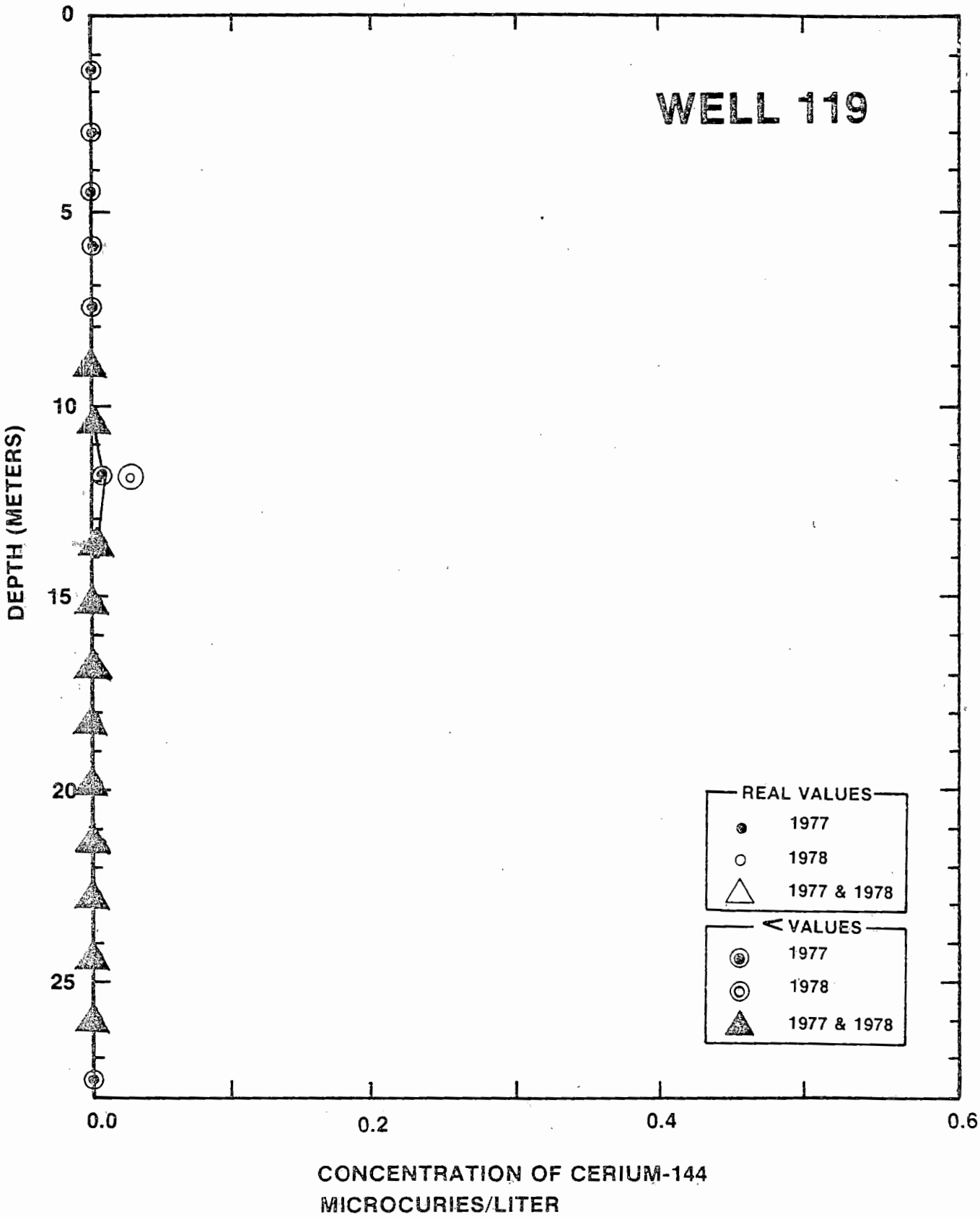

9 2 1 2 4 6 6 1 4 2 5

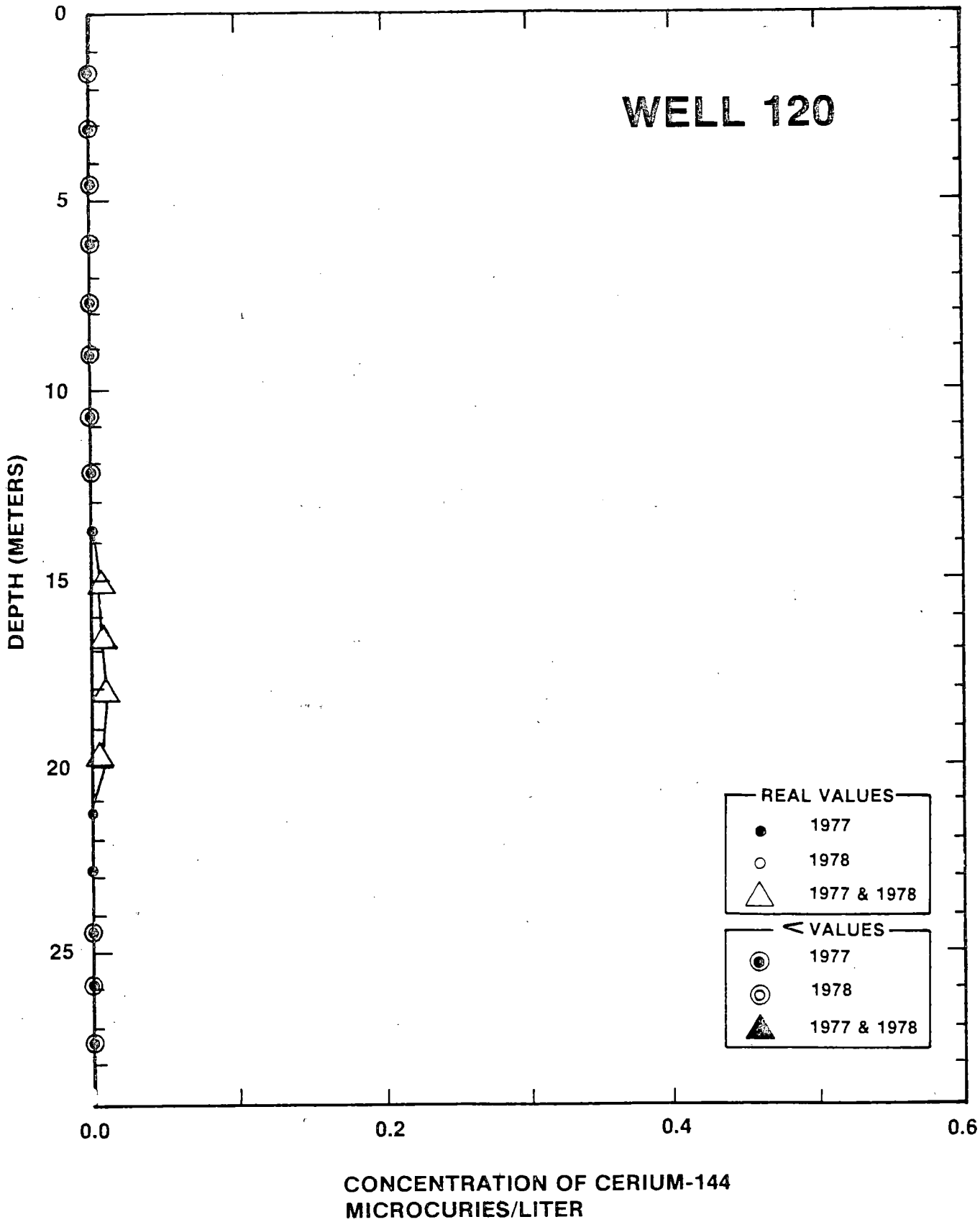

9 2 1 2 4 6 6 1 4 2 6

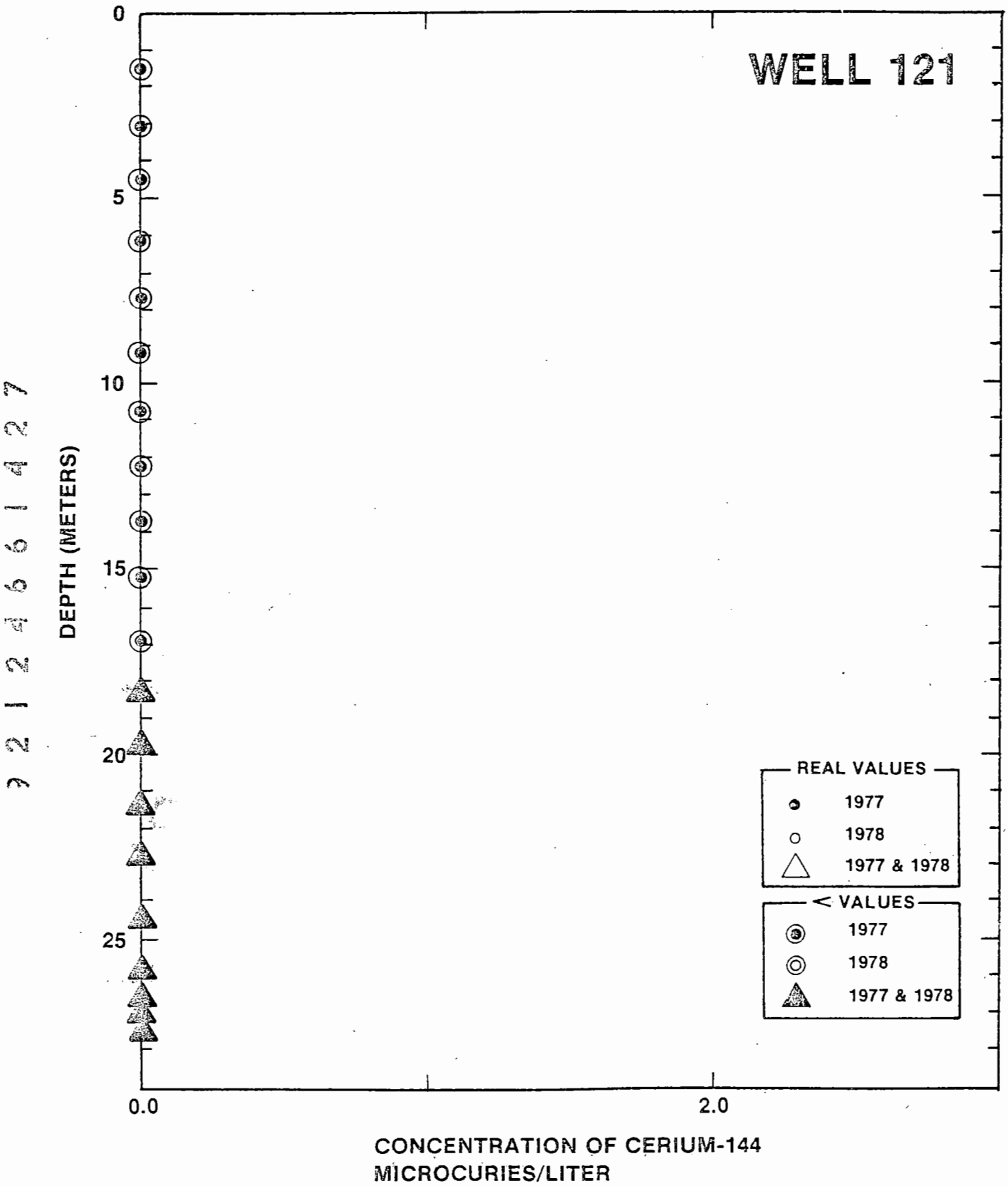
WELL 121
DEPTH (METERS)
0
5
10
15
20
25
0.0
2.0
CONCENTRATION OF CERIUM-144
MICROCURIES/LITER
REAL VALUES
1977
1978
1977 & 1978
< VALUES
1977
1978
1977 & 1978

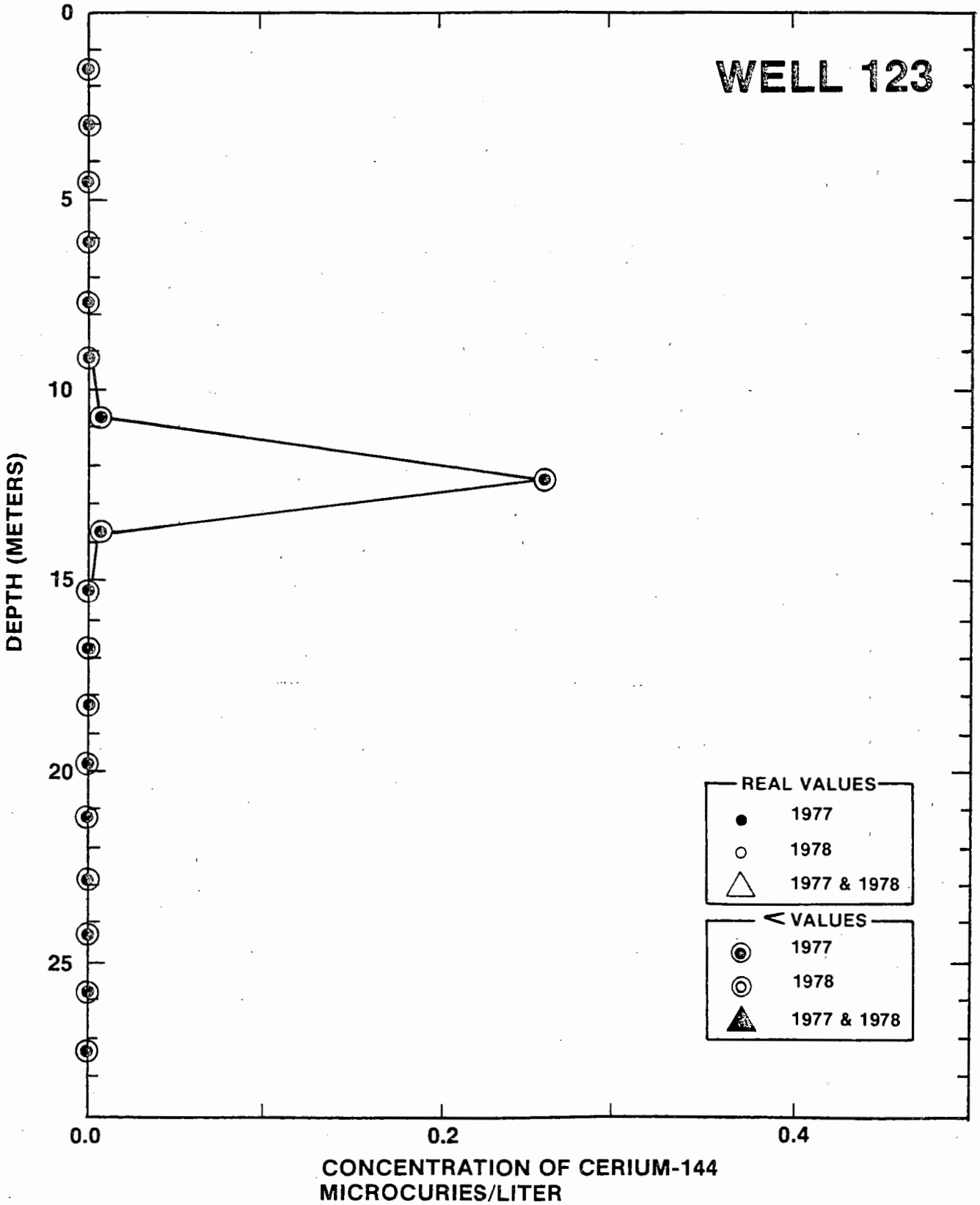

9 2 1 2 4 6 6 1 4 2 8

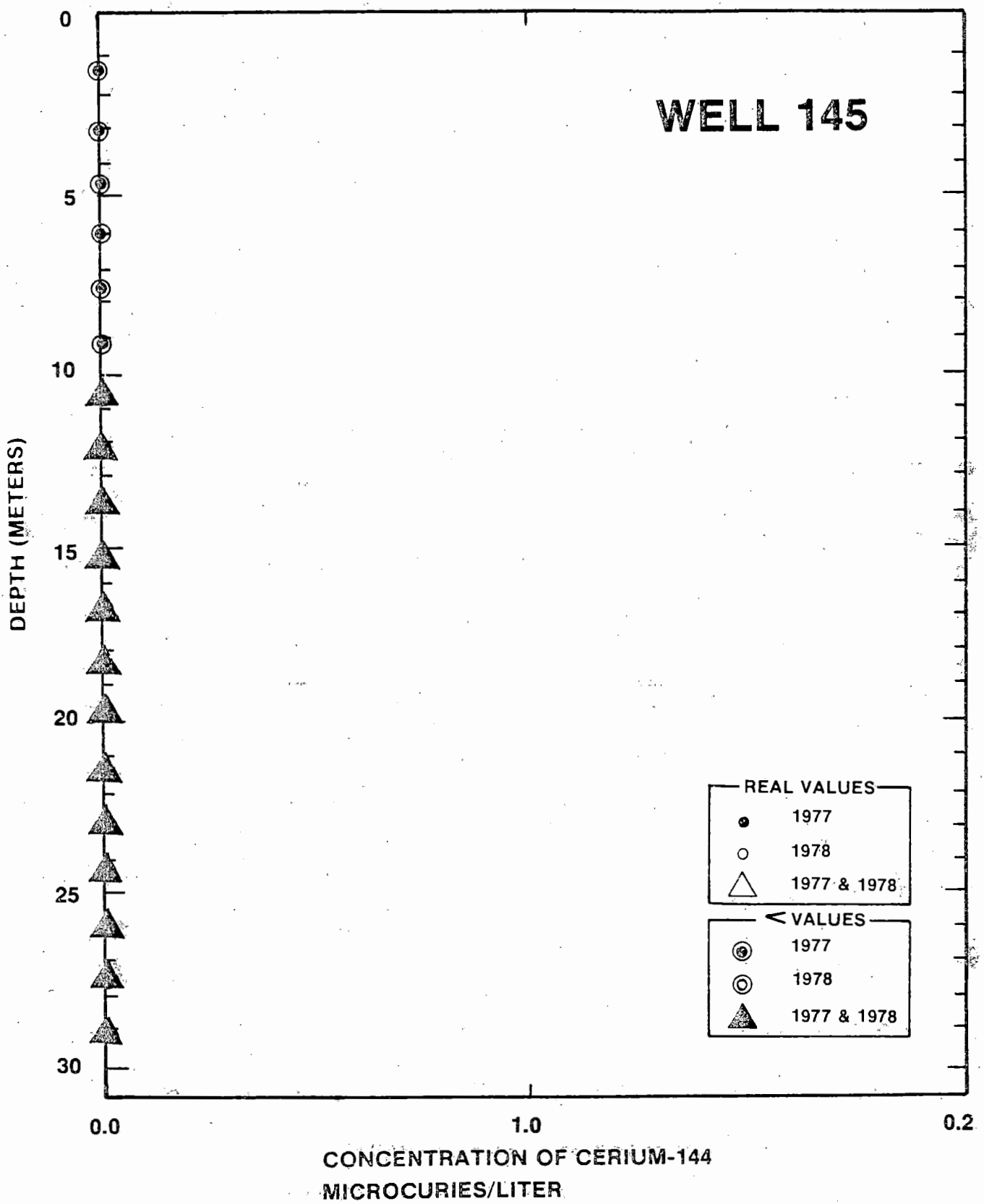

9 2 1 2 4 6 6 1 4 2 9

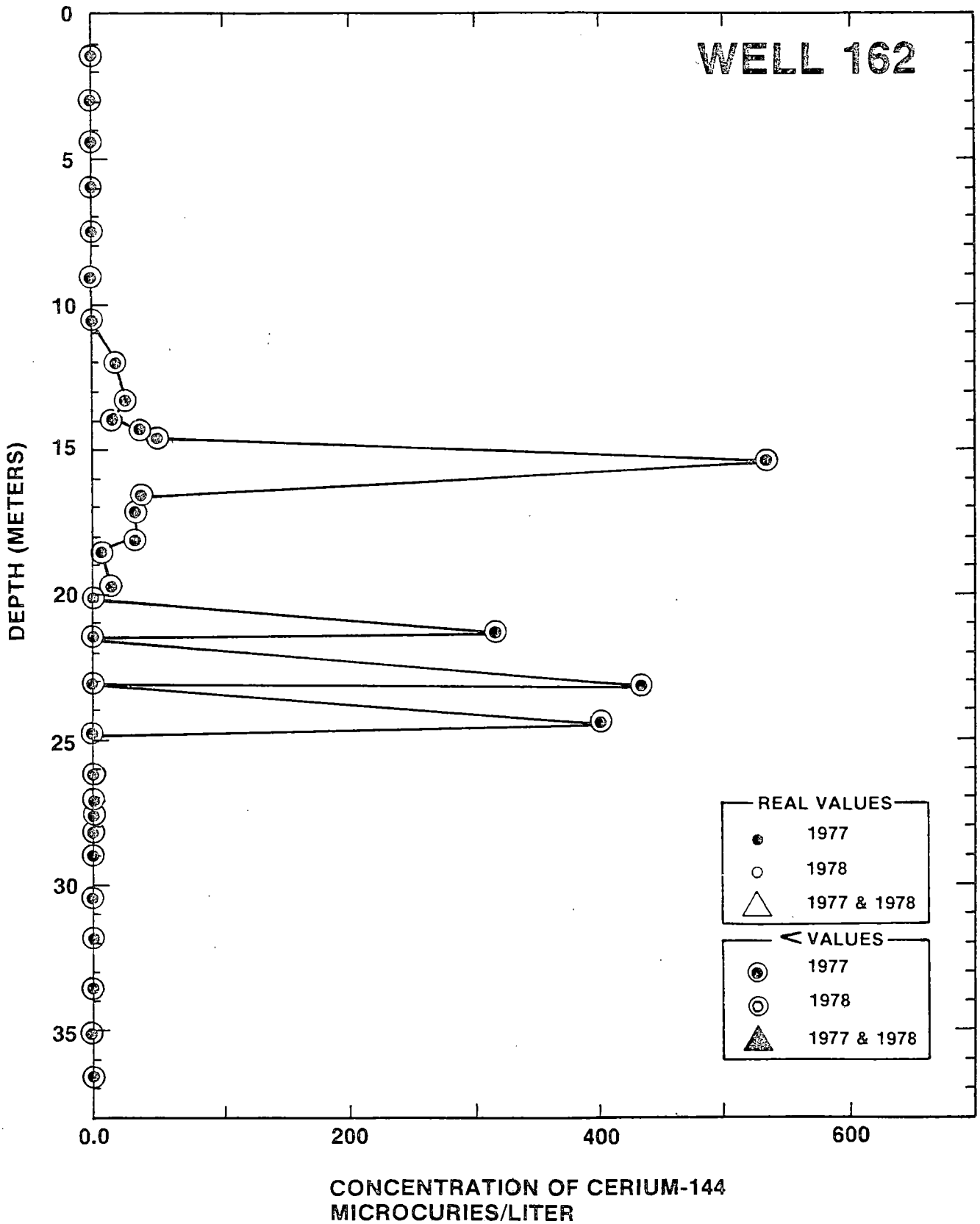
WELL 162
DEPTH (METERS)
0
5
10
15
20
25
30
35
0.0
200
400
600
CONCENTRATION OF CERIUM-144
MICROCURIES/LITER
REAL VALUES
1977
1978
1977 & 1978
< VALUES
1977
1978
1977 & 1978

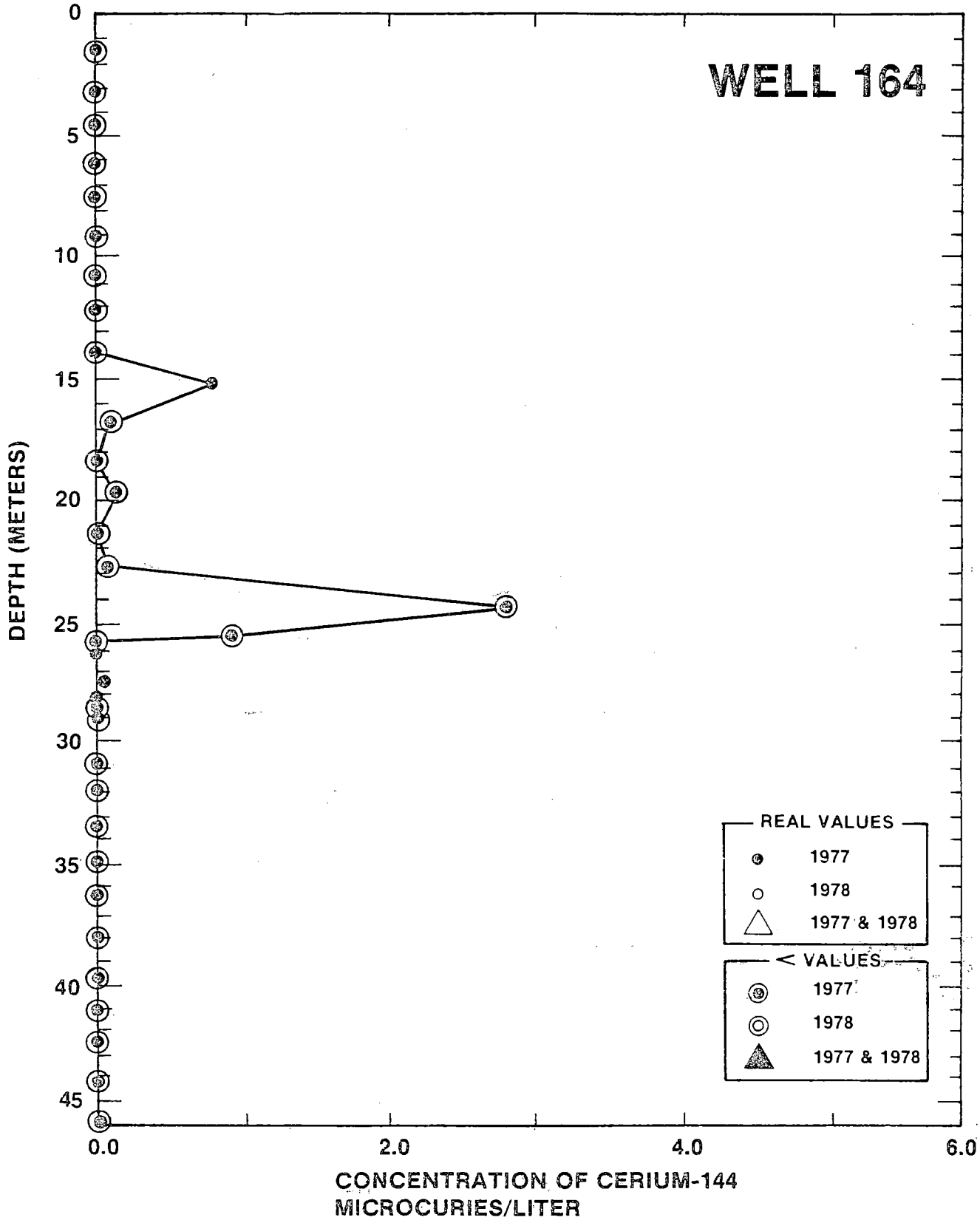
WELL 164
DEPTH (METERS)
0
5
10
15
20
25
30
35
40
45
0.0
2.0
4.0
6.0
CONCENTRATION OF CERIUM-144
MICROCURIES/LITER
REAL VALUES
1977
1978
1977 & 1978
< VALUES
1977
1978
1977 & 1978

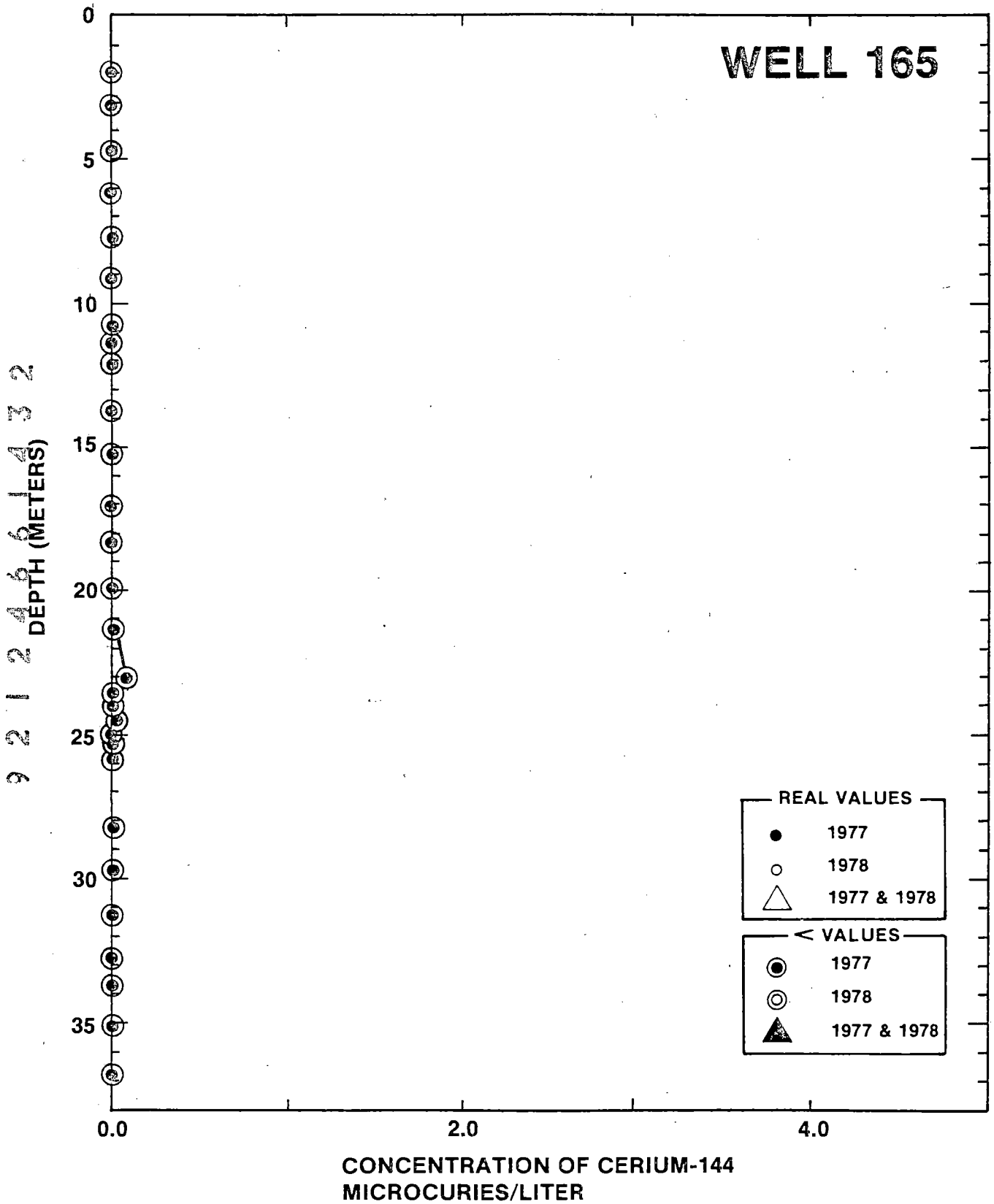
WELL 165
DEPTH (METERS)
0
5
10
15
20
25
30
35
0.0
2.0
4.0
CONCENTRATION OF CERIUM-144
MICROCURIES/LITER
REAL VALUES
1977
1978
1977 & 1978
< VALUES
1977
1978
1977 & 1978

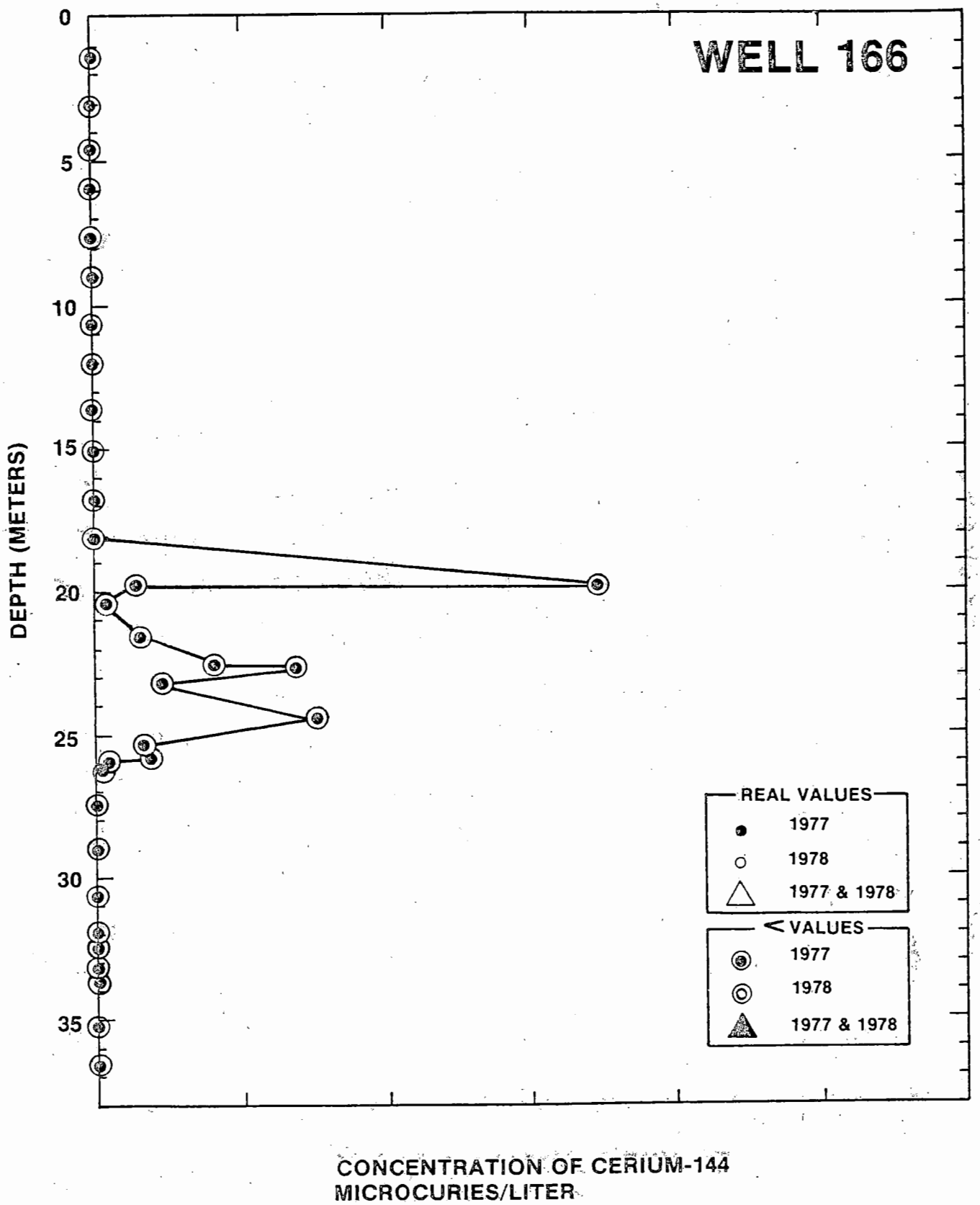
WELL 166
DEPTH (METERS)
0
5
10
15
20
25
30
35
REAL VALUES
1977
1978
1977 & 1978
< VALUES
1977
1978
1977 & 1978
CONCENTRATION OF CERIUM-144
MICROCURIES/LITER

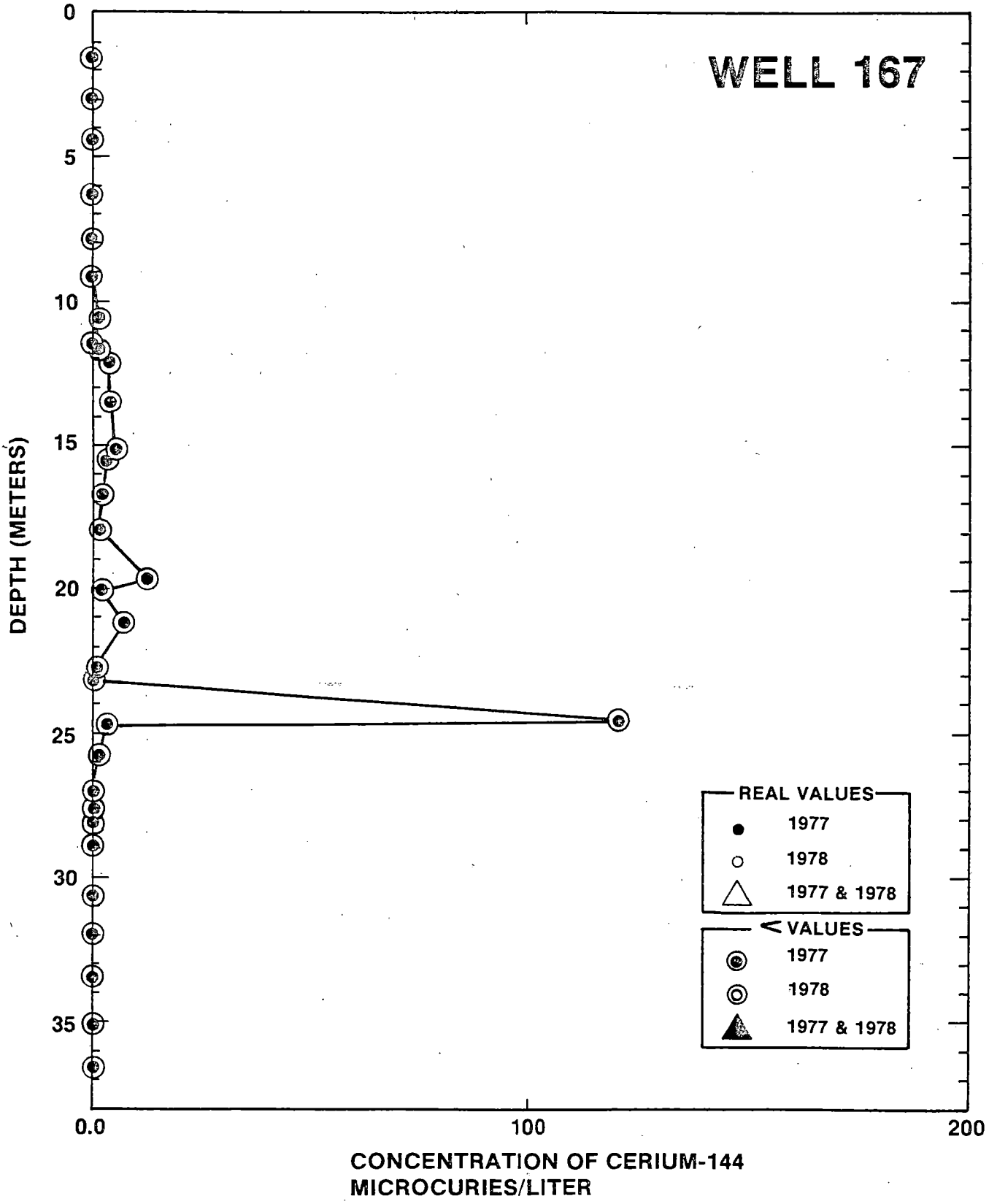
WELL 167
DEPTH (METERS)
0
5
10
15
20
25
30
35
0.0
100
200
CONCENTRATION OF CERIUM-144
MICROCURIES/LITER
REAL VALUES
1977
1978
1977 & 1978
< VALUES
1977
1978
1977 & 1978

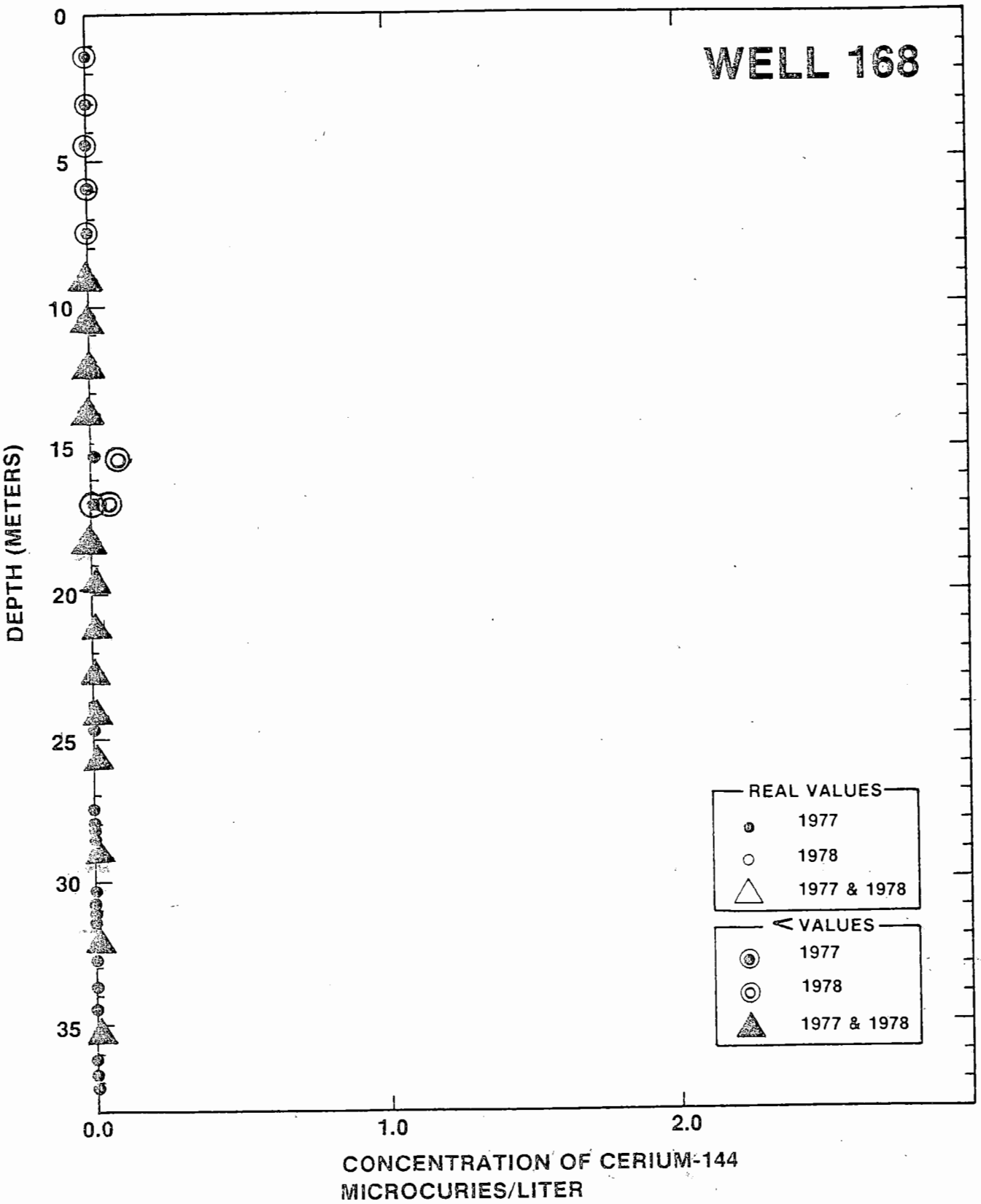
WELL 168
DEPTH (METERS)
0
5
10
15
20
25
30
35
0.0
1.0
2.0
CONCENTRATION OF CERIUM-144
MICROCURIES/LITER
REAL VALUES
1977
1978
1977 & 1978
< VALUES
1977
1978
1977 & 1978

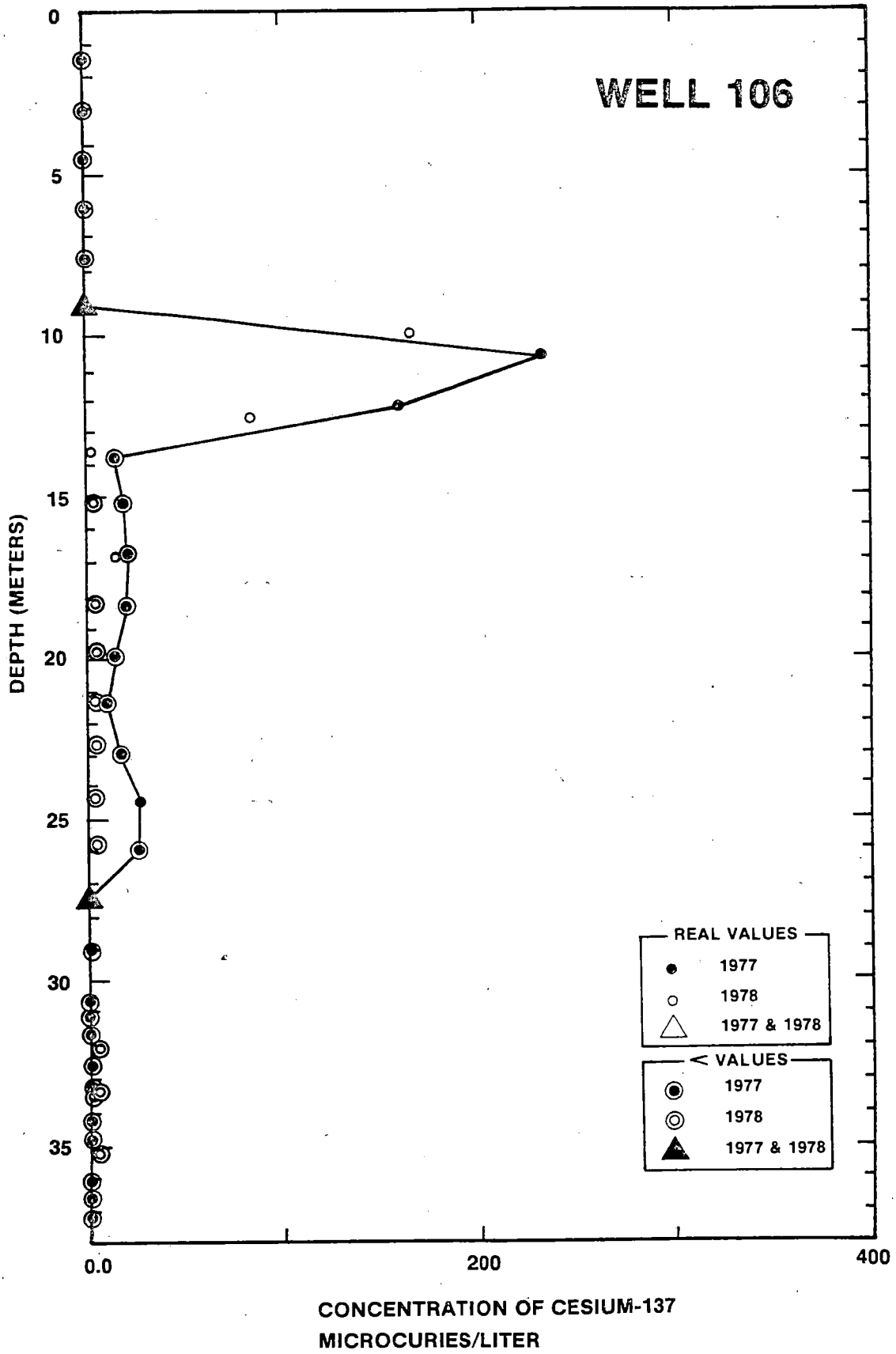

9 2 1 2 4 6 6 1 4 3 6

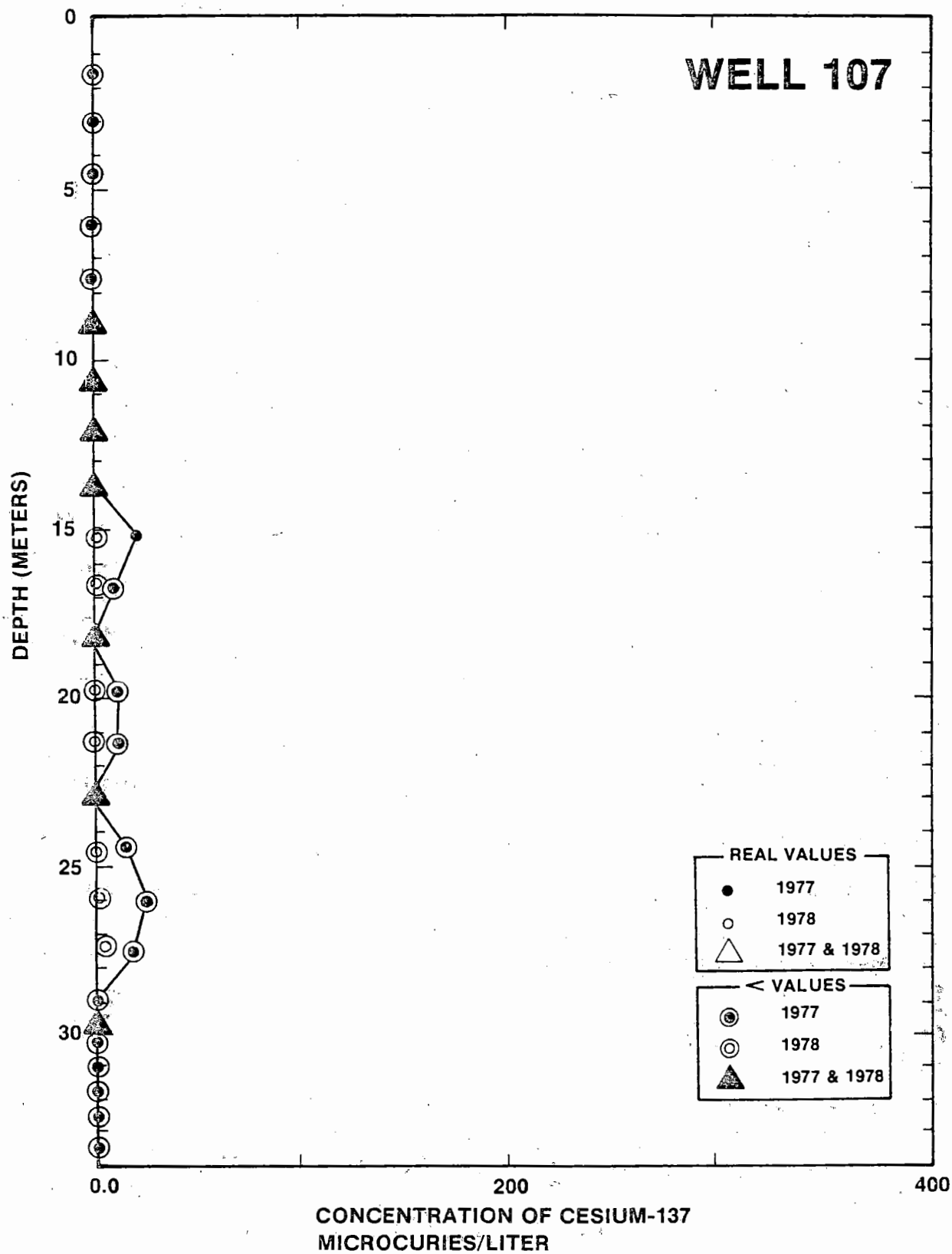

9 2 1 2 4 6 6 1 4 3 7

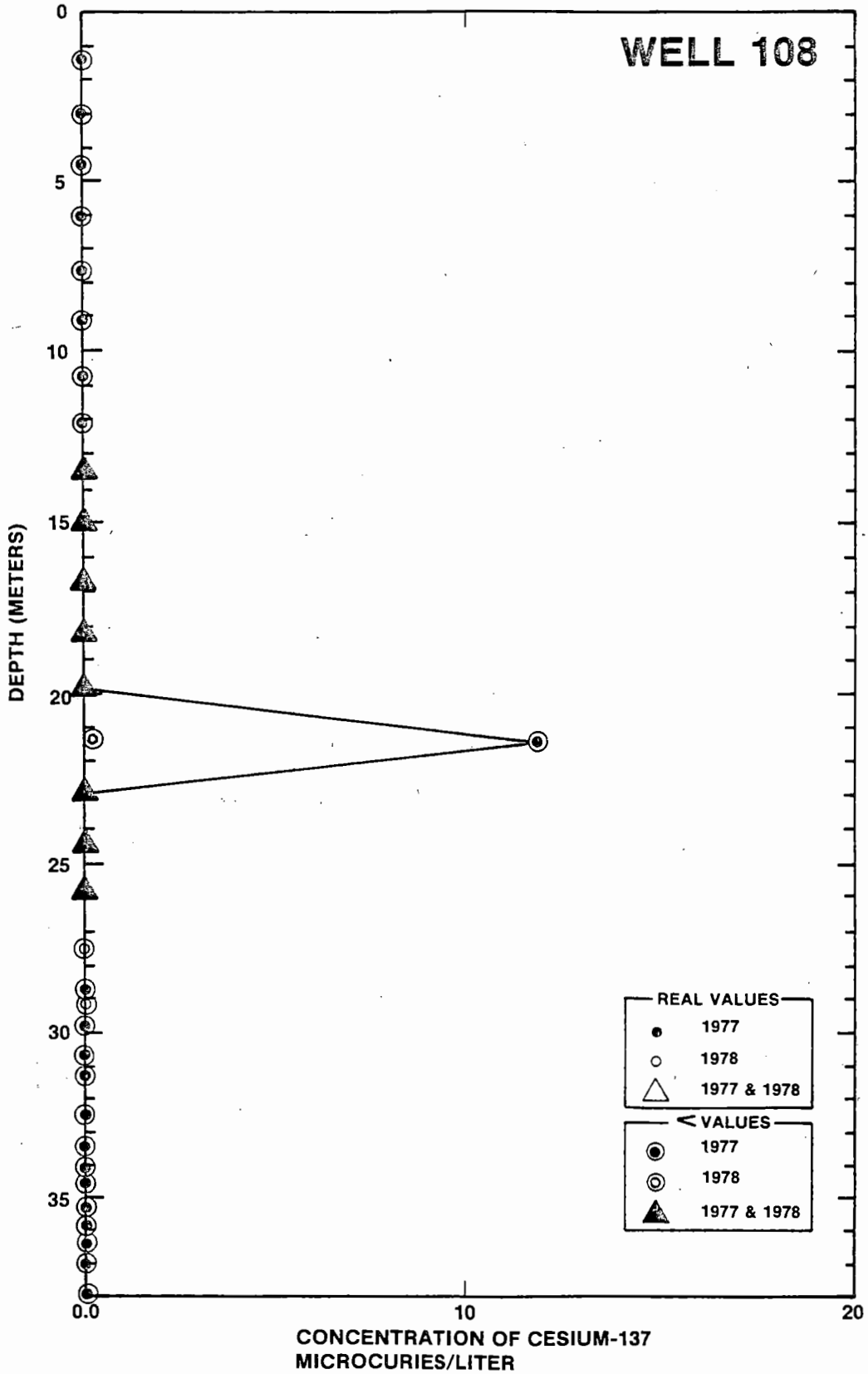

9 2 1 2 4 6 6 1 4 3 8

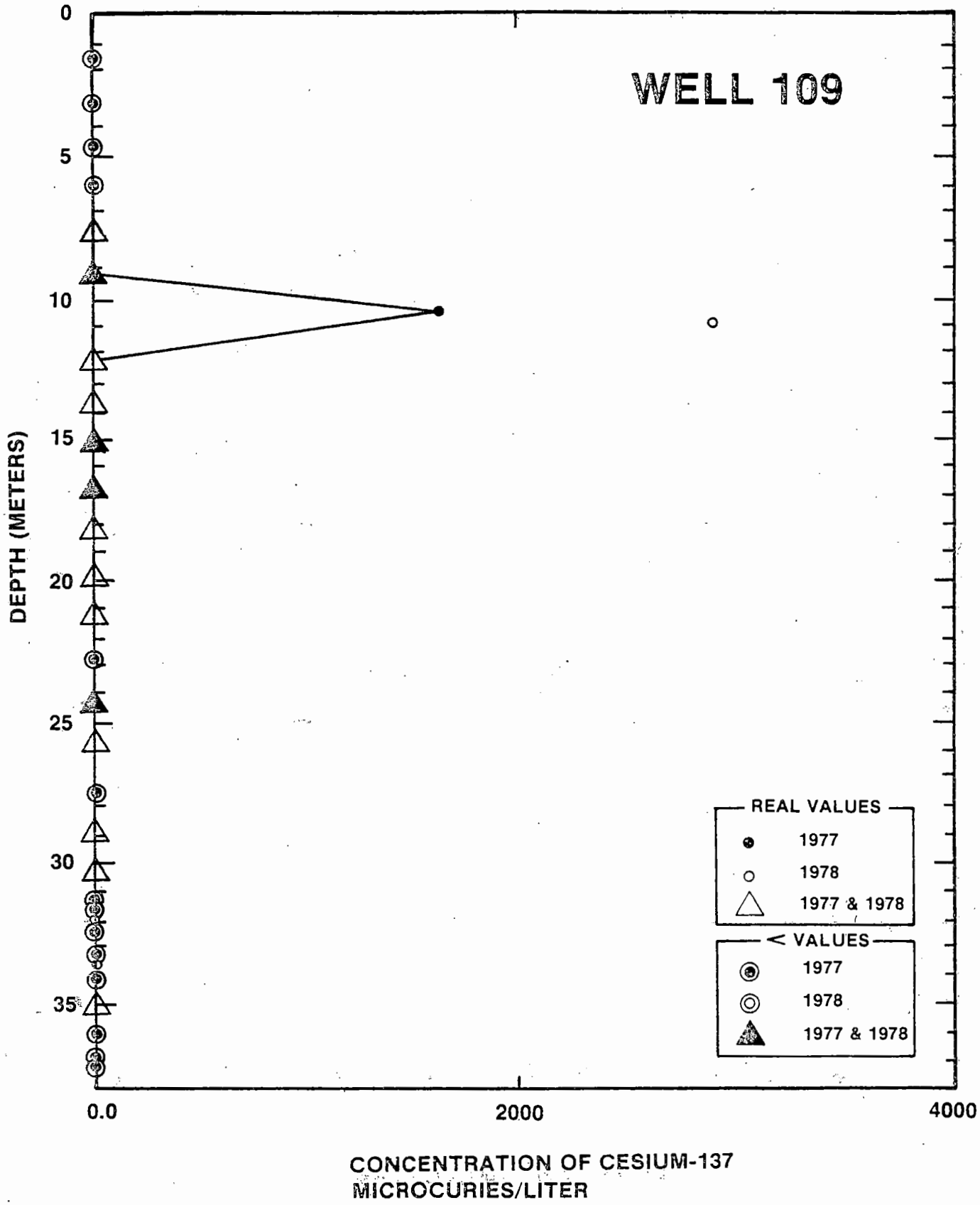

9 2 1 2 4 6 6 1 4 3 9

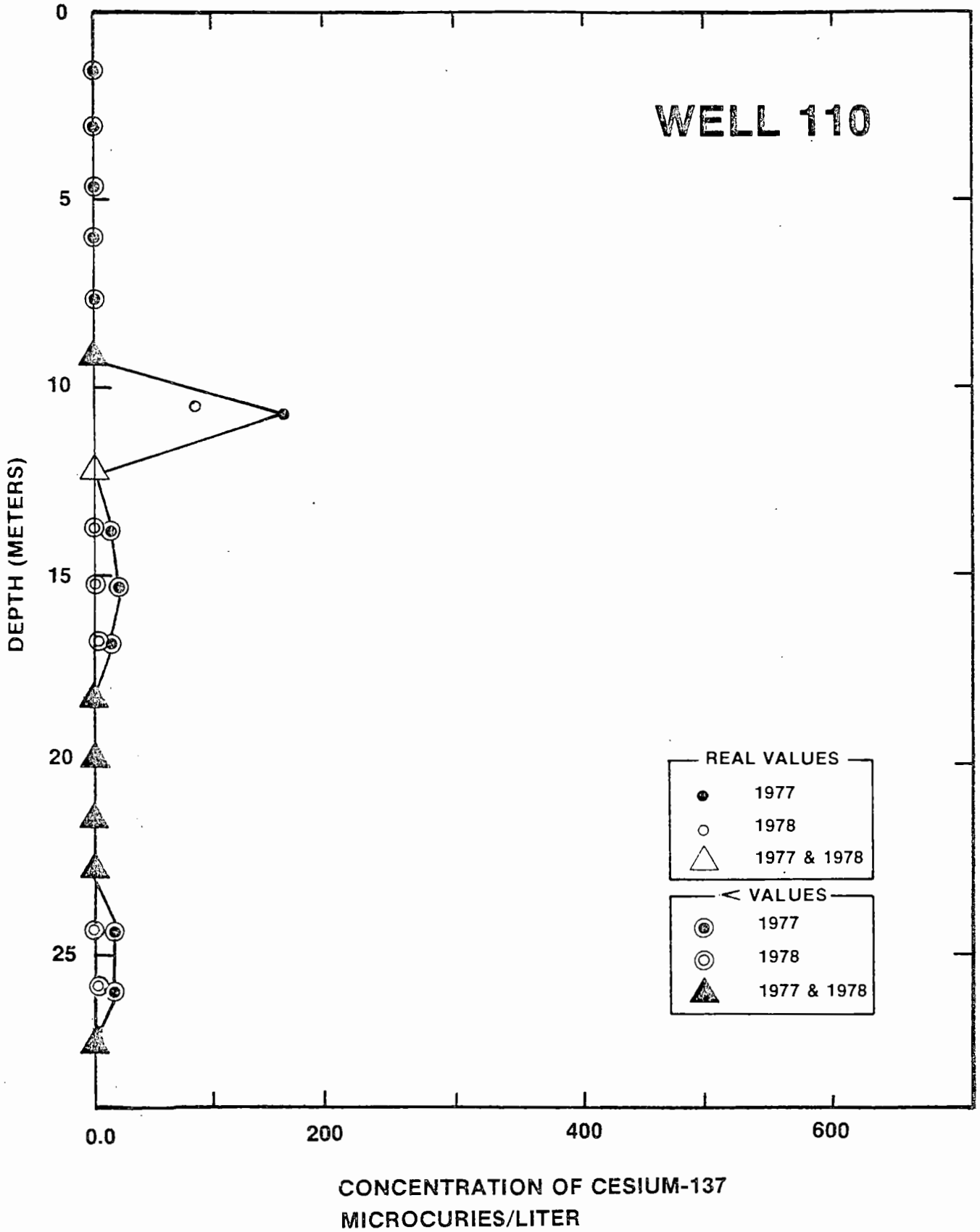
WELL 110
DEPTH (METERS)
0
5
10
15
20
25
0.0
200
400
600
CONCENTRATION OF CESIUM-137
MICROCURIES/LITER
REAL VALUES
1977
1978
1977 & 1978
< VALUES
1977
1978
1977 & 1978

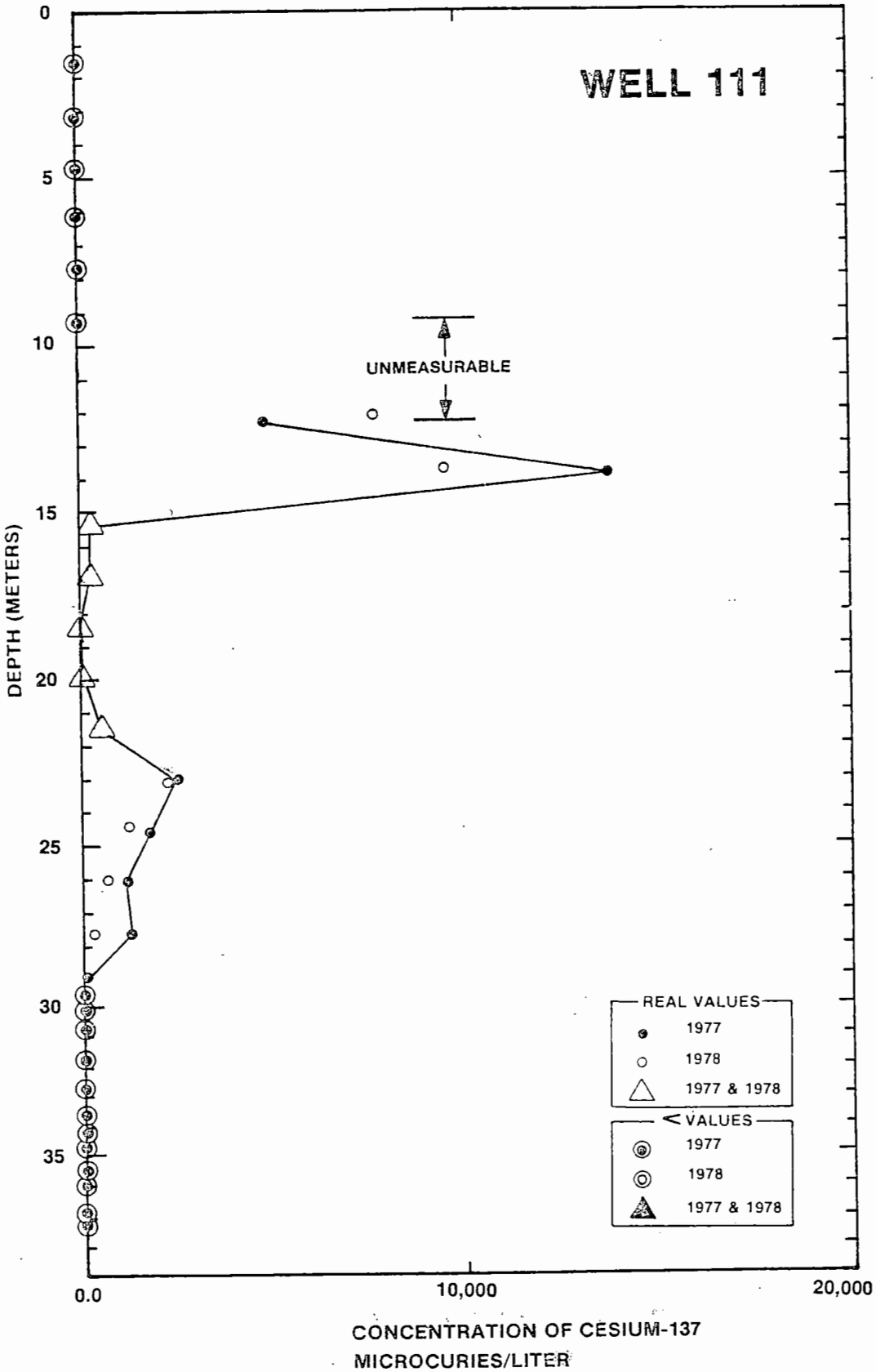
WELL 111
UNMEASURABLE
DEPTH (METERS)
0
5
10
15
20
25
30
35
0.0
10,000
20,000
CONCENTRATION OF CESIUM-137
MICROCURIES/LITER
REAL VALUES
1977
1978
1977 & 1978
< VALUES
1977
1978
1977 & 1978

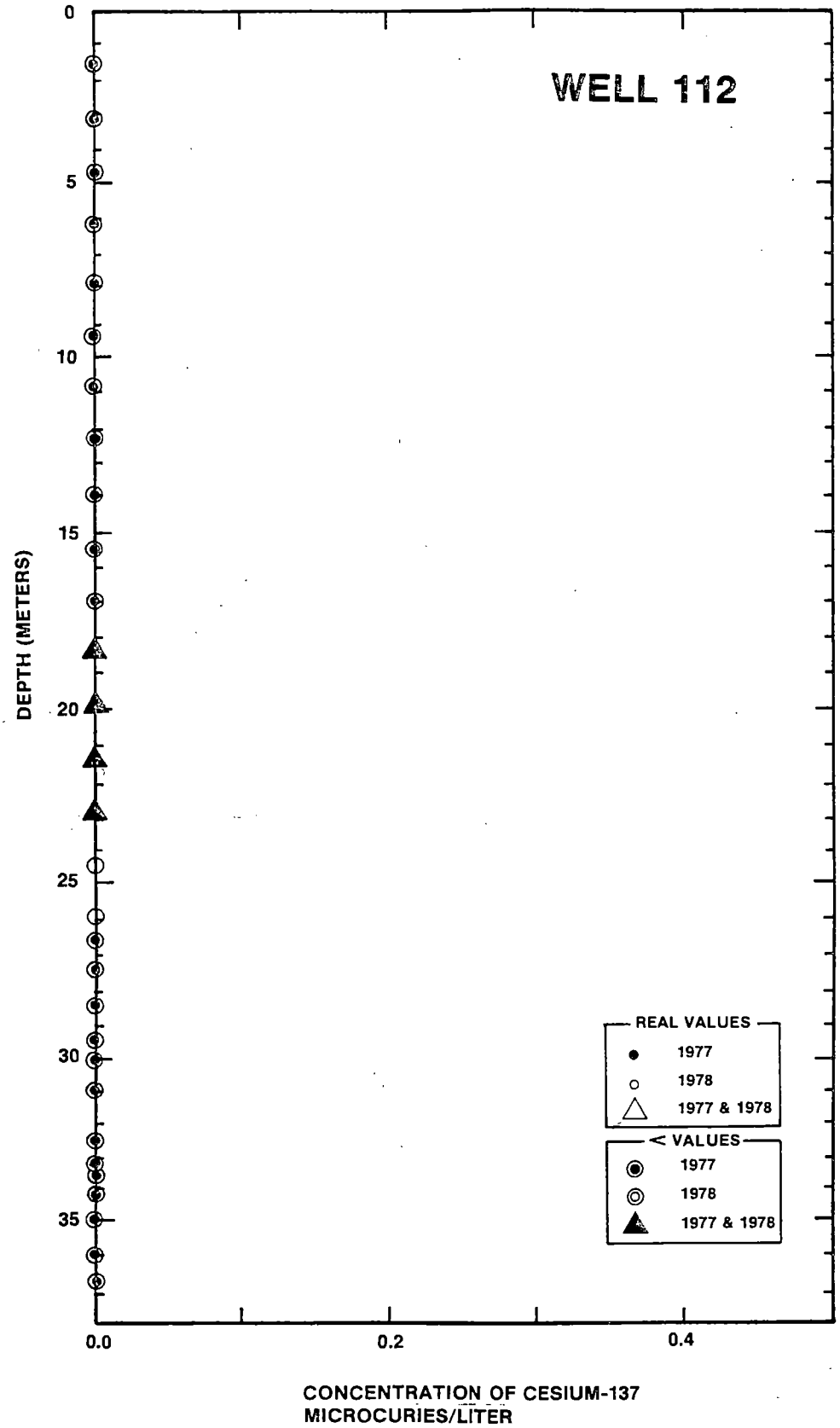

9 2 1 2 4 6 6 1 4 4 2

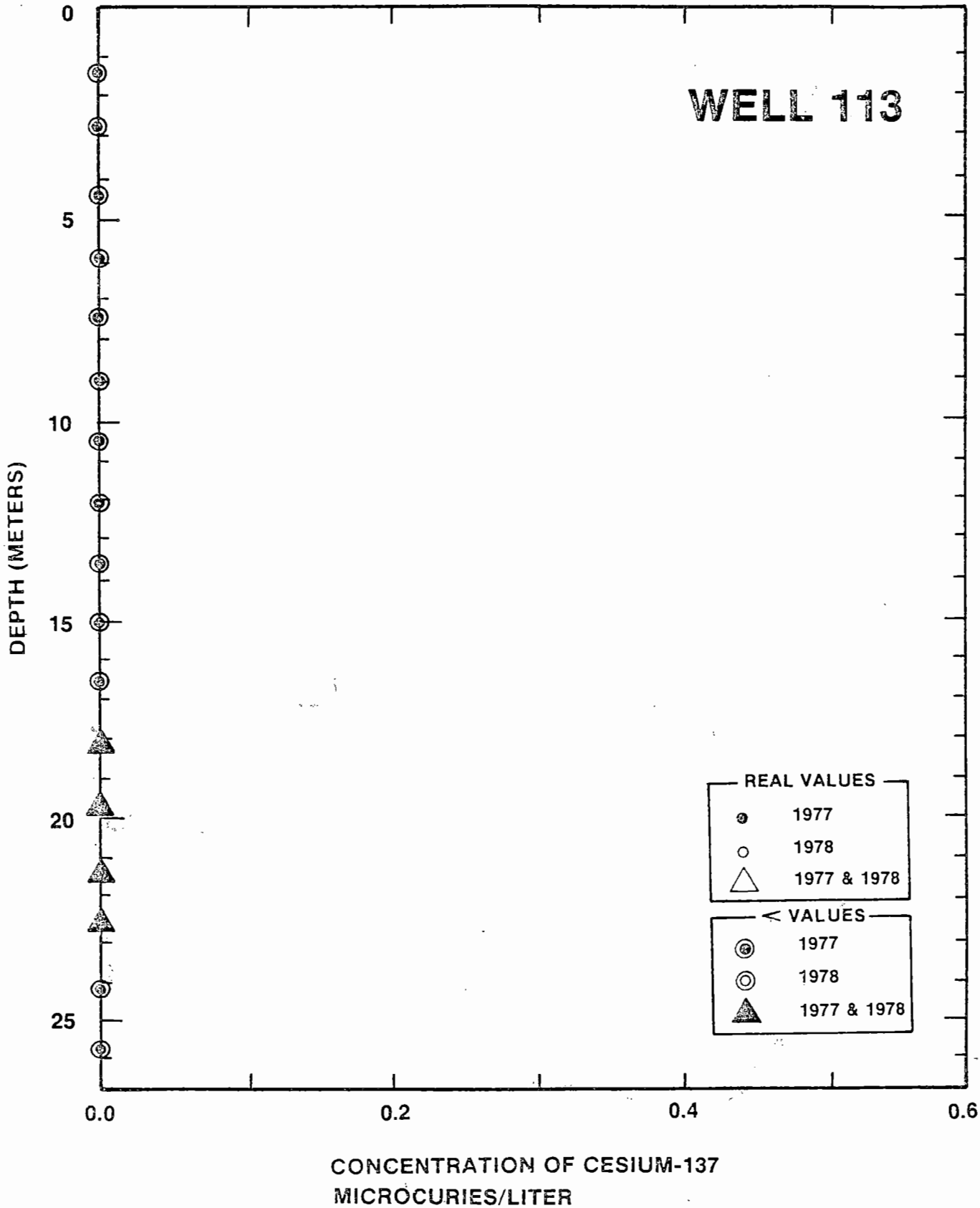
WELL 113
DEPTH (METERS)
0
5
10
15
20
25
0.0
0.2
0.4
0.6
CONCENTRATION OF CESIUM-137
MICROCURIES/LITER
REAL VALUES
1977
1978
1977 & 1978
< VALUES
1977
1978
1977 & 1978

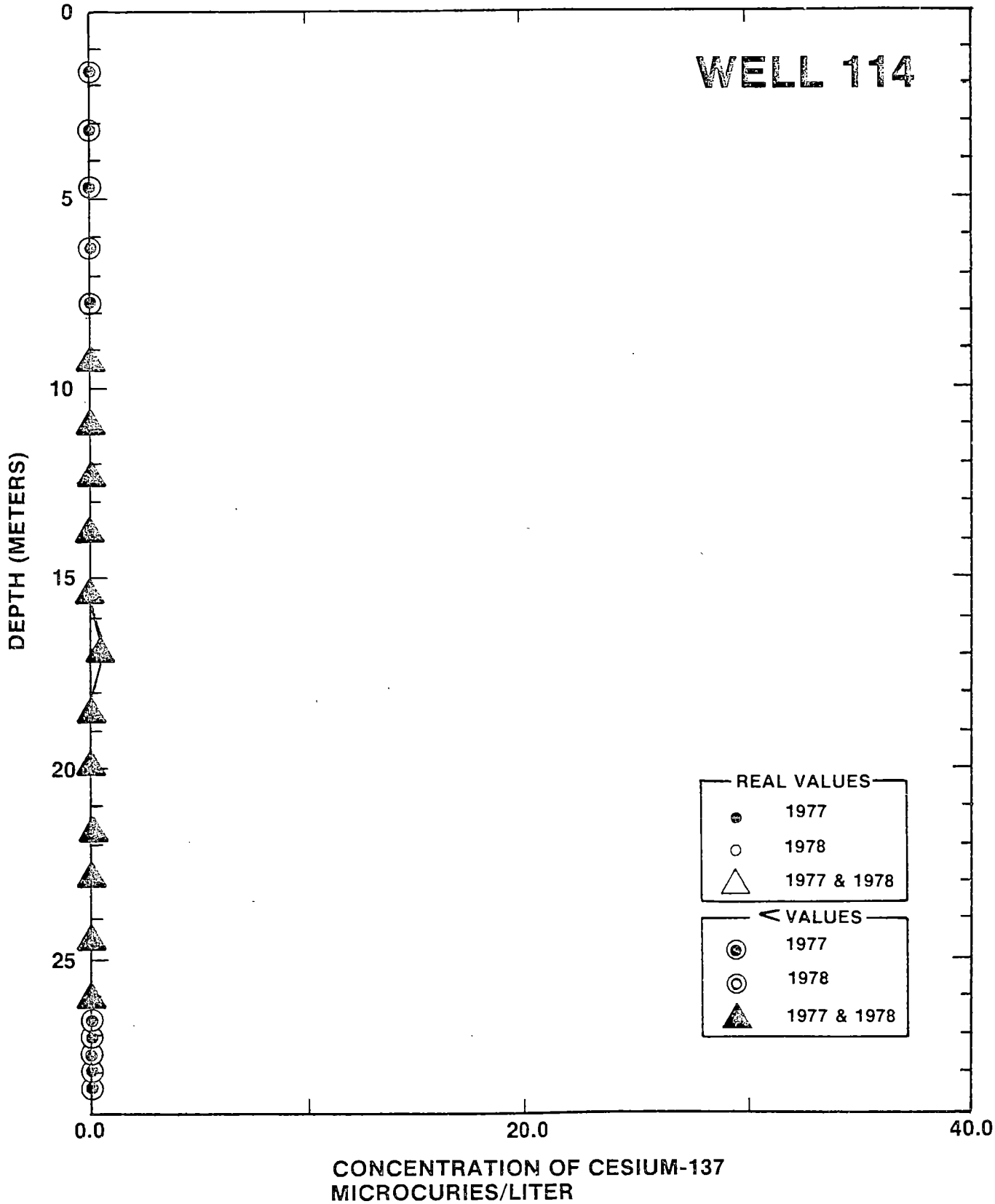
WELL 114
DEPTH (METERS)
0
5
10
15
20
25
0.0
20.0
40.0
CONCENTRATION OF CESIUM-137
MICROCURIES/LITER
REAL VALUES
1977
1978
1977 & 1978
< VALUES
1977
1978
1977 & 1978

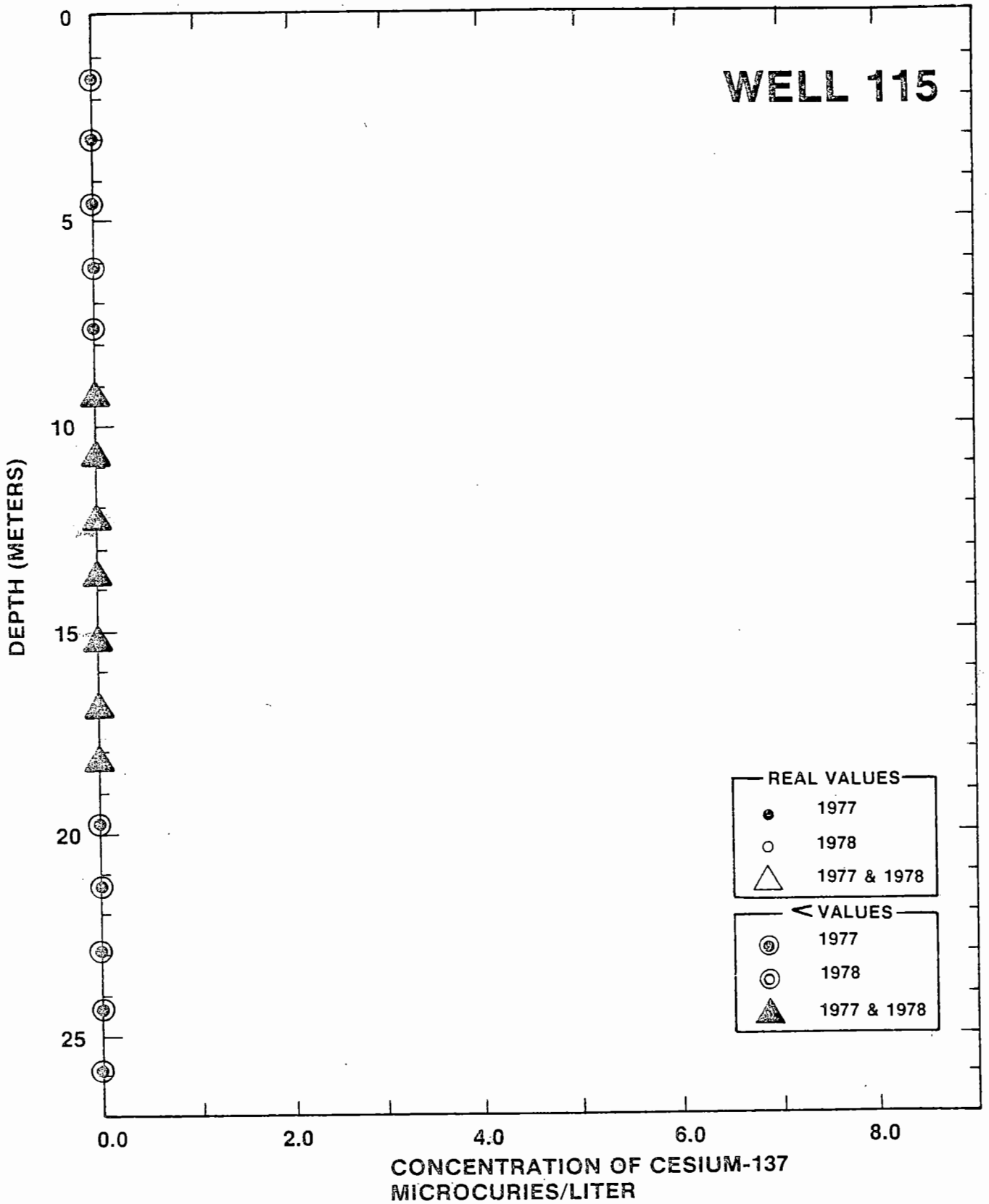
WELL 115
DEPTH (METERS)
0
5
10
15
20
25
0.0
2.0
4.0
6.0
8.0
CONCENTRATION OF CESIUM-137
MICROCURIES/LITER
REAL VALUES
1977
1978
1977 & 1978
< VALUES
1977
1978
1977 & 1978

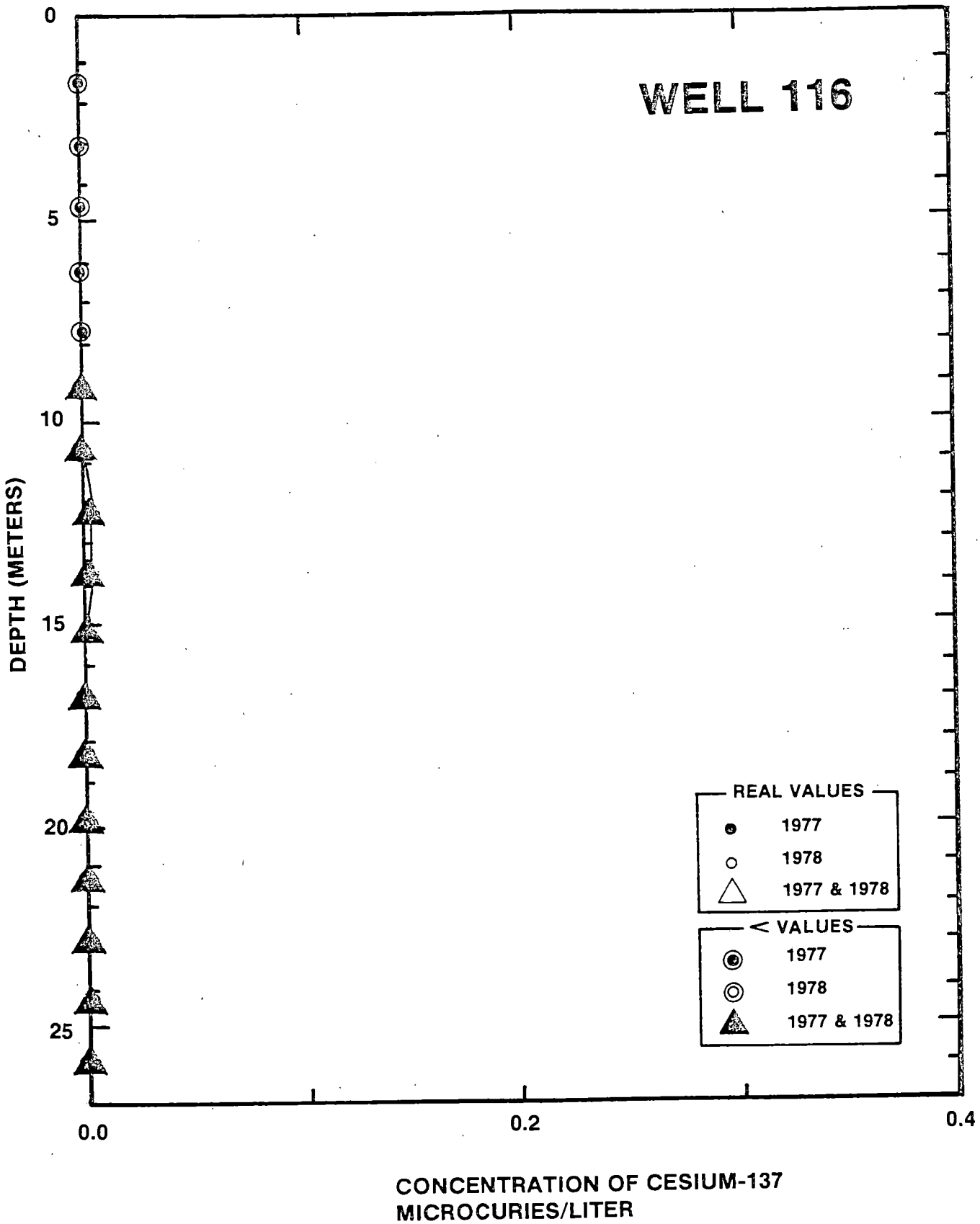
WELL 116
DEPTH (METERS)
0
5
10
15
20
25
0.0
0.2
0.4
CONCENTRATION OF CESIUM-137
MICROCURIES/LITER
REAL VALUES
1977
1978
1977 & 1978
< VALUES
1977
1978
1977 & 1978

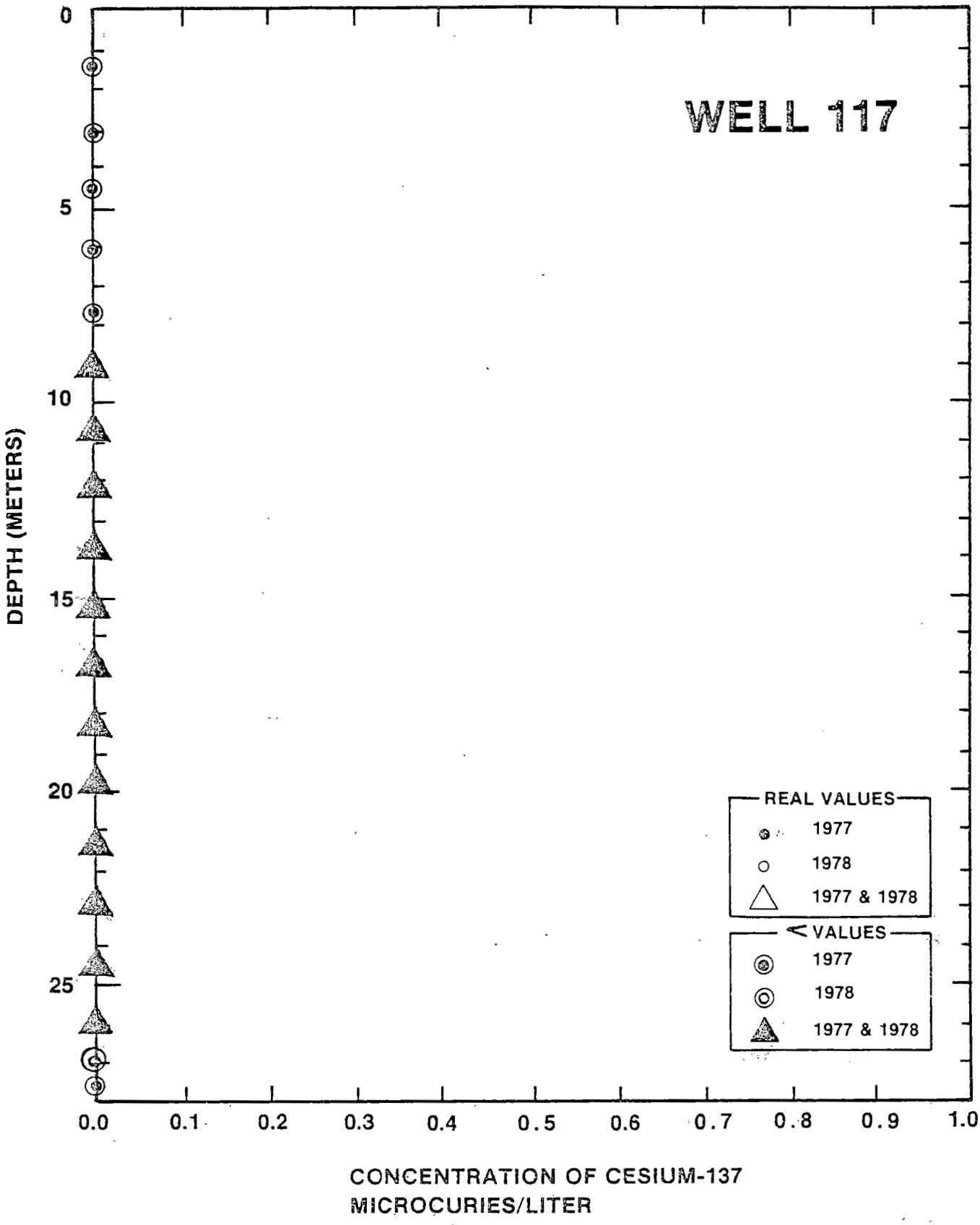
WELL 117
DEPTH (METERS)
0
5
10
15
20
25
0.0
0.1
0.2
0.3
0.4
0.5
0.6
0.7
0.8
0.9
1.0
CONCENTRATION OF CESIUM-137
MICROCURIES/LITER
REAL VALUES
1977
1978
1977 & 1978
< VALUES
1977
1978
1977 & 1978

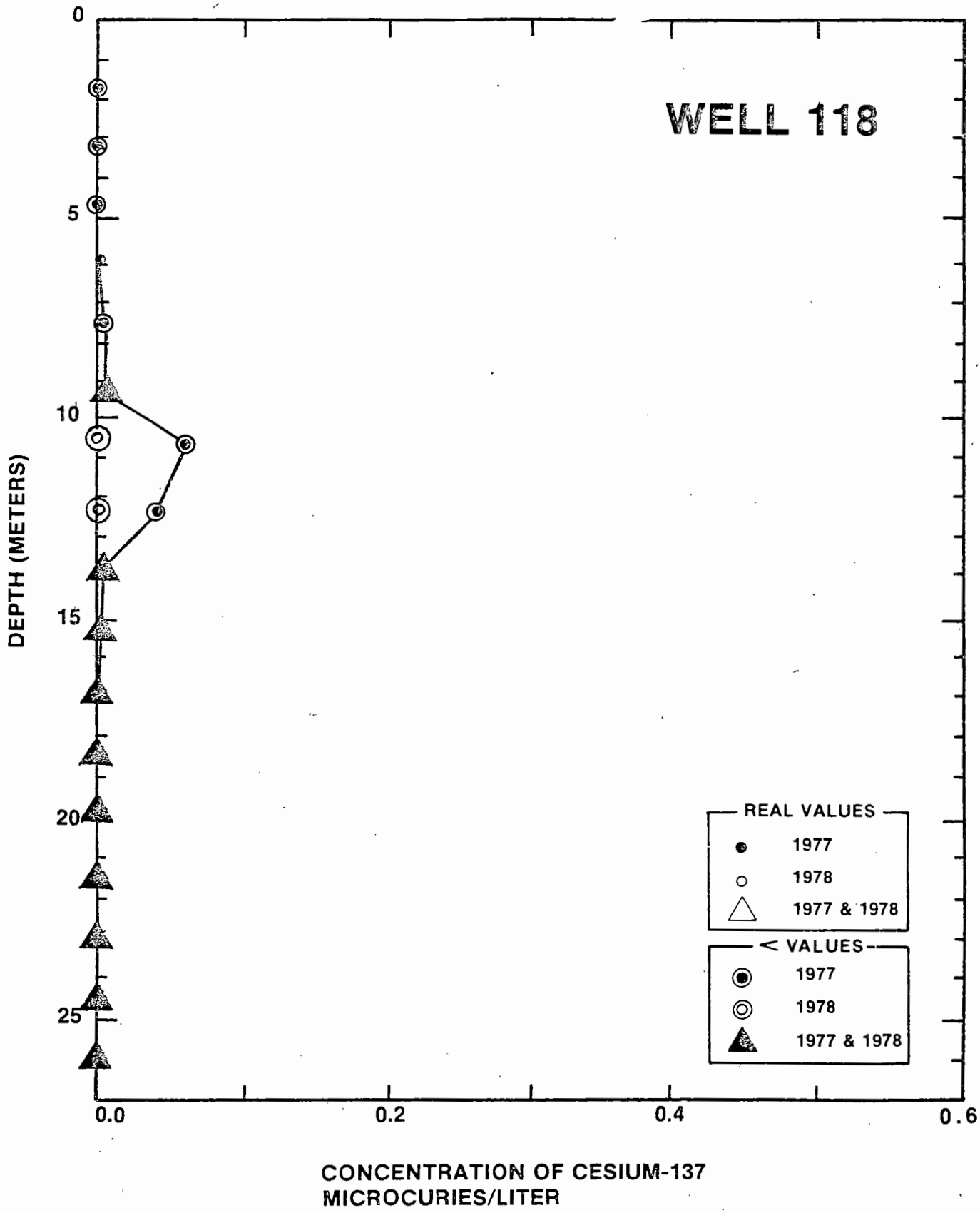
WELL 118
DEPTH (METERS)
0
5
10
15
20
25
0.0
0.2
0.4
0.6
CONCENTRATION OF CESIUM-137
MICROCURIES/LITER
REAL VALUES
1977
1978
1977 & 1978
< VALUES
1977
1978
1977 & 1978

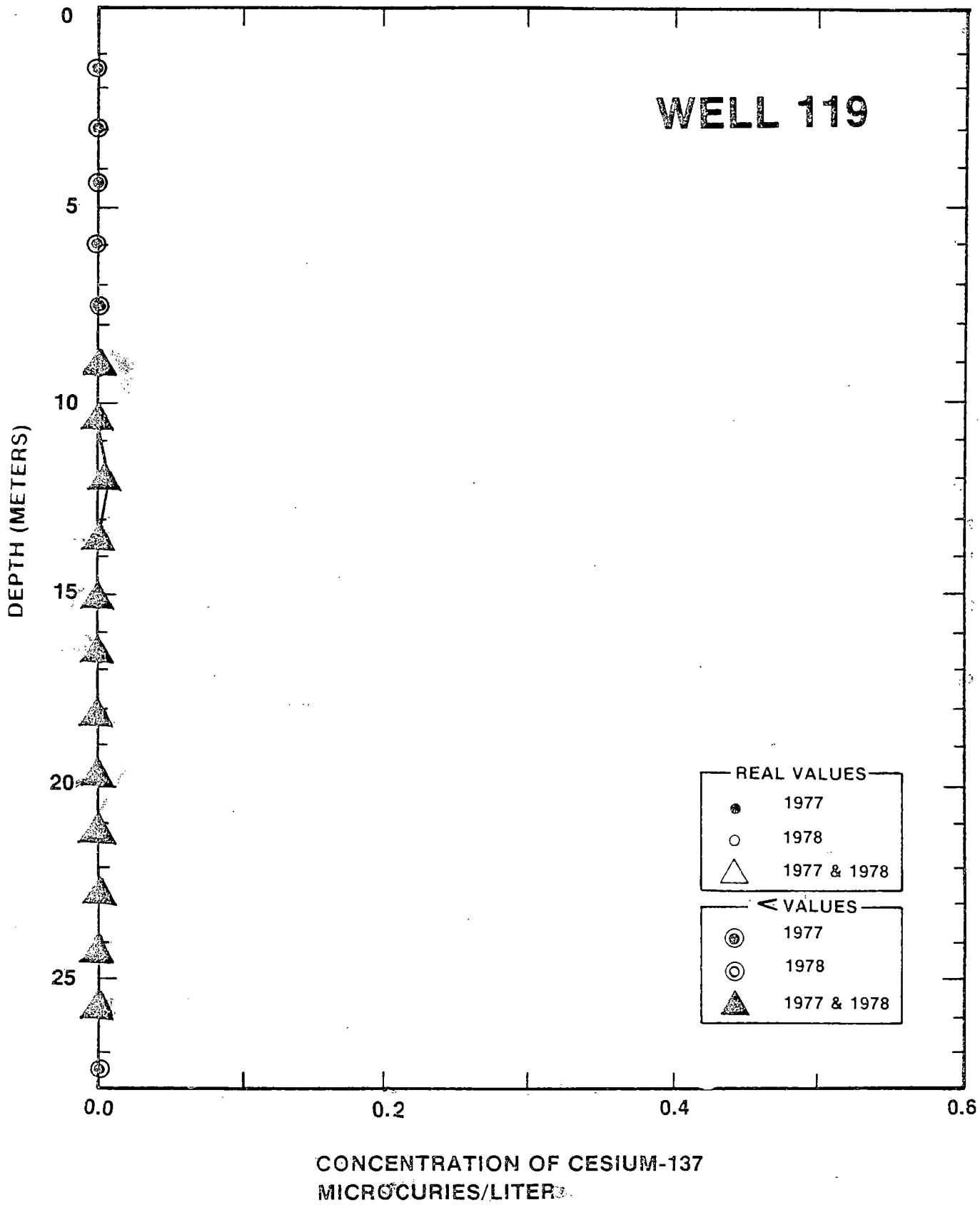
WELL 119
DEPTH (METERS)
0
5
10
15
20
25
0.0
0.2
0.4
0.6
CONCENTRATION OF CESIUM-137
MICROCURIES/LITER
REAL VALUES
1977
1978
1977 & 1978
< VALUES
1977
1978
1977 & 1978

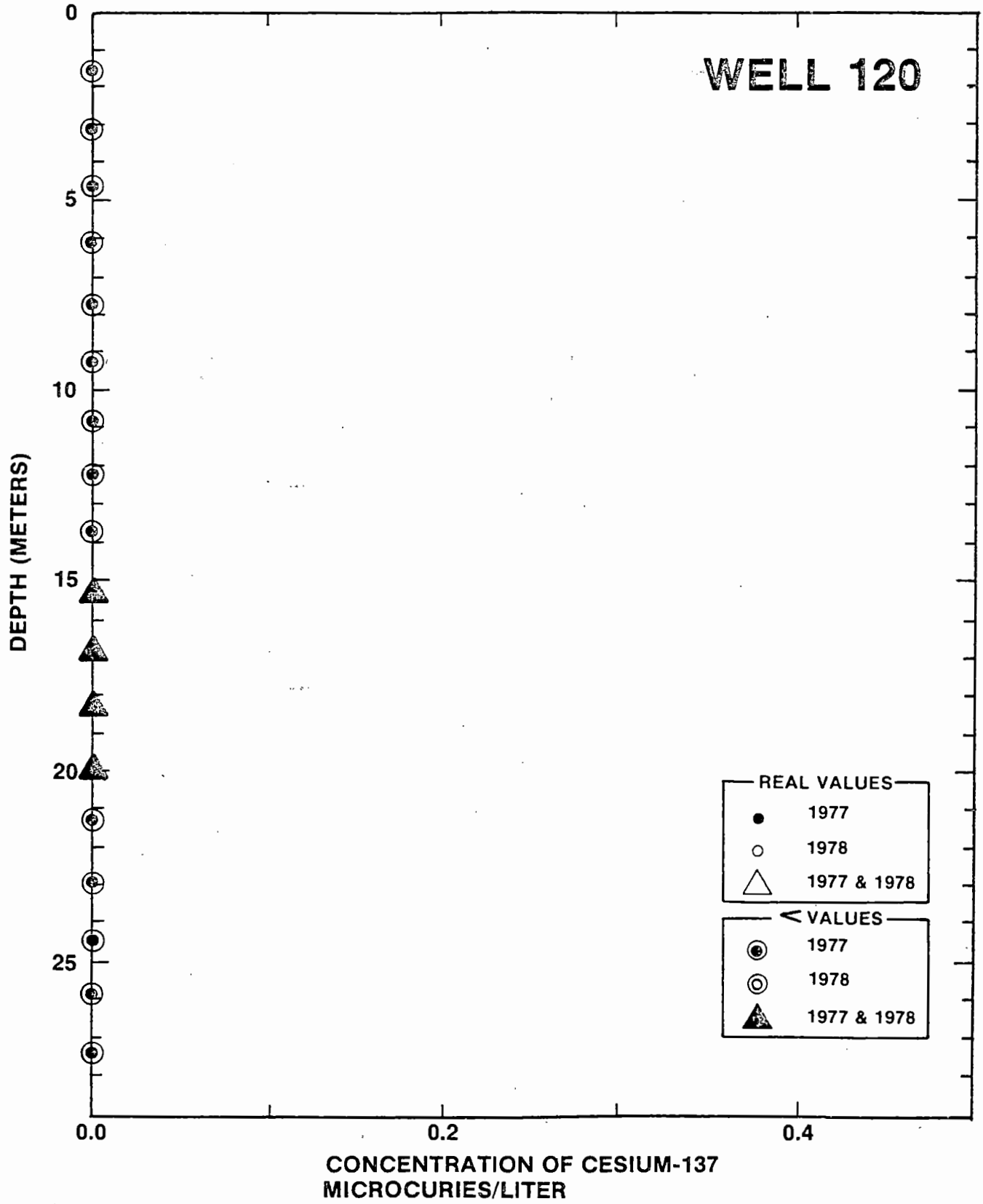
WELL 120
DEPTH (METERS)
0
5
10
15
20
25
0.0
0.2
0.4
CONCENTRATION OF CESIUM-137
MICROCURIES/LITER
REAL VALUES
1977
1978
1977 & 1978
< VALUES
1977
1978
1977 & 1978

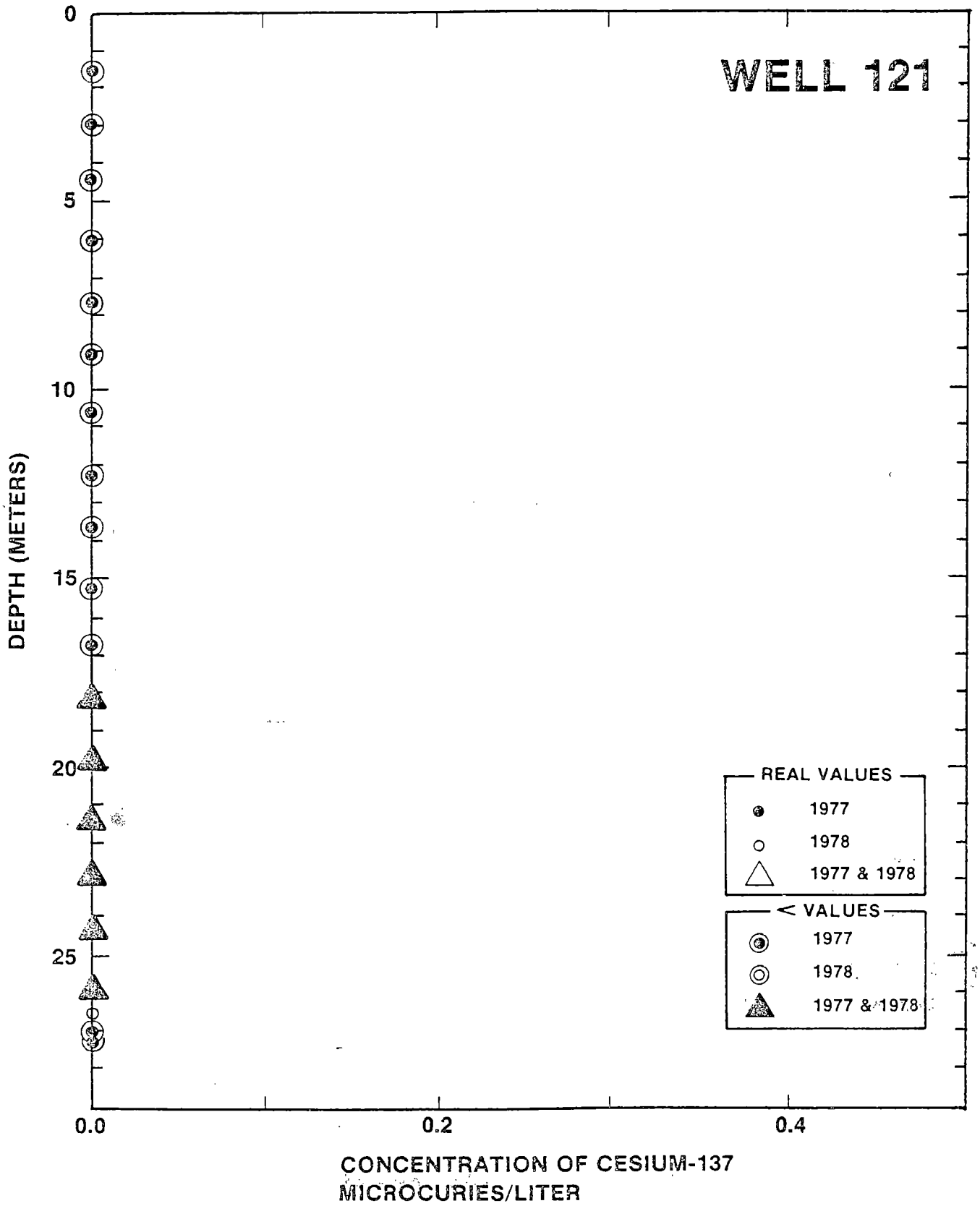
WELL 121
DEPTH (METERS)
0
5
10
15
20
25
0.0
0.2
0.4
CONCENTRATION OF CESIUM-137
MICROCURIES/LITER
REAL VALUES
1977
1978
1977 & 1978
< VALUES
1977
1978
1977 & 1978

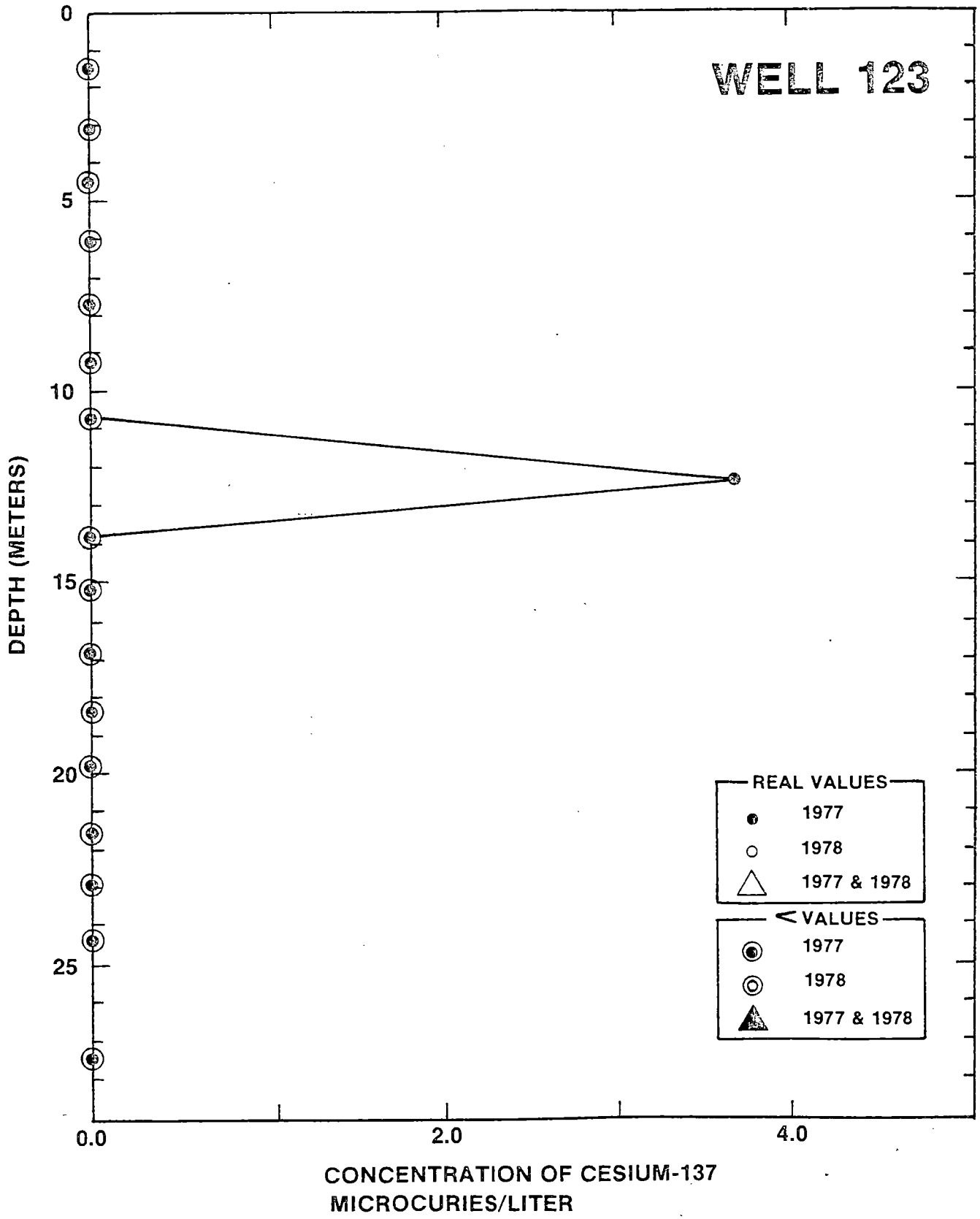
WELL 123
DEPTH (METERS)
0
5
10
15
20
25
0.0
2.0
4.0
CONCENTRATION OF CESIUM-137
MICROCURIES/LITER
REAL VALUES
1977
1978
1977 & 1978
< VALUES
1977
1978
1977 & 1978

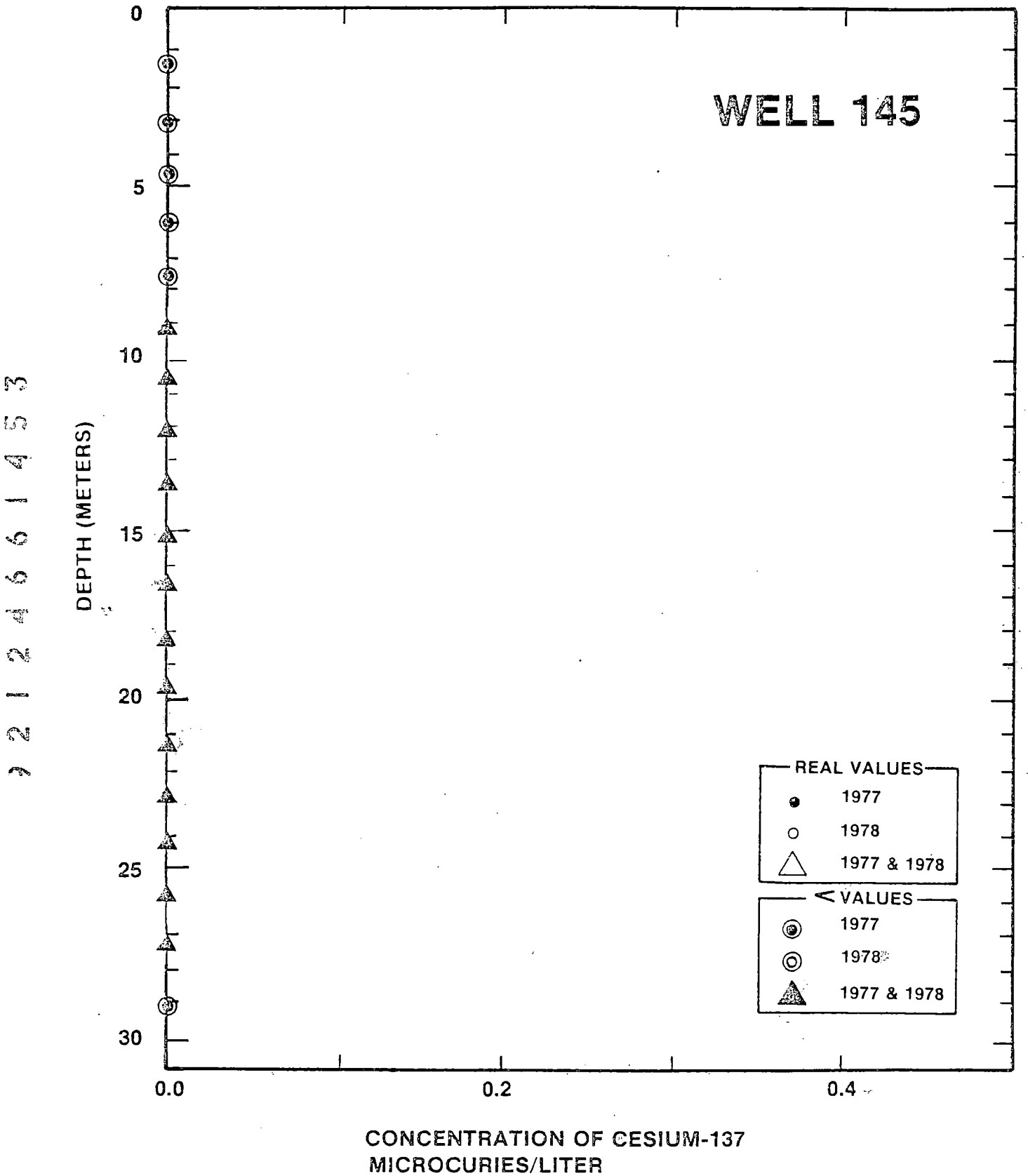
WELL 145
DEPTH (METERS)
0
5
10
15
20
25
30
0.0
0.2
0.4
CONCENTRATION OF CESIUM-137
MICROCURIES/LITER
REAL VALUES
1977
1978
1977 & 1978
< VALUES
1977
1978
1977 & 1978

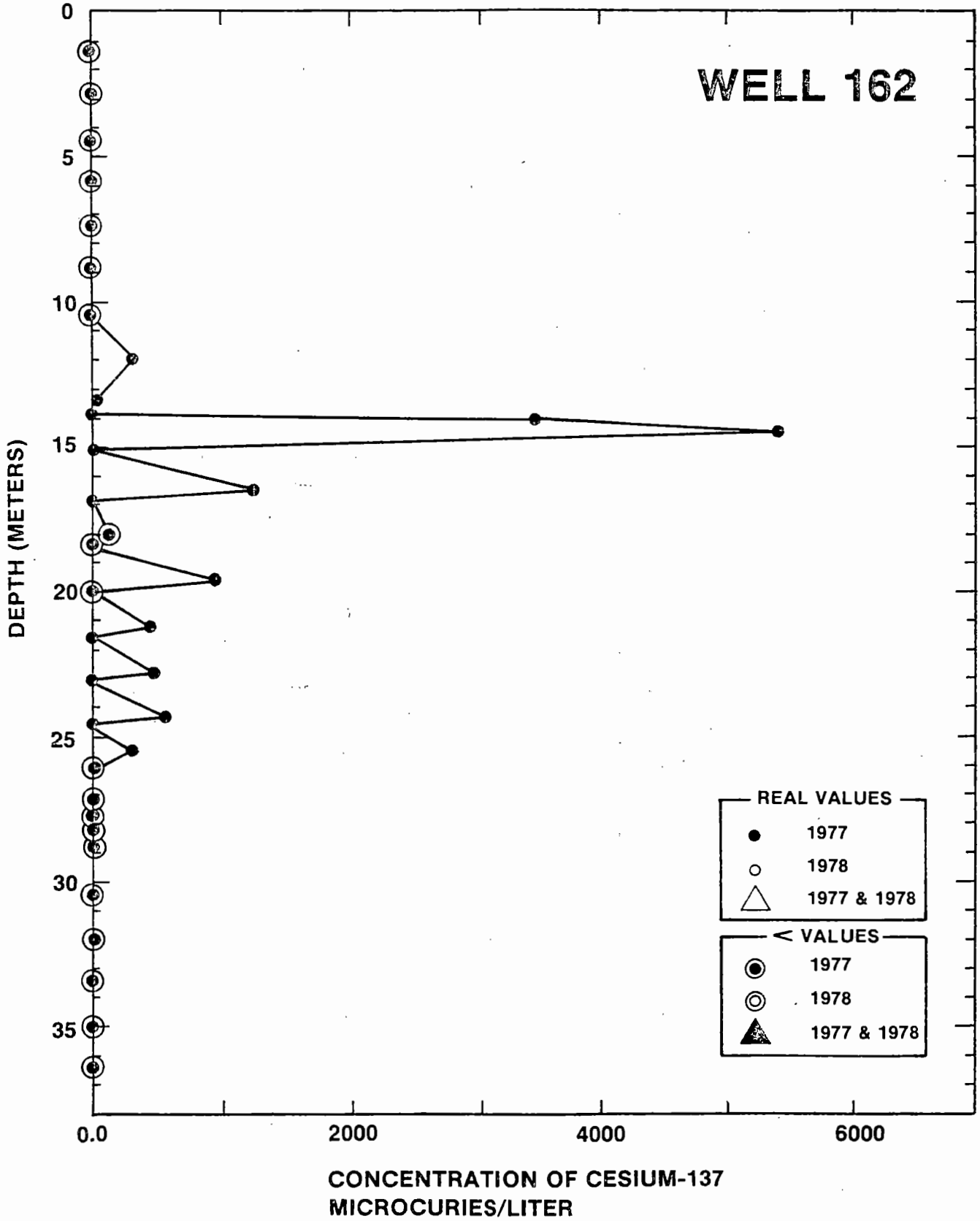

9 2 1 2 4 6 6 1 4 5 4

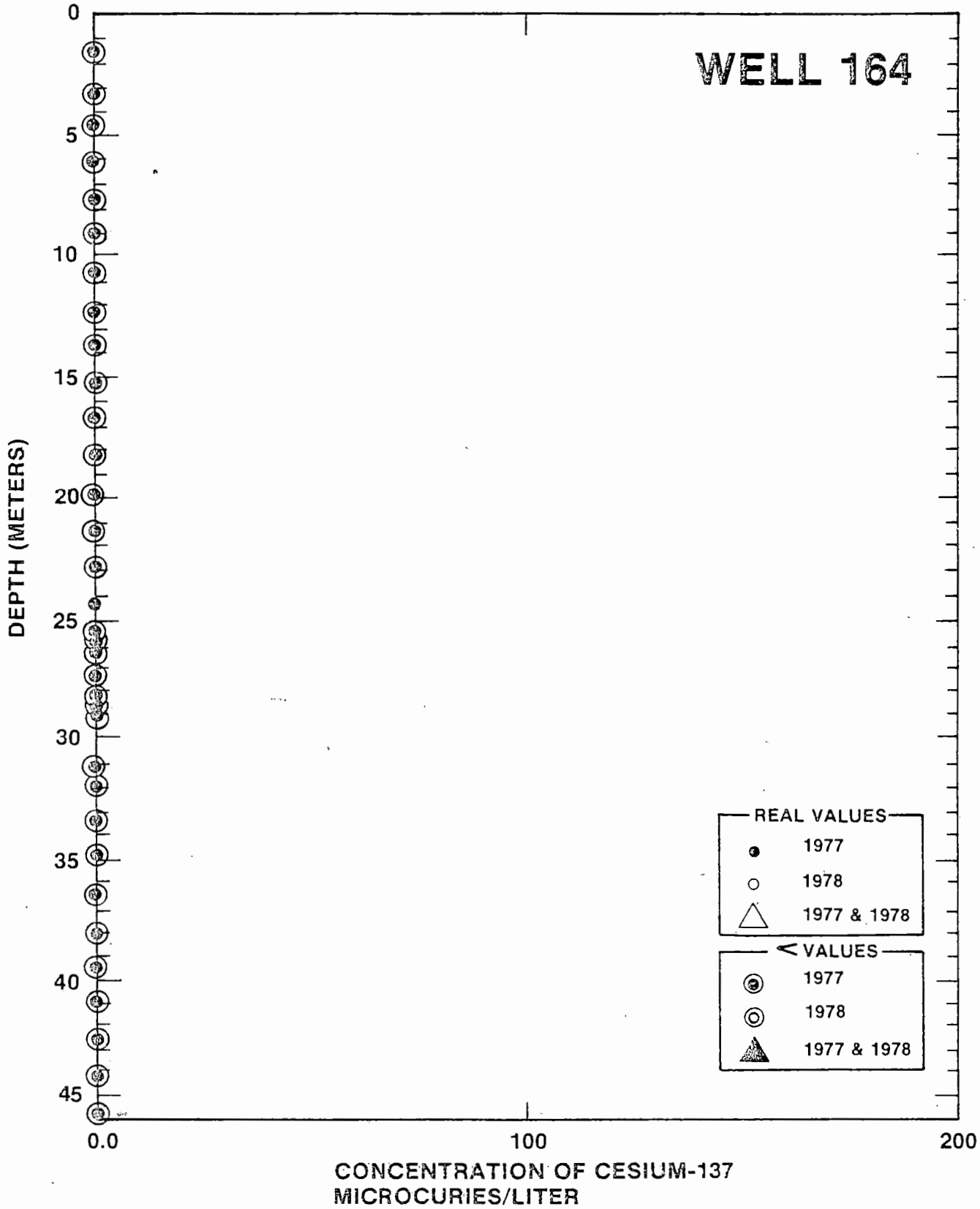
WELL 164
DEPTH (METERS)
0
5
10
15
20
25
30
35
40
45
0.0
100
200
CONCENTRATION OF CESIUM-137
MICROCURIES/LITER
REAL VALUES
1977
1978
1977 & 1978
< VALUES
1977
1978
1977 & 1978

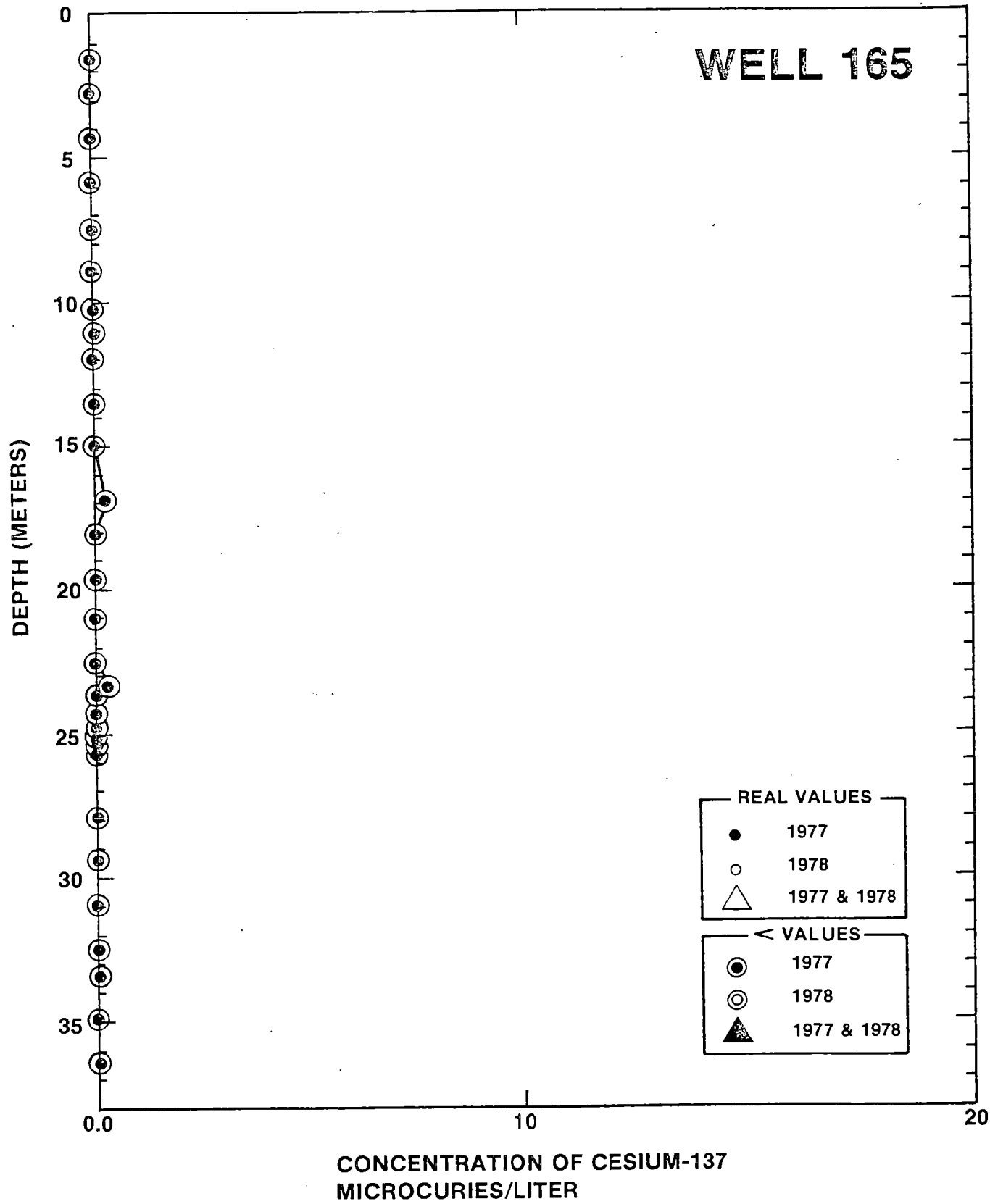
WELL 165
DEPTH (METERS)
0
5
10
15
20
25
30
35
0.0
10
20
CONCENTRATION OF CESIUM-137
MICROCURIES/LITER
REAL VALUES
1977
1978
1977 & 1978
< VALUES
1977
1978
1977 & 1978

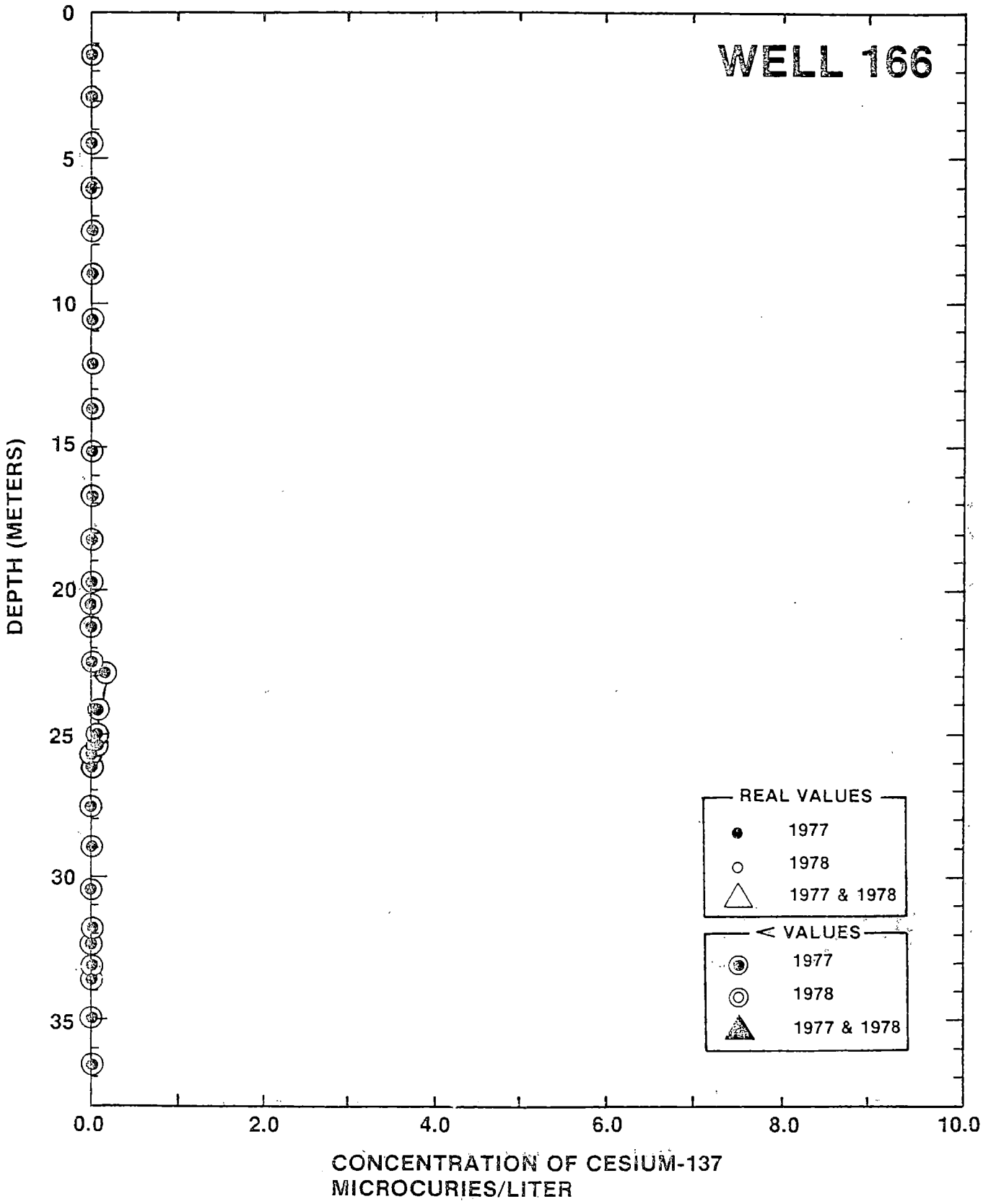
WELL 166
DEPTH (METERS)
0
5
10
15
20
25
30
35
0.0
2.0
4.0
6.0
8.0
10.0
CONCENTRATION OF CESIUM-137
MICROCURIES/LITER
REAL VALUES
1977
1978
1977 & 1978
< VALUES
1977
1978
1977 & 1978

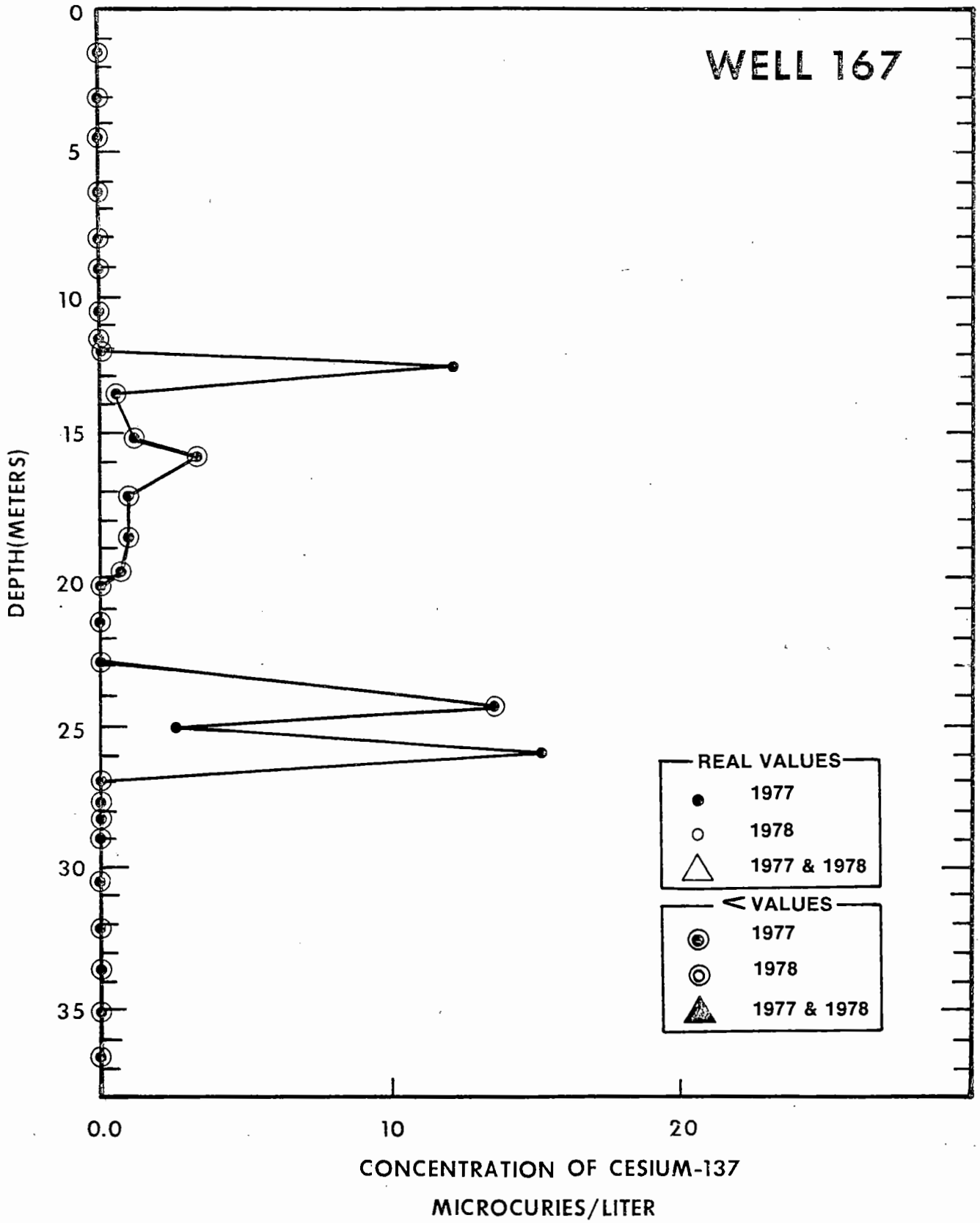

9 2 1 2 4 6 6 1 4 5 8

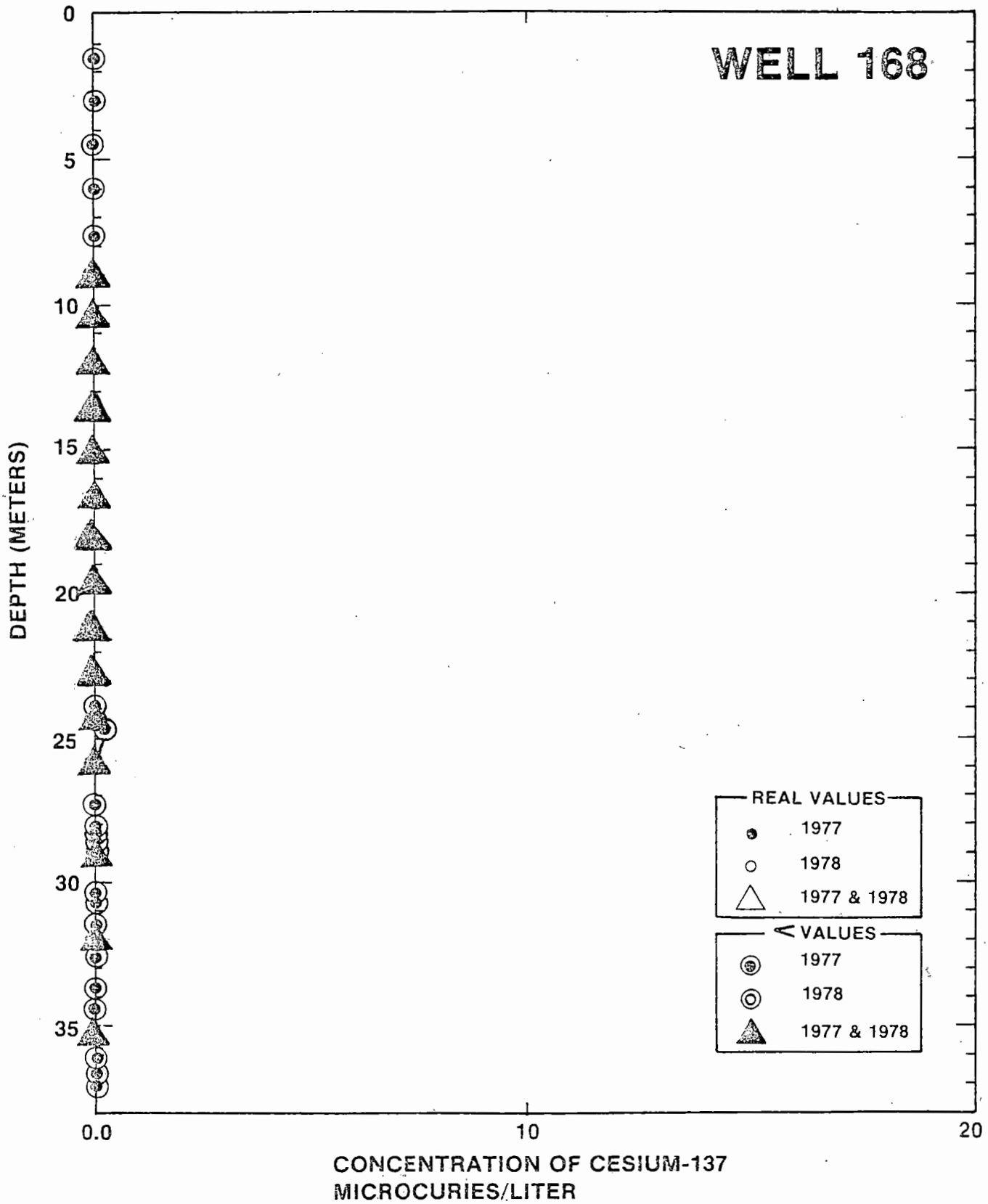
WELL 168
DEPTH (METERS)
0
5
10
15
20
25
30
35
0.0
10
20
CONCENTRATION OF CESIUM-137
MICROCURIES/LITER
REAL VALUES
1977
1978
1977 & 1978
< VALUES
1977
1978
1977 & 1978

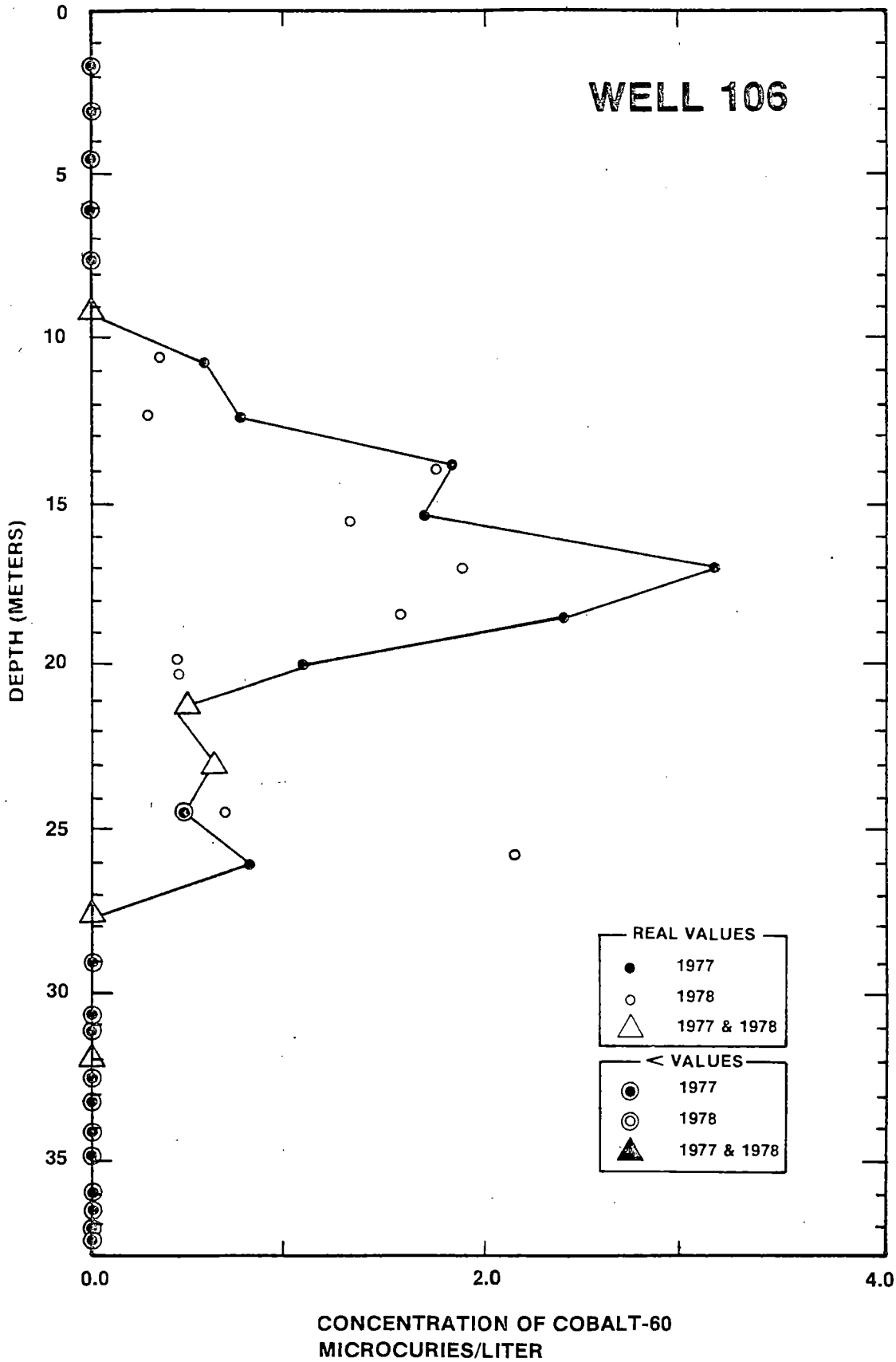

9 2 1 2 4 6 6 1 4 5 0

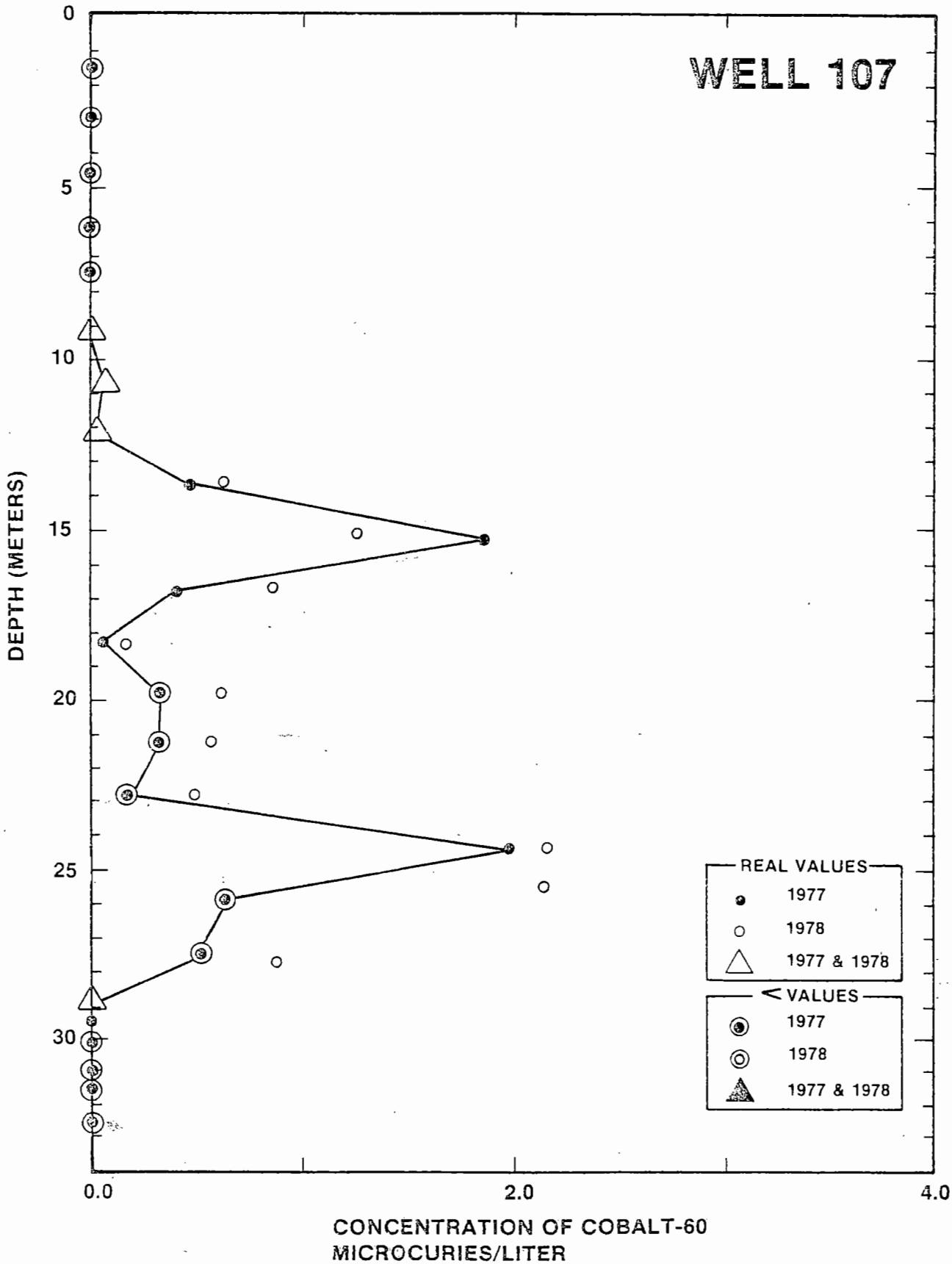
WELL 107
DEPTH (METERS)
0
5
10
15
20
25
30
0.0
2.0
4.0
CONCENTRATION OF COBALT-60
MICROCURIES/LITER
REAL VALUES
1977
1978
1977 & 1978
< VALUES
1977
1978
1977 & 1978

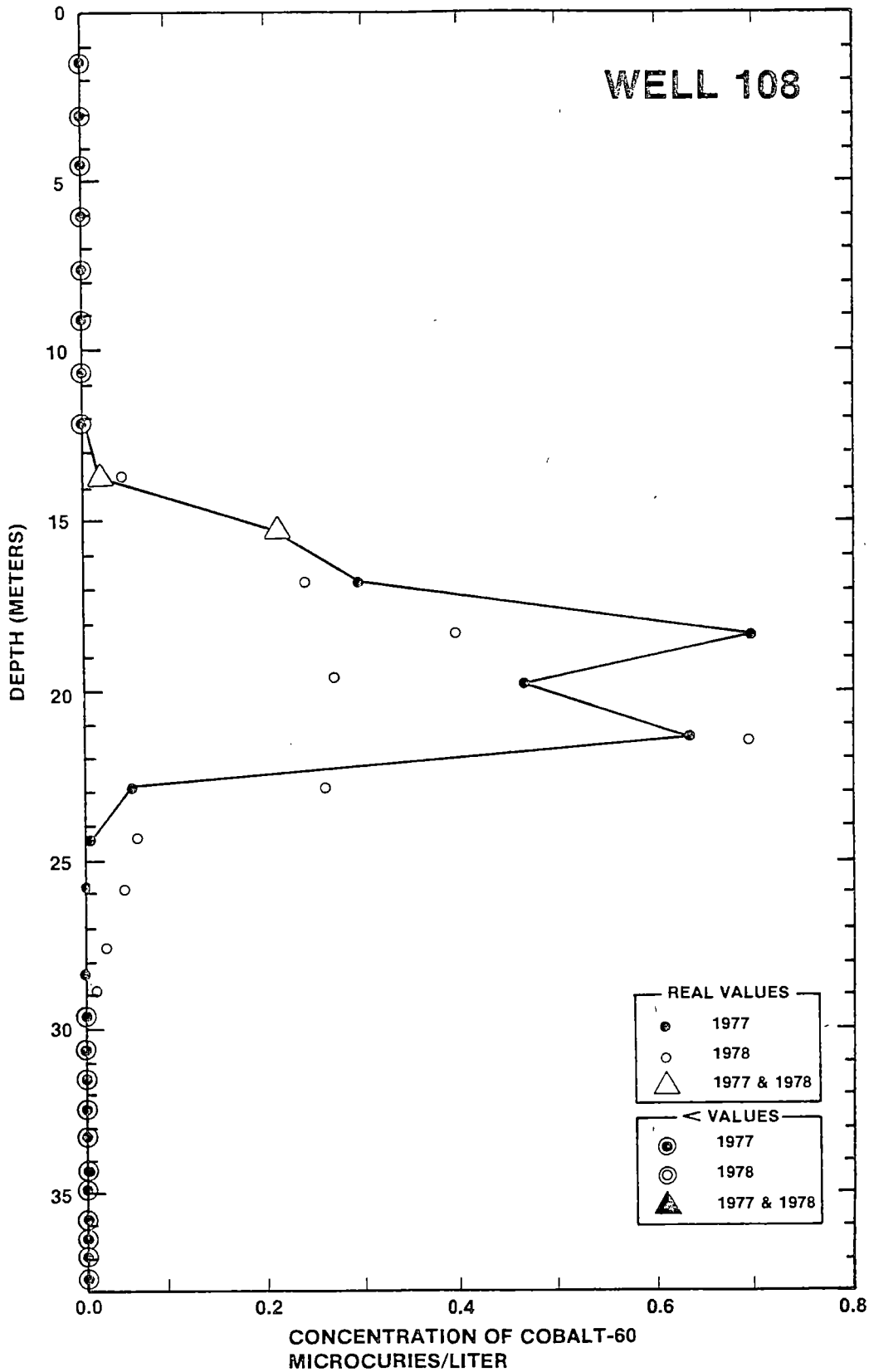
WELL 108
DEPTH (METERS)
0
5
10
15
20
25
30
35
0.0
0.2
0.4
0.6
0.8
CONCENTRATION OF COBALT-60
MICROCURIES/LITER
REAL VALUES
1977
1978
1977 & 1978
< VALUES
1977
1978
1977 & 1978

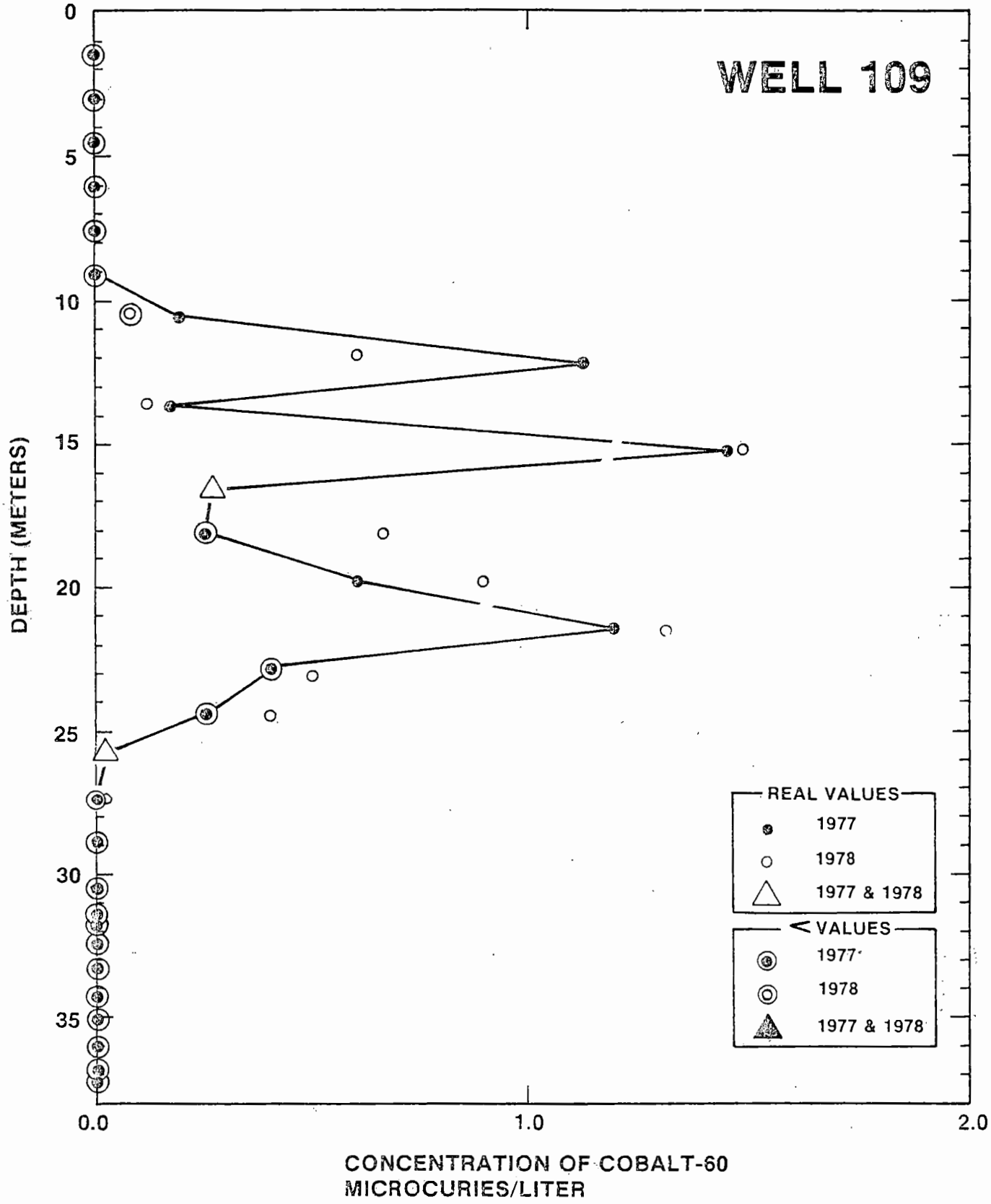
WELL 109
DEPTH (METERS)
0
5
10
15
20
25
30
35
0.0
1.0
2.0
CONCENTRATION OF COBALT-60
MICROCURIES/LITER
REAL VALUES
1977
1978
1977 & 1978
< VALUES
1977
1978
1977 & 1978

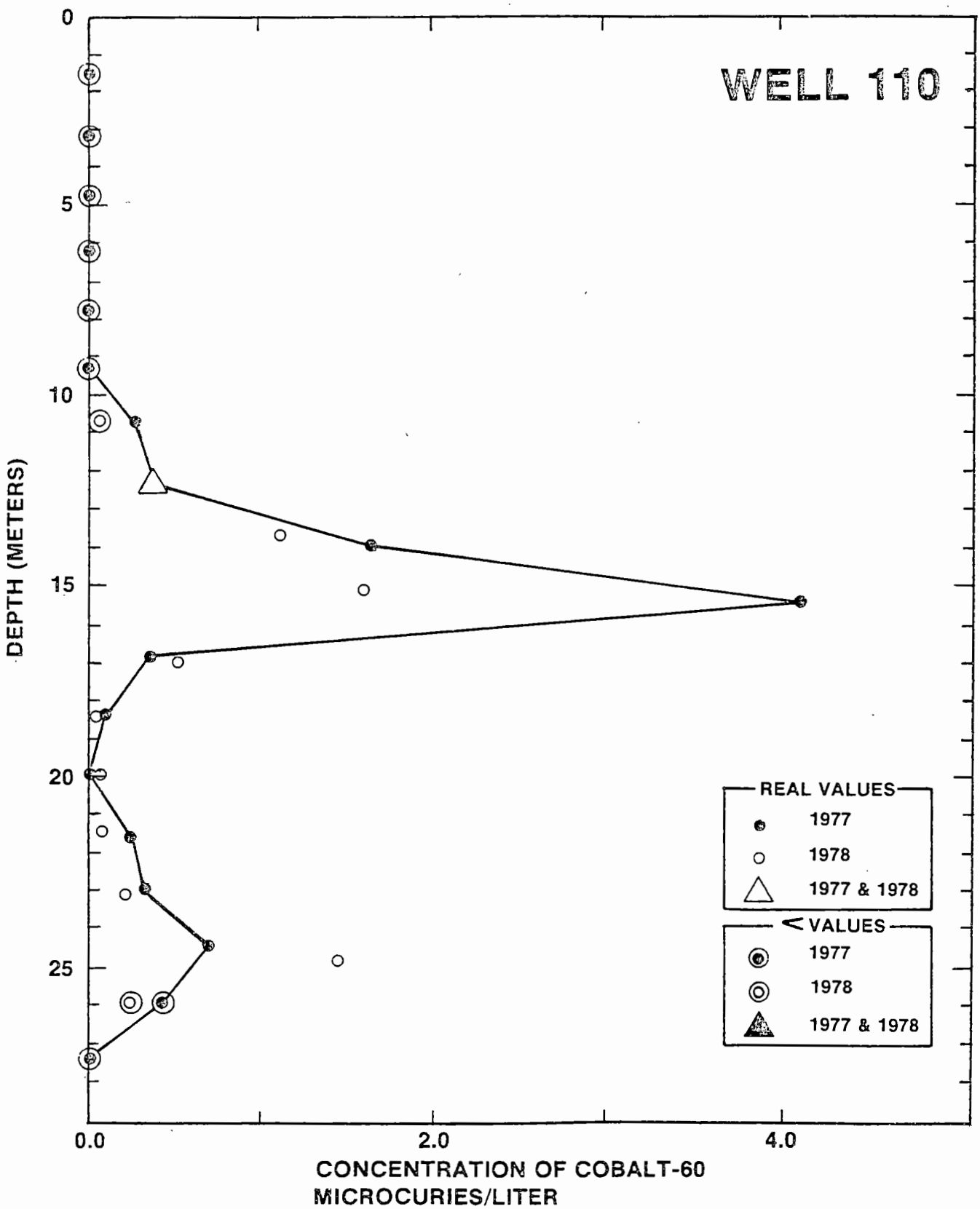
WELL 110
DEPTH (METERS)
0
5
10
15
20
25
0.0
2.0
4.0
CONCENTRATION OF COBALT-60
MICROCURIES/LITER
REAL VALUES
1977
1978
1977 & 1978
< VALUES
1977
1978
1977 & 1978

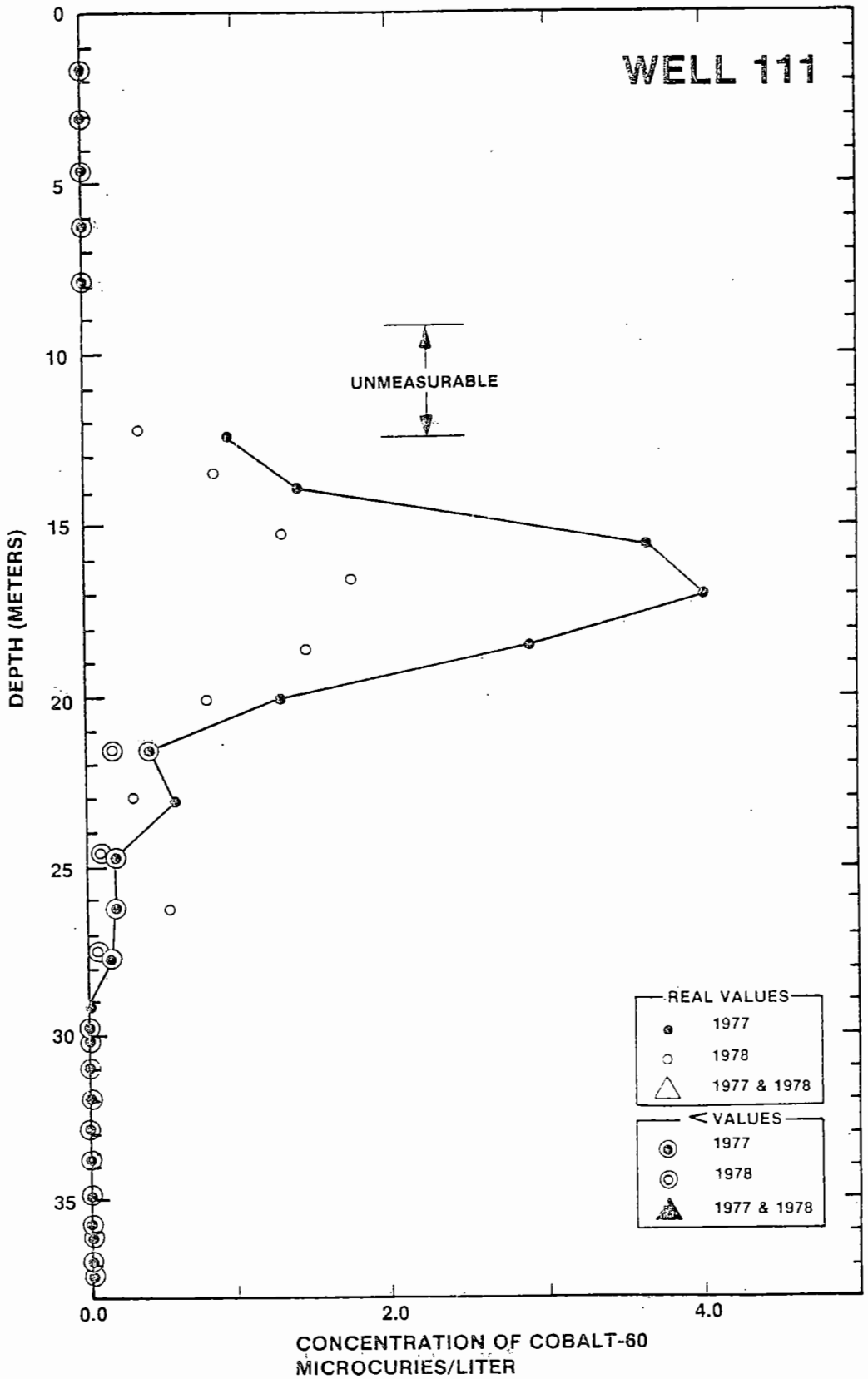
WELL 111
UNMEASURABLE
DEPTH (METERS)
0
5
10
15
20
25
30
35
0.0
2.0
4.0
CONCENTRATION OF COBALT-60
MICROCURIES/LITER
REAL VALUES
1977
1978
1977 & 1978
< VALUES
1977
1978
1977 & 1978

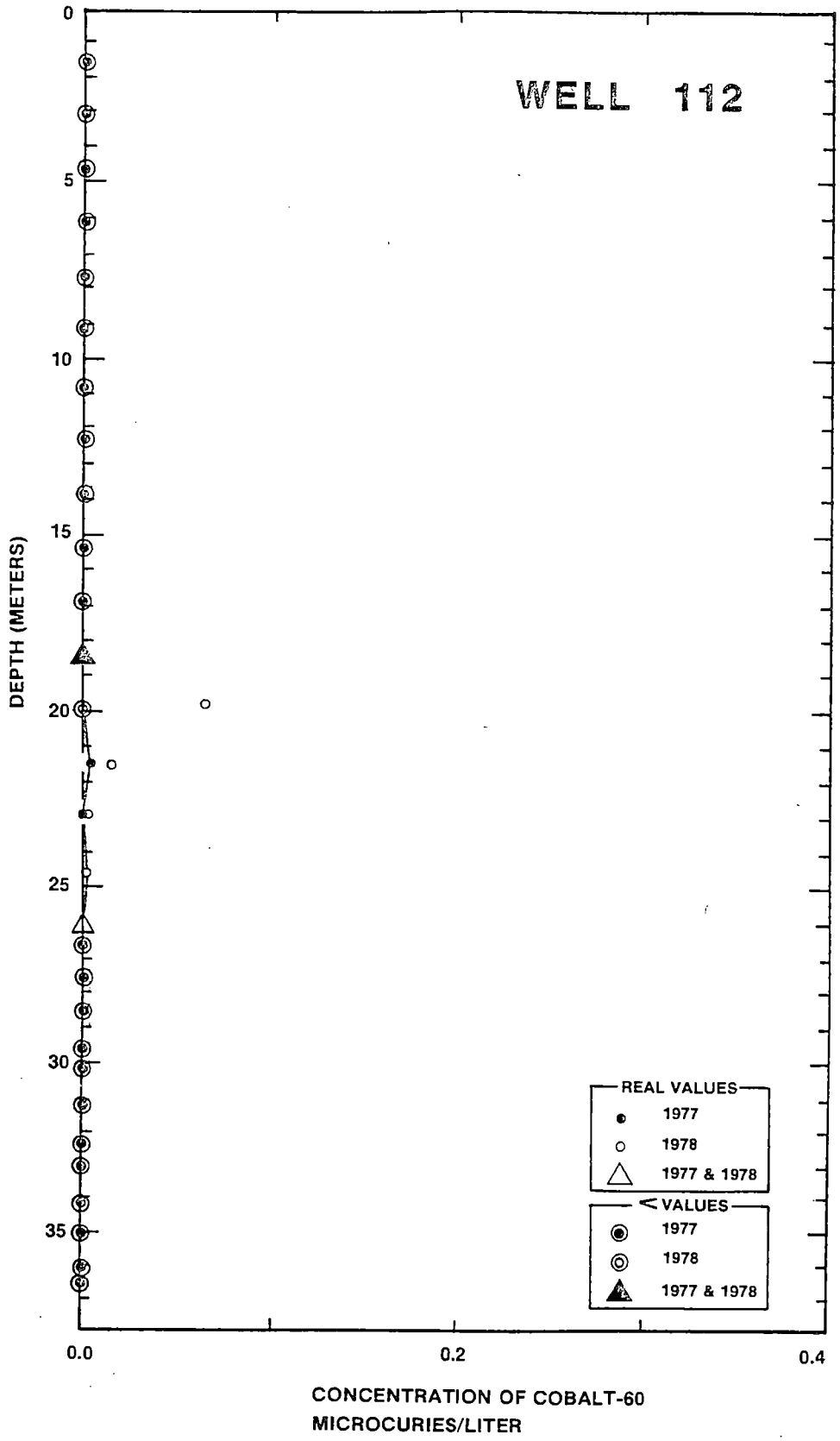
WELL 112
DEPTH (METERS)
0
5
10
15
20
25
30
35
0.0
0.2
0.4
CONCENTRATION OF COBALT-60
MICROCURIES/LITER
REAL VALUES
1977
1978
1977 & 1978
< VALUES
1977
1978
1977 & 1978

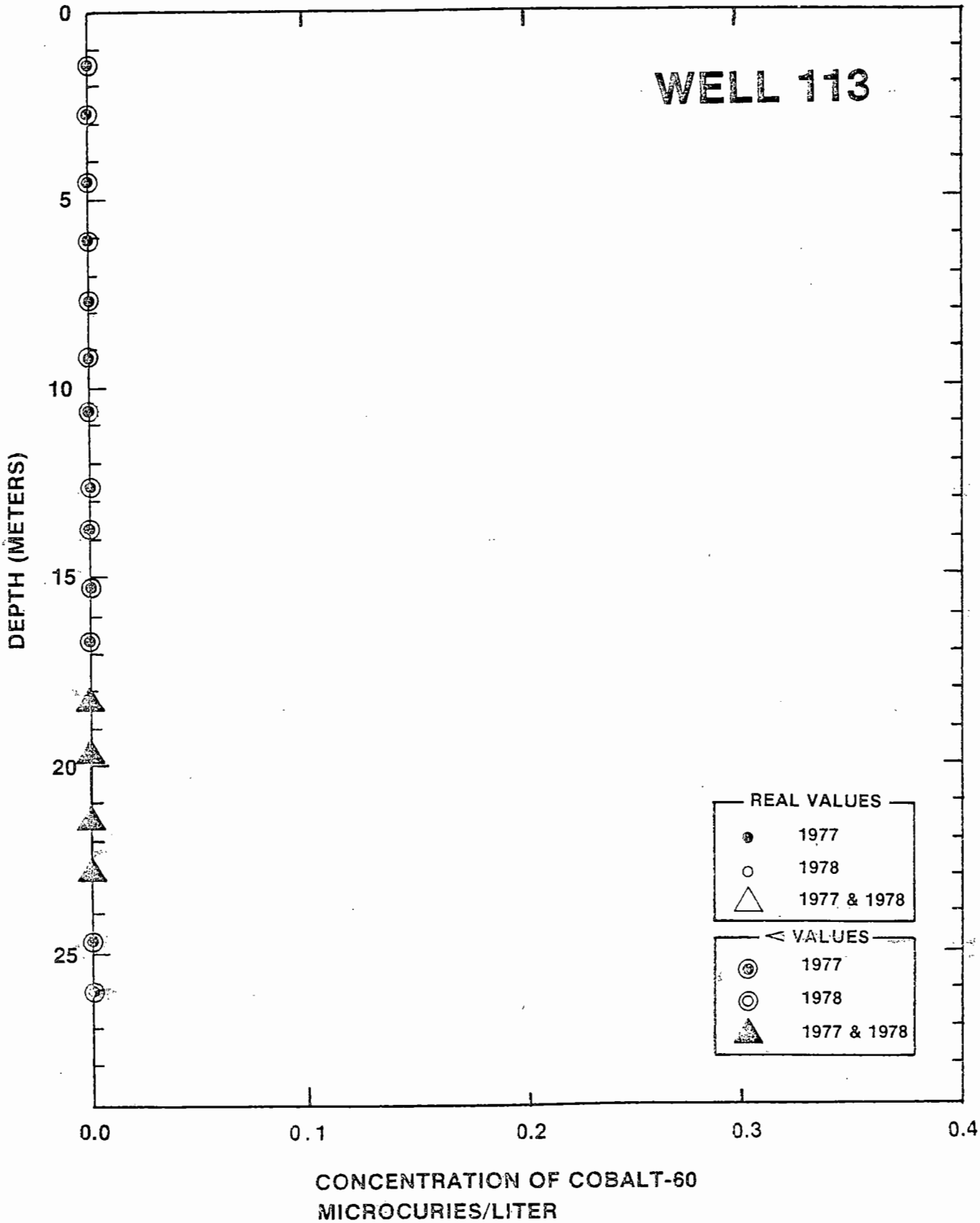
WELL 113
DEPTH (METERS)
0
5
10
15
20
25
0.0
0.1
0.2
0.3
0.4
CONCENTRATION OF COBALT-60
MICROCURIES/LITER
REAL VALUES
1977
1978
1977 & 1978
< VALUES
1977
1978
1977 & 1978

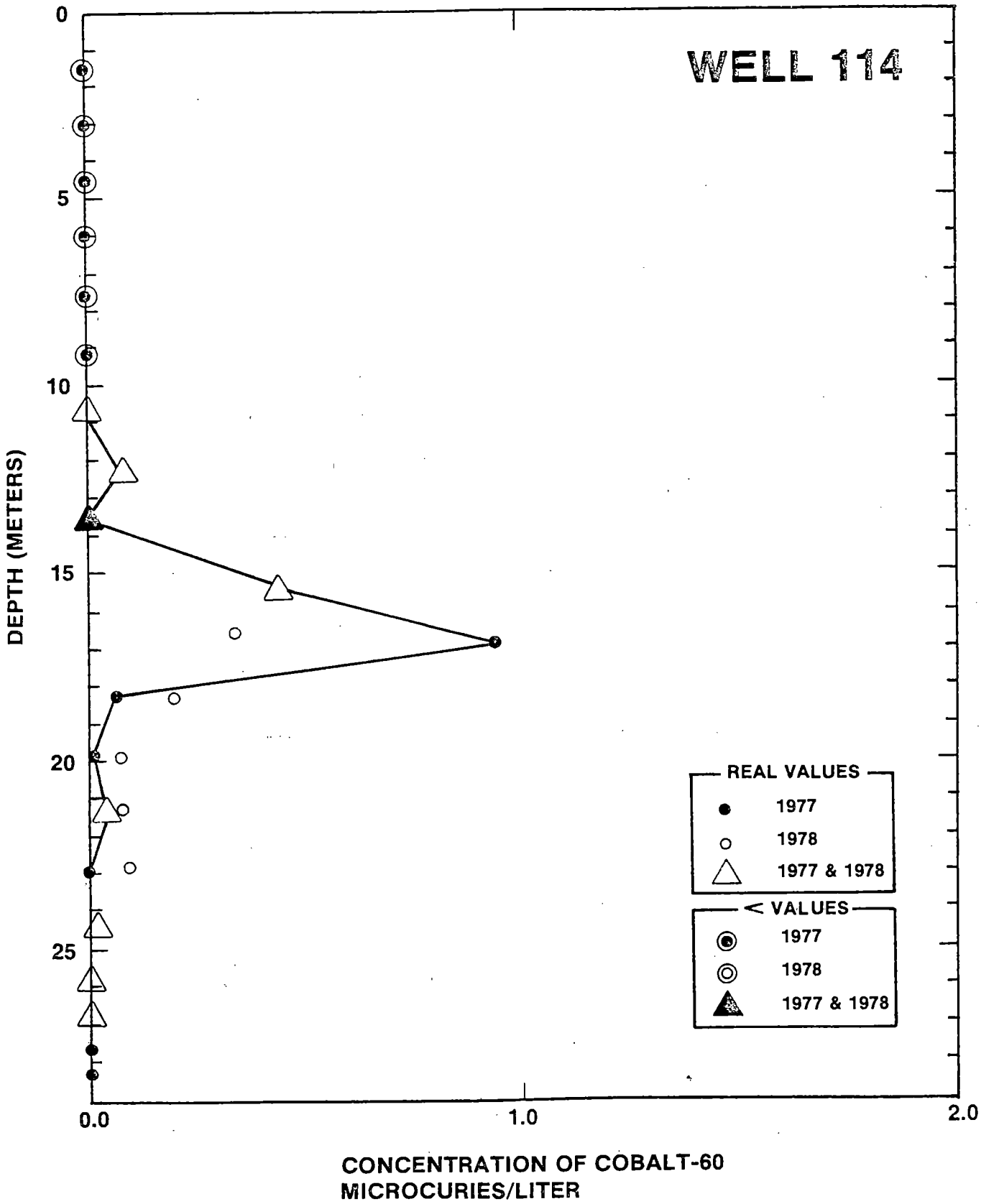
WELL 114
DEPTH (METERS)
0
5
10
15
20
25
0.0
1.0
2.0
CONCENTRATION OF COBALT-60
MICROCURIES/LITER
REAL VALUES
1977
1978
1977 & 1978
< VALUES
1977
1978
1977 & 1978

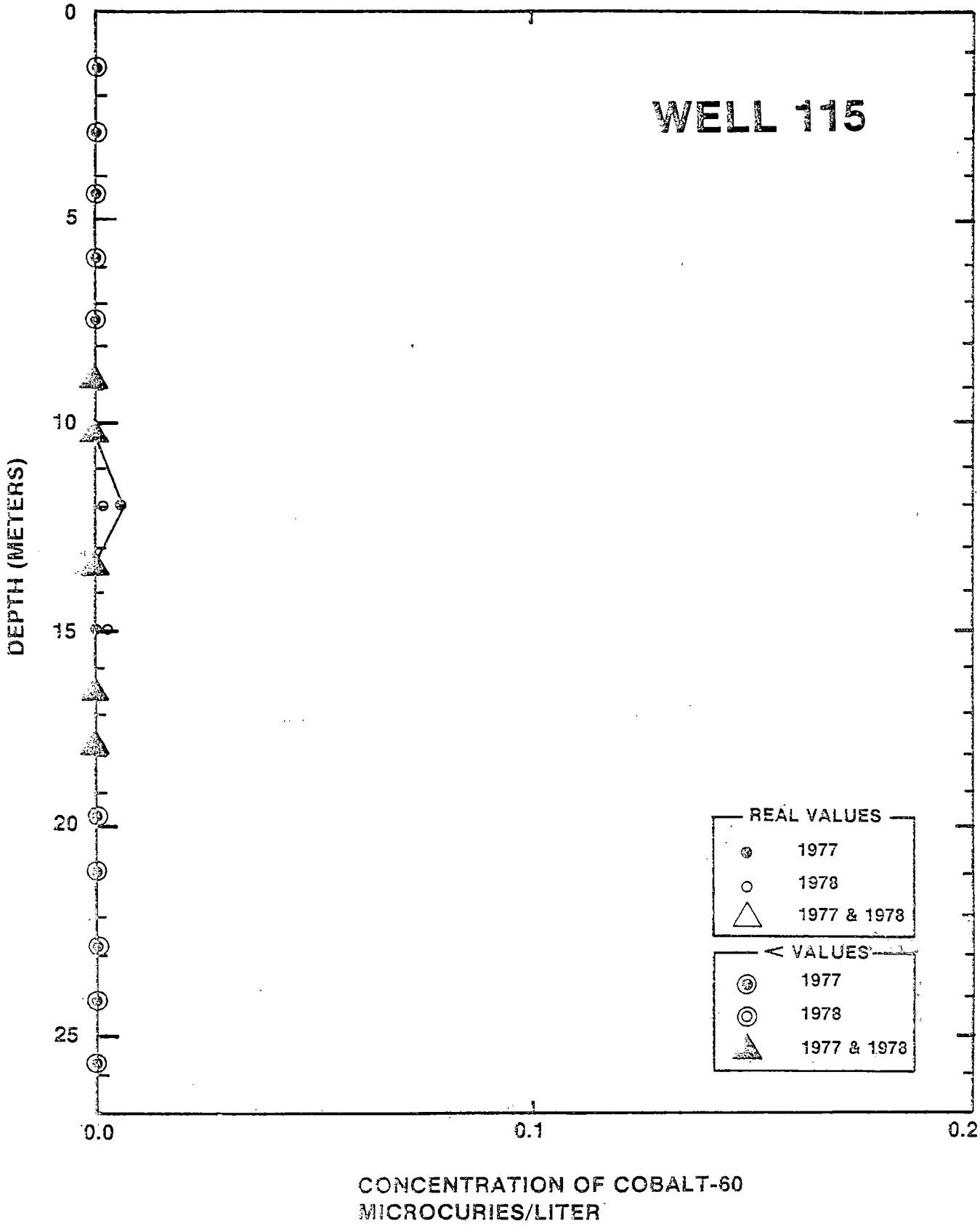
WELL 115
DEPTH (METERS)
0
5
10
15
20
25
0.0
0.1
0.2
CONCENTRATION OF COBALT-60
MICROCURIES/LITER
REAL VALUES
1977
1978
1977 & 1978
< VALUES
1977
1978
1977 & 1978

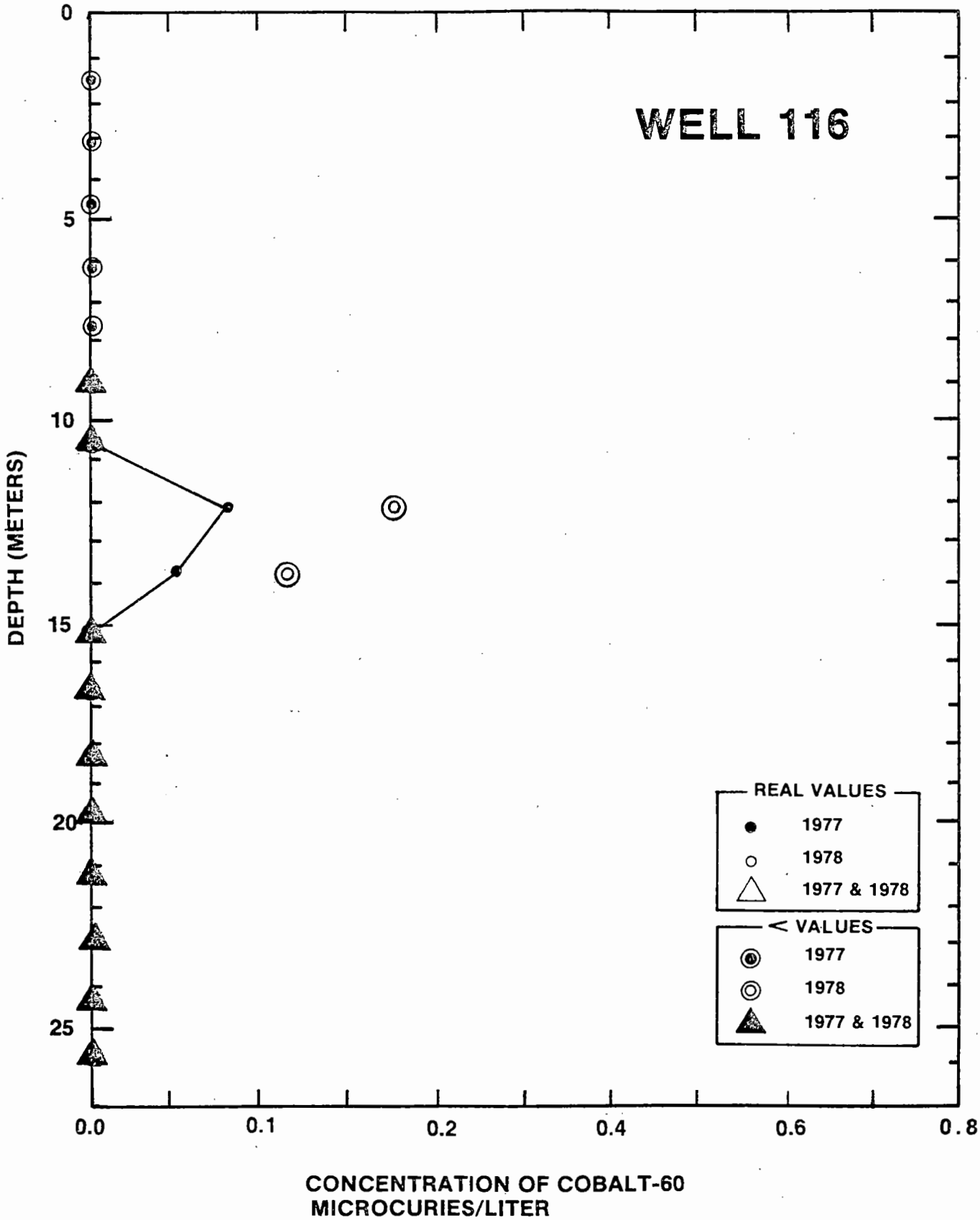

2 2 1 2 4 5 6 1 4 7 0

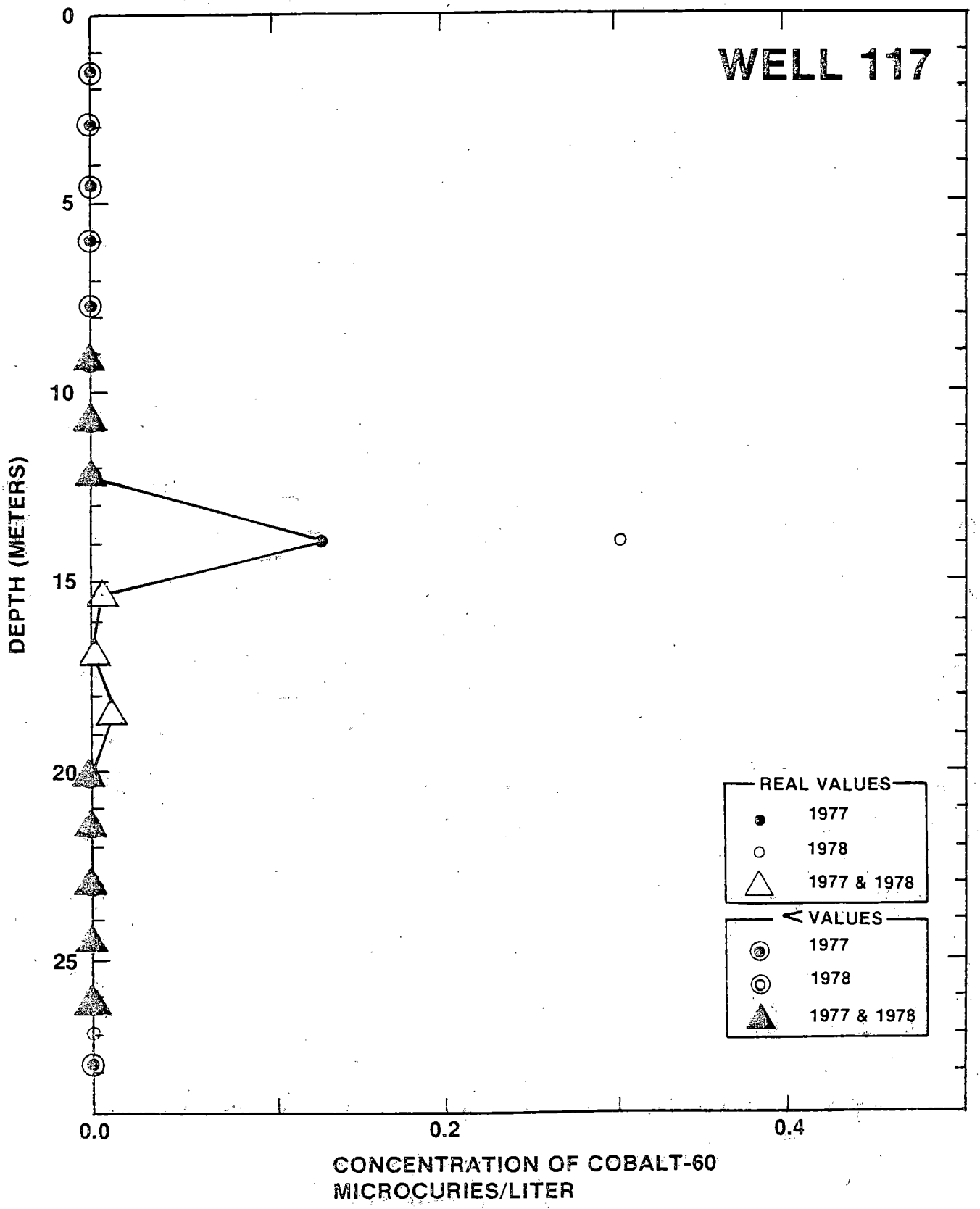
WELL 117
DEPTH (METERS)
0
5
10
15
20
25
0.0
0.2
0.4
CONCENTRATION OF COBALT-60
MICROCURIES/LITER
REAL VALUES
1977
1978
1977 & 1978
< VALUES
1977
1978
1977 & 1978

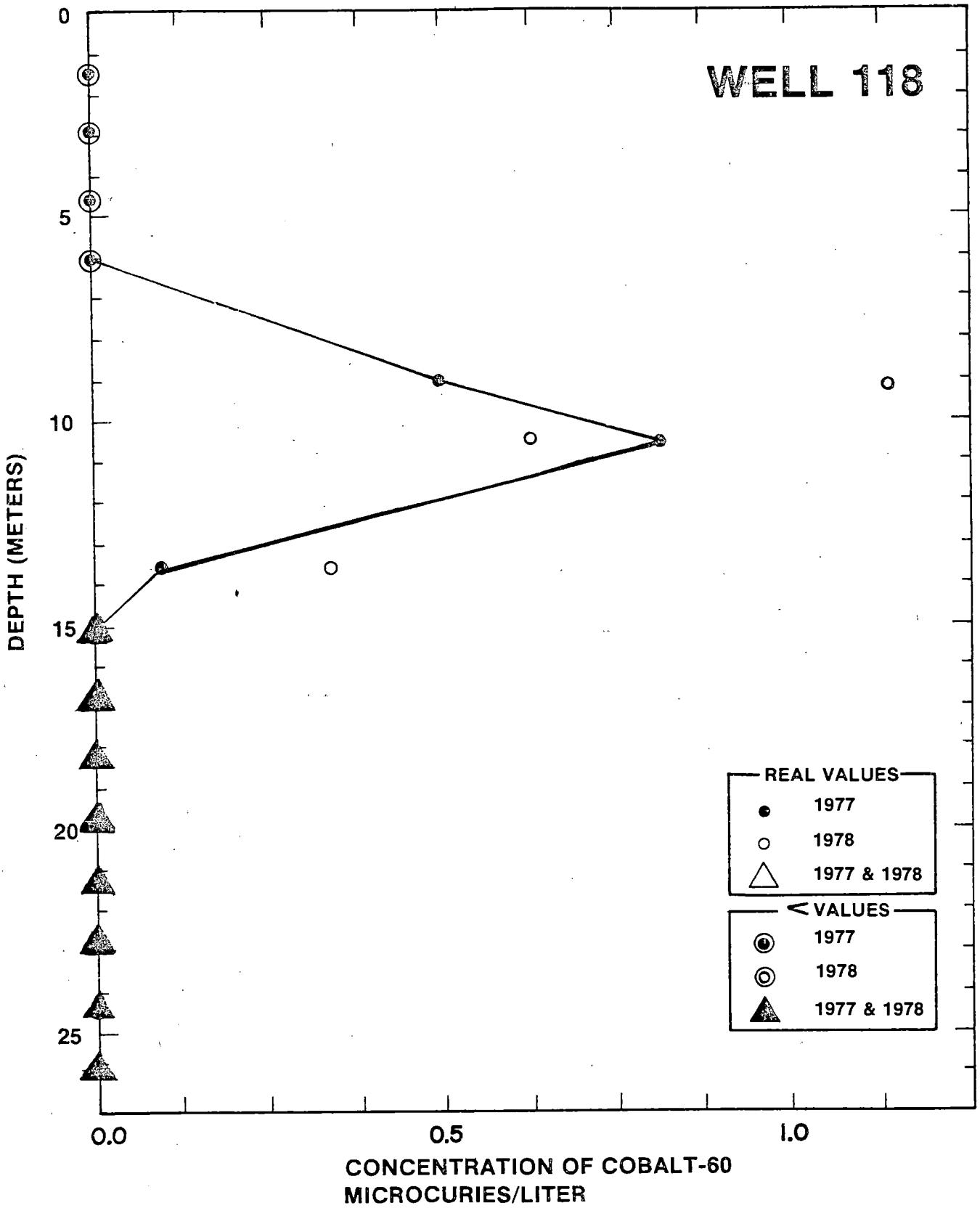
WELL 118
DEPTH (METERS)
0
5
10
15
20
25
0.0
0.5
1.0
CONCENTRATION OF COBALT-60
MICROCURIES/LITER
REAL VALUES
1977
1978
1977 & 1978
< VALUES
1977
1978
1977 & 1978

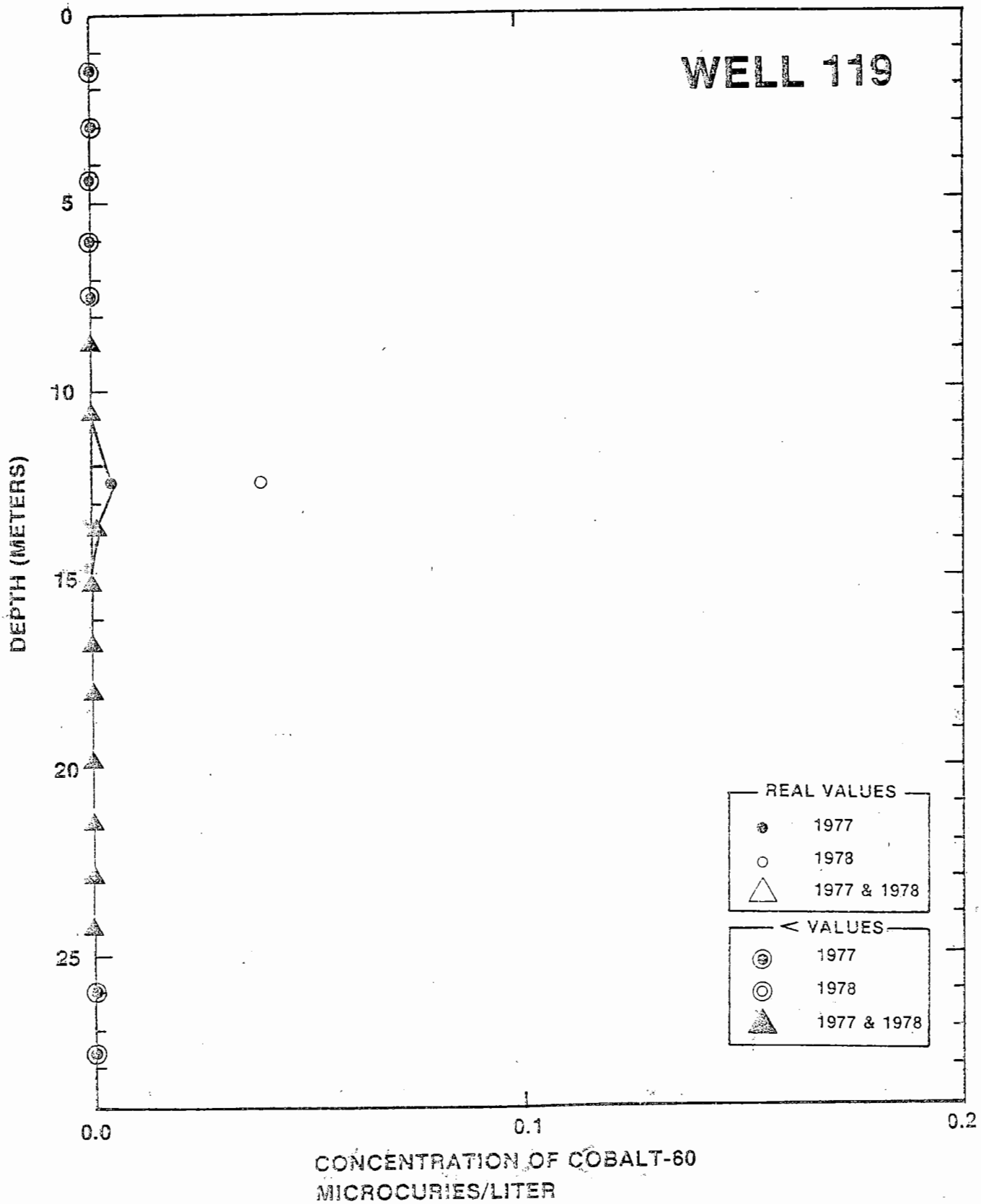

9 2 1 2 4 5 6 1 4 7 3

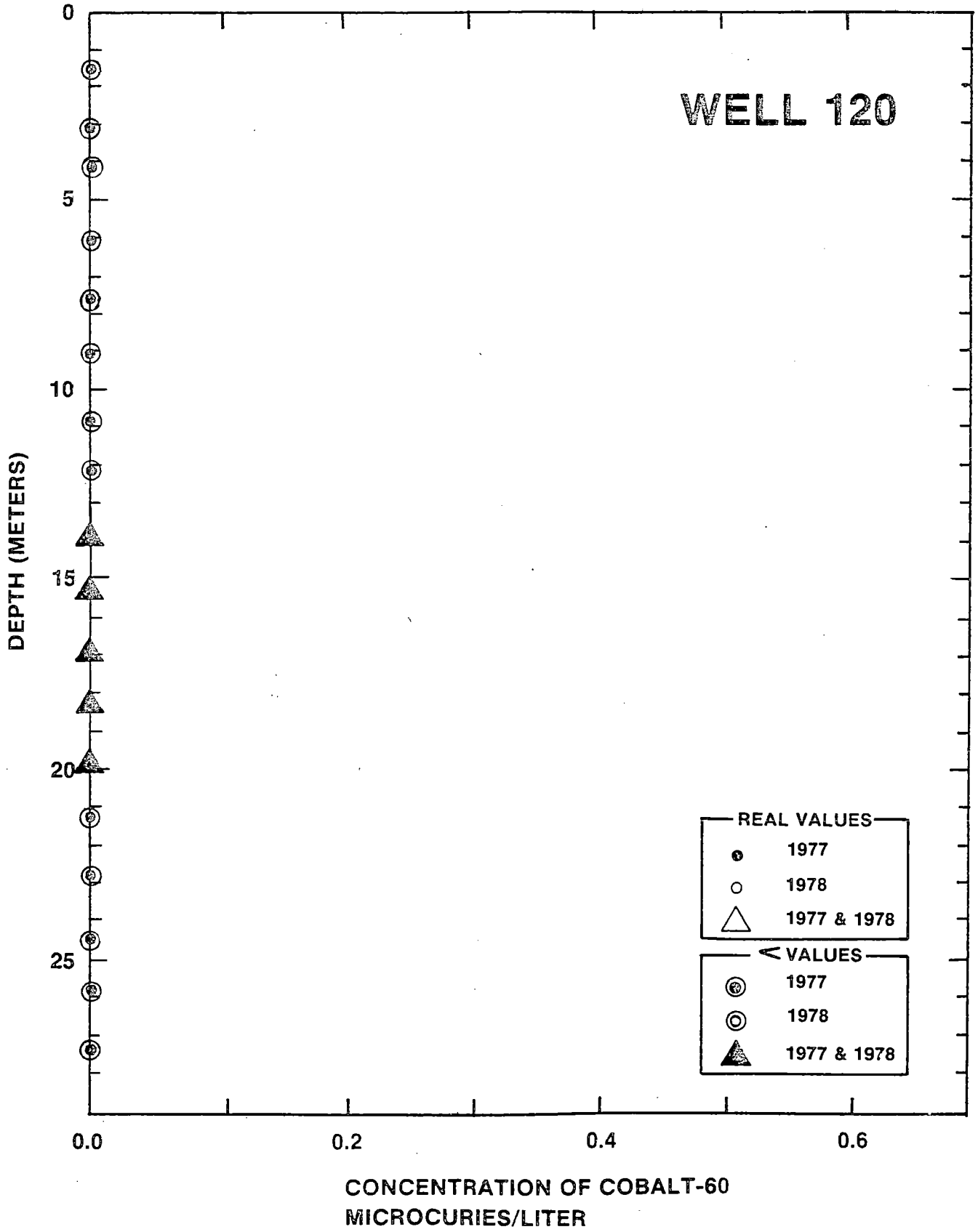
WELL 120
DEPTH (METERS)
0
5
10
15
20
25
0.0
0.2
0.4
0.6
CONCENTRATION OF COBALT-60
MICROCURIES/LITER
REAL VALUES
1977
1978
1977 & 1978
< VALUES
1977
1978
1977 & 1978

2124661474

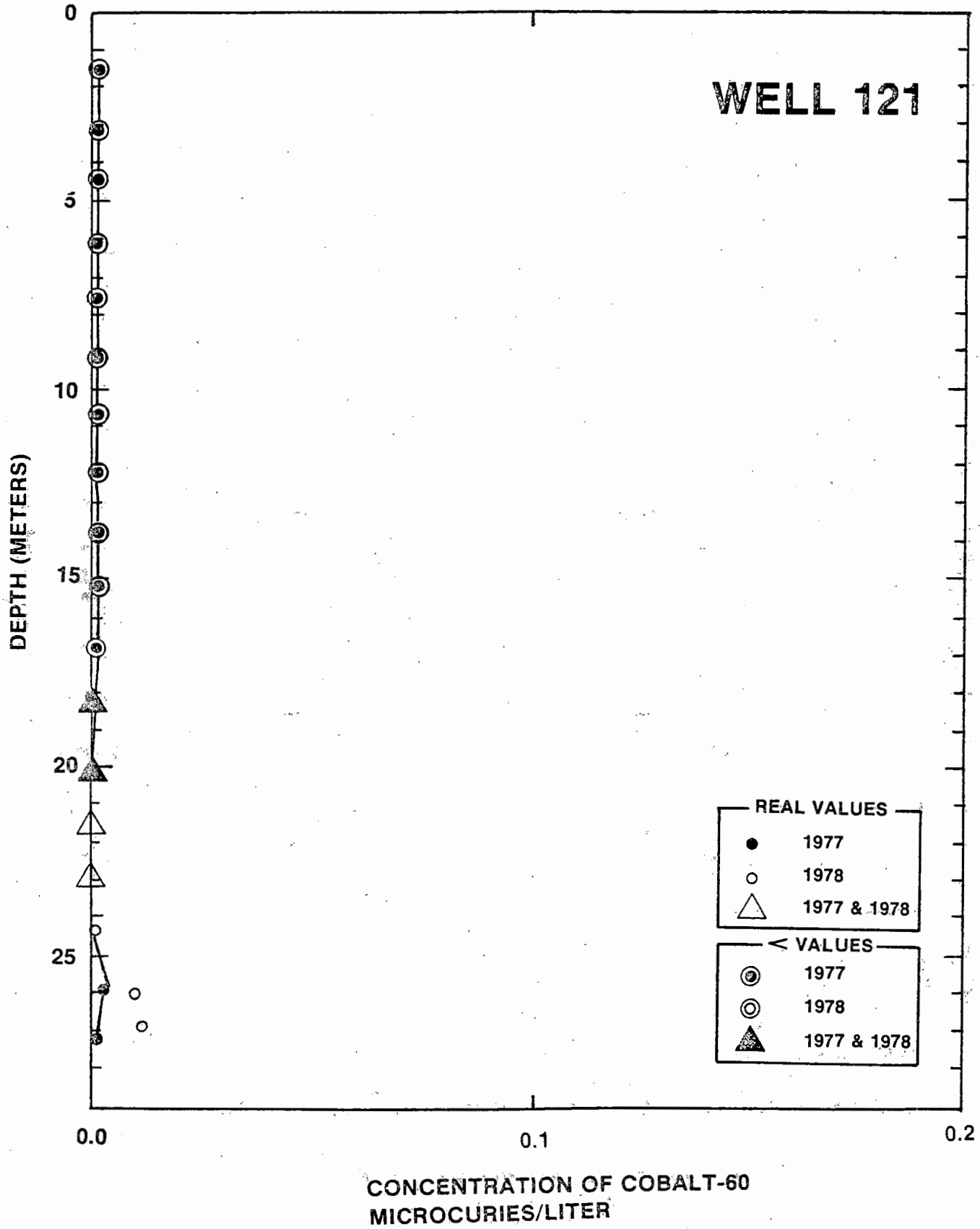
WELL 121
DEPTH (METERS)
0
5
10
15
20
25
0.0
0.1
0.2
CONCENTRATION OF COBALT-60
MICROCURIES/LITER
REAL VALUES
1977
1978
1977 & 1978
< VALUES
1977
1978
1977 & 1978

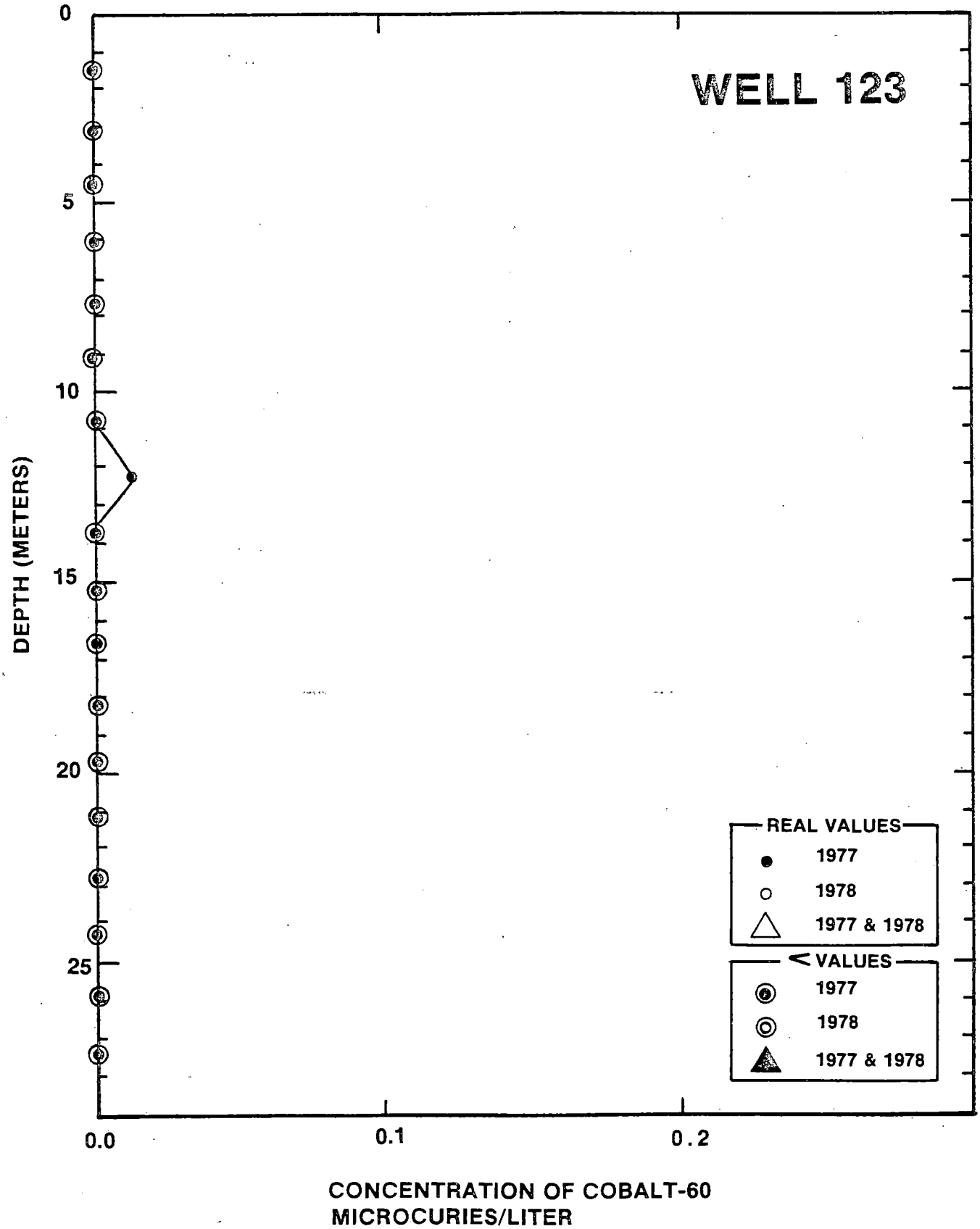

9 2 1 2 4 8 6 1 4 7 6

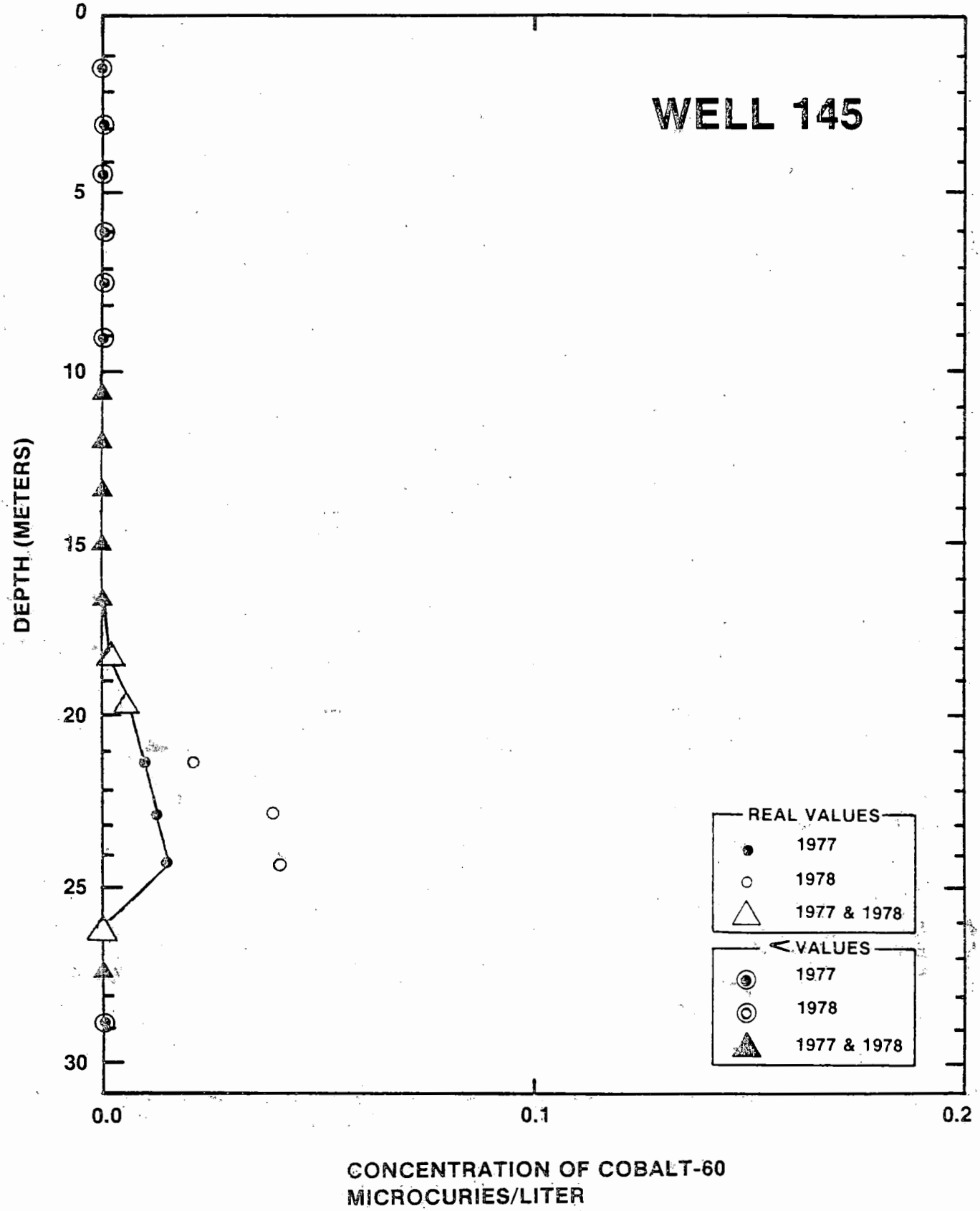
WELL 145
DEPTH (METERS)
0
5
10
15
20
25
30
0.0
0.1
0.2
CONCENTRATION OF COBALT-60
MICROCURIES/LITER
REAL VALUES
1977
1978
1977 & 1978
< VALUES
1977
1978
1977 & 1978

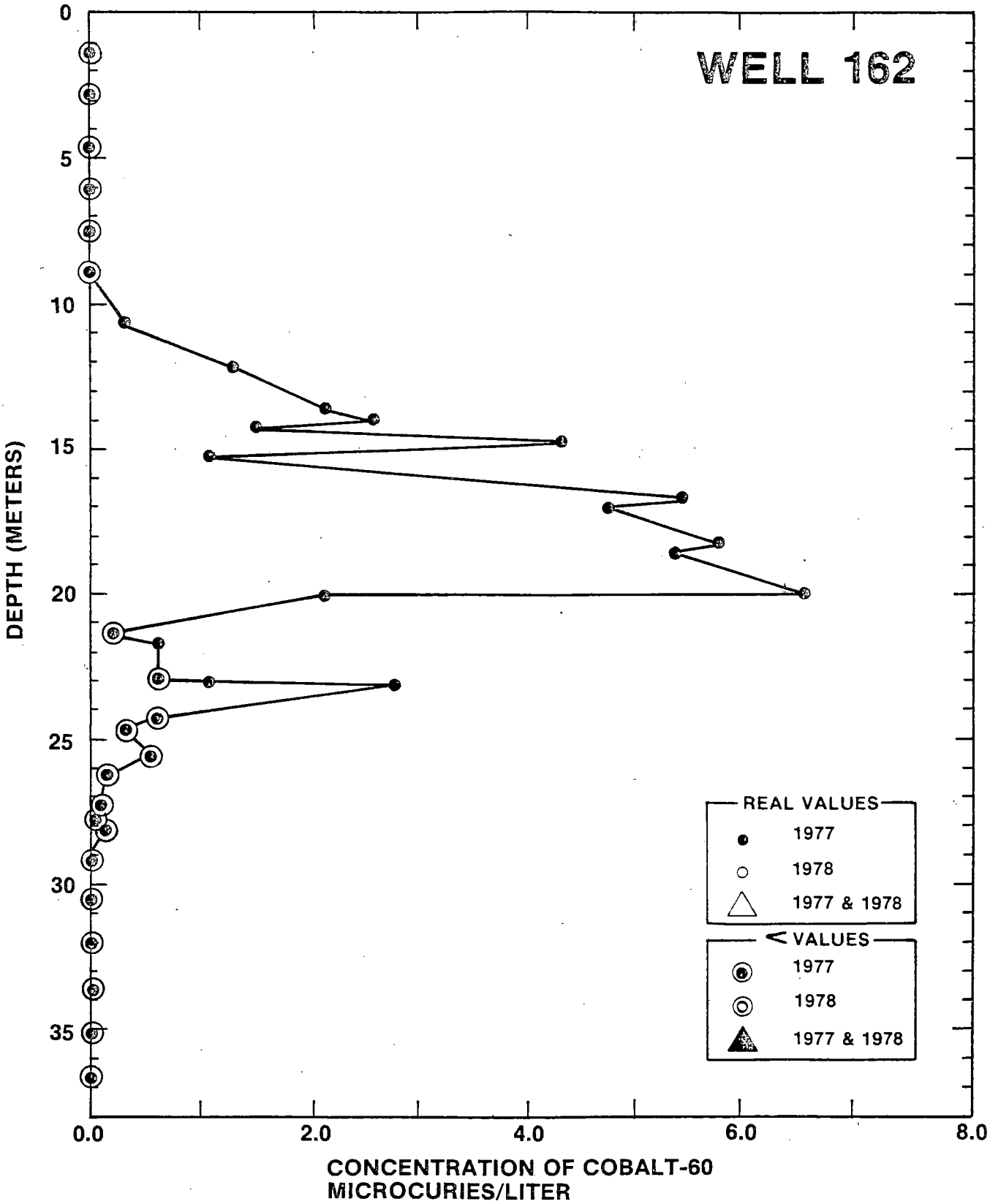
WELL 162
DEPTH (METERS)
0
5
10
15
20
25
30
35
0.0
2.0
4.0
6.0
8.0
CONCENTRATION OF COBALT-60
MICROCURIES/LITER
REAL VALUES
1977
1978
1977 & 1978
< VALUES
1977
1978
1977 & 1978

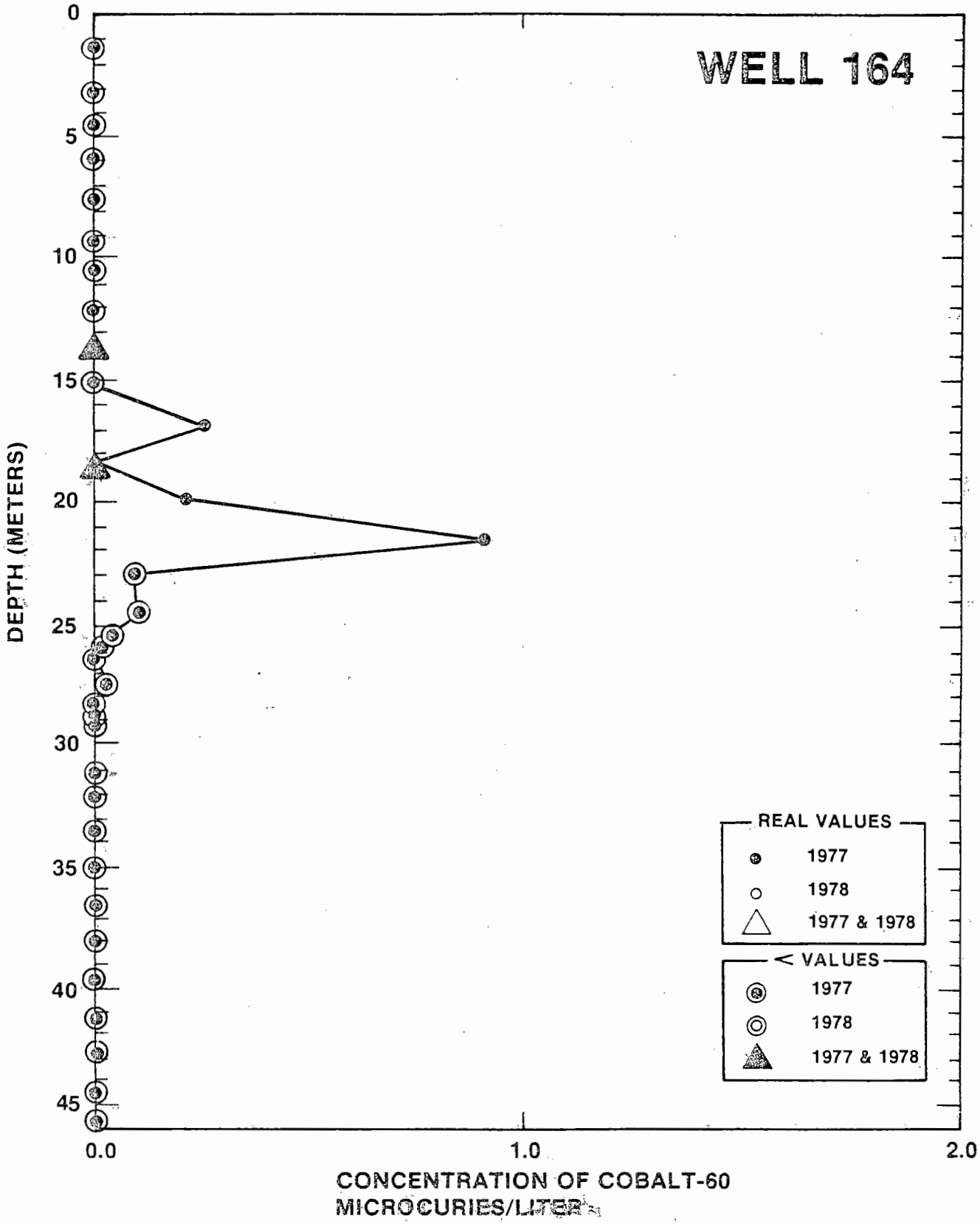
WELL 164
DEPTH (METERS)
0
5
10
15
20
25
30
35
40
45
0.0
1.0
2.0
CONCENTRATION OF COBALT-60
MICROCURIES/LITER
REAL VALUES
1977
1978
1977 & 1978
< VALUES
1977
1978
1977 & 1978

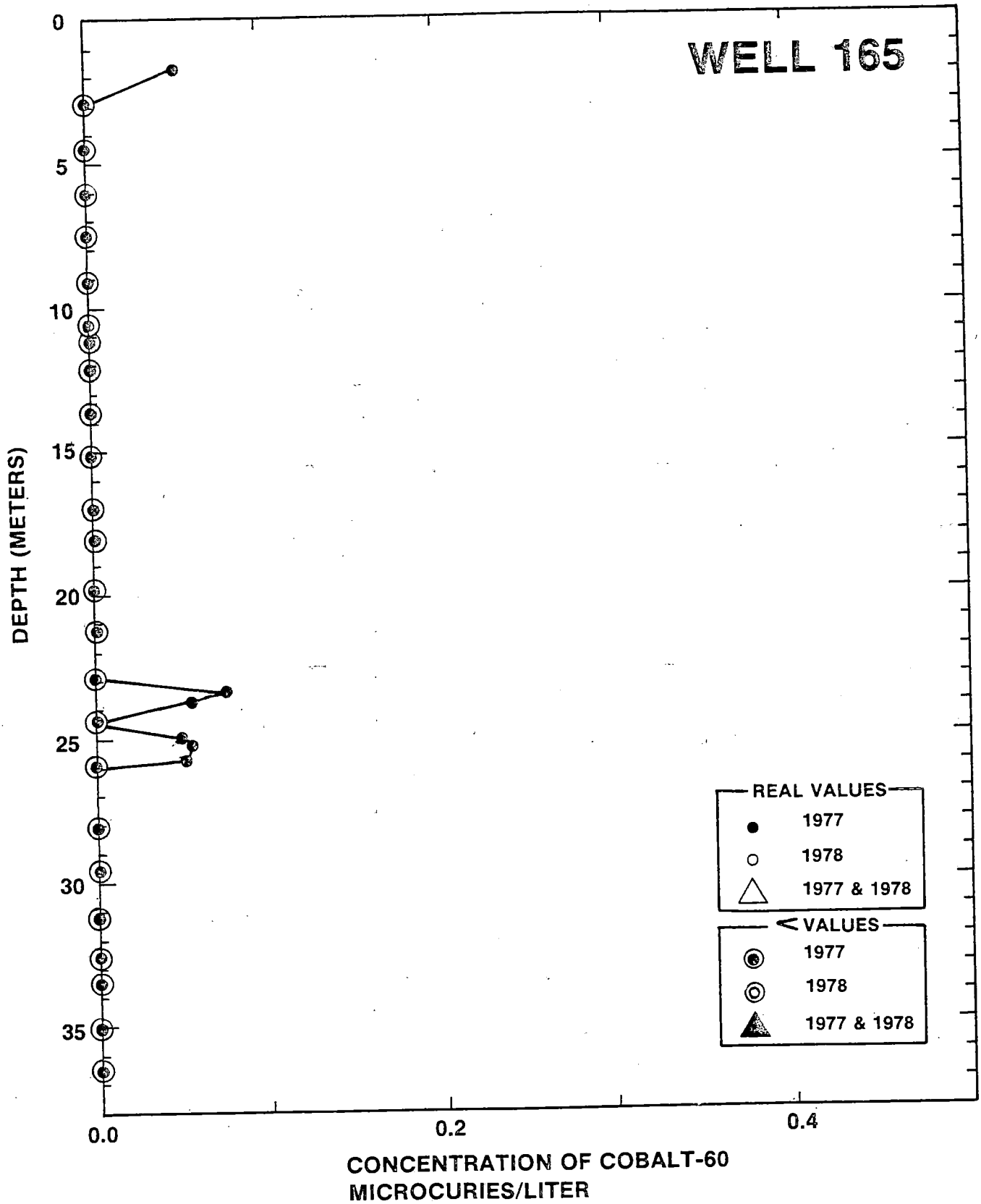

9 2 1 2 4 6 6 1 4 8 0

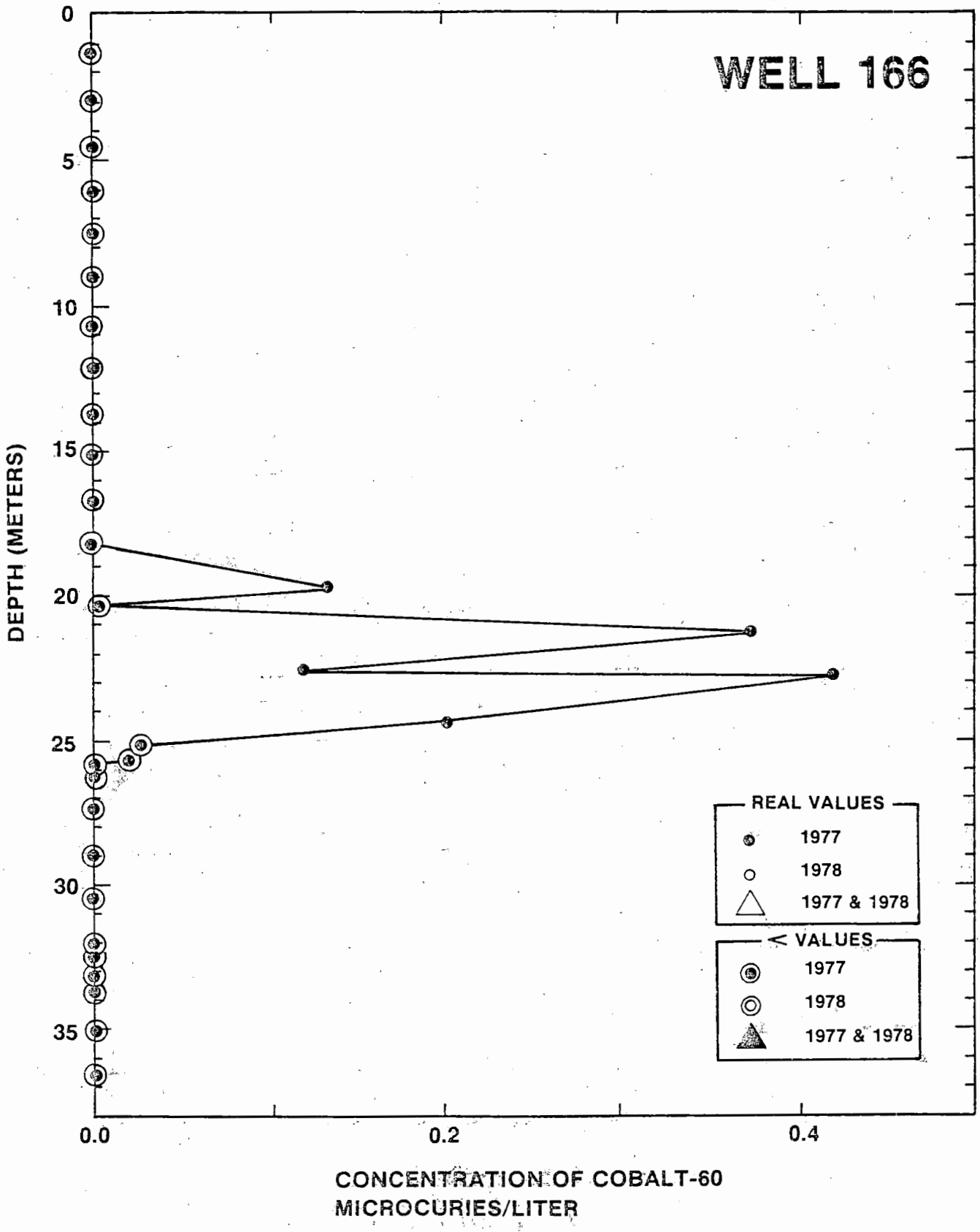
WELL 166
DEPTH (METERS)
0
5
10
15
20
25
30
35
0.0
0.2
0.4
CONCENTRATION OF COBALT-60
MICROCURIES/LITER
REAL VALUES
1977
1978
1977 & 1978
< VALUES
1977
1978
1977 & 1978

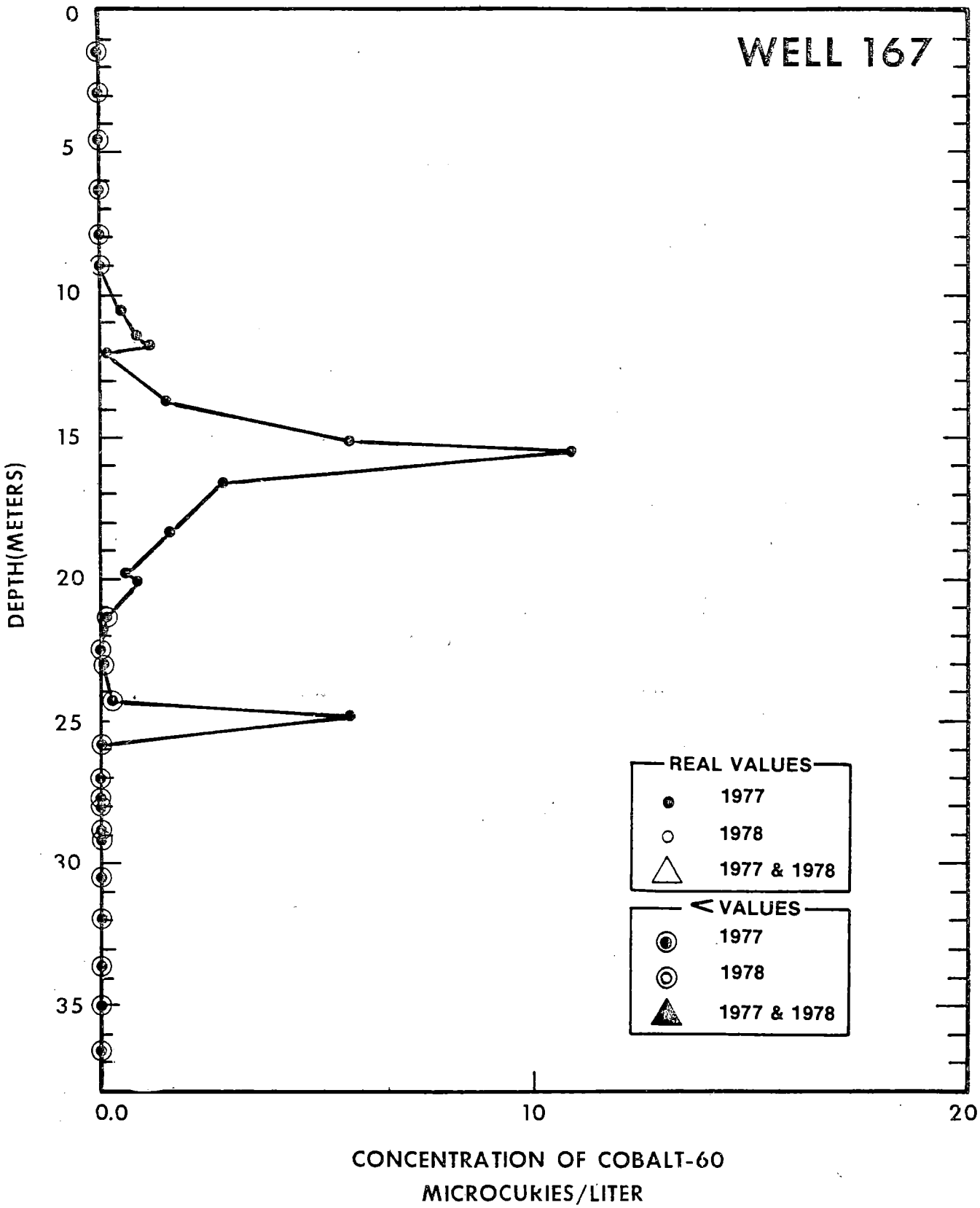
WELL 167
DEPTH(METERS)
0
5
10
15
20
25
30
35
0.0
10
20
CONCENTRATION OF COBALT-60
MICROCURIES/LITER
REAL VALUES
1977
1978
1977 & 1978
< VALUES
1977
1978
1977 & 1978

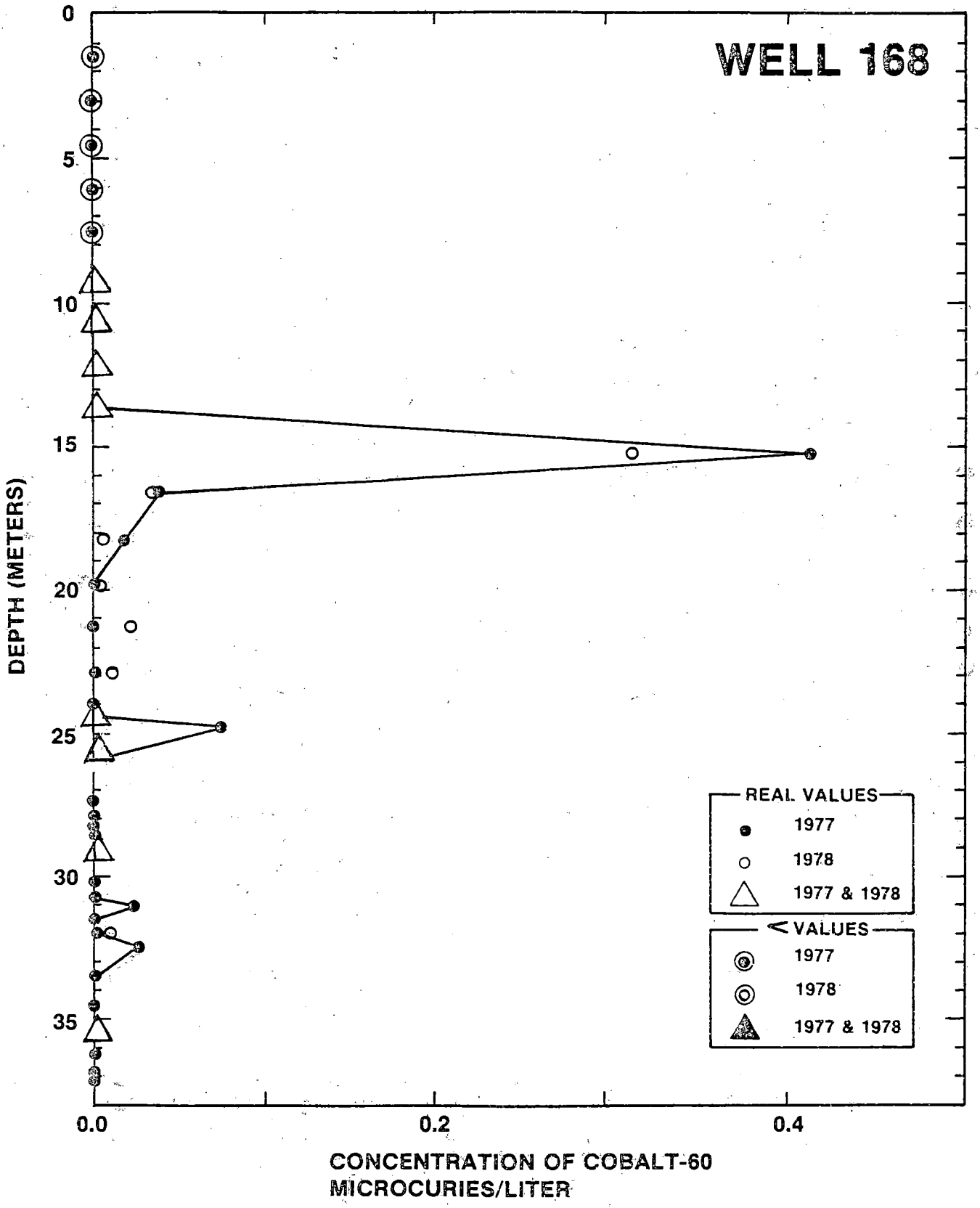
WELL 168
DEPTH (METERS)
0
5
10
15
20
25
30
35
0.0
0.2
0.4
CONCENTRATION OF COBALT-60
MICROCURIES/LITER
REAL VALUES
1977
1978
1977 & 1978
< VALUES
1977
1978
1977 & 1978

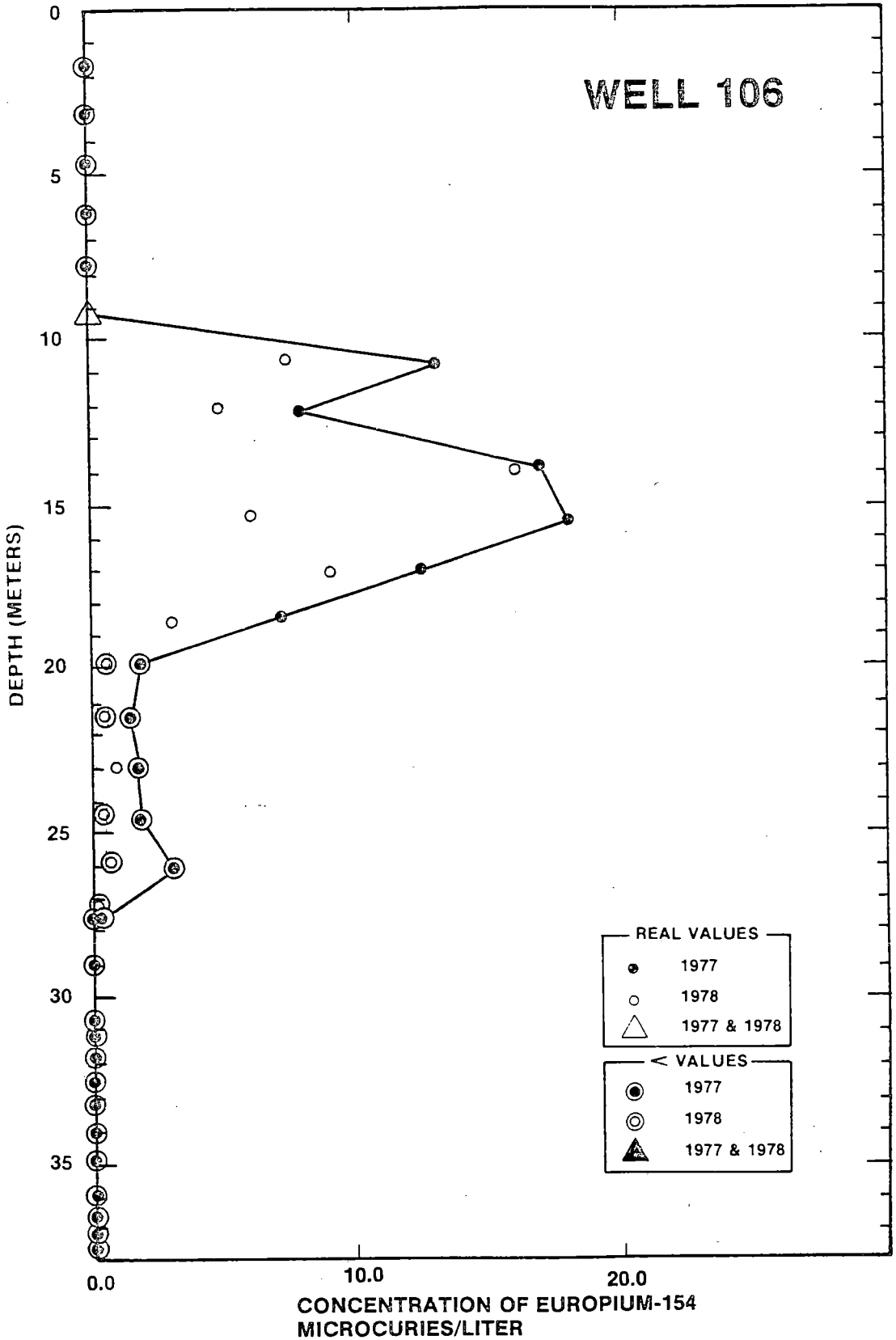

9 2 1 2 4 5 6 1 4 8 4

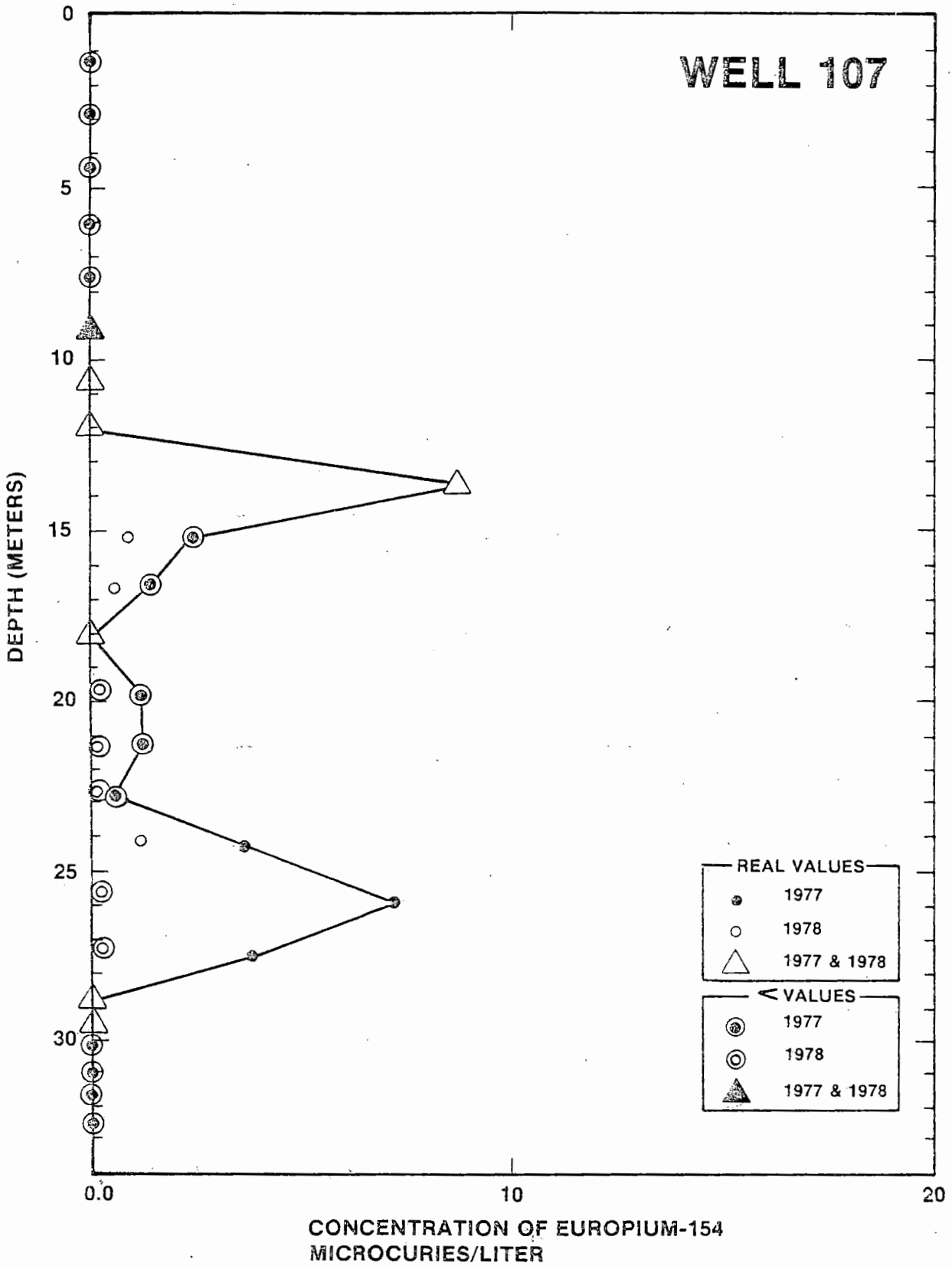
WELL 107
DEPTH (METERS)
0
5
10
15
20
25
30
0.0
10
20
CONCENTRATION OF EUROPIUM-154
MICROCURIES/LITER
REAL VALUES
1977
1978
1977 & 1978
< VALUES
1977
1978
1977 & 1978

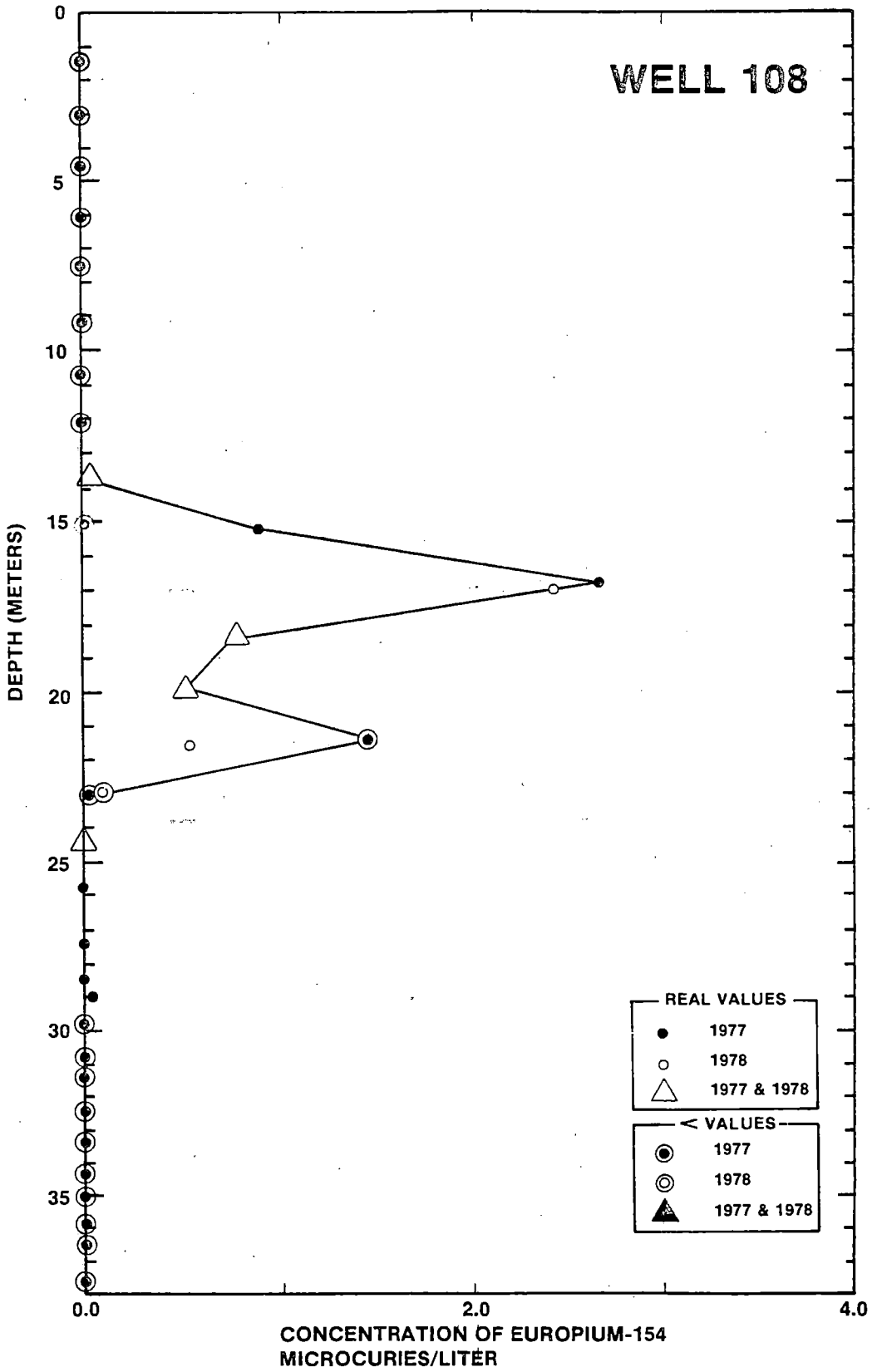

9 2 1 2 4 6 6 1 4 8 6

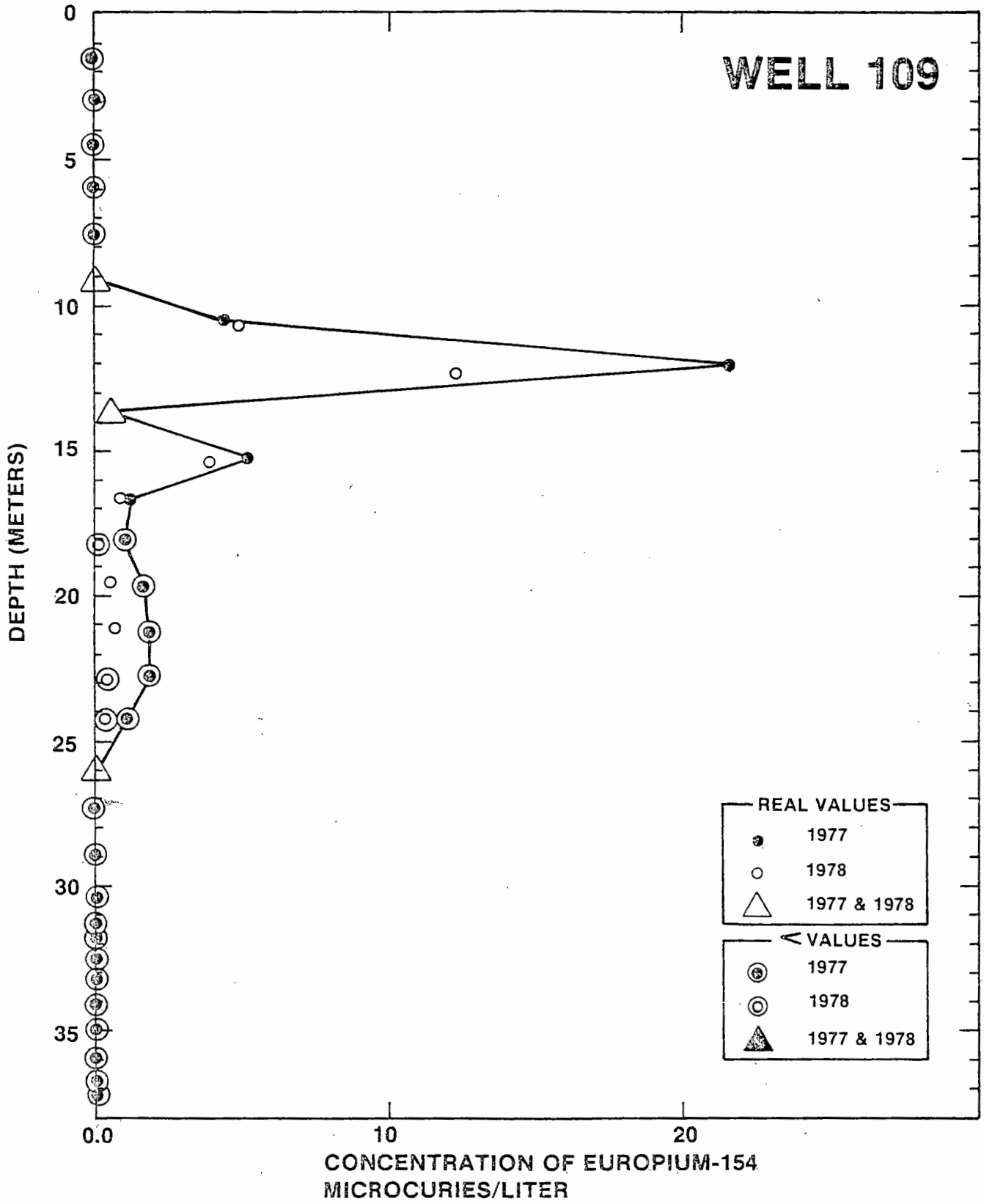
WELL 109
DEPTH (METERS)
0
5
10
15
20
25
30
35
0.0
10
20
CONCENTRATION OF EUROPIUM-154
MICROCURIES/LITER
REAL VALUES
1977
1978
1977 & 1978
< VALUES
1977
1978
1977 & 1978

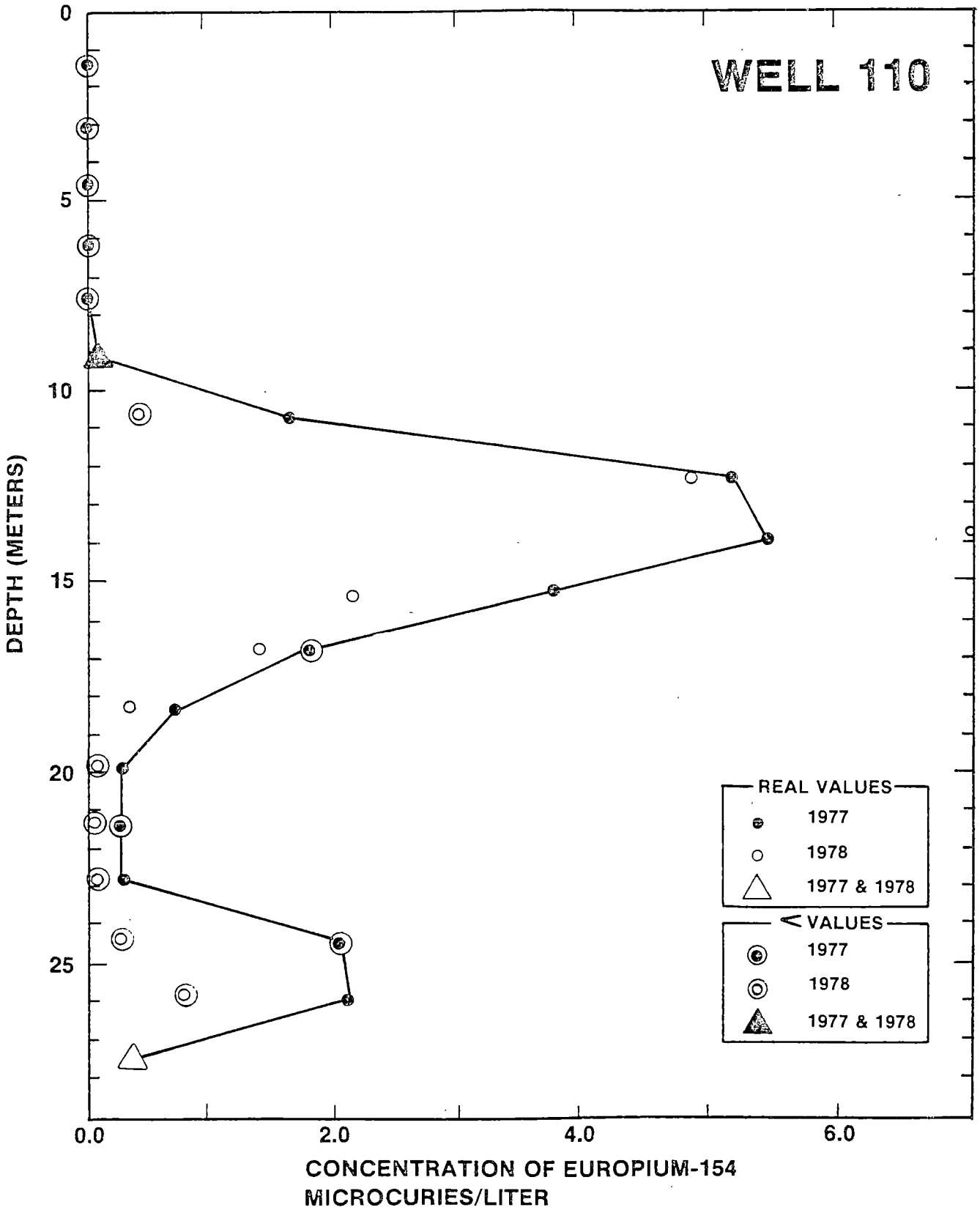
WELL 110
DEPTH (METERS)
0
5
10
15
20
25
0.0
2.0
4.0
6.0
CONCENTRATION OF EUROPIUM-154
MICROCURIES/LITER
REAL VALUES
1977
1978
1977 & 1978
< VALUES
1977
1978
1977 & 1978

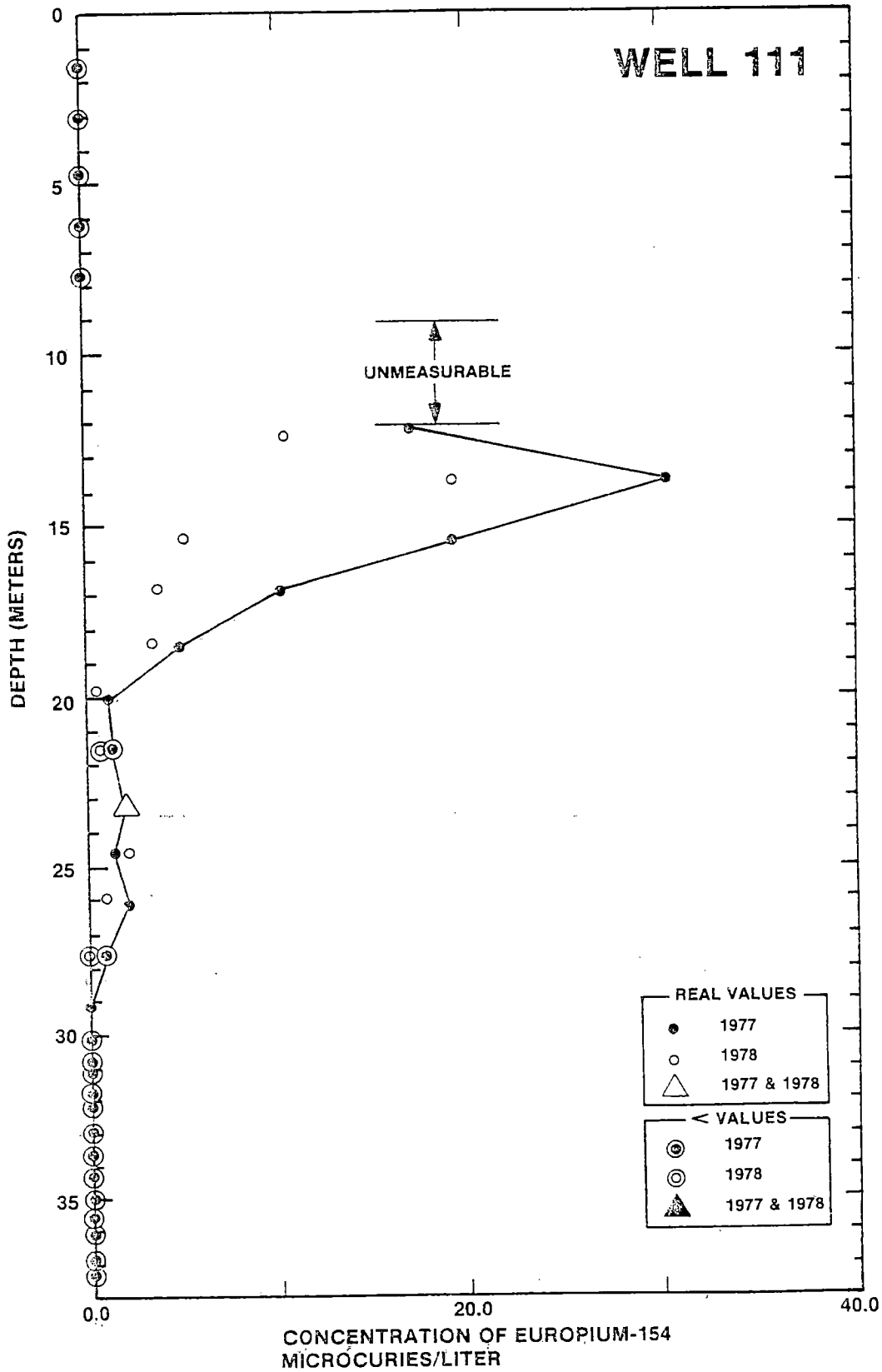
WELL 111
UNMEASURABLE
DEPTH (METERS)
0
5
10
15
20
25
30
35
0.0
20.0
40.0
CONCENTRATION OF EUROPIUM-154
MICROCURIES/LITER
REAL VALUES
1977
1978
1977 & 1978
< VALUES
1977
1978
1977 & 1978

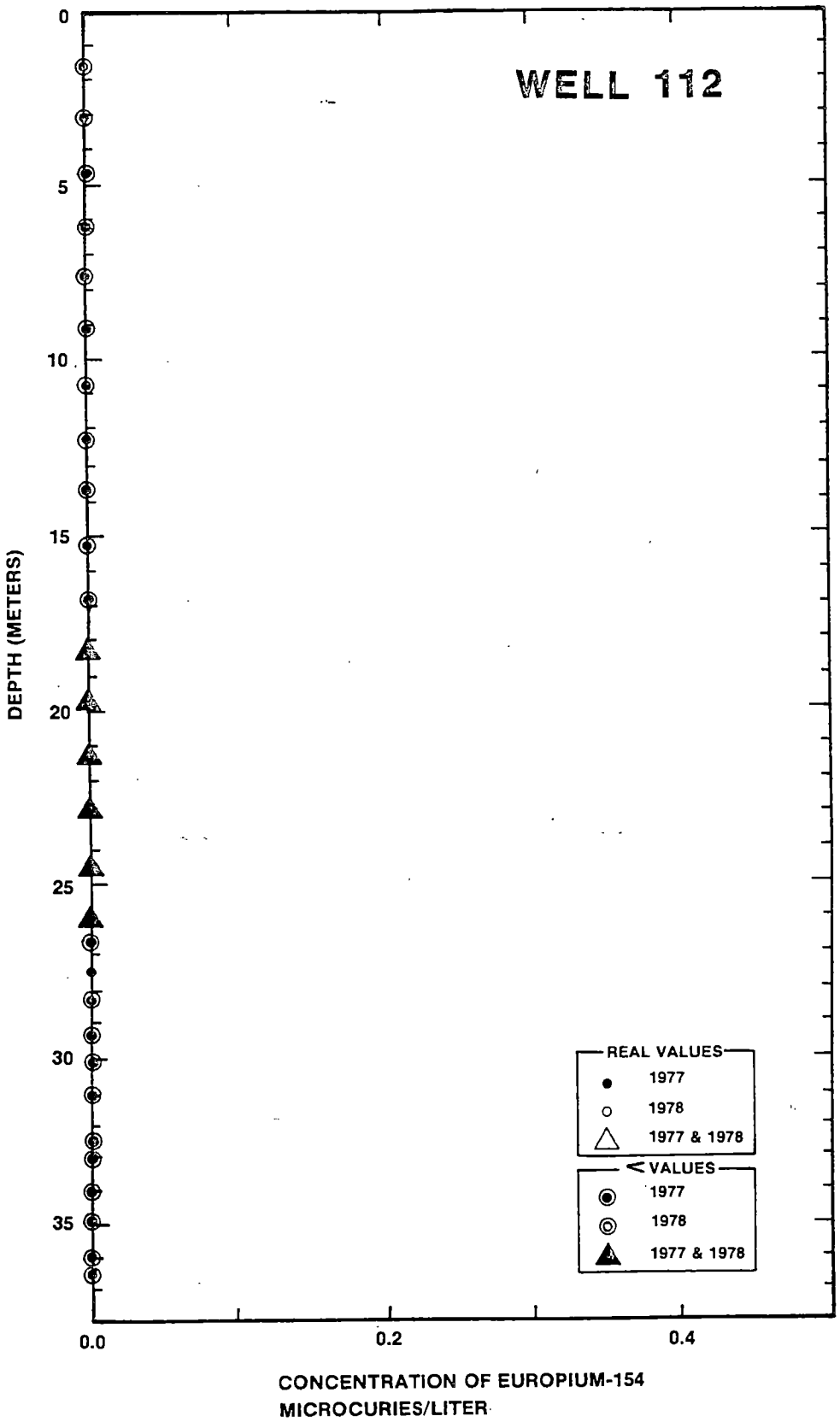

9 2 1 2 4 6 6 1 4 9 0

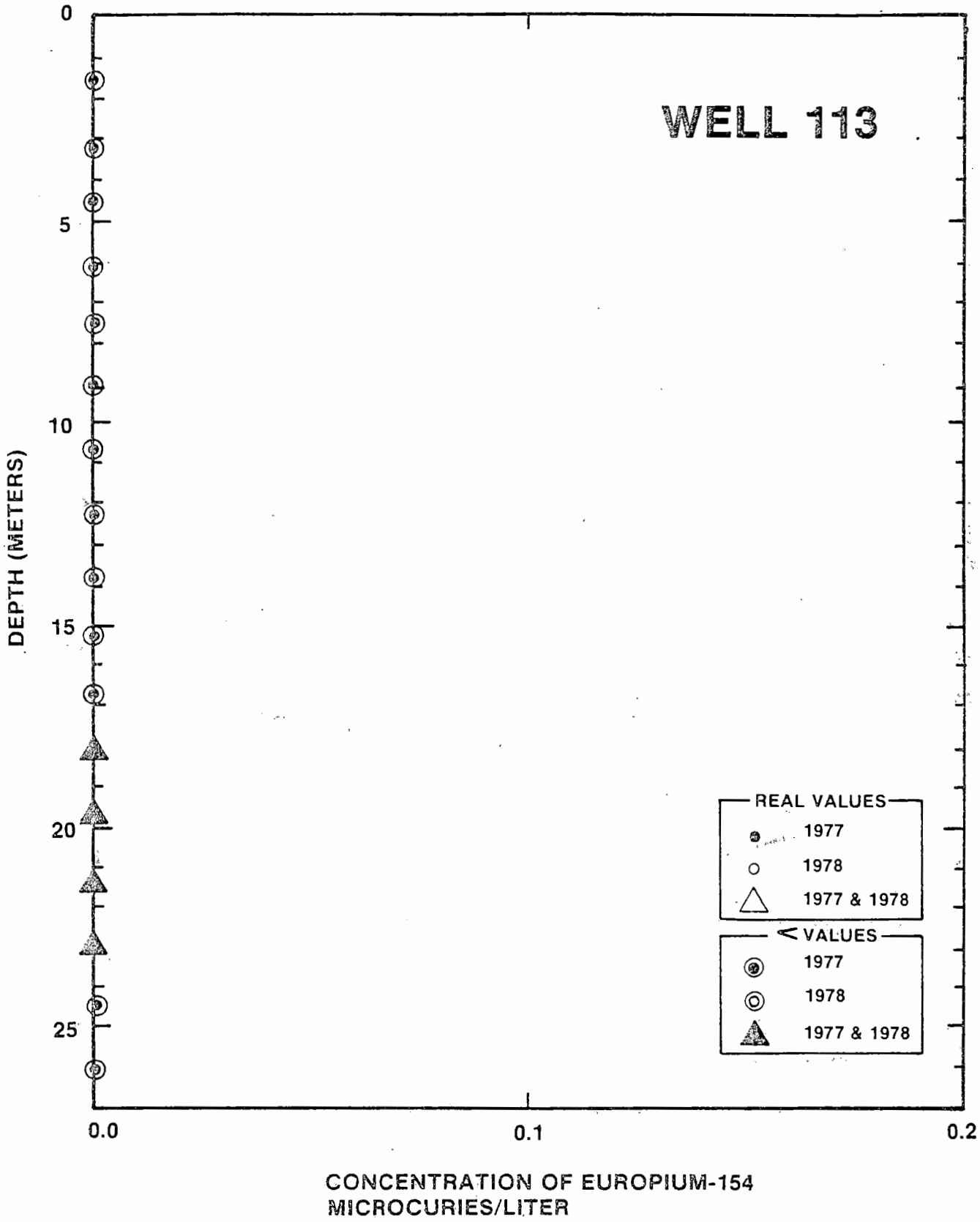
WELL 113
DEPTH (METERS)
0
5
10
15
20
25
0.0
0.1
0.2
CONCENTRATION OF EUROPIUM-154
MICROCURIES/LITER
REAL VALUES
1977
1978
1977 & 1978
< VALUES
1977
1978
1977 & 1978

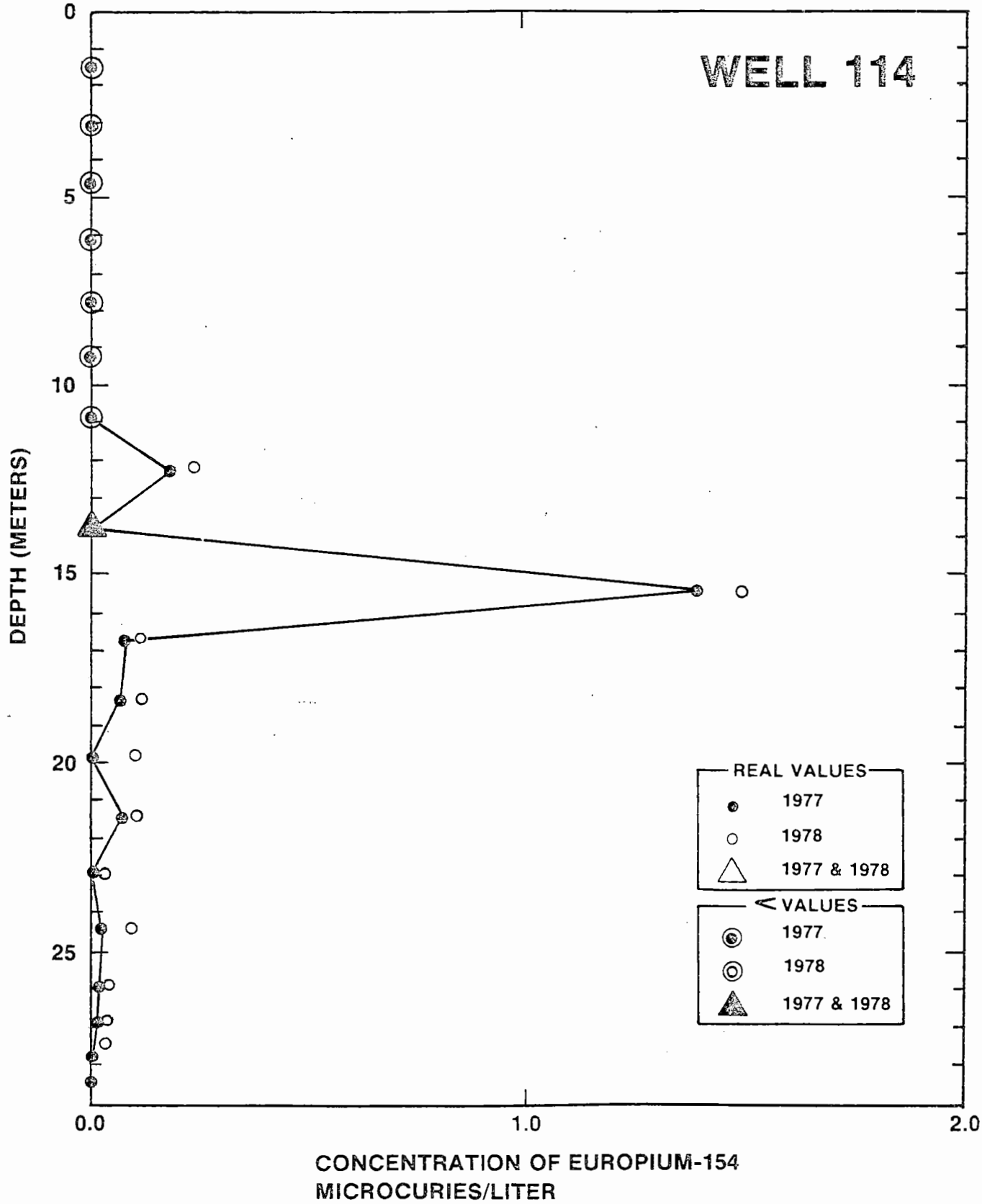
WELL 114
DEPTH (METERS)
0
5
10
15
20
25
0.0
1.0
2.0
CONCENTRATION OF EUROPIUM-154
MICROCURIES/LITER
REAL VALUES
1977
1978
1977 & 1978
< VALUES
1977
1978
1977 & 1978

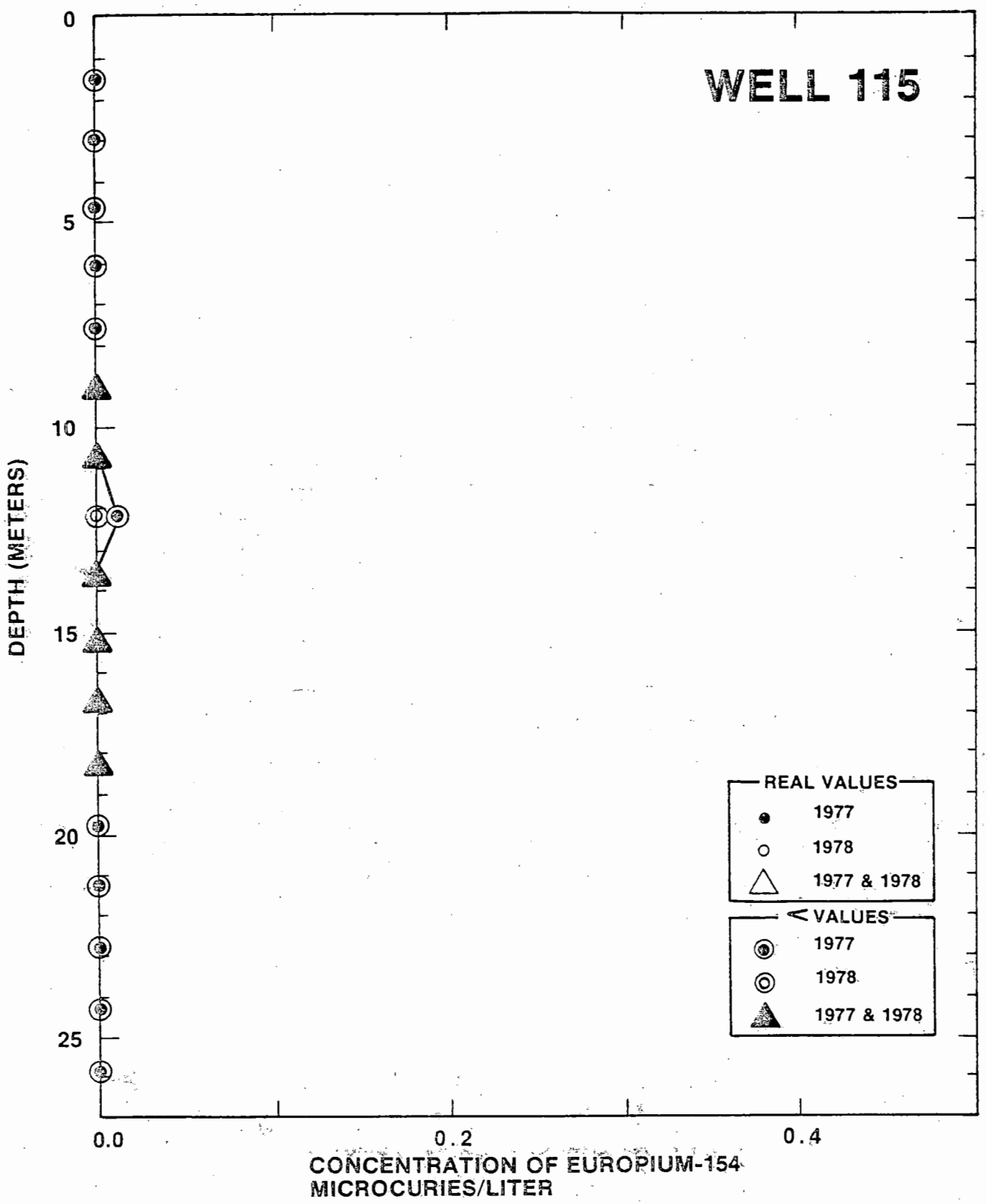

9 2 1 2 4 6 6 1 4 9 3

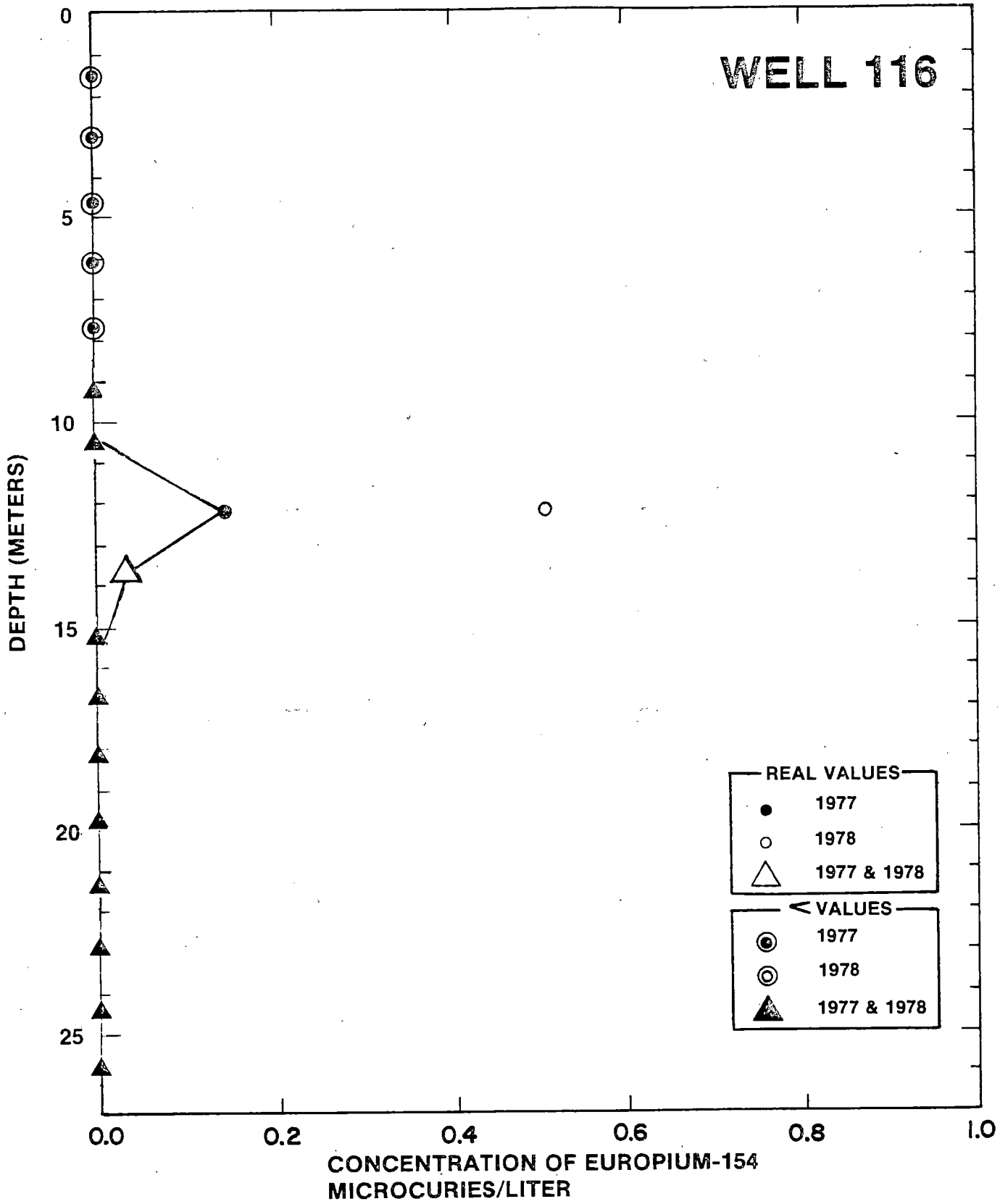

9 2 1 2 4 6 6 1 4 9 4

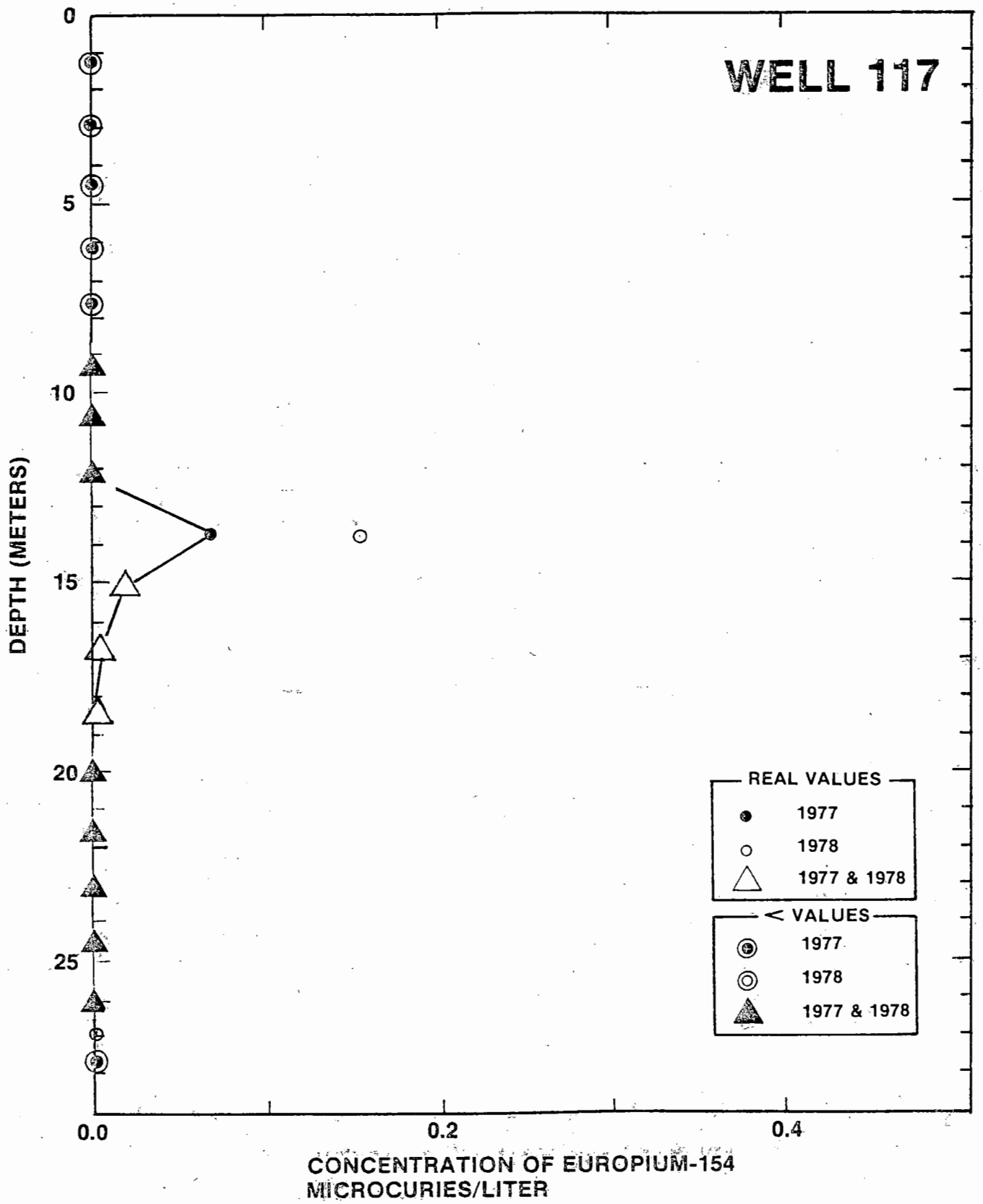

9 2 1 2 4 6 6 1 4 9 5

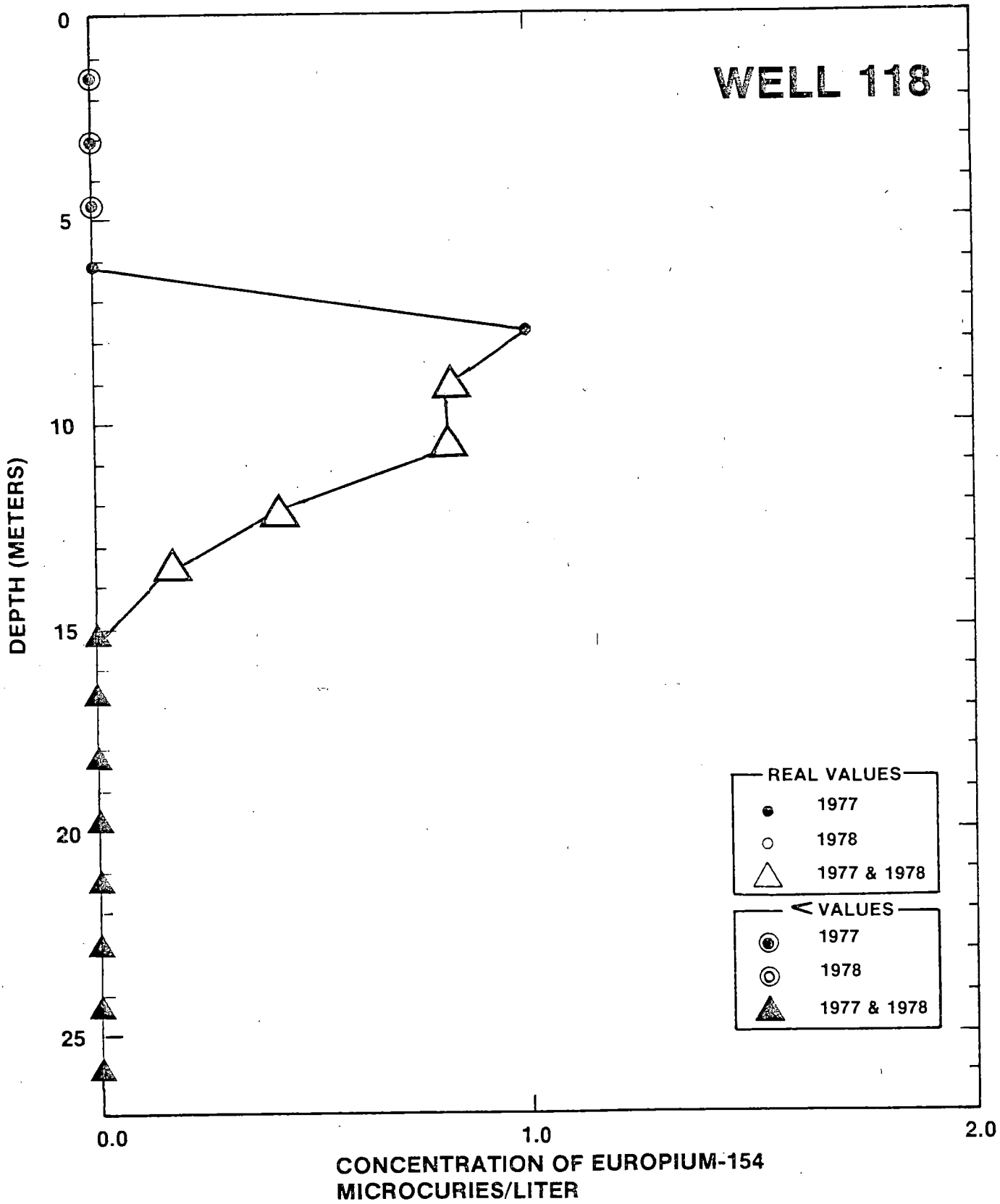

9 2 1 2 4 6 6 1 4 9 6

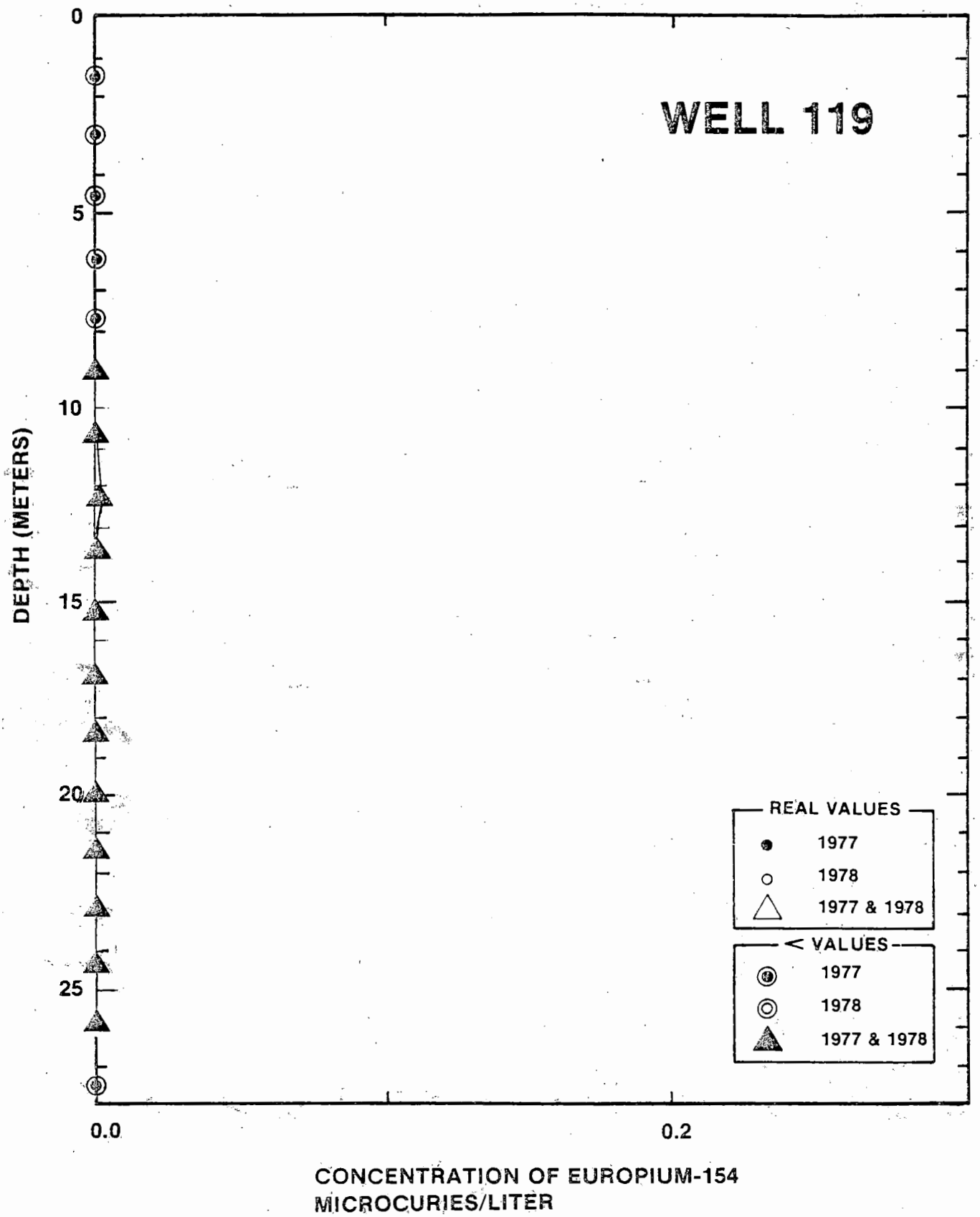

9 2 1 2 4 5 6 1 4 9 7

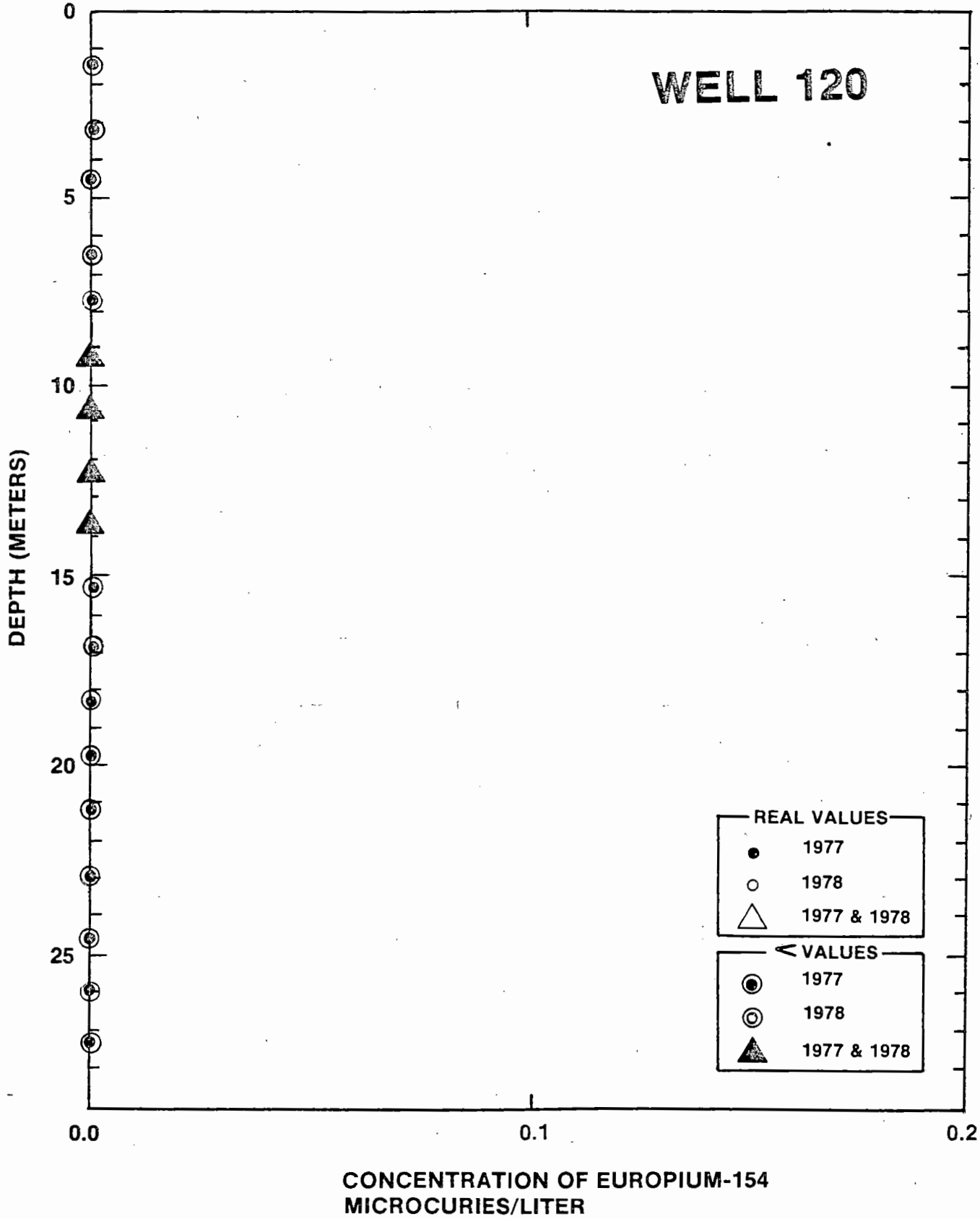

9 2 1 2 4 6 6 1 4 9 8

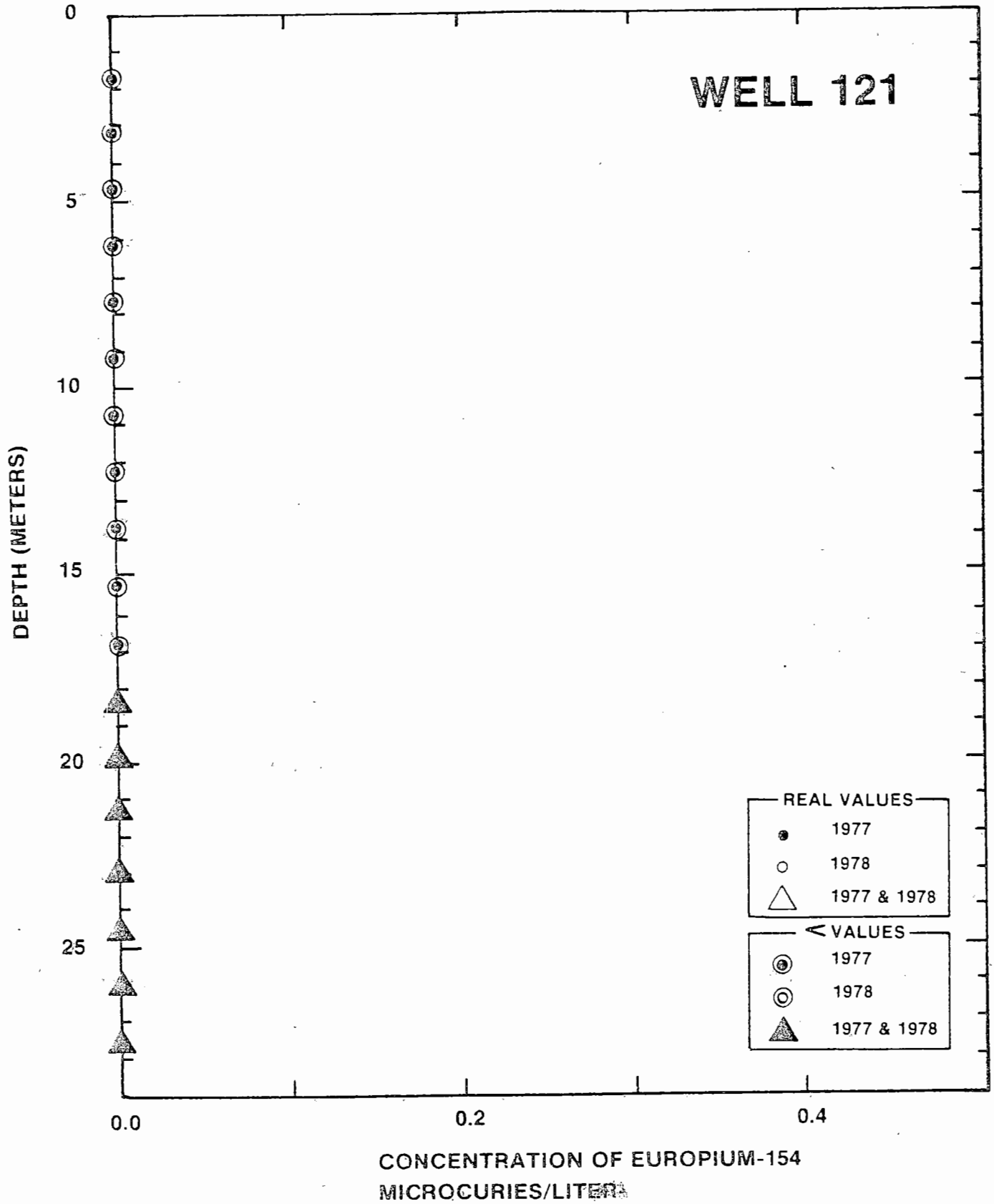

9 2 1 2 4 6 6 1 4 9 9

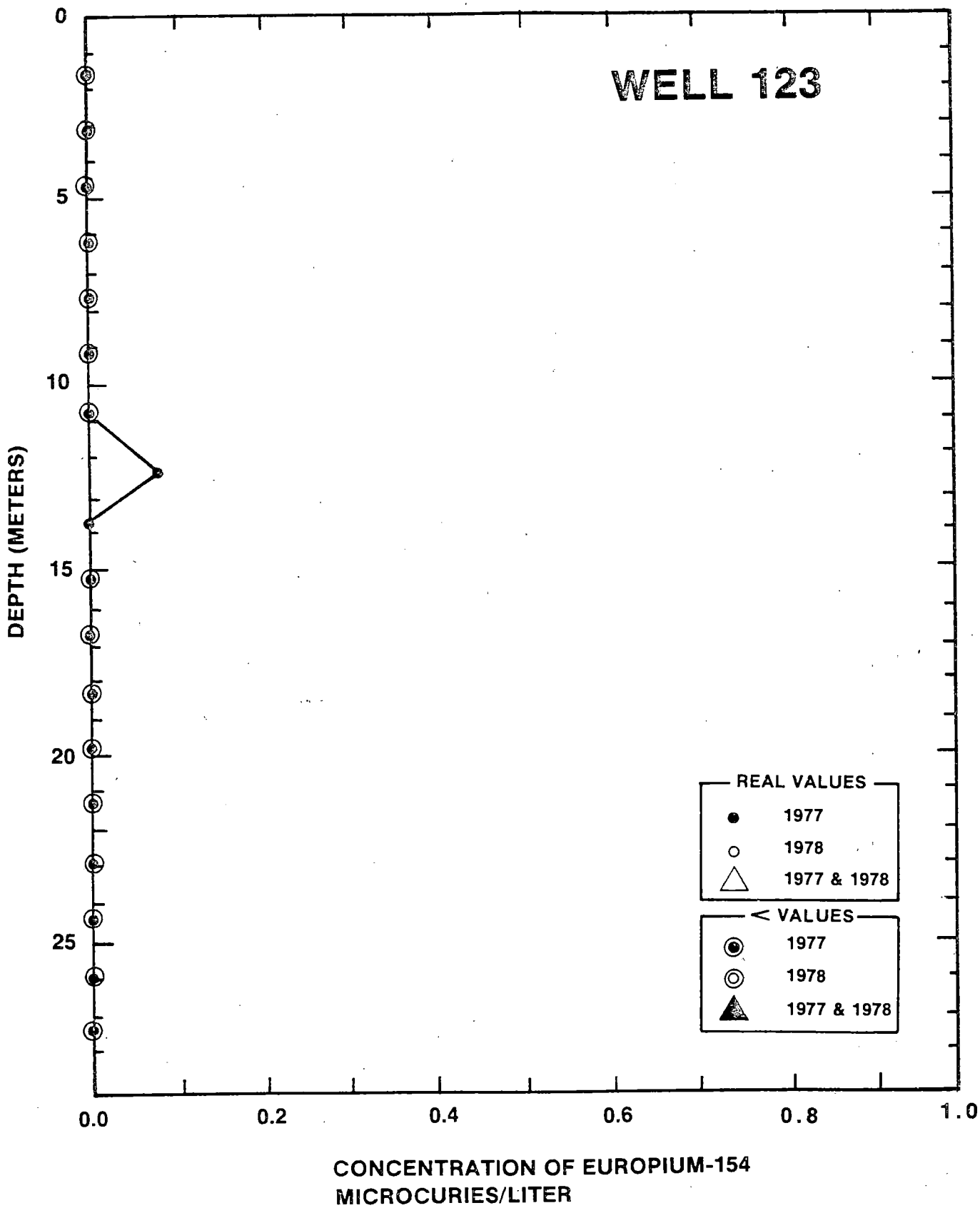

9 2 1 2 4 6 6 1 5 0 0

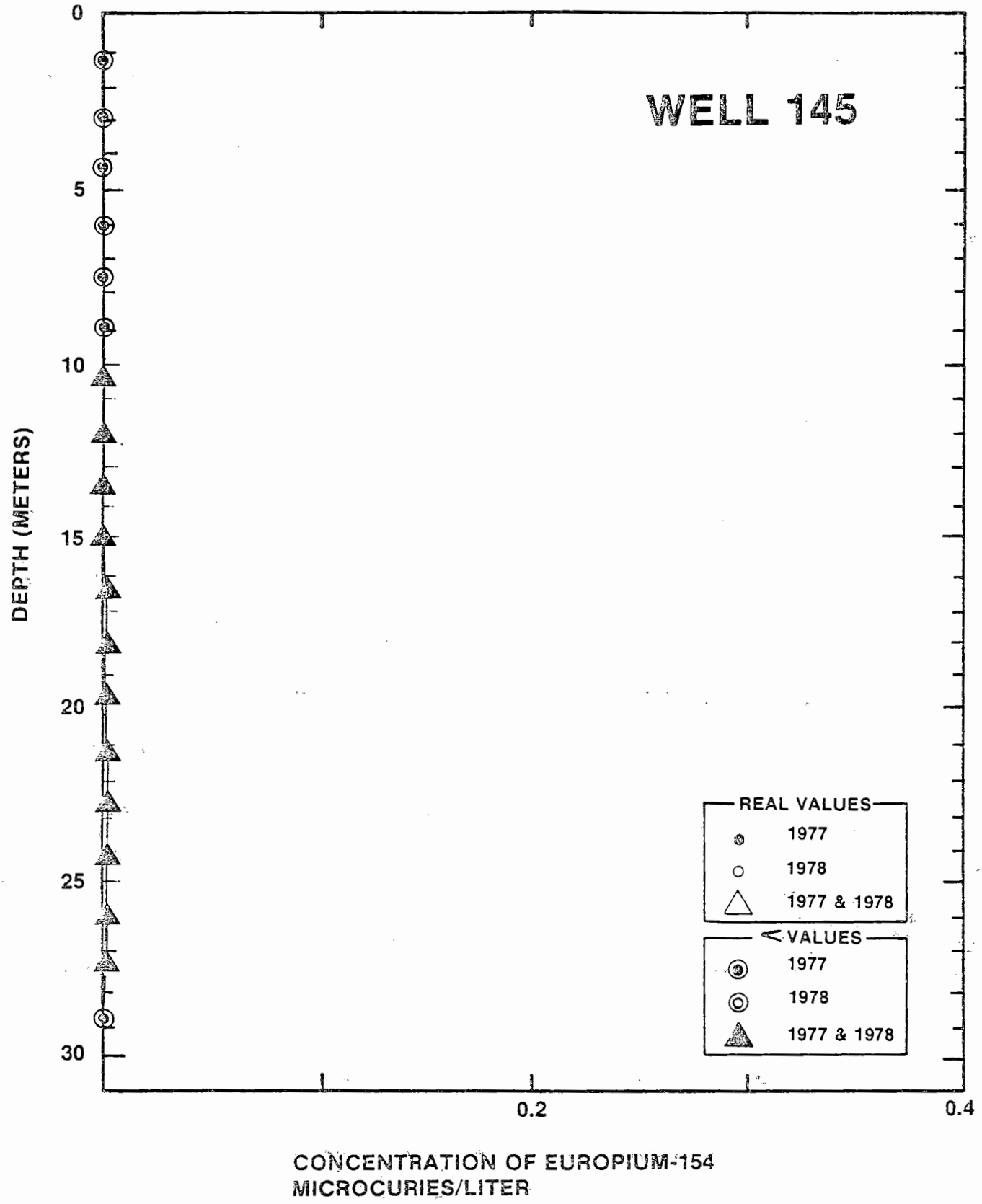
WELL 145
DEPTH (METERS)
0
5
10
15
20
25
30
0.2
0.4
REAL VALUES
1977
1978
1977 & 1978
< VALUES
1977
1978
1977 & 1978
CONCENTRATION OF EUROPIUM-154
MICROCURIES/LITER

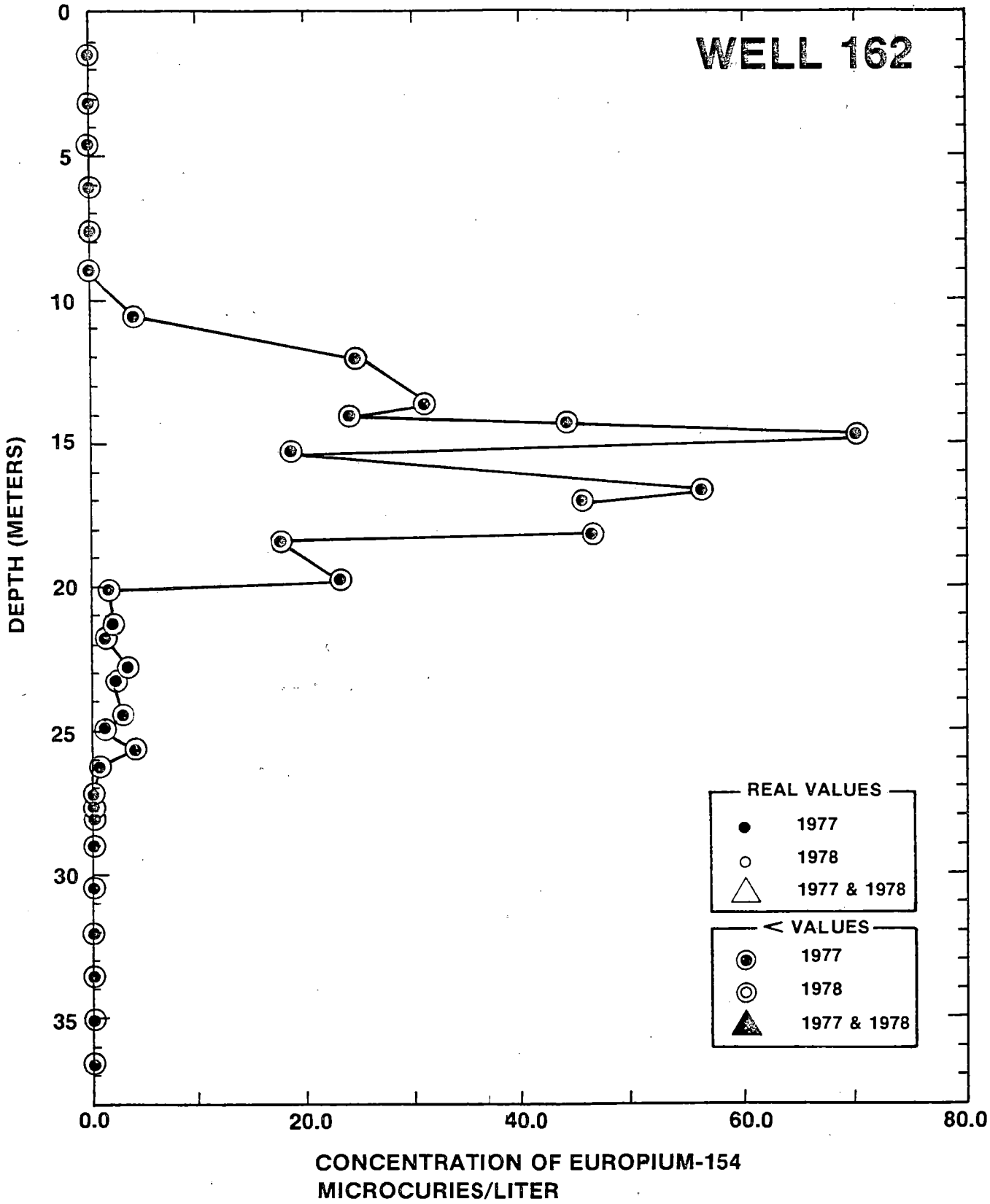

9 2 1 2 4 6 6 1 5 0 2

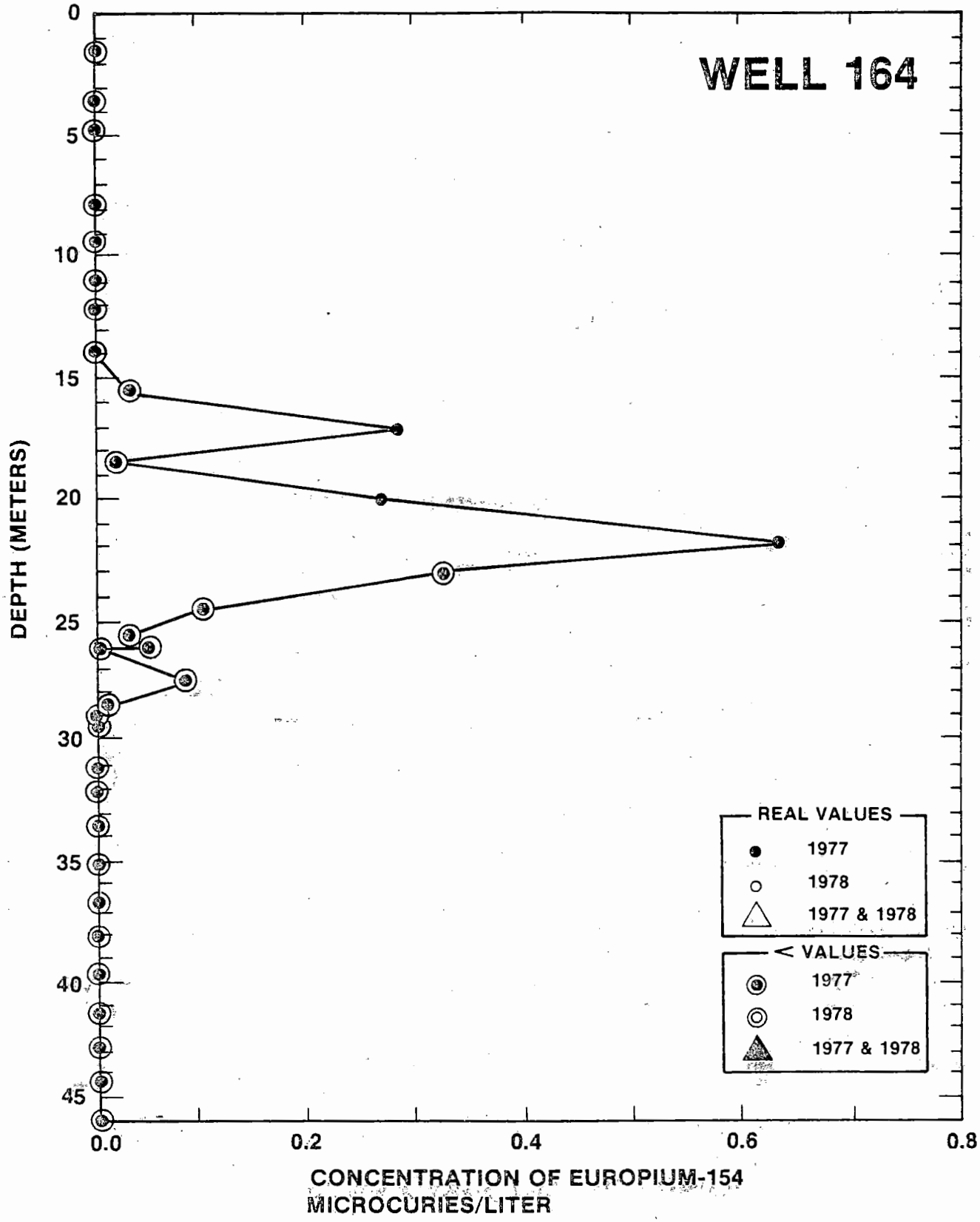

9 2 1 2 4 6 6 1 5 0 3

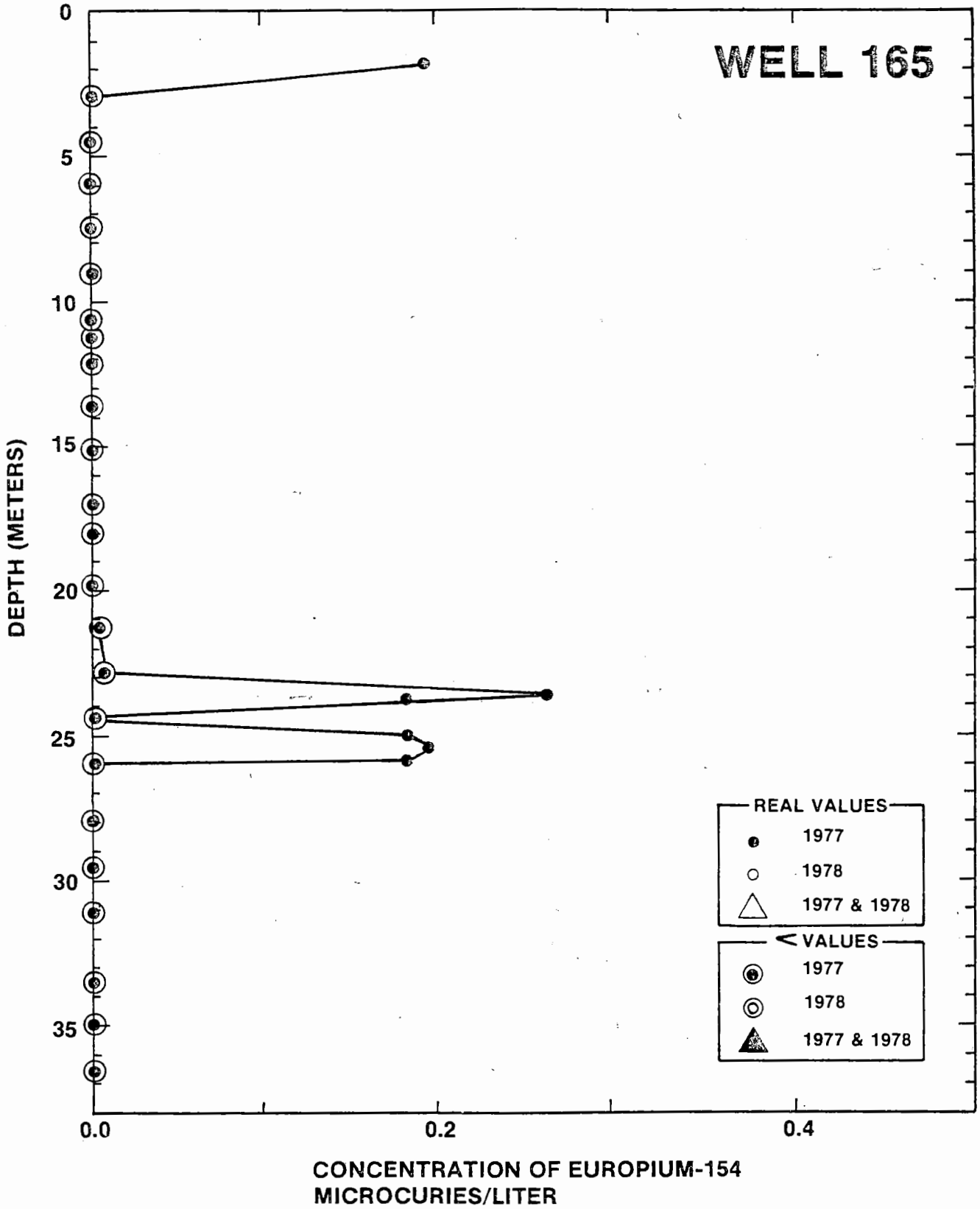

9 2 1 2 4 6 6 1 5 0 4

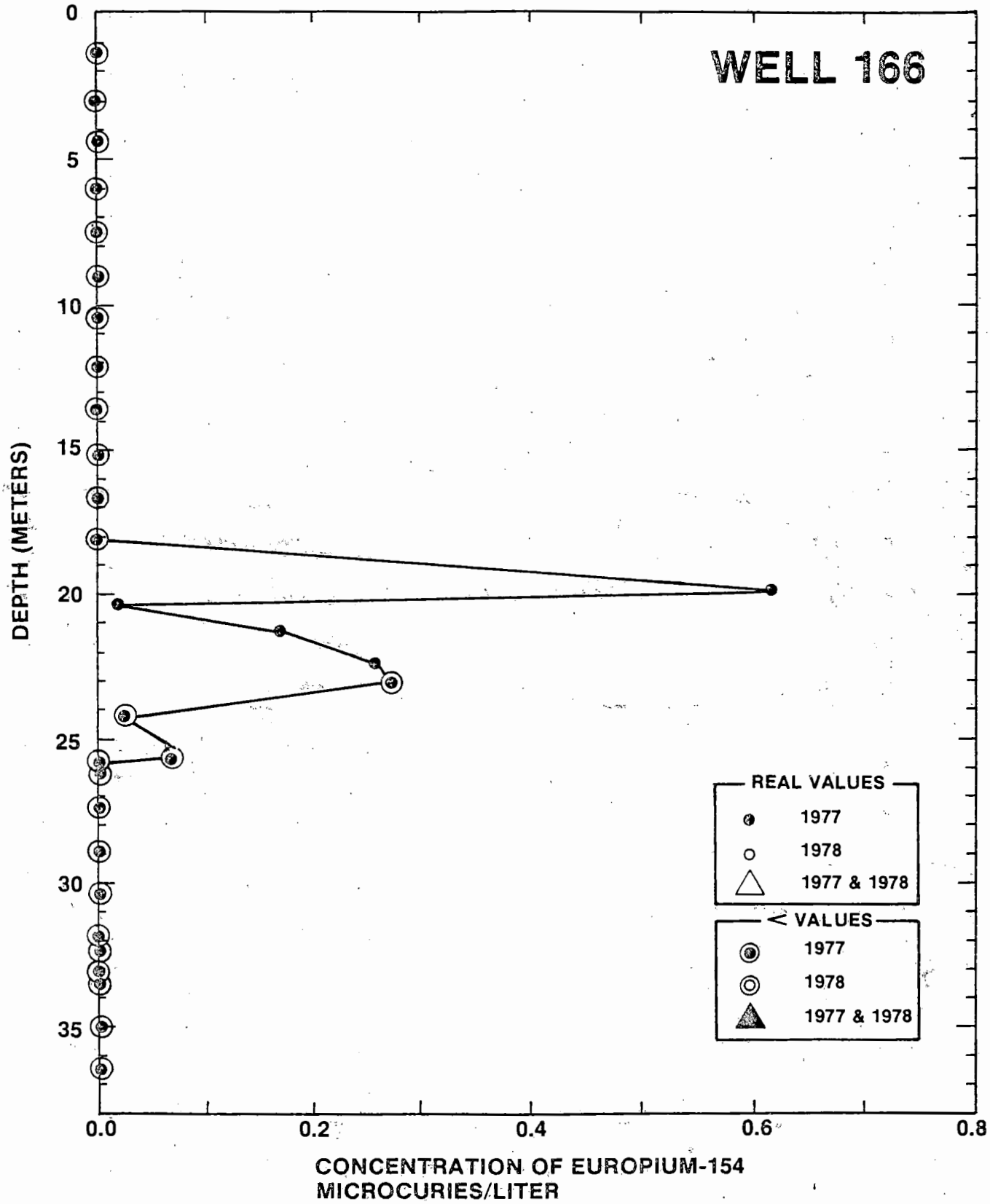
WELL 166
DEPTH (METERS)
0
5
10
15
20
25
30
35
0.0
0.2
0.4
0.6
0.8
CONCENTRATION OF EUROPIUM-154
MICROCURIES/LITER
REAL VALUES
1977
1978
1977 & 1978
< VALUES
1977
1978
1977 & 1978

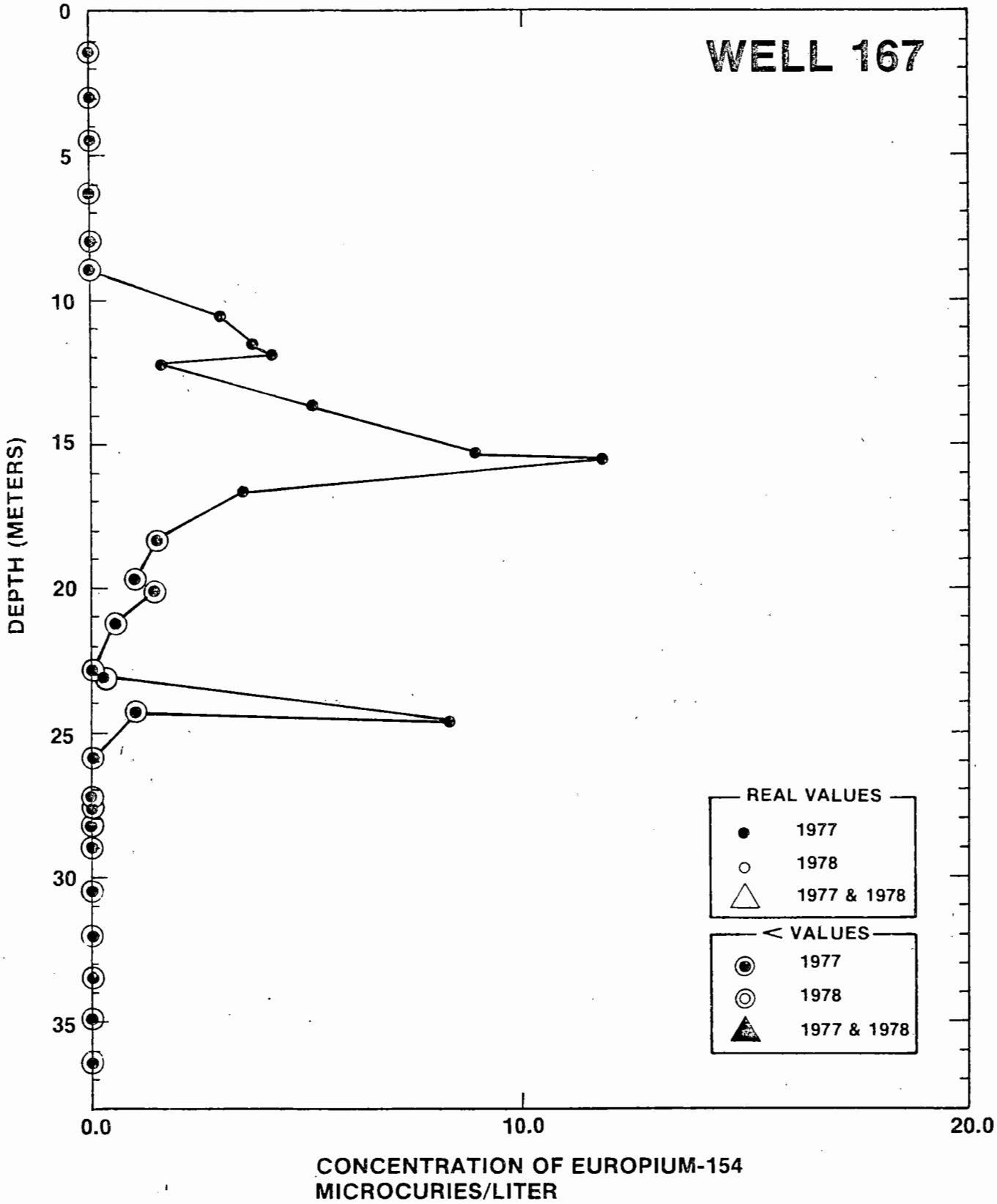

9 2 1 2 4 6 6 1 5 0 6

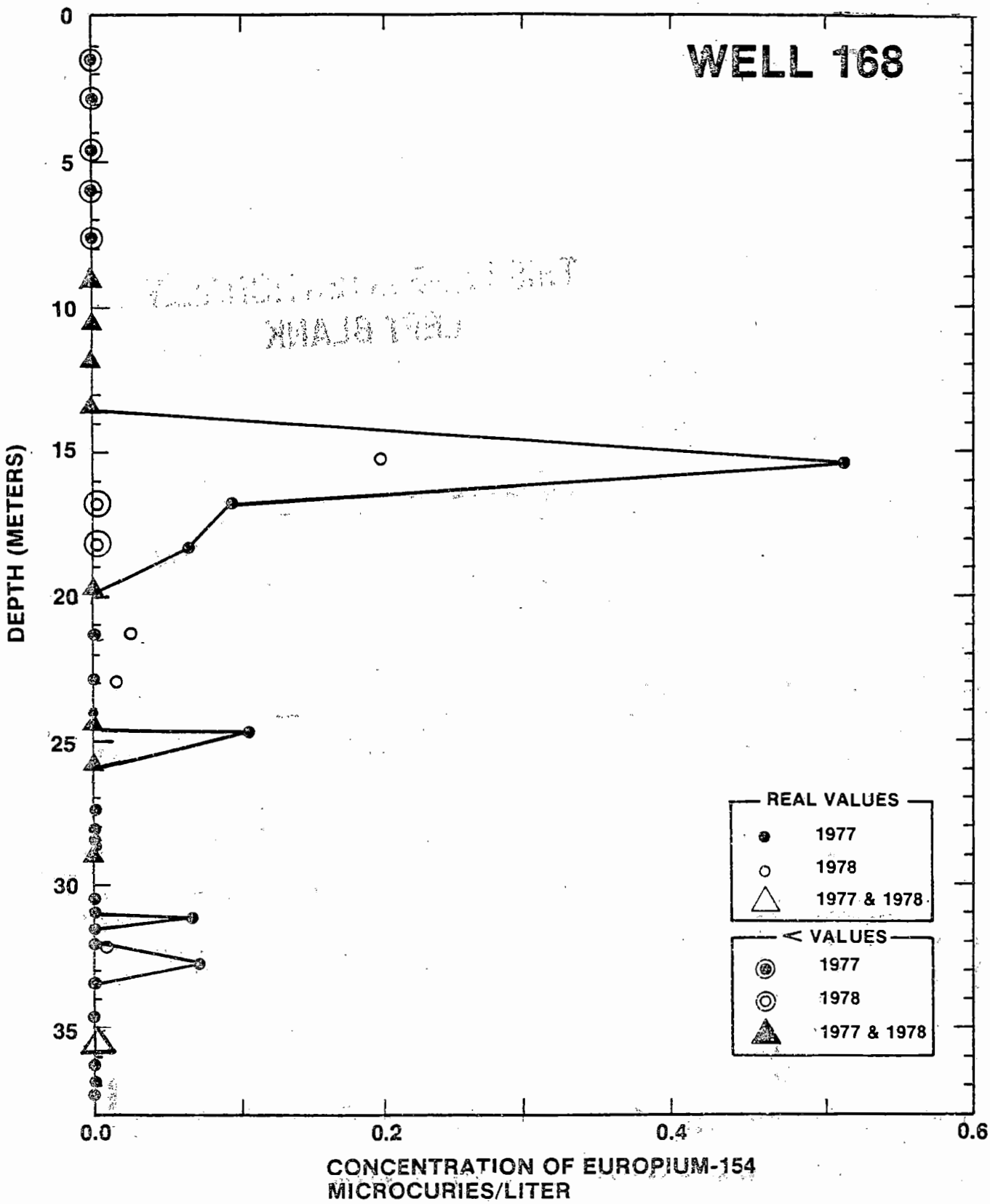

9 2 1 2 4 6 6 1 5 0 7

THIS PAGE INTENTIONALLY
LEFT BLANK

APPENDIX L

1978 PLAN AND SECTION VIEWS OF THE ^{106}Ru, ^{144}Ce AND ^{137}Cs ACTIVITY NEAR THE 241-T-106 TANK

Appendix L illustrates the 1978 plan and section views of ^{106}Ru, ^{144}Ce, and ^{137}Cs radioactivity near the 241-T-106 Tank based on the 1977 and 1978 ^{106}Ru, ^{144}Ce, and ^{137}Cs concentrations ($\mu Ci/\ell$) illustrated in Appendix K. Contours are hand drawn.

9212466150 8

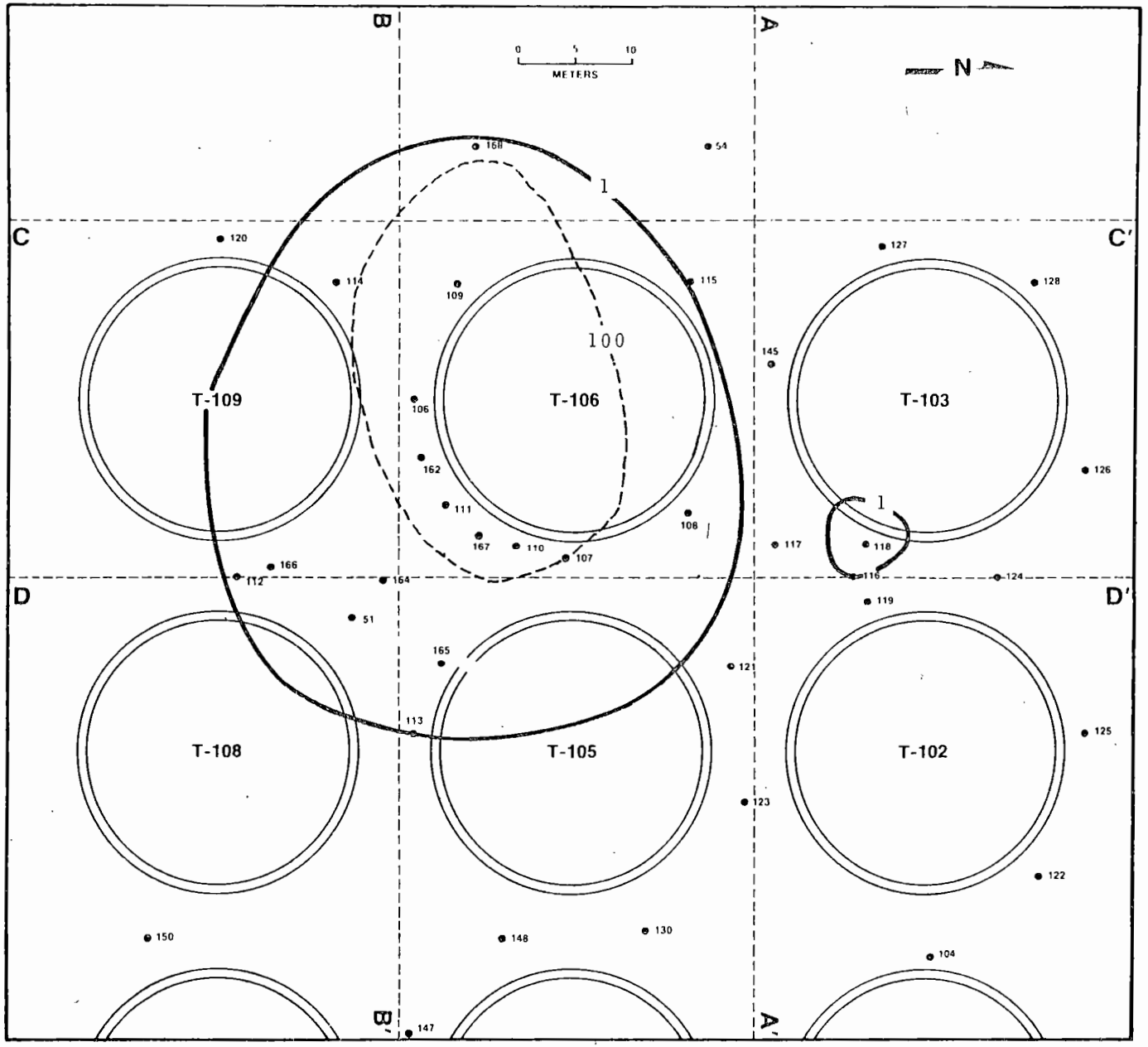

FIGURE L-1. Plan View Delineating 1.0- and 100.0-μCi/ℓ ^{106}Ru Isopleths at a Depth of 15.2 Meters

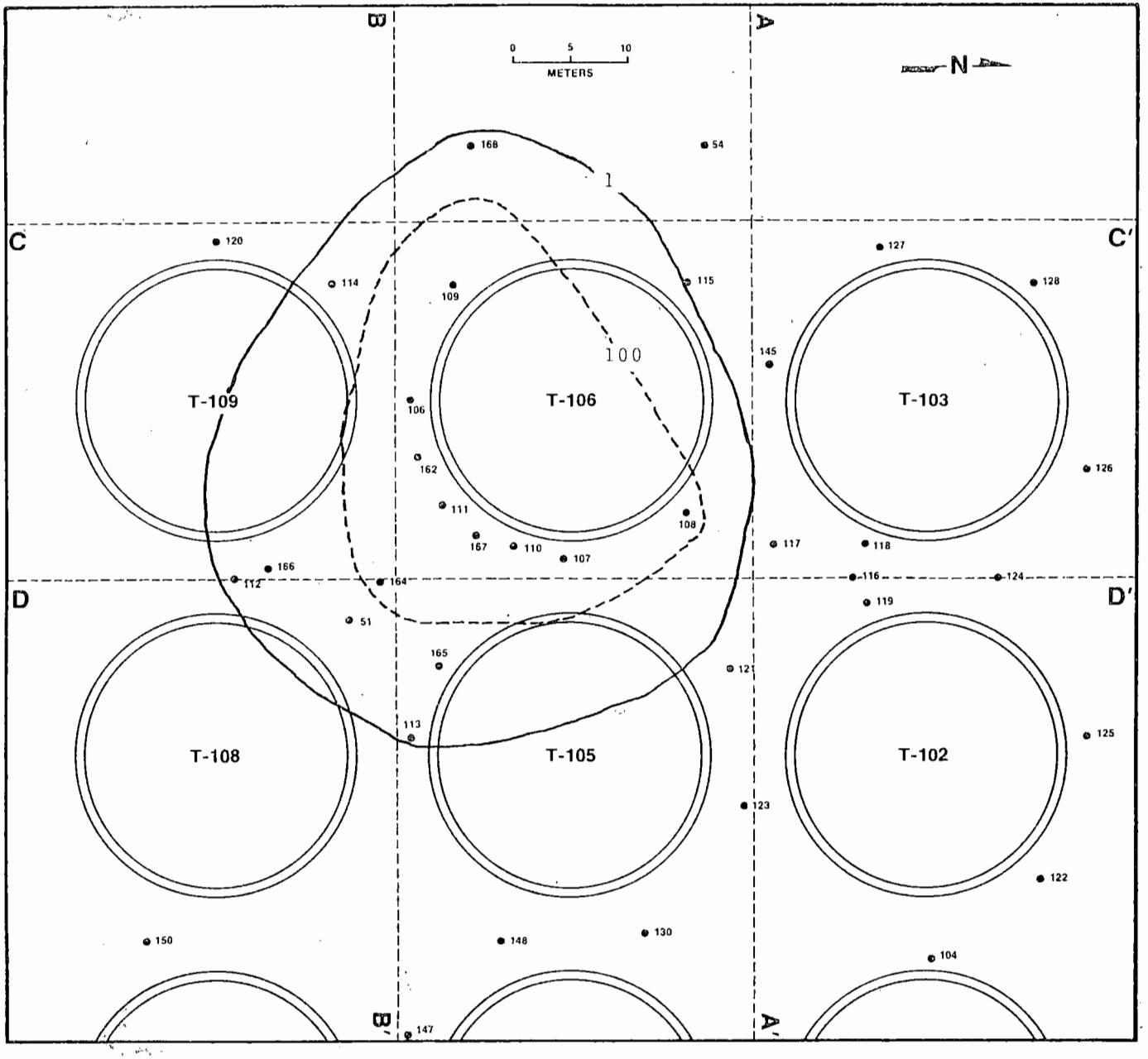

FIGURE L-2. Plan View Delineating 1.0- and 100.0-μCi/ℓ ^{106}Ru Isopleths at a Depth of 22.9 Meters.

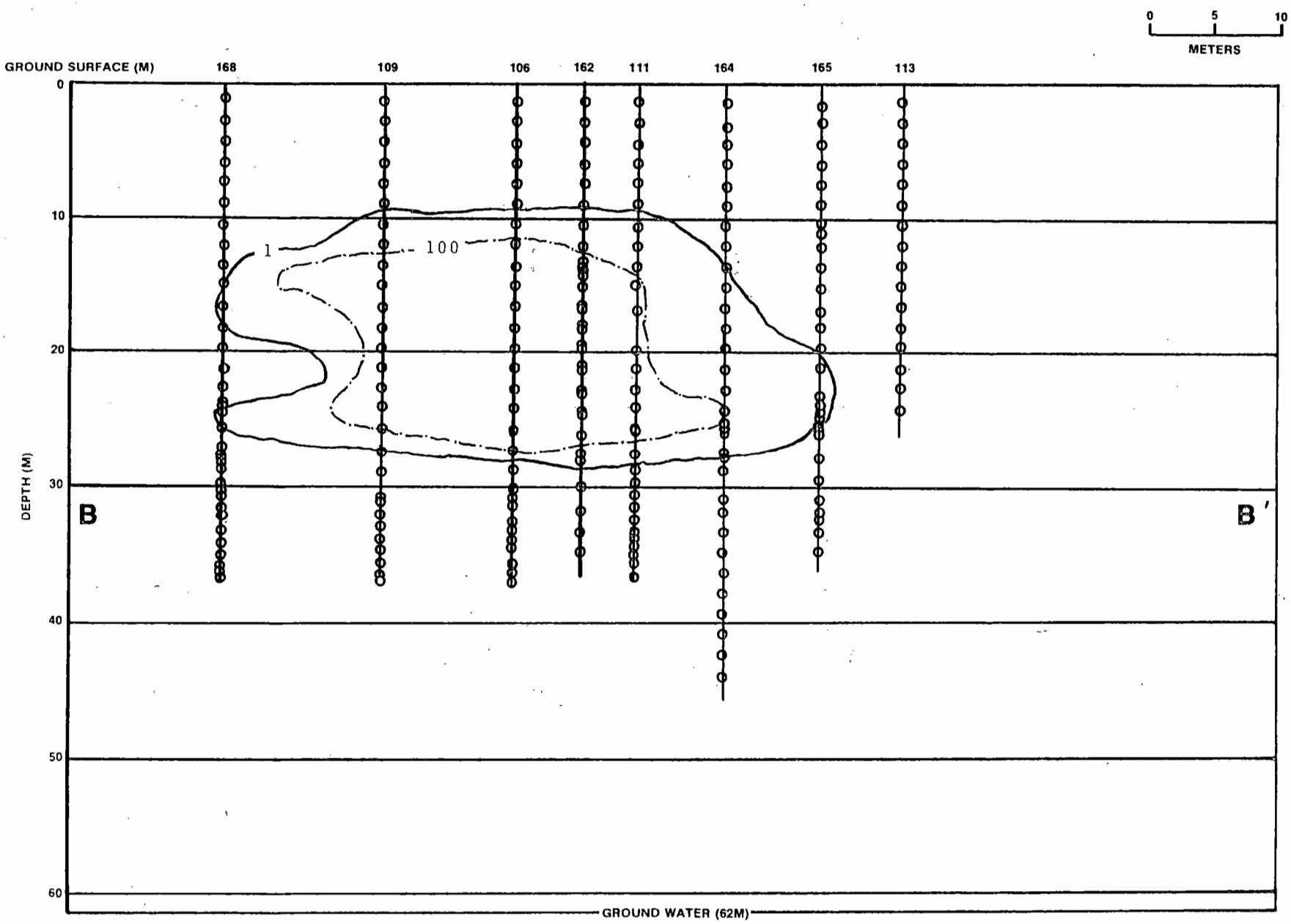

FIGURE L-3. Section View B-B' Delineating 1.0- and 100.0-μCi/ℓ ^{106}Ru Isopleths.

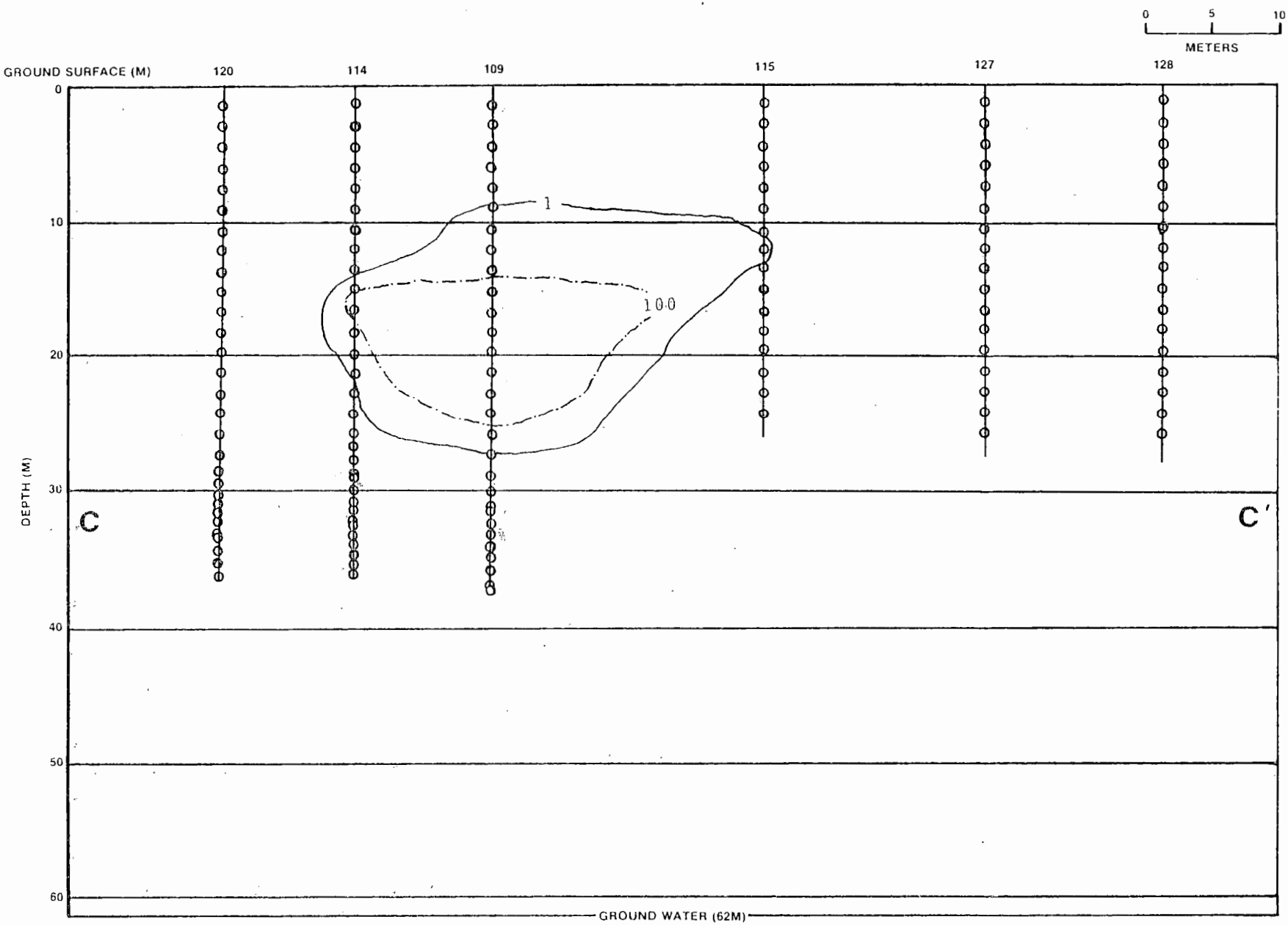

FIGURE L-4. Section View C-C' Delineating 1.0- and 100.0-μCi/ℓ ^{106}Ru Isopleths.

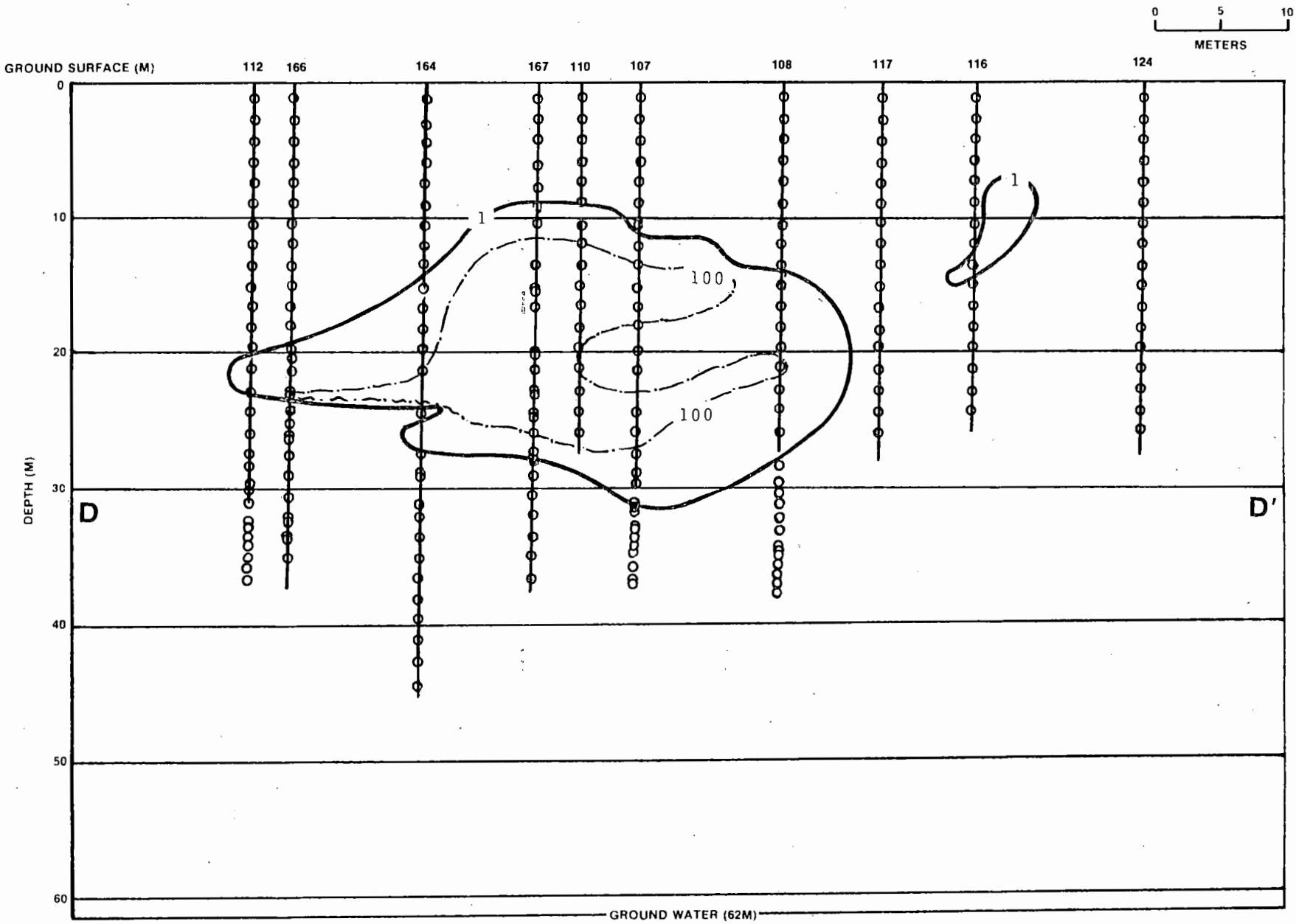

FIGURE L-5. Section View D-D' Delineating 1.0- and 100.0-μCi/ℓ ^{106}Ru Isopleths.

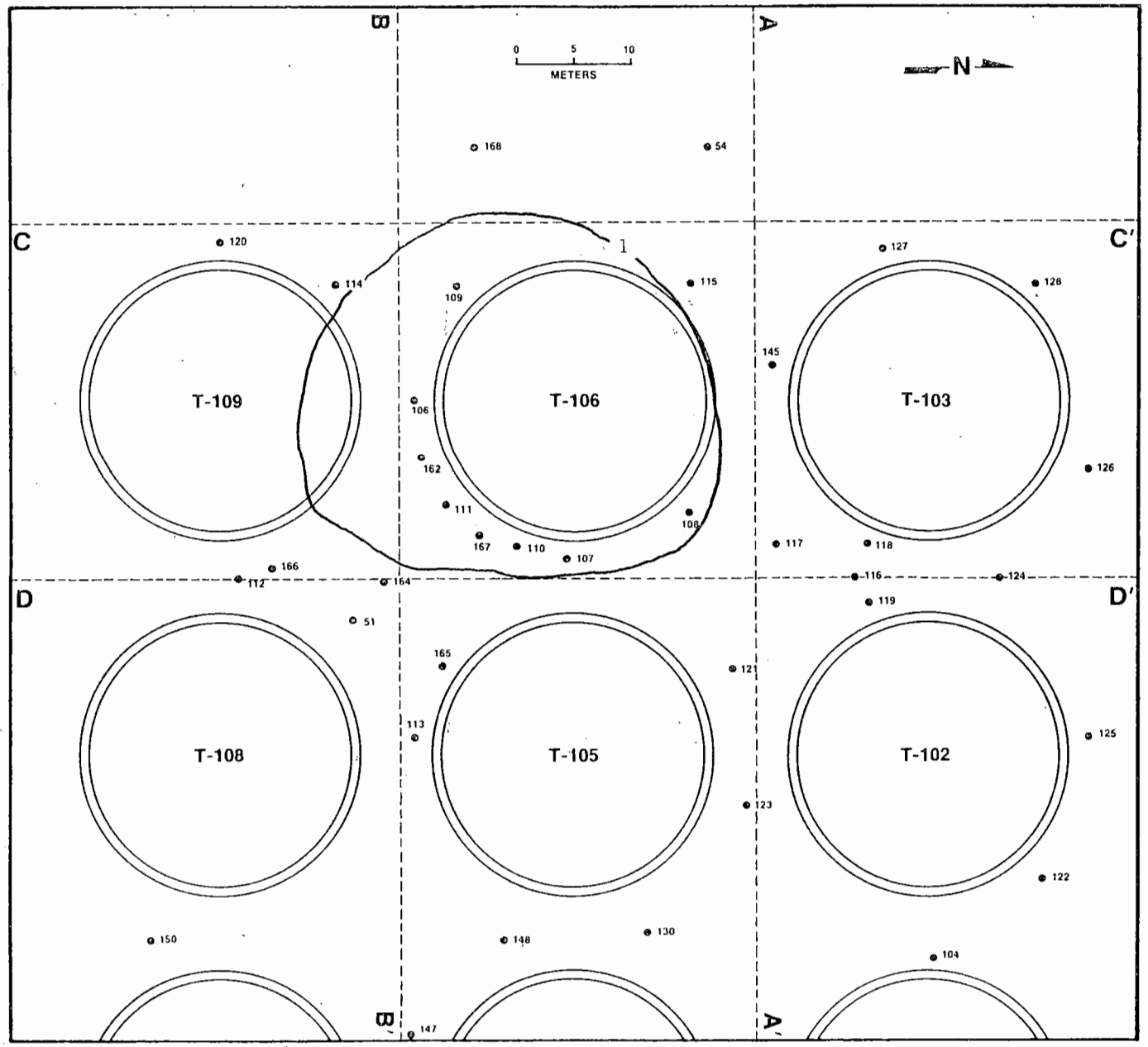

FIGURE L-6. Plan View Delineating 1.0-μCi/ℓ ^{144}Ce Isopleths at a Depth of 15.2 Meters.

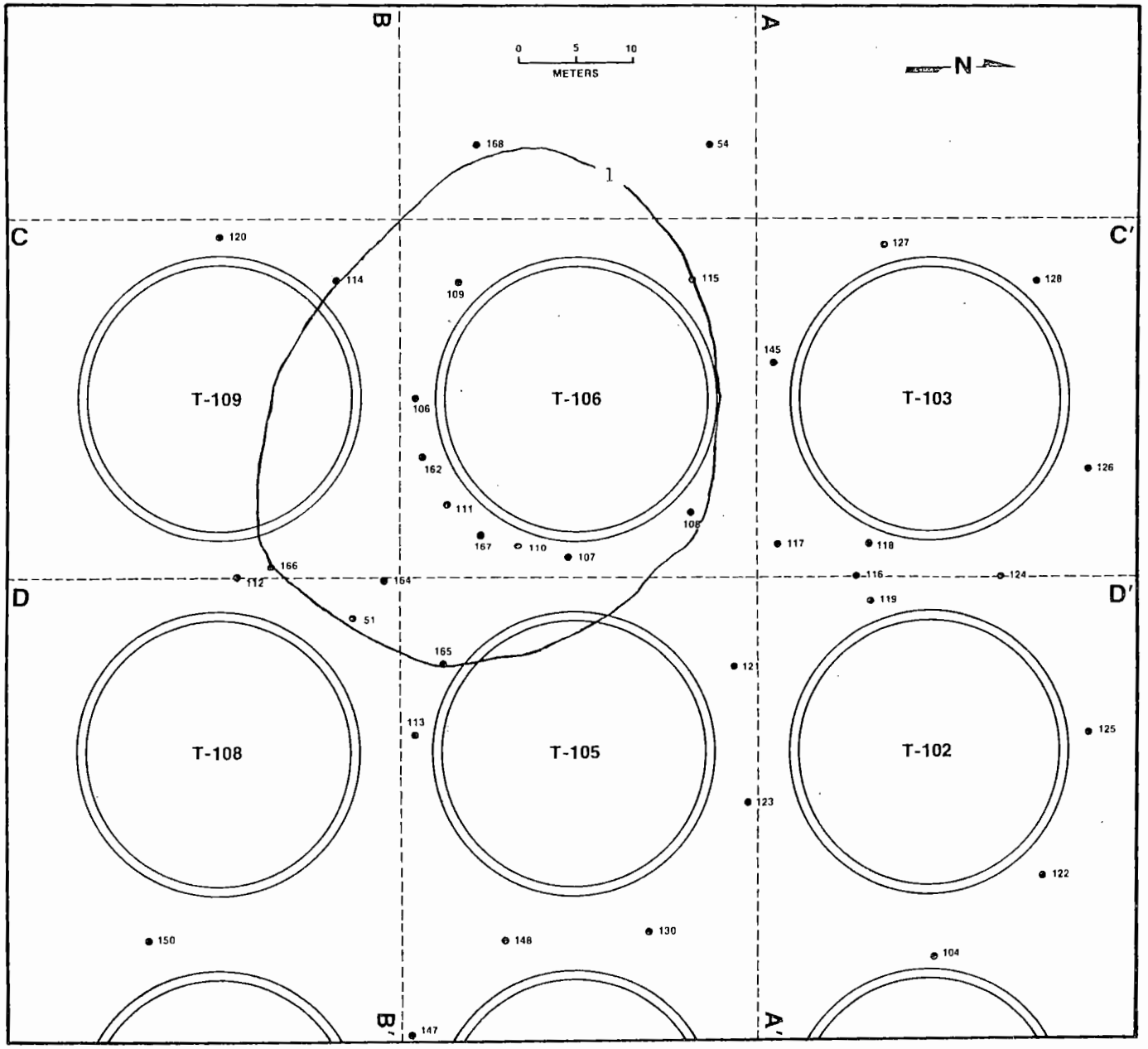

FIGURE L-7. Plan View Delineating 1.0-μCi/ℓ ^{144}Ce Isopleths at a Depth of 21.3 Meters.

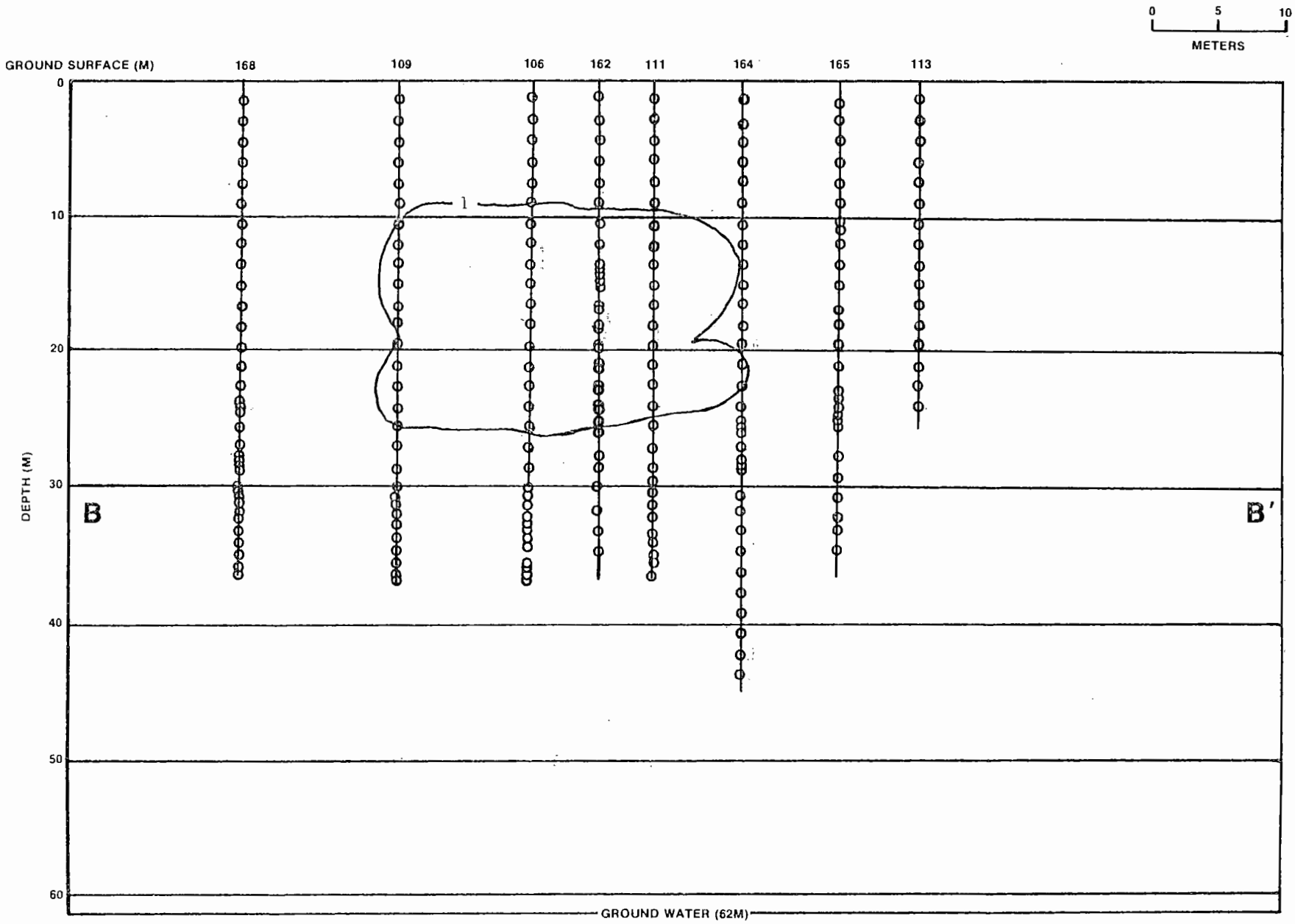

FIGURE L-8. Section View B-B' Delineating 1.0-μCi/ℓ ^{144}Ce Isopleths.

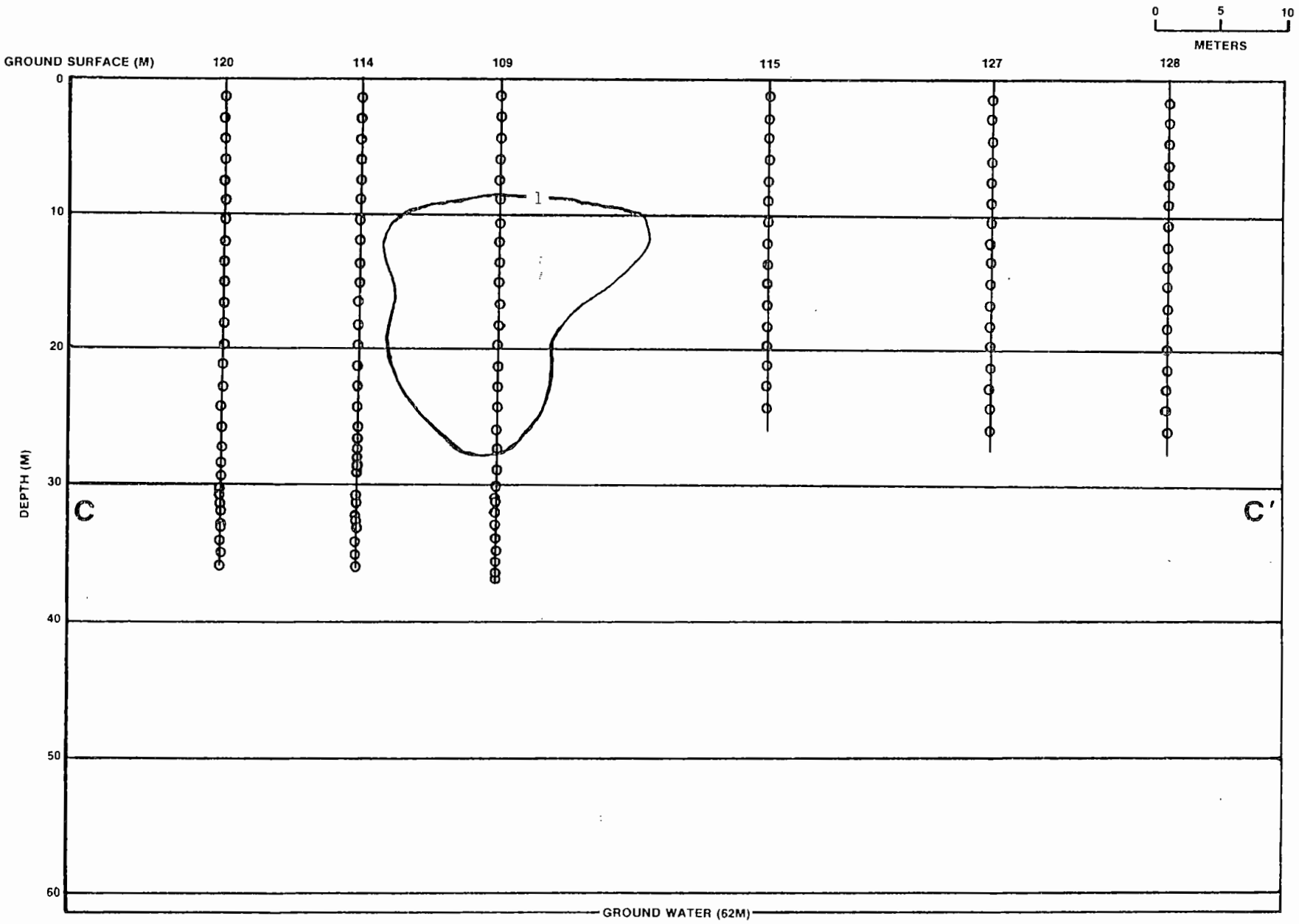

FIGURE L-9. Section View C-C' Delineating 1.0-μCi/ℓ ^{144}Ce Isopleths.

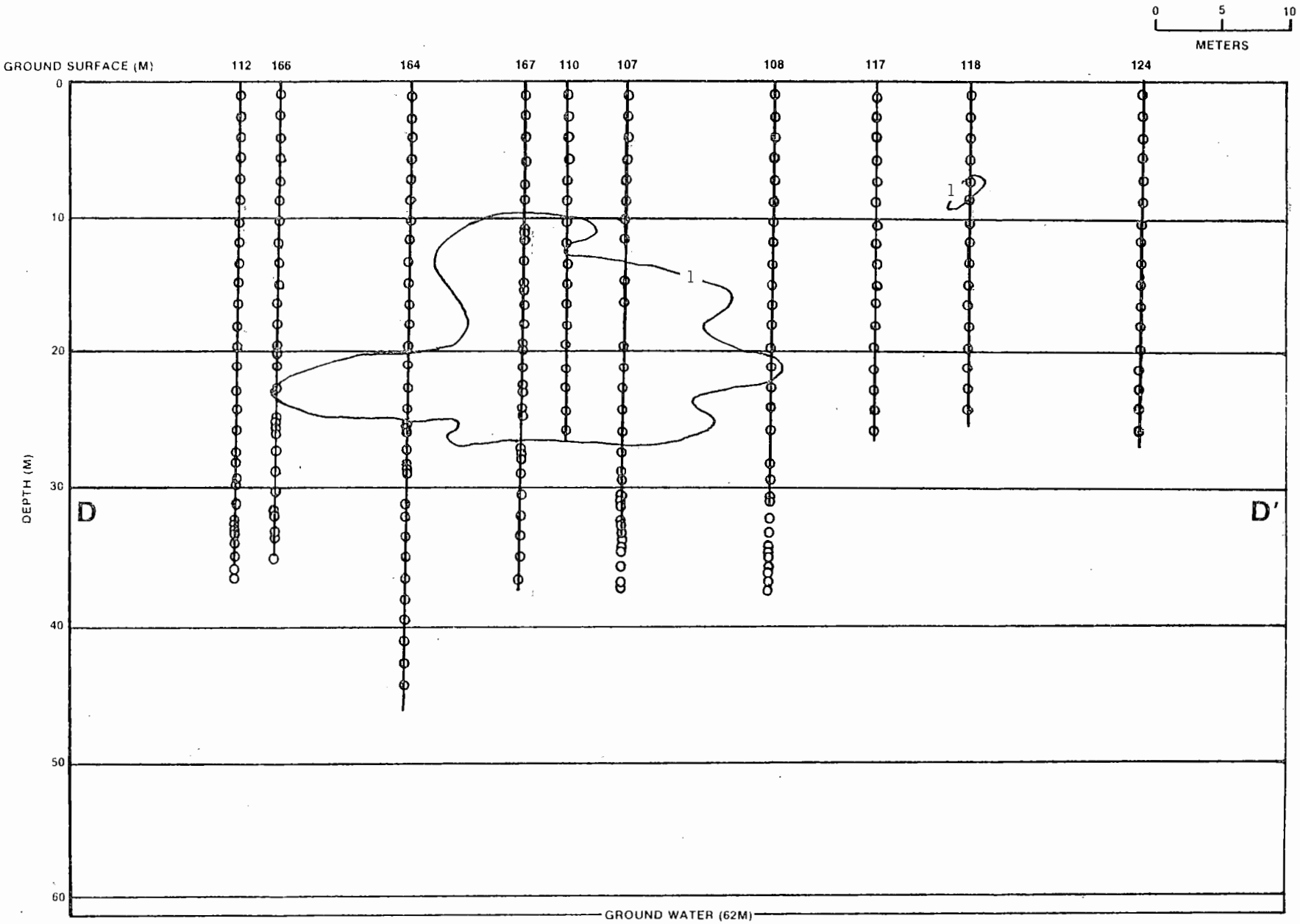

FIGURE L-10. Section View D-D' Delineating 1.0-μCi/ℓ ^{144}Ce Isopleths.

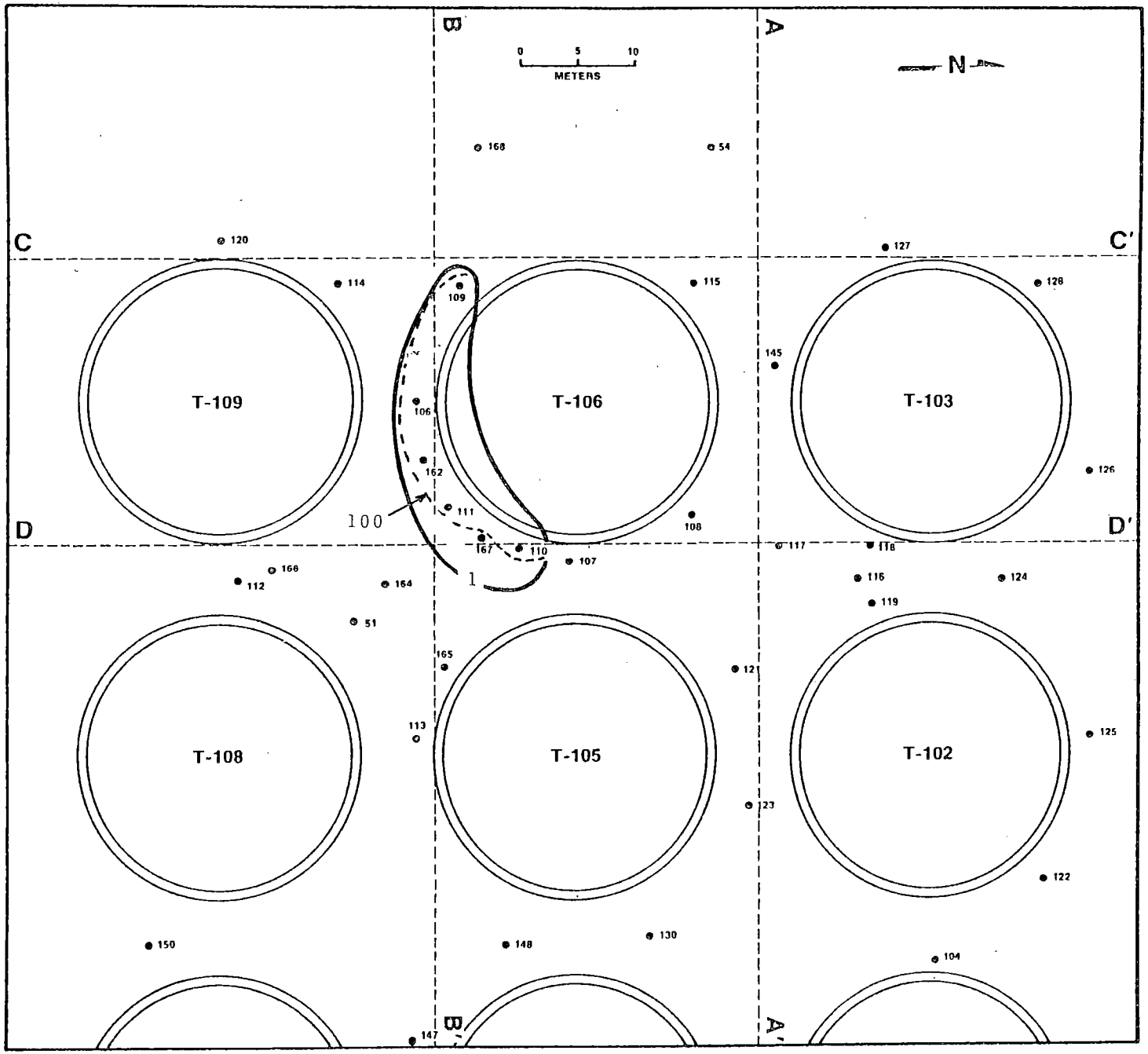

FIGURE L-11. Plan View Delineating 1.0- and 100.0-μCi/ℓ ^{137}Cs Isopleths at a Depth of 10.7 Meters.

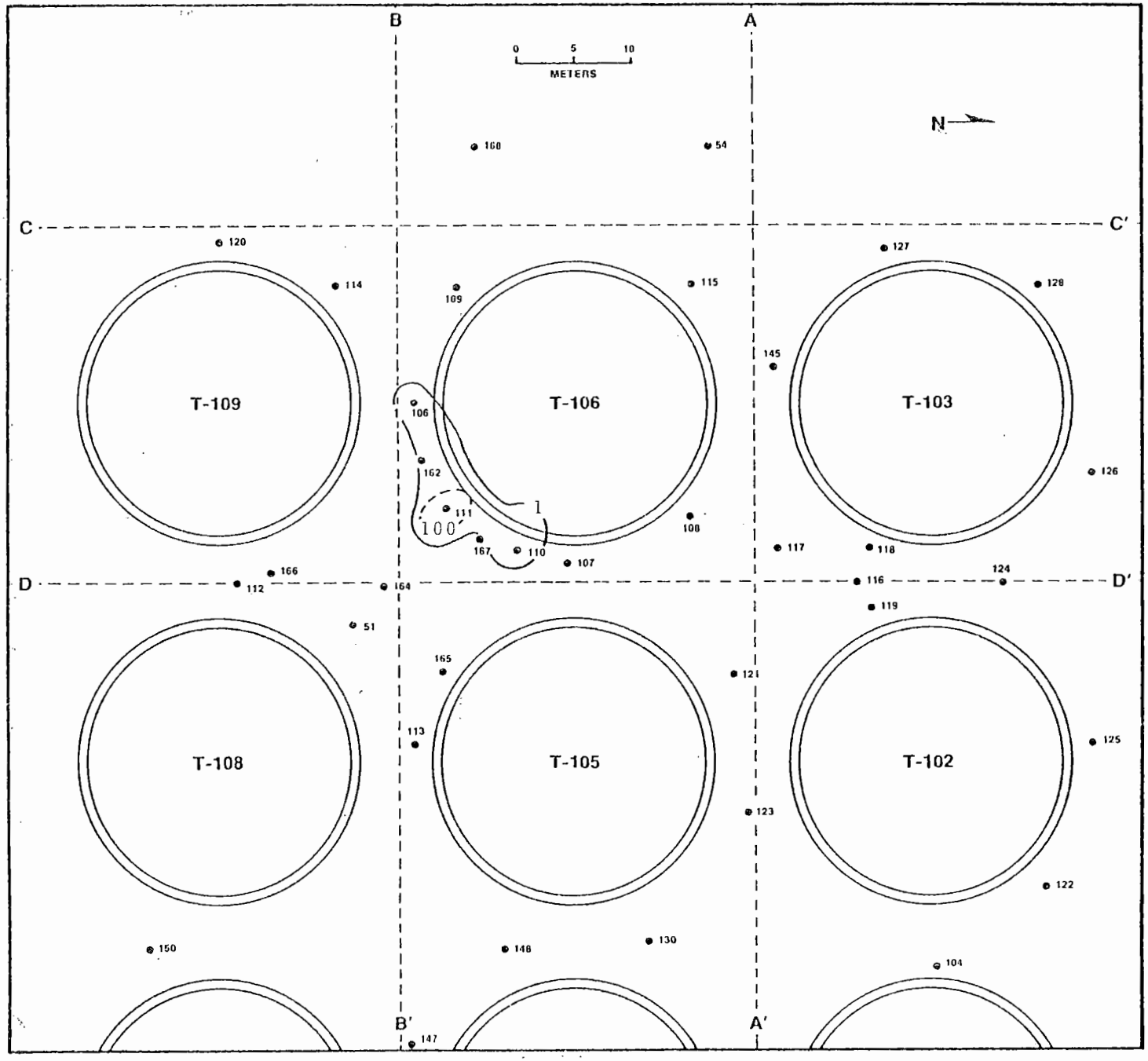

FIGURE L-12. Plan View Delineating 1.0- and 100.0-μCi/ℓ ^{137}Cs Isopleths at a Depth of 22.9 Meters.

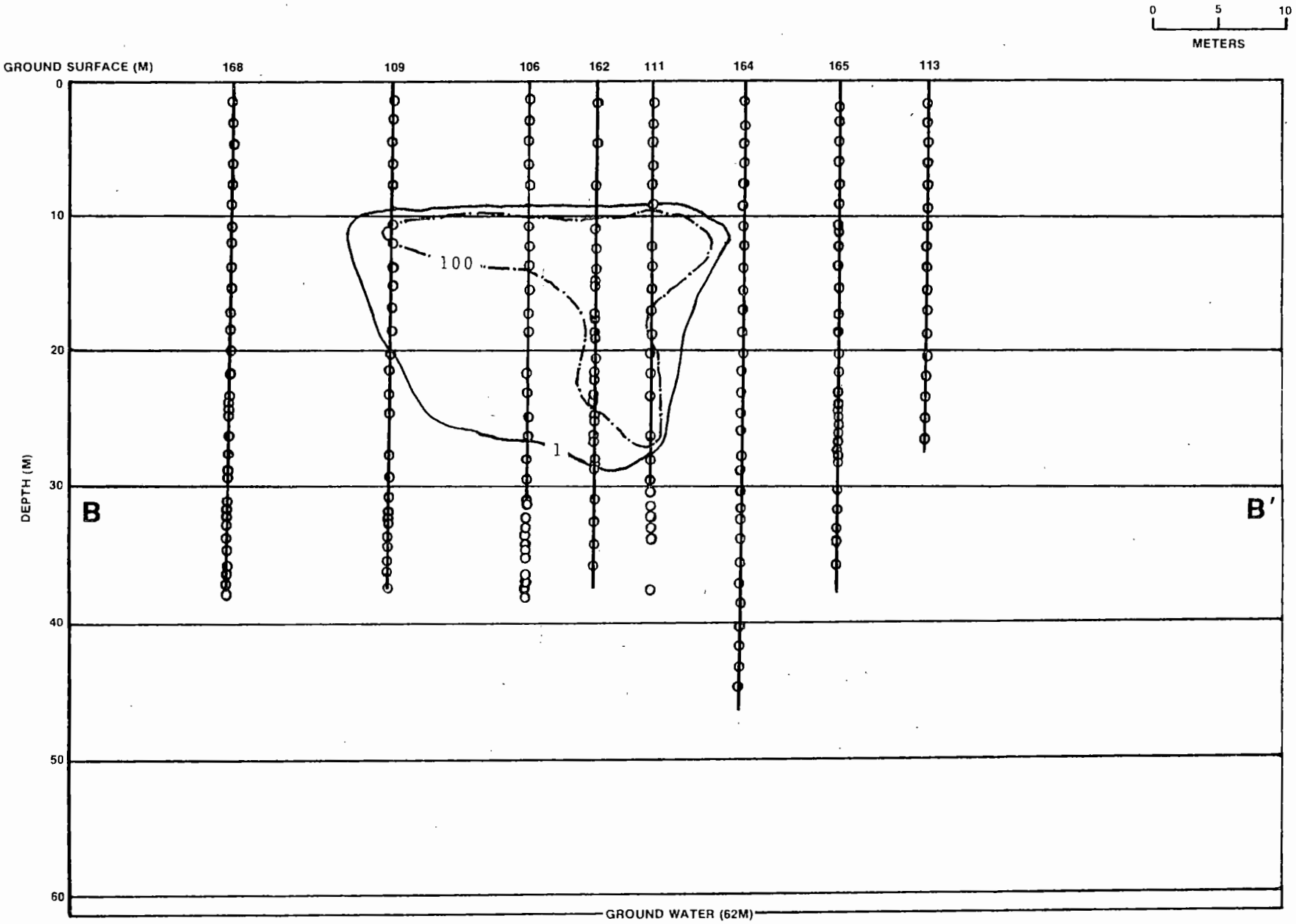

FIGURE L-13. Section View B-B' Delineating 1.0- and 100.0-μCi/ℓ ^{137}Cs Isopleths.

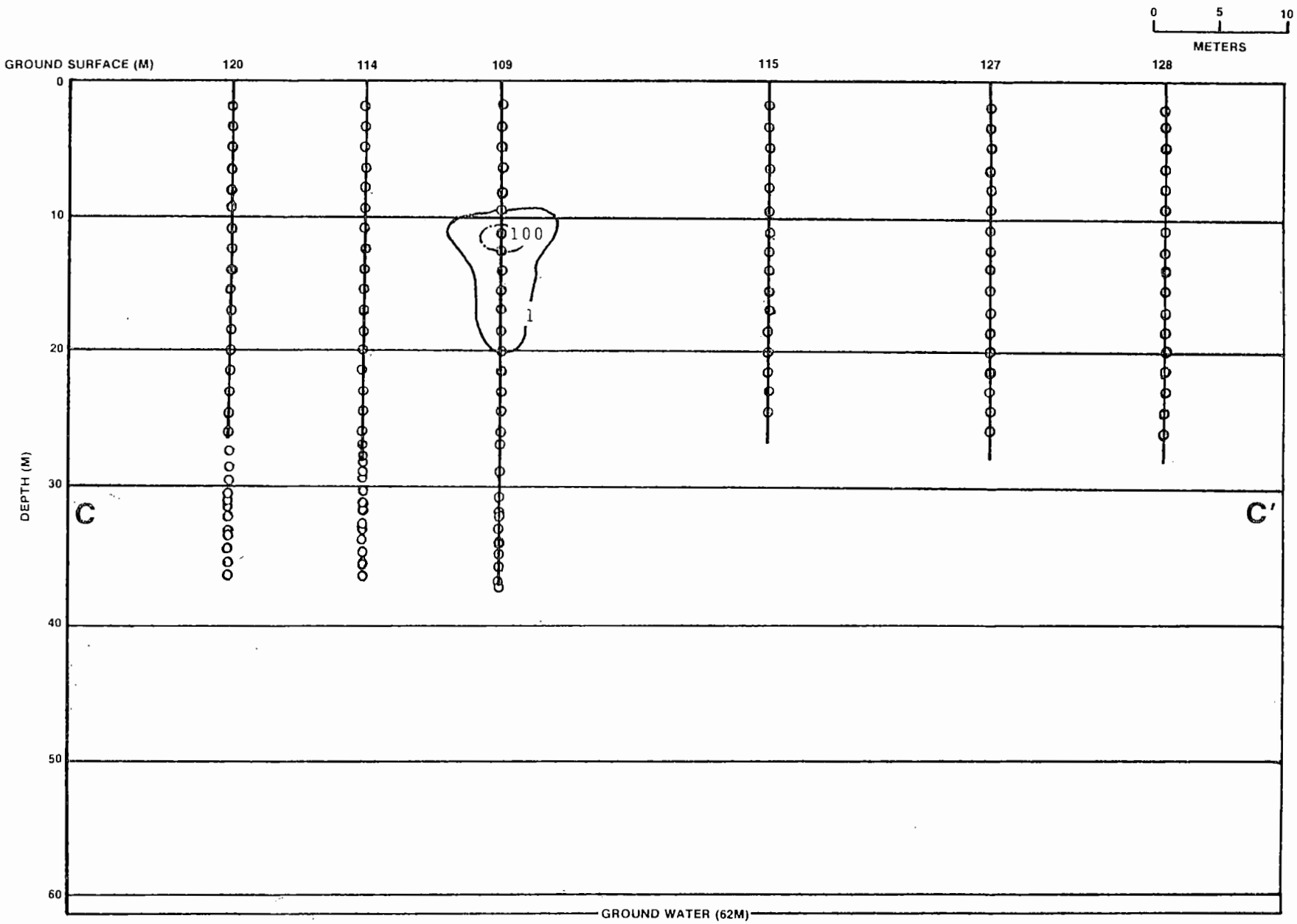

FIGURE L-14. Section View C-C' Delineating 1.0- and 100.0-μCi/ℓ ^{137}Cs Isopleths.

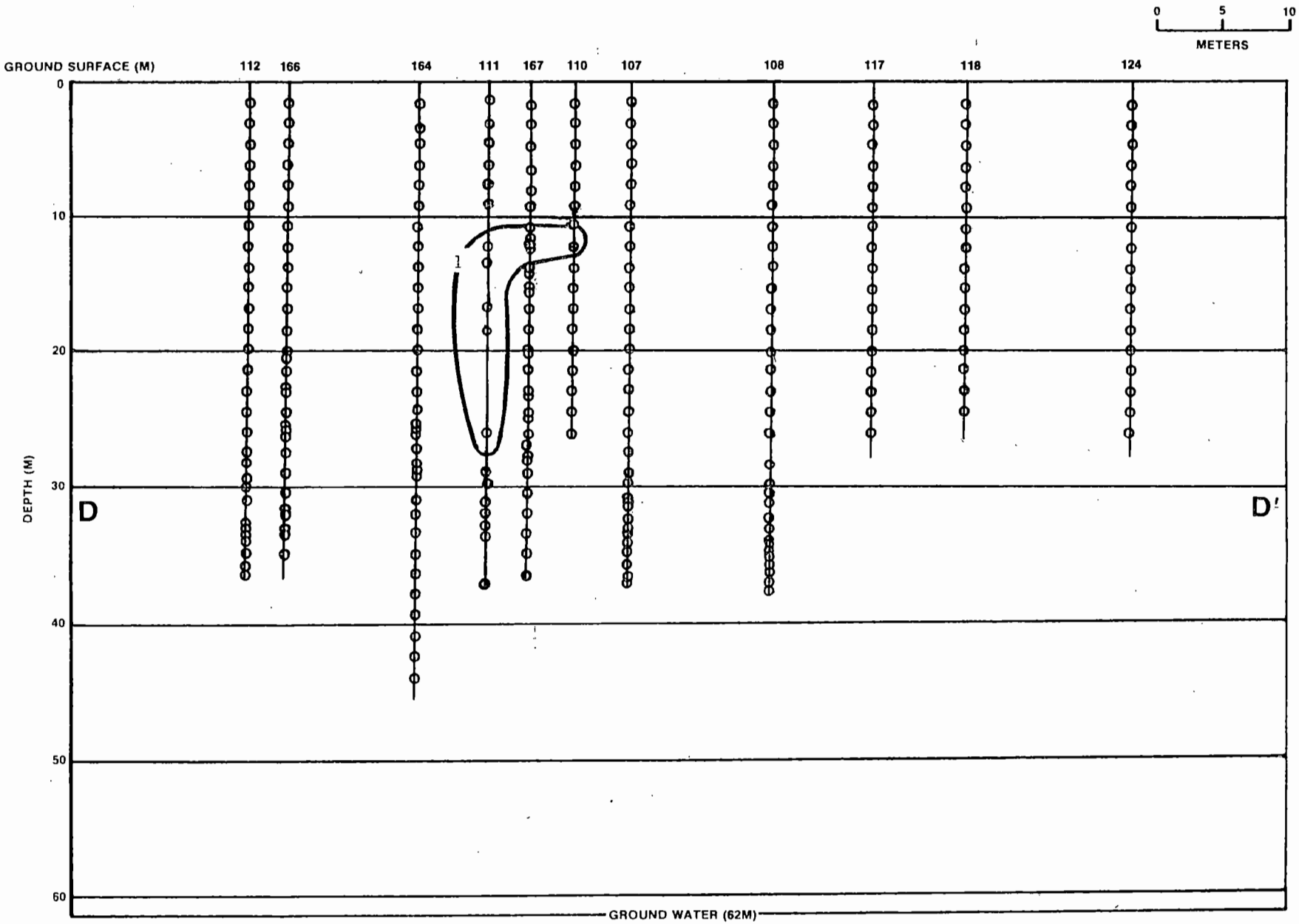

FIGURE L-15. Section View D-D' Delineating 1.0-μCi/ℓ ^{137}Cs Isopleth.

APPENDIX M

REGRESSION ANALYSIS OF THE LOGARITHM OF THE IN-WELL TOTAL GAMMA COUNTS WITH TIME

x = months since 6-1-73

y = cpm/1,000

z = linear fit

ln = natural logarithm

r^2 = squared regression coefficient

9 2 1 2 4 6 6 1 5 2 4

WELL 51 AT 22.5 METERS

$z = \ln y = 5.846 - .05955\ x$

Standard error estimate of z = .105

Standard deviation of x = .0032

$r^2 = 0.896$

t = 18.75

Run	X	Y	Calc. z	Diff.	Sum	Rn	Calc. y	Diff.
1	.10	300.00	5.8403	.1366	.1366	1.337	343.9	43.9
2	.20	328.00	5.8344	.0414	.1780	.405	341.8	13.8
3	.35	337.00	5.8255	.0054	.1834	.053	338.8	1.8
4	.70	334.00	5.8046	-.0064	.1769	.063	331.8	-2.1
5	.85	304.00	5.7957	.0787	.2556	.767	328.8	24.8
6	1.05	314.00	5.7838	.0344	.2901	.335	324.9	10.9
7	1.40	318.00	5.7629	.0009	.2910	.009	318.2	.2
8	1.70	322.00	5.7451	-.0294	.2616	.286	312.6	-9.3
9	1.80	304.00	5.7391	.0221	.2837	.214	310.8	6.8
10	1.95	296.00	5.7302	.0398	.3235	.387	308.0	12.0
11	2.05	282.00	5.7242	.0828	.4059	.799	306.2	24.2
12	2.20	286.00	5.7153	.0593	.4652	.575	303.4	17.4
13	2.45	270.00	5.7004	.1020	.5673	.575	303.4	17.4
14	2.60	295.00	5.6915	.0045	.5718	.043	296.3	1.3
15	2.80	275.00	5.6795	.0628	.6346	.608	292.8	17.8
16	3.10	294.00	5.6617	-.0218	.6128	.211	287.6	-6.3
17	3.30	315.00	5.6498	-.1027	.6100	.993	284.2	-30.7
18	3.60	294.00	5.6319	-.0516	.4584	.498	279.2	-14.7
19	3.85	272.00	5.6170	.0112	.4697	.108	275.0	3.0
20	4.10	300.00	5.6021	-.1016	.3681	.980	271.0	-28.9
21	4.30	265.00	5.5902	.0105	.3786	.101	267.8	2.8
22	4.50	247.00	5.5783	.0689	.4476	.665	264.6	17.6
23	4.75	264.00	5.5634	-.0124	.4351	.120	260.7	-3.2
24	4.95	220.00	5.5515	.1579	.5930	1.523	257.6	37.6
25	5.20	270.00	5.5366	-.0617	.5313	.595	253.8	-16.1
26	5.40	287.00	5.5247	-.1347	.3965	1.299	250.8	-36.1
27	5.75	265.00	5.5039	-.0758	.3207	.730	245.6	-19.3
28	5.95	312.00	5.4920	-.2510	.0697	2.419	242.7	-69.2
29	6.20	275.00	5.4771	-.1396	-.0698	1.346	239.1	-35.8
30	6.40	245.00	5.4652	-.0360	-.1059	.347	236.3	-8.6
31	6.65	290.00	5.4503	-.2195	-.3255	2.117	232.8	-57.1
32	6.90	235.00	5.4354	-.0241	-.3496	.233	229.3	-5.6
33	7.15	220.00	5.4205	.0269	-.3227	.259	225.9	5.9
34	14.50	134.00	4.9828	.0775	-.2452	.775	145.8	10.8
35	14.70	111.00	4.9708	.2613	.0161	2.618	144.1	33.1
36	15.10	124.50	4.9470	.1227	.1888	1.234	140.7	16.2
37	15.40	120.00	4.9292	.1417	.2806	1.429	138.2	18.2
38	16.09	135.00	4.8881	-.0171	.2634	.174	132.7	-2.2
39	16.13	165.00	4.8857	-.2202	.0432	2.237	132.3	-32.6
40	16.23	133.00	4.8797	-.0105	.0326	.107	131.6	-1.3
41	16.35	135.00	4.8726	-.0326	-.0000	.332	130.6	-4.3

9 2 1 2 4 6 1 5 2 5

WELL 106 AT 16.0 METERS

$z = \ln y = 6.226 - .08476\ x$

Standard error estimate of z = .105

Standard deviation of x = .0036

$r^2 = 0.937$

t = -23.44

Run	X	Y	Calc. z	Diff.	Sum	Rn	Calc. y	Diff.
1	1.50	425.00	6.0988	.0467	.0467	.462	445.3	20.3
2	1.95	392.00	6.0606	.0894	.1361	.882	428.6	36.6
3	2.50	362.00	6.0140	.1224	.2585	1.203	409.1	47.1
4	2.85	325.00	5.9843	.2005	.4590	1.967	397.1	72.1
5	3.05	400.00	5.9674	-.0240	.4350	.235	390.5	-9.5
6	3.30	440.00	5.9462	-.1405	.2945	1.374	382.3	-57.6
7	3.60	380.00	5.9208	-.0193	.2751	.189	372.7	-7.2
8	3.80	310.00	5.9038	.1672	.4424	1.632	366.4	56.4
9	4.10	398.00	5.8784	-.1080	.3344	1.052	357.2	-40.7
10	4.35	350.00	5.8572	-.0006	.3337	.006	349.7	-.2
11	4.50	337.00	5.8445	.0244	.3581	.237	345.3	8.3
12	4.70	317.00	5.8275	.0686	.4268	.667	339.5	22.5
13	4.90	285.00	5.8100	.1581	.5849	1.535	333.8	48.8
14	5.15	315.00	5.7894	.0368	.6218	.357	326.8	11.8
15	5.40	340.00	5.7682	-.0606	.5611	.588	319.9	-20.0
16	5.55	307.00	5.7555	.0286	.5898	.277	315.9	8.9
17	5.90	350.00	5.7258	-.1320	.4577	1.278	306.6	-43.3
18	6.10	324.00	5.7089	-.0718	.3859	.695	301.5	-22.4
19	6.30	315.00	5.6919	-.0606	.3253	.586	296.4	-18.5
20	6.60	290.00	5.6665	-.0033	.3220	.032	289.0	-.9
21	6.85	297.00	5.6453	-.0483	.2736	.467	282.9	-14.0
22	7.10	260.00	5.6241	.0634	.3371	.613	277.0	17.0
23	7.40	287.00	5.5987	-.0607	.2763	.586	270.0	-16.9
24	7.60	304.00	5.5817	-.1352	.1411	1.306	265.5	-38.4
25	8.20	277.00	5.5309	-.0930	.0480	.899	252.3	-24.6
26	8.45	287.00	5.5097	-.1497	-.1017	1.446	247.0	-39.9
27	8.60	270.00	5.4970	-.1013	-.2031	.979	243.9	-26.0
28	9.15	267.00	5.4504	-.1368	-.3399	1.323	232.8	-34.1
29	14.30	170.00	5.0139	-.1218	-.4618	1.208	150.4	-19.5
30	14.50	120.00	4.9969	.2094	-.2524	2.080	147.9	27.9
31	15.10	132.00	4.9460	.0632	-.1891	.632	140.6	8.6
32	15.40	117.00	4.9206	.1584	-.0306	1.587	137.0	20.0
33	16.09	219.00	4.8621	.0023	-.0282	.023	129.3	.3
34	16.13	138.00	4.8587	-.0684	-.0967	.690	128.8	-9.1
35	16.23	117.00	4.8503	.0881	-.0085	.890	127.7	10.7
36	16.30	135.00	4.8443	-.0608	-.0694	.615	127.0	-7.9
37	16.35	118.00	4.8401	.0694	-.0000	.702	126.4	8.4

9 2 1 2 4 6 6 1 5 2 6

WELL 107 AT 25.0 METERS

$z = \ln y = 6.131 - .0516\ x$

Standard error estimate of z = .103

Standard deviation of x = .0046

$r^2 = 0.826$

t = -11.33

Run	X	Y	Calc. z	Diff.	Sum	Rn	Calc. y	Diff.
1	3.80	390.00	5.9348	-.0312	-.0312	.319	378.0	-11.9
2	4.10	400.00	5.9194	-.0720	-.1033	.734	372.1	-27.8
3	4.50	360.00	5.8987	.0126	-.0906	.128	364.5	4.5
4	5.00	290.00	5.8729	.2030	.1124	2.050	355.3	65.3
5	5.40	350.00	5.8523	-.0055	.1068	.056	348.0	-1.9
6	5.70	310.00	5.8368	.1002	.2071	1.006	342.7	32.7
7	5.90	395.00	5.8265	-.1523	.0548	1.526	339.1	-55.8
8	6.20	340.00	5.8110	-.0178	.0369	.178	333.9	-6.0
9	6.60	345.00	5.7904	-.0531	-.0161	.529	327.1	-17.8
10	6.90	320.00	5.7749	.0066	-.0095	.065	322.1	2.1
11	7.20	275.00	5.7594	.1426	.1331	1.417	317.1	42.1
12	7.50	330.00	5.7439	-.0551	.0780	.546	312.3	-17.6
13	7.80	310.00	5.7205	-.0080	.0699	.079	307.5	-2.4
14	8.10	305.00	5.713	-.0072	.0626	.072	302.7	-2.2
15	8.50	330.00	5.6975	-.1015	-.0388	1.004	298.1	-31.8
16	8.80	310.00	5.6769	-.0506	-.0985	.589	292.0	-17.9
17	9.20	255.00	5.6562	.1150	.0164	1.136	286.0	31.0
18	9.70	290.00	5.6304	-.0094	-.0229	.389	278.7	-11.2
19	14.30	282.00	5.3931	-.2487	-.2716	2.514	219.8	-62.1
20	14.50	210.00	5.3828	.0357	-.2359	.361	217.6	7.6
21	14.70	174.00	5.3724	.2134	-.2359	.361	217.6	7.6
22	15.10	201.00	5.3513	.0485	.0260	.494	210.9	9.9
23	15.40	186.00	5.3363	.1106	.1366	1.131	201.1	-2.8
24	16.03	204.00	5.0038	-.0142	.1223	.147	201.1	-2.8
25	16.13	214.00	5.2987	-.0672	.0551	.695	200.0	-13.9
26	16.23	207.00	5.2936	-.0391	.0159	.405	199.0	-7.9
27	16.35	201.00	5.2873	-.0159	-.0000	.165	197.8	-3.1

9 2 1 2 4 6 6 1 5 2 7

WELL 108 AT 17.0 METERS

$z = \ln y = 5.902 - .0894\ x$

Standard error estimate of z = .115

Standard deviation of x = .0038

$r^2 = 0.934$

t = -23.27

Run	X	Y	Calc. z	Diff.	Sum	Rn	Calc. y	Diff.
1	1.25	294.00	5.7902	.1067	.1067	.959	327.1	33.1
2	1.55	284.00	5.7634	.1144	.2212	1.026	318.4	34.4
3	1.80	314.00	5.7411	-.0082	.2129	.074	311.4	-2.5
4	2.05	295.00	5.7187	.0317	.2446	.283	304.5	9.5
5	2.40	307.00	5.6874	-.0394	.2052	.351	295.1	-11.8
6	2.80	245.00	5.6516	.1504	.3556	1.337	284.7	39.7
7	3.15	294.00	5.6203	-.0632	.2924	.561	275.9	-18.0
8	3.40	325.00	5.5979	-.1858	.1066	1.647	269.8	-55.1
9	3.65	275.00	5.5756	-.0411	.0654	.364	263.9	-11.0
10	3.80	270.00	5.5622	-.0362	.0292	.320	260.3	-9.6
11	4.15	310.00	5.5309	-.2056	-.1763	1.817	252.3	-57.6
12	4.25	252.00	5.5219	-.0463	-.2227	.409	250.1	-11.8
13	4.45	257.00	5.5040	-.0450	-.2677	.397	245.6	-11.3
14	4.65	247.00	5.4861	-.0232	-.2909	.204	241.3	-5.6
15	4.90	205.00	5.4688	.1408	-.1501	1.240	235.9	30.9
16	5.40	250.00	5.4191	-.1023	-.2525	.900	225.6	-24.3
17	5.80	172.00	5.3833	.2358	-.0166	2.073	217.7	45.7
18	5.95	264.00	5.3699	-.2060	-.2227	1.810	214.8	-49.1
19	6.20	220.00	5.3475	-.0460	-.2688	.404	210.0	-9.9
20	6.60	200.00	5.3117	.0134	-.2553	.118	202.7	2.7
21	6.85	185.00	5.2894	.0690	-.1863	.606	198.2	13.2
22	7.15	167.00	5.2625	.1445	-.0417	1.268	192.9	25.9
23	7.50	178.00	5.2312	.0494	.0077	.434	187.0	9.0
24	7.80	187.00	5.2044	-.0266	-.0189	.234	182.0	-4.9
25	8.10	180.00	5.1776	-.0153	-.0342	.134	177.2	-2.7
26	8.50	176.00	5.1418	-.0286	-.0629	.251	171.0	-4.9
27	8.75	170.00	5.1194	-.0163	-.0792	.143	167.2	-2.7
28	9.25	155.00	5.0747	.0313	-.0479	.275	159.9	4.9
29	9.70	160.00	5.0344	-.0406	-.0886	.357	153.6	-6.3
30	14.30	105.00	4.6230	-.0309	-.1195	.278	101.8	-3.1
31	14.50	90.00	4.6051	.1053	-.0142	.949	99.9	9.9
32	14.70	84.00	4.5872	.1564	.1422	1.413	98.2	14.2
33	15.10	91.50	4.5514	.0351	.1773	.318	94.7	3.2
34	15.20	72.00	4.5425	.2658	.4432	2.412	93.9	21.9
35	15.40	93.00	4.5246	-.0079	.4353	.072	92.2	-.7
36	16.13	105.00	4.4593	-.1946	.2407	1.781	86.4	-18.5
37	16.23	100.50	4.4504	-.1597	.0809	1.464	85.6	-14.3
38	17.90	80.00	4.3010	-.0809	-.0000	.757	73.7	-6.2

9 2 1 2 4 6 6 1 5 2 8

WELL 109 AT 15.0 METERS

$z = \ln y = 5.938 - .0781\ x$

Standard error estimate of z = .127

Standard deviation of x = .0046

$r^2 = 0.904$

t = 16.78

Run	X	Y	Calc. z	Diff.	Sum	Rn	Calc. y	Diff.
1	2.10	330.00	5.7741	-.0249	-.0249	.204	321.8	-8.1
2	2.30	280.00	5.7585	.1237	.0988	1.014	316.8	36.8
3	2.70	237.00	5.7273	.2592	.3581	2.118	307.1	70.1
4	3.15	315.00	5.6921	-.0603	.2977	.491	296.5	-18.4
5	3.30	290.00	5.6804	.0105	.3083	.086	293.0	3.0
6	3.60	320.00	5.6570	-.1112	.1970	.903	286.2	-33.7
7	3.85	265.00	5.6375	.0577	.2548	.468	280.7	15.7
8	4.20	295.00	5.6101	-.0768	.1780	.621	273.1	-21.8
9	4.50	267.00	5.5867	-.0005	.1775	.004	266.8	-.1
10	5.00	195.00	5.5476	.2746	.4521	2.212	256.6	61.6
11	5.20	250.00	5.5320	.0106	.4628	.085	252.6	2.6
12	5.40	270.00	5.5164	-.0819	.3808	.659	248.7	-21.2
13	5.70	250.00	5.4939	-.0284	.3523	.228	242.9	-7.0
14	5.90	280.00	5.4773	-.1573	.1949	1.263	239.2	-40.7
15	6.15	255.00	5.4578	-.0833	.1116	.668	234.5	-20.4
16	6.40	220.00	5.4383	.0447	.1563	.358	230.0	10.0
17	6.70	237.00	6.4149	-.0531	.1031	.425	224.7	-12.2
18	6.90	235.00	5.3992	-.0602	.0428	.482	221.2	-13.7
19	7.10	220.00	5.3836	-.0099	.0329	.079	217.8	-2.1
20	8.30	245.00	5.2899	-.2113	-.1783	1.689	198.3	-46.6
21	8.75	210.00	5.2548	-.0923	-.2706	.738	191.4	-18.5
22	14.30	110.00	4.8213	.1208	-.1498	.992	124.1	14.1
23	14.50	102.00	4.8057	.1807	.0309	1.486	122.2	20.2
24	14.70	96.00	4.7900	.2257	.2566	1.860	120.3	24.3
25	15.10	216.00	4.7588	-.0774	.1792	.640	116.6	-9.3
26	15.40	96.00	4.7354	.1710	.3503	1.419	113.9	17.9
27	16.03	114.00	4.6862	-.0499	.3003	.417	108.4	-5.5
28	16.13	124.00	4.6784	-.1337	.1665	1.119	107.5	-15.4
29	16.23	117.00	4.6705	-.0915	.0749	.767	106.7	-10.2
30	16.35	114.00	4.6612	-.0749	-.0000	.629	105.7	-8.2

9 2 1 2 4 6 6 1 5 2 9

WELL 110 AT 15.0 METERS

$z = \ln y = 6.251 - .0632\ x$

Standard error estimate of z = .142

Standard deviation of x = .0056

$r^2 = 0.992$

t = 11.33

Run	X	Y	Calc. z	Diff.	Sum	Rn	Calc. y	Diff.
1	2.45	400.00	6.0958	.1043	.1043	.770	443.9	43.9
2	2.80	372.00	6.0736	.1547	.2591	1.139	434.2	62.2
3	3.10	446.00	6.0547	-.0455	.2135	.334	426.1	-19.8
4	3.40	430.00	6.0357	-.0280	.1855	.205	418.1	-11.8
5	3.70	380.00	6.0167	.0766	.2621	.559	410.2	30.2
6	3.82	380.00	6.0092	.0690	.3312	.503	407.1	27.1
7	4.10	425.00	5.9915	-.0605	.2706	.440	400.0	-24.9
8	5.00	280.00	5.9346	.2998	.5704	2.169	377.8	97.8
9	5.22	357.00	5.9207	.0429	.6134	.310	372.6	15.6
10	5.40	384.00	5.9093	-.0413	.5721	.298	368.4	-15.5
11	5.75	390.00	5.8872	-.0789	.4931	.568	360.3	-29.6
12	6.20	348.00	5.8587	.0065	.4997	.047	350.2	2.2
13	6.45	364.00	5.8429	-.0541	.4455	.389	344.7	-19.2
14	6.80	345.00	5.8208	-.0227	.4228	.163	337.2	-7.7
15	7.12	320.00	5.8006	.0322	.4551	.231	330.5	10.5
16	7.92	447.00	5.7500	-.3525	.1026	2.525	314.2	-132.7
17	8.10	357.00	5.7386	-.1390	-.0364	.996	310.6	-46.3
18	8.30	300.00	5.7260	.0222	-.0142	.159	306.7	6.7
19	8.45	338.00	5.7165	-.1065	-.1207	.762	303.8	-34.1
20	8.75	350.00	5.6975	-.1603	-.2810	1.148	298.1	-51.8
21	9.25	285.00	5.6659	.0134	-.2676	.096	288.8	3.8
22	9.70	330.00	5.6375	-.1615	-.4291	1.158	280.7	-49.2
23	14.50	174.00	5.3340	.1750	-.2541	1.290	207.2	33.2
24	14.70	150.00	5.3214	.3108	.0566	2.296	204.6	54.6
25	15.10	171.00	5.2961	.1545	.2111	1.146	199.5	28.5
26	15.40	171.00	5.2772	.1355	.3466	1.009	195.8	24.8
27	16.03	201.00	5.2373	-.0659	.2807	.494	188.1	-12.8
28	16.13	207.00	5.2310	-.1016	.1791	.764	186.9	-20.0
29	16.23	207.00	5.2247	-.1079	.0711	.812	185.8	-21.1
30	16.35	198.00	5.1171	-.0711	-.0000	.536	184.4	-13.5

9 2 1 2 4 6 6 1 5 3 0

WELL 114 AT 16.5 METERS

$z = \ln y = 5.232 - .0787\ x$

Standard error estimate of z = .224

Standard deviation of x = .0056

$r^2 = 0.999$

t = -13.95

Run	X	Y	Calc. z	Diff.	Sum	Rn	Calc. y	Diff.
1	1.85	205.00	5.0837	-.2393	-.2393	1.099	161.3	-43.6
2	2.00	200.00	5.0718	-.2264	-.4657	1.039	159.4	-40.5
3	2.20	178.00	5.0561	-.1256	-.5913	.576	156.9	-21.0
4	2.50	188.00	5.0325	-.2039	-.7952	.933	153.3	-34.6
5	2.65	200.00	5.0207	-.2775	-1.0728	1.270	151.5	-48.4
6	2.80	150.00	5.0089	-.0017	-1.0746	.007	149.7	-.2
7	3.20	175.00	4.9774	-.1873	-1.2619	.855	145.0	-29.9
8	3.40	172.00	4.9616	-.1858	-1.4477	.847	142.8	-29.1
9	3.65	168.00	4.9419	-.1819	-1.6297	.828	140.0	-27.9
10	3.80	172.00	4.9301	-.2173	-1.8470	.989	138.4	-33.5
11	4.15	154.00	4.9026	-.1343	-1.9813	.610	134.6	-19.3
12	4.40	144.00	4.8829	-.0868	-2.0682	.394	132.0	-11.9
13	4.60	122.00	4.8672	.0631	-2.0050	.286	129.9	7.9
14	4.75	132.00	4.8554	-.0274	-2.0324	.124	128.4	-3.5
15	5.00	110.00	4.8357	.1352	-1.8972	.612	125.9	15.9
16	5.20	125.00	4.8199	-.0083	-1.9055	.037	123.9	-1.0
17	5.90	125.00	4.7648	-.0634	-1.9689	.286	117.3	-7.6
18	6.15	117.00	4.7451	-.0169	-1.9859	.076	115.0	-1.9
19	6.40	95.00	4.7255	.1716	-1.8143	.774	112.7	17.7
20	6.65	97.00	4.7058	.1311	-1.6832	.591	110.5	18.5
21	6.85	92.00	4.6900	.1682	-1.5149	.759	108.8	16.8
22	7.05	87.00	4.6743	.2084	-1.3065	.939	107.1	20.1
23	7.45	92.00	4.6428	.1210	-1.1854	.545	103.8	11.8
24	7.80	97.00	4.6152	.0405	-1.1448	.182	101.0	4.0
25	8.05	97.00	4.5956	.1297	-1.0151	.583	99.0	12.0
26	8.30	75.00	4.5759	.2584	-.7567	1.162	97.1	22.1
27	8.50	80.00	4.5601	.1781	-.5785	.801	95.6	15.6
28	8.70	72.00	4.5444	.2677	-.3107	1.204	94.1	22.1
29	8.80	70.00	4.5365	.2880	-.0227	1.295	93.3	23.3
30	9.15	70.00	4.5090	.2605	.2378	1.171	90.8	20.8
31	9.50	62.00	4.4814	.3543	.5921	1.592	88.3	26.3
32	9.70	72.00	4.4657	.1890	.7811	.849	86.9	14.9
33	10.15	80.00	4.4302	.0482	.8294	.216	83.9	3.9
34	10.35	80.00	4.4145	.0325	.8619	.146	82.6	2.6
35	10.50	102.00	4.4027	-.2222	.6397	.999	81.6	-20.3
36	10.80	67.00	4.3791	.1744	.8141	.784	79.7	12.7
37	11.05	77.00	4.3594	.0156	.8297	.070	78.2	1.2
39	11.40	95.00	4.3318	-.2219	.8204	.998	76.0	-18.9
40	11.80	100.00	4.3003	-.3047	.5156	1.371	73.7	-26.2
41	12.15	55.00	4.2728	.2655	.7811	1.195	71.7	16.7
42	12.30	55.00	4.2610	.2537	1.0348	1.142	70.8	15.8
43	12.60	75.00	4.2374	-.0800	.9547	.360	69.2	-5.7
44	13.10	52.00	4.1980	.2468	1.2015	1.112	66.5	14.5
45	13.25	70.00	4.1862	-.0622	1.1393	.280	65.7	-4.2

9 2 1 2 4 6 6 1 5 3 1

Run	X	Y	Calc. z	Diff.	Sum	Rn	Calc. y	Diff.
46	13.40	82.00	4.1744	-.2322	.9070	1.047	65.0	-16.9
47	13.70	37.00	4.1508	.5499	1.4469	2.437	63.4	26.4
48	14.00	81.50	4.1272	-.2733	1.1735	1.235	62.0	-19.4
49	14.03	72.80	4.1248	-.1628	1.0106	.735	61.8	-10.9
50	14.30	35.00	4.1035	.5482	1.5589	2.479	60.5	25.5
51	14.50	60.00	4.0878	-.0065	1.5524	.029	59.6	-.3
52	14.70	48.00	4.0720	.2008	1.7533	.909	58.6	10.6
53	15.10	55.20	4.0406	.0296	1.7829	.134	56.8	1.6
54	15.20	44.4040327		.2394	2.0224	1.085	56.4	12.0
55	15.40	54.00	4.0169	.0280	2.0504	.127	55.5	1.5
56	15.90	69.80	3.9776	-.2680	1.7824	1.218	53.3	-16.4
57	16.06	46.50	3.9650	.1255	1.9080	.571	52.7	6.2
58	16.10	59.40	3.9618	-.1224	1.7856	.556	52.5	-6.8
59	16.13	60.60	3.9595	-.1447	1.6408	.658	52.4	-8.1
60	16.23	60.00	3.9516	-.1426	1.4981	.649	52.0	-7.9
61	16.37	58.80	3.9406	-.1335	1.3646	.608	51.4	-7.3
62	17.50	80.40	3.8516	-.5353	.8293	2.450	47.0	-33.3
63	17.70	79.27	3.8359	-.5369	.2923	2.460	36.3	-32.9
64	17.90	59.30	3.8201	-.2624	.0299	1.203	45.6	-13.6
65	18.16	48.00	3.7997	-.0714	-.0415	.328	44.6	-3.3
66	18.42	42.00	3.7792	.0415	-.0000	.191	43.7	1.7

THIS PAGE INTENTIONALLY
LEFT BLANK

DISTRIBUTION

Number of Copies

OFFSITE

267 U.S. Technical Information Center
Oak Ridge, TN 20545

ONSITE

7 U.S. Department of Energy - RL

T. A. Bauman
O. J. Elgert (3)
R. G. Harris
F. R. Standerfer
M. W. Tiernan

10 Pacific Northwest Laboratory

L. L. Ames
R. L. Brodzinski
D. B. Clearlock
P. A. Eddy
J. R. Eliason
O. F. Hill
R. W. Perkins
S. J. Phillips
R. J. Serne
R. E. Wildung

1 United Nuclear Industries, Inc.

H. F. Jenson

96 Rockwell Hanford Operations

B. W. Anderson
H. Babad
J. W. Bailey
D. C. Bartholomew
D. J. Brown (10)
L. E. Bruns
C. R. Carter
D. J. Cockeram
J. L. Deichman (5)
R. A. Deju
J. W. Donahue
G. T. Dukelow
J. B. Fecht
K. R. Fecht
R. D. Fox
P. J. Fritch
J. H. Garbrick
R. J. Gimera
D. J. Gustavson
R. D. Hammond
W. F. Heine
R. E. Isaacson
J. E. Kinzer
E. J. Kosiancic
A. G. Law
H. B. Lindberg
R. Y. Lyon
C. W. Manry (2)

9 2 1 2 4 6 6 1 5 3 3

DISTRIBUTION (Continued)

Rockwell Hanford Operations (cont'd)

H. E. McGuire
L. P. McRae
P. F. Mercier
D. L. Merrick
P. M. Nugent
G. C. Owen
J. V. Panesko
W. H. Price (5)
R. D. Prosser (5)
I. E. Reep
R. C. Roal
J. H. Roecker
R. C. Routson (10)
W. W. Schulz
H. P. Shaw
D. F. Shepard
M. J. Smith
D. Summer
J. A. Teal
H. H. Wang
C. T. Webster
T. J. Wood
D. C. Wodrich
Earth Sciences Library (10)
Document Control (4)

9 2 1 2 4 6 6 1 5 3 4